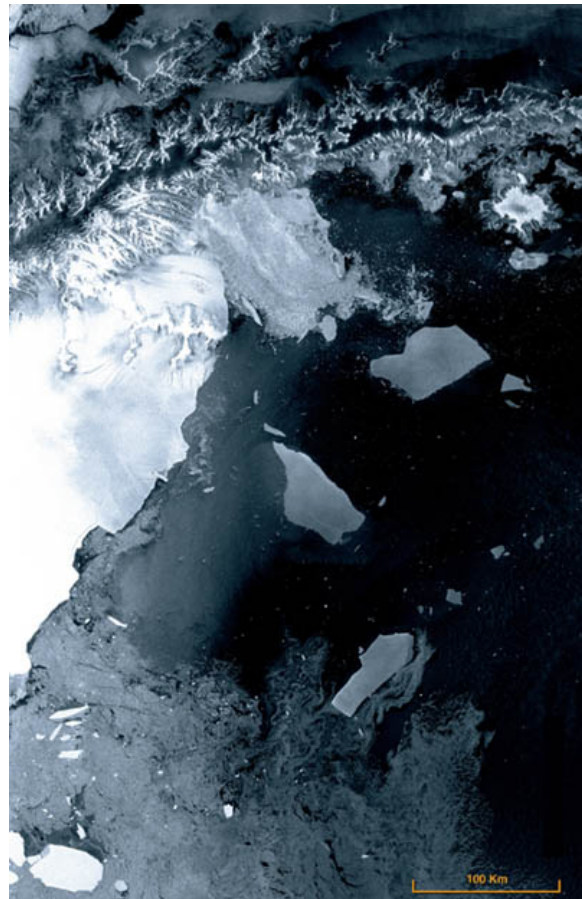




## ASAR Product Handbook



European Space Agency - EnviSat ASAR Product Handbook, Issue 2.2, 27 February 2007

---

Copyright 2000-2007, European Space Agency, All rights reserved



# Table of contents

---

ASAR Product Handbook	
1 The ASAR User Guide	13
1.1 How to Choose ASAR Data	13
1.1.1 Geophysical Measurements	14
1.1.2 Scientific Background	17
1.1.2.1 Radar Imaging	17
1.1.2.1.1 Polarisation	19
1.1.2.1.2 Backscatter	19
1.1.2.2 Real Aperture Radar (RAR)	20
1.1.2.2.1 Spatial Resolution	20
1.1.2.2.2 Range Resolution	21
1.1.2.2.3 Azimuth Resolution	21
1.1.2.3 Synthetic Aperture Radar (SAR)	21
1.1.2.4 Image Interpretation	23
1.1.2.4.1 Geometric Characteristics	23
1.1.2.4.2 Electrical Characteristics	25
1.1.2.4.3 Responses of Soil, Vegetation, Mountains, Water and Ice	25
1.1.2.4.3.1 Soil	25
1.1.2.4.3.2 Vegetation	25
1.1.2.4.3.3 Mountains	26
1.1.2.4.3.4 Water and Ice	27
1.1.2.5 General Rules for SAR Image Interpretation	28
1.1.2.6 References	28
1.1.3 Principles of Measurement	28
1.1.4 Geophysical Coverage	36
1.1.5 Special Features of ASAR	38
1.1.5.1 Dual Polarisation	38
1.1.5.2 Selectable Incidence Angles	50
1.1.5.3 Wide Area Coverage and Frequency of Coverage	56
1.1.5.4 Interferometry	61
1.1.5.4.1 Principles	62
1.1.5.4.2 Across-track Interferometry (InSAR)	64
1.1.5.4.3 Along-track Interferometry	67
1.1.5.4.4 Differential Interferometry (D-InSAR)	67
1.1.5.4.5 Coherence Evaluation	69
1.1.5.4.6 Low Resolution Interferometry	70
1.1.5.4.7 Conclusions	71
1.1.5.4.8 References	71
1.1.5.5 Wave Spectra	73
1.1.5.6 Simultaneous Observations	79
1.1.6 Summary of Applications vs Products	82
1.1.6.1 Summary of Applications Introduction	82
1.1.6.1.1 Remote Sensing Science	83
1.1.6.1.2 Earth Science	85

1.1.6.1.3 Commercial Applications	87
1.1.6.2 Ocean Applications	88
1.1.6.2.1 Wave Characteristics	89
1.1.6.2.2 Ocean Fronts	92
1.1.6.2.3 Coastal Dynamics	92
1.1.6.2.4 Oil Slicks and Ship Traffic	94
1.1.6.3 Land Applications	97
1.1.6.3.1 Global Vegetation Monitoring	99
1.1.6.3.2 Forestry	101
1.1.6.3.3 Geology and Topography	103
1.1.6.3.4 Agriculture	106
1.1.6.3.5 Natural Hazards	108
1.1.6.3.6 Flooding, Hydrology and Water Management	114
1.1.6.3.7 Urban Studies	116
1.1.6.3.8 References	118
1.1.6.4 Sea Ice Applications	118
1.1.6.4.1 Sea Ice Applications - Ice Sheet Dynamics	123
1.1.6.4.2 Sea Ice Applications - Snow Cover	127
1.1.6.4.3 Sea Ice Applications - Sea Ice Mapping	132
1.1.6.4.4 Sea Ice Application - Ship Routing through Sea Ice	134
1.2 How to Use ASAR Data	135
1.2.1 Software Tools	136
1.2.1.1 General Software Tools	136
1.2.1.2 EnviView	137
1.2.1.3 ASAR Toolbox	139
1.3 Further Reading	140
1.4 Image Gallery	144
2 ASAR Products and Algorithms	160
2.1 Products and Algorithms Introduction	161
2.1.1 Child Products	169
2.1.1.1 Definition	169
2.1.1.2 Child Product Extraction Requirements	170
2.1.1.2.1 Data Set Selection	170
2.1.1.2.2 ISP Subsets Selection (Extracted Instrument Headers)	171
2.1.1.2.3 Common Archiving Facility Requirements	171
2.1.2 Organisation of Products	172
2.2 Definitions and Conventions	178
2.3.1 Definitions	178
2.3.1.1 Global and Regional Coverage	178
2.3.1.2 Auxiliary Data	178
2.3.1.3 Geolocation and Geocoding	179
2.3.1.4 Product Confidence Data	179
2.3.1.5 Calibration	180
2.3.1.6 Processed Product Sizes and Coverage	180
2.3.2 Conventions	181
2.3.2.1 ENVISAT: General product structure	181
2.3.2.2 Main Product Header (MPH)	182
2.3.2.3 Specific Product Header (SPH)	184
2.3.2.4 Data Set Descriptors (DSD)	184
2.3.2.5 Data Set (DS)	189
2.4 Product Evolution History	190
2.5 ASAR Level 0 Products	191
2.5.1 Introduction	191
2.5.1.1 ASAR Instrument Source Packet	191
2.5.1.2 Level 0 Products	191
2.5.1.2.1 Processing Performed	192
2.5.1.2.2 High Data Rate Level 0 Products	192
2.5.1.2.2.1 Image Mode (ASA_IM_0P)	193

2.5.1.2.2.2 Alternating Polarisation (AP) Mode	193
2.5.1.2.2.3 Wide Swath (WS) Mode (ASA_WS_0P)	194
2.5.1.2.2.4 Level 0 External Characterisation (ASA_EC_0P)	195
2.5.1.2.3 Low Data Rate Level 0 Products	195
2.5.1.2.3.1 Global Monitoring (GM) Mode (ASA_GM_0P)	196
2.5.1.2.3.2 Wave Mode (WV) Level 0 Product (ASA_WV_0P)	196
2.5.1.2.3.3 Level 0 Module Stepping Mode (ASA_MS_0P)	197
2.5.1.3 Level 0 Formats	198
2.5.2 Level 0 Instrument Source Packet Description	199
2.6 Level 1B Products	209
2.6.1 ASAR Level 1B Algorithms	209
2.6.1.1 ASAR Level 1B Algorithm Physical Justification	209
2.6.1.1.1 Introduction	209
2.6.1.1.2 Radar Geometry	209
2.6.1.1.3 Pulse Compression	210
2.6.1.1.4 SAR Signal	211
2.6.1.1.5 Continuous versus Burst Data	213
2.6.1.1.6 Image Cross Spectra	214
2.6.1.2 ASAR Level 1B Algorithm Descriptions	215
2.6.1.2.1 Preprocessing	216
2.6.1.2.2 Doppler Frequency Estimator	217
2.6.1.2.2.1 Introduction	217
2.6.1.2.2.2 Madsen's Method	219
2.6.1.2.2.3 Multi-Look Cross Correlation (MLCC) Method	219
2.6.1.2.2.4 Look Power Balancing	222
2.6.1.2.2.5 PRF Diversity Method	225
2.6.1.2.2.6 Notes	226
2.6.1.2.2.7 References	227
2.6.1.2.3 Range-Doppler	227
2.6.1.2.3.1 Introduction	227
2.6.1.2.3.1.1 Overview	227
2.6.1.2.3.1.2 Range Compression	229
2.6.1.2.3.1.3 Azimuth FFT	230
2.6.1.2.3.1.4 Range Cell Migration Correction (RCMC)	230
2.6.1.2.3.1.5 Azimuth Compression	231
2.6.1.2.3.1.6 Summary	233
2.6.1.2.3.1.7 References	233
2.6.1.2.3.2 Processing Algorithms For AP SLC	233
2.6.1.2.3.2.1 Introduction	233
2.6.1.2.3.2.2 Background	234
2.6.1.2.3.2.3 Burst Mode Interferometry	235
2.6.1.2.3.2.4 Modifications To Range Doppler Algorithm	241
2.6.1.2.3.2.5 Conclusions	243
2.6.1.2.3.2.6 References	243
2.6.1.2.4 SPECAN	243
2.6.1.2.4.1 Introduction	244
2.6.1.2.4.1.1 Overview	244
2.6.1.2.4.1.2 Range Compression	245
2.6.1.2.4.1.3 Linear Range Cell Migration Correction (RCMC)	245
2.6.1.2.4.1.4 Azimuth Processing	246
2.6.1.2.4.1.5 Look Summation and Resampling	248
2.6.1.2.4.1.6 Product Processing	248
2.6.1.2.4.1.7 Summary	249
2.6.1.2.4.1.8 References	249
2.6.1.2.4.2 Descalloping	249
2.6.1.2.4.2.1 Scalloping	249
2.6.1.2.4.2.2 Methods for Scalloping Correction	251
2.6.1.2.4.2.2.1 Azimuth Descalloping Function Application	252

2.6.1.2.4.2.2.2 Doppler Centroid Frequency Estimation in the context of Burst Mode Data_____	252
2.6.1.2.4.2.3 Notes_____	253
2.6.1.2.4.2.4 References_____	253
2.6.1.2.4.3 ScanSAR Beam Merging_____	253
2.6.1.2.4.3.1 Determine a reference point in the blend region_____	254
2.6.1.2.4.3.2 Determine the limits of the blend region_____	254
2.6.1.2.4.3.3 Merge the data in the two beams corresponding to the blend region according to a predefined rule_____	254
2.6.1.2.4.4 Global Monitoring Mode Inverse Filter_____	255
2.6.1.2.5 ASAR Strip Line Product Processing_____	257
2.6.1.2.5.1 2.6.1.2.5.1 Introduction_____	257
2.6.1.2.5.1.1 Slice Size and Overlap_____	259
2.6.1.2.5.1.2 Processing Parameters Affected By Strip Line Product Continuity Requirements_____	259
2.6.1.2.5.2.1 I And Q Channel Statistics_____	260
2.6.1.2.5.2.2 Chirp Replica_____	260
2.6.1.2.5.2.3 Antenna Elevation Gain Correction_____	261
2.6.1.2.5.2.4 Doppler Centroid Estimation_____	261
2.6.1.2.5.2.5 along-track Pixel Spacing/Start Position_____	261
2.6.1.2.5.2.6 Slant Range/Ground Range (SR/GR) Conversion To Output Grid_____	262
2.6.1.2.5.2.7 FM Rate_____	262
2.6.1.2.5.2.8 First Output Range Sample_____	262
2.6.1.3 Level 1B Accuracies_____	263
2.6.2 Level 1B Products_____	264
2.6.2.1 Level 1B High Level Organisation of Products_____	264
2.6.2.1.1 Level 1B Image Products_____	266
2.6.2.1.1.1 Image Product Structure_____	266
2.6.2.1.1.1.1 Image Product Data Sets_____	268
2.6.2.1.1.1.2 Stand-Alone (On-Request) Image Products_____	268
2.6.2.1.1.2.1 Stand-Alone Product Types_____	269
2.6.2.1.1.2.1.1 Image Mode Single-Look Complex_____	269
2.6.2.1.1.2.1.2 Image Mode Precision Image_____	270
2.6.2.1.1.2.1.3 Image Mode Ellipsoid Geocoded Image_____	270
2.6.2.1.1.2.1.4 Alternating Polarisation Mode Single-Look Complex_____	271
2.6.2.1.1.2.1.5 Alternating Polarisation Mode Precision Image_____	272
2.6.2.1.1.2.1.6 Alternating Polarisation Ellipsoid Geocoded Image_____	273
2.6.2.1.1.2.2 Input Data_____	274
2.6.2.1.1.2.3 Auxiliary Data Used_____	274
2.6.2.1.1.3 Stripline Processed Image Products_____	275
2.6.2.1.1.3.1 Stripline Product Types_____	276
2.6.2.1.1.3.1.1 Image Mode Medium-resolution Image_____	277
2.6.2.1.1.3.1.2 Alternating Polarisation Medium-resolution Image_____	277
2.6.2.1.1.3.1.3 Wide Swath Medium-resolution Image_____	278
2.6.2.1.1.3.1.4 Global Monitoring Mode Image Product_____	279
2.6.2.1.1.3.2 Input Data_____	279
2.6.2.1.1.3.3 Auxiliary Data Used_____	279
2.6.2.1.1.3.4 Product Structure_____	279
2.6.2.1.2 Level 1B Wave Products_____	281
2.6.2.1.2.1 Product Types_____	281
2.6.2.1.2.1.1 Wave Mode SLC Imagette and Imagette Cross-Spectra_____	281
2.6.2.1.2.1.2 Wave Mode Imagette Cross-Spectra_____	282

2.6.2.1.2.2 Input Data	283
2.6.2.1.2.3 Auxiliary Data Used	283
2.6.2.1.2.4 Processing Performed	283
2.6.2.1.2.4.1 Wave Mode Error Handling	284
2.6.2.1.2.5 Product Structure	284
2.6.2.1.2.5.1 Main Product Header	285
2.6.2.1.2.5.2 Specific Product Header	285
2.6.2.1.2.5.3 Data Set Names	286
2.6.2.1.2.5.4 Data Sets	286
2.6.2.1.2.5.4.1 MDS Containing Imagettes	287
2.6.2.1.3 Browse Products	287
2.6.2.1.3.1 Product Types	288
2.6.2.1.3.1.1 Image Mode Browse Image	288
2.6.2.1.3.1.2 Alternating Polarisation Browse Image	289
2.6.2.1.3.1.3 Wide Swath Browse Image	290
2.6.2.1.3.1.4 Global Monitoring Mode Browse Image	291
2.6.2.1.3.2 Processing Performed	291
2.6.2.1.3.3 Product Structure	292
2.6.2.1.3.3.1 Browse SQ ADS	292
2.6.2.1.3.3.2 Subsampled Geolocation Grid ADS	292
2.6.2.2 Level 1B Engineering Quantities	293
2.6.2.2.1 Image Products	293
2.6.2.2.1.1 Medium Resolution Products	293
2.6.2.2.1.1.1 Image Mode Medium-resolution Image (ASA_IMM_1P)	293
2.6.2.2.1.1.2 Alternating Polarisation Medium-resolution Image (ASA_APM_1P)	293
2.6.2.2.1.1.3 Wide Swath Medium-resolution Image (ASA_WSM_1P)	294
2.6.2.2.1.2 Single-Look Complex (SLC) Products	295
2.6.2.2.1.2.1 Image Mode Single-Look Complex (ASA_IMS_1P)	295
2.6.2.2.1.2.2 Alternating Polarisation Mode Single-Look Complex (ASA_APS_1P)	295
2.6.2.2.1.3 Precision Image Products	296
2.6.2.2.1.3.1 Image Mode Precision Image (ASA_IMP_1P)	296
2.6.2.2.1.3.2 Alternating Polarisation Mode Precision Image (ASA_APP_1P)	297
2.6.2.2.1.4 Ellipsoid Geocoded Products	297
2.6.2.2.1.4.1 Image Mode Ellipsoid Geocoded Image (ASA_IMG_1P)	298
2.6.2.2.1.4.2 Alternating Polarisation Ellipsoid Geocoded Image (ASA_APG_1P)	298
2.6.2.2.1.5 Global Monitoring Products	299
2.6.2.2.1.5.1 Global Monitoring Mode Image Product (ASA_GM1_1P)	299
2.6.2.2.2 Wave Products	300
2.6.2.2.2.1 Imagette Cross-Spectra Products	300
2.6.2.2.2.1.1 Wave Mode SLC Imagette and Imagette Cross-Spectra (ASA_WVI_1P)	300
2.6.2.2.2.2 Single-Look Complex (SLC) Imagette Products	301
2.6.2.2.2.2.1 Wave Mode Imagette Cross-Spectra (ASA_WVS_1P)	301
2.6.2.3 Level 1B Essential Product Confidence Data	301
2.7 Level 2 Product and Algorithms	303
2.7.1 ASAR Level 2 Algorithms	303
2.7.1.1 General Description	304
2.7.1.2 Processing Steps	304

2.7.2 Level 2 Product	309
2.8 Instrument-specific Topics	315
2.9 Auxiliary Products	315
2.9.1 Summary of Auxiliary Data Sets	316
2.9.1.1 Auxiliary Data Files	316
2.9.1.2 Naming Strategy	316
2.9.1.3 Auxiliary Data Structure	317
2.9.1.4 Auxiliary Data MPH	318
2.9.1.5 Auxiliary Data SPH Structure	319
2.9.1.6 Auxiliary Data Sets	319
2.9.2 Auxiliary Data Sets for Level 1B Processing	319
2.9.3 Common Auxiliary Data Sets	321
2.9.3.1 FOS Orbit State Vectors	321
2.9.3.2 DORIS Preliminary Orbit State Vectors	322
2.9.3.3 DORIS Precise Orbit State Vectors	322
2.9.3.4 DORIS Navigator Level 0	323
2.9.3.5 UTC/SBT Time Conversion File	323
2.9.3.6 ECMWF Data Files	324
2.10 ASAR Latency Throughput and Data Volume	325
2.10.1 Latency	325
2.10.2 Throughput	326
2.10.2.1 Product parameters	326
2.10.3 Data Volume	326
2.10.3.1 Product Sizes for Disk Storage	326
2.11 ASAR Characterisation and Calibration	327
2.11.1 Introduction	327
2.11.2 Pre-flight Characterisation Measurements	328
2.11.3 Internal Calibration	329
2.11.3.1 Elevation Gain Monitoring	331
2.11.3.2 Chirp Replica Construction	333
2.11.3.3 PF-ASAR Normalisation	334
2.11.3.4 Module Stepping	334
2.11.4 External Characterisation	334
2.11.4.1 Characterisation of the Antenna Beam Pattern	335
2.11.4.2 Gain Calibration	335
2.11.4.3 Global Monitoring Mode	336
2.11.5 The Derivation of Backscattering Coefficients and RCSs in ASAR Products	336
2.11.6 Notes	338
2.11.7 References	338
2.12 ASAR Data Handling Cookbook	339
2.12.1 Hints and Algorithms for Data Use	339
2.12.1.1 Extracting Grid Information To Do Plots	339
2.12.1.2 Locating the Error Information	340
2.12.1.3 Converting Units of Engineering/Geophysical parameters	340
2.12.1.4 Displaying 'Scientific' PCD Information	340
2.12.2 Hints and Algorithms for Higher Level Processing	340
3 The ASAR Instrument	341
3.1 Instrument Description	342
3.1.1 Payload Description and Position on the Platform	347
3.1.1.1 ASA Subsystem	348
3.1.1.2 CESA Subsystem	354
3.1.1.2.1 Data Subsystem	354
3.1.1.2.2 Radio Frequency (RF) Subsystem	355
3.1.1.2.3 Control Subsystem (CSS)	357
3.1.1.2.4 Power Conditioning Unit (PCU)	357
3.1.2 ASAR Instrument Functionality	358
3.1.2.1 Global Mission	358

3.1.2.2 Regional Mission	359
3.1.3 Internal Data Flow	361
3.2 Instrument Characteristics and Performance	362
3.2.1 Preflight Characteristics and Expected Performance	362
3.2.2 Inflight Performance Verification	368
4 ASAR Frequently Asked Questions	377
5 ASAR Glossary Terms	388
5.1 Acronyms and Abbreviations	388
5.2 RADAR and SAR Glossary	393
5.3 Product Terms	403
5.4 ASAR Instrument Glossary	410
5.5 Geometry Glossary	411
5.6 Oceans Glossary	418
5.7 Land Glossary	419
5.8 Sea Ice Glossary	420
6 ASAR Data Formats Products	421
6.1 Level 2 Products	421
6.1.1 ASA_WVV_2P: ASAR Wave Mode Wave Spectra	422
6.2 Level 1 Products	422
6.2.1 ASA_APG_1P: ASAR Alternating Polarization Ellipsoid Geocoded Image	422
6.2.2 ASA_APM_1P: ASAR Alternating Polarization Medium Resolution Image product	423
6.2.3 ASA_APP_1P: ASAR Alternating Polarization Mode Precision Image	424
6.2.4 ASAAPS_1P: ASAR Alternating Polarization Mode Single Look Complex	425
6.2.5 ASA_GM1_1P: ASAR Global Monitoring Mode Image	425
6.2.6 ASA_IMG_1P: ASAR Image Mode Ellipsoid Geocoded Image	426
6.2.7 ASA_IMM_1P: ASAR Image Mode Medium Resolution Image	427
6.2.8 ASA_IMP_1P: ASAR Image Mode Precision Image	427
6.2.9 ASA_IMS_1P: ASAR Image Mode Single Look Complex	428
6.2.10 ASA_WSM_1P: ASAR Wide Swath Medium Resolution Image	429
6.2.11 ASA_WVI_1P: ASAR Wave Mode SLC Imagette and Imagette Cross Spectra	429
6.2.12 ASA_WVS_1P: ASAR Wave Mode Imagette Cross Spectra	436
6.2.13 ASA_WSS_1P: Wide Swath Mode SLC Image	437
6.3 Level 0 Products	437
6.3.1 ASA_APc_0P: ASAR Alternating Polarization Level 0 (Copolar)	438
6.3.2 ASAAPH_0P: ASAR Alternating Polarization Level 0 (Cross polar H)	438
6.3.3 ASA_APV_0P: ASAR Alternating Polarization Level 0 (Cross polar V)	439
6.3.4 ASA_EC_0P: ASAR Level 0 External Characterization	440
6.3.5 ASA_GM_0P: ASAR Global Monitoring Mode Level 0	440
6.3.6 ASA_IM_0P: ASAR Image Mode Level 0	441
6.3.7 ASA_MS_0P: ASAR Level 0 Module Stepping Mode	441
6.3.8 ASA_WS_0P: ASAR Wide Swath Mode Level 0	442
6.3.9 ASA_WV_0P: ASAR Wave Mode Level 0	442
6.4 Browse Products	443
6.4.1 ASA_AP_BP: ASAR Alternating Polarization Browse Image	443
6.4.2 ASA_GM_BP: ASAR Global Monitoring Mode Browse Image	444
6.4.3 ASA_IM_BP: ASAR Image Mode Browse Image	444
6.4.4 ASA_WS_BP: ASAR Wide Swath Browse Image	445
6.5 Auxillary Products	446
6.5.1 ASA_CON_AX: ASAR Processor Configuration	446
6.5.2 ASA_INS_AX: ASAR Instrument characterization	446
6.5.3 ASA_XCA_AX: ASAR External calibration data	447

6.5.4 ASA_XCH_AX: ASAR External characterization data	448
<b>6.6 Records</b>	<b>448</b>
6.6.1 Main Product Header	448
6.6.2 ASAR processor configuration data	453
6.6.3 ASAR instrument characterization data	465
6.6.4 ASAR external calibration data	488
6.6.5 ASAR external characterization data	490
6.6.6 Antenna Elevation pattern	492
6.6.7 Chirp parameters	493
6.6.8 Doppler Centroid parameters	495
6.6.9 Geolocation Grid ADSRs	496
6.6.10 Measurement Data Set 1	498
6.6.11 ASAR Image Products SPH	499
6.6.12 Main Processing parameters	505
6.6.13 Map Projection parameters	513
6.6.14 Ocean Wave Spectra	516
6.6.15 Measurement Data Set containing spectra. 1 MDSR per spectra.	519
6.6.16 SQ ADSRs	521
6.6.17 Slant Range to Ground Range conversion parameters	524
6.6.18 ASAR Wave Mode Products Base SPH	525
6.6.19 Wave Mode Geolocation ADS	530
6.6.20 Wave Mode processing parameters	531
6.6.21 SQ ADSRs	543
6.6.22 ASAR WV Product SPH	546
6.6.23 SPH for auxiliary data with N=1 DSDs	552
6.6.24 Level 0 MDSR	552
6.6.25 Level 0 SPH	554
6.6.26 Doppler Centroid parameters	558
<b>7 Credits</b>	<b>560</b>

# Abstract

The ASAR Handbook has been produced as a part of the ENVISAT Handbook and is designed to provide detailed information concerning the instrument, its data, and data uses. This is a living document. The parameters and values provided may change as the ground segment processing becomes better defined.

The handbook has been organised into the following sections:

- The ASAR Products User Guide- The User Guide will provide the reader with information on the special features of ASAR data, as well as how to select the type of products best suited for specific requirements. It will also discuss how to use the data, and provide a selection of sources for further reading.
- ASAR Products and Algorithms - This section will provide detail on all of the ASAR products and associated algorithms, including a discussion on ASAR characterisation and calibration as well as hints on data handling.
- The ASAR Instrument - Here is where the reader will find the specifics concerning the ASAR instrument itself. Topics covered include the payload description, instrument functionality, characteristics and performance expectations.
- Frequently Asked Questions (FAQs) - This section will be populated over time.
- Glossary - A list of all acronyms, abbreviations, and terms used throughout the ASAR handbook.
- Data Formats - A summary of all ASAR products and a detailed description of each record within each ASAR product.
- Credits - A list of the agencies who have contributed data or information to this document.

# Chapter 1

---

## The ASAR User Guide

The Advanced Synthetic Aperture Radar (ASAR) instrument on board the ENVISAT satellite extends the mission of the Active Microwave Instrument (AMI) Synthetic Aperture Radar (SAR) instruments flown on the European Remote Sensing (ERS) Satellites ERS-1 and ERS-2. ASAR uses an active phased-array [antenna](#), with [incidence angles](#) between 15 and 45 degrees. Applications for this sensor will include the study of ocean waves, sea ice extent and motion, and land surface studies such as deforestation and desertification, to name a few.

This User Guide will provide the reader with information on the special features of ASAR data, as well as how to select the type of products best suited for specific requirements. It also discusses how to use the data, and provides a list of sources for further reading.

### 1.1 How to Choose ASAR Data

---

The Advanced Synthetic Aperture [Radar](#) (ASAR) instrument is capable of retrieving a variety of geophysical measurements. In order to exploit these effectively, it is necessary to understand exactly what ASAR measures, why the instrument has been designed to operate in this way, and how these measurements are made.

ASAR data also offers a number of unique capabilities and advantages over data from similar imaging instruments, which are highlighted in the following sections.

The result of these features is data suitable for a wide range of potential applications. A summary of products and applications is provided to assist the user in identifying the most suitable product for his or her particular needs and use.

### 1.1.1 Geophysical Measurements

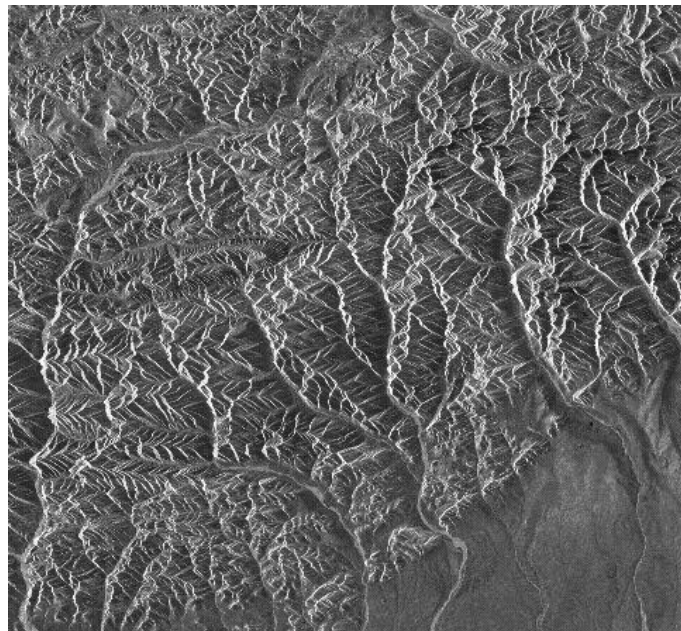


Figure 1.1 ERS-1 image Aug. 5, 1992 Brooks Range - Bathtub Ridge (Copyright ESA, 1992)

The [ENVISAT](#) mission has both global and regional objectives, with the corresponding need to provide data to scientific and application users on various time scales.

Following on from the very successful [ERS-1/2 SARs](#), [ASAR](#) is an all-weather, day-and-night, [high-resolution imaging](#) instrument that will provide [radar backscatter](#) measurements indicative of terrain structure, surface [roughness](#), and dielectric constant. Important new capabilities of ASAR include beam steering for acquiring images with different [incidence angles](#), dual polarisation, and wide [swath](#) coverage.

Important contributions of ASAR to the global mission include:

- measuring sea state conditions at various scales
- mapping ice sheet characteristics and dynamics
- mapping sea ice distribution and dynamics
- detecting large scale vegetation changes
- monitoring natural and man-made pollution over the ocean

ASAR will make a major contribution to the regional mission by providing continuous and reliable data sets for applications such as:

- offshore operations in sea ice
- snow and ice mapping
- coastal protection and pollution monitoring
- ship traffic monitoring
- agriculture and forest monitoring
- soil moisture monitoring
- geological exploration
- topographic mapping
- predicting, tracking and responding to natural hazards
- surface deformation

Some of the global and regional objectives (sea state condition, sea ice applications, marine pollution, maritime traffic, hazard monitoring, etc.) require near real-time (NRT) data products (within a few hours from sensing). Some of these products are generated systematically since they are assimilated by meteorological offices (e.g. wave and wind information from wave mode acquisitions) while others are generated according to user requests. Other applications (e.g., agriculture, soil moisture, etc.) require fast turnaround data services (within a few days).

As well as using ASAR to satisfy specific operational and commercial requirements, major systematic data collection programmes will be undertaken, to build up archives for scientific research purposes.

ASAR will provide continuity of the ERS SAR Image and Wave Modes but with the opportunity for better temporal frequency of coverage. The nominal spatial resolution (30 m) and swath coverage of ASAR Image Mode (100 km) are the same as the ERS Image Mode, and ASAR will also be in a 35-day repeat orbit. However, using beam steering, it will be possible to obtain images of the same area on the ground from different orbits with different incidence angles. This gives a revisit frequency varying from daily coverage near the poles to weekly coverage at the equator.

ASAR has dual polarisation capabilities and a special Alternating Polarisation Mode has been implemented that permits half of the looks from a scene to be acquired with horizontal

---

and half with vertical polarisation, thereby considerably increasing the target classification capability (especially if used in conjunction with multi-temporal imaging).

Wide area coverage will be achieved by switching between different swaths using the ScanSAR technique. This will enable 405 km coverage at resolutions of either 150 m or 1 km. At the 1 km resolution the data rate is low enough for tape recording on board the spacecraft and the recording capacity will be sufficient for downloading low-resolution global coverage through a single receiving station.

#### Incidence Angle

In contrast to the ERS SARs, which had a fixed swath position (23° mid-swath incidence angle), ASAR Image Mode will provide data acquisition in seven different swath positions (i.e., IS1 to IS7), giving incidence angles ranging from 15° to 45°. This subject is discussed in the section "[Selectable Incidence Angles](#)" [1.1.5.2](#).

#### Dual Polarisation

Imaging radars can transmit horizontal or vertical electric field vectors, and receive either horizontal or vertical return signals, or both. The basic physical processes responsible for the like-polarised return are quasi-specular surface reflection and surface or volume scattering. The cross-polarised return is usually weaker, and often associated with multiple scattering due to surface roughness or multiple volume scattering. Scattering mechanisms and the returns from different surfaces may also vary markedly with incidence angle. For a further discussion of this topic see the section entitled "[Dual Polarisation](#)." [1.1.5.1](#).

#### Wide Area and Frequent Coverage

ASAR medium and low-resolution images, provided by the Wide Swath and Global Monitoring Modes, open up new possibilities for applications requiring large area coverage and/or more frequent revisit. Both modes will provide 405 km swath coverage with a spatial resolution of 150 m for the Wide Swath and 1000 m for the Global Monitoring. For applications where higher resolution is necessary, better than a 5-day repeat interval is possible for approximately 100 km x 100 km areas using Image Mode. For a further discussion on this topic, see the section entitled "[Wide Area Coverage and Frequency of Coverage](#)." [1.1.5.3](#).

#### Interferometry

ASAR offers continuity with 35-day repeat images for SAR interferometry, although interferometric pairs will need to be taken with the same incidence angles. The availability of ASAR interferometric pairs acquired at higher incidence angles will be useful for improving the visibility of steeper slopes, and there will also be new possibilities for low-resolution interferometry. For a further discussion on this topic, see the section entitled "[Interferometry](#)." [1.1.5.4](#).

#### Wave Spectra

ASAR Wave Mode will provide wave spectra derived from imagettes of minimum size (5 km x 5 km), similar to the ERS AMI-Wave Mode, spaced 100 km along-track in VV polarisation. For a further discussion on this topic, see the section entitled "[Wave Spectra](#)." [1.1.5.5](#).

## 1.1.2 Scientific Background



Figure 1.2 ERS-1 image, May 17, 1992 Mt. Redoubt, Southern Alaska (Copyright ESA, 1992)

### 1.1.2.1 Radar Imaging

Radar is the commonly used acronym for Radio Detection and Ranging. Radio waves are that part of the electromagnetic spectrum that have wavelengths considerably longer than visible light, as shown in [figure 1.3](#) below.

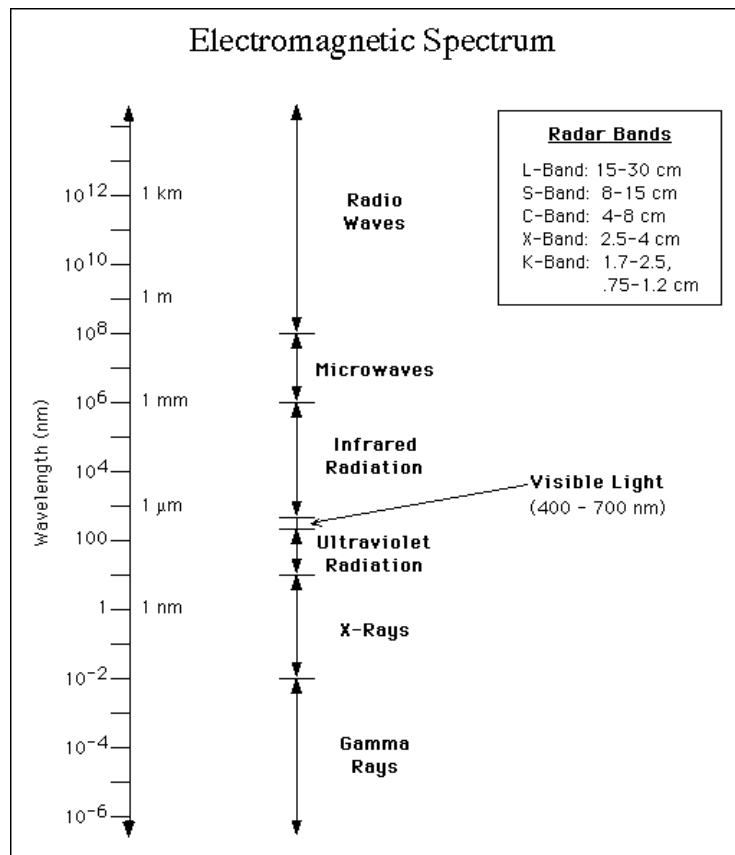


Figure 1.3 The Electromagnetic Spectrum

Imaging radar is an active illumination system, in contrast to passive optical imaging systems that require the Sun's illumination. An antenna, mounted on an aircraft or spacecraft, transmits a radar signal in a [side-looking direction](#) towards the earth's surface. The reflected signal, known as the echo, is [backscattered](#) from the surface and received a fraction of a second later at the same antenna, as shown in [figure 1.4](#) below. The brightness, or amplitude (A), of this received echo is measured and recorded and the data are then used to construct an image. For coherent Radar systems such as Synthetic Aperture Radar (SAR), the phase of the received echo is also measured and used to construct the image.

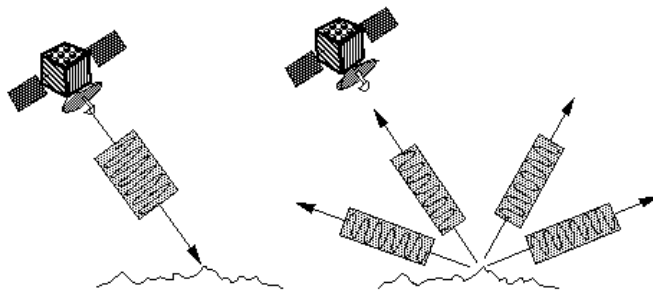


Figure 1.4 Echoes received back by antenna

Radar uses a single frequency for illumination; therefore there is no color associated with raw Radar imagery (unlike optical imagery which is illuminated by all the various colours from the ambient visible light.) However, Radar provides at least two significant benefits from its not being dependent on natural light: the ability to image through clouds, and the ability to image at night. The wavelength of the microwaves used in Radar are longer than those of visible light, and are less responsive to the boundaries between air and the water droplets within the clouds. The result is that, for Radar, the clouds appear homogeneous with only slight distortions occurring when the waves enter and leave the clouds.

#### 1.1.2.1.1 Polarisation

Irrespective of wavelength, radar signals can be transmitted and/or received in different modes of polarisation. Being electromagnetic waves, microwaves are transverse; that is the vibrations are perpendicular to the direction of wave propagation (unlike sound waves which are longitudinal and vibrate in the same direction as the wave propagation.) For Radar, the waves are typically polarised in a plane, either horizontal or vertical; although it is also possible for the waves to not be restricted to a plane (they could be elliptically or circularly polarised).

#### 1.1.2.1.2 Backscatter

Radar images are composed of many picture elements referred to as pixels. Each pixel in the radar image represents an estimate of the radar backscatter for that area on the ground. Darker areas in the image represent low backscatter, while brighter areas represent high backscatter. Bright features mean that a large fraction of the radar energy was reflected back to the radar, while dark features imply that very little energy was reflected. Backscatter for a target area at a particular wavelength will vary for a variety of conditions, such as the physical size of the scatterers in the target area, the target's electrical properties and the moisture

content, with wetter objects appearing bright, and drier targets appearing dark. (The exception to this is a smooth body of water, which will act as a flat surface and reflect incoming pulses away from a target. These bodies will appear dark). The wavelength and polarisation of the Radar pulses, and the observation angles will also affect backscatter

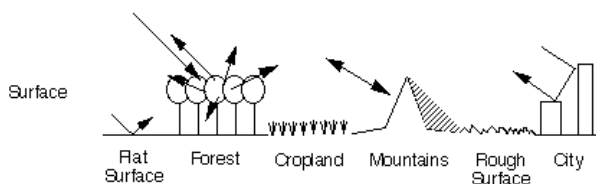


Figure 1.5 Backscatter from various surfaces types

A useful rule-of-thumb in analysing radar images is that the higher or brighter the backscatter on the image, the rougher the surface being imaged. Flat surfaces that reflect little or no radio or microwave energy back towards the radar will always appear dark in radar images. Vegetation is usually moderately rough on the scale of most radar wavelengths and appears as grey or light grey in a radar image. Surfaces inclined towards the radar will have a stronger backscatter than surfaces which slope away from the radar and will tend to appear brighter in a radar image. Some areas not illuminated by the radar, like the back slope of mountains, are in shadow, and will appear dark. When city streets or buildings are lined up in such a way that the incoming radar pulses are able to bounce off the streets and then bounce again off the buildings (called a double-bounce) and directly back towards the radar they appear very bright (white) in radar images. Roads and freeways are flat surfaces and so appear dark. Buildings which do not line up so that the radar pulses are reflected straight back will appear light grey, like very rough surfaces.

### 1.1.2.2 Real Aperture Radar (RAR)

Before considering the properties of a Synthetic Aperture Radar system, we will consider a Real Aperture System. Aperture means the opening used to collect the reflected energy that is used to form an image. In the case of radar imaging this is the antenna. For RAR systems, only the amplitude (and not the phase) of each echo return is measured and processed.

#### 1.1.2.2.1 Spatial Resolution

The spatial resolution of a Real Aperture Radar system is determined by, among other things, the size of the antenna used. For any given wavelength, the larger the antenna the better the spatial resolution. Other determining factors include the pulse length and the

antenna [beamwidth](#). The pulse length of the radar signal is determined by the length of time that the antenna emits its burst of energy.

Consider an image to be a set of values  $A(x,y)$ , where the x coordinate is in the direction of platform motion and the y coordinate is in the direction of illumination. Then the value of y, or [range direction](#), and its resolution (range resolution) is based on the pulse length, the arrival time of the echo, and the timing precision of the radar. The value of x, which is [azimuth](#) direction (also referred to as the along-track direction), and its resolution (azimuth resolution) depends on the position of the platform that carries the transmitting antenna and the beamwidth of the radar.

### 1.1.2.2 Range Resolution

For a Radar system to image separately two ground features that are close together in the range direction, it is necessary for all parts of the two objects' reflected signals to be received separately by the antenna. Any time overlap between the signals from two objects will cause their images to be blurred together.

### 1.1.2.3 Azimuth Resolution

As mentioned above, the azimuth resolution is affected by the beamwidth. As the antenna beam fans out with increasing distance from the earth to the platform carrying the pulse transmitting source and receiver, the azimuth resolution deteriorates. The beamwidth of the antenna is directly proportional to the wavelength of the transmitted pulses and inversely proportional to the length of the antenna.

So, for any given wavelength, antenna beamwidth can be best controlled by one of two different means:

- by controlling the physical length of the antenna, or
- by synthesising an effective length of the antenna

Those systems where beamwidth is controlled by the physical antenna length are referred to as Real Aperture, or Noncoherent Radars and the natural resolution of such an orbiting radar instrument, observing from 1000 km, is typically 10 km on the ground. While these systems enjoy relative simplicity of design and data processing, the resolution difficulties restrict them to short-range, low altitude operation and the use of relatively short wavelengths. These restrictions limit the area of coverage obtainable and the short wavelengths experience more atmospheric dispersion.

### 1.1.2.3 Synthetic Aperture Radar (SAR)

Synthetic Aperture Radar (SAR) takes advantage of the [Doppler](#) history of the radar echoes generated by the forward motion of the spacecraft to synthesise a large antenna, enabling high azimuthal resolution in the resulting image despite a physically small antenna, as shown in [figure 1.6](#). As the radar moves, a pulse is transmitted at each position. The return echoes pass through the receiver and are recorded in an echo store.

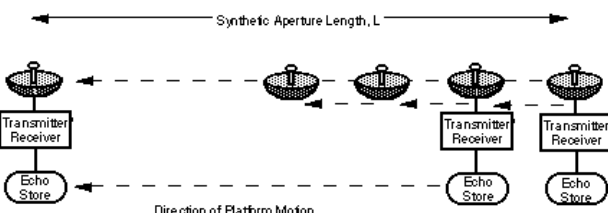


Figure 1.6 Constructing a synthetic antenna

SAR is a [coherent](#), active, microwave imaging method that improves natural radar resolution by focusing the image through a process known as synthetic aperture processing. This typically requires a complex integrated array of onboard navigational and control systems, with location accuracy provided by both Doppler and inertial navigation equipment. For a C band instrument, (such as ERS-1, ERS-2 or ASAR) 1000 km from its target, the area on the ground covered by a single transmitted EM pulse, known as the radar footprint, is on the order of 5 km long in the along-track (azimuth) direction. In SAR, the satellite must not cover more than half of the azimuth antenna length between the emission of successive pulses, so as not to degrade the [range resolution 1.1.2.2.2](#). For example, a 10 m antenna should advance only 5 m between pulses, to produce a 5 m long final elementary resolution cell, or [pixel](#). Therefore, each 5 km long footprint is a collection of signals, each one of which is a mixture of a thousand 5 m samples, each of which contributes to a thousand signals. Focusing is the reconstruction of the contribution of each 5 m cell, which results in an improvement of resolution of approximately a thousand times of a Real Aperture Radar. This effectively provides a synthetic aperture of a 20 km antenna.

In essence, return signals from the centre portion of the beamwidth are discriminated by detecting Doppler frequency shifts, which is a change in wave frequency resulting from the relative velocities of a transmitter and a reflector. Within the wide antenna beam, returns from features in the area ahead of the platform will have upshifted, or higher, frequencies resulting from the Doppler effect. Conversely, returns from features behind the platform will have downshifted, or lower, frequencies. Returns from features near the centreline of the beamwidth (the so-called Zero-Doppler line) will experience no frequency shift.

The amplitude and phase of the signals returned from objects are recorded in the echo store throughout the time period in which the objects are within the beam of the moving antenna. By processing the return signals according to their Doppler shifts, a very narrow effective

---

antenna beamwidth can be achieved, even at far ranges, without requiring a physically long antenna or a short operating wavelength.

Because the signals received by a SAR system are recorded over a long time period, the system translates the real antenna over a correspondingly long distance, which becomes the effective length of the antenna. The [azimuth resolution 1.1.2.3.](#), with this synthetic antenna length is greatly improved, due to the effective narrowing of the beamwidth. The azimuth resolution is also essentially independent of range, because at long range an object is in the beam longer, meaning that returns from it are recorded over a longer distance.

#### 1.1.2.4 Image Interpretation

Determining and describing how various objects reflect radar energy has been mostly derived from empirical observation. It has been found that the primary factors influencing an object's return signal intensity are their geometric and electrical characteristics, as well as their general composition. That is, radar waves interact differently with soil, vegetation, water, ice, or man-made objects.

##### 1.1.2.4.1 Geometric Characteristics

One of the most readily apparent features of radar imagery is its sidelighted character, which arises through variations in the relative sensor to terrain geometry. Shadow areas and radar [backscatter 1.1.2.1.2.](#) are affected by different surface properties over a range of [incidence angles](#).

For flat terrain, the local reflection angle is the same as the incidence angle; most of the incident energy is reflected away from the sensor, resulting in a very low return signal. Rough surfaces, on the other hand, will scatter incidence energy in all directions and return a significant portion of the incident energy back to the antenna, as show in the scattering mechanisms figure below.

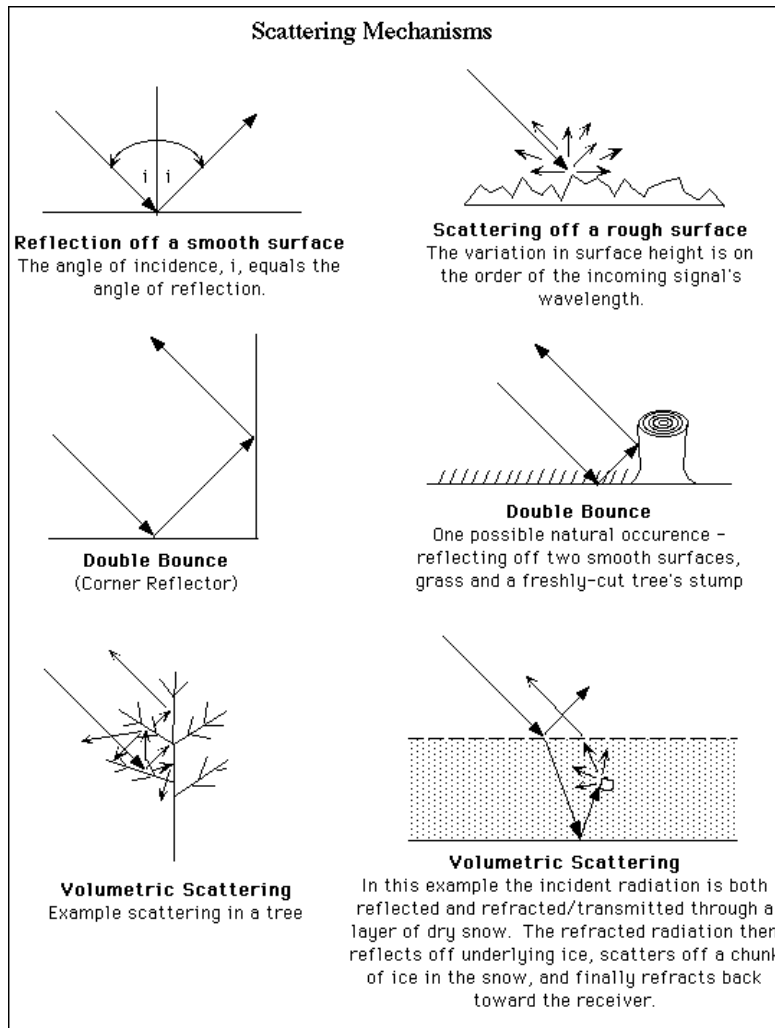


Figure 1.7 Scattering mechanisms

The shape and orientation of objects must be considered, as well as their surface roughness, when evaluating radar returns. For instance a particularly bright response will come from a corner reflector, which will produce a double bounce, as shown above. It is also worth noting that some features, such as corn fields, might appear rough when seen in both the visible and microwave portion of the spectrum, whereas other surfaces, such as roads, may appear rough in the visible range but look smooth in the microwave spectrum. In general, SAR images will manifest many more smooth, or specular, surfaces than those produced with optical sensors.

Since one factor affecting backscatter is the polarisation used, as was discussed previously [1.1.2.1.2.](#), those SAR systems that can transmit pulses in either horizontal (H) or vertical (V) polarisation and receive in either H or V, such as the ASAR sensor, can better utilise this property for image interpretation.

In addition, SARs measure the phase of the incoming pulse and can therefore measure the phase difference in the return of the HH and VV signals. This difference can be thought of as a difference in the round-trip times of HH and VV signals and is frequently the result of the structural characteristics of the scatterers, or targets. The phase information in the products from these SARs can be used to derive an estimate of the correlation coefficient for the HH and VV returns, which can be considered as a measure of how alike the HH and VV scatterers are.

As an aside, the phase information derived by a SAR may also be exploited in Interferometric SAR (InSAR). InSAR requires the phase differences of at least two complex-valued SAR images, acquired from different orbit positions and/or at different times. These phase differences can be compared after proper image registration and produce a new kind of image called an interferogram. This subject is discussed in greater detail in the section entitled "[Interferometry 1.1.5.4.](#)".

#### 1.1.2.4.2 Electrical Characteristics

The electrical characteristics of terrain features interact with their geometric characteristics to determine the intensity of radar returns. One measure of an object's electrical character is the 'complex dielectric constant', which is a parameter that indicates the reflectivity and conductivity of various materials. As reflectivity and conductivity increases, so does the value of this constant.

In the microwave region of the spectrum, most natural materials have a dielectric constant in the range of 3 to 8 when dry, whereas water has a dielectric constant of approximately 80. This means that the presence of moisture in either soil or vegetation will result in significantly greater reflectivity. Other examples of sources of high reflectivity are metal bridges, silos, and railroad tracks.

#### 1.1.2.4.3 Responses of Soil, Vegetation, Mountains, Water and Ice

##### 1.1.2.4.3.1 Soil

Because the dielectric constant for water is at least 10 times that for dry soil, the presence of water in the top few centimetres of bare, unvegetated soil can be detected in radar imagery, becoming particularly apparent at longer wavelengths.

##### 1.1.2.4.3.2 Vegetation

A vegetation canopy will interact with radar waves as a group of volume scatterers, as shown in [figure 1.7](#) above. The canopy is composed of a large number of discrete plant components, such as leaves, stems, stalks, limbs and so on. In addition, the canopy is underlain by soil that may result in surface scattering of the energy that penetrates the vegetation canopy. In general, shorter wavelengths, of approximately 2 to 6 cm, are best for sensing crop canopies and tree leaves, because at these wavelengths volume scattering predominates and surface scattering from the underlying soil is minimised. However, longer wavelengths, of approximately 10 to 30 cm are best for sensing tree trunks or limbs.

Another factor influencing the affect of radar backscatter from vegetation is the [polarisation](#) of the beam, with like-polarised waves (HH or VV) penetrating vegetation more than cross-polarised (HV or VH) waves. In addition, more energy is returned from crops having their rows aligned in the [azimuth](#) direction than from those aligned in the [range](#) direction, especially in the case of like-polarised beams.

#### 1.1.2.4.3.3 Mountains

When a spaceborne SAR looks down and to the side toward a steep mountain, many objects on the mountain's facing slope may appear to be located at the same distance from the spacecraft, as though the farther out in range an object is, the higher, or closer, to the spacecraft the ground is raised by the mountain to compensate. Since those many objects are located at nearly the same distance from the SAR, their backscattered signals will return to the spacecraft at about the same time. The SAR will conclude that the object located at that distance backscattered brightly, mapping all those responses into one location while in truth they came from many. This is called [foreshortening](#), or layover in the extreme case where responses from, say, a mountain's peak are positioned before surrounding locations. This is depicted in the figure below entitled "Geometric Distortions".

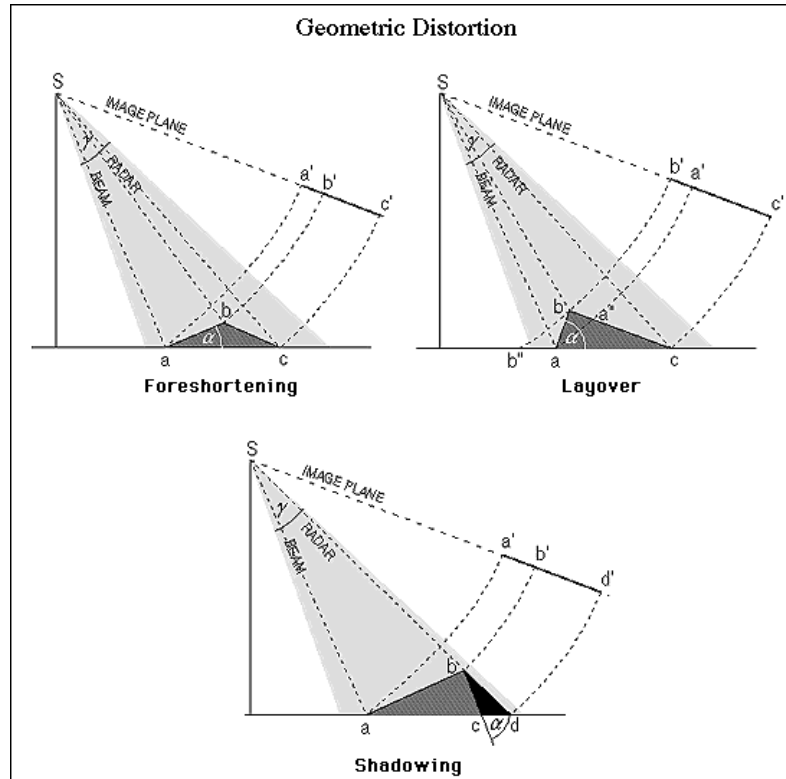


Figure 1.8 Geometric distortions

The resulting SAR image will show much of the mountain's bright facing slope was mapped onto a few pixels, while the darker backfacing slope was considered to cover many more pixels. Therefore it appears as though the mountains are lying over. Steeper topography or a smaller SAR look angle can worsen foreshortening effects.

#### 1.1.2.4.3.4 Water and Ice

Smooth water surfaces yield no returns to the antenna, but rough water surfaces return radar signals of varying strengths. In addition, waves moving in the range direction, that is moving toward or away from the radar system, are easier to detect than waves moving in the azimuthal direction.

Radar backscatter from sea ice is dependent on the dielectric properties and spatial distribution of the ice. Such factors as ice age, surface roughness, internal geometry, temperature, and snow cover will also all play a role in the effect of radar backscatter.

Each of these above topics are discussed in more detail in the sections within the handbook

relating to these applications.

### 1.1.2.5 General Rules for SAR Image Interpretation

In summary, the general rules for SAR Image Interpretation are as follows:

- Regions of calm water and other smooth surfaces will appear black, because the incident radar reflects away from the spacecraft.
- Surface variations near the size of the radar's wavelength cause strong backscattering.
- A rough surface backscatters more brightly when it is wet.
- Wind-roughened water can backscatter brightly when the resulting waves are close in size to the incident radar's wavelength.
- Hills and other large-scale surface variations tend to appear bright on the side that faces the sensor and dim on the side that faces away from the sensor. Mountains show this effect to the extreme, in part due to increased foreshortening.
- Due to the reflectivity and angular structure of buildings, bridges, and other human-made objects, these targets tend to behave as corner reflectors and show up as bright spots in a SAR image.
- A particularly strong response, say from a corner reflector, can look like a bright cross in a processed SAR image.

### 1.1.2.6 References

#### Ref 1.1

T.M. Lillesand, R.W. Kiefer, "Remote Sensing and Image Interpretation", 2nd ed, Wiley 1987.

#### Ref 1.2

D. Massonet, K.L.Feigl, "Radar interferometry and its application to changes in the earth surface", Reviews of Geophysics Vol. 36, Number 4, Nov. 1998.

#### Ref 1.3

R. Bamler, P. Hartl, "Synthetic aperture radar interferometry", 1998.

#### Ref 1.4

ALASKA Sar Facility, [www.asf.alaska.edu](http://www.asf.alaska.edu)

## 1.1.3 Principles of Measurement

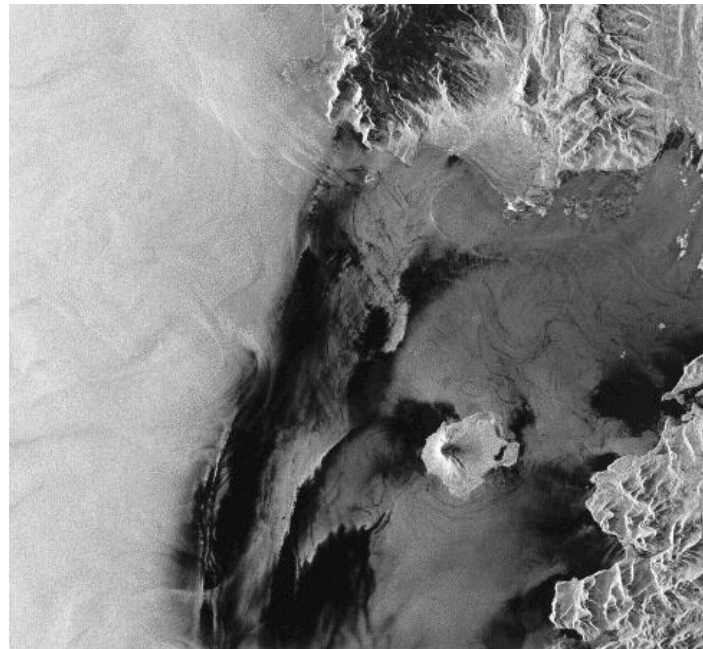


Figure 1.9 ERS-1 image June 21 1992, Mt. St. Augustine Volcano, Cook Inlet (Copyright ESA, 1992)

The antenna beam of a side-looking [radar](#) is directed perpendicular to the flight path and illuminates a [swath](#) parallel to the platform ground track. Due to the motion of the satellite, each target element is illuminated by the [beam](#) for a period of time (integration time). As part of the on-ground processing, the complex echo signals received during this period are added coherently. This process is equivalent to synthetically forming a long [antenna](#) (called Synthetic Aperture).

Assuming a constant angular beam width [along-track](#) (azimuth) for the entire swath, the achievable synthetic aperture increases with the distance(slant range) between radar and target.

The [range resolution](#) of a pulsed radar system is limited fundamentally by the [bandwidth](#) of the transmitted [pulse](#) (slant range [resolution](#) =  $c/2B$  hence the wider the bandwidth, the better the [range](#) resolution). A wide bandwidth can be achieved by a short duration pulse. However, the shorter the pulse, the lower the transmitted energy (for a fixed-peak power limitation) and the poorer the signal-to-noise ratio, hence the radiometric resolution. To preserve the radiometric resolution, the technique adopted by ASAR is to generate a long pulse with a linear [frequency](#) modulation (or chirp). The length of the pulse is defined to be consistent with the requirement for the signal-to-noise ratio. The chirp bandwidth is defined by the required range resolution. After the received signal has been compressed, the range resolution will be optimised without loss of radiometric resolution.

The azimuth resolution of a [real aperture radar](#) system is a function of the antenna length (the larger the antenna, the better the azimuth resolution). It can be shown that a spaceborne real aperture radar, giving a useful azimuth resolution for points on the Earth's surface, will require an impractically large antenna. Aperture synthesis, therefore, offers a means of greatly improving the [azimuth resolution](#) for a given antenna length.

The measurement principle of ASAR depends on the use of coherent radiation, together with precise knowledge of the transmit and receive point of the radar pulse. For a given target, as the platform moves, the distance from the radar to the target (i.e., the slant range) changes continuously, hence the [phase](#) of the reflected signal changes according to a law given by the geometry of observation. As this law is deterministic, it is therefore possible to correctly phase the return signals with respect to each other so that the net effect is equivalent to them all having been received simultaneously by an antenna of length equal to the path length over which the radar signals were collected (i.e., the synthetic aperture). In this way, the synthesised antenna can be thought of as a number of independently radiating elements (i.e., the real aperture), whose separation is established by the [Pulse Repetition Frequency](#) (PRF) and the platform velocity. The change of phase with respect to time is the Doppler angular frequency. The azimuth resolution is determined by the Doppler bandwidth of the received signal. For ASAR, the bandwidth of target returns, in azimuth, is defined by the Doppler bandwidth covered between the half-power points of the [one-way](#) azimuth pattern. This implies that pulses must be transmitted with a repetition frequency greater than the azimuth bandwidth in order to satisfy the Nyquist sampling criterion.

There is an upper limit on the PRF imposed by the geometry. If the PRF is so high that return signals from two consecutively transmitted pulses arrive simultaneously at the receiver, there will be ambiguities in the response. This will, therefore, define a set of unambiguous intervals for a given geometry and PRF, which corresponds to constraining the [ground range](#) extent of the region illuminated within the elevation beamwidth of the antenna footprint (i.e., the swath width).

As a consequence of the ASAR antenna being used for pulse transmission and echo reception, there will be echoes that are not received due to periods when the antenna is transmitting pulses and hence not receiving echo returns. For a given geometry and PRF, these "blind" intervals will lie at constant ground range positions.

The return from [nadir](#) (the ground point vertically below the satellite) will be significantly larger than the returns from the required swath, because of its close range and high reflectivity. To avoid this unwanted signal saturating any other returns arriving at the same time, the PRFs and swaths for ASAR are chosen such that the nadir returns do not occur in the imaging window.

The significant feature of the ASAR [instrument](#) is the active phased array antenna, which allows independent control of the phase and [amplitude](#) of the transmitted radiators from different regions of the antenna surface. It also provides independent weighting of the received signal to each of these regions. This offers great flexibility in the generation and control of the radar beam, giving the ASAR instrument the capability to operate in a number of different modes. These modes use two principal methods of taking measurements; the

ASAR instrument may operate as a conventional stripmap SAR or as a ScanSAR.  
 ASAR Stripmap Modes (Image, Wave)

When operating as a stripmap SAR, the phased array antenna gives ASAR the flexibility to select an imaging swath by changing the beam incidence angle and the elevation beamwidth. In addition, the appropriate PRF required to ensure acceptable ambiguity performance and to suppress unwanted nadir returns is selected.

In the Image Mode, ASAR operates in one of seven predetermined swaths with either vertically or horizontally polarised radiation; the same polarisation is used for transmit and receive (i.e., HH or VV). See [figure 1.10](#).

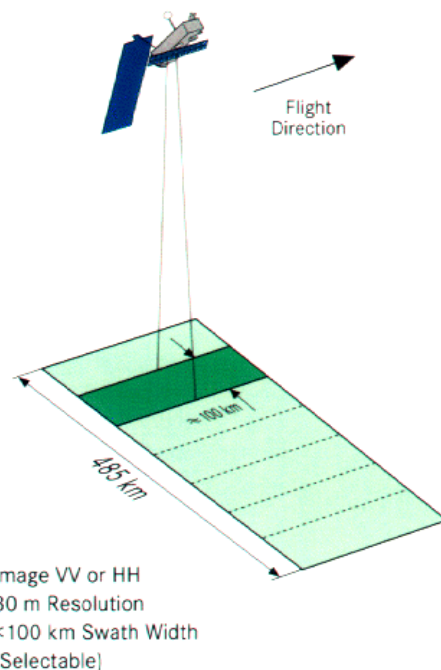


Figure 1.10 Image Mode

The Wave Mode uses the same swaths and polarisations as Image Mode. However, a continuous strip of data is not required. Instead, small areas of the ocean are imaged at regular intervals along the swath. This intermittent operation provides a low data rate, such that the data can be stored on board the satellite, rather than being downlinked immediately to the ground station. See [figure 1.11](#).

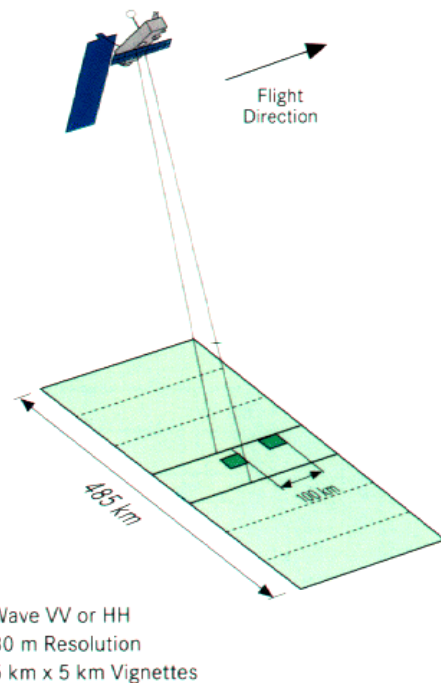


Figure 1.11 Wave Mode

### ASAR ScanSAR Modes (Wide Swath, Global Monitoring, and Alternating Polarisation)

While operating as a stripmap SAR, ASAR is limited to a narrow swath which is imposed by the ambiguity limitation. This constraint can be overcome by utilising the ScanSAR principle, which achieves swath widening by the use of an antenna beam which is electronically steerable in elevation.

Radar images can then be synthesised by scanning the incidence angle and sequentially synthesising images for the different beam positions. The area imaged from each particular beam is said to form a sub-swath. The principle of the ScanSAR is to share the radar operation time between two or more separate sub-swaths in such a way as to obtain full image coverage of each.

The system transmits pulses to, and receives echoes from, a sub-swath for a period long enough to synthesise a radar image of the area within the beam footprint at the required resolution. It then switches beams to illuminate a different sub-swath and continues in this manner until the full-wide swath is covered, at which point it returns to the original sub-swath and the scanning cycle is repeated.

The imaging operation is, therefore, split into a series of bursts of pulses, each burst

providing returns from one of the sub-swaths. Each burst will be processed to provide an image of a section of the corresponding sub-swath. The imaging operations must therefore be such that it cycles around the full set of sub-swaths sufficiently rapidly for the imaged sections in any one sub-swath to be adjoining or overlapping.

ASAR operates according to the ScanSAR principle, as described above, in two measurement modes: the Wide Swath Mode and Global Monitoring Mode. These use five predetermined overlapping antenna beams which cover the wide swath.

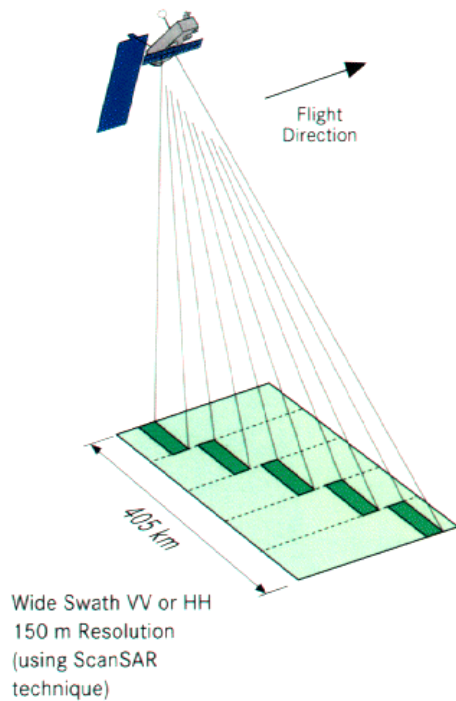


Figure 1.12 Wide Swath Mode

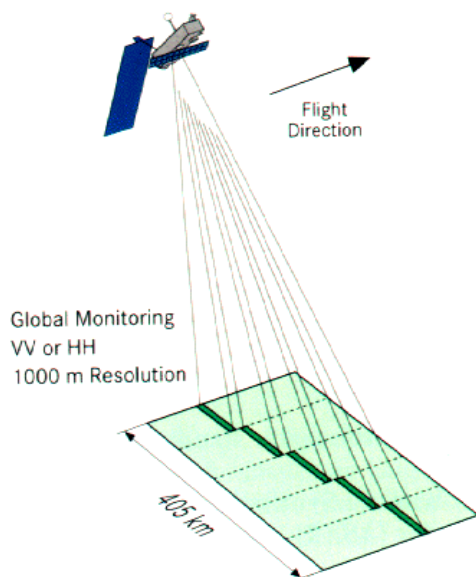


Figure 1.13 Global Monitoring Mode

An additional ASAR measurement mode, called Alternating Polarisation Mode, has also been defined which employs a modified ScanSAR technique. Instead of scanning between different elevation sub-swaths, the Alternating Polarisation Mode (co-polar) scans between two polarisations, HH and VV, within a single swath (which is preselected, as for Image and Wave Modes). In addition, there are two cross-polar modes, where the transmit pulses are all H or all V polarisation, with the receive chain operating alternatively in H and V, as in the CO-polar mode.

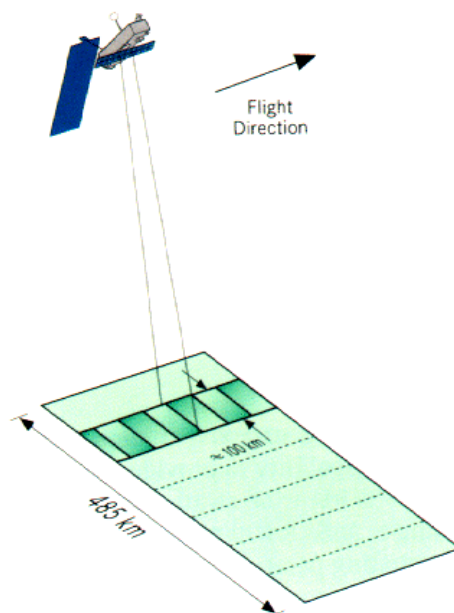


Figure 1.14 Alternating Polarisation Mode

## The ASAR Instrument's Capabilities

[Table 1.1](#) summarises the ASAR capabilities.

Table 1.1 Summary of ASAR capabilities

Instrument Parameters	Image Mode	Alternating Polarisation Mode	Wide Swath Mode	Global Monitoring Mode	Wave Mode
Swath width	up to 100 km	up to 100 km	> 400 km	> 400 km	5 km vignette
Operation time	up to 30 min per orbit rest of orbit				
Data Rate	up to 100 Mbit/s 0.9 Mbit/s				
Power	1365 W	1395 W	1200 W	713 W	647 W

The use of the ASAR generic processor for near real-time (NRT) and off-line processing in the processing and archiving centres (PACs) and national stations offering ESA services, is a simplification for processing and product validation. This allows full product compatibility between the different processing centres.

## 1.1.4 Geophysical Coverage

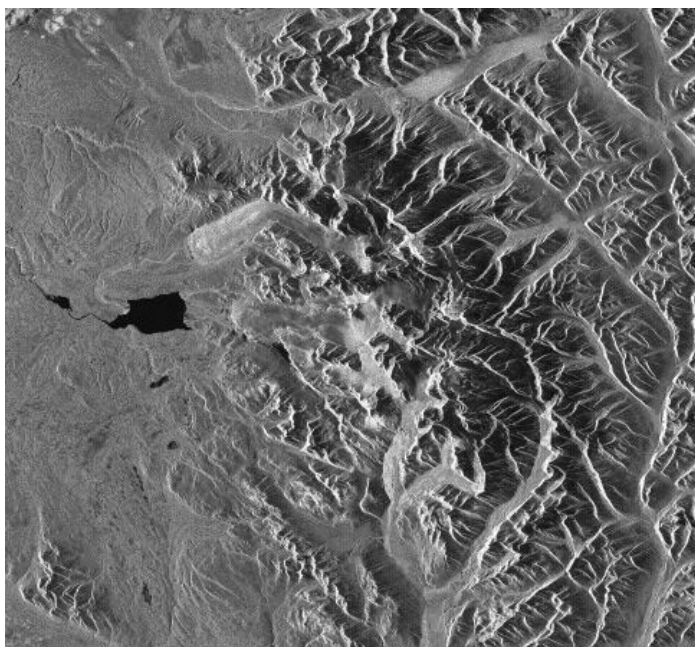


Figure 1.15 ERS-1 image Aug. 30, 1992 Mt. Spurr, Southern Alaska (Copyright ESA, 1992)

The orbit selected for ENVISAT will provide a 35-day repeat cycle, the same as the ERS-2 mission. Since the [orbit](#) track spacing varies with latitude (the orbit track spacing at 60° latitude is half that at the equator), the density of observations and/or revisit rate is significantly greater at higher latitudes than at the equator. The flexible [swath](#) positioning in Image Mode greatly increases the potential temporal coverage [frequency](#) compared to ERS. Coverage is also affected by the different swath widths of IS1 to IS7. [Table 1.2](#) below shows the repeat coverage capability as a function of latitude and incidence angle variation (note: only for descending tracks). If there are no incidence angle constraints, average revisit will be 7 days at the equator, improving to nearly every 2 days at 70° latitude.

Table 1.2 Average revisit frequency per 35-day orbit cycle as a function of latitude and incidence angle variation to illustrate ASAR revisit time capability (only for descending path)

Incidence Angle	0°	45°	60°	70°
Latitude				
No Constraints	5	7	11	16
<5°	3	4	6	9
<20°	1	1.4	2	3
Exact repeat	1	1	1	1

ASAR will operate simultaneously with the other ENVISAT instruments. [Figure 1.16](#) below shows the swath positioning of ASAR together with [AATSR](#) and MERIS coverage. Overlap with AATSR is seen to be quite limited, but ASAR IS1 to IS5 and most of Wide Swath/Global Monitoring Mode coverage falls within the MERIS cover.

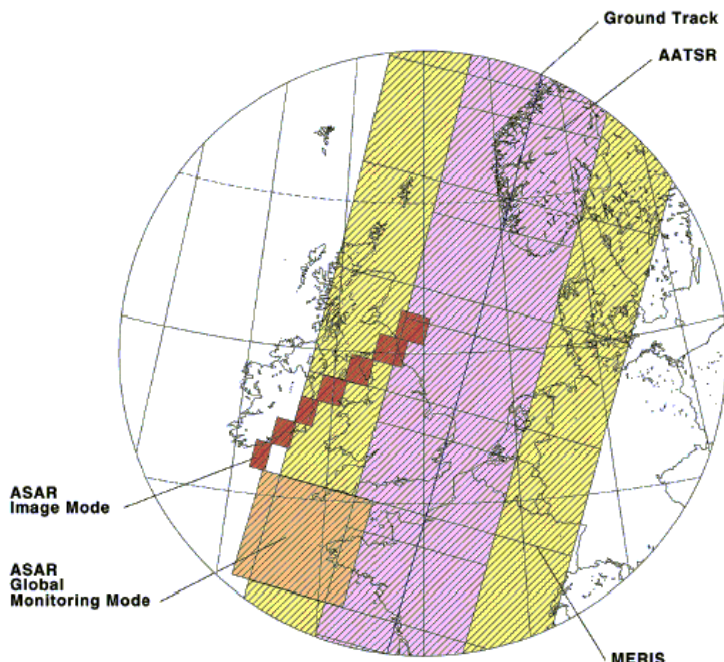


Figure 1.16 Comparative simultaneous coverage of ASAR Image (red), Wide Swath - Global (orange), AATSR (violet) and MERIS (yellow).

The ENVISAT Swath and Orbit Visualisation (ESOV) software provides visualisation of the ENVISAT orbits, instrument swaths and ground station visibility. It is a free tool available to any user involved in ENVISAT data acquisition planning.

For an in-depth discussion on wide area coverage, see the section "[Wide Area Coverage and Frequency of Coverage.](#)" [1.1.5.3.](#)

## 1.1.5 Special Features of ASAR



Figure 1.17 ERS-1 image Sept. 23, 1992 Methane Emissions, Tundra, Alaska North Slope  
(Copyright ESA, 1992)

ASAR has a number of special features (see the index)

### 1.1.5.1 Dual Polarisation

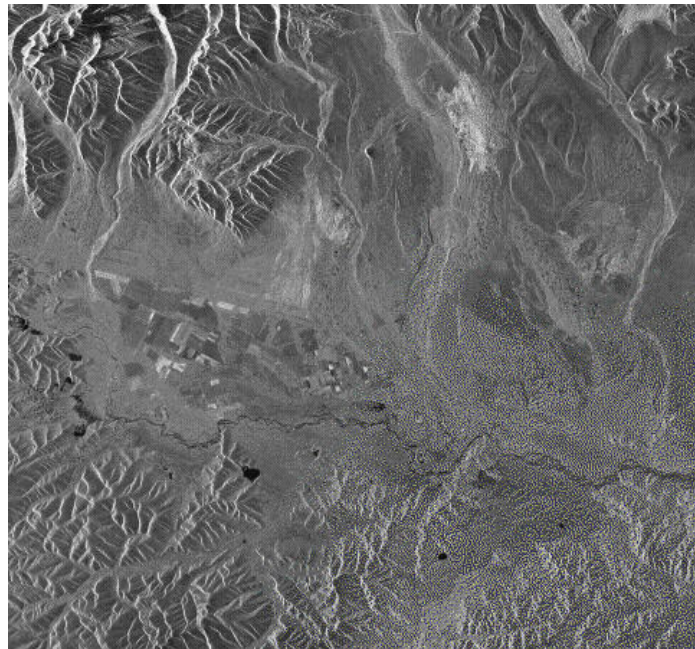


Figure 1.18 ERS-1 image Aug.2, 1992 Tanana Valley Alaska (Copyright ESA, 1992)

Imaging radars can transmit horizontal (H) or vertical (V) electric-field vectors, and receive either horizontal or vertical return signals, or both. The basic physical processes responsible for the like-polarised return are quasi-specular surface reflection and surface or volume scattering. The cross-polarised return is usually weaker, and often associated with multiple scattering due to surface roughness or multiple volume scattering. Scattering mechanisms and the returns from different surfaces may also vary markedly with incidence angle.

To illustrate the effect of polarisation, consider the very simple model of a vegetation canopy consisting of short vertical scatterers over a rough surface, as shown in the [figure 1.19](#) below:

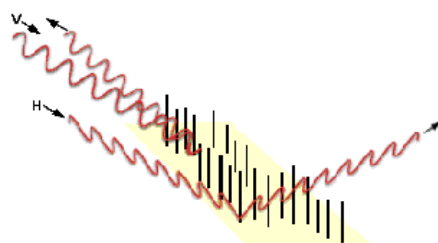


Figure 1.19 Electromagnetic Wave Orientation

Assuming that the scatterers will act as short vertical dipoles, then incident, horizontally polarised microwave energy will not interact with the canopy and will scatter from the surface underneath. Conversely, vertically polarised microwave energy will interact strongly with the dipoles.

ASAR provides dual-channel data. In Alternating [Polarisation](#) Mode (AP Mode), it provides one of three different channel combinations:

- VV and HH
- HH and HV
- VV and VH

Dual [polarisation](#) data is important for a wide range of applications such as bare soil, vegetation studies, sea ice applications, etc.

Vertical Transmit/Vertical Receive (VV) - Like Polarisation

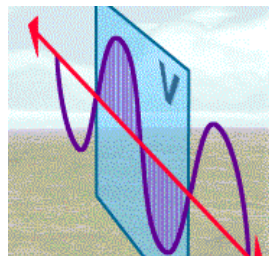


Figure 1.20 VV Polarisation

VV polarisation, shown in [figure 1.20](#), is the preferred polarisation configuration in a number of applications. For instance, in studying the small-scale roughness of (capillary) waves on the water surface, VV is better than HH or cross-polarised combinations, which means it is used extensively for surface wind speed extraction.

Horizontal Transmit/Horizontal Receive (HH) - like polarisation

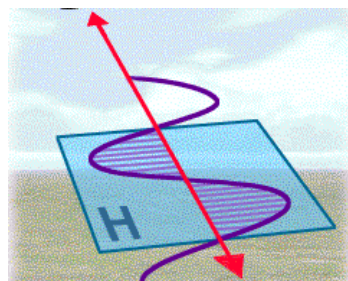


Figure 1.21 HH Polarisation

HH polarisation, shown in [figure 1.21](#), is the preferred polarisation configuration in a number of applications. For instance, in the study of soil moisture, if we ignore the crop density differences, then the vertically oriented crops (e.g., wheat and barley) have improved penetration with HH, allowing the [backscatter](#) to represent the soil moisture regime better rather than the crop geometry. HH is very suitable for separating marine ice and water, since it is less sensitive to water roughness than VV polarisation, thus producing an improved contrast between the two target types. For a similar reason, HH is used for ship detection.

Vertical Transmit/Horizontal Receive (VH) - cross polarisation

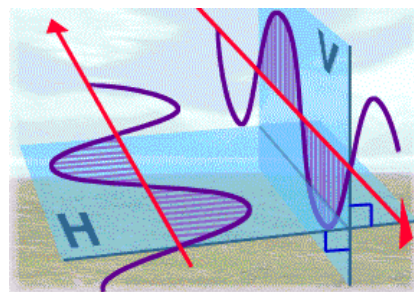


Figure 1.22 VH Polarisation

Horizontal Transmit/Vertical Receive (HV) - Cross Polarisation

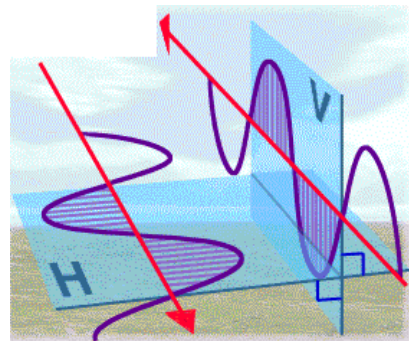


Figure 1.23 HV Polarisation

Since the backscatter from water surfaces is reduced under cross-polarised SAR illumination/detection, using the VH or HV technique is very suitable for detecting targets on the water surface, which accommodate multiple scattering necessary for depolarisation. Such targets are, for example: ship superstructures and various ice deformations (ridging, fractures and rubble). For a similar purpose, the separation of broadleaf from grain crops, for example, benefits from cross-polarised SAR imaging, since [depolarisation](#) is much stronger with the geometries of broadleaf vegetation where multiple scattering of the radar beam is much more likely. There are also indications that the detection of geological linear

benefits from cross polarisation when the look angle is acute.

For studies of bare soil, where attention focuses on the retrieval of soil moisture and soil roughness, the use of different polarisations will improve the inversion into soil parameters. Cross polarisation provides an important improvement for soil moisture retrieval since the radar backscatter is less sensitive to surface roughness, row direction, etc.

For many vegetation studies, the use of different polarisations, in particular cross polarisation, will improve the discrimination between vegetation (volume scattering) and soil (surface scattering). In the case of forestry, the use of cross polarisation will improve the forest/non-forest discrimination and the retrieval of low biomass values (forest regeneration, regrowth, plantation). Two examples are provided below ([figure 1.24](#) and [figure 1.25](#)) showing how the use of dual polarisation data can improve the information content.

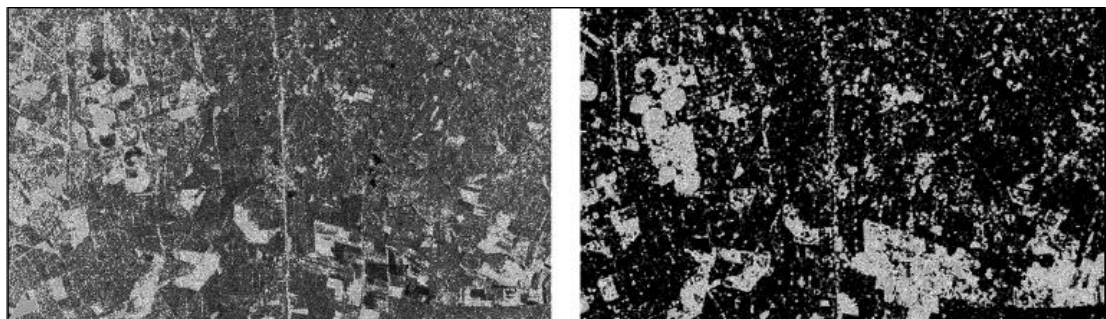


Figure 1.24 SIR-C data (C-band, 26.5°) over Les Landes test site, France. Left image is backscatter intensity (VV polarisation) and right image is HH/VV correlation image.

(Acknowledgement: Souyris et al, 1998.)

In [figure 1.24](#) above, the SIR-C backscatter intensity image (left) shows poor discrimination between vegetated and non-vegetated areas. This is because of large variations in the backscatter of bare soil surfaces related to different soil roughness and moisture conditions and is similar for both VV and HH polarisation images. However, using both polarisations to produce a HH/VV correlation image (below), it becomes possible to discriminate between non-vegetated (high-correlation) and vegetated (low-correlation) areas. On this image, the high-correlation (bright) areas correspond to recently harvested cornfields. In contrast, the different states of tillage are seen to produce large variations in backscatter intensity in the single-channel image.

[figure 1.25](#) , [figure 1.26](#) and [figure 1.27](#) below illustrates differences between like-polarised and cross-polarised images of urban areas. Three different polarisation images are shown for an area in southern Germany which was imaged by the JPL AIRSAR during the MAC Europe campaign in 1989. The area is 12 km wide, and includes forests, cultivated fields and urban areas. The two like-polarised images are seen to be very similar. However, on the cross-polarised image, urban areas are seen to be much less bright. This is because the cross-polarised return only appears through multiple scattering, while the urban areas are

---

characterised by man-made objects that act like corner reflectors.

Three different C-band polarisation images for an area in southern Germany imaged by the JPL AIRSAR during the 1989 MAC Europe Campaign.

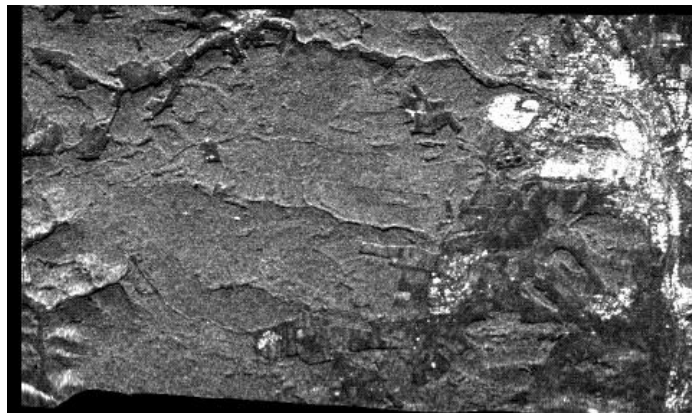


Figure 1.25 C-band HH polarisation

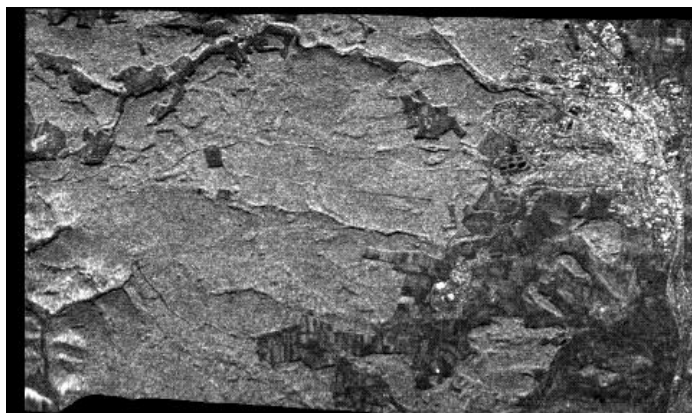


Figure 1.26 C-band HV polarisation

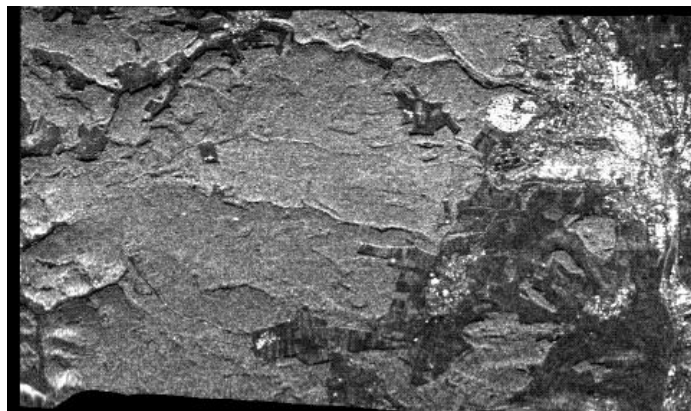


Figure 1.27 C-band VV polarisation

It is possible to simulate Alternating Polarisation images (VV/HH) using ERS and Radarsat data. [figure 1.28](#) shows a combination of ERS and Radarsat images taken one day apart, for an area in Oxfordshire, UK. In this example a large number of agricultural fields are seen to have a blue colour which is indicative of a high backscatter in HH polarisation compared with VV. Since these fields are all cereal fields, this is a good indication of the value of [alternating polarisation](#) images for improving

crop classification. Over the remainder of the image, urban areas, woodland and grassland all have grey tones indicating no significant differences in HH and VV backscatter.

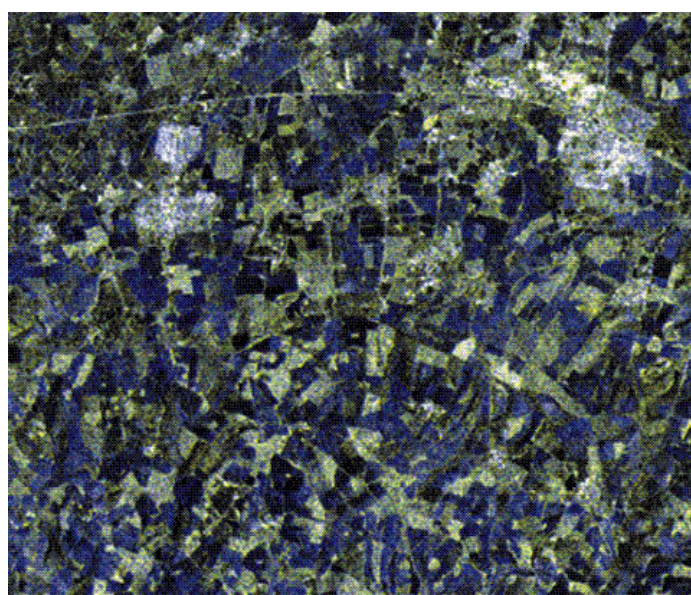


Figure 1.28 Simulated Alternating Polarisation image (VV&HH) of an area in Oxfordshire, UK. (Red & Green: ERS 26/5/97. Blue: Radarsat 27/5/97). Acknowledgement: Remote

---

### Sensing Applications Consultants, UK

There is considerable interest in the Alternating Polarisation Mode for sea ice applications. From current research results using ERS and RADARSAT data, it is still not clear whether VV or HH polarisation is generally better for mapping sea ice. One of the current problems using either ERS or RADARSAT data at low incidence angles is that ice/water discrimination can sometimes be poor. Alternating polarisation, HH and VV data, will give improved ice edge/water discrimination. Cross polarisation data is expected to be particularly useful for mapping ice topography (ridging, rubble), and is also likely to give improved ice type discrimination.

[Figure 1.29](#) below, showing ERS and RADARSAT images from the Arctic acquired less than 2 hours apart, provides a very striking example of the differences that can occur between VV and HH polarisation images, although in this case it should be noted that the radar viewing directions were virtually opposite. Over much of the area one can see large signature reversals between the VV and HH images. Differences show up primarily over open water. The wind speeds recorded on board the icebreaker Oden, 55 km away from the scene centre, were 8 and 14 m/s respectively. The incidence angle varies between 21 and 26 degrees over the ERS-2 sub-image and between 29 and 34 degrees over the RADARSAT sub-image. The different VV and HH responses to wind roughening can be used for wind determination, and the sea ice differences can help in classifying ice properties.

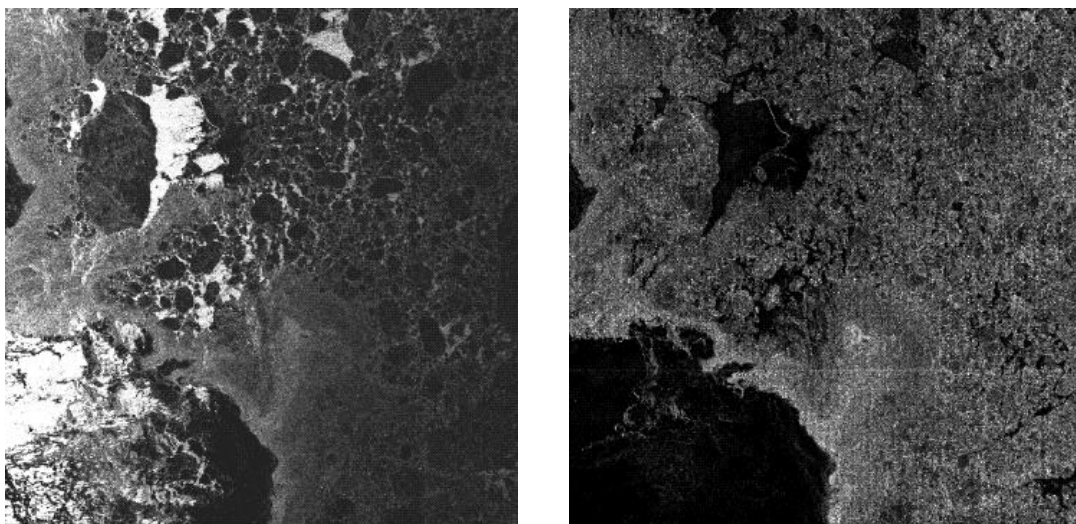


Figure 1.29 Almost simultaneous ERS and RADARSAT images covering 80 x 80 sq km centred around 82°N 12°E. The ERS image was acquired from a descending orbit at 12:88 and the RADARSAT (which has been rotated by 90 degrees) from an ascending orbit at 14:33, both on 19 September 1996. The images have been averaged to the same pixel spacing and intensity stretched. (Acknowledgement: J. Askne and A. Li. Chalmers Univ. of Technology, Sweden.)

The EMAC-95 airborne radar experiment demonstrated the value of dual polarised data for discriminating sea ice types. [Figure 1.30](#) shows an EMISAR C-band co-polarisation ratio VV/HH image covering Baltic Sea Ice (Dierking et al., 1997 [Ref. \[1.5\]](#)). The green and yellow areas on this image have co-polarisation ratios larger than 1, and correspond to level ice and thin ice/open water. The largest values (green) are associated with smooth ice surfaces. A low co-polarisation ratio around 1 (blue) is observed for highly deformed areas and ridges, where the return radar signal is dominated by coherent (specular) scattering.

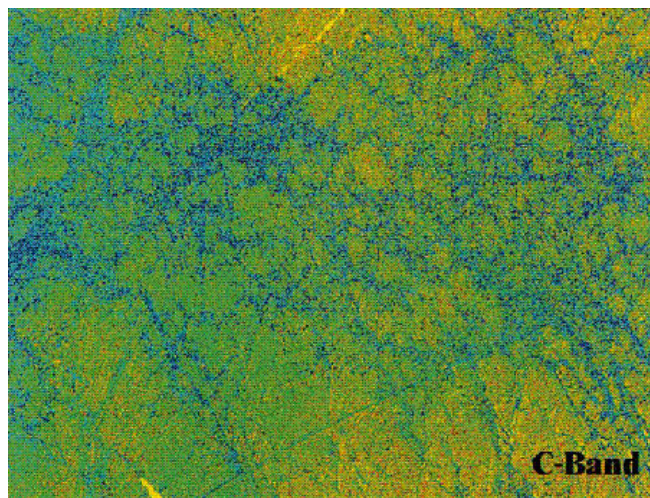


Figure 1.30 Copolarisation ratio VV/HH image for the Baltic Sea Ice site imaged by EMISAR during EMAC-95. (Acknowledgement: Dierking et al., 1997).

Another example illustrating the value of the ratio VV/HH for discriminating ice/no ice is provided in [figure 1.31](#), which shows HH, VV and VV/HH ratio images of a mixed pack ice and open water scene in the Gulf of St. Lawrence, imaged by the SIR-C radar. Discrimination of ice/water is complicated by incidence angle and wind conditions, and is not always distinguishable with either HH or VV polarisations. However, since the ratio of VV to HH backscatter is larger than 1 for open water, but close to 1 for pack ice, the sea ice is seen to be much darker on the VV/HH ratio image, independent of incidence angle or wind conditions.

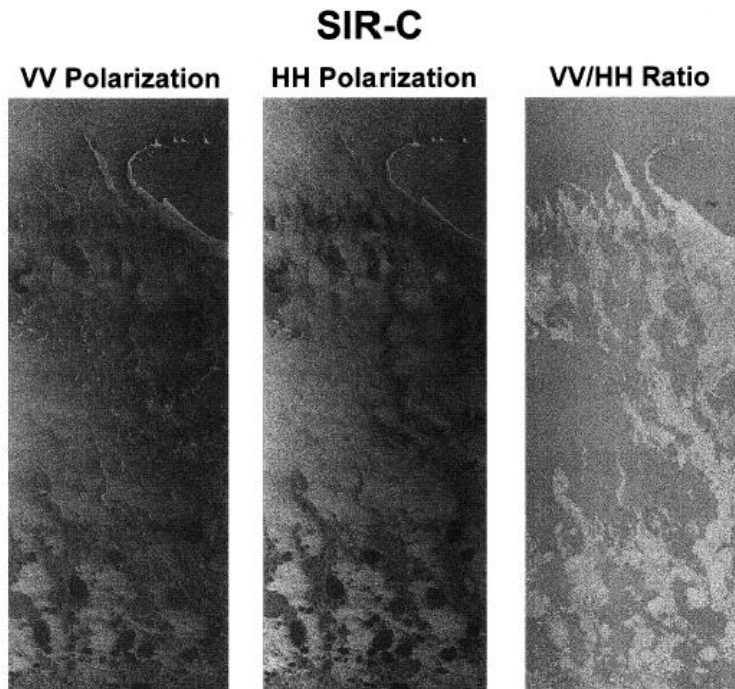


Figure 1.31 Dual polarisation images (VV, HH and VV/HH ratio) from SIR-C for the Gulf of St. Lawrence. (Acknowledgement: L. Gray, CCRS, Canada.)

Over the oceans, the backscattering signal is stronger with VV than with HH polarisation. Experimental results indicate that oceanic features such as internal waves, fronts and sea floor topography tend to appear somewhat better with HH than with VV polarisation. [Figure 1.32](#), RADARSAT HH polarisation, shows internal waves in the Straits of Gibraltar particularly well. In contrast, sea surface imprints of atmospheric features (in particular, convective cells) appear to be more visible with VV polarisation than with HH polarisation.

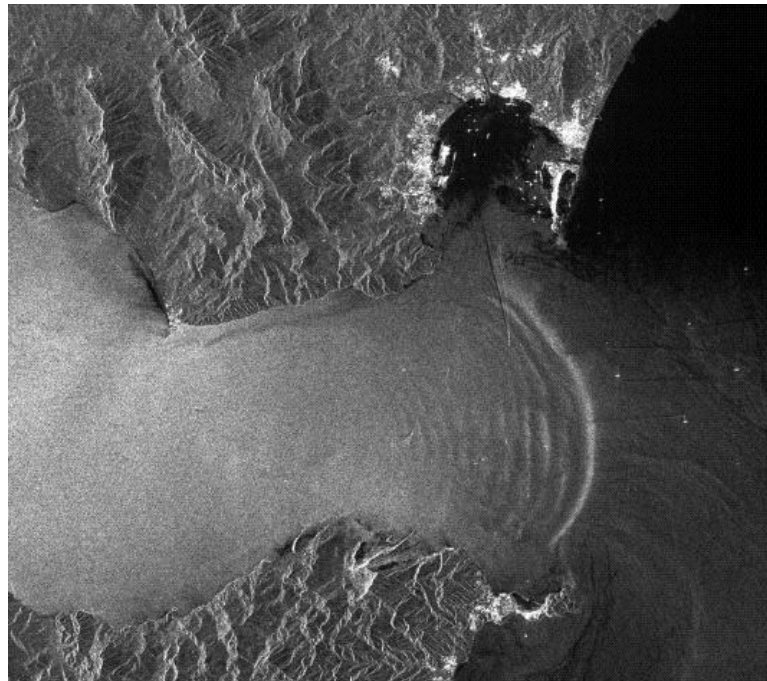


Figure 1.32 Internal wave packet seen on a RADARSAT image of the Straits of Gibraltar.  
(Acknowledgement: Space Dept., DERA, UK: Data copyright Canadian Space Agency.)

There are many excellent examples of atmospheric phenomena seen with VV polarisation ERS images, such as those illustrated in [figure 1.33](#) below.

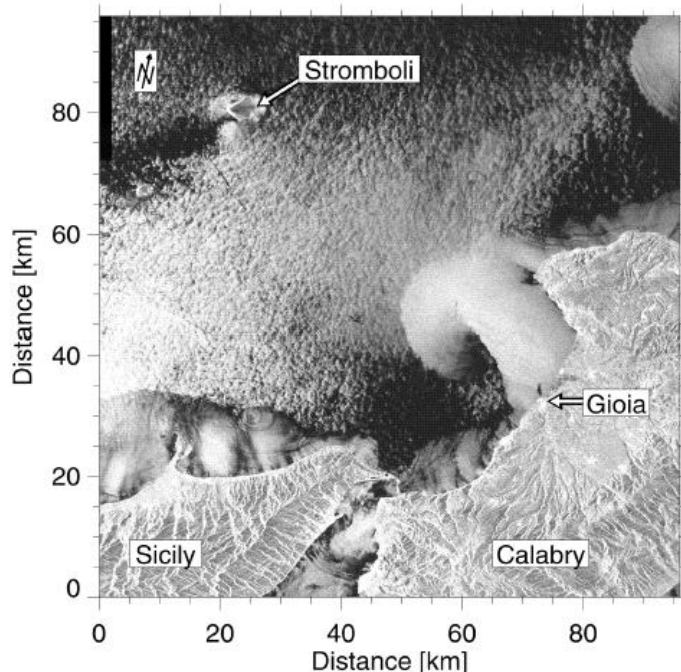


Figure 1.33 ERS-1 SAR VV image (100 km x 100 km) of the Mediterranean Sea north of the Strait of Messina acquired on September 8, 1992. (Acknowledgement: W. Alpers, Univ. Hamburg, Germany.)

To the north-west of Gioia there are surface manifestations of a katabatic wind (bright area). Furthermore, between the island of Stromboli and the Sicilian coast there is a granular pattern, which is interpreted as sea surface "imprints" of atmospheric convective cells. This cellular structure is destroyed in the vicinity of the Sicilian coast by the katabatic wind blowing from the mountains onto the sea. In the lower section of the image, an oceanic internal wave train can be delineated propagating southwards in the Strait of Messina.

The ASAR Alternating Polarisation Mode is therefore of strong interest for ocean studies. Simultaneous dual polarisation images will allow discrimination between similar signatures of oceanic/atmospheric features (e.g., fronts, internal waves). The most favourable can be chosen for detection of oceanic/atmospheric features or for special applications. Wind vector retrieval from SAR images and the tuning of imaging models (e.g., in bathymetric assessment systems) becomes easier if backscatter variations with HH and VV polarisations are known.

#### References

##### Ref 1.5

ASAR Science Advisory Group, Editor R.A.Harris, European Space Agency 1998, "ASAR Science and Applications", ESA SP-1225

##### Ref 1.6

Dierking W., Askne J. & Pettersson M.I., 1997, "Baltic Sea Ice Observations during EMAC-95 using Multi-frequency Scatterometry and EMISAR Data.", Workshop Proceedings" EMAC 94/95, "Final Results", ESA WPP-136,

September 1997.

Ref 1.7

Le Toan T., Smacchia P., Souyris J. C., Beaudoin A., Merdas M., Wooding M., & Lichtenegger J., 1994, "On the Retrieval of Soil Moisture from ERS-1 SAR Data", Proceedings of the Second ERS-1 Symposium "Space at the Service of our Environment", ESA SP-361 Vol. II, pp 883 to 888, January 1994.

### 1.1.5.2 Selectable Incidence Angles

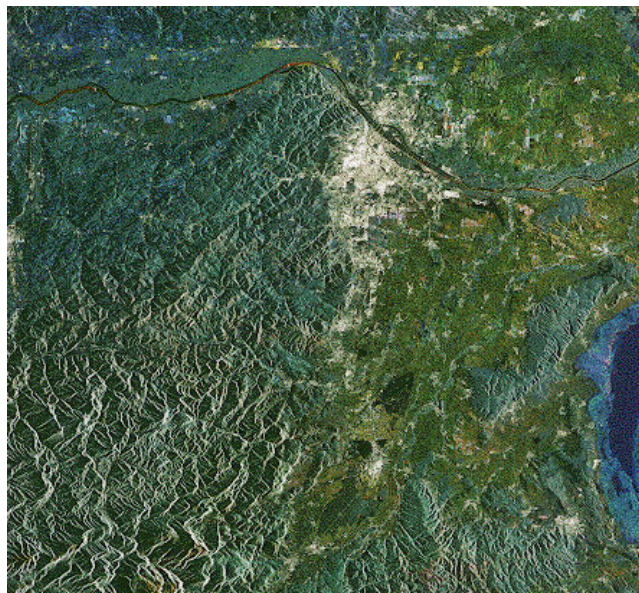


Figure 1.34 ERS-1 image, Wien Austria, Acquired at Fucino (I), 4 Jan 1993 (red) 17 August 1992 (green) 4 May 1992 (blue). Processed by I-PAF (Copyright ESA 1993)

The incidence angle is defined as the angle formed by the [radar beam](#) and a line perpendicular to the surface at the point of incidence. [Microwave](#) interactions with the surface are complex, and different scattering mechanisms may occur in different angular regions. Returns due to surface scattering are normally strong at low incidence angles and decrease with increasing incidence angle, with a slower rate of decrease for rougher surfaces. Returns due to volume scattering from a heterogeneous medium with low dielectric constant tend to be more uniform for all incidence angles. Thus, radar [backscatter](#) has an angular dependence, and there is potential for choosing optimum configurations for different

applications.

The incidence angle range for each of the [Swath](#) positions and the slightly narrower range of incidence angles for [Wide Swath](#) and Global Monitoring Modes are shown in [table 1.3](#) below:

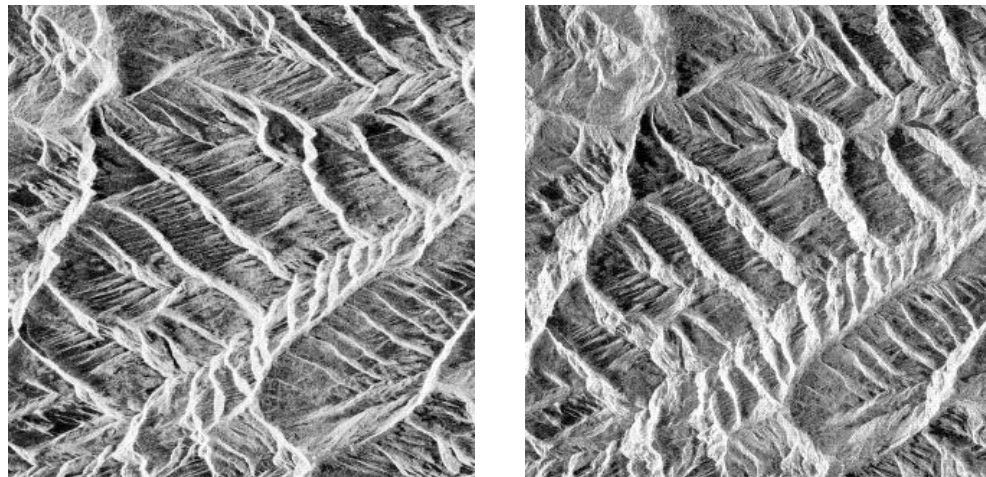
Table 1.3 Specifications for ASAR Image Mode Swaths (for satellite altitude of 786 km).

Image Swath	Swath Width(km)	Ground, position from nadir (km)	Incidence Angle Range	Worst Case Noise Equivalent Sigma Zero
IS1	105	187 - 292	15.0 - 22.9	-20.4
IS2	105	242 - 347	19.2 - 26.7	-20.6
IS3	82	337 - 419	26.0 - 31.4	-20.6
IS4	88	412 - 500	31.0 - 36.3	-19.4
IS5	64	490 - 555	35.8 - 39.4	-20.2
IS6	70	550 - 620	39.1 - 42.8	-22.0
IS7	56	615 - 671	42.5 - 45.2	-21.9

One significant advantage of higher incidence angles is that terrain distortion is reduced. This is well illustrated by a comparison of ERS-2 and RADARSAT images of the Zillertal region in the Austrian Alps, shown in [figure 1.35](#) below. This region includes narrow valleys which range from 600 m at Mayrhofen, up to 3500 m on the highest peaks. Up to about 1900 m, the slopes are partly forested, with alpine vegetation (grass, sedge, etc.), rocks and moraines at higher levels. The two images were obtained within a few days of one another, with a very similar viewing direction. Looking first at the ERS-2 image, obtained with incidence angles of 24° to 26° from near to far range, one sees extreme terrain distortion in the form of severe foreshortening and layover (brightening) of slopes facing the radar, combined with significant lengthening of the slopes facing away from the radar. In contrast, these distortions are seen to be much less in the RADARSAT image where the incidence angle varies between 41° and 44° from near to far range on this image extract. One clear benefit of the higher incidence angle is the extra information which can be observed on the bright steep slopes facing the radar, and this has been found to greatly improve the value of the image for classification of surface classes such as moraine, bare soil and vegetation types.

Figure 1.35 Terrain distortion effects on SAR images obtained with different incidence angles: Zillertal Region, Austrian Alps. Area covered is approx. 36 km x 40 km.  
(Acknowledgement: H. Rott, University of Innsbruck.)

Look Direction → Flight Direction ↑



With a range of different incidence angles available, it becomes possible to select optimum angles for different applications, or to use acquisitions from two separate passes for multi-angle analysis. In the context of vegetation and soil applications, there are some general points which can be made, based on previous research results:

- For soil moisture and soil roughness studies, the combination of different incidence angles is of interest, with the condition that there be short time intervals between acquisitions.
- For agriculture, the use of particular incidence angles will improve selective observation of vegetation (high incidence angles) or underlying soil (low incidence angles).
- For forestry, the use of low incidence angles enhances the sensitivity to biomass, whereas the use of high incidence angles enhances the discrimination of forest types through interaction with forest structure.

Figure 1.36 below illustrates the importance of the incidence angle in isolating the radar response due to the vegetation canopy from that of the underlying soil. Each curve represents the simulated response, with C-band W polarisation, of a soybean canopy for varying gravimetric soil moisture ranging from 20% to 30% (from bottom to top). Whilst the backscatter at 20° incidence angle is still sensitive to underlying soil conditions, that at 40° is stable and invariant with respect to soil moisture.

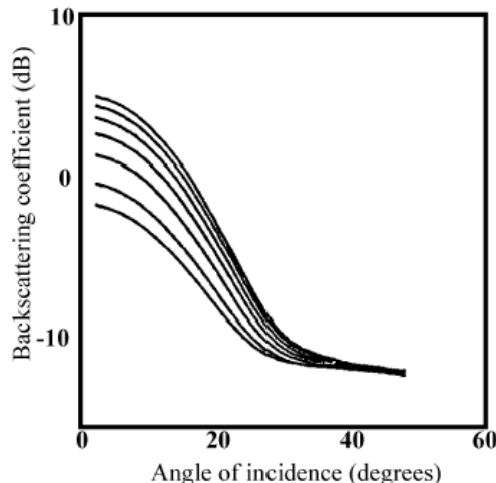


Figure 1.36 Simulated backscatter for a soybean canopy showing increased sensitivity to soil moisture at low incidence angles. (Acknowledgement: Nghiem et al, 1993.)

[Figure 1.37](#) below provides an excellent example of how vegetation mapping can be enhanced by using high incidence angle data. This pair of RADARSAT images shows discrimination of forest clearcuts in Whitecourt, Alberta, an active logging area in the foothills of the Rocky Mountains. On the first image, acquired at an incidence angle of 20° to 27° there is poor contrast between the clearcuts and the forest. On the second image, which was acquired at a much larger incidence angle of 43° to 46°, the dark tones of the clearcut areas contrast strongly with the brighter returns from the surrounding forest.

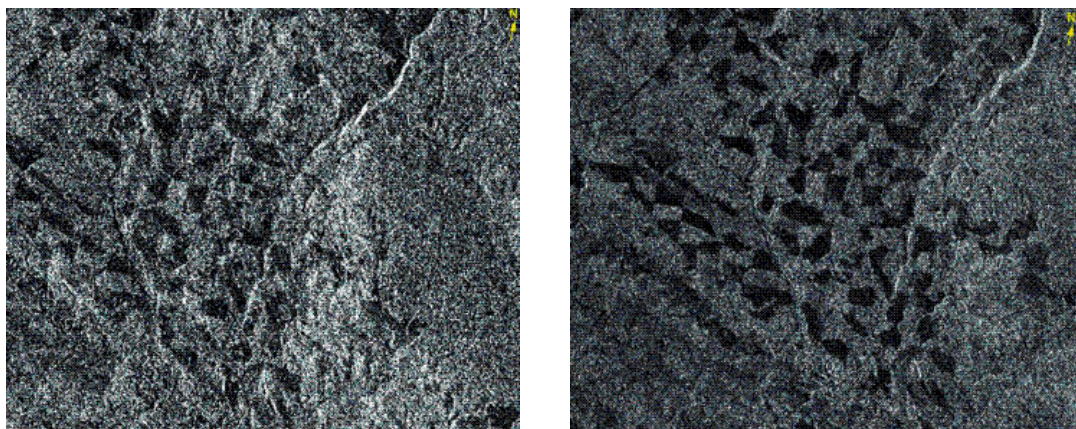


Figure 1.37 RADARSAT images acquired at different incidence angles (a. 20° to 27°. b. 43° to 46°), showing Forest Clearcuts in Alberta, Canada. (Acknowledgement: L. Gray, CCRS, Canada.)

Images acquired with different incidence angles may be used in combination to improve land cover discrimination, but since each image has to be acquired on a different day, any composite image will also include a temporal change component.

Images acquired with different incidence angles may be used in combination to improve land cover discrimination, but since each image has to be acquired on a different day, any composite image will also include a temporal change component.

[Figure 1.38](#) below provides an illustration of the use of multiple incidence angles to improve land cover discrimination for an area near Oxford, UK.

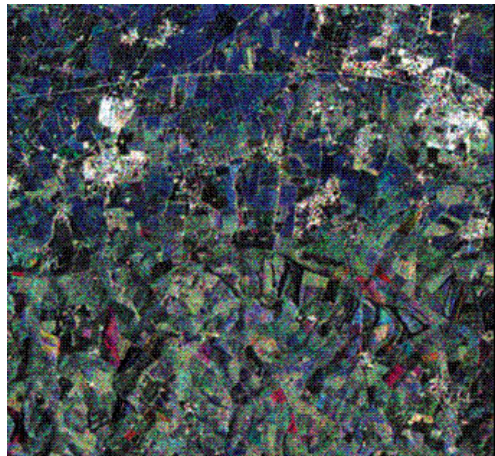


Figure 1.38 Multiple incidence angle image of Oxfordshire area, UK. Composite of Radarsat images: Blue: 23° - 23/3/97, Green: 37° - 13/3/97, Red: 43° - 3/3/97. (Acknowledgement: Remote Sensing Application Consultants, UK)

In this case, 3 Radarsat images taken within a period of 10 days have been combined (Blue - 23° 23 rd March 97, Green - 37° 13 th March 97, Red - 43° 3 rd March 97). Most of the coloured areas on the image, indicative of

backscatter differences related to incidence angle, are bare soil fields, while grassland, woodland and urban areas tend to have grey tones, showing a similar backscatter at the different incidence angles. In the northern half of the area, which has clay soils, practically all bare soil fields have a blue colour, indicating higher backscatter at the lowest incidence angle, as one would expect. In the southern half of the area which has chalk soils, some of the bare soil fields also have blue colours, but some of the fields coloured red are also bare soil fields and this seems something of an anomaly. Possible explanations are that these fields have marked differences in soil roughness, or possibly that cultivation changes took place during the period over which the 3 images were acquired.

---

Ship detection with ERS data was limited to a certain extent by the steep incidence angles. As illustrated in [figure 1.39](#), RADARSAT has now clearly demonstrated the benefits of higher incidence angle data for the detection of ocean-going trawlers (typically, 55 m long) and RADARSAT images are already used pre-operational for monitoring fishing activity in the Barents Sea. The pattern of trawlers seen on this image shows a marked concentration in International Waters along the boundary with Norwegian Waters. Several of the outer ASAR standard beams will be capable of detecting trawlers, although in a rather narrow swath. Also, cross-polarised images from the Alternating Polarisation Mode should further improve detection capability at steeper incidence angles.

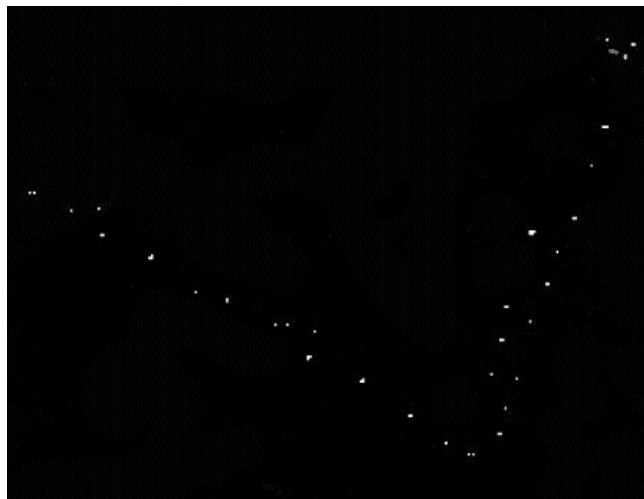


Figure 1.39 RADARSAT image showing fishing vessels in the Barents Sea, similar to what will be possible with ASARs higher incidence angles (26 km scene width). (Data copyright Canadian Space Agency.)

Although higher incidence angles are preferable for ship detection, wide swath and ScanSAR images, such as that shown in [figure 1.40](#) below, can be used across most of the incidence angle range, giving excellent wide area coverage.

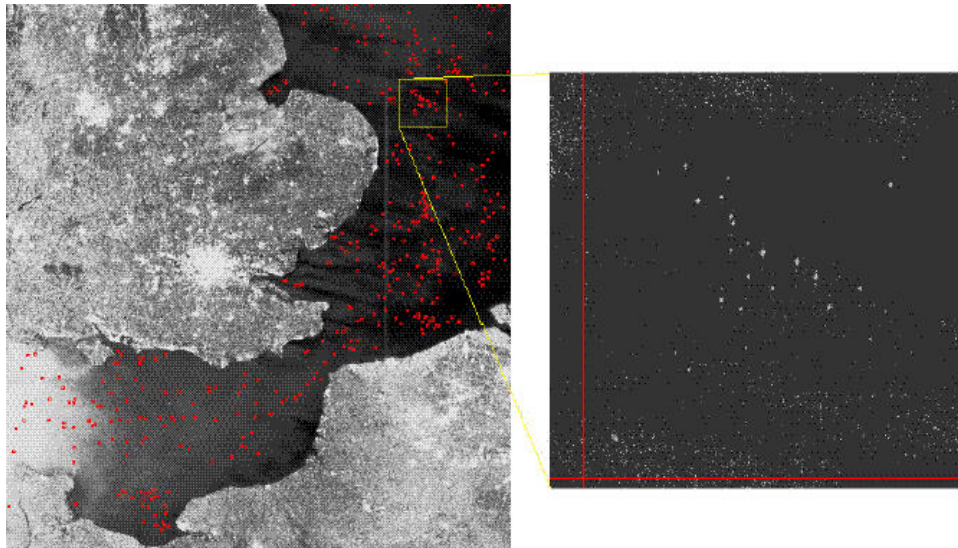


Figure 1.40 RADARSAT ScanSAR image of the English Channel and North Sea showing ship/oil rig detections. The enlarged inset shows a cluster of oil rigs in the North Sea.  
(Acknowledgement: Space Dept., DERA, UK; Data copyright Canadian Space Agency.)

For a further discussion of this subject see the section entitled "[Ocean Applications.](#)"  
[1.1.6.2.4.](#)

### 1.1.5.3 Wide Area Coverage and Frequency of Coverage

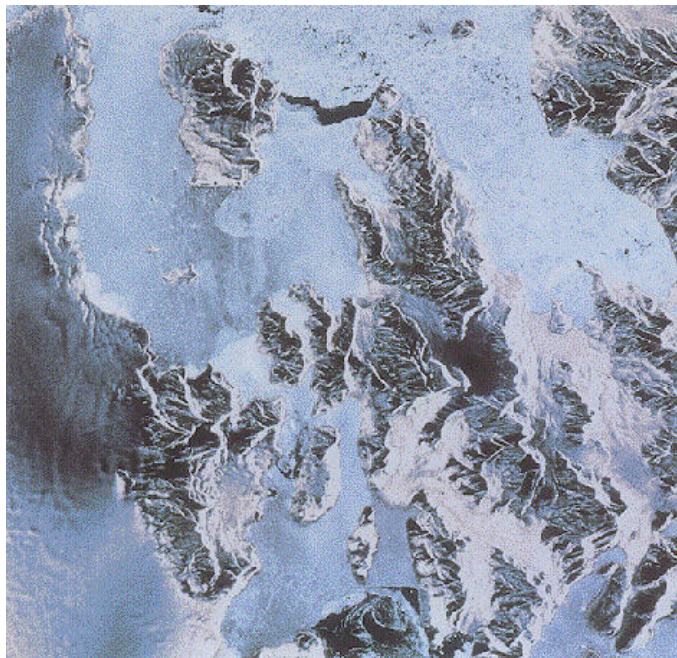


Figure 1.41 ERS-1 SAR image, Adelaide Island Antarctica Nov. 3, 1991 (Copyright ESA 1992)

ASAR [low-resolution](#) images provided by the Wide [Swath](#) and Global Monitoring Modes open up new possibilities for applications requiring large area coverage and/or more frequent revisit. Both modes will provide 105 km swath coverage for applications where higher [resolution](#) is necessary (better than a 5-day frequency).

ASAR [Wide Swath](#) is aimed primarily at sea ice and other oceanographic applications, where there is a special interest in obtaining a wide area view with high temporal frequency. (See [Figure](#) in the section entitled "Geophysical Coverage" to view a graphic portrayal of the comparative swaths for the [ENVISAT](#) instruments). [figure 1.42](#) below shows a [RADARSAT](#) wide swath [image](#) of the Gulf of St. Lawrence on which ice types are seen in various shades of light grey, in contrast with water which has the darkest tones. Such images are now used routinely by the Canadian Coast Guard for ice breaker operations and routing of ships in the Gulf.

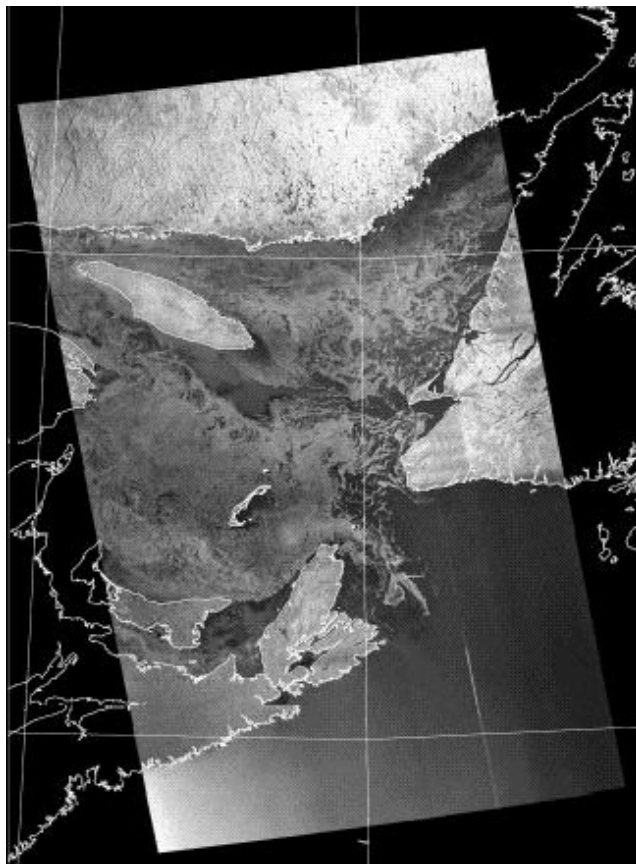


Figure 1.42 Sea Ice Monitoring using RADARSAT ScanSAR data in the Gulf of St. Lawrence, Canada, March 6, 1996. Swath coverage is 450 km, with 250 m pixel spacing. (RADARSAT Data Copyright Canadian Space Agency/Agence spatiale canadienne 1996.)

Received by the Canada Centre for Remote Sensing. Processed and distributed by RADARSAT International. Imagery enhanced and interpreted by CCRS.)

The ASAR Global Monitoring images, with low data rates, promise to be particularly valuable for sea ice mapping over extensive areas. [figure 1.43](#) below shows a simulation of an ASAR Global Monitoring Mode image for regional ice reconnaissance. The simulation is based on a RADARSAT ScanSAR wide, C(HH), image of the southern Beaufort Sea. The original 100 m resolution, 500 km image, which was acquired on October 11, 1996, shows the Mackenzie delta and Tuktoyuktuk peninsula to the south, the new ice and open water in the lead just north of the shore-fast ice, and the pack ice to the north occupy most of the image. The simulation was obtained by reducing the swath from 500 km to 400 km, then sub-sampling and smoothing the image to simulate both the spatial resolution (1 km) and the radiometric resolution of the ASAR Global Monitoring Mode. The simulation shows the potential value of the resulting product. Although the transition from land to shore-fast ice is not distinct, there is still sufficient detail in the ice imagery to recognise areas of slightly lower pack ice concentration (to the east), and to recognise the westward drift of the pack ice just

---

north of the shore-fast ice. This is consistent with the normal clockwise ice movement in the Beaufort Sea gyre.

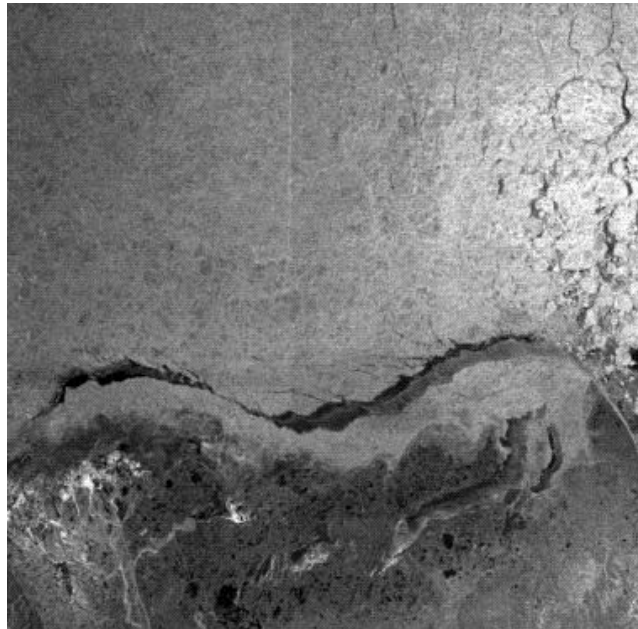


Figure 1.43 ASAR Global Monitoring Mode simulation using RADARSAT ScanSAR wide data. (Acknowledgement: L. Gray, CCRS.)

The frequent large area coverage which ASAR is able to provide is also important for monitoring ice sheets. Of course, ERS already provides frequent revisits of polar regions and the value of this has been well demonstrated in a study of the collapse of the northern Larsen Ice Shelf, Antarctica (Rott et al, 1996). [Figure 1.44](#) below shows two ERS-1 SAR images of the Larsen Ice Shelf. The first (left image) is a strip of three 100 km x 100 km images from a descending pass on January 30, 1995, in which the ice sheet can be seen to be breaking up. Looking at the second (right) image, which was taken just five days earlier, one sees the ice shelf still largely intact. Such images provide valuable information on the timing and rates of change, in this case illustrating the extremely rapid disintegration of the ice shelf over a few days at the end of January 1995. ASAR will be able to provide daily coverage of such phenomena in the polar regions and another important advantage will be the on-board storage capability. For Antarctica, the O' Higgins ERS receiving station currently operates only for two 5-week periods per year.

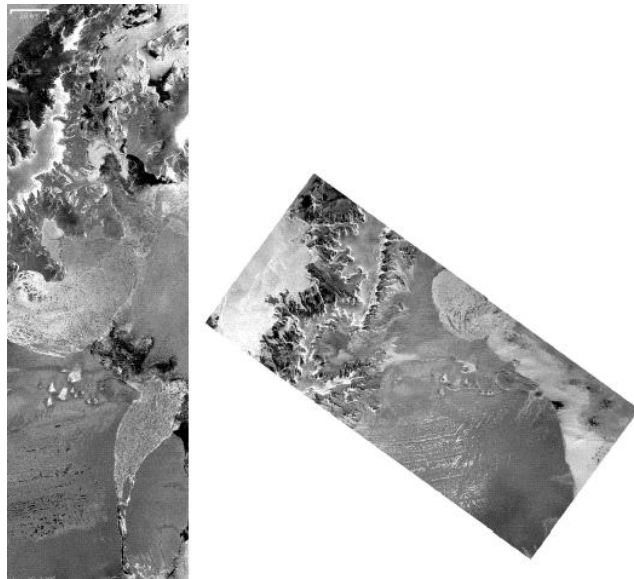


Figure 1.44 ERS SAR images of the Larsen Ice Shelf, Antarctica. The left image is a strip of 3 standard 100 km x 100 km images (descending pass) taken on January 30, 1995, showing break-up of the ice shelf. The right image is another strip of 100 km images (ascending pass) taken on January 25, 1995, when the ice shelf can be seen to be largely intact.

(Acknowledgement: H. Rott, University of Innsbruck, Austria.)

Over the land, interests focus on the potential of low-resolution SAR data for soil moisture and vegetation monitoring.

Previous work carried out over land using ERS Wind Scatterometer data has already shown that low-resolution measurements, in this case 50 km spatial resolution, can provide useful information concerning vegetation dynamics and freeze/thaw on a continental and regional scale (Wisemann & Boehnke, 1994). [Figure 1.45](#) shows how the ERS Wind Scatterometer has been used to monitor seasonal variations over the African continent. Besides the scatterometer image for summer 1993, the so-called Hovmoeller diagram shows a slice through Africa from 35°N to 35°S extending longitudinally from 20° to 26°E. Monthly averages of the radar intensity are plotted for the period from 1991 to 1997. The predominant signal in the Hovmoeller diagram is the annual variation in radar backscatter in the savannah region north and south of the rain forest, and it can be seen how the pattern of increased backscatter in 1992 is repeated every year. The much better resolution of the ASAR Global Monitoring Mode will provide a significantly improved capability for continental or regional scale measurements.

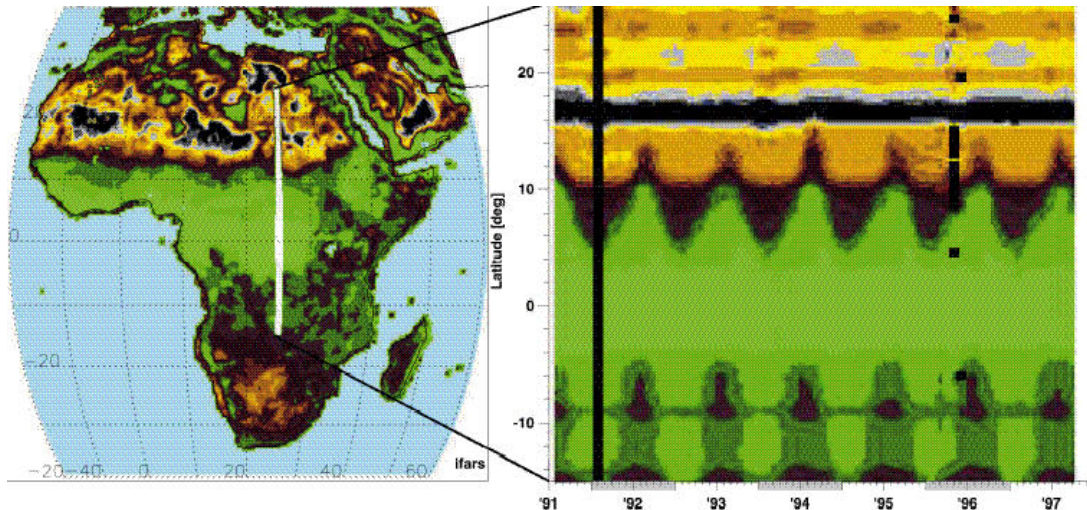


Figure 1.45 ERS-1 scatterometer map of Africa and a Hovmoeller diagram for a slice through Africa from 35°N to 35°S at a longitude of 20°E. Monthly averages are plotted for 1991 to 1997. (Acknowledgement: V Wismann and H. Bohnke, WARS, Germany.)

The availability of approximately 5-day revisit coverage (in Central Europe) using Image Mode promises to be particularly important for flood mapping. For floodplain mapping and emergency management, a resolution of around 30 m is required, with frequent coverage. The much improved temporal coverage possible using ASAR is vital for developing operational systems. In addition, the high incidence angles and HH polarisation capabilities of ASAR will give better mapping of flood extent.

For applications where this improved temporal coverage is important, the main issue then becomes the utility of data acquired at a wide range of different incidence angles. Combined use of images acquired with different incidence angles poses a new set of challenges.

#### 1.1.5.4 Interferometry



Figure 1.46 ERS-1 Interferogram, Feb. 7 2002, Bay of Naples/Vesuvius Italy (Copyright (c) 2001 by SRC SASA, original data by ESA)

#### 1.1.5.4.1 Principles

As was discussed in the section entitled "[Scientific Background](#)" [1.1.2.3.](#), a SAR works by illuminating the Earth with a beam of [coherent](#) microwave radiation, retaining both amplitude and phase information in the radar echo during data acquisition and subsequent processing. This radiation can be described by three properties:

- Wavelength - the distance between peaks on the wave.
- Amplitude - the displacement of the wave at the peak.
- Phase - describes the shift of the wave from some other wave. Phase is usually measured in angular units, like degrees or radians.

Synthetic Aperture Radar (SAR) interferometry exploits this [coherence](#), using the phase measurements to infer differential range and range change in two or more [complex-valued](#) SAR images of the same surface, thereby deriving more information about an object than is obtainable with one single image.

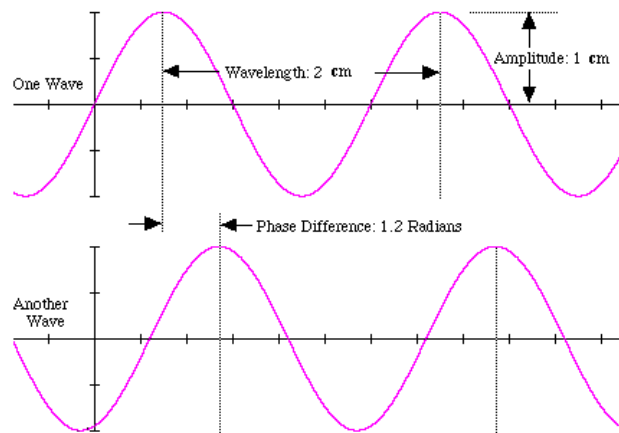


Figure 1.47 Phase shift

The resulting difference of phases is a new kind of image, called an interferogram, which is a pattern of fringes containing all of the information on relative geometry. [Figure 1.48](#) below, offers an example of such an image.

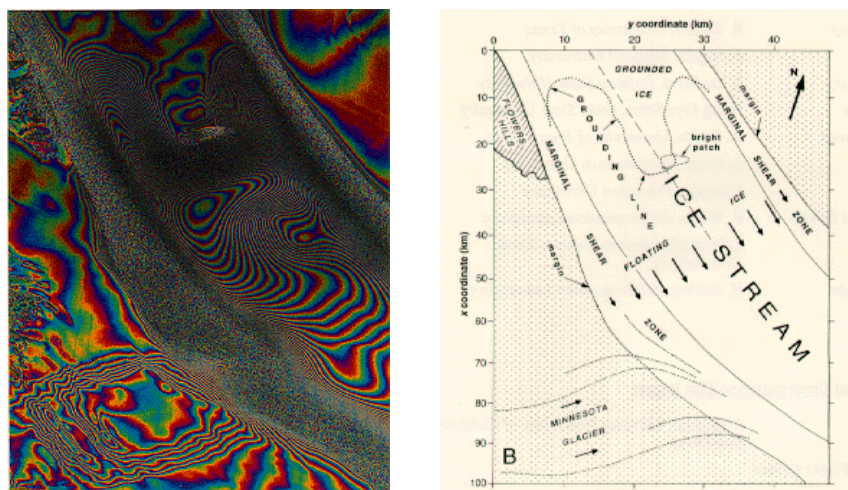


Figure 1.48 Radar interferogram of a portion of the Rutford ice stream in Antarctica, based on two ERS-1 images taken six days apart. The fringe pattern (colour cycle) is essentially a map of ice flow velocity, with one fringe representing 28 mm of range change along the radar line of site. (Image courtesy Jet Propulsion Laboratory, California Institute of Technology)

For a second SAR image to provide additional information, it must be acquired from a different sensor position or at a different time. The difference between the acquisitions of the first and second images determines the type of interferometer that results. Some of the most common forms are:

- Across-track - used primarily for topographical information, this type utilises a difference in across-track position, or look angle.
- Along-track - used primarily for ocean currents information and moving object detection, this type utilises a difference in the along-track position, which can be achieved by a small difference in acquisition time, on the order of microseconds to seconds.
- Differential - this method utilises a difference in time, on the order of days to years, and is used primarily to observe glacier (ice field) or lava flows, if the time difference is within days. If the time difference is measured in days to years, it can be a very useful method of observing subsidence, seismic events, volcanic activity, or crustal displacement.

Each of these types will be touched on briefly below.

#### 1.1.5.4.2 Across-track Interferometry (InSAR)

The best known application of SAR Interferometry is the reconstruction of the Earth topography by using different look angles to compare the same object. This is what is referred to as across-track interferometry. Across-track is also known as the range direction, defined as the dimension of an image perpendicular to the line of flight of the radar.

Consider two radar antennas, A<sub>1</sub> and A<sub>2</sub>, simultaneously viewing the same surface and separated by a baseline vector B with length B and angle  $\alpha$  with respect to horizontal, as shown in [figure 1.49](#) below. A<sub>1</sub> and A<sub>2</sub> may also represent a single antenna viewing the same surface on two separate passes.

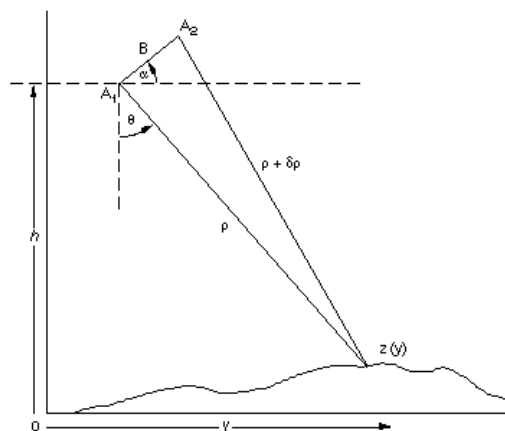


Figure 1.49 Basic imaging geometry for InSAR

A1 is located at height  $h$  above some reference surface. The distance between A1 and the point on the ground being imaged is the slant range  $r$ , while  $r + \delta r$  is the distance between A2 and the same point.

In the case of simultaneous imaging from two separate antennas, one antenna both transmits and receives the radar signal. This antenna is known as the master. The second antenna, known as the slave, only receives. This method is sometimes referred to as single-pass interferometry.

In the case where a single-antenna SAR system revisits the same position and images the same area on the ground after several days or weeks, the repeat-pass interferometry method is used. With this method, each antenna acts as both transmitter and receiver, as depicted in [figure 1.50](#) below.

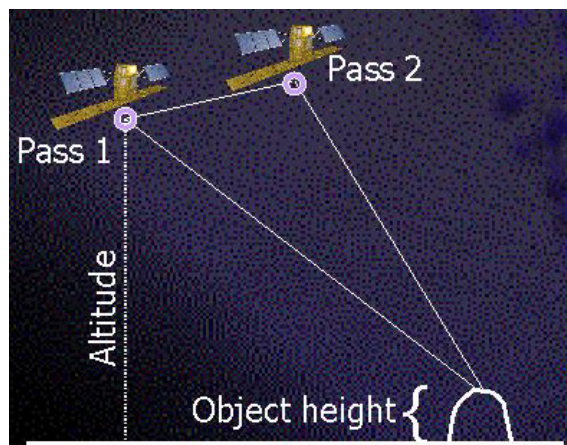


Figure 1.50 InSAR Data Collection

The [phase](#) of pixel value in a complex SAR image depends on the scattering mechanism in the resolution cell, and the distance from the antenna to the point. If the scattering mechanism in the two images is similar, then the phase difference between the two complex SAR images is proportional to the difference in [slant range](#) from the two antenna to the point.

The similarity in scattering mechanism in the two images is indicated by the correlation coefficient of the image, which is also called [coherence](#) in SAR interferometry literature. Any dissimilarity of the scattering mechanism between the two images, indicated by a low

coherence, results in phase noise. A certain loss of coherence results from the different [look angles](#) from two antenna to the point, and from receiver noise. Coherence loss can also result from changes in the surface between acquisitions, in the case of repeat-pass interferometry.

The difference between  $\rho$  and  $\rho + \delta\rho$  can be measured by the phase difference between the two [complex](#) SAR images. That is, by multiplying one image by the [complex conjugate](#) of the other image, an interferogram is formed whose phase is proportional to the range difference to the point. The phase of the interferogram, displayed as an image, contains fringes that trace the [topography](#) like contour lines, as shown in [figure](#) above.

Interferograms are often displayed by showing the phase difference as colour, and the SAR [amplitude](#) as brightness (see [figure 1.51](#) below).

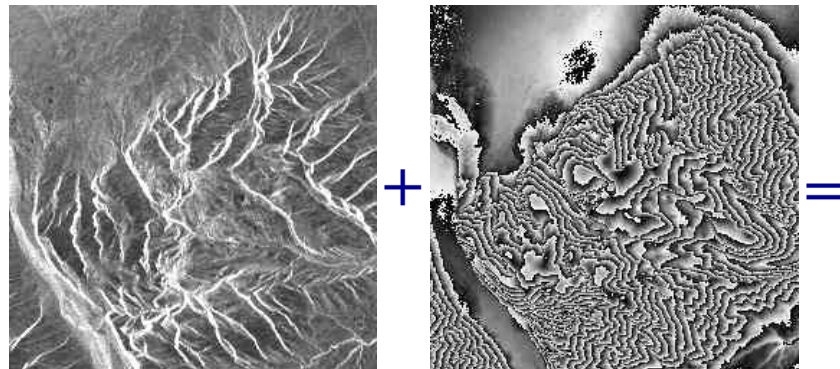
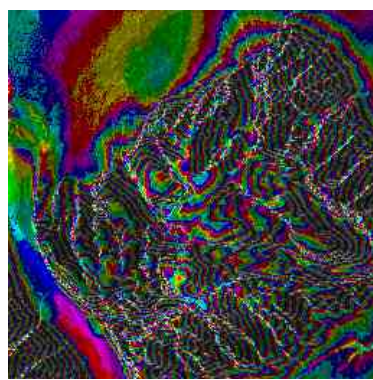


Figure 1.51 Interferogram creation

SAR Amplitude (0..300) + Phase Difference (-pi..pi) =



The phase of the above interferogram shows the topography of an imaged mountain.

The slant range difference is proportional to the full phase or absolute phase of the complex-valued interferogram. However, the measured phase values of the interferogram can only take values between 0 and  $2\pi$ . That is, the phase is 'wrapped'. Thus, in order to

---

compute the slant range difference which is needed to compute topography, the  $2\pi$  ambiguity inherent in the phase measurements must be solved, using techniques of '[phase-unwrapping](#)'.

Once the absolute phase of each pixel of the interferogram is known, the geometry of the figure can be used to compute the topography  $z(y)$ , if the baseline vector (vector B in [figure 1.49](#)) is known. The result is a [Digital Elevation Model \(DEM\)](#) of the observed area.

#### 1.1.5.4.3 Along-track Interferometry

[Along-track](#) (azimuth) interferometry uses two antennas; the master that transmits and receives, and the slave that receives only. Such a system takes two images of the same target, with a time delay that results in an along-track difference in position. Typically, this time delay is between 10 microseconds (ms) and 100 ms. If the target remains stationary between acquisitions, the two data sets are ideally identical (i.e. in the absence of any system phase noise) and the interferometric phase is zero. However, any relative range shift of the targets between the two images will result a non-zero interferometric phase. The along-track interferometric method is most often used when detecting relatively fast motion, such as ocean currents.

#### 1.1.5.4.4 Differential Interferometry (D-InSAR)

The temporal separation in [repeat-pass interferometry](#) of days, months, or even years, can be used to advantage for long term monitoring of geodynamic phenomena, in which the target has changed position at a relatively slow pace. This would be true when monitoring glacial or lava flows. It is also useful for analysing the results of single dramatic events, such as earthquakes. If two acquisitions are made at different times from the same position, so there is no [across-track](#) baseline, then the [phase](#) of the interferogram depends only on the change in [topography](#) between the acquisition times. In general, a difference in across-track, ([azimuth](#)), position of the acquisitions also exists. In this case, multiple acquisitions can be made to measure the topography, and measure the change in topography (differential effects) over time.

The block diagram below depicts a typical D-InSAR processor using one SAR and one [ScanSAR](#) image, that incorporates a [Digital Elevation Model \(DEM\)](#).

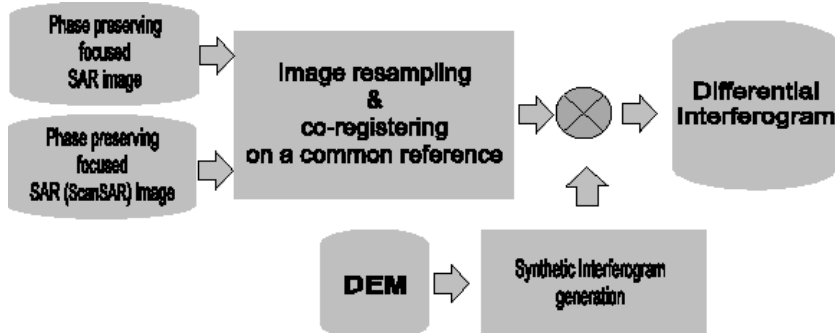


Figure 1.52 Block diagram of a typical D-InSAR processor.

In the 35 day repeat orbit scenario, the wide swath capabilities of ASAR, combined with the predictable high reliability and repeatability of the orbits, will allow the retrieval of extremely useful data for differential interferometry (D-InSAR). Another

important benefit of ASAR will be the availability of different viewing angles and in particular higher off-nadir angles, that enhance the interferometric visibility of steeper slopes, which are otherwise in layover with the 23° incidence angle of ERS-1/2. As for ERS, in order that terrain can be imaged with differential interferometry the surface conditions should be stable enough so that more than 30-40% of the strong scatterers remain unchanged in two images acquired 35 days apart.

ASAR will be able to measure very small terrain displacements due to co-seismic motions, subsidence, volcanic upswelling, landslides, ice movement and possibly oscillatory effects like earth tides and the loading of sea tides on the continental shelf. ( See section entitled "[Land Applications](#)" )

An excellent example of the detection of surface subsidence is shown in [figure 1.53](#) below. The image displays an exaggerated three dimensional (3D) perspective view of the Belridge (middle left) and Lost Hills (lower left) Oil Fields, California, viewed from the north-west. Both oil fields are located in the San Joaquin Valley. The surface deformation derived from ERS-1 data collected in September and November 1992 (70 days time difference), shows subsidence of up to 6 cm.

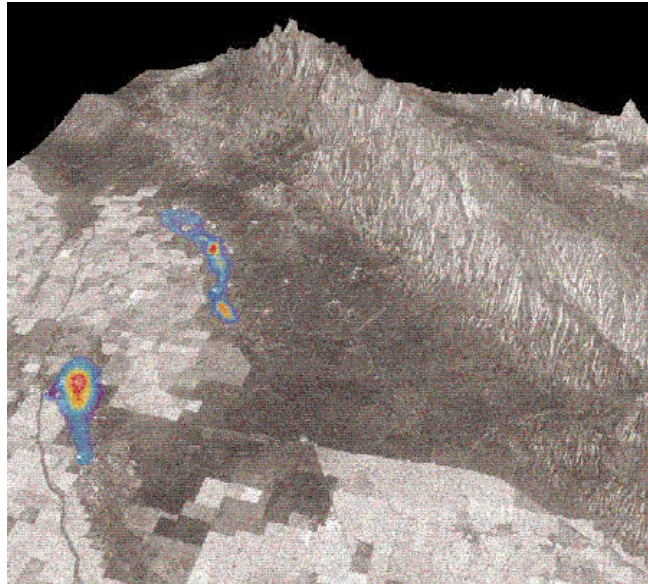


Figure 1.53 Subsidence in the Belridge Oilfields, California. The colours derived from ERS-1 data collected in September and November 1992 (70 days time difference) show subsidence ranging from 1 cm (blue) to 6 cm (red-brown). The 3D view has been produced using the DEM generated from the ERS tandem pair, combined with a Radarsat image.  
 (Acknowledgement: M. van der Kooij, Atlantis Scientific Inc.; Radarsat Data Copyright Canadian Space Agency/Agence spatiale canadienne 1996)

Usually, D-InSAR surveys are generated starting from two full resolution SAR images. Yet, it is possible to combine low-resolution, [Wide Swath \(WS\)](#) images with full resolution ones to give high quality D-InSAR images. See [Low Resolution Interferometry 1.1.5.4.6.](#) below.

#### 1.1.5.4.5 Coherence Evaluation

[Coherence](#), when associated with interferometry, is related to phase variance between the two SAR images. For the purpose of processing the interferometry data into [topography](#) of motion information, the coherence can be a useful tool in indicating areas of noisy phase. For example, during [phase unwrapping](#), areas of noisy phase - as indicated by a low value of coherence - can be avoided.

In addition, coherence is another useful parameter that can be extracted from [repeat-pass interferograms](#). Coherence provides information on stability over time, or temporal stability, and is therefore an important feature for land cover classification. Temporal decorrelation can be caused by such things as changes in vegetation, freezing and thawing, or human activities like plowing. All of these changes are observed over periods of days to years, whereas some changes to water surfaces can occur in a matter of milliseconds.

#### 1.1.5.4.6 Low Resolution Interferometry

Pairs of complete [Wide Swath \(WS\)](#) or [Global Monitoring \(GM\) Mode](#) images will be unsuitable for interferometry because, in the lower resolution modes, the data are sampled in bursts along the [azimuth direction](#) (along-track). For interferometry the sampling bursts need to be spatially aligned in the two interfering frames. However, there are interesting possibilities for using low resolution images in conjunction with full resolution, [Image Mode \(IM\)](#) images. A full resolution image with the same [incidence angle](#) as the subswath of the Wide Swath or Global Monitoring Mode image is needed.

Once a worldwide archive of Wide Swath or Global Monitoring Mode images is built up it will be possible to obtain interferometric pairs of particular areas of interest within 35 days, by acquiring full resolution (IM) data with the same imaging geometry as the relevant portion of the low resolution image. Because the previously acquired burst images are of low resolution, the quality of the fringes will be proportionally lower than if two full resolution images had been used.

[Figure 1.54](#) is a simulation of [co-seismic](#) motion retrieval using low resolution differential interferometry. In this example ERS SAR images for the Landers 1992 earthquake have been used to simulate interferograms, using an Image Mode image together

with either Wide Swath Mode or Global Monitoring Mode images. On these images one fringe corresponds to half a wavelength displacement along the radial direction.

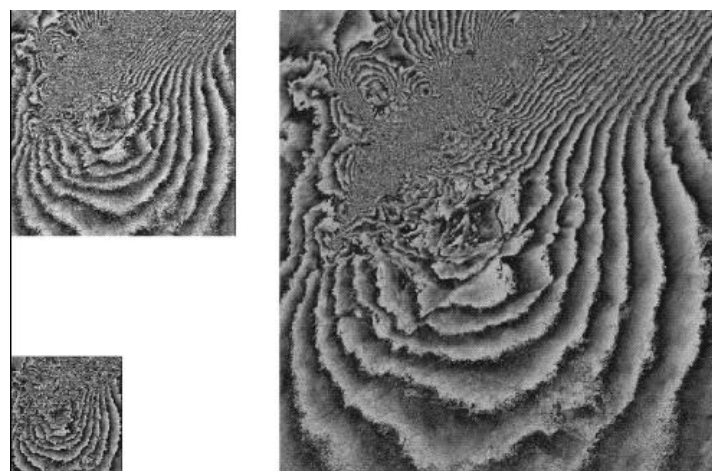


Figure 1.54 Simulation of low resolution interferograms of the Landers 1992 earthquake,

---

using ERS SAR data. Image Mode (right), Wide Swath Mode (top left) and Global Monitoring Mode (bottom left), for an area of 48 km x 45 km. (Acknowledgement: F. Rocca, Politecnico di Milano, Italy).

#### 1.1.5.4.7 Conclusions

The above discussion of interferometry only scratches the surface of a rich and complex branch of remote sensing and the list of references provided below offers just a small portion of the wealth of material dedicated to this expanding area of research.

It is now well established that SAR interferometry provides a valid form of geophysical measurement. The huge archive of data acquired by the [C-band](#) sensors [ERS-1 and ERS-2](#) has imposed a de facto standard for interferometry. The Advanced Synthetic Aperture Radar (ASAR) sensor, which is also a C-band instrument, will provide considerably higher flexibility compared with the two ERS SARs. ASAR provides a choice of two [polarisations](#) (out of H, VV, and VH) as well as a variety of imaging modes, such as different [incidence](#) angles, standard and [ScanSAR](#) wide swath modes. ( Refer to the other subsections within "[Special Features of ASAR](#)" [1.1.5.](#) for more information on these topics ). In particular, since ASAR can provide higher off-[nadir](#) angles than was the case with the ERS-1/2 sensors, the problems of [layover](#) will be reduced, thereby enhancing the interferometric visibility of steeper slopes.

#### 1.1.5.4.8 References

##### Ref 1.8

ASAR Science Advisory Group, Editor R.A.Harris, European Space Agency 1998, "ASAR Science and Applications", ESA SP-1225

##### Ref 1.9

Bamler, R., P. Hartl, "Synthetic aperture radar interferometry", R. Bamler, P. Hartl, Inverse Problems 14, pp. R1-R54, 1998

##### Ref 1.10

Dixon, T. H, "Report of a Workshop Held in Boulder, Colorado : February 3-4, 1994", prepared by the Jet Propulsion Laboratory, California Institute of Technology, under a contract with the National Aeronautics and Space Administration.

##### Ref 1.11

Feigl, K. L., A. Sergent, and D. Jacq, "Estimation of an earthquake focal mechanism from a

satellite radar interferogram": application to the December 4, 1992 Landers aftershock, *Geophys. Res. Lett.*, in press, 1994.

#### Ref 1.12

Geudtner, D., "The interferometric processing of ERS-1 SAR data", European Space Agency, Technical Translation of DLR-FB 95-28, ESA-TT-1341, 1995.

#### Ref 1.13

Goldstein, R. M., H. Engelhardt, B. Kamb, and R. M. Frolich, "Satellite radar interferometry for monitoring ice sheet motion: application to an Antarctic ice stream", *Science*, 262, 1525-1530, 1993.

#### Ref 1.14

Goldstein, R. M., H. A. Zebker, and C. Werner, "Satellite radar interferometry: two-dimensional phase unwrapping", *Radio Science*, 23, 713-720, 1988.

#### Ref 1.15

Graham, L. C., "Synthetic interferometer radar for topographic mapping", *Proc. IEEE*, 62, 763-768, 1972.

#### Ref 1.16

Li, F., and R. M. Goldstein, "Studies of multibaseline spaceborne interferometric synthetic aperture radars", *IEEE Trans. Geosci. Remote Sensing*, 28, 88-97, 1990.

#### Ref 1.17

Massonnet, D., K.L.Feigl, "Radar interferometry and its application to changes in the earth surface", *Reviews of Geophysics* Vol. 36, Number 4, Nov. 1998, pp.441-500.

#### Ref 1.18

Massonnet, D., M. Rossi, C. Carmona, F. Adragna, G. Peltzer, K. Feigl, and T. Rabaute, "The displacement field of the Landers earthquake mapped by radar interferometry", *Nature*, 364, 138-142, 1993.

#### Ref 1.19

Massonnet, D., K. Feigl, M. Rossi, and F. Adragna, "Radar interferometric mapping of deformation in the year after the Landers earthquake", *Nature*, 369, 227-230, 1994.

#### Ref 1.20

Massonnet, D., and K. L. Feigl, "Discriminating geophysical phenomena in satellite radar interferograms", *Geophys. Res. Lett.*, in press, 1995a.

#### Ref 1.21

Monti Guarnieri, A., Prati, C., Rocca, F., and Desnos, Y-L, "Wide Baseline Interferometry With Very Low Resolution SAR Systems", Dipartimento di Elettronica e Informazione - Politecnico di Milano, ESTEC (available on-line at: <http://www.elet.polimi.it/users/dei/sections/telecom/andrea.montiguarnieri/papers/ceos/>)

**Ref 1.22**

Peltzer, G., K. Hudnut, and K. Feigl, "Analysis of coseismic surface displacement gradients using radar interferometry: new insights into the Landers earthquake", *J. Geophys. Res.*, 99, 21971-21981, 1994.

**Ref 1.23**

Rodriguez, E., and J. Martin, "Theory and design of interferometric SARs", *Proc. IEEE*, 139, 147-159, 1992. [Ref. \[1.22\]](#) Solaas, G.A., "ERS-1 interferometric baseline algorithm verification", *ESA Tech. Note ES-TN-DPE-OM-GS02*, 69 p., 1994.

**Ref 1.24**

Zebker, H., and R. Goldstein, "Topographic mapping from interferometric synthetic aperture radar observations", *J. Geophys. Res.*, 91, 4993-5001, 1986.

**Ref 1.25**

Zebker, H., and J. Villasenor, "Decorrelation in interferometric radar echoes", *IEEE Trans. Geosci. Rem. Sensing*, 30, 950-959, 1992.

**Ref 1.26**

Zebker, H., P. Rosen, R. Goldstein, A. Gabriel, and C. Werner, "On the derivation of coseismic displacement fields using differential radar interferometry: the Landers earthquake", *J. Geophys. Res.*, 99, 19617-19634, 1994a. [Ref. \[1.25\]](#) Zebker, H.A., C. Werner, P.A. Rosen, and S. Hensley, "Accuracy of topographic maps derived from ERS-1 interferometric radar", *IEEE Trans. Geosci. Rem. Sens.*, 32, 823-836, 1994c.

### 1.1.5.5 Wave Spectra

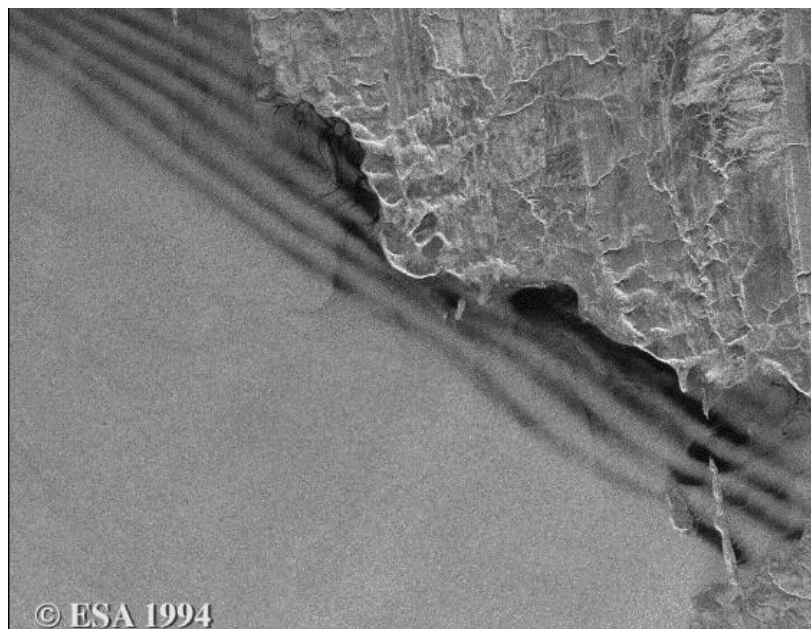


Figure 1.55 ERS-1 SAR image, Dundas Peninsula (in the Parry Islands of northern Canada), Aug. 17, 1994 (Copyright ESA 1994)

The exchange of energy between the ocean and atmosphere, between the upper layers of the ocean and the deep ocean, and transport within the ocean, all have a role in controlling the rate of global climate change and the patterns of regional change. Long continuity of measurements of sea surface temperature, winds, topography, geostrophic currents and ocean colour is essential.

[Figure 1.56](#) below, of the Gulf of Gaeta, Italy, shows the first multitemporal ERS-2/ERS-1 image acquired at Fucino (I) and Kiruna (S), processed by ESA/ESRIN: 578x900 pixels, 475 Kb. The ERS-1 and ERS-2 images of May 1st and 2nd reveal a difference in soil moisture due to changed weather conditions, shown by the greenish land colour. The colours of the sea correspond to different wind and current conditions during the three acquisitions, while black indicates calm areas at all acquisition dates.

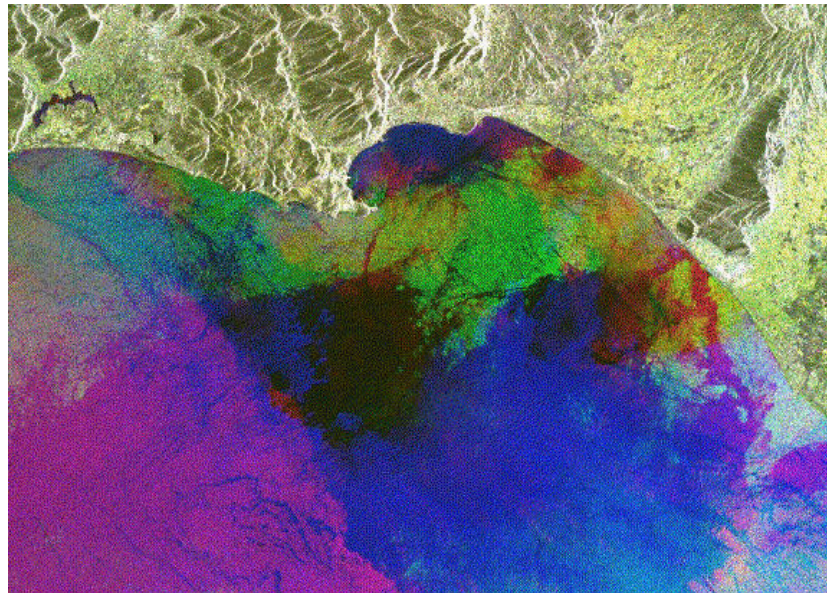


Figure 1.56 Gulf of Gaeta, Italy ERS-1 ( blue: acquired Mar 27, 1995. green acquired May 1, 1995 ) and ERS-2 ( red: acquired May 2, 1995 )

ASAR products of interest to ocean scientists include wind speed and wave spectra from the Wave Mode. Other [ASAR modes](#) are of interest for wind field measurement, studies of internal waves and eddies and the [detection](#) of atmospheric phenomena, with Wide [Swath](#) and Global Monitoring Modes being of particular interest because of the larger area and more frequent coverage.

ASAR Wave Mode will provide wave spectra derived from imagettes of minimum size (5 km x 5 km), similar to the ERS [AMI](#) Wave Mode, spaced 100 km [along-track](#) in either HH or VV polarisation. The position of the imagette [across-track](#) can be selected to be either constant or alternating between two across-track positions over the full swath width.

ERS Wave Mode products are based on image spectra (wave number and direction) estimated from SAR intensity imagettes using standard Fourier Transform techniques. These products are therefore symmetric containing 180° propagation ambiguity. Techniques involving the use of Wave Model predictions have been developed to solve the ambiguity problem, though this can be subject to error when opposite or near opposite wave components exist.

For ASAR, this problem was solved by using the new wave product preserving the phase and a new algorithm called "inter-look cross spectral processing," whereby information on the wave propagation direction is computed from pairs of individual look images separated in time by a fraction of the dominant wave period. (Engen & Johnsen, 1995.) [Figure 1.57](#) shows a simulated ASAR Wave Mode Spectrum, with the top left plot being the real part of the

cross spectrum (symmetric and equivalent to an ERS product) and the top right plot the new imaginary part (asymmetric, giving wave propagation direction).

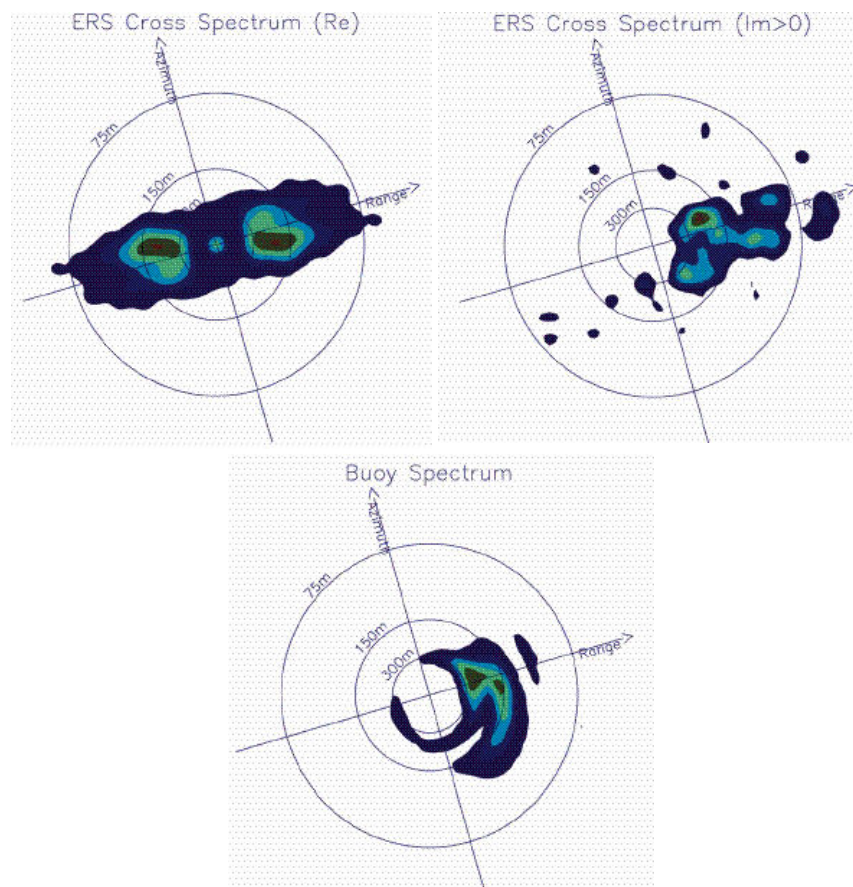


Figure 1.57 SAR ocean image cross spectrum (real and imaginary part) processed from ERS-1 data using the ENVISAT ASAR Wave Mode Cross Spectra algorithm. The corresponding directional buoy spectrum is also shown. (Acknowledgement: NORUT IT, Norway.)

In the above example, the output from the new algorithm is seen to correspond with the wave direction provided by buoy measurements, as shown in the bottom of the figure.

[Figure 1.58](#) shows an example of a Level 1B ASAR wave spectra, as displayed by [EnviView 1.2.1.2](#). Note that the image is anti-symmetric in this case. The image is a polar plot of ASAR wave spectrum data placed into discrete bins. Each wave spectra image is composed of 864 bins arranged in a polar plot.

- The first bin (1,1) is at the top (from 0° to 10°) of the image.
- The spectrum image is divided up into 36 sectors or 'spokes', each 10° wide. Note that the data is redundant due to the symmetry of the spectra, so only data from the first 180° of the spectra are provided (sectors 1 to 18). The other half of the

- spectrum display (sectors 19 to 36) can be constructed from the first half, as the spectrum is either symmetric or anti-symmetric.
- Each radial sector or 'spoke' contains 24 bins, numbered from 1 at the outside edge of the spectra display to 24 at the centre.

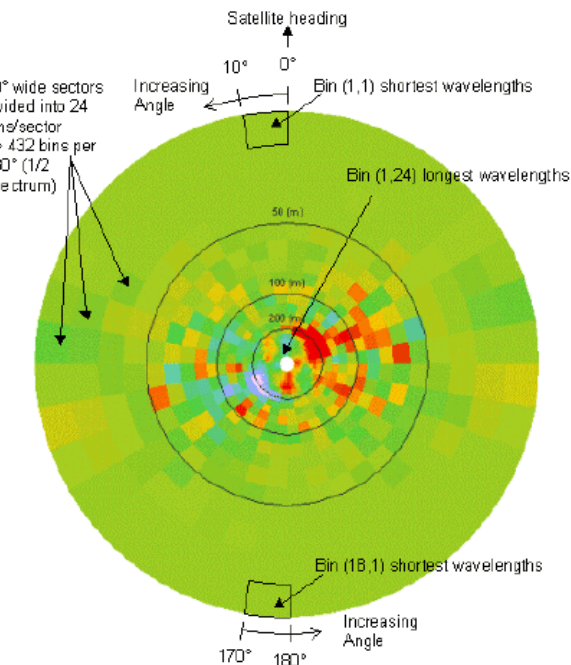


Figure 1.58 Level 1B ASAR wave spectra image. Each bin is colour-coded based on the value of the bin data mapped onto a colour scale shown to the right-hand side of the image.

[Figure 1.59](#) below provides the Wave Mode Cross Spectra Format

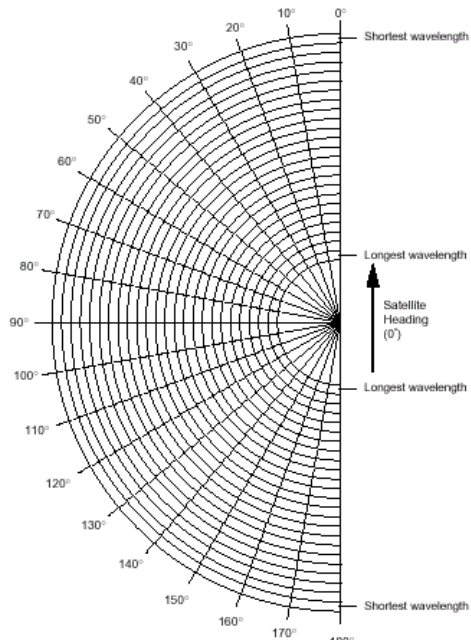


Figure 1.59 Wave Mode Cross Spectra Format

The method for reconstructing the entire cross spectrum from that stored in the cross spectrum [Measurement Data Set \(MDS\)](#) is shown below in [Figure 1.60](#).

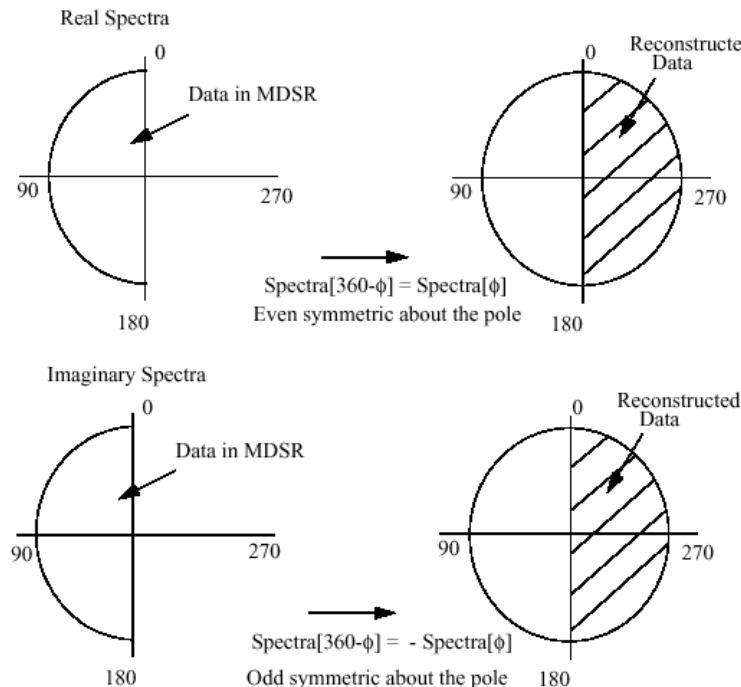


Figure 1.60 Method to reconstruct full cross spectra from product cross spectra

### 1.1.5.6 Simultaneous Observations

The ENVISAT Mission offers simultaneous acquisition of ASAR and MERIS data, and this promises to be particularly valuable for ocean and coastal studies. With MERIS having a swath width of 1150 km around nadir, simultaneous data acquisition is possible up to ASAR incidence angles of approximately 34°, therefore including IS1 to IS5 in Image Mode, and all but the outer edge of the [low-resolution](#) modes. It will be possible to use ASAR data together with [AATSR](#) data, but simultaneous data acquisition is restricted to a narrow overlapping swath.

[Figure 1.61](#) provides an illustration of the type of simultaneous SAR and optical large area data acquisition that will be possible. In this example a low pressure system is seen on both a Wide Swath Radarsat image and a NOAA [AVHRR](#) image acquired within 30 minutes of each other. On the SAR image one sees the differences in sea surface [roughness](#) associated with the depression, while on the AVHRR image the same feature is depicted through cloud patterns.

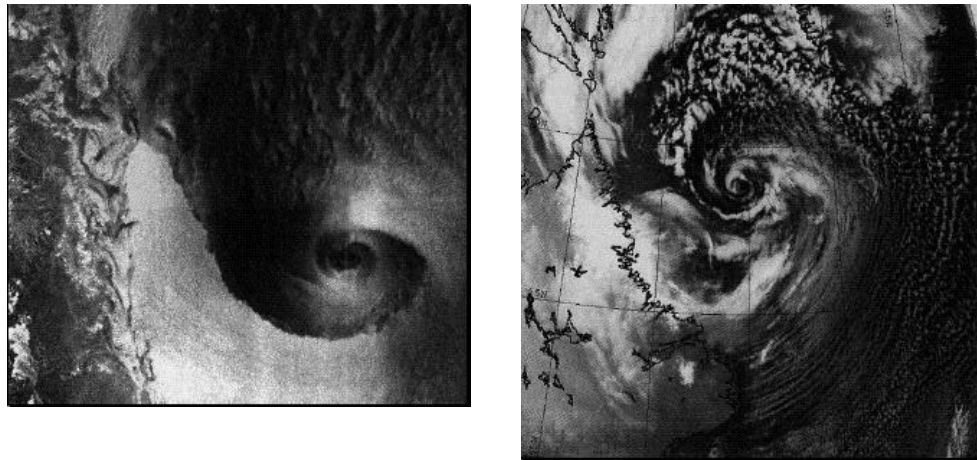


Figure 1.61 A low pressure system seen on Radarsat Wide Swath (left) and NOAA AVHRR (right) images acquired on 30/3/97. Area shown on the Radarsat image is 500 km x 700 km.  
 (Radarsat Data Copyright Canadian Space Agency/Agence spatiale Canadienne 1996.  
 Received by the Canada Centre for Remote Sensing. Processed and distributed by Radarsat International. Imagery enhanced and interpreted by CCRS)

[Figure 1.62](#) below shows the combination of a SAR image and satellite derived sea surface temperatures. The ERS and

AVHRR images were acquired on 3 rd October 1992, off the west coast of Norway. In the AVHRR IR image the surface temperature decreases from nearly 14°C (white) in the coastal water to 12°C (purple) in the Atlantic water offshore. The pattern of the sea surface temperature field with the curvilinear temperature fronts represents meso-scale variability of

10 to 50 km, characteristic of the unstable Norwegian Coastal Current (Johannessen et al., 1994). The ERS image, acquired 7 hours later, contains frontal features at a scale, configuration and orientation that are in good agreement with those seen in

the IR image. The SAR image shows both bright and dark radar modulations of various width across the boundaries, which clearly show current boundaries including meanders.

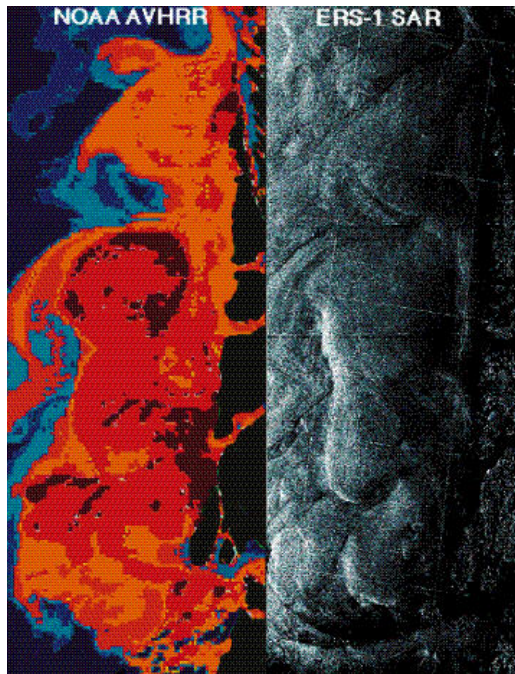


Figure 1.62 Comparison of a 1 km resolution AVHRR image acquired at 14:20 on 3/10/92 (white is 14°C and purple is 12°C; + denotes buoy position; land is masked in green and clouds in black) and a 100m resolution ERS-1 SAR ( Copyright ESA 1992 ) image acquired at 21:35 on 3/10/92. Both images cover the same 100 km x 300 km region off the west coast of Norway between 59°N and 62°N. (Acknowledgement: J.A. Johannessen et al., 1994).

In [figure 1.63](#) below, the temperature information provided by the Advanced Very High Resolution Radiometer (AVHRR) satellite combined with the resolution of ERS-1 SAR data, both acquired on February 24, 1992, aids in calculating heat fluxes and in deriving salt fluxes for coastal shelf processes and global climate models. In the composite image of St. Lawrence Island shown below, the land mask is shown in blue.

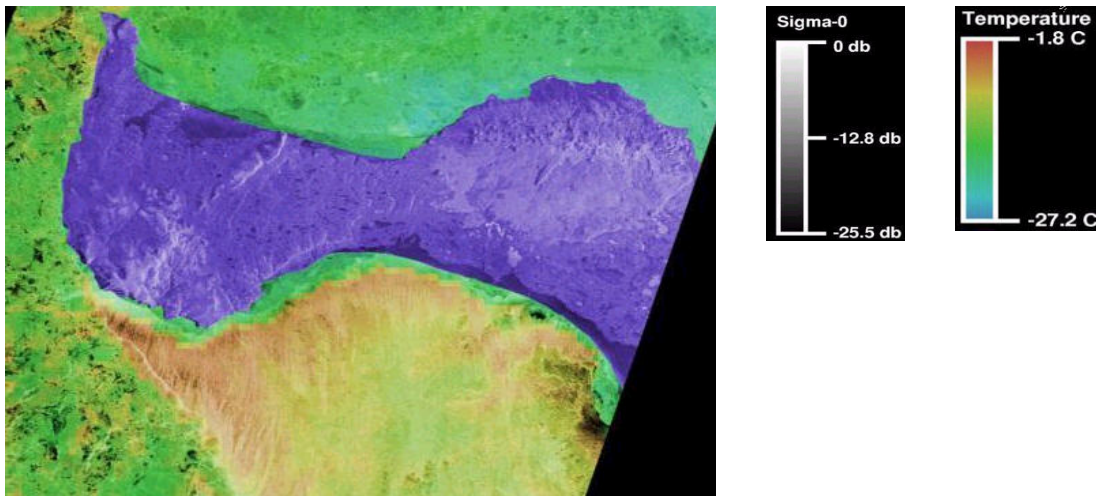


Figure 1.63 Combined AVHRR and ERS-1 Image of St. Lawrence Island Alaska (image courtesy of the Alaska SAR Facility).

## References

### Ref 1.27

ASAR Science Advisory Group, Editor R.A.Harris, European Space Agency 1998, "ASAR Science and Applications", ESA SP-1225

### Ref 1.28

Johannessen J.A., Digranes G., Esdedal H., Johannessen O.M., Samuel P, Browne D, & Vachon P., 1994, "ERS-1 SAR Ocean Feature Catalogue", ESA SP-1174. October 1994.

## 1.1.6 Summary of Applications vs Products

### 1.1.6.1 Summary of Applications Introduction

The original focus of the ERS missions was oceans and ice monitoring, and there has been an impressive range of scientific investigations in oceanography, polar science, glaciology, and climate research which will be supported by ASAR. These include measurements of ocean surface features (currents, fronts, eddies, internal waves), directional ocean wave spectra, sea floor topography, snow cover and ice sheet dynamics. Operational systems have been

developed for mapping sea ice, oil slick monitoring and ship detection.

The ASAR Instrument will provide continuity and improvement upon the ocean, coastal one, and land cover monitoring capabilities of the previous ERS SAR instruments. ASAR promises to be important for modelling changes in vegetation, oceans, ice sheets, snow and sea ice. Data is required in order to initiate or validate models, and for long-term monitoring over global to regional scales, as well as smaller areas of particular interest.

Three different groups of users of ASAR data are:

1. Remote Sensing Science
2. Earth Science Community
3. Commercial Applications

#### 1.1.6.1.1 Remote Sensing Science

A considerable amount of research has been undertaken into the processing and use of spaceborne SAR data from ERS-1 and ERS-2, as well as other SAR instruments. The need for further research will continue, both in data processing and analysis techniques, and in the development of geophysical retrieval models. Research will be undertaken by a range of users from universities and research institutes, to value-added companies and industries seeking to improve the product or service they are selling or using. The availability of multi-polarised data and data from the [Global Monitoring Mode](#) will be of particular interest.

Preliminary processing of data at ground stations and by value-added companies includes calibration and validation of data, feature detection, texture analysis, reduction of speckle, image registration, geocoding and radiometric corrections. Techniques are continually being developed; particularly when data from a new sensor like ASAR becomes available. Data from all modes will be required for specific study sites over land, ocean and ice.

The availability of data from multiple incidence angles provides opportunities to develop new data processing techniques which may give new information on soil moisture, forest characteristics, geological structure, etc. Data will be required at all modes and polarisations for specific study sites covering a range of incidence angles.

#### Algorithm Development

Considerable ocean-related research is currently being undertaken by defence departments to monitor fishing boats and ships in busy traffic lanes. The likelihood of detecting ships and ship wakes will improve with the use of multi-polarised data. In the coastal zones, research is currently being undertaken to develop methods of mapping shorelines and the sea bottom in shallow areas. Some of these applications are now operational and will continue to expand with ASAR.

Much of the basic research on classification of ice types has been carried out, and good

algorithms are available. The value of multi-polarised data for ice type discrimination, especially during the ice formation and ice melting periods has been demonstrated using airborne systems. Data from both the [Alternating Polarisation](#) and Wide Swath (HH and VV) Modes available with ASAR will be utilised throughout the year for test areas in the Arctic Ocean.

To develop agricultural and vegetation products, multi-temporal data across the major crop and cover types, from which backscatter models of crop type, area, height and condition will be developed.

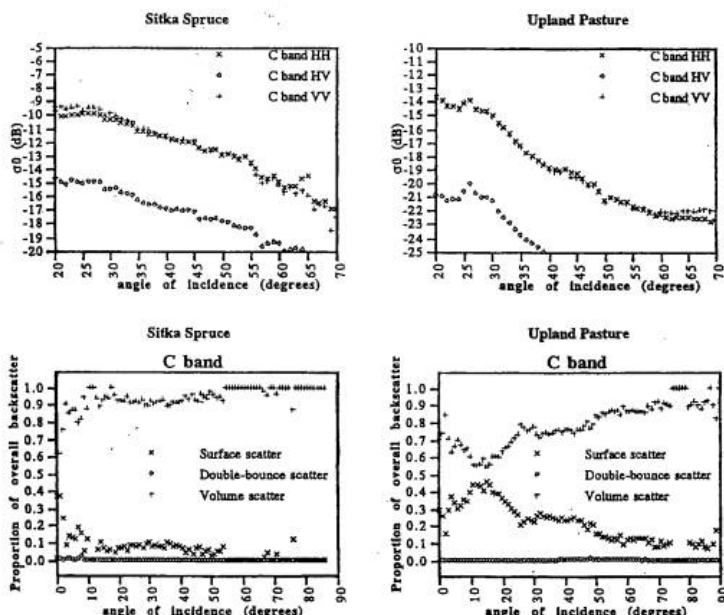


Figure 1.64 Backscatter of Sitka Spruce and Upland Pasture at Llyn Brianne, Wales.  
(Acknowledgement: Luckman and Baker, 1995.) Above: Polarisation and incidence angle effects on backscattering. Below: Relative contributions of surface, double-bounce and volume scattering.

Forest mapping is of particular interest in the humid tropics and other persistently cloudy areas. Important research topics include the classification of forest types, identification of burned forest, assessment of forest stress and monitoring of logging concessions. The availability of multi-polarised and variable incidence angle data from ASAR should improve on the accuracy of ERS results. For example, [figure 1.64](#) above shows how backscatter varies with VV, HH and HV polarisations across a range of incidence angles, for Sitka Spruce and Upland Pasture, and how these measurements have been used in a decomposition model to determine the relative contribution of surface, double-bounce and volume scattering mechanisms.

Many hydrological and agricultural applications use soil moisture data. Current research is

investigating the relationship between soil moisture and backscatter across a range of soil conditions (Le Toan et al, 1994). The use of multi-polarised and multi-incidence angle data should increase the accuracy of models by reducing the effect of surface roughness and vegetation. There is a strong interest in the use of Wide Swath and Global Monitoring Modes, because of the much improved temporal frequency of coverage (Zmuda et al, 1997). Snow melt and hydrology applications require information on snow cover distribution and snow water equivalent.

[Table 1.4](#) provides a list of the ASAR modes for applications being addressed by remote sensing science. In particular, it shows a very strong demand for Alternating Polarisation (AP) Mode. The other modes shown are: Image (IM) Mode and Wide Swath (WS) Mode.

Table 1.4 ASAR Modes for Remote Sensing Science

	Mode	Polarisation	Swath	Remarks
Agriculture	AP	VV/VH	IS4-6	Multi-temporal
Land cover	AP	VV/VH	IS4-6	Multi-temporal
Forestry	AP	VV/VH'	IS4-6	Multi-temporal and interferometry
Soil moisture	AP	VV/VH	IS1-3	High revisit
Snow melt	IM	HH or VV	IS3-7	High revisit
Hydrology	AP	VV/VH	IS2-5	High revisit
Geology	IM	HH	IS4-7	
Urban mapping	AP	HH/HV	IS3-7	
Inland water	IM	VV	IS2-4	
Oceanography	AP	VV/HH	IS2-6	
Coastal phenomena	AP	VV/HH	IS2-6	
Sea ice	AP	VV/HH	IS2-6	
Ship detection	AP	HH/HV	IS2-7	
Marine meteorology	AP	VV/HH	IS2-6	
Pollution monitoring	WS	VV		

### 1.1.6.1.2 Earth Science

The past decade has seen increasing public concern about the Earth, its environment and mankind's impact upon it. Global threats such as climate warming, stratospheric ozone depletion, tropospheric pollution and, more recently, regional events such as the very intense El Niño, the fires in S.E. Asia, and the floods in mid Europe and China, have left us more concerned than ever about the need to monitor and understand what is going on in the Earth's environment. There are many aspects of the complex evolving Earth System that we still do not understand.

These concerns have led to the establishment of the concept of a Global Climate Observing System (GCOS), including both space- and surface-based systems, to measure on a routine basis all major elements of the global climate system. [Table 1.5](#) below provides a summary of the principal observations required in support of GCOS.

Ultimately, the way in which our understanding of the Earth will improve, is by the

development of Earth System models which integrate into data from various sources. Earth observation from space is a critical tool in this task because of the unique synoptic view and high repeat frequency that it provides. Some of the earliest initiatives, including [METEOSAT](#) and SPOT, have already developed into long-term applications programmes integrated into regular operational use. The ERS satellites have made major contributions in areas as diverse as global and regional ocean and atmospheric science, sea ice, glaciology and snow cover investigations, land surface studies and the dynamics of the Earth's crust (seismology and volcanology). ENVISAT will provide new capabilities to monitor atmospheric composition and chemistry, with ASAR providing continuity and improvement upon the ocean, coastal zone and land cover monitoring capabilities of the ERS SAR instruments.

ASAR promises to be particularly important for modelling and monitoring changes in vegetation, oceans, ice sheets, snow and sea ice.

Table 1.5 Summary of GCOS principal observations

Planet Earth	PRINCIPAL SYSTEM	GCOS MISSIONS	PRINCIPAL OBSERVATIONS
			Cloud Amount
			Cloud Drop Size Distribution
			Surface Fluxes (heat, water)
	Global		Solar Irradiance
	Radiative		Surface Radiation Fluxes
	Properties		Earth Radiation Budget
GLOBAL			Multispectral Albedo
			Aerosols
			Ocean Colour
			Ocean Topography/Geoid
	Ocean		Sea Ice Cover
	Characteristics		Sea Surface Temperature
			Ocean Salinity
			Sea Surface Temperature
	Ocean		Ocean Wind Vectors/Seed
	Atmosphere		Sea Ice Cover (as tracer)
	Boundary		Ocean Wave Height Spectra
OCEANS			Atmospheric Surface Pressure
			Temperature Profile
			Cloud Clearing
	Atmospheric		Wind Profile
	Thermodynamics		Liquid Water/Ice
			Precipitation
			Humidity (profile/total)
			Constituents (total/profile)
	Atmospheric		Atmospheric Dynamics
	Composition		Ozone (total/profile)
ATMOSPHERE	& Chemistry		Aerosols (total/role)
			Vegetation Characteristics
	Land		Soil Moisture
	Atmosphere		Snow & Ice Cover
	Interaction		Land Surface Temperature
			Evaporation
			Vegetation Change
	Land		Land Use Change
LAND	Biosphere Climate Response		

The following applications are considered to be the major areas of use for ASAR data within Earth Sciences:

- Vegetation Monitoring
- Sea Ice Monitoring
- Glaciology and Snow Mapping
- Oceanography
- Coastal Zone Processes

These primary ASAR applications are described in more detail in the following sections.

[\*\*Table 1.6\*\*](#) below gives a summary of the ASAR modes mostly likely to meet the various needs of the Earth Sciences community.

Table 1.6 ASAR Modes for earth science

	Mode	Polarisation	Swath	Remarks
Vegetation maps	WS	VV or HH		Large area cover, multi-temporal
Soil moisture estimation	WS	VV		
Surface motion and subsidence	IM	VV or HH	IS2-5	Using interferometry
Oceanography	WS	HH		
Coastal phenomena	AP	VV/HH	IS2-6	
Marine meteorology	WS	VV		
Wind/Wave Models	WM	VV		
Glacier/ice sheet motion	IM	HH or VV	IS3-6	
Ice sheet extent and melt areas	WS	HH or VV		
Snow climatology	WS and GM	HH or VV		
Wetlands	WS	VV		
Sea Ice	WS and GM	HH		

### 1.1.6.1.3 Commercial Applications

The growing availability of Earth observation data is encouraging increased involvement and investment by value-added organisations and end-users. These include government departments with responsibility for agriculture, the environment, pollution control, meteorology, coastal protection, transport (especially coastal, marine and ice), fisheries and hazard management.

The following applications are considered to be the major areas for commercial exploitation of ASAR data:

- Ship Routing through Sea Ice
- Sea Ice Monitoring
- Ocean Monitoring
- Monitoring Oil Slicks
- Nowcasting of ocean fronts, eddies and current shears
- Agricultural Monitoring

- Forestry
- Hydrology and Water Management
- Flood Mapping

These commercial ASAR applications are described in more detail in following sections.

Table 1.7 ASAR Modes for commercial applications

	Mode	Polarisation	Swath	Remarks
Ship routing in sea ice				
Sea ice extent	WS	HH		
Ocean monitoring				
Surface features	AP	HH/HV	IS2-6	
Oil slicks	WS	VV		
Ship detection	APorIM	HH/HVHH	IS2-7, IS5-7	
Bathymetry	IM	HH	IS2-5	
Agricultural monitoring				
Crop area	AP	VV/VH or VV/HH	IS4	
Crop condition	IM	VV or HH	IS2-7	
Soil moisture	WS	VV		High repeat
Forestry				
Forest area/type/condition	AP	VV/VH	IS4-6	
Hydrology, and water management				
Runoff forecasts	WS	VV		High repeat
Flooding	WS	HH		High repeat
Oil and as industry				
Geological ma	IM	HH	IS4-7	
Natural hazards				
Earthquakes/volcanoes /land subsidence	IM	VV or HH	IS1-7	

### 1.1.6.2 Ocean Applications

The oceans not only provide valuable food and biophysical resources, they also serve as transportation routes, are crucially important in weather system formation and CO<sub>2</sub> storage, and are an important link in the Earth's hydrological balance. Understanding ocean dynamics is important for fish stock assessment, ship routing, predicting global circulation consequences of phenomena such as El Niño, forecasting and monitoring storms so as to reduce the impact of disaster on marine navigation, offshore exploration, and coastal settlements. Studies of ocean dynamics include wind and wave retrieval (direction, speed, height), mesoscale feature identification, bathymetry, water temperature, and ocean productivity.

Ocean feature analysis includes determining current strength and direction, amplitude and direction of surface winds, measuring sea surface temperatures, and exploring the dynamic relationship and influences between ocean and atmosphere. Knowledge of currents, wind speed, tides, storm surges and surface wave height can facilitate ship routing. Sea floor modelling supports waste disposal and resource extraction planning activities.

Ocean circulation patterns can be determined by the examination of mesoscale features such

---

as eddies, and surface gravity waves. This knowledge is used in global climate modelling, pollution monitoring, navigation and forecasting for offshore operations.

Remote sensing offers a number of different methods for acquiring information on the open ocean and coastal region. Scatterometers collect wind speed and direction information, altimeters measure wave height, and identify wind speed. SAR is sensitive to spatially varying surface [roughness](#) patterns caused by the interaction of the upper ocean with the atmosphere at the marine boundary layer, and scanning radiometers and [microwave](#) sounders collect sea surface temperature data. Buoy-collected information can be combined with [remote sensing](#) data to produce [image](#) maps displaying such things as hurricane structure with annotated wind direction and strength, and wave height. This information can be useful for offshore engineering activities, operational fisheries surveillance and storm forecast operations.

ASAR provides an option for acquiring information on the open ocean and coastal region. Several new SAR ocean applications can be expected to reach pre-operational or operational status during the lifetime of ENVISAT, notably in the areas of pollution monitoring, ship detection, and ocean feature nowcasting. This information can be useful for offshore engineering activities, operational fisheries surveillance, and storm forecast operations.

Some of the key areas of interest will include the following:

- Wave Characteristics
- Ocean Fronts
- Coastal Dynamics
- Oil Slicks and Ship Traffic

Wide area coverage is useful for monitoring and surveillance applications including ship traffic, fisheries monitoring, oil spill mapping, and ocean circulation mapping. Intermediate area coverage is useful for monitoring ship traffic, near-shore fisheries activities, oil spill mapping, and inter-tidal feature mapping. Small area coverage is useful for harbour traffic monitoring, aquaculture site location and small spill mapping.

#### 1.1.6.2.1 Wave Characteristics

For general sea-state information (waves, currents, winds), the data is usually time-sensitive; meaning that the information is only valuable if it is received while the conditions exist. ASAR data is expected to play a key role in the study of wave characteristics.

Certain wind speed conditions are necessary in order for the SAR to receive signal information from the ocean surface. At very low wind speeds (2 to 3m/s) the SAR is not sensitive enough to detect the ocean "clutter" and at very high wind speeds (greater than 14 m/s) the ocean [clutter](#) masks whatever surface features may be present. The principal scattering mechanism for ocean surface imaging is Bragg scattering, whereby the short waves on the ocean surface create spatially varying surface patterns. The [backscatter](#) intensity is a

---

function of the incidence angle and [radar](#) wavelength, as well as the sea state conditions at the time of imaging. The surface waves that lead to Bragg scattering are roughly equivalent to the wavelength used by ASAR and [RADARSAT](#) (5.3 cm). These short waves are generally formed in response to the wind stress at the upper ocean layer. Modulation in the short (surface) waves may be caused by long gravity waves, variable wind speed, and surface currents associated with upper ocean processes such as eddies, fronts and internal waves. These variations result in spatially variable [surface roughness](#) patterns which are detectable on SAR imagery, as shown in [figure 1.65](#).

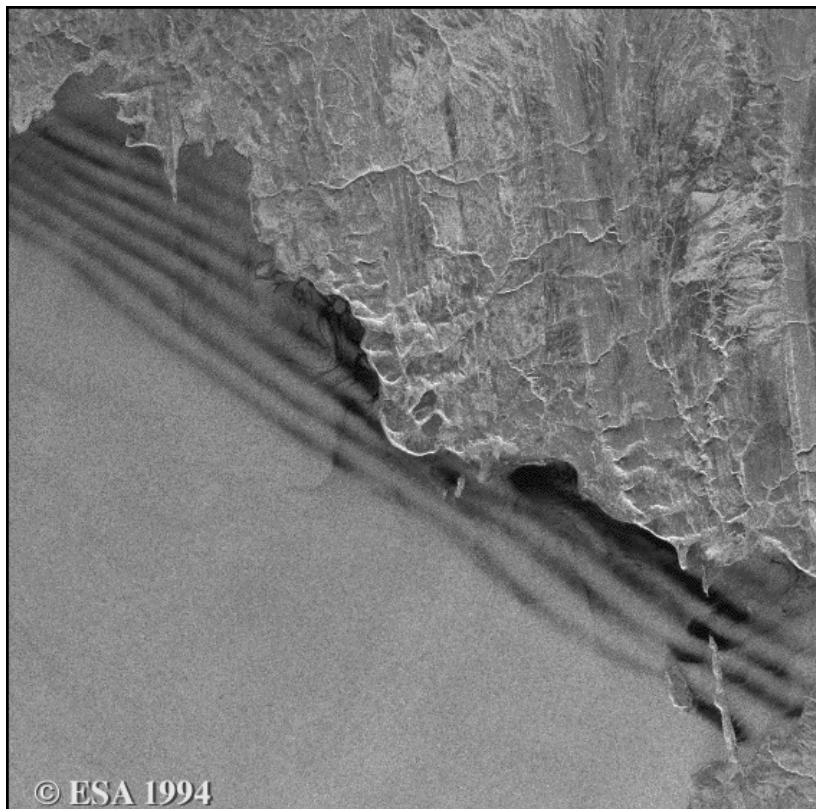


Figure 1.65 Atmospheric Waves (Copyright 1994, European Space Agency)

The SAR data for this image was taken by the European Space Agency's ERS-1 satellite on August 17, 1994. The scene shows the southern coast of Melville Island's Dundas Peninsula (in the Parry Islands of northern Canada), with north pointing about 30 degrees to the right.

Internal waves form at the interfaces between layers of different water density, which are associated with velocity shears (i.e., where the water above and below the interface is either moving in opposite directions or in the same direction at different speeds). Oscillations can occur if the water is displaced vertically resulting in internal waves. Internal waves in general occur on a variety of scales and are widespread phenomena in the oceans. The most important are those associated with tidal oscillations along continental margins. The internal waves are large enough to be detected by satellite imagery. In the image shown below, the

internal waves, are manifested on the ocean surface as a repeating curvilinear pattern of dark and light banding, a few kilometres east of the Strait of Gibraltar, where the Atlantic Ocean and Mediterranean Sea meet. Significant amounts of water move into the Mediterranean from the Atlantic during high tide and/or storm surges. (See [figure 1.66](#) )

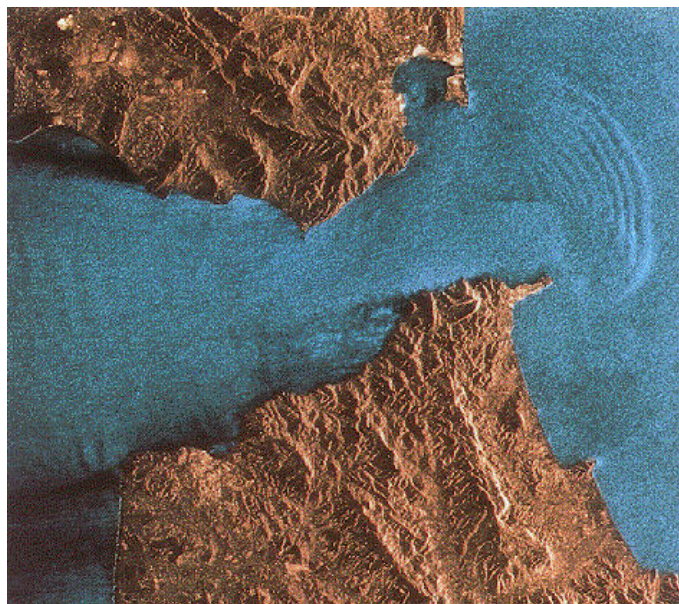


Figure 1.66 ERS 1 scene of internal waves: Strait of Gibraltar ( ESA 1992)

One ASAR study being proposed by Dr. Olga Lavrova, a senior scientist at the Space Research Institute Russian Academy of Sciences in Russia, plans to investigate circulation processes in the ocean and atmosphere (transformation of speed field, energy and momentum transfer) for the case of a stratified flow running against natural obstacles. The study will employ theoretical and experimental investigation of the spatial and temporal structure and dynamics of waves, vortexes, and vortex streets that emerge behind small islands, capes, rocks, and underwater rapids in the presence of currents in the ocean, and due to air flows on the shore and islands in the atmosphere. In addition to the study of forms and parameters of these lee structures, their relation to the speed of the run-against flow, the stratification of the media and the morphometry of the obstacle will be considered. This paves the way for the estimation of flow speed and media density stratification from space.

This project envisages development of numerical models based on the classical hydrodynamic theory of stratified fluid running against an obstacle. Process hydrodynamic characteristics retrieved from ASAR images will serve as input parameters for the models. The models will be used to retrieve current characteristics in ocean and wind fields in atmosphere above ocean from remote sensing data. Experimental tests based on the models will allow to observe in time and space the stages of circulation processes around natural obstacles to flows.

### 1.1.6.2.2 Ocean Fronts

There is increasing interest in the maritime community in high-precision nowcasting of ocean fronts, eddies and current shears. Important application areas could be: piloting of large transport ships, fisheries and fish farming, sea floor operations and autonomous underwater vehicles, acoustic sensors and acoustic communication. Also, ASAR imagery, together with data from other ENVISAT instruments such as MERIS and [AATSR](#), will significantly enhance the nowcasting of ocean features in coastal waters.

Open ocean applications include the study of large-scale ocean features manifested at the ocean surface by the interaction of wind-driven currents with the marine boundary layer. The principle scattering mechanism for ocean surface imaging is Bragg scattering, whereby the short waves create spatially varying surface patterns. The backscatter intensity is a function of the incidence angle and radar/wavelength, as well as the wind and wave condition at the time of imaging. For RADARSAT (5.3 cm wavelength), the surface waves that lead to Bragg scattering are roughly equivalent to its wavelength. These short waves are generally formed in response to the wind stress at the marine boundary layer. Modulation in the short waves may be caused by long gravity waves, variable wind speed, and surface currents associated with upper ocean processes such as eddies, fronts, and internal waves. These variations result in spatially variable surface roughness pattern which is imaged by the SAR.

### 1.1.6.2.3 Coastal Dynamics



Figure 1.67 RADARSAT image of coastal region (courtesy Radarsat International)

Coastlines are environmentally sensitive interfaces between the ocean and the land, and respond to changes brought about by economic development and changing land-use patterns. Often coastlines are biologically diverse inter-tidal zones and can also be highly urbanised. With over 60% of the world's population living close to the ocean, the coastal zone is a region subject to increasing stress from human activity. Government agencies concerned with the impact of human activities in this region need new data sources with which to monitor such diverse changes as coastal erosion, loss of natural habitat, urbanisation, effluents and

---

offshore pollution. Many of the dynamics of the open ocean and changes in the coastal region can be mapped and monitored using remote sensing techniques.

Coastal zone monitoring implies observation of the interaction of oceanographic and atmospheric phenomena with human activities in the near-shore region. The key issues include the delineation of the coastline, defining areas of erosion and sedimentation, mapping the inter-tidal vegetation, and identifying areas of human settlement and accompanying activities. The coastal zone is an environmentally sensitive region subject to increasing stress from economic development, and government agencies concerned with the impact of human activities in the near-shore region are looking for new data sources with which to monitor this region.

An excellent coastal zone application of radar is aquaculture site monitoring. These man-made structures provide higher signal returns than the surrounding water.

The main areas of interest in the coastal zone are changes in sea level and in suspended sediment, carbon, and nutrients. Activities are being undertaken, at a range of scales, using diverse data sets for ocean measurements, land use, vegetation and coastal morphology. There are numerous local, national, regional, and international programmes involved in the coastal zone. Major programmes include the International Oceanographic Commission, the MAST programme organised by the EC, and the IGBP Land-Ocean Interactions in the Coastal Zone (LOICZ) programme to determine how changes in the Earth's system are affecting coastal zones and altering their role in global cycles.

ASAR data will certainly be used within the range of activities in the coastal zone. Examples of current use of SAR data in the coastal zone include: topographic maps of tidal flats, sea bed topography, sediment distribution in The Netherlands, an inter-tidal digital terrain model of the Wash in the UK, and coastal erosion in French Guiana.

The availability of multi-polarised data and data at different incidence angles, or at a specific incidence angle, should improve the accuracy and quality of products for many applications. The Wide Swath (WS) and Global Monitoring (GM) Modes will provide data that is not currently available, for applications requiring large area coverage.

For example, a new conceptual scheme in coastal research being proposed by Dr. Francis Gohin, a Physical Oceanographer at IFREMER in France, is to deploy optical instruments, combined with airborne and spaceborne spectral and SAR imagers like ASAR, to provide an up-to-date means of observing the narrow bands of red tides. By integrating colour data obtained from aircraft and satellites in classical data sets, a 3-D numerical model will provide estimation of the chlorophyll content and the suspended matter concentration on the continental shelf of the Bay of Biscay. Remote sensing methods can be used in the validation of such models. In return, these models help to include passive remote sensing data, poorly sampled in time because of clouds, in a regular set of simulations.

In addition, a study being proposed by researcher Samuray Elitas M.Sc. of the TUBITAK Marmara Research centre in Turkey, envisions ASAR data being used to analyse coastal regions there. As ASAR and multicolour MERIS images for the project area arrive, the most

recent and/or simultaneous pollution mapping of the Marmara Sea will be evaluated by relating other geographical information data like bathymetrical information and land usage information. Consequently, geographical information systems for the Marmara marine environment, supported by ASAR and MERIS images will be established as a whole database.

The effects of bathymetry are visible in near-shore regions under light wind conditions. Small incidence angles are better suited to imaging inter-tidal features such as mudflats, shoals and sandbars.

Large incidence angles provide a larger radar backscatter contrast which improves the discrimination of the water/land boundary. The smooth surface of a water body acts as a specular reflector in contrast to the diffuse scattering which occurs over land. Open water surfaces will appear dark in comparison to the brighter returns from land. Shoreline detection and the identification of areas of erosion or sedimentation can be improved by acquiring multi-temporal data with different look directions (e.g., ascending or descending).

#### 1.1.6.2.4 Oil Slicks and ShipTraffic

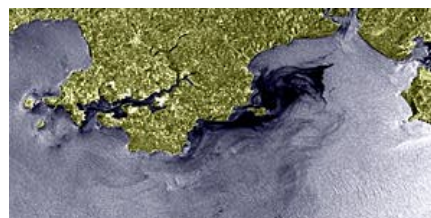


Figure 1.68 RADARSAT image of coastal oil spill, Wales (Courtesy CCRS)

Oil spills can destroy marine life as well as damage habitat for land animals and humans. The majority of marine oil spills result from ships emptying their bilge tanks before or after entering port. Large area oil spills result from tanker ruptures or collisions with reefs, rocky shoals, or other ships. These spills are usually spectacular in the extent of their environmental damage and generate wide spread media coverage. Routine surveillance of shipping routes and coastal areas is necessary to enforce maritime pollution laws and identify offenders.

Remote sensing offers the advantage of being able to observe events in remote and often inaccessible areas. For example, oil spills from ruptured pipelines may go unchecked for a period of time because of uncertainty of the exact location of the spill, and limited knowledge of the extent of the spill. Remote sensing can be used to both detect and monitor spills.

For ocean spills, remote sensing data can provide information on the rate and direction of oil movement through multi-temporal imaging and input to drift prediction modelling, and may assist in targeting cleanup and control efforts. Remote sensing devices used include infrared video and photography from airborne platforms, thermal infrared imaging, airborne laser fluourosensors, airborne and spaceborne optical sensors, as well as airborne and spaceborne SAR. SAR sensors have an advantage over optical sensors in that they can provide data under poor weather conditions and during darkness. Users of remotely sensed data for oil spill applications include the Coast Guard, national environmental protection agencies and departments, oil companies, shipping industry, insurance industry, fishing industry, national departments of fisheries and oceans, and departments of defence.

Oil slicks and natural surfactants are imaged through the localised suppression of Bragg scale waves. Under calm conditions, natural surfactants may form over large areas of the ocean, along current boundaries, and in areas of upwelling. The accumulation of natural surfactants at these boundaries can delineate the general circulation pattern and are visible on the radar image as curvilinear features with a darker tone than the surrounding ocean. Oil spills also have a darker tone with respect to the surrounding ocean background. The detection of an oil spill is strongly dependent upon the wind speed. At wind speeds greater than 10 m/s, the slick will be broken up and dispersed, making it difficult to detect. Another factor that can play a role in the successful detection of an oil spill is the difficulty in distinguishing between a natural surfactant and an oil spill. Multi-temporal data and ancillary information can help to discriminate between the two phenomena. Wind shadows near land, regions of low wind speed, and grease ice can also be mistaken for oil spills and ancillary data (or an experienced user) is necessary to distinguish between these features and a spill.

Oil companies are now actively using ERS SAR imagery in their search for new oil fields (oil seepage from the ocean floor is an important indicator). The ASAR Wide Swath Mode in VV polarisation will be a unique instrument for detection of oil slicks on the ocean surface, offering a very good combination of wide coverage and radiometric quality. The fourfold increase in coverage capability compared to ERS will make routine services feasible also at lower latitudes.

Small incidence angles are optimum for oil spill detection. Detection will also depend on the spill size, sea state conditions and image resolution.

At the Norwegian Computing Centre, senior research scientist Anne Solberg proposes to modify algorithms for automatic detection of oil spills originally developed for ERS SAR images, for use with ASAR images. Methods have been developed for automatic detection of oil spills in ERS images as part of the Norwegian oil spill project and the European Union project ENVISYS. ASAR Wide Swath data will have a different pixel size and a different radiometric resolution than the ERS SAR images, and these will be incorporated in the detection and classification algorithms. The new project will use ASAR data from four test sites with a high probability of observing oil slicks: the North Sea, the English Channel, and two sites in the Mediterranean.

The image shown in [figure 1.69](#) below, taken over the "Flemish Cap," an area in the Atlantic Ocean south east of the coast of Newfoundland Canada, shows two natural slicks (A) and five ships. Two of the ships can be identified to the east of the slicks and three are clustered to the south. Wakes are clearly visible behind the three ships at the bottom of the image. This information can be used to determine their speed and direction of travel.



© CSA / ASC, 1996

Figure 1.69 RADARSAT image of 'Flemish Cap,' east coast of Canada (courtesy of CCRS)

With larger incidence angles, the ocean background clutter effects are reduced, improving the detection of ships, coastline and ice edges. For example, a ship is a bright point target against the ocean background clutter and can be detected using image thresholding techniques. However, as the ocean clutter increases with increasing wind speeds, ship detection becomes more difficult. At wind speeds greater than 10 m/s it is difficult to detect small fishing vessels. This relationship with wind speed is a critical factor for ship detection as well as oil spill mapping and feature detection. As the wind speeds increase, the radar cross-section of the ocean increases, reducing the contrast between the feature of interest and the surrounding ocean.

Ship detection is a good example of the operational role of radar. A wide range of ship sizes

---

may be detected under a variety of sea-state conditions. Radar can infer ship size, and if a wake is present, its speed and direction of travel. It should be noted that an HH polarisation is less sensitive to wake detection and, in studies to date, wakes are infrequently detected. Potential users of this information include agencies who monitor ship traffic, authorities responsible for sovereignty and fisheries surveillance, as well as customs and excise agencies charged with stopping illegal smuggling activities. (See [figure 1.70](#) )



© ESA 1992

Figure 1.70 Ship Wake. ESA image courtesy of the Alaska SAR Facility (copyright ESA)

Large incidence angles are optimum for ship target detection. Detection depends on ship size and type, heading with respect to look angles, and sea state conditions at the time of imaging.

#### 1.1.6.3 Land Applications



Figure 1.71 Multi-temporal, artificially coloured image ERS-1 SAR image, Germany-Darmstadt and Odenwald, Nov.11, 1991 (Copyright ESA 1991)

Although the terms land cover and land use are often used interchangeably, their actual meanings are quite distinct. Land cover refers to the surface cover on the ground, whether vegetation, urban infrastructure, water, bare soil or other. Identifying, delineating and mapping land cover is important for global monitoring studies, resource management, and planning activities. Identification of land cover establishes the baseline from which monitoring activities (change detection) can be performed, and provides the ground cover information for baseline thematic maps.

Land use refers to the purpose the land serves, for example, recreation, wildlife habitat, or agriculture. Land use applications involve both baseline mapping and subsequent monitoring, since timely information is required to know what current quantity of land is in what type of use and to identify the land use changes from year to year. This knowledge will help develop strategies to balance conservation, conflicting uses, and developmental pressures. Issues driving land use studies include the removal or disturbance of productive land, urban encroachment, and depletion of forests.

It is important to distinguish this difference between land cover and land use, and the information that can be ascertained from each. The properties measured with remote sensing techniques relate to land cover, from which land use can be inferred, particularly with ancillary data or a priori knowledge.

Resource managers involved in parks, oil, timber, and mining companies, are concerned with both land use and land cover, as are local resource inventory or natural resource agencies.

---

Changes in land cover will be examined by environmental monitoring researchers, conservation authorities, and departments of municipal affairs, with interests varying from tax assessment to reconnaissance vegetation mapping. Governments are also concerned with the general protection of national resources, and become involved in publicly sensitive activities involving land use conflicts.

[C-band Synthetic Aperture Radar \(SAR\)](#) satellites sensors, such as [ERS-1, ERS-2](#) and [ASAR](#), allow the agricultural industry to acquire imagery anytime, using [microwave energy 1.1.2.1.](#) to penetrate darkness, clouds, rain or haze ( See "[Scientific Background" 1.1.2.](#) ). As such, they have become an invaluable source of information in mapping the aftermath of natural disasters like hail storms, floods and hurricanes.

As a result of observing the land surface with the [ERS Synthetic Aperture Radar \(SAR\)](#) sensors a large number of land applications has emerged, several based on important developments which have been made in the field of [SAR Interferometry 1.1.5.4.](#) . SAR data are being used for agricultural monitoring, forest mapping, geological exploration and flood mapping, while SAR Interferometry measurements of [topography](#) and small topographic changes are making major contributions to environmental risk assessment from earthquakes and land [subsidence](#). The Advanced Synthetic Aperture Radar (ASAR) sensor will be used for numerous land-based applications which include:

- Global Vegetation Monitoring
- Forestry
- Geology and Topography
- Agriculture
- Natural Hazards
- Flooding, Hydrology and Water Management
- Urban Studies

#### 1.1.6.3.1 Global Vegetation Monitoring

Land cover is defined as the observed physical cover, including vegetation and human constructions, of the Earth's surface.

For many ecological studies, there is a need for current information on the distribution and amount of vegetation. This need has not been fully addressed by a quarter century of spaceborne remote sensing systems operating in the visible and near-infrared region of the [electromagnetic spectrum 1.1.2.1.](#) . Collection of visible/near-infrared imagery over ecologically important regions on a continuous basis is often limited by cloud cover, particularly in tropical and boreal biomes. However, radar data can be acquired at any time since imagery acquisition is not hindered by atmospheric conditions or darkness ( See "[Scientific Background" 1.1.2.](#) ).

Radar data can be used in applications supporting land cover delineation, base mapping and updating, and environmental monitoring. In these applications, radar data is used as a tool for distinguishing differences in surface [roughness](#), moisture content, and geometric shape associated with different land uses and covers, which in turn allows the delineation and

identification of land cover types and related land use and cultural features. By using the [backscatter models 1.1.2.4.1.](#) of crop types, area, height and condition changes, through the application of [multitemporal imagery](#), changes in land use and land cover over time can be assessed.

The image shown in [figure 1.72](#) below provides an example of 25 km resolution global backscatter data from the [ERS](#) Scatterometer, which contains information on vegetation type, standing biomass and active vegetation. In comparison, the Advanced Synthetic Aperture Radar (ASAR) [Global Monitoring Mode \(GM\)](#) will provide the much improved [spatial resolution 1.1.2.2.1.](#) of 1 km, similar to that of [AVHRR](#).

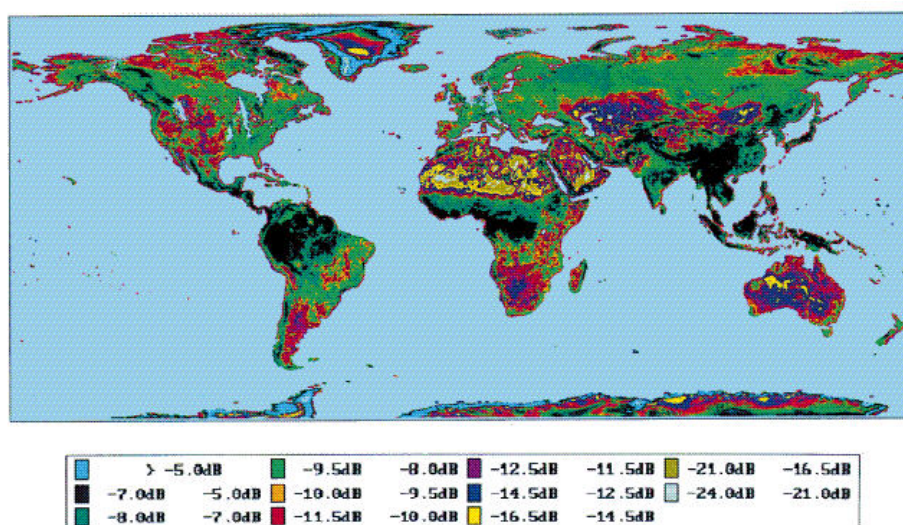


Figure 1.72 Global backscatter data collected by the ERS Scatterometer in August 1993, showing major vegetation types and morphological units (i.e. tropical rain forest, savannah, deserts, mountain ranges, tundra). Acknowledgement: E. Mougin, P. Frison, CESR, Toulouse; Y. Kerr, LERTS/CESBIO, Toulouse, France.

One of the the main aims of global vegetation mapping is to characterise the function of biomes within the climate change models, and to quantify the extent to which changes in global vegetation distribution may affect the climate. Climate data are the main inputs for these models. When radar data are acquired for the quantitative study of land use and land cover, it is important that data are calibrated, since this allows image [brightness](#) values to be more directly related to target [backscatter](#). When radar data are acquired over a number of time periods, for the purposes of monitoring change for land use and land cover applications, it is again important that data are calibrated. Image calibration for change detection ensures that any change in the image are a result of a change in the target and not from a change in the sensor. [ASAR](#) products will be used, along with other remote sensing data, for initialising, parameterising, and calibrating models, on a global and regional scale, and for the monitoring of changes in vegetation type and status. ASAR data and products developed from the [Global Monitoring \(GM\)](#) and [Wide Swath Modes \(WS\)](#) are of particular interest.

### 1.1.6.3.2 Forestry

Accurate and consistent mapping is essential for the successful management of forests. Global forests provide invaluable benefits and resources, both of an ecological and economic nature, to the world's population. Not only do forests provide a supply of fuel and building material, but they also retain soil, regulate run-off, minimise the siltation of water, and provide fruits, nuts, tree extracts and medicinal plants. As the large proportion of the Earth's surface is occupied by forests, which are continually changing, a management tool is required that is capable both of covering large areas of the Earth's surface, as well as revisiting those areas with some frequency.

The ability of spaceborne radar sensors to image the globe in a short period of time, unimpaired by such atmospheric effects as light rain and cloud, is well known. ( See section entitled "[Scientific Background](#)" [1.1.2](#) ). As with other applications, this ability is well-suited to forestry applications, as a large proportion of the world's forests are found in tropical areas where there is cloud cover for much of the year or at high latitudes where there are long periods of darkness during the winter months. By using [multi-temporal](#) analysis and [interferometric](#) techniques, [ERS](#) data are beginning to be used in operational mapping programmes.

The image shown in [figure 1.73](#) below gives an indication of the deforestation that is occurring in the Brazil.



Figure 1.73 Brazil Deforestation. This artificially coloured ERS-1 SAR image, covering an area 75 km x 75 km, shows the Teles Pires river in Brazil (Mato Grosso State). A regular pattern of deforestation is clearly seen in the rectangular patches of destroyed forest extending over areas as large as 20 kilometres ( copyright ESA 1992 )

Radar is particularly effective for the delineation of burned areas because of its sensitivity to differences in structure and moisture content. ( See "[Scientific Background](#)" [1.1.2](#) ). Several months after a forest fire, burnt forest areas dry out and leaves and small twigs drop from the trees which results in a contrast in structure and moisture content between burnt and unaffected areas. On radar imagery, this produces a contrast in backscatter, where the burnt areas appear darker than the unaffected forested areas.

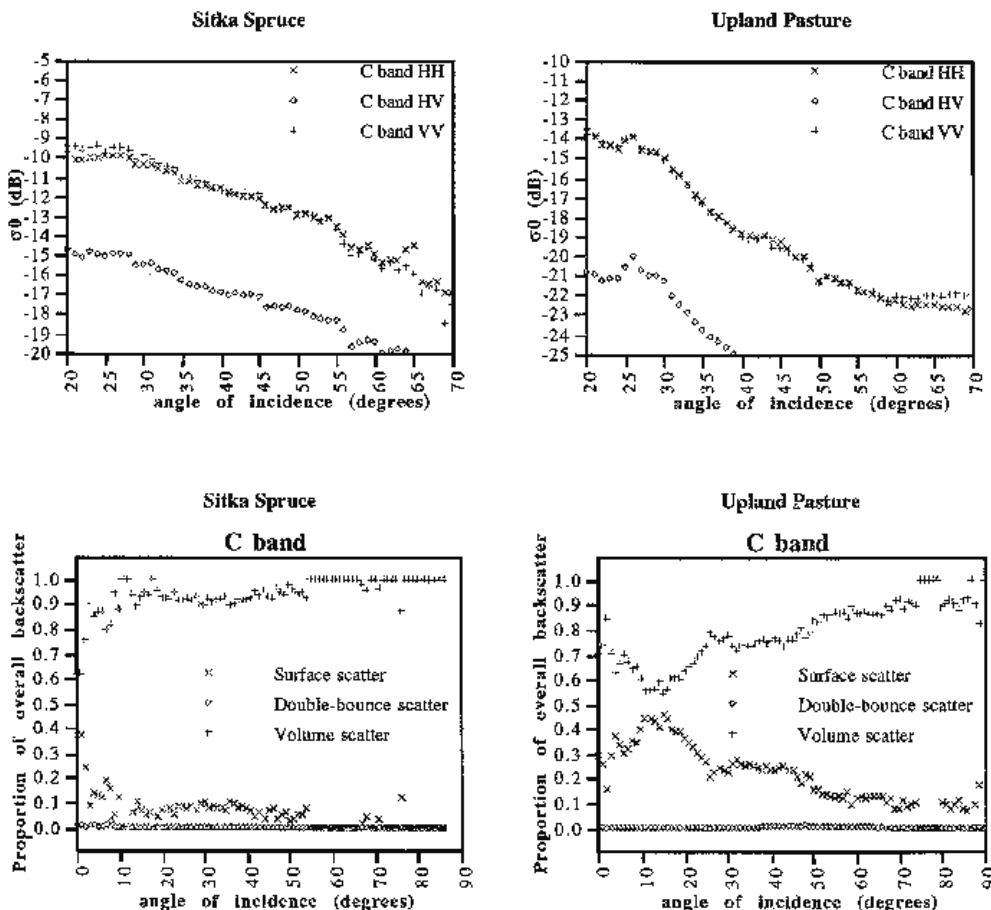
The ability of [C-band](#) radar to discriminate between some forest types has been shown in a range of forest environments. In areas of mixed deciduous and coniferous forests, separation of general forest type is accomplished through the use of [multitemporal](#) data; the leaf-on and leaf-off conditions of deciduous species results in a seasonal change in [backscatter](#) which contrasts with that of the coniferous species which do not experience leaf-off. It is important to note that in order to acquire useful information on general forest type, using radar satellites, stands will have to be large and of uniform composition. Species differentiation is more difficult in general at [microwave frequencies](#) [1.1.2.1](#), then with optical data because of overlap in signatures between species.

The higher [incidence angles](#) [1.1.5.2](#), and [dual polarisation](#) [1.1.5.1](#), data from [ASAR](#) will improve the potential for forestry applications. Use of low incidence angles enhances the sensitivity to biomass, whereas the use of high incidence angles improves mapping of deforestation. Dual polarisation will improve discrimination of forest types.

The graphs in [figure 1.74](#) below show how [backscatter](#) [1.1.2.1.2](#), varies with [VV](#), [HH](#) and [HV polarisations](#) across a range of [incidence angles](#), for Sitka Spruce and Upland Pasture, and how these measurements have been used in a decomposition model to determine the relative contribution of surface, double-bounce and volume scattering mechanisms.( See "[Scattering Mechanisms](#)" [1.7](#) in the section entitled "[Scientific Background](#)" [1.1.2](#) ).

In the two upper graphs shown below polarisation and incidence angle effects on backscattering are shown, and in the bottom two graphs relative contributions of surface, double-bounce and volume scattering are shown.

Figure 1.74 Backscatter of Sitka Spruce and Upland Pasture at Llyn Brianne, Wales.  
(Acknowledgement: Luckman and Baker, 1995).



The multipolarisation, multi-swath modes of [ASAR](#) ( see section entitled "["Principles of Measurement" 1.1.3.](#)" ) offer a greatly enhanced capability for forest assessment over any previous spaceborne SAR mission. New research being proposed brings together expertise in SAR data, software, ecology, and forestry, as well as a long history of ground data. The application of ASAR to the quantitative assessment of forest characteristics such as yield, species, and phenology will be demonstrated for tropical, boreal and temperate forests.

### 1.1.6.3.3 Geology and Topography

Traditionally geological information for mapping at local and regional scales has been acquired through field work by qualified geoscientists. Optical remote sensing from air- and spaceborne platforms provide a synoptic view of the terrain which allows geological information to be collected over a larger region. Geological information from optical sensors are however, hindered by cloud cover, identification of features restricted by illumination conditions, and the delineation of geological structure dependent on the angle and elevation of the sun. Radar remote sensing has proven to be an effective tool for the extraction of geological information, unhindered by external illumination and weather conditions. ( [See "Scientific Background" 1.1.2.](#) ).

The [side-looking configuration](#) of spaceborne [Synthetic Aperture Radar \(SARs\)](#) [1.1.2.3.](#) highlights relief, which assists in [topographic](#) mapping for [terrain analysis](#). When relief information provided by radar is combined with optical data, an image is created that provides valuable terrain information. The use of shallow [incidence angles](#) produces a shading effect or [shadowing](#) which can emphasise even subtle slopes in the landscape. These are often attributable to underlying geological units and structures.

The image in [figure 1.75](#) below, shows excellent imaging of faults and contrasts, using enhanced ERS-1 (SAR) imagery.

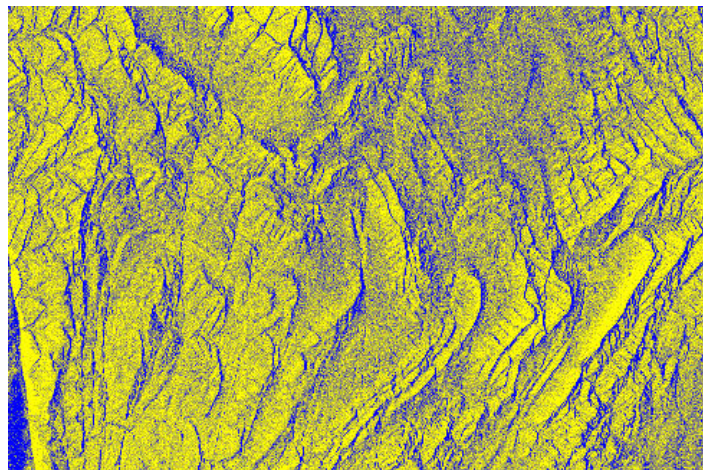


Figure 1.75 ERS-1 SAR enhanced and enlarged image of Penzhinskaya Guba, North Kamchatka, Russia. ( Image created by Dr. William Harbert of the Geophysics Department, University of Pittsburgh )

Geological mapping with SAR data has become well established and a number of organisations offer a commercial service for mapping structure, but the effect of [layover](#) in hilly terrain prevents widespread use of the data. ASAR [Image Mode \(IM\)](#) products, with high [incidence angles](#) will be of particular interest to reduce terrain distortions. The [Alternating Polarisation Mode \(AP\)](#) products may be of value for texture analysis in arid areas. [Wide Swath Mode \(WS\)](#) products will be useful for looking at regional and continental geological structures.

Other remotely sensed data can be integrated with SAR data to provide additional information for an imaged area, thus creating an enhanced image map for interpretation. Another valuable combination is with the varied data sets generated by modern geophysical surveying, which is widespread in mineral exploration. Combined with radar imagery, it provides a means of correlating, or at least locating, inferred subsurface mineral horizons, structural features, or lithologies with respect to surface relief.

In the creation of the image shown in [figure 1.76](#) below, topographic phase recovery from

stacked ERS [SAR interferometry 1.1.5.4.](#), and a low resolution [Digital Elevation Model \(DEM\)](#) were used.

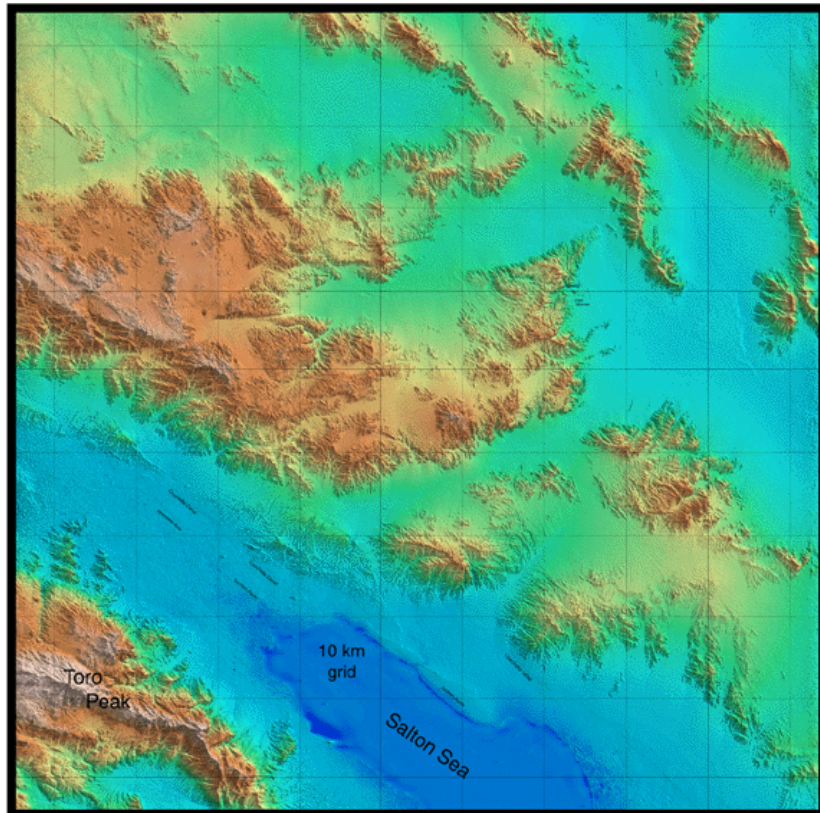


Figure 1.76 Interferogram created by using 25 ERS SAR images from an area of Southern California containing 2700 m of relief; compared with the topography measured by the Shuttle Radar Topography Mission. Fringes from two major earthquakes and a seismic slip on the San Andreas Fault are clearly isolated. ( Image created by David T. Sandwell and Lydie Sichoux at the Institute of Geophysics and Planetary Physics, Scripps Institution of Oceanography, La Jolla, CA

Radar has also proven to be a promising tool for mineral and hydrocarbon exploration. Certain types of mineralization and hydrocarbon resources are often associated with specific geological structures thus, the [mapping](#) of these structures when topographically expressed can assist in the identification of areas of high mineral and hydrocarbon potential. Often radar data are merged with geophysical data. The radar data allows the [delineation](#) of topographically expressed structures, while the geophysical data aids in the identification of strong magnetic signature. Resulting composites show the correlation between geological structure and magnetic anomalies which aid in the planning of detailed ground surveys.

#### 1.1.6.3.4 Agriculture

The use of Earth-observation satellite data can provide agriculture and its related industries, such as food and insurance, with cost-effective methods for wide-scale and localised monitoring of crop output and condition factors. Optical and radar satellite imagery can be used as a tool for recording important information that is needed before and during the growing season. The information derived from this imagery can be of particular importance to individuals and organisations in the agriculture industry including farmers, agricultural co-operatives, agribusiness and food companies.

Earth-observation data can provide:

- Soil moisture detection and monitoring
- Crop studies and acreage determination
- Hail, flood, and hurricane damage mapping

The ERS programme has demonstrated the ability of satellite radars, independently of weather conditions, to identify crops, detect soil moisture and monitor seasonal land cover changes. [Multi-temporal](#) techniques are used, which involve the collection and analysis of SAR data on a series of different dates over the period of interest. [Interferometric coherence](#) has also been used to improve land cover discrimination.

**Soil Moisture and Detection:**

Soil moisture variability is an important factor in many agricultural business processes. It is a valuable input into crop yield prediction models and helps in the determination of plant stress zones for the management of agricultural inputs. Radar imagery can be used to create moisture maps and for irrigation management, as well as to monitor the effectiveness of central pivot irrigation systems. A further use in this area involves developing moisture level base maps for monitoring regions of high flood probability.

The [ASAR Wide Swath \(WS\)](#) and [Global Monitoring \(GM\)](#) Modes will be of most interest to soil moisture and large area vegetation mapping.

**Crop studies and acreage determination**

Satellite imagery is a valuable tool in determining varying levels of crop vigour within fields or agricultural management zones. Plant stress can be monitored and growth inputs applied in a more timely and efficient manner when the different areas of stress are available in a single image to the farm manager. Satellite imagery can therefore increase the efficiency of crop scouting practices by more precisely targeting areas that need to be examined or tested. Imagery can be used to produce vigour maps that can be linked to geospatial information and allow the farmer to determine the relative health of all planted areas at one time.

An increasing aspect of precision farming is the management of agricultural zones within

fields. Soil type, crop vigour, and irrigation levels, as revealed by Earth-observation data, can be delivered to the customer and input into field management [GIS](#) to aid in the efficient application of fertiliser and other agricultural input chemicals.

[ERS](#) data are now being used operationally within major European programmes concerned with agricultural statistics (MARS STAT) and the control of agricultural subsidies (MARS PAC). Within MARS STAT the use of ERS data has improved the estimates of crop area early in the crop growing season. ERS data are used as a substitute for optical data in the MARS PAC control activity when cloudy conditions are encountered at key times during the crop growing season.

[Figure 1.77](#) below shows the use of [multi-temporal](#) ERS data for mapping the areas using different rice cropping systems in the Mekong Delta of Vietnam.

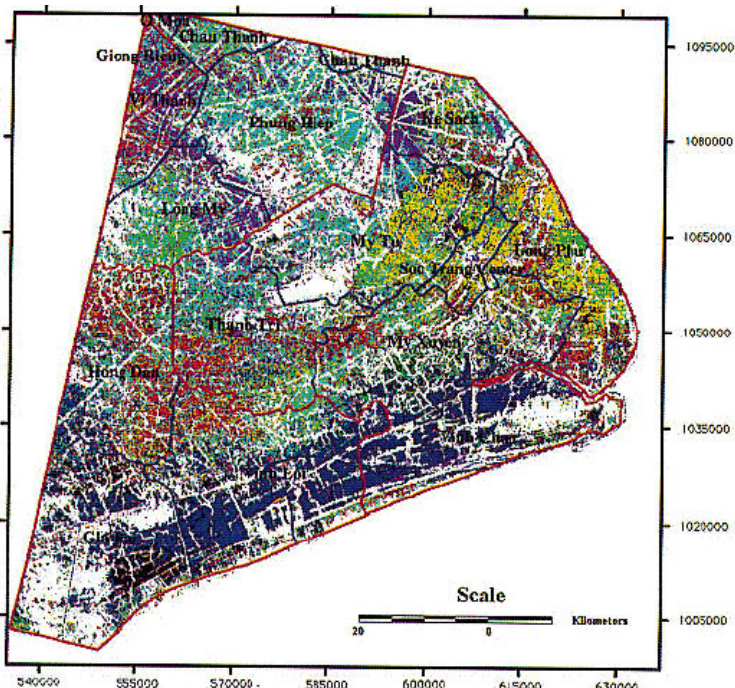


Figure 1.77 Map of different rice cropping systems in the Mekong Delta, derived from classification of seven ERS SAR images acquired over the period May to December 1996.  
 (Acknowledgement: Balababa et al. 1997).

**Legend**

	Non-ice
	Single cropped
	Rainfed: He Thu - Mua (1)
	Rainfed: He Thu - Mua (2)
	Irrigated: Dong Xuan - He Thu (2)
	Rainfed: He Thu - Mua (3)
	Irrigated: Dong Xuan - He Thu (1)
	Forest / Roads / Canals / Shrimp area
	District boundary
	Province boundary



ASAR [Image Mode \(IM\)](#) offers continuity for agricultural applications, enhanced by the ability of variable [incidence angles](#). The [Alternating Polarisation Mode \(AP\)](#) will greatly improve crop classification.

#### 1.1.6.3.5 Natural Hazards

A number of areas of study relating to natural hazards will utilise [ASAR](#) data. These include:

- [volcanic activity](#)
- [earthquakes](#)
- [land subsidence](#)

Volcanic Activity:

The Afar triangle, located in the Republic of Djibouti of East Africa and shown in the image below, is the only place on Earth where the mid-ocean ridge is visible as a rift in an arid desert. It is thus a uniquely privileged site for long-term study by radar [interferometry](#).

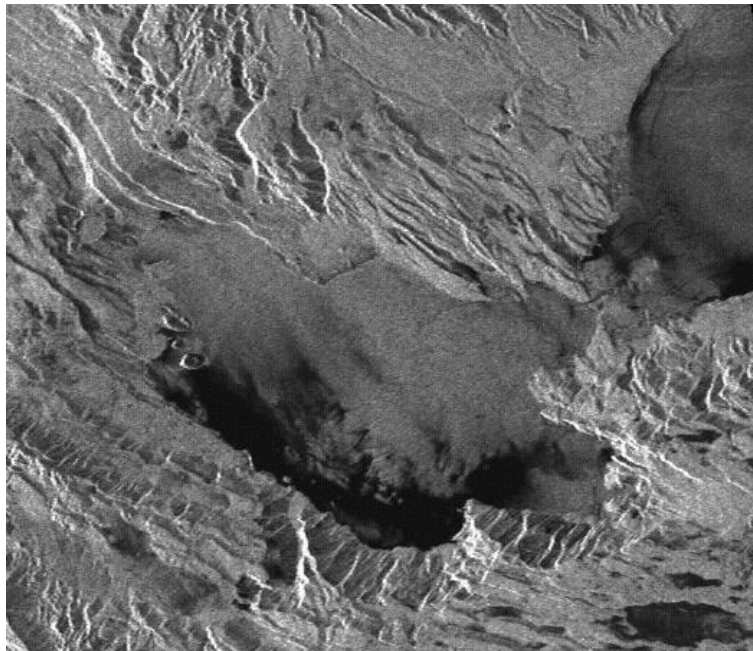


Figure 1.78 ERS-2 Image of the Afar Triangle in East Africa

The area shown above has experienced damage in this century by volcanic eruptions and large earthquakes. To evaluate the risk of such events in the future, it is essential to understand the geophysical signatures recorded in the topographic relief and the deformation field. The [ASAR](#) instrument can measure both of these signals with [SAR interferometry 1.1.5.4.](#). The [imaging geometry](#), surface conditions, and climate are optimal for SAR interferometry.

#### Earthquakes:

To study seismically active fault systems, it is important to measure both the long-term rate of deformation averaged over several seismic cycles and the short-term deformation associated with the seismic activity along individual faults. The first type of measurement requires accurate topographic maps to quantify the cumulative displacement of Quaternary surfaces and geomorphic structures, such as alluvial fans or glacial moraines. The second type of measurements requires the capacity of estimating subtle displacements of the ground at the millimetre level of precision over short time intervals. With the advent of spaceborne radar systems, such as [ERS-1, ERS-2](#), and now [ASAR](#), the technique of [SAR interferometry 1.1.5.4.](#) is becoming a new tool for active tectonics by providing both mm-precision surface change maps spanning periods of days to years and m-precision, high resolution topographic maps for measuring crustal strain accumulated over longer periods of time.

A strong earthquake shook northwestern Turkey, levelling buildings, and cutting power and phone lines. The quake had a magnitude of 7.8, making it nearly as powerful as the 7.9-magnitude San Francisco quake, which killed 700 people in 1906. The [digital elevation](#)

model (DEM) of this area, shown below, was produced by interferometric analysis of synthetic aperture radar (SAR) data from the ESA ERS-1 and ERS-2 satellites . Pairs of SAR images from tandem acquisitions, with temporal separation of one day, were processed separately to produce a height map in ground range coordinates. Then the height maps were projected into UTM coordinates. Final elevations in the DEM are the average of the overlapping SAR interferometric height maps.

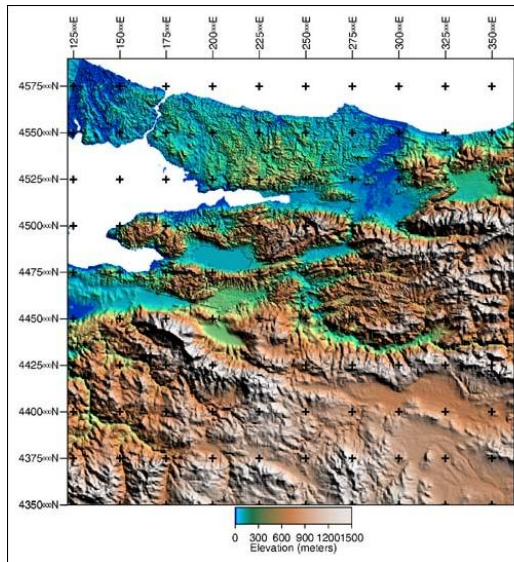


Figure 1.79 Izmit Earthquake digital Elevation Model from ERS SAR Interferometry ERS data ESA (1995,1996,1999),DEM Eric Fielding, Oxford (1999) Shaded relief image of interferometric DEM from three descending and one ascending ERS SAR Tandem pairs, with GTOPO30 filling in gaps.

In the ERS-1 SAR interferometric map below, created at the Jet Propulsion Laboratories (JPL), the post seismic surface movements following the Landers 1992 earthquake are clearly evident Ref.[1.29].

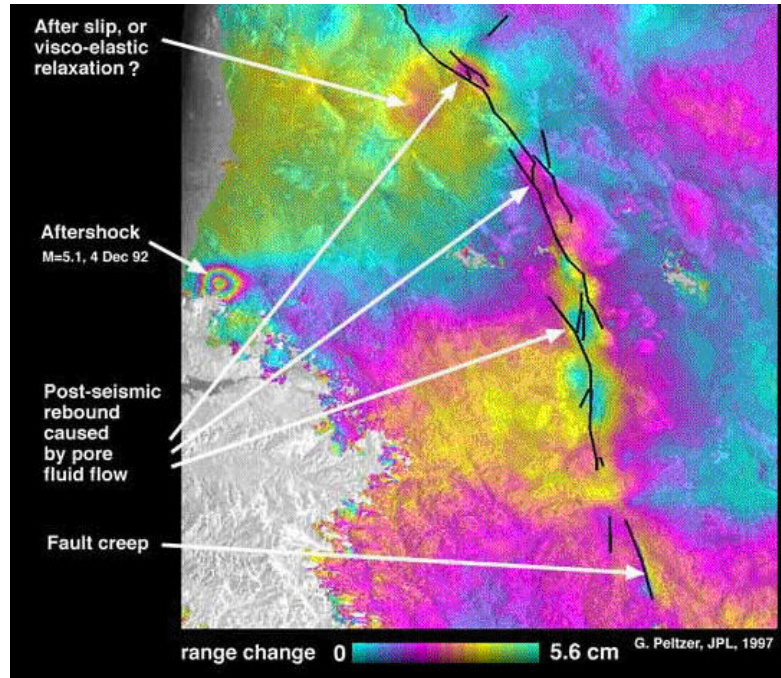


Figure 1.80 ERS-1 Interferometric map, Landers 1992 earthquake. Images used were from Sep. 27, 1992 to Jan 23, 1996. Map created by JPL.

The [Interferometric SAR](#) data revealed several centimetres of post-seismic rebound in step-overs of the 1992 break with a characteristic decay time of 0.7 years. Such a rebound can be explained by shallow crustal fluid flow associated with the dissipation of pore pressure gradients caused by [co-seismic](#) stress changes.

In [figure 1.81](#) below, SAR images spanning three different time intervals in the three years following the earthquake were combined. In the left panel the interferogram covers 41 days after the event, starting on 7 August 1992. The most striking features are the localised strain along three sections of the 1992 surface rupture where the rupture changed direction or jumped to another fault branch and formed two pull-apart structures and a compressive jog (boxes in left panel). The observed displacement in the fault step-overs is consistent with surface uplift in the pull-apart structures and subsidence in the compressive jog, i.e., opposed to the direction of the co-seismic movements, which is shown in the panel on the right.

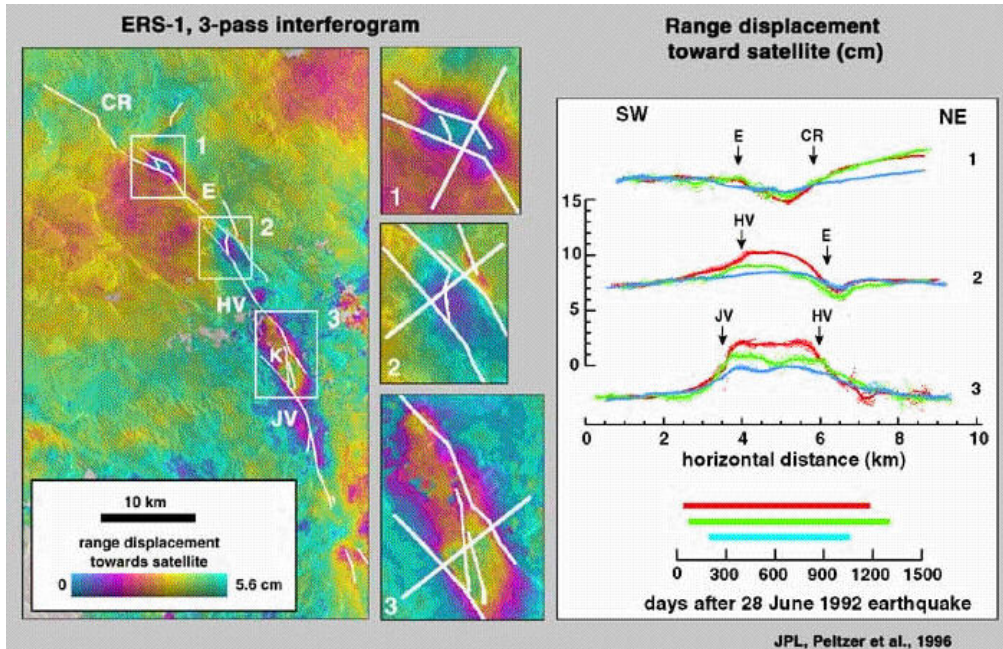


Figure 1.81 ERS-1 3 pass interferogram of Landers earthquake (JPL 1996)

### Land Subsidence:

Subsidence is the sinking of the Earth's surface in response to geological or man-induced causes. This surface displacement is shown by the image below, created from [ERS-1](#) SAR data by the Jet Propulsion Laboratory (JPL). In this image, which shows the location of existing and future Global Positioning System (GPS) stations of the Southern California Integrated GPS Network (SCIGN), the colours of the radar image represent the change in range due to surface displacement toward the satellite antenna, which is illuminating the area from the east with an [incidence angle](#) of 23 deg.off the vertical. The black lines are mapped as active faults. One full colour cycle represents 5.6 cm of range change between the dates of acquisition of the radar data (20 October, 1993 - 22 December, 1995). Grey areas within the radar [swath](#) are zones where the radar correlation is lost due to steep slopes and seasonal change of the vegetation.

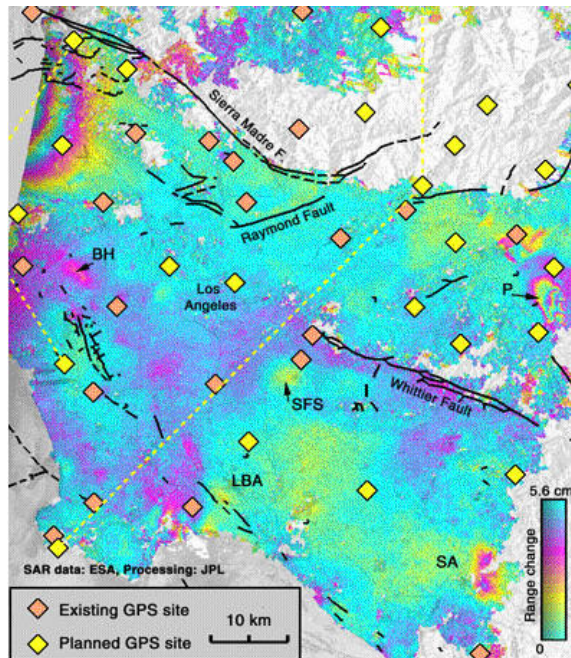


Figure 1.82 ERS-1 SAR 3-pass interferogram showing subsidence in Panoma California.  
Image created by JPL

Although surface displacement in this region is primarily due to the tectonic activity, as shown in the above image by the concentric rings visible along the western edge of the SAR swath, other features visible on the image are related to human activity such as water and oil withdrawal. Regions of ground subsidence include the Pomona (P) area (water), the Beverly Hills (BH) oil field (oil) and localised spots in the San Pedro and Long Beach airport (LBA) area (probably oil industry activity). Noticeable surface uplift is observed in the Santa Fe Springs oil field (SFS) and east of Santa Ana (SA). Surface uplift in these areas may result from the recharge of aquifers or oil fields with water, or from the poro-elastic response of the ground subsequent to water or oil withdrawal.

The relationship between the sinking of the earth's surface and how this is displayed by the [SAR interferogram 1.1.5.4.](#) is depicted in [figure 1.83](#) below.

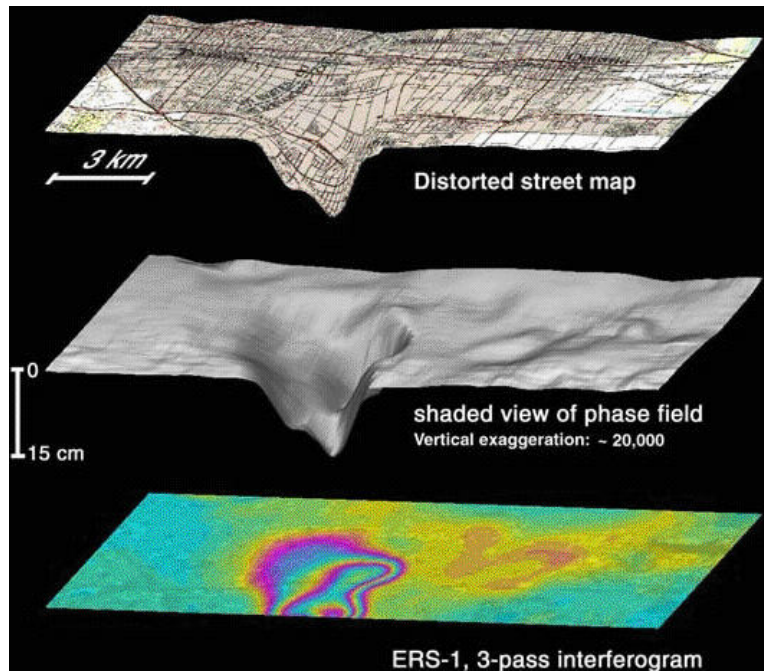


Figure 1.83 Relationship between ERS-1 SAR Interferogram and Panoma Subsidence.  
Image generated by JPL

In the interferogram, the colours depict the displacement of the ground along the radar line of sight (23 degree off vertical) having occurred between October 20, 1993 and December 22, 1995. The shaded view in the centre is the radar phase field displayed with 20,000 vertical exaggeration. The top view gives a street map wrapped on the phase field.

#### 1.1.6.3.6 Flooding, Hydrology and Water Management

Floods are among the most frequent of all natural hazards. They are extreme events that are usually sudden and short-lived, and

can cause considerable economic loss due to damage to buildings, destruction of infrastructure as well as the loss of human

lives. One of the biggest problems during such an emergency is to obtain an overall view of the phenomenon, with a clear idea

of the extent of the flooded area, and to predict the likely developments.



Figure 1.84 Extensive flooding near Oxford, UK. (Courtesy Institute of Hydrology, UK)

ERS [SAR](#) products, such as those created by [ERS-1 and ERS-2](#), as well as [ASAR](#), can be used in the event of flooding to permit immediate assessments of the areas at risk and aid decision-making on relief and cleanup operations. Products derived from archived SAR data may provide accurate spatial information on the extent of previous flood events. This is being used for management planning for preventative measures in areas where flooding occurs regularly. ERS SAR data can serve as up-to-date information in the absence of conventional optical satellite or other data. This is often the case in bad weather conditions which accompany flooding events.

The low resolution ERS SAR images shown below, which were obtained from the Rapid Information Dissemination System (RAIDS) of the UK, gives an indication of how SAR imagery can be used to monitor a floods progression.

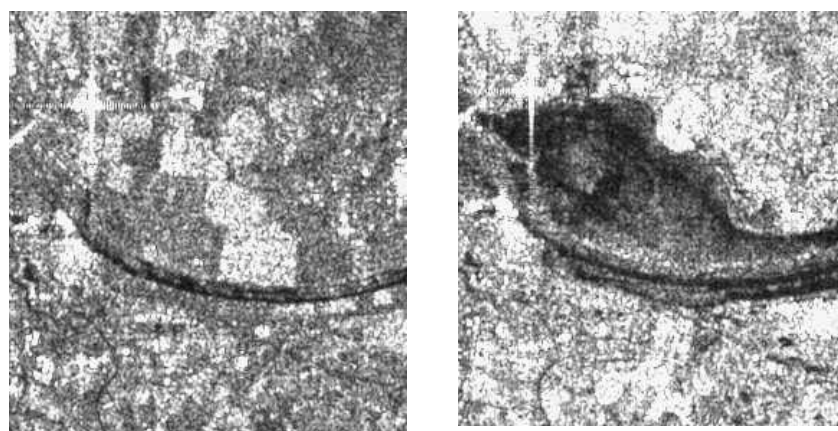


Figure 1.85 Reduces Resolution images ( 100 km x 100 km. pixel size 400m ) of the River Maas in the Netherlands shown before (left) and during (right) flooding (Imagery 1994-95  
ESA)

The image below gives an example of the hybrid change detection procedure used to detect human induced land cover changes in Southwest Florida [Ref. \[1.35\]](#). The work carried out at the Environmental Research Institute of Michigan, Duke University, was to advance techniques for monitoring and predicting changes in the hydrologic condition of regional scale wetland ecosystems in the south Florida region. The objectives were to integrate satellite remote sensing data with hydrologic models and field data to improve capabilities for monitoring and understanding processes controlling surface water flow in Florida wetlands. It was found that the herbaceous wetlands in their study area exhibited a wide range of conditions, from dry to saturated soils to flooded, which are readily detected by the [C-Band](#) ERS-2 SAR sensor.

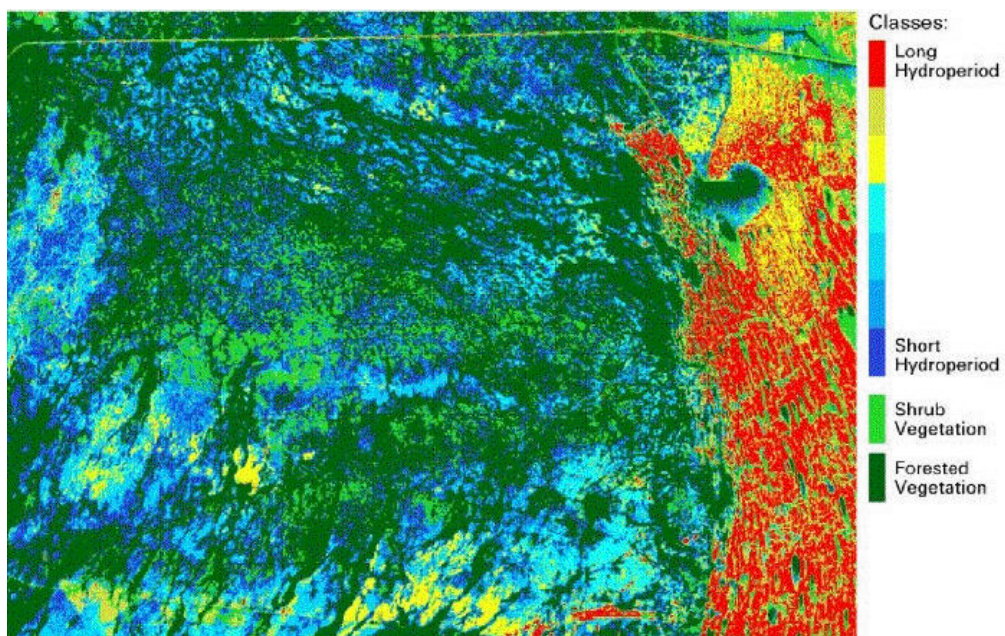


Figure 1.86 Vegetation and hydropattern dynamics of Big Cypress National Preserve PCA - Unsupervised classification of 1997 - 1998 ERS-2 SAR imagery. ( Image courtesy of Environmental Research Institute of Michigan, Duke University)

ASAR will add a new wealth of data for such research around the world.

#### 1.1.6.3.7 Urban Studies

The interrelated issues of urban sprawl, traffic congestion, noise, and air pollution are major socio-economic problems faced by most major cities. Though it is desirable to know about

---

the storage of heat in a particular city and how that amount of heat changes from day to night and from one day to the next, the information is difficult to obtain because of the complex three-dimensional structure of the urban surface and the variety of materials involved. Structures, pavements, vegetation and the ground itself must all be taken into account. Large bodies of water nearby are a further complication.

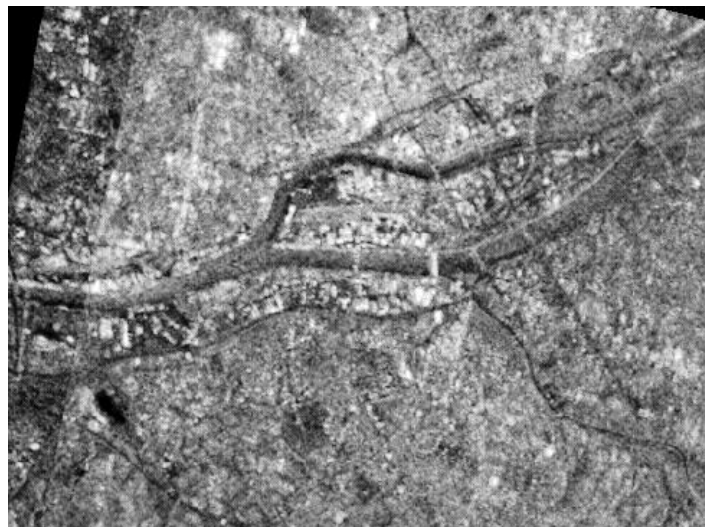


Figure 1.87 Mean image computed from five ERS SAR images, of the city of Nantes. The island is the island of Beaulieu. The Loire river appears in grey, crossed by several bridges in bright. In dark are the major roads, and the airport in the lower left corner. (copyright ESA 1994)

In the above image the importance of the relative direction of the target with respect to the radial direction of the radar wave clearly impacts the results. If the relative direction is perpendicular to the radial direction, then this object is clearly visible, even if it is flat such as a road or a railway track within a flat area. If the object is orientated in the same direction than the radar wave, then it is not visible. This is the case for the central station of Nantes and of the large railway complex in the western part of the Beaulieu island. However if the same object is surrounded by e. g. buildings reflecting the radar signal, it will be perceived because of the created contrast.

The direct analysis of the [ASAR](#) measurements, with many different [polarisations](#) and viewing angles, allows the recognition of different urban environments. The interferometric analysis of the same data, acquired in more than one passage, can be used for the 3D characterisation of a zone.

### 1.1.6.3.8 References

#### Ref 1.29

Peltzer, Gilles, "Crustal Deformation Studies Using SAR Interferometry", Jet Propulsion Laboratories at the California Institute of Technology and the Earth and Space Science Division of the University of California Los Angeles.

#### Ref 1.30

ASAR Science Advisory Group, Editor R.A.Harris, European Space Agency 1998, "ASAR Science and Applications", ESA SP-1225

#### Ref 1.31

Sandwell, David T., and Sichoux, L., "Topographic Phase Recovery From Stacked ERS Interferometry and a Low Resolution Digital Elevation Model", Institute of Geophysics and Planetary Physics, Scripps Institution of Oceanography, La Jolla, CA. Submitted to Journal of Geophysical Research, March 1, 2000

#### Ref 1.32

Harbert, Dr. W., "Geological Interpretation of North Kamchatka, Russia: Constraints from Synthetic Aperture Radar, Digital Elevation Models and Digital Residual Magnetics", Geophysics Department, University of Pittsburgh. Abstract published in Earth Observation Magazine, September 1992, pp. 45-47.

#### Ref 1.33

Pailou, P., "Arid Sub-Surface Imaging using Radar Techniques", Observatoire Astronomique de Bordeaux, BP 89, 33270 Floirac, France, web: <http://www.observ.u-bordeaux.fr/~pailou/pailou.html>

#### Ref 1.34

Wright, T., Fielding, E., Parsons, B., "The 17 August 1999, Izmit Earthquake Displacements and Topography from SAR Interferometry", [www.earth.ox.ac.uk/~geodesy/izmit.html](http://www.earth.ox.ac.uk/~geodesy/izmit.html).

#### Ref 1.35

Kasischke, E.S., et. al, "Monitoring Regional-Scale Hydrologic Processes in the South Florida Ecosystem", Environmental Research Institute of Michigan, Duke University, US., January 31, 2000.

### 1.1.6.4 Sea Ice Applications

There is a wide range of sea ice data applications in the marine community and across a

number of industrial sectors. Industries and agencies operating in ice-infested waters include commercial shippers, offshore oil exploration companies, fisheries, military, regulatory agencies, and research institutions. Other industrial sectors use ice information when designing ship hulls and offshore drilling platforms, to perform risk assessment, and to establish insurance premiums.

The sea ice markets include agencies in the USA, Canada, Japan, Russia, Norway, and the Baltic countries. SAR data are combined with other sources of data to optimise sea ice forecasts, and are also transmitted directly to ice breakers and ships operating near the ice edge.

Ice information is required at continental or global scales. As described by Manore et al. (1991), the requirement for these scales comes largely from the global ice studies community, which has interests in:

- monitoring global sea ice extent as an indicator of climatic change
- providing better parameterizations of sea ice in ocean-ice-atmosphere global circulation models
- better understanding of the processes of heat and mass exchange between the ocean, ice, and the atmosphere

Radar data can aid in areas of study such as ice concentration determination, ice type classification, ice feature identification, ice motion monitoring, and iceberg tracking. Information on total ice concentration, location of the ice edge, ice type and thickness, ice topography, the presence and location of leads, ice pressure, state of ice decay, and iceberg and ice island location can be derived directly from [radar](#) imagery.

Note that HH [polarisation](#) differentiates between open water and ice better than VV polarisation. Also note that the appearance of a given ice feature may differ significantly in wet versus dry conditions. When surface meltwater is on the ice or ocean spray is on the surface at the ice edge, feature [brightness](#) may differ from that encounter in dry conditions. When wet surface conditions prevail, it is useful to have a reference [image](#) acquired before the onset of melt conditions.

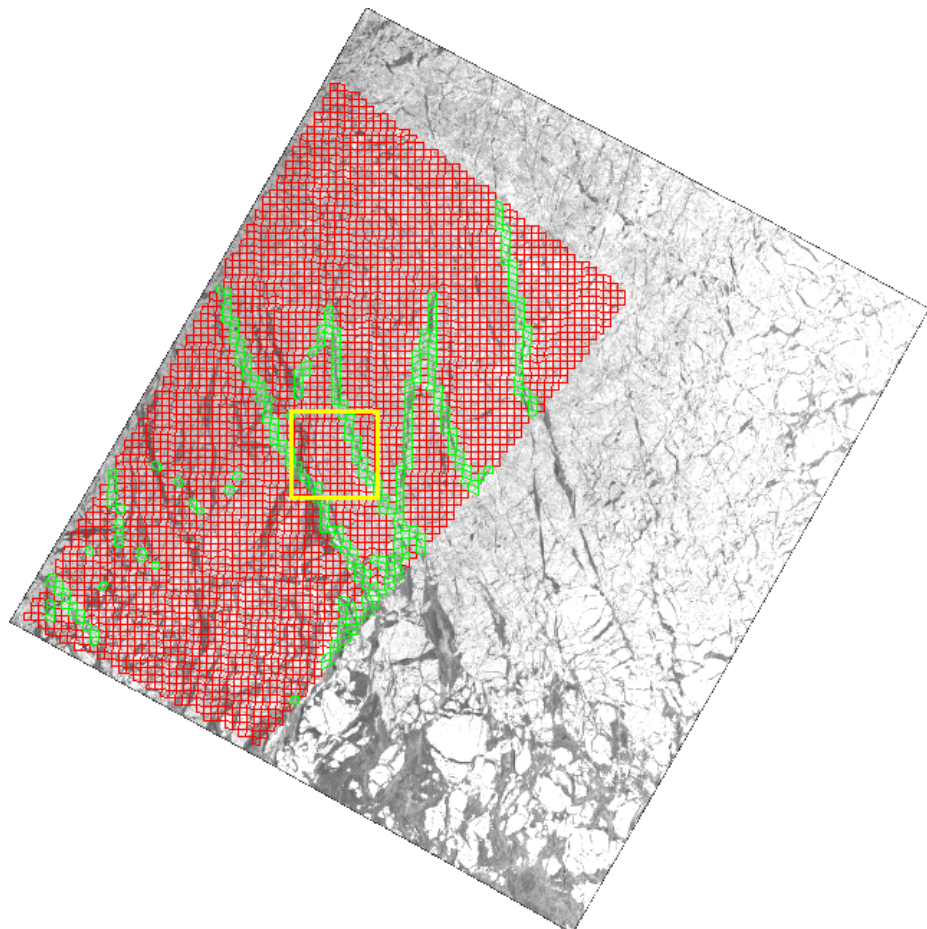


Figure 1.88 RADARSAT SAR Image With Sea Ice Deformation (SAR image is Copyright CSA 1998. Grid produced by the Radarsat Geophysical Processor System)

The above is a RADARSAT ScanSAR Wide B geocoded image of sea ice in the Beaufort Sea on January 11, 1998, that has been block-averaged (10 x 10) to 1000 metre pixel size.

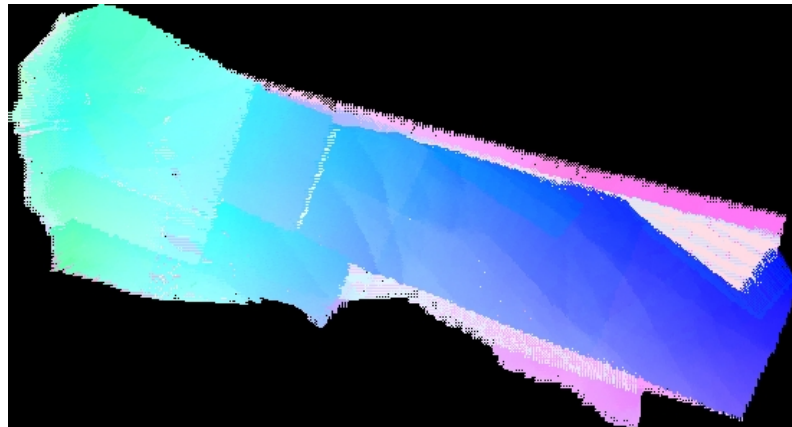


Figure 1.89 RGPSS Lagrangian Ice Motion Visualization( Using data produced by the Radarsat Geophysical Processor System )

The above image is an early attempt to visualize the RGPSS Ice Motion product. RGPSS is the Radarsat Geophysical Processor System under development by the Polar Remote Sensing Group at JPL. The visualization is an ASF Science Division project directed by Dr. Mitchell Roth, UAF Professor of Computer Science, with Richard Guse, CS graduate student. The data is derived from arctic snapshot data of an area in the Beaufort Sea acquired by ASF in November of 1996. This datatake is cycle 15 based on 143 ScanSAR B images. Ice motion is visualized using a colourwheel (shown below.) The direction is given by colour (1-1 correspondence with the colourwheel) & the magnitude of its movement is given as the saturation (white being slow and full colour being fast, not necessarily 1-1).

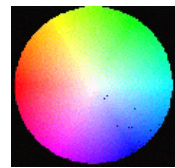


Figure 1.90 Colour Wheel

This visualization is a 'composite' of vectors in 3-space, the z-coordinate (out of the screen) represents the time the vector is computed with more recent vectors on top.

### Sea Ice Motion Derived from Satellite Imagery

Sea ice motion data are utilized both in fundamental scientific research and for practical

---

every-day purposes. Ice motion data help scientists in many research endeavors such as: analyzing the polar regions' latent heat advection; determining the local oceanic surface stresses; passively tracing currents; tracking new areas of open water (formed by ice divergence and shear); and understanding the effects of icebreaker vessels. In addition to furthering this fundamental research, the data are also used to help forecast weather and ice conditions, evaluate possible hazards, and contribute to the overall understanding of environmental impacts in the Arctic region.

Traditionally there have been many obstacles in acquiring sea ice motion data. Sea ice is by nature located in remote, inaccessible regions, and the ice extends over a large area. Though ice motion can be determined by placing sensors directly onto ice floes, the cost of installing and maintaining many field instruments is prohibitively high. It is similarly prohibitive for scientists to stay in the field and monitor the sea ice motion themselves! One can readily see the benefits of studying sea ice remotely, from satellites.

There are also complications with monitoring sea ice from space, however. Cloudy skies hide the sea ice from some sensors, and long winter nights thwart the ability to image polar regions with visible light. The research community therefore turned to the Synthetic Aperture Radar (SAR) as a viable sea ice imager. Since a SAR emits its own signals (similar to a camera's flash), it works during the day or night. The radar signals also penetrate through cloud cover, a characteristic which is especially valuable to oceanographers. Scientists determined that a satellite-borne SAR could routinely and reliably image large regions of sea ice.

The SAR-carrying ERS-1 satellite, launched in July 1991, provided many scientists the chance to study sea ice with SAR. The Geophysical Processor System (GPS), an effort led by Ron Kwok of JPL, was designed to facilitate this research. The GPS generated sea ice motion, sea ice classifications, and ocean wave spectra data from ASF's collection of ERS-1 SAR imagery. Scientists could then use the derived geophysical information for their various research projects.

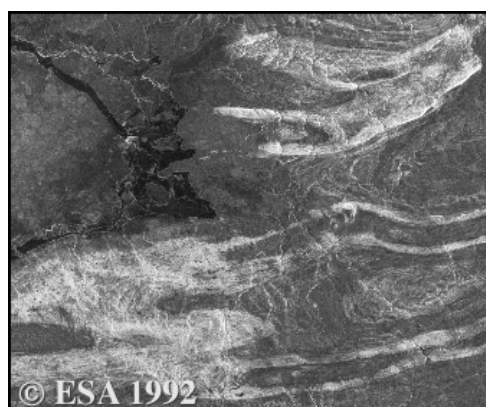


Figure 1.91 Melville Island Canada Copyright 1992, European Space Agency

---

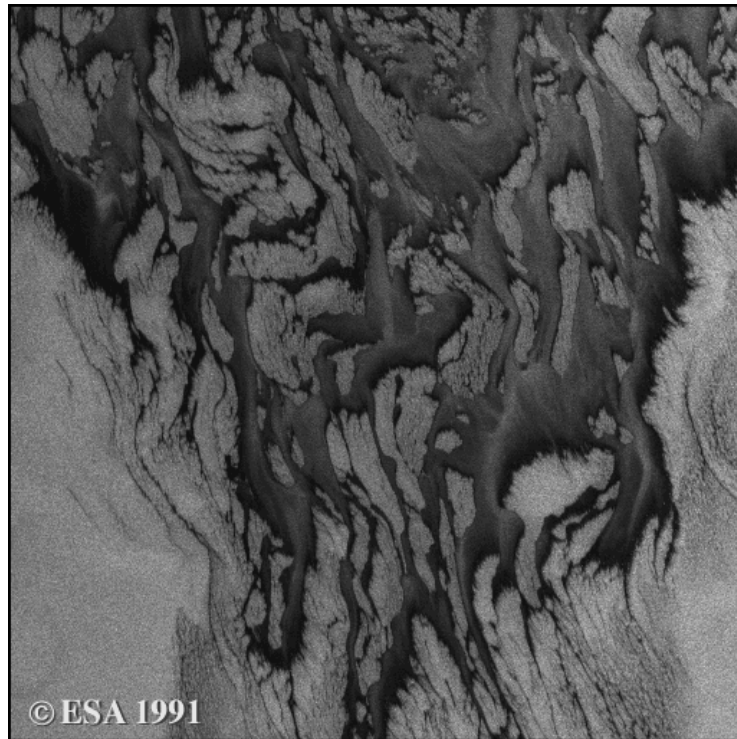
This image above was derived from SAR data obtained by the European Space Agency's ERS-1 satellite on October 11, 1992. This scene shows a portion of Melville Island, way up in northern Canada (108 W, 75 N), and should be of particular interest to you geologists. The image covers about 65 km by 55 km. North points approximately 33 degrees counter-clockwise from the top of this scene, and the spacecraft was descending "down" the right side of the image, so the scene's radar illumination is from the right.

#### 1.1.6.4.1 Sea Ice Applications - Ice Sheet Dynamics

Radar is sensitive to the physical properties of sea ice (salinity, microstructure, and surface roughness) that vary with ice concentration, type, age and thickness. Elements that are employed to visually discriminate ice types in SAR imagery include the structural characteristics of floes, such as the shape and presence of ridges, fractures, and melt ponds. The ability to discriminate ice types is highly dependent on the geographic region and the season of imaging because different ice types exist in different regions and at different times of the year. The most promising season is winter when the snowpack is dry and cold. During the drier months of winter the surface texture is the primary key for discrimination. In the warmer months, when free water is present, the differences between old and first-year ice become more difficult to discriminate, in particular when the overlying snow pack is saturated and the differences in [backscatter](#) are significantly reduced. Classification ambiguity can be reduced by consulting the past history of ice features in a particular region, ice climatology, and current meteorological conditions (Ramsay et al, 1993).

The identification of specific structural features within the sea ice is also important for navigation because they pose hazards to vessels. The identification of leads and floes is used to optimise route selection, and RADARSAT's sensitivity to surface roughness and its fine spatial resolution permit the detection of ice ridges and their orientation.

The image shown in [figure 1.92](#), available through the [Alaska SAR Facility Ref. \[1.37\]](#), shows an example of grease ice.



© ESA 1991

Figure 1.92 Grease Ice(Copyright 1991, European Space Agency)

The SAR data for this image was taken by the European Space Agency's ERS-1 satellite on October 2, 1991. The centre location of the complete image is 73.58 N, 166.60 E, north of Siberia in the East Siberian Sea. North points approximately 30 degrees counter clockwise from the top of this scene.

In addition to the detection of ice structures, knowledge of the state of decay or growth of sea ice is important to infer its strength. During periods of decay when temperatures are above freezing, the ice is relatively weak and can be more easily traversed by an ice-strengthened vessel. However, during an extended period of ice growth when temperatures fall below freezing, the same ice could be impassable. Ongoing monitoring of sea ice to identify the onset of melt and freeze-up may aid in route selection (Ramsay et al, 1993).

Another factor that can impede the progress of ice-strengthened vessels is the continual movement of the sea ice in response to wind and ocean currents, and the pressure that is created within the ice floes. Because these movements are continual, monitoring must be an ongoing activity, requiring frequent and sequenced imaging.

Icebergs of all sizes, including those less than 5 m in size (referred to as bergy bits), are of interest to shipping and offshore operators because of the hazard they pose to ships and structures such as oil platforms. Steep incidence angles and the low-resolution of reconnaissance-scale imagery, pose problems in detecting icebergs in pack ice and in open

water. In open water, the sea conditions and orientation of larger icebergs with respect to the SAR will determine whether they can be detected. In pack ice, the signature of an iceberg is often lost in the backscatter from the surrounding sea ice.

Areas of glaciology to which ASAR contributes include: monitoring the ice extent and the boundaries of ice sheets, and mapping the motion of ice sheets and glaciers. [figure 1.93](#) provides a simple example of the use of ERS data for mapping changes in the extent of the Larsen Ice Shelf, Antarctica. There are many similar examples. SAR data is still being used on an irregular basis when something interesting happens, rather than as a monitoring tool. [Interferometry](#) and correlation measurements which show movement of the ice sheets are very important to this work. ASAR will provide valuable continuity in the supply of data started with ERS.

Mass balance and ice dynamics are the key scientific questions, with the parameters to be derived from ASAR including:

1. Ice boundaries (every 2 weeks)
2. Ice export due to calving (every 2 weeks)
3. Extent of melt zones (2 weeks during summer; Greenland and Antarctic Peninsula)
4. Snow and ice faces (once a year)
5. Ice motion by means of feature tracking (once a year)
6. Surface morphology (flow lines, rifts, crevasse zones etc.) (once a year).

Depending on the topography and the requirements for spatial detail, the ice sheets may be separated into the boundary zone (including the ice shelves) and the interior part. Baseline operation for the boundary zones is considered to be the Wide Swath Mode for the measurement of parameters (1), (2) and (3) above. Baseline operation mode for the interior could be the Global Monitoring Mode, for the measurement of parameters (3) and (4). The preferred operation modes for selected zones (ice streams) are Image Modes at higher incidence angles (IS3 to IS7), for measurement of (5) and (6) above with approximately annual repetition of observations.

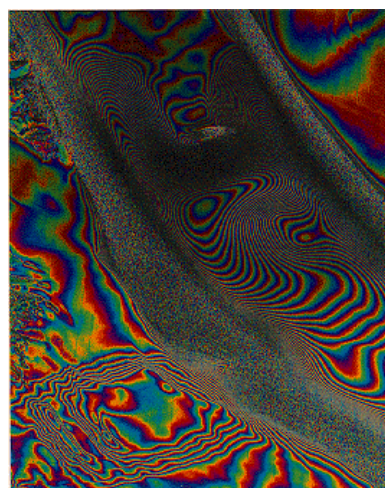


Figure 1.93 Radar interferogram of a portion of the Rutford ice stream in Antarctica, based on two ERS-1 images taken six days apart. The fringe pattern (colour cycle) is essentially a

map of ice flow velocity, with one fringe representing 28 mm of range change along the radar line of site.(From Goldstein et al, 1993)

There are a number of key studies in this field being proposed that will utilise ASAR data to a great extent. Some of these are briefly discussed below.

One study, to be conducted by Dr. Massimo Frezzotti at the ENEA Environmental Department in Italy, will focus on using ENVISAT ASAR data to study the XXI century iceberg calving of East Antarctic. The objective is to study the iceberg calving process, to perform monitoring of ice front change, and to evaluate a century behaviour of iceberg calving. Comparisons are to be made using new ASAR images and previous data (aerial photographs, satellite images), taken several years apart (1947 - 65; 1972 - 73; 1988 - 93; 1996) to estimate the XXI century of ice front fluctuation and of iceberg discharge. The study of the dynamics of seaward extension of floating glaciers will allow the investigators to hypothesise the ice ocean interaction.

Another area of research, to be carried out by Dr. Eric Rignot at the Jet Propulsion Laboratory in the United States, will study two related ice sheet dynamics and evolution problems that are addressable with ENVISAT data:

1. The stability of the onset areas of fast-moving glaciers in Greenland and Antarctica using SAR interferometry.
2. The time evolution of surface rifting, crevasse development and meltwater production on Antarctica's floating ice shelves using dual polarisation SAR data.

The two research topics are related because fast moving glaciers are strongly influenced by the presence or absence of buttressing ice shelves (Antarctica) or floating ice tongues (north Greenland).

The first topic will attempt at detecting mechanical instabilities (surge) of large ice streams draining polar ice sheets in response to climate change (e.g., enhanced melting at the coast). The second topic will provide new insights into the physical mechanisms (rift propagation, meltwater accumulation) controlling tabular iceberg production in the Antarctic.

At the British Antarctic Survey, Dr. Christopher Doake and associates propose to use ENVISAT data to investigate two important components of the Antarctic Ice Sheet:

1. the ice streams draining the West Antarctic Ice Sheet (WAIS)
2. the climatically sensitive ice shelves

The ice streams that drain the WAIS are the key controls on its size and configuration. Dr. Doake will use ASAR brightness data and interferometry to investigate the current dynamics of these ice streams and use velocity fields to calculate ice flux, searching for changes that could indicate a state of imbalance. The WAIS ice streams will then be contrasted with an ice

---

station in East Antarctica, that drains a similar area of ice sheet but has a different dynamical character. Dr. Doake's team has recently shown that the ice shelves along the Antarctic Peninsula are sensitive indicators and integrators of a regional climate change. The ENVISAT data will be used to monitor the predicted changes and to determine the flow regime of the ice shelves.

Yet another study being proposed comes from director Kenneth Jezek at the Byrd Polar Research centre in the United States. This project will concentrate on compiling an ENVISAT SAR mosaic of Antarctica. The acquisitions will be coordinated with planned acquisitions by the Canadian RADARSAT. The intent is to answer important questions about seasonal processes such as calving, melting, coastal polynya formation and the consequences on glacier flow. The possibility of complete, simultaneous interferometric coverage of Antarctica offers the greatest scientific payoff and could revolutionise our understanding of how Antarctica responds to changing global climate.

And Dr. Johnathan Bamber at the Centre for Remote Sensing, University of Bristol in the UK, will use Interferometric ASAR data to provide information on the dynamics and temporal stability of the flow of the ice sheets and Arctic ice masses.

These are but a few of the areas of ice dynamics research in which ASAR data will be of major benefit. Incidence angle is not a critical factor in sea ice monitoring. However, shallow incidence angles are more effective in highlighting surface topography, separating the ice/water boundary, and detecting icebergs.

#### References:

##### Ref 1.36

Report of a Workshop Held in Boulder, Colorado: February 3 - 4, 1994, Timothy H. Dixon, Editor , University of Miami, Rosenstiel School of Marine and Atmospheric Science. available at <http://southport.jpl.nasa.gov/scienceapps/dixon/index.html>

##### Ref 1.37

Alaska SAR Facility, web site [www.asf.alaska.edu](http://www.asf.alaska.edu)

#### 1.1.6.4.2 Sea Ice Applications - Snow Cover

In many areas of the world, the majority of freshwater available for consumption and irrigation results from snowpack runoff. Snow wetness, snow-water equivalent and the aerial extent of the snow cover are the most important parameters in predicting total runoff. Mapping the extent of wet snow is possible using SAR data (Rott et al, 1988) as wet snow produces a low radar return in contrast to dry snow which is essentially transparent at C-band.

The ice sheets of Antarctica and Greenland are the principal stores of fresh water in the

Earth's hydrological system and changes in their mass balance affect the mean sea level. Changes in the height of ice sheets can indicate changes in the mass balance. Snow cover, snow accumulation, and ice type information are also required for monitoring, detection of change and process studies at high latitudes and high altitudes.

The presence of snow on the ground has a significant influence on the radiative balance of the Earth's surface and on the heat exchange between the surface and atmosphere. ERS has demonstrated the value of SAR data for mapping snow cover, and the Global Monitoring Mode is of special interest for monitoring the areal extent of snow and the temporal dynamics during the melt period, on a weekly basis for climate research purposes.

Snow mapping is also important for hydrology and water management. Snow cover extent data are required every 2 weeks during the melting season, and the baseline operation in mountainous areas should be Image Mode at high incidence angles (IS4 to IS7).

Scientists Craig Lingle, Carl Benson, and Kristina Ahlnaes, of the Geophysical Institute, use Synthetic Aperture Radar (SAR) imagery to monitor glaciers. At the fall 1996 meeting of the American Geophysical Union (AGU), these researchers presented a poster which detailed how glacier facies (zones) can be examined through satellite SAR imagery. They focused their attention on the Nabesna Glacier, which flows down the slopes of Mt. Wrangell in south-central Alaska.

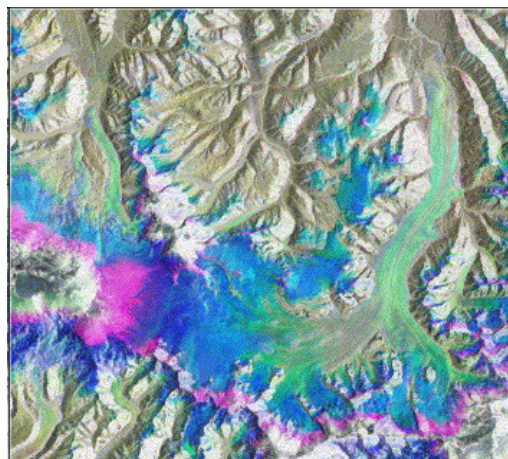


Figure 1.94 Glacier facies on Mt. Wrangell, Alaska, examined with SAR imagery. image size was greatly reduced for display here) ( Copyright ERS)

The image above is a multi-temporal image of Mt. Wrangell and Nabesna Glacier derived from midsummer, late-summer, and winter ERS-1 SAR data. Mt. Wrangell is located at left-centre, with Nabesna Glacier flowing to the east (right) before turning north (up). The glacier's wet snow facies (zone) is outlined by the blue region. The pink areas mark the upper extent of summer snow melt.

The SAR imagery (shown in [figure 1.94](#)) is particularly effective at distinguishing between a glacier's characteristic zones. Near its terminus the glacier is covered by rocks which scatter the transmitted radar signals back to the SAR sensor. Consequently, the glacier's terminus appears rather bright in the SAR imagery. Above the terminus lies the ablation area. The relatively smooth ice in this region is specular; it "forward scatters" a significant portion of the radar signals away from the spacecraft. The ablation area is therefore assigned a medium to dark grey image intensity. The light streaks seen in the ablation area correspond to medial moraines: lines of rock debris on the glacier's surface which strongly backscatter radar.

The radar response from the next zone, termed the "wet snow facies," changes dramatically with the seasons. In summer this snow is wet and dense. Small pools of water may form on the glacier's surface. These surface characteristics imply that nearly all of the radar signals are forward scattered away from the spacecraft. As a result, this zone looks very dark in the summer SAR imagery (See [figure 1.95](#).)



© ESA, 1993

Figure 1.95 ERS-1 SAR image for June 23, 1993 The wet snow facies (zone) is dramatically outlined as the dark region between the lower ablation area and the bright percolation facies.

In early autumn, however, it's a different story. The wet snow freezes into coarse crystals which cause strong backscatter. To the SAR sensor, the wet snow zone then appears much brighter. Higher still, the "dry snow facies" lies on and near Mt. Wrangell's summit, where the weather is cold and dry. The radar signals pass right through the summit's homogenous, dry snow and are almost entirely absorbed. Since few signals are backscattered from this region, Mt. Wrangell's crater appears dark, as seen in the December SAR image. Due to the stable snow characteristics atop Mt. Wrangell, this area has a consistent radar signature year-round. (See [figure 1.96](#).)



Figure 1.96 ERS-1 SAR image for September 29, 1993

In the above image, water in the wet snow facies is re-freezing, resulting in similar radar responses from that zone and the neighbouring ablation area. The upper boundary of melted snow (the dark region below Mt. Wrangell's base) stands out in this early autumn image.

The dramatic differences between the dark wet snow facies and the bright percolation facies during summer, and between the bright wet snow facies and the relatively dark ablation area in winter, allow researchers to map the extent of a glacier's facies. This information is very important because it is closely related to mass balance: the amount of new snow accumulated versus the amount of meltwater lost. Shifts in facies' boundaries are also indications of climate change; glaciers react significantly to small variations in climate.



Figure 1.97 ERS-1 SAR image for December 30, 1992

Mt. Wrangell's crater (left-centre) contains the dry snow facies, where radar signals are primarily absorbed. The arrow marks the late-summer snow line; above this boundary, snow remains on the glacier's surface throughout the year.

A project was undertaken at the Alaska SAR Facility, by visiting scientist Kim Partington, to try and determine if both the ablation/wet snow and wet snow/percolation boundaries could be seen in a single image, if that image was the result of combining imagery from various seasons into one year.

A blue colour scheme was applied to the December image, red to the June image, and green to the September image. The three colour images were then merged. If the red, green, and blue values were all of similar strength, the result was simply a shade of grey. This would imply no change in radar response between the seasons. The percolation facies on Wrangell's upper volcanic cone is white; this zone backscatters brightly year-round. The darker radar signature from the dry snow facies within the crater is similarly stable throughout the year. Blue patches indicate that the corresponding regions backscattered the radar most brightly in winter. The wet snow zone, which has low radar response in the summer but backscatters strongly in the winter, is therefore coloured blue. The pink regions were least bright in late summer and hence mark the upper extent of snow melt. The green area surrounding Mt. Wrangell's summit, implying brightest radar backscatter in September, is believed to be caused by the development of hoar frost at that time of year.

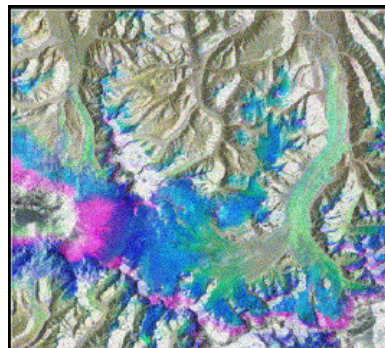


Figure 1.98 Multi-temporal image which combines the June, September, and December SAR images into one product. Nabesna Glacier's wet snow facies is represented by the blue region.

The upper boundary of the pink region marks the highest extent of summer snow melt.

ASAR data will provide scientists with a valuable new tool in their investigations into snow cover studies. One such study being proposed by Dr. Jan-Gunnar Winther, head of the Antarctic Section of the Norwegian Polar Institute, is to use ASAR and MERIS data for studies of snow distribution, and glacier characteristics, and to evaluate how these sensors can improve our present use of satellite data for studies of how the cryosphere responds to climate change, as well as for applications within hydropower production management. In particular, the goal is to determine:

- how snow distribution on Svalbard affects regional climate
- snow distribution in mountainous areas of Norway, for updating hydrological models used for management of hydropower production

---

as well as to monitor glaciers on Svalbard for studies of mass balance, surge mechanisms, calving and sensitivity to climate change.

#### References:

##### Ref 1.38

Alaska SAR Facility web site: [www.asf.alaska.edu/user\\_serv/features](http://www.asf.alaska.edu/user_serv/features)

#### 1.1.6.4.3 Sea Ice Applications - Sea Ice Mapping

Radar data can be used in applications supporting regional sea ice mapping and monitoring, iceberg monitoring, as well as marine transport and fisheries support. In the remote and extensive areas affected by sea ice, radar remote sensing has been able to provide comprehensive, timely, and accurate information.

Active microwave remote sensing instruments are particularly effective for sea ice mapping because of their all-weather, day-and-night and high-resolution imaging capability. As well, to be an effective information tool, the imagery must be captured on a regular basis if imaging in Arctic regions.

Sea ice research is currently concentrating on increasing our understanding of the processes operating in local areas and on continuous monitoring to identify seasonal changes. Sea ice models, used to estimate surface flux and understand process behaviour, require information on ice extent, concentration, and leads at varying resolutions appropriate to the use of Image (IM) and Wide Swath (WS) Mode data. Monthly, seasonal, and annual products are required. Areas of special interest are monitored continuously, while other areas require data only during times of fieldwork. Some large-scale monitoring is undertaken for which a large swath width is required.

The most important features of interest to potential users are ice concentration and delineation of ice edges. Information regarding the location of the ice edge is vital, since most ships are not ice-strengthened and any contact with ice is potentially dangerous. The discrimination between new ice and water is also required.

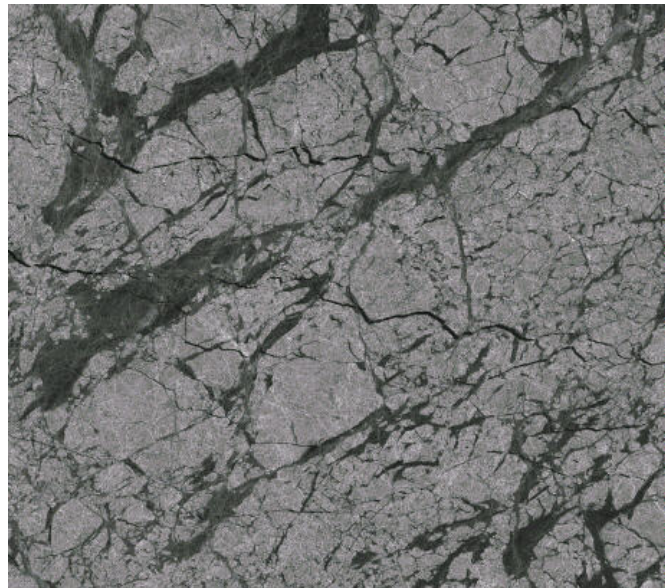


Figure 1.99 ERS-1 SAR image showing sea ice signatures, fall freeze-up, Beaufort Sea  
(image courtesy of Alaska SAR Facility)

ASAR offers data similar to both ERS SAR and RADARSAT, both of which are being used extensively for sea ice research. Both Wide Swath and Image Modes will provide valuable data.

Some ambiguity in the interpretation of newly formed ice and smooth water may occur under calm conditions because the water surface is very similar to that of new ice. In general, the new sea ice, although a relatively flat surface, is "rougher" than a calm water surface (because of the presence of ridges and rafting) and is therefore distinguishable on radar imagery. Generally, the images are interpreted with the use of ancillary data such as meteorological records, recent and historical ice records, bathymetry, and data on ocean and coastal currents and winds.

The identification and mapping of ice types is another feature of interest to navigators. Ice-type definitions are based on the age of the sea ice, which is directly correlated to its thickness and strength. Of greatest importance to navigators is the differentiation between new, first year and multi-year ice. Because of their strength and hardness, multi-year sea ice and icebergs are significant hazards to ships and offshore structures (Ramsay et al, 1993).

There are several cooperative projects collecting and analysing sea ice information. For example, the Arctic Climate System Study (ACSYS), a regional project within the World Climate Research Programme (WCRP), is a ten-year programme that began in 1994. Its objectives are to improve understanding of the processes within the Arctic Ocean, including

assembling a basin-wide climatological database of sea ice extent and concentration (from satellite observations) and of ice thickness and motion (using underwater sonars) and drifting ice buoys.

Another investigation, being led by Dr. Son V. Nghiem, at the Jet Propulsion Laboratory in the United States, will develop new algorithms using ENVISAT ASAR and MERIS for sea ice mapping, iceberg tracking, and studying sea ice surface thermal effects. ENVISAT-RADARSAT synergy will be used to enhance sea ice operational applications. The approach is to use ASAR data at different polarisations to classify open ocean and ice for ice mapping, lead detection, and iceberg tracking.

To study sea ice surface thermal effects under clouds, ASAR is used to detect surface temperature change and map melt pond areas under both clear sky and cloudy conditions with MERIS for cloud detection. ASAR Wide Swath imagery is combined with the RADARSAT ScanSAR product to provide a near daily revisit at high latitude with added polarisation diversity to improve ice mapping ambiguities.

#### 1.1.6.4.4 Sea Ice Application - Ship Routing through Sea Ice

Satellite SAR data is particularly useful for mapping the extent and type of sea ice for ship routing due to the availability of data in all-weather conditions and during darkness. There can be significant benefits in improving the efficiency of offshore operations. Since the launch of ERS-1, systems have been developed which send information and images directly to ice breakers and ice-strengthened ships, and images are also sent to Ice Centres that produce forecasts of ice conditions.

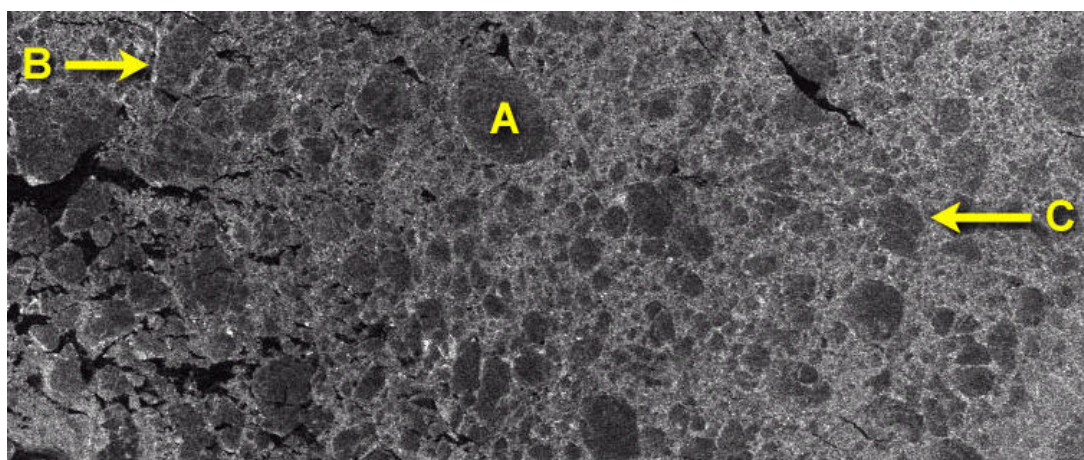


Figure 1.100 RADARSAT image of the Gulf of St Lawrence, Eastern Canada (image courtesy of CCRS)

[Figure 1.100](#) above shows a number of different ice types present in the Gulf of St Lawrence

---

in Canada. The Synthetic Aperture Radar (SAR) is sensitive to variations in the salinity, surface roughness and surface wetness of ice.

This type of imagery is very useful to agencies for locating, monitoring and evaluating the movement of sea ice. The ability to determine ice type and monitor ice motion are extremely important to ship navigation. Based on this kind of information, navigators can determine the path of least resistance and plan the ships' routes through the ice. The area indicated by (A) depicts first year ice floes. Rough "brash ice", indicated as (B) and pressure ridges (C) are also clearly visible.

One-to-three day coverage is required for ice forecasting and ship routing. The temporal repeat time is of greater importance than a high spatial resolution and current use of ERS SAR and RADARSAT data has shown that 100 m data will meet the product specification. RADARSAT or ASAR Wide Swath Mode is the obvious choice in order to have the wide area coverage.

Ship navigation requires information at a scale which is useful when supporting ship routing decisions over regions of 1 to 50 km. High-resolution data is required to identify individual ice features, so that in case of an emergency, immediate ship routing decisions can be made. Specific features of interest on acquired imagery include the size and thickness (or type) of ice floes, ice ridges, leads, and icebergs. For navigation, coverage is also required for areas of 100 to 2000 km in extent, at spatial resolutions of 1 to 50 km. At this scale, broad ice conditions can be assessed and ship operators can identify the overall least costly or least hazardous route. The information requirements for these applications include ice edge location, ice concentration and type determination, and lead detection (open areas or cracks in the ice).

Small-scale (large area) imagery provides regional mapping capability for sea ice concentration, ice edge location, ice motion tracking, and ice type classification. This information can be useful for tactical navigation depending on the actual ice environment. Intermediate-scale imagery provides detail for medium-scale mapping and tactical navigation support.

## 1.2 How to Use ASAR Data

There are a number of ways to visualise and process ASAR data. The following subsections provide information on the software tools available, plus key features of ASAR product format and contents which should be taken into consideration before using the data. A discussion of the possible software tools that may be used with ASAR data is given in the following subsections (see index)



## 1.2.1 Software Tools

ASAR products are delivered in the standard ENVISAT data format. Having received the data, the following categories of software tools can be used to explore ASAR products (see index)

### 1.2.1.1 General Software Tools

Users may wish to directly decode data in the ENVISAT format themselves, to allow subsequent visualisation and further processing in languages such as C, or in commonly available software packages such as IDL, ENVI and Erdas Imagine.

The EnviView tool, which is discussed in detail in the ENVISAT Handbook, can also be used to convert ENVISAT data into hdf files. As briefly discussed in the next section, "[EnviView](#)," [1.2.1.2](#), this ENVISAT tool is not intended for the detailed analysis, visualisation, and processing of ENVISAT data. Other commercial and proprietary tools provide these facilities in great detail and with many specialised options. The difference between such tools and EnviView is that they are usually aimed at certain classes of data, such as images or atmospheric data, or even data for a particular instrument. EnviView, however, is a single solution for all ENVISAT products. EnviView is intended as a stepping stone between these tools and the proprietary data format used for ENVISAT data. The data can then be automatically read by any software supporting this format.

Some other tools that may be used for more detailed analysis are provided below. Some are not ASAR specific.

- IDL (Interactive Data Language) <http://www.rsinc.com> a general purpose graphical and scientific computing system
- CAESAR image processing (speckle reduction) from NAS Software at <http://www.nasoftware.co.uk>
- DORIS Insar software (open-source) at <http://www.geo.tudelft.nl/fmr/research/insar/sw/doris/index.html.cgi>
- Earthview InSAR from PGI Geomatics at <http://www.pcigeomatics.com>
- ENVI from Research Systems at <http://www.rsinc.com> based on the IDL product
- ERS SAR toolbox described at <http://esapub.esrin.esa.it/eq/eq64/toolbox.pdf> and available at <http://earth.esa.int/STBX/>
- GAMMA <http://www.gamma-rs.ch> sells modular SAR processor software, and interferometric SAR and differential SAR processors
- GEOimage <http://www.geoimage.fr> software for processing Earth-observation imagery
- Geomatica (remote-sensing image processing, cartography, photogrammetry) <http://www.pcigeomatics.com>
- IMAGINE Professional (remote sensing scene analysis, radar analysis, mapping) <http://www.erdas.com>
- Matlab <http://www.mathworks.com> includes a number of optional toolboxes

including Signal Processing, System Identification, Fuzzy Logic, Image Processing, Mapping, Neural Networks.

- Mathematica <http://www.wolfram.com/>
- Noesys (data exploration and visualisation) from Research Systems <http://www.rsinc.com>
- PulSAR from Phoenix Systems, <http://www.phoenixsystems.co.uk>
- PV-WAVE <http://www.vni.com> data manipulation, visualisation, statistics. Image Processing and Signal Processing toolkits available.
- SARscape <http://www.sarmap.ch>

### 1.2.1.2 EnviView

The EnviView tool, developed by ESA, is described in detail in the ENVISAT Handbook. In general, however, EnviView is a tool capable of opening and decoding data in a format exclusive to the ENVISAT Ground Segment, known as Payload Data Segment (PDS) format. It then displays the data as simple text in HTML format, as graphs, or as images when these are appropriate.

As with the data from all of the ENVISAT instruments, the EnviView is a simple tool to provide a first look at ASAR data files in the PDS format. It uses a graphical user interface for data exploration and visualisations and is intended for the following purposes:

- To be able to open any Level 0, 1b, Level 2 or auxiliary PDS data file.
- To determine and display the contents of a file and the value of any given fields in any data set, except raw source packets (level 0 data).
- To provide basic visualisation of data through simple 2D graphs and images.
- To visualise certain high level data sets in a meaningful manner where a 2D graph conveys little information, especially:
  - ASAR image data sets
  - ASAR Wave spectra.
- To provide a representation of the geographic coverage on a rectangular map projection.
- To export selected data to HDF, ASCII or binary data files, for analysis in COTS tools such as Mathematica, IDL, Excel, and so on..
- To save the contents of a record as HTML text for inclusion in reports.

- To provide support for printing and system clipboard (cut/paste) where possible.
- To be highly portable and to reach as wide an audience as possible.
- To be guaranteed to run on Unix, Windows and MacOS and potentially other platforms too.

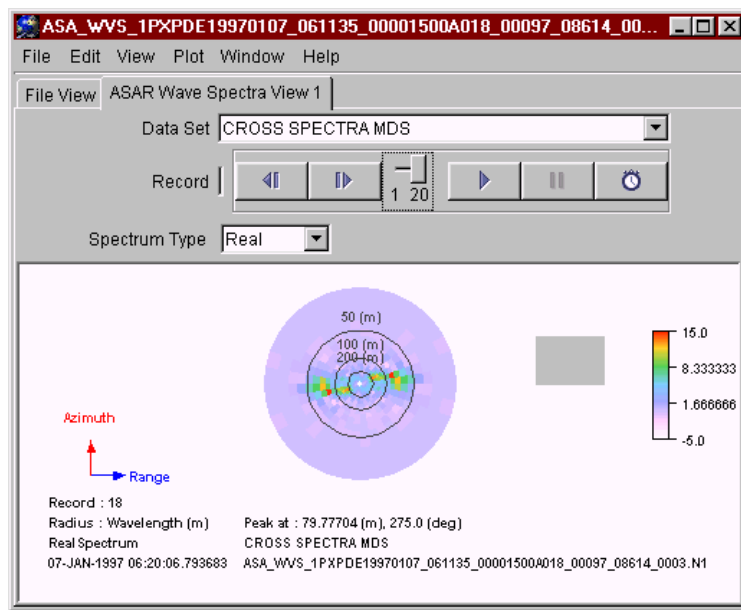


Figure 1.101 Example of Level 1B Wave Product Cross Spectra

[Figure 1.101](#) is an example of a level 1b wave product, as seen using the EnviView ASAR Wave Spectra View window. (See section entitled [Wave Spectra 1.1.5.5](#).). A wave spectrum viewer displays a false colour polar plot showing level 1B or level 2 ASAR wave spectra data. Since the data values are complex, having both real and imaginary parts, various representations of the spectra are possible. Data from one record at a time is displayed with the option of displaying record data sequentially as a movie.

The ASAR level 1B wave spectrum data is complex, containing both real and imaginary parts. EnviView only displays scalar (1 dimensional) values on the ASAR wave spectrum viewer, which means that it can only display either the real parts, the imaginary parts, or some scalar combination of the real and imaginary parts.

ASAR Level 2 data is not complex, hence there is no need to have selection provided for different display types when viewing such a data set. Level 2 data is neither symmetric nor anti-symmetric, and contains information for the entire 360 spectrum.

The complete instructions for the use and application of the EnviView viewer are provided in the EnviView User Guide that is included with the viewer when it is delivered to the customer.

### 1.2.1.3 ASAR Toolbox

The Basic Envisat SAR Toolbox (BEST) is a collection of executable software tools that has been designed to facilitate the use of ESA SAR data. The purpose of the Toolbox is not to duplicate existing commercial packages, but to complement them with functions dedicated to the handling of SAR products obtained from ASAR (Advanced Synthetic Aperture Radar) and AMI (Active Microwave Instrument) onboard Envisat and ERS 1&2 respectively.

The Toolbox operates according to user-generated parameter files. The software is designed with an optional graphical interface that simplifies specification of the required processing parameters for each tool and (for Windows versions only) sets it running.

The interface doesn't include a display function. However, it includes a facility to convert images to TIFF or GeoTIFF format so that they can be read by many commonly available visualisation tools. Data may also be exported in the BIL format for ingestion into other image processing software, and the tools may be integrated within (for example) IDL.

The tools are designed to achieve the following functions:

- Data Import and Quick Look: generation of quick-look and full resolution internal format files from a variety of ESA SAR products and import of TIFF and GeoTIFF images and generic raster data.
- Data Export: output of data to selected common formats (TIFF, Geo TIFF and BIL).
- Data Conversion: conversion between different image formats (e.g. power to amplitude) and transformation of the data by flipping or slant range to ground range reprojection.
- Statistical: calculation of global or local statistical parameters from real image data and computation of the principal components of multiple images. Resampling: over- and under-sampling of an image by means of spatial and spectral methods.
- Co-registration and Coherence Generation: automatic co-registration of both real and complex images, calculation of interferometric coherence and application of automatic geo-correction.
- Radiometric Resolution Enhancement: improvement of the radiometric resolution of a backscatter image.
- Calibration: radiometric correction of an input image to a variety of levels.

The Toolbox has been designed to handle ESA data products from both the Envisat ASAR instrument and the AMIs on ERS 1&2.

ASAR data acquired in Image Mode, Wide Swath Mode, Alternating Polarisation Mode and Global Monitoring Mode, processed to Level 0 or Level 1b (SLC, Precision, Medium Resolution or Ellipsoid Geo-coded), is supported.

Image Data from ERS SAR, processed as RAW, SLC, SLCI, PRI, GEC or GTC, is also supported.

The Toolbox handles the standard Envisat product file format. For ERS data, products generated within the ESA ERS ground segment at D-PAF, I-PAF, UK-PAF and ESRIN are supported, plus data from non-ESA PAF stations, if they are delivered with ESA CEOS annotations.

More information is available from the envisat web site at <http://envisat.esa.int/best>

## 1.3 Further Reading

Further information on the ASAR instrument can be found in documentation available from ENVISAT <http://envisat.esa.int/>

Additional reference sources:

### Ref 1.39

ASAR Science Advisory Group, Editor R.A.Harris, European Space Agency 1998, "ASAR Science and Applications", ESA SP-1225

### Ref 1.40

C H Buck, J-L Suchail, R Torres and M Zink (ESA-ESTEC, NL). "ASAR Performance", ENVISAT Payload Division, Keplerlaan 1, 2200 AG.

### Ref 1.41

R. Torres, C. H. Buck, J-L. Suchail, M. Zink (ESA-ESTEC, NL). "In-Orbit Calibration and Maintenance of the ENVISAT ASAR Antenna Beams", ENVISAT Programme, Keplerlaan 1, 2200 AG.

### Ref 1.42

R. Torres, C. Buck, J. Guijarro and J-L. Suchail (ESA-ESTEC, NL). "ESA's Ground Breaking Synthetic Aperture Radar: The ENVISAT-1 ASAR Active Antenna". APS'99.

### Ref 1.43

J-L. Suchail, C. Buck, J. Guijarro and R. Torres (ESA-ESTEC, NL). "The Development of ENVISAT-1 Advanced Synthetic Aperture Radar". RADAR'99.

### Ref 1.44

P. Mancini, J-L. Suchail, R. Torres, J. Guijarro and C. Buck (ESA-ESTEC, NL). "The

**ENVISAT-1 Advanced Synthetic Aperture Radar. The Development Status". CEOS'98.**

**Ref 1.45**

J. Guijarro, C. Buck, P. Mancini, J-L. Suchail and R. Torres (ESA-ESTEC, NL). "The Development of the ENVISAT-1 ASAR". IGARSS'96.

**Ref 1.46**

J-L. Suchail, C. Buck, A. Schnenberg, R. Torres, M. Zink, ESA/ESTEC. "The ASAR Instrument Verification: Results from the Pre-Flight Test Campaign". Proc. CEOS SAR Workshop April 2001, Tokyo, Japan.

**Ref 1.47**

H Jackson ESA/ESTEC, I. Sinclair, S. Tam. MPB Technologies Inc. "ENVISAT ASAR Precision Transponders". CEOS SAR Workshop 26-29 October 1999, ESA-SP450

**Ref 1.48**

R.K. Hawkins, et al. "RADARSAT Precision Transponders". Adv. Space Res. Vol. 19, No. 9, pp. 1455-1465, 1997.

**Ref 1.49**

C H Buck, J-L Suchail, R Torres and M Zink, "ASAR Performance", Proc. of CEOS SAR Workshop 2001, Tokyo, Japan, 2.-5. April 2001.

**Ref 1.50**

R. Torres, C. H. Buck, J-L. Suchail, M. Zink, "In-Orbit Calibration and Maintenance of the ENVISAT ASAR Antenna Beams", Proc. of CEOS SAR Workshop 2001, Tokyo, Japan, 2.-5. April 2001.

**Ref 1.51**

F.H. Wong, I.G. Cumming, "A Combined SAR Doppler Centroid Estimation Scheme Based Upon Signal Phase", IEEE Trans Geoscience and Remote Sensing, 34-3, May 1996

**Ref 1.52**

T.M. Lillesand, R.W. Kiefer, "Remote Sensing and Image Interpretation", 2nd ed, Wiley 1987

**Ref 1.53**

Alley, R. B., and J. M. Whillans, "Changes in the west Antarctic ice sheet", Science, 254, 959-963, 1991.

**Ref 1.54**

Blakenship, D.D., R. E. Bell, S. M. Hodge, J. M. Brozena, J. C. Behrendt, and C. A. Finn, "Active volcanism beneath the West Antarctic ice sheet and implications for ice-sheet stability", *Nature*, 361, 526-529, 1993

**Ref 1.55**

Bilham, R., "Earthquakes and sea level: space and terrestrial geodesy on a changing planet", *Rev Geophys.*, 29, 1-29, 1991.

**Ref 1.56**

Bull, W. B., "Geomorphic responses to climatic change", Oxford University Press, 326 p, 1991.

**Ref 1.57**

Burke, K., and T. H. Dixon, "Topographic Science Working Group Report to the Land Processes Branch, Earth Science and Applications Division", NASA, Lunar and Planetary Institute, 64 p., 1988.

**Ref 1.58**

Dahlen, F. A., and T. D. Barr, "Brittle frictional mountain building 1. Deformation and mechanical energy budget", *J. Geophys. Res.*, 94, 3906-3922, 1989.

**Ref 1.59**

Dixon, T. H., M. Bursik, S. Kornreich-Wolf, M. Heflin, F. Webb, F. Farina, and S. Robaudo, "Constraints on deformation of the resurgent dome, Long Valley caldera, California, from space geodesy, in Contributions of Space Geodesy to Geodynamics", D. Smith and D. Turcotte, eds., American Geophysical Union Geodynamics Series, 23, 193-215, 1993

**Ref 1.60**

Elachi, C., "Spaceborne imaging radar: geologic and oceanographic applications", *Science*, 209, 1073-1082, 1980

**Ref 1.61**

Francis, O., and P. Mazzega, "Global charts of ocean tides loading effects", *J. Geophys. Res.*, 95, 11411-11424, 1990.

**Ref 1.62**

Hahn, C.J., S.G. Warren, J. London, R.L. Jenne, and R.M. Chervin, "Climatological data for clouds over the globe from surface observations", Report NDP-026, Carbon Dioxide Information Center, Oak Ridge TN, 57 p. (also available as CD-ROM), 1987.

**Ref 1.63**

Harding, D.J., J.L. Bufton, and J.J. Frawley, "Laser altimetry of terrestrial topography: vertical accuracy as a function of surface slope, roughness, and cloud cover", *IEEE Trans. Geosci. Rem. Sens.*, in press, 1994a.

**Ref 1.64**

Harrison, C. G. A., "Rates of continental erosion and mountain building", *Geol. Rundsch.*,

83, 431-447, 1994.

**Ref 1.65**

Herzfeld, U. C., "A method for seafloor classification using directional variograms, demonstrated for data from the western flank of the Mid-Atlantic Ridge", *Math. Geology*, 25, 901-924, 1993.

**Ref 1.66**

Herzfeld, U.C., I. I. Kim, J. A. Orcutt, and C. G. Fox, "Fractal geometry and seafloor topography: theoretical concepts versus data analysis for the Juan de Fuca Ridge and the East Pacific Rise", *Ann. Geophysicae*, 11, 532-541, 1993.

**Ref 1.67**

Meier, M. F., "Contribution of small glaciers to global sea level", *Science*, 226, 1418-1421, 1984.

**Ref 1.68**

Meier, M. F., "Role of land ice in present and future sea level change, Sea Level Change", National Academy Press, 171-184, 1990.

**Ref 1.69**

Milliman, J. D., and R. H. Meade, "World-wide delivery of river sediment to the oceans", *J. Geol.*, 91, 1-21, 1983.

**Ref 1.70**

Mueller, I. I. and S. Zerbini (eds), "The interdisciplinary role of space geodesy", Erice, Sicily Workshop Proceedings, Lecture Notes in Earth Sciences, 22, Springer-Verlag, Berlin, 1989.

**Ref 1.71**

Balababa L., Schumann R., Adrianasolo H., & Tinsley R., 1997, "Identification of Rice Cropping Areas in the Mekong Delta (Vietnam) using Radar Imagery", ESA EOQ No. 56-57, December 1997.

**Ref 1.72**

Engen G. & Johnsen H., "SAR Ocean Wave Inversion using Image Cross Spectra", *IEEE Trans. Geosci. Remote Sensing*, Vol. 33, No.4, pp.1047-1056.

**Ref 1.73**

ESA, 1995, "New Views of the Earth: Scientific Achievements of ERS-1", ESA SP-1176/I.

**Ref 1.74**

ESA, 1996, "New Views of the Earth: Applications Achievements of ERS-1", ESA SP-1176/II.

**Ref 1.75**

ESA, 1997a, "New Views of the Earth: Engineering Achievements of ERS-1", ESA

SP-1176/III.

Ref 1.76

ESA, 1997b, "Fringe 96 Workshop ERS SAR Interferometry", ESA SP-406, Vol. I, March 1997 & Vol. II, December 1997.

Ref 1.77

ESA, 1998, "Envisat Mission: Opportunities for Science and Applications", ESA SP-1218.

Ref 1.78

Luckman A.J., Baker J.R., 1995, "The Effects of Topography on Radar Scattering Mechanisms from Coniferous Forest and Upland Pasture", MAC Europe 91 Final Results Workshop Proceedings, ESA WPP-88, January 1995.

Ref 1.79

Mastenbroek K., 1998, "High resolution wind fields from ERS SAR", ESA EOQ No. 59, June 1998

## 1.4 Image Gallery

Multi-look SAR Image

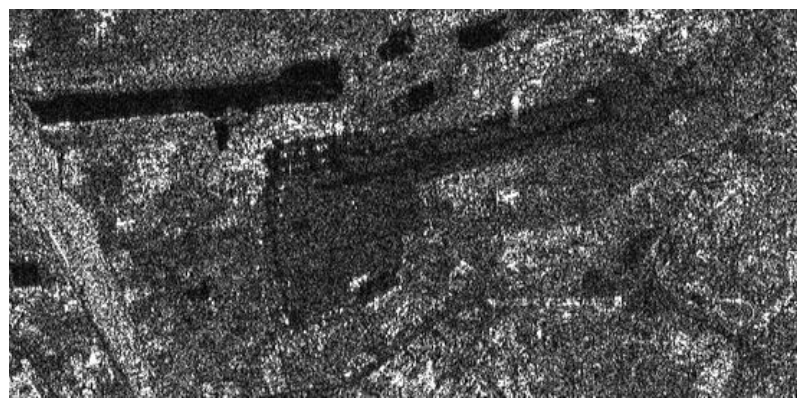


Figure 1.102 One look radar image showing speckled appearance



Figure 1.103 Multi-look radar image resulting from combining several images

The signal from the synthetic aperture radar can be exploited to produce an image. The radar image differs substantially from an optical image: it is, in reality, a map of apparent radar backscattering (coded as different grey levels), which not only depends on the target reflectivity at microwave wavelengths, but also depends on the viewing geometry. One additional salient feature of a microwave image, which makes it different from any optical image we are used to, is that the incoming light (in this case, the transmitted radar signal) is a monochromatic coherent light. As a result, the image appears speckled (see [figure 1.102](#) above). To reduce this effect several images are incoherently combined as if they corresponded to different looks of the same scene. The resulting improvement of the image interpretability is shown in the [figure 1.103](#).

New ASAR Features



Figure 1.104 ASAR image using one polarisation choice



Figure 1.105 ASAR image of same area as in the other figure using different polarisation choice

Among the many new features that ASAR will present when compared, not only to ERS-1/2 but, to any other spaceborne flying SAR is the capability to transmit and receive signals with different polarisations (either vertical or horizontal). Because any given target responds in a different way when illuminated with a different polarisation (see example in the figure aside), the potential of this technique in terms of applications like classification, agriculture, detection are enormous.

ASAR will also be characterised by the capability to image large areas (up to 400 km swath width), thus reducing the revisiting time compared to ERS-1/2.

### Glacial Topography

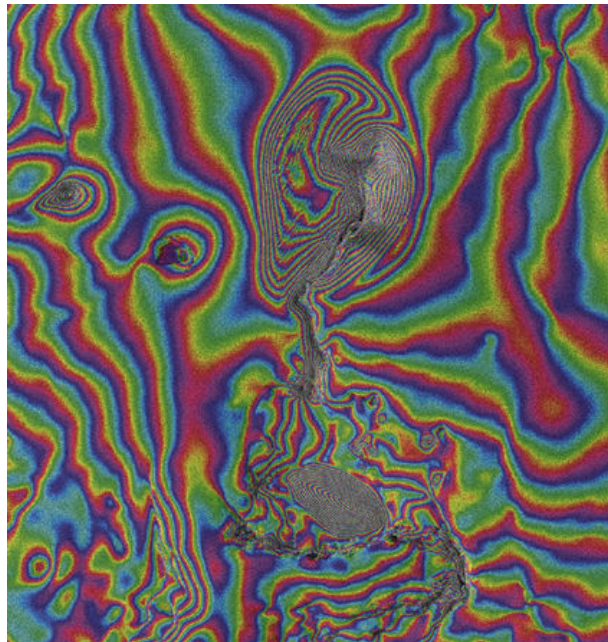


Figure 1.106 Interferogram from ERS tandem mission of part of the Vatnajokull Glacier, Iceland, May 1997

This is an interferogram from ERS tandem mission of part of the Vatnajokull Glacier, Iceland, May 1997. This shows glacial topography, including a major depression (400-600 m deep) in the upper central part of the image, caused by sub-glacial volcanic eruption (acknowledgement: H. Rott, Institut fr Meteorologie und Geophysik, Innsbruck, Austria). In this example, by comparing the phase difference between the images of the same scene taken by two slightly displaced points in space, a so-called interferogram is built. This example is from the ERS-1/2 tandem mission. Observations from separate ASAR passes can achieve a similar result.

#### Earth Movements Due To Earthquake

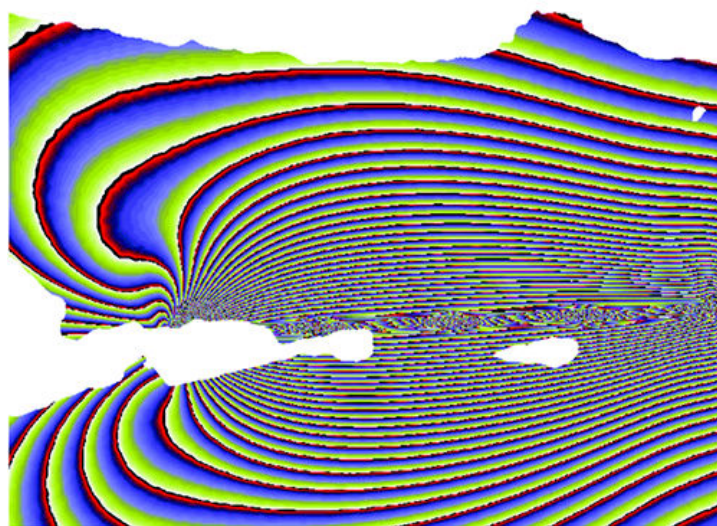


Figure 1.107 SAR differential interferogram in an area between Istanbul and the Lake of Sapanca showing ground displacement of 28 mm

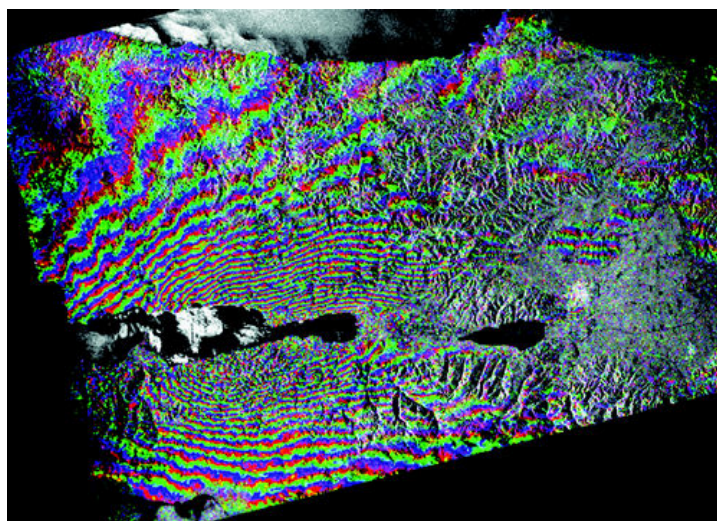


Figure 1.108 SAR differential interferogram showing the surface deformation in an area between Istanbul and the Lake of Sapanca showing deformation of about 80 cm.

SAR interferometry can be used to quantify the dislocation produced by an earthquake. ERS-1 and 2 data were used to obtain a SAR differential interferogram showing the surface deformation in an area between Istanbul and the Lake of Sapanca. A theoretical

---

deformation model derived from geophysical data was compared with the ERS SAR-derived phase interferogram.

The result of the modelled earthquake movement can be recomputed and displayed as fringes. The geophysical interpretation of the model is that the rupture occurred along an east-west fault, causing a predominantly horizontal movement (right-lateral strike). In the interferogram in [figure 1.107](#), each colour cycle from red to yellow corresponds to a ground displacement of 28 mm in the slant range direction (ERS satellite's viewing direction). By counting the number of fringes, one can calculate the co-seismic deformation. In the [figure 1.108](#),  $28 \pm 2$  fringes can be observed across the image. They suggest a deformation of about 80 cm.

#### Wind Field Distribution

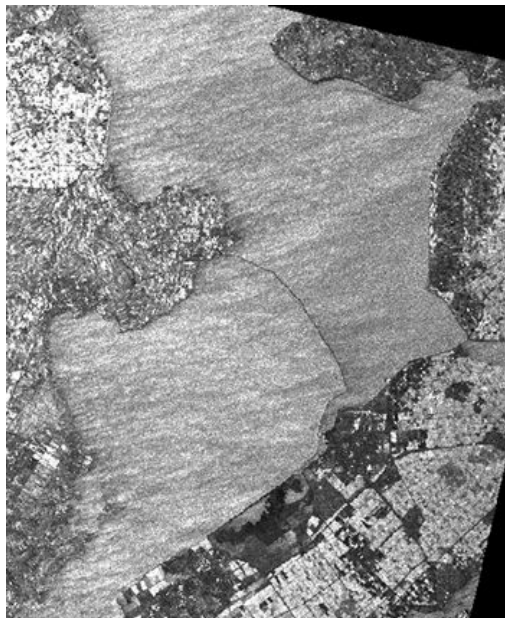


Figure 1.109 Large part of Lake Ijssel in The Netherlands

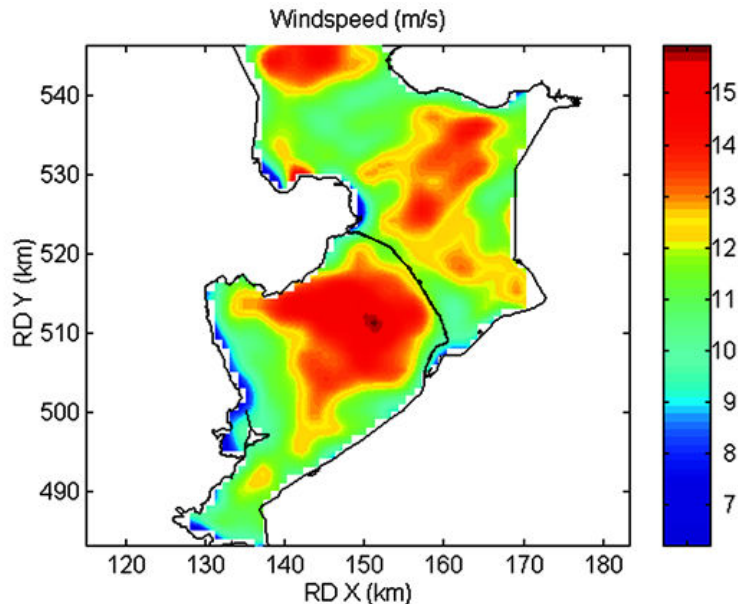


Figure 1.110 Large part of Lake Ijssel in The Netherlands showing wind field obtained from the SAR

The ERS-1/2 missions have successfully demonstrated that the radar cross-section measured over the oceans can be related to wind speed. The retrieval of the wind field from a SAR image is split into two parts. First, the wind direction is determined from wind-rows, which are often visible on the SAR image. In the second stage, the radar backscatter measured by the SAR is related to the wind speed, given the wind direction from the wind streaks.

The top SAR image, [figure 1.109](#), shows a large part of Lake Ijssel in The Netherlands. The wind field obtained from the SAR image is shown below it in [figure 1.110](#).

Forest Cover Classification

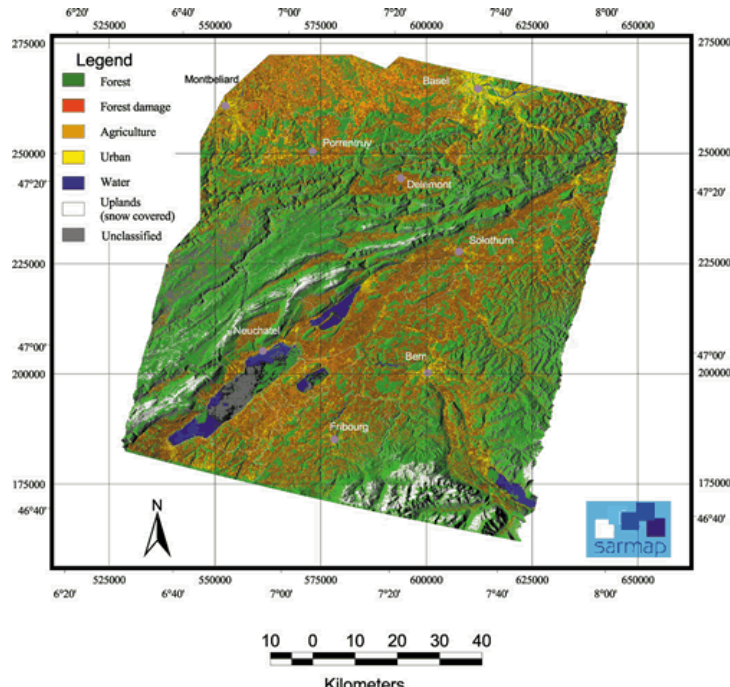


Figure 1.111 Classified forest image overlayed on a DEM, generated using InSAR techniques

Comparing imagery from sequential SAR passes shows different degrees of coherence. Bare or sparsely vegetated soil has a high degree of coherence as there is little or no change in the scatterer properties between the two acquisitions. Forested areas, on the other hand, show a low degree of coherence, as the elementary scatterers (i.e. leaves) in each pixel move between the two acquisitions, mainly due to wind and, hence, lead to decorrelation in the imagery. This fact can be exploited to discriminate between forest and non-forest vegetation. Moreover, in this case, given two coherence images, one prior to the storm (4/5 April 1999) and one after the storm (9/10 January 2000), a change within forested areas from low coherence to high coherence should be indicative of forest damage. Using the coherence combined with the backscatter data, a supervised classification was carried out to identify forest areas damaged, as well as the other cover types in the scene. The classified image overlayed on a DEM, generated using InSAR techniques, is shown [figure 1.111](#) above.

## Ice Classification

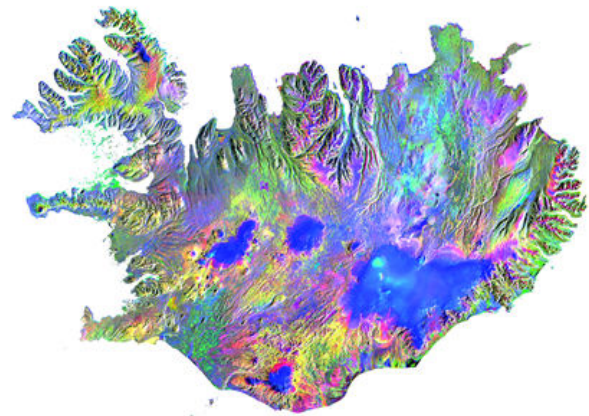


Figure 1.112 A multi-temporal image of Iceland

By combining three images acquired over different passes (over Iceland, in the figure above), a multi-temporal image can be produced (the colours blue, green and red are assigned in increasing date order).

#### Snow Cover

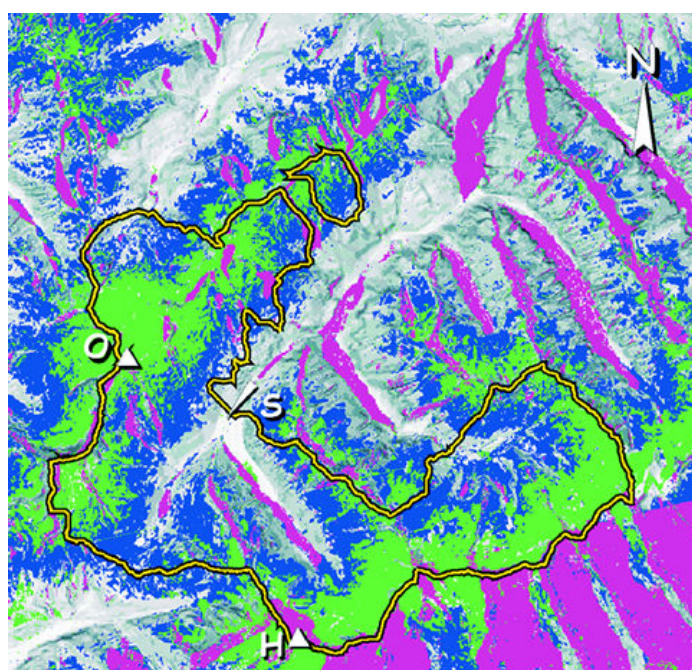


Figure 1.113 ERS-2 ascending and descending passes showing snowmelt runoff

The extent of snow covered area is a key parameter for snowmelt runoff modelling and forecasting. Because SAR sensors provide repeat pass observations, irrespective of cloud coverage, they are of interest for operational snowmelt runoff modelling and forecasting.

The algorithm for mapping melting snow is based on repeat pass images of C-band SAR and applies change detection to eliminate the topographic effects of backscattering. At C-band dry snow is transparent and backscattering from the rough surfaces below the snowpack dominates. This is the reason why the return signal from dry snow and snow-free areas is very similar. When the snow becomes wet, backscattering decreases significantly. Therefore wet snow can be detected by the backscatter changes when compared to dry snow or snow-free conditions [Nagler,1996 ].

An example of snow maps derived from ERS-2 ascending and descending passes are shown above figure in [figure 1.113](#) (on 12 May 1997 in blue and green and on 16 June 1997 in green only),

#### Storm Damage Assessment

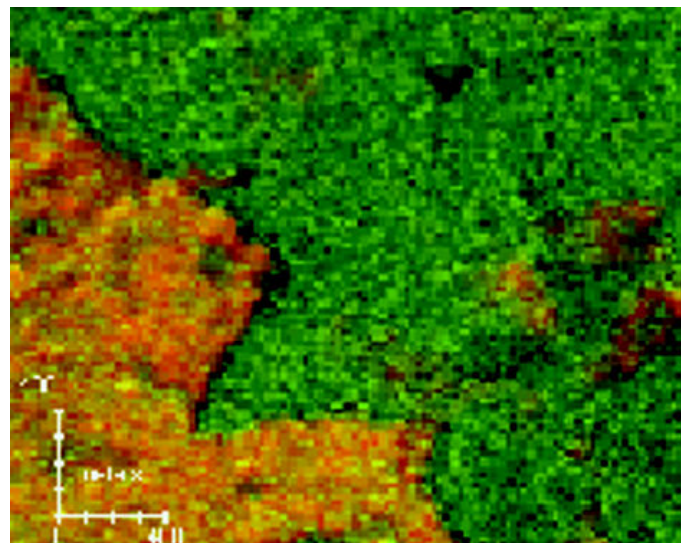


Figure 1.114 Land cover measured with SAR before a storm in the forest of Haguenau, 30 km north of Strasbourg

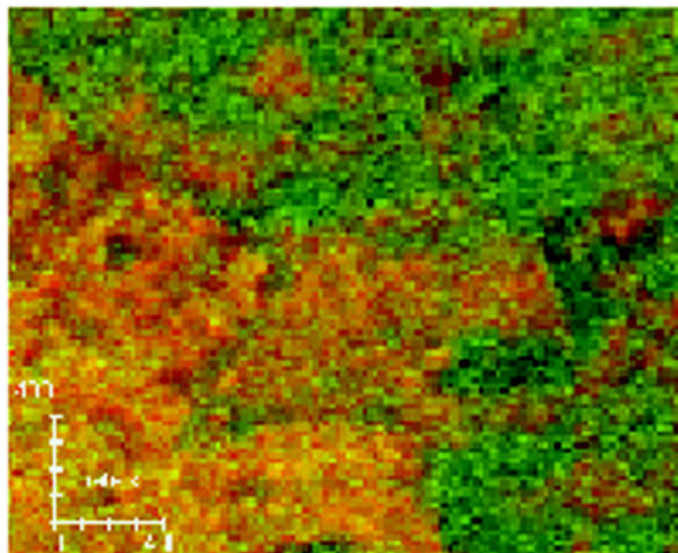


Figure 1.115 Land cover measured with SAR after a storm in the same forest of Haguenau, as shown in the figure above showing a strong increase of the coherence level within forested areas.

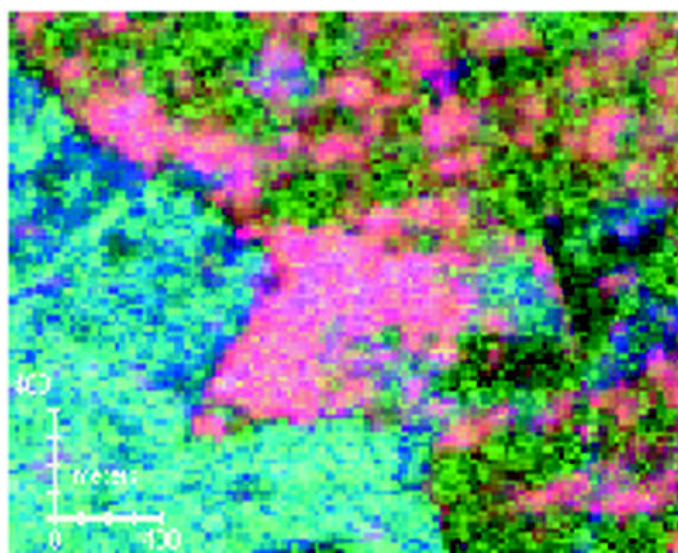


Figure 1.116 Damage image composite of the land cover measured with SAR after a storm in the same forest of Haguenau, as shown above.

[Figure 1.114](#) , [figure 1.115](#) and [figure 1.116](#) above show the comparison of land cover

measured with SAR before ([figure 1.114](#)) and after ([figure 1.115](#) and [figure 1.116](#)) a storm in the forest of Haguenau, 30 km north of Strasbourg. The top image is a coherence standard product showing bare soils and cultivated areas as orange-red, and wooden areas as green.

After the storm, the coherence product shown in [figure 1.115](#), indicates a strong increase of the coherence level within forested areas.

In the 'damage' image composite, shown in [figure 1.116](#), pink tones provide an estimate of the level of the damage. In this case, a level of damage of 50% had been reported by the forest service which corresponds to the increase of coherence over the area. This imagery was taken 31 Oct 1999 and 9 January 2000.

#### Flood Monitoring

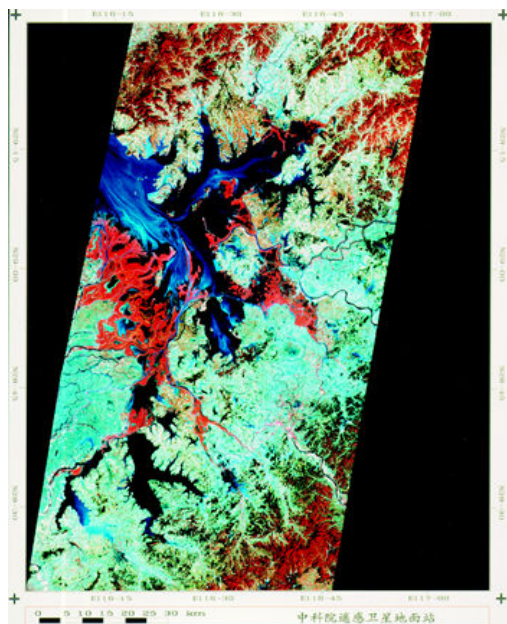


Figure 1.117 SAR image of flooded area

Floods are among the most severe risks on human lives and properties. The forecast and simulation of floods is essential for planning and operation of civil protection measures (e.g. dams, reservoirs) and for early flood warning (evacuation management). The economic importance of flood forecasting becomes clear considering that 85 % of civil protection measures taken by the EC Member States are concerned with floods (EC Report Task Force Water, 1996). Floods can be monitored in real time by ASAR as shown by the example given in [figure 1.117](#) above..

#### Soil Moisture And Flood Forecasting

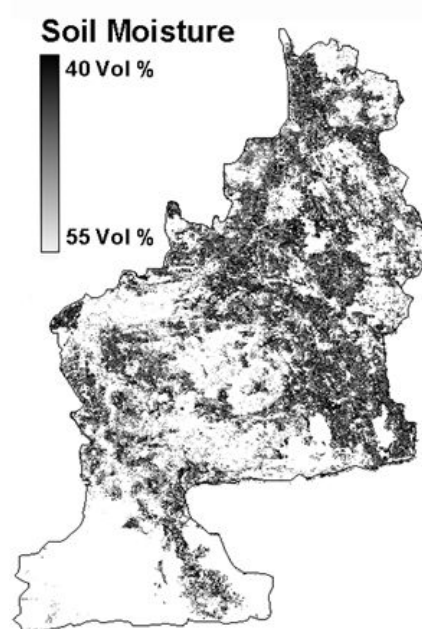


Figure 1.118 An example of top soil moisture distribution

Hydrological modelling for flood forecast is widely applied and makes use of satellite remote sensing data. A remotely sensed, interferometrically derived, elevation model is used to determine topographic information on the watershed. Together with a soil map, the watershed is then classified into hydrologically relevant classes of water storage capacity.

For the dynamic part of the system, which deals with a specific flood event, rainfall information is required as driving variable. In addition, soil moisture information is of relevance for runoff modelling because it determines the extent of saturation of the watershed and thereby the partitioning of rainfall into surface runoff and infiltration. The same amount of rainfall, which normally does not lead to a significant increase in water level, can cause a severe flood, if the soil has already been filled with water and the storage capacity is close to zero.

SAR data is used in the model also to derive soil moisture distributions to improve the antecedent moisture characterisation of the watershed. The basis of the approach for surface soil moisture determination from SAR is an algorithm developed for ERS data (Mauser et al. 1995) which was already successfully used in a series of applications (Rombach & Mauser 1997, Schneider & Oppelt 1998). An example of top soil moisture distribution is illustrated in [figure 1.118](#) above.

Sea Ice Navigation

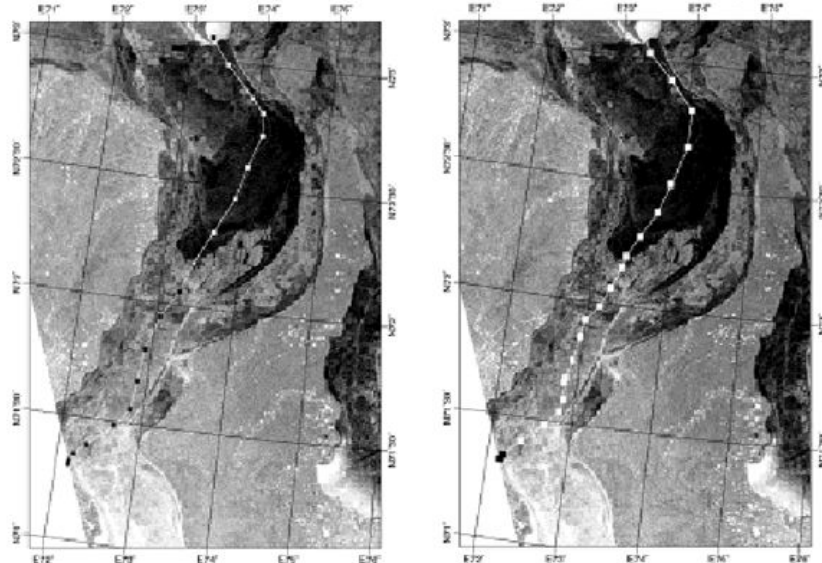


Figure 1.119 Ship performance plotted on an ERS-SAR scene (Image courtesy of Nansen Environmental and Remote Sensing Center)

Radar extracted sea-ice information can satisfy operational needs for navigation, offshore operations and weather forecasting.

Radar images downloaded via the Internet are used in real time to organise icebreaker interventions and to address vessel routes. The image in [figure 1.119](#) above illustrates ship performance plotted on an ERS-SAR scene (left: four days after the pass of an icebreaker, right: eight days after). The distance between each point represents one hour of sailing. Use of lower resolution modes, such as wide swath and global monitoring modes, provided from ASAR will offer the possibility to monitor larger areas with more frequent revisits. The variable incidence angle can be used to enhance sea-ice edges. Polarisation will allow improved ice-type discrimination and probably will help in forecasting of leads or ice pack development.

Image Mode Medium-Resolution ASAR Image

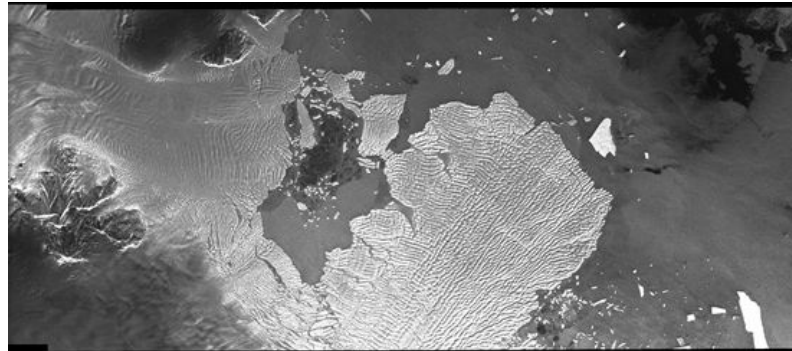


Figure 1.120 Image Mode Medium-Resolution Image of Walgreen Coast, Antarctica generated from ERS raw data using the ASAR processing algorithm

#### Image Mode Precision ASAR Image



Figure 1.121 Image Mode Precision Image, generated from ERS raw data using the ASAR Processor, of Bathurst Island, Canada.

Pixel = 12.5 m

Spatial Res. = 30 m



---

ENL = 3.9

Coverage = 56 to 107 km width x 100 km

---

# Chapter 2

## ASAR Products and Algorithms

In general, the ENVISAT product strategy is to offer a simple, flexible product format and structure, featuring a unique format, as well as stripwise processing and a floating scene concept. ENVISAT product data sets will extend over a five-year period, and will include data from a number of instruments and operating modes collected in continuous operation or discrete segments. In order to handle this volume and range of data, it is necessary to separate the data into manageable sizes and deliver them as product files. The product strategy is based on:

- a systematic processing of all acquired data into medium resolution of [stripwise](#) products in order to have a reference archive with no discontinuities between pixels [along-track](#)
- child products extracted from parent products at Level 0, Level 1B or Level 2
- a [floating scene](#) concept to allow flexibility for users to order a portion of the stripwise the product that fulfils their needs.
- processing of precision, high resolution products on request

Furthermore, as a design rule, the number of facilities generating and using product information has been minimised to limit the effect of any changes in the contents of the

---

product header in the application software.

The general layout for all ENVISAT includes the following records:

- Main Product Header (MPH) - The MPH has a fixed length and the format is identical for all ENVISAT products.
- Specific Product Header (SPH) - The SPH is defined for each product and provides additional information, applicable to the whole product, related to the processing.
- Data Set (DS) - The DS contains the instrument's scientific measurements. Product Confidence Data (PCDs) - The PCD provides an evaluation of the overall quality of the product.

This chapter of the ASAR Handbook will provide detail on all of the ASAR products and associated algorithms, including a discussion on ASAR characterisation and calibration, as well as hints on data handling. The details of the layouts for each product will be found in chapter "[Data Formats.](#)" ([Chapter 6.](#))

## 2.1 Products and Algorithms Introduction

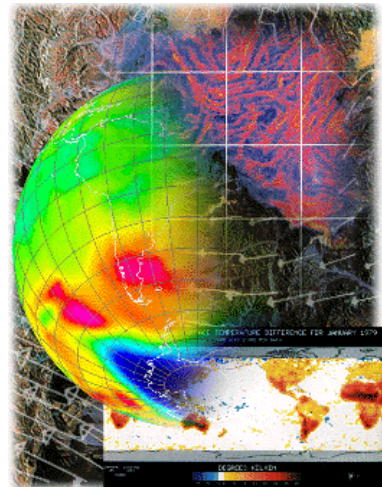


Figure 2.1

The specifications for the standard [Advanced Synthetic Aperture Radar \(ASAR\)](#) data products are shown in [table 2.1](#) below. Many of the product types and definitions are similar to those used for the [European Remote Sensing Satellite \(ERS\)](#). For instance, [Precision](#), [Ellipsoid Geocoded](#), and [Single-Look Complex](#) images have the same nominal [resolution](#)

and [pixel](#) spacing as their ERS equivalents. (For a discussion on the differences between resolution and pixel spacing see )

## ASAR Measurement Modes

The Advanced Synthetic Aperture Radar is a high-resolution [imaging radar](#) that can be operated in 5 distinct Measurement Modes:

- [Image Mode \(IM\)](#)
- [Alternating Polarisation Mode \(AP\)](#)
- [Wide Swath Mode \(WS\)](#)
- [Global Monitoring Mode \(GM\)](#) and
- [Wave Mode \(WV\).](#)

Within each mode, several different image [swaths](#) may be used. IM, AP, and WS modes are designated as High Rate (HR) modes, and have a downlink rate of 100 Mbps. GM and WV are Low Rate (LR) modes and have a data generation rate of 0.9 Mbps.

In addition, ASAR supports 2 Auxiliary Modes (Test Mode and [Module Stepping Mode 2.5.1.2.3.3.](#)) and one Calibration Mode ([External Characterisation Mode 2.5.1.2.2.4.](#)), which are used for testing, calibration and instrument monitoring.

Table 2.1 Standard specifications for ASAR data products

Product ID	Product Name	Nominal Resolution(m) (range x azimuth)	Nominal Pixel Spacing (m) (range x azimuth)	Approx.Coverage (km) (range x azimuth)	Equivalent No. of Looks
IMP	<a href="#">Image Mode Precision 2.6.2.1.1.2.1.2.</a>	30 x 30	12.5 x 12.5	56-100 x 100	> 3
IMS	<a href="#">Image Mode Single-Look Complex 2.6.2.1.1.2.1.1.</a>	9 x 6 - -	natural	56-100 x 100	1
IMG	<a href="#">Image Mode high-resolution Ellipsoid Geocoded 2.6.2.1.1.2.1.3.</a>	30 x 30	12.5 x 12.5	56-100 x 100	> 3
IMM	<a href="#">Image Mode medium-resolution 2.6.2.1.1.3.1.1.</a>	150 x 150	75 x 75	56-100 x 100	40
IMB	<a href="#">Image Mode Browse 2.6.2.1.3.1.1.</a>	450 x 450	225 x 225	56-100 x 100	80
APP	<a href="#">Alternating Polarisation Precision Image 2.6.2.1.1.2.1.5.</a>	30 x 30	12.5 x 12.5	56-100 x 100	> 1.8
APS	<a href="#">Alternating Polarisation Single-Look Complex 2.6.2.1.1.2.1.4.</a>	9 x 12	natural	56-100 x 100	1
APG	<a href="#">Alternating Polarisation Mode high-resolution Ellipsoid Geocoded 2.6.2.1.1.2.1.6.</a>	30 x 30	12.5 x 12.5	56-100 x 100	> 1.8
APM	<a href="#">Alternating Polarisation Mode medium-resolution 2.6.2.1.1.3.1.2.</a>	150 x 150	75 x 75	56-100 x 100	50
APB	<a href="#">Alternating Polarisation Mode Browse 2.6.2.1.3.1.1.</a>	450 x 450	225 x 225	56-100 x 100	75
WSM	<a href="#">Wide Swath Mode medium-resolution 2.6.2.1.1.3.1.3.</a>	150 x 150	75 x 75	400 x 400	11.5
WSB	<a href="#">Wide Swath Mode Browse 2.6.2.1.3.1.3.</a>	1800 x 1800 (approximately)	900 x 900	400 x 400	30 to 48
WVI	<a href="#">Wave Mode Imagger and Imagger Power Spectrum 2.6.2.1.2.1.1.</a>	9 x 6	natural	5 x 5	1
WVS	<a href="#">Wave Mode Image Spectra 2.6.2.1.2.1.2.</a>	N/A	N/A	5 x 5	N/A
GMI	<a href="#">Global Monitoring Mode Image 2.6.2.1.1.3.1.4.</a>	1000 x 1000	500 x 500	400 x 400	7 - 9
GMB	<a href="#">Global Monitoring Mode Browse</a>	2000 X 2000	1000 x 1000	400 x 400	11 - 15

---

Product ID	Product Name	Nominal Resolution(m) (range x azimuth)	Nominal Pixel Spacing (m) (range x azimuth)	Approx.Coverage (km) (range x azimuth)	Equivalent No. of Looks
	<a href="#">2.6.2.1.3.1.4.</a>				

For additional product summary tables refer to "[Organisation of Products. 2.2.](#)"

### Product Generation

Product generation may fall into two major classes. These are:

- Systematic - Medium resolution and browse products are generated automatically for all received data in strip-line format.
- On Request - Products are not generated unless specifically requested by a user, such as Precision, Ellipsoid Geocoded and Single-Look Complex images.

In addition, the systematic products may be subdivided into two categories based on the production time:

- Near Real Time - There are two types of Near Real Time (NRT) products, those to be produced within 3 hours and those to be produced within one day.
- Off-line - Some products will be processed off-line. The availability time depends on the complexity of the processing and the availability of auxiliary data. Delivery time ranges from two business days to four weeks. Off-line products benefit from the more precise orbit information which becomes available later.

### Stripline Products

Stripline products are generated along a complete segment or an orbit. Geometric and radiometric continuity are ensured along the complete segment or orbit. Scenes can be ordered from within a stripline, then extracted and distributed via the PDS User Services. Scene sized is based on granules, an area consisting of the along-track distance by the full swath width. The framing constraints are that the scene must contain an integer number of granules, beginning and ending anywhere within the stripline and must be a full swath width. Child products may be sized to be any multiple of a granule. Stripline processing of browse, medium- and low-resolution data will produce products for up to 10 minutes data acquisition in Image, Alternating Polarisation and Wide Swath Modes, and up to a full orbit for Global Monitoring Mode.

In order to achieve stripline processing, the full data segment is divided across multiple PF-ASAR processors, as shown in [figure 2.2](#) below. The output of each processor is called a slice, and the slices are concatenated together to form the final stripline product. Each slice is divided into an integer number of granules, which are used to facilitate child product extraction.

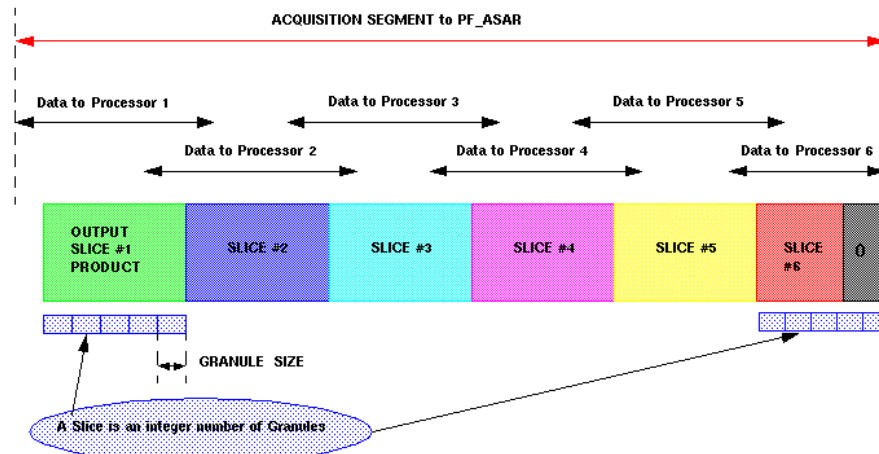


Figure 2.2 System design for stripline processing

For a detailed description of strip-line processing see the section entitled "["ASAR Stripline Product Processing" 2.6.1.2.5.](#)

#### Floating Scene Concept on Archived Products

There is no reason why a user's region of interest should be limited to that which matches the archived product, either in terms of size or geographical position. For these reasons, production has been disassociated from the dissemination and, according to the floating scene concept, a multiple of the minimum scene size only can be disseminated if necessary. The size of a product can be anything from the whole data downlink segment to the minimum scene size, without any constraint on the beginning of the product. Regardless of the size, the extracted product will have a size equal to a multiple of the minimum scene size.

For ASAR, the minimum product size is a single granule, which is a pre-defined, along-track distance by the full swath width.

This flexibility is obtained by the Archiving Facility (ARF), which allows a product to be selectively extracted from an existing archived product without any processing. This corresponds to the child product concept, which is discussed below. (Also see "["Floating scene concept for NRT products"](#) discussed below.)

For products processed systematically, the user selects the position of one or more scenes along the acquired data segment. The scene starts at granule boundary, as shown in [figure 2.3](#) below.

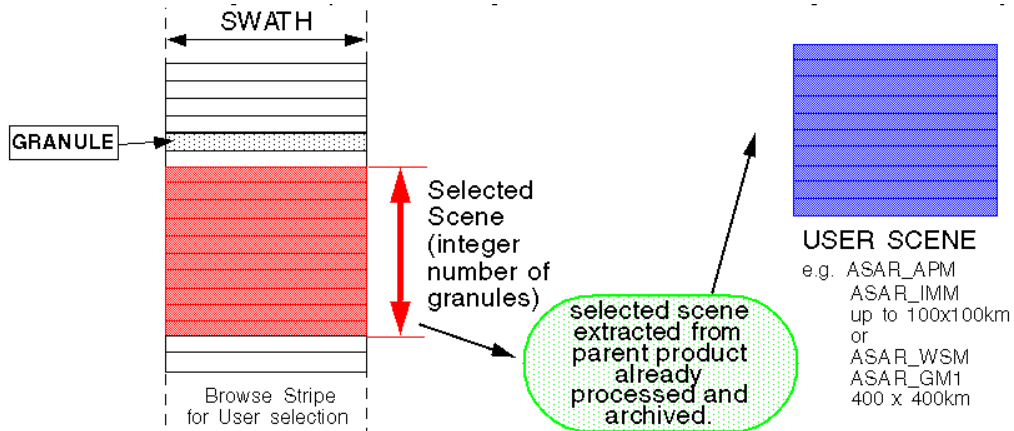


Figure 2.3 The selection of the scene starts at granule boundary

For products generated on request, such as Alternating Polarisation (AP) and Image Mode (IM) precision products, the user can select a scene starting from any time along the acquisition data segment (no framing constraint), as shown in [figure 2.4](#) below. These products have fixed sizes.

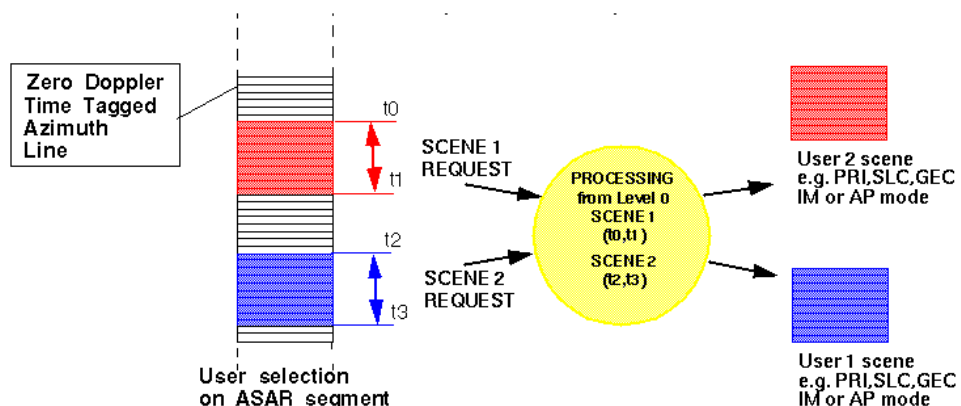


Figure 2.4 The selection of a scene can start from any time along the acquisition data segment

### Child Product Concept

A child is the result of the extraction of a set of data from a parent product (Level 0, Level 1B, Level 2). Generation of child products can be formulated in terms of time, Data Set

(DS), or Instrument Source Packet (ISP) selection, in terms of either segments or scenes; that is:

- time window
- geographic zone (search using the LADS with the help of the PDS inventory)
- data subset

For generation of scenes, the only extraction criteria available are times. When performing child extraction, it is possible to output either a segment corresponding to the time window, or a set of scenes containing the time window, as depicted in [figure 2.5](#) below.

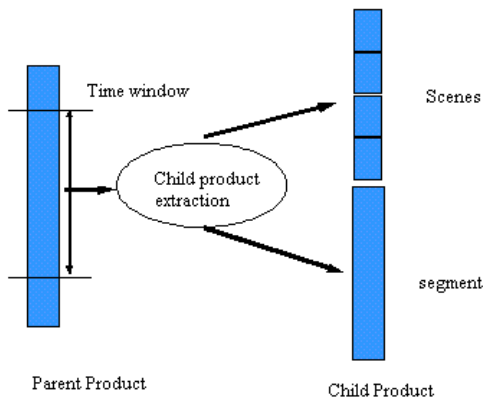


Figure 2.5 Child product extraction

When a child extraction is required against consecutive slices archived at the ARF, the child product generation can apply to several parent products. These parent products are identified through their physical names and their Stripline Continuity Indicators (SCI).

Again, the result of such a child product extraction could be formulated in terms of either segment or scenes.

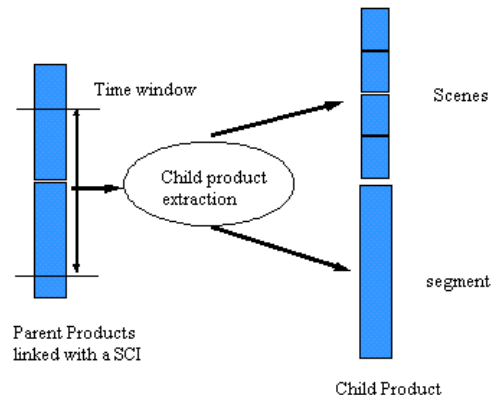


Figure 2.6 Child product extraction from consecutive slices

For a further discussion of these products, as they relate to ASAR, refer to ["Child Products"](#) [2.1.1.](#).

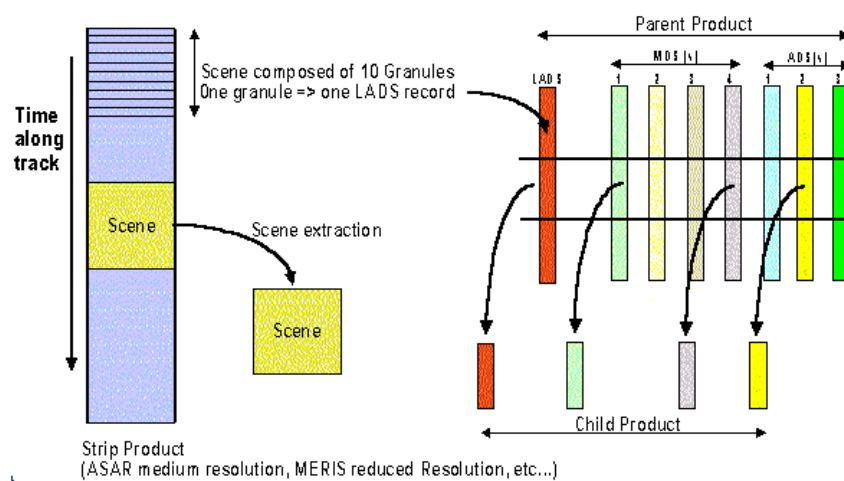


Figure 2.7 Product generation and extraction

Floating scene concept for NRT products

The ARF will be able to generate and distribute scenes associated to the concatenation or

the extraction of the different consecutive slices it has received. For NRT mode distribution, the ARF will transmit as quickly as possible each scene to the DF, not waiting for the reception of the set of complete slices before building and transmitting the associated scenes.

Each scene will be transmitted immediately as it becomes complete.

The NRT scene generation is illustrated below:

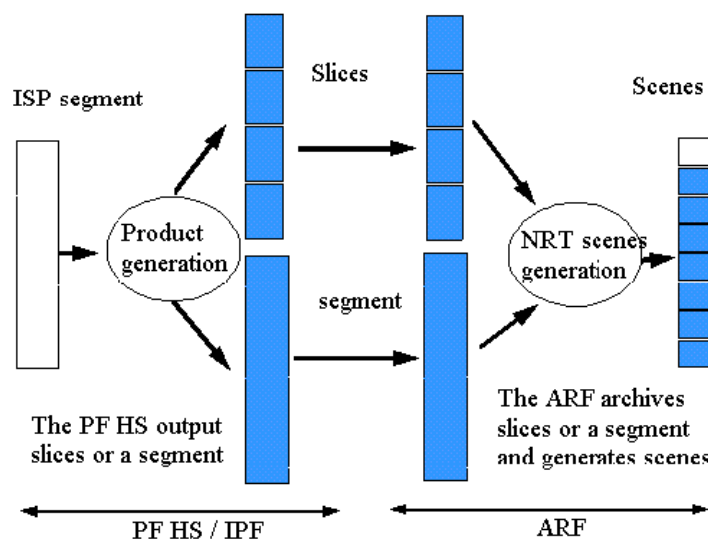


Figure 2.8 Scene generation in NRT

## General Product Layout

The data production format for one product will consist of:

- One file [Main Product Header \(MPH\)](#) - common format for all products
- [Specific Product Header \(SPH\)](#) - common format in Level 0 products, specific format in Level 1B and in Level 2 products.
  - [Data Set Descriptor \(DSD\)](#) - (included in SPH): common format in all products
  - [Data sets \(DS\)](#):
    - [Global Annotation Data Set](#) (GADS): ADS which contains [Data Set Records](#) (DSRs) without time tag.
    - [Measurement Data Set](#) (MDS): The MDS-DSRs are time tagged in [MJD2000](#).
    - [Auxiliary Data Set](#) (ADS): The ADS-DSRs are time tagged in [MJD2000](#).

- 
- [Localisation ADS](#) (LADS): only in Level 1B and Level 2 products, specific format for each product ID. Inventory has a subsampled LADS, called SLADS. The LADS-DSRs are time tagged in MJD2000.
  - [Summary Quality ADS](#) (SQ ADS): ADS of quality parameters, stored in Inventory. ( The SQADS-DSRs are time tagged in MJD2000.)

All data sets are filled with DSRs, and each DSR starts with a time entry. The time entry permits correlation between all data sets at record level and permits subset extraction as will be defined later. The GADS is an exception to this rule.

For a further discussion on each of these components, refer to the section entitled "[Definitions and Conventions](#)." 2.3.

## 2.1.1 Child Products

### 2.1.1.1 Definition

Child products are the result of the extraction from existing [Level 0](#), [Level 1B](#) or [Level 2](#) parent products, and they own the same format and file name principles as any other ENVISAT Payload Data Segment (PDS) product (child product does not apply to future products). Also, there is no [child product](#) extraction from [Auxiliary Data](#). The child products are generated by the Archiving Facility (ARF) and they consist of one segment, or separated consecutive scenes.

The product structure is provided in the previous section, entitled "[Products and Algorithms Introduction](#)"

Each child product contains an integer number of granules, which is a part of the product that corresponds to the time window covered by a [Data Set Record \(DSR\)](#) of the [Location Annotation Data Set \(LADS\)](#). The start time of the granule is the time label of the LADS DSR. For the [Advanced Synthetic Aperture Radar \(ASAR\)](#) instrument, the stop time of the granule immediately precedes the time label of the following LADS DSR in the product.

In [table 2.2](#) below, examples are given for full scenes, relative to the specific product mode described, and scenes the size of only one granule.

Table 2.2 Child product scene sizes

Products	Full Scene Size	Granule Size
<a href="#">IM, AP</a>	100 Km x 100 Km (10 granules)	10% of the full scene 10 Km along-track
<a href="#">WS, GM</a>	400 Km x 400 Km (10 granules)	10% of the full scene 40 Km along-track
<a href="#">WV</a>	One imagette for ASAR WV ( one granule )	One imagette for ASAR WV

The Extracted Instrument Header (EIH) product is extracted from a Level 0 product. It contains a suite of [Instrument Source Packet \(ISP\)](#) fields for a selected time interval. Its structure is the following:

- [Main Product Header \(MPH\)](#): It is identical to the MPH of the Level 0 product from which the data is being extracted, except for the time and positioning information which are updated to reflect the extracted region.
- [Specific Product Header \(SPH\)](#): It contains sensing time information, offset and length in MDS-DSR of each field (one or several fields) extracted from ISP of the parent product.
- [Measurement Data Set \(MDS\)](#): Each [Data Set Record \(DSR\)](#) of the MDS contains one or several fields extracted from ISP.
- The file name also changes to "C"; that is ASA\_IMM\_1C.

### 2.1.1.2 Child Product Extraction Requirements

As was first discussed in the [Introduction](#), the ASAR child product is extracted from a parent product already archived in the [ARF](#). However, the ARF does not archive the child product, and it does not update the inventory. After completion of the instruction, the ARF sends back an instruction report to the Centre Monitoring and Control (CMC).

The ASAR child products extraction criteria is defined as follows:

Table 2.3 ASAR child product extraction criteria

Product Level	Time	Location	Bands	Data Set	Extracted Ins. Header
Level 0	Yes	Yes	No	No	Yes
Level 1B and Level 2	Yes	Yes	No	Yes	N/A

#### 2.1.1.2.1 Data Set Selection

The ARF shall select the Data Set (DS) of the parent product based on data set names in

each [Data Set Descriptor \(DSD\)](#) of the [Specific Product Header \(SPH\) 2.3.2.3.](#) to extract child products with a DS extraction criterion. All [Global ADS \(GADS\)](#) shall be kept in the child product.

### 2.1.1.2.2 ISP Subsets Selection (Extracted Instrument Headers)

The [ARF](#) shall extract from the [Level 0](#) products the [Extracted Instrument Headers \(EIH\)](#), by selection of one or several sets of selected [Instrument Source Packets \(ISPs\)](#).

### 2.1.1.2.3 Common Archiving Facility Requirements

1. The external auxiliary data [DSD](#) records shall always be kept in the child product.
2. The [GADS](#) shall always be kept in the child product.
3. The [MPH](#) of the extracted child product shall be copied from the parent product, and then updated with the following parameters:
  - sensing start day and start time (t0)
  - sensing stop day and stop time (TL)
  - duration of the product (t 140)
  - processing centre
  - processing time
  - total size
  - size of each [DS](#)
  - number of DS
4. The name of the extracted child product shall be updated according to the parameters updated in the MPH.
5. The [SPH](#) shall be copied from the parent product.
  - Time information.
  - Location information of the products determined by reading the [LADS](#) in [Level 1B](#) or [Level 2](#) products, if the product has a LADS. This information contains at least the four corners of the product area expressed in latitude and longitude, including the first and last sample latitude and longitude (determined from the LADS).

The following parameters shall be updated for each DSD describing a data set in the extracted child product:

- filename: set to "NOT \_USED" if the DS corresponding to the DSD is empty, when the DS is not kept during a data set extraction
- data set offset
- total size of data set
- number of [DSRs](#) within the data set

## 2.2 Organisation of Products

The data from all the ENVISAT instruments is classified according to a hierarchical data product scheme. Details of this scheme are as follows:

Raw Data is data as it is received from the satellite (serial data stream, not demultiplexed). Raw data is recorded from the X and Ka band demodulator output interfaces and stored on High-Density Data Tapes (HDDTs). The Raw Data is not considered a product, and its structure is not defined in this document.

Level 0 is reformatted, time-ordered satellite data (no overlap), in computer-compatible format. The Level 0 product is the lowest level product in the ENVISAT PDS. [Table 2.7](#) in the section "Level 0 Products" shows a full list of ASAR Level 0 products.

Level 1B products are geolocated engineering foundation products in which data has been converted to engineering units, auxiliary data has been separated from measurements, and selected calibrations have been applied to the data. These products are the foundation from which higher level products are derived.

The Level 0 product is transformed into a Level 1B Product by application of algorithms and calibration data to form a baseline engineering product. The Level 1B product may be based on the whole of the source Level 0 product, or only a selected set of instrument packets from within the Level 0 product, based on a time range or other selection criteria.

Level 1B products may be produced in the following ways:

- Unconsolidated: generated in Near Real Time (NRT); an intermediate step in near real time processing, used for instrument performance monitoring. It is produced in NRT using available NRT auxiliary data (i.e., may not contain the most precise orbit vectors or calibration information).
- Fully Consolidated: generated off-line, time ordered, no overlap, no data gaps (except where the instrument has been turned off), fully validated; the basis for any further off-line processing. It is produced using the most precise auxiliary information available. It is compiled to respect the defined product boundaries (e.g., ascending node to ascending node at the equator for full orbit products).
- Partially Consolidated: a product that has been consolidated in all ways except that it does not use the most precise auxiliary data possible to perform processing. Since several different levels of accuracy exist for auxiliary data (e.g., 5 possible orbit state vector sources), varying levels of consolidation may exist for a product.

Level 1B products make up the majority of ASAR products, and are outlined in the section "[Level 1B Products](#)" [2.6](#). [Table 2.39](#) in that section provides a summary of these products.

Level 2 consists of geolocated geophysical products:

- 
- Near Real Time: generated in near real time from unconsolidated Level 1B products
  - Off-line: generated from consolidated Level 1B products

In general, the Level 1B product is transformed into one or more Level 2 products through higher-level processing to convert engineering units into geophysical quantities and to form a more directly interpretable and useful measurement data set. The Level 1B products used are created at the time of Level 2 processing.

The general rule for product structure is that NRT and off-line versions of Level 2 products share the same structure, the only difference being that the off-line product is of better quality due to the fact that more accurate (fully consolidated) data is used during production than for the NRT product; and that the start and stop times of the data may be different to reflect consolidation of the data to standardised portions of the orbit. Level 2 products may be processed systematically or upon user request.

At present, there is only one ASAR Level 2 product, which is the "Wave Mode Ocean Wave Spectra" product (ASA\_WVW\_2P). This is discussed more fully in the section "[Level 2 Products and Algorithms.](#)" [2.7.](#)

#### Browse

Browse products are decimated images which can be ordered from the ENVISAT inventory. These products are very small to support electronic transmission while querying the catalogues. They may be further reduced in size through the use of standardised data compression algorithms.

Browse products will be generated systematically for ASAR (except wave mode) and will contain image lines derived from a data segment (up to a full orbit of data).

The user will view the browse product to assist in ordering the required products by displaying scenes starting anywhere in the browse product. A comprehensive description of the Browse products is provided in the section entitled "[Browse Products.](#)" [2.6.2.1.3.](#)

[Figure 2.9](#) below shows the generalised product tree:

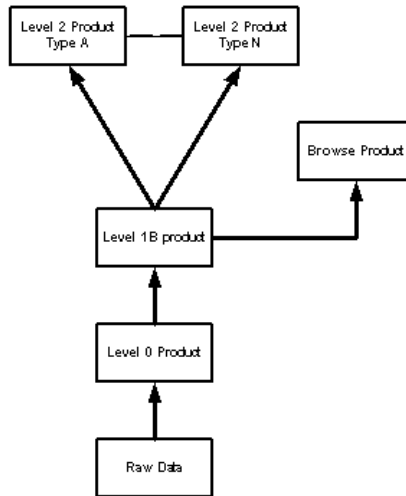


Figure 2.9 The Generalised Product Tree

As discussed in the [Introduction 2.1](#), ASAR products can be classified according to the mode in which the SAR instrument is operating. These are:

- [Image](#) (IM) Mode - these products are high-resolution, narrow swath products based on data acquired at one of seven subswaths.

The Precision Image product is a multi-look, ground range, digital image (in either [Horizontal Polarisation Transmitted/Horizontal Polarisation Received \(HH\)](#) or [Vertical Polarisation Transmitted/ Vertical Polarisation Received \(VV\)](#) polarisation) suitable for most applications. It is intended for [multi-temporal](#) analysis and for deriving [backscatter](#) coefficients. Engineering corrections and relative [calibration](#) are applied to compensate for well understood sources of system variability. Absolute calibration parameters are provided in the product annotations.

The Ellipsoid Geocoded Image product is similar to a Precision Image, but with rectification to a map projection. It is geocoded using a map projection selectable by the user, such as UTM, or Polar Stereographic. Absolute calibration parameters are provided in the product annotations.

Single-Look Complex (SLC) image data is intended for SAR image quality assessment, calibration and interferometric or wind/wave applications. A small number of corrections and interpolations are performed on the data in order to allow freedom in the derivation of higher-level products. Absolute calibration parameters are provided in the product annotations.

A Medium-Resolution Image product will be available at 150 m resolution, which is

specifically aimed at sea ice and oceanography applications. Absolute calibration parameters are provided in the product annotations.

- Alternating Polarisation (AP) Mode - these products are similar to Image Mode products but include a second image acquired using a second polarisation combination. The raw data is acquired in bursts of alternating polarisation.

The polarisation combinations are:

- the co-polarisation submode (one image HH and one image VV)
- the cross-H polarisation submode (one image HH and one image HV)
- the cross-V polarisation submode (one image VV and one image VH)

Products contain two images corresponding to one of the three polarisation combination submodes, at reduced spatial resolution in comparison to Image Mode.

- Wide Swath (WS) Mode - these products provide greater swath width at reduced spatial resolution through the use of the ScanSAR technique.

The standard product available for Wide Swath Mode will be a 150 m resolution image with the full 405 km swath width.

- Wave (WV) Mode - these products are similar to those in Image Mode but are much smaller, covering an area of approximately 5 km by 5 km. Wave mode products may also contain secondary information like cross spectra.

ASAR Wave Mode products are based on small high-resolution, complex images of ocean scenes also called imagettes. These are processed to derive spectra of the ocean backscatter and consequently the wavelength and direction of ocean waves.

An SLC Imagette and Imagette Cross Spectrum is the basic Level 1B product from the ASAR Wave Mode. A minimum number of corrections and interpolations are performed on the SLC data in order to allow freedom in the derivation of higher-level products. Absolute calibration parameters are provided in the product annotations.

ASAR Ocean Wave Mode Spectra are available as a Level 2 product. A Level 2 product is an ocean wave wavelength and direction measurement.

- Global Monitoring (GM) Mode - is similar to WS mode, but has a lower data rate since the data is subsampled on board the satellite.

The Global-Monitoring Mode product is a 1 km resolution image with a 405 km swath width, suitable for dissemination by electronic links in near real time.

The nominal characteristics of the various ASAR measurement modes are summarised in the following table:

Table 2.4 Nominal characteristics of ASAR measurement modes

VV or HH polarisation images from any of 7 selectable swaths. Swath width between approximately 56 km (swath 7) and 100 km (swath 1) across-track. Spatial resolution of approximately 30 m (for precision product).
ASAR Alternating Polarisation Mode (AP)
Two co-registered images per acquisition, from any of 7 selectable swaths. HH/VV HH/HV or VV/VH polarisation pairs possible. Spatial resolution of approximately 30 m (for precision product)
ASAR Wide Swath Mode (WS)
400 km by 400 km wide swath image. Spatial resolution of approximately 150 m by 150 m for nominal product. VV or HH polarisation.
ASAR Global Monitoring Mode (GM)
Spatial resolution of approximately 1000 m in azimuth by 1000 m in range for nominal product. Up to a full orbit of coverage, HH or VV polarisation.
ASAR Wave Mode (WV)
A small imagette (dimensions range between 10 km by 5 km, to 5 km by 5 km) is acquired at regular intervals of 100 km along-track. The imagette can be positioned anywhere in an Image Mode swath. Up to two positions in a single swath or in different swaths may be specified, with acquisitions alternating between one and the other (successive imagettes will hence have a separation of 200 km between acquisitions at a given position). HH or VV polarisation may be chosen. Imagettes are converted to wave spectra for ocean monitoring.

[Table 2.5](#) below gives a summary of the ASAR products, categorised by product level, and [Table 2.5](#) below gives a product summary categorised by mode. As for all ENVISAT instruments, the interface for browsing and ordering these products is via the PDS User Service Facility (USF).

Table 2.5 Summary of ASAR data products

Mode	Product Level	Product ID	Product Name
IM	Level 0	<a href="#">ASA_IM_0P 2.5.1.2.2.1</a>	ASAR Image Mode source packets
AP	Level 0	<a href="#">ASA_AP_H_0P 2.5.1.2.2.2</a>	ASAR Alternating Polarisation Mode source packets cross-polarised H (HH/HV= H transmit H and V received)
AP	Level 0	<a href="#">ASA_AP_V_0P 2.5.1.2.2.2</a>	ASAR Alternating Polarisation Mode source packets cross-polarised V (VV/VH= V transmit V and H received)
AP	Level 0	<a href="#">ASA_AP_C_0P 2.5.1.2.2.2</a>	ASAR Alternating Polarisation Mode source packets co-polarised C (HH/VV= H and H received/V transmit and V received)
WS	Level 0	<a href="#">ASA_WS_0P 2.5.1.2.2.3</a>	ASAR Wide Swath Mode source packets
WV	Level 0	<a href="#">ASA_WV_0P 2.5.1.2.3.2</a>	ASAR Wave Mode (low rate)
GM	Level 0	<a href="#">ASA_GM_0P 2.5.1.2.3.1</a>	ASAR Global Monitoring Mode (low rate)
IM	Level 1b	<a href="#">ASA_IM_P 2.6.2.1.1.2.1.2</a>	ASAR Image Mode Precision Image (high-resolution)
IM	Level 1b	<a href="#">ASA_IMS_1P 2.6.2.1.1.2.1.1</a>	ASAR Image Single-look Complex (high-resolution)
IM	Level 1b	<a href="#">ASA_IMG_1P 2.6.2.1.1.2.1.3</a>	ASAR Image Mode ellipsoid Geocoded image (high-resolution)
AP	Level 1b	<a href="#">ASA_APP_1P 2.6.2.1.1.2.1.5</a>	ASAR Alternating Polarisation Precision image
AP	Level 1b	<a href="#">ASA_APG_1P 2.6.2.1.1.2.1.6</a>	ASAR Alternating Polarisation Mode Ellipsoid Geocoded image
AP	Level 1b	<a href="#">ASAAPS_1P 2.6.2.1.1.2.1.4</a>	ASAR Alternating Polarisation Mode Complex image (high-resolution)
WS	Level 1b	<a href="#">ASA_WSM_1P 2.6.2.1.1.3.1.3</a>	ASAR Wide Swath standard image
IM	Level 1b	<a href="#">ASA_IMM_1P 2.6.2.1.1.3.1.1</a>	ASAR Image Mode Medium-resolution image
AP	Level 1b	<a href="#">ASA_APM_1P 2.6.2.1.1.3.1.2</a>	ASAR Alternating Polarisation Medium-resolution image
WV	Level 1b	<a href="#">ASA_WVI_1P 2.6.2.1.2.1.1</a>	ASAR Wave Mode SLC imagette and Imagette Cross Spectra
WV	Level 1b	<a href="#">ASA_WVS_1P 2.6.2.1.2.1.2</a>	ASAR Wave Mode Imagette Cross Spectra
GM	Level 1b	<a href="#">ASA_GMI_1P 2.6.2.1.1.3.1.4</a>	ASAR Global Monitoring Mode Image
WV	Level 2	<a href="#">ASA_WVW_2P</a>	ASAR Wave Mode Ocean Wave Spectra
GM	browse	<a href="#">ASA_GM_BP 2.6.2.1.3.1.4</a>	ASAR Global Monitoring Mode Browse Image
IM	browse	<a href="#">ASA_IM_BP 2.6.2.1.3.1.1</a>	ASAR Image Mode Browse Image
AP	browse	<a href="#">ASA_AP_BP 2.6.2.1.3.1.2</a>	ASAR Alternating Polarisation Browse Image

WS	browse	<a href="#">ASA_WS_BP 2.6.2.1.3.1.3.</a>	ASAR Wide Swath Browse Image
----	--------	--	------------------------------

To view the summary table that provides the standard specifications for ASAR data products, see ["Products and Algorithms Introduction." 2.1.](#)

The Image Mode (IM), Alternating Polarisation mode (AP), and the Wide Swath modes (WS) are all high data rate products. [Figure 2.10](#) below gives the generalised product tree for high data rate products.

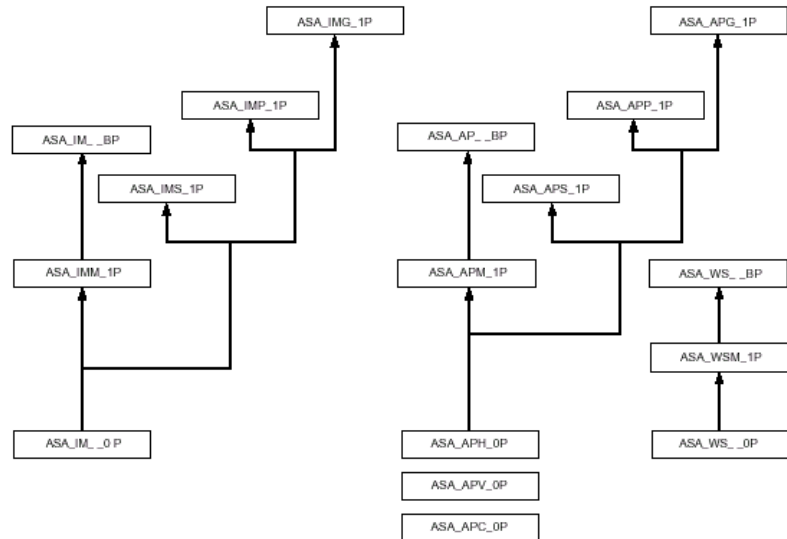


Figure 2.10 ASAR high data rate product tree

The Global Monitoring (GM) and Wave Modes (WV) are low data rate products. The generalised trees for these products is given below in [Figure 2.11](#).

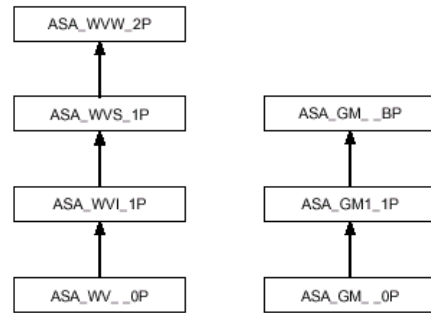


Figure 2.11 ASAR low data rate product tree

## 2.3 Definitions and Conventions

### 2.3.1 Definitions

#### 2.3.1.1 Global and Regional Coverage

Depending upon the instrument and operating mode, ENVISAT products may be either Global or Regional. A global product contains coverage for the entire length of an orbit. A regional product may only cover a specific segment of an orbit.

#### 2.3.1.2 Auxiliary Data

Auxiliary data is defined as all other data required for the processing of a product which is not part of the primary measurement data received from the instrument while in the nominal measurement mode. Auxiliary data may come from the satellite itself, sources external to the ADS, or be created by instrument processing facilities within the ADS. A comprehensive description of the Auxiliary Products is provided in the section entitled "[Auxiliary Products](#)." [2.9.](#)

### 2.3.1.3 Geolocation and Geocoding

Geolocation information is provided in the product header in the form of latitude and longitude information that allow the user to determine the area covered by the data from a simple inspection of the header. For image data, a geolocation grid may also be provided as an auxiliary data set in the product to allow for precise pixel geolocation.

Some image products may also be geocoded, which is the process of resampling the data to conform to a standard map projection with known coordinates.

### 2.3.1.4 Product Confidence Data

Product Confidence Data provides an evaluation of the overall quality of the product. As such, it is an evaluation of the product statistics as reported by various pieces of equipment and processors in the processing chain. Product confidence data is thus best represented by evaluating product statistics against predetermined thresholds to determine if the product meets the minimum quality requirements defined by the thresholds. If a product does not measure up to the predefined quality level, the error threshold is exceeded and a flag is set. (See also the section "["Level 1B Essential Product Confidence Data." 2.6.2.3.](#)" )

- PCD in the MPH

The MPH is a generic header (i.e., instrument unspecific), and so any product confidence data (PCD) contained within must be applicable to all instrument types.

PCD applications include:

- summary quality; high-level quality indicator for product
- acquisition and de-multiplexing; this is related to the data commutation and downlink performance aspects which are independent of product type

### PCD in the SPH

The PCD in the SPH may only contain information pertaining to the entire product length and relates to the execution of the product generation command (since a product will be generated by a single command). Examples include:

- arithmetic error during product generation
- auxiliary data files available/used during processing

- 
- mode usage statistics during orbital revolution
  - time relations used (predicted or precise)

## PCD in the DSR

The PCD in the DSR, which was called Measurement Confidence Data (MCD) in ERS is referred to as PCD in the ENVISAT payload data segment. The DSR PCD provides details on individual source packet quality. It is related directly to the engineering aspects and details of the ground processing algorithms.

### 2.3.1.5 Calibration

[Calibration](#) data is classified as auxiliary data within the ADS

[Internal calibration 2.11.3.](#) data, contained within the instrument source packet, is used during the product generation process. The internal calibration information is generated by the instrument itself during the nominal measurement mode, or as part of a dedicated calibration mode.

[External calibration 2.11.4.](#) data, generated by on-ground or orbit calibration activities, is also used during the product generation process. The external calibration data is measured on ground, before launch, or in orbit during the commissioning phase or during periodic calibration activities.

### 2.3.1.6 Processed Product Sizes and Coverage

The Maximum Size of any product will be the smallest of:

- Data from a full orbit (100 minutes + potentially 10%, depending on [OBR](#) tape dump and specific acquisition downlink timing),
- Or, data from maximum continuous processed instrument/mode on-time (e.g., ASAR stripline [IM, AP, and WS modes] = 10 minutes),
- Or, the amount of data to fill a 2 Gbyte file. (In order to use standard UNIX file system capabilities, this limitation may be adjusted or removed as extended file sizes are fully supported.) If the amount of data is greater than 2 GBytes, the product is contained in multiple files, each no larger than 2 GB and each having its own MPH and SPH.

The Minimum Coverage of any product will be the size of a scene specified by ESA for selected imagery sensors (nominal sizes specified):

- ASAR IM/AP 100 km \* 56 km (it may be larger (up to 100 km) for different swath choices)

- 
- ASAR WS or GM 400 km \* 400 km

## 2.3.2 Conventions

### 2.3.2.1 ENVISAT: General product structure

The following convention has been defined for all ENVISAT products:

#### ASCII Header Conventions

The Main Product Header (MPH) and Specific Product Header (SPH) of ENVISAT products follow the following conventions:

- Headers use only ASCII characters.
- They are fixed size structures (i.e., the SPH may vary across products, but within each product it is a fixed number of bytes long).
- Each entry in the MPH and SPH will follow a keyword-value<units>-terminator structure.

**KEYWORDS:** Keywords are limited to the set of ASCII characters which include the capital English alphabet [A...Z], and the numbers [0...9]. The only other characters allowed in a keyword is the underscore (\_), and the equal sign (=). A keyword is a single word, or several words connected by underscore characters, followed by an equal sign.

**VALUES:** All values are expressed in ASCII format and follow immediately after the equal sign in the keyword (i.e., no white space in between keyword and value). Values may be of two classes: numeric values, or string-values. Numeric values are those which would normally be expressed as an integer or floating point value. String values are those values which would normally be expressed in ASCII characters regardless of their location in the product. String values fall into two types: single-character entries, and multi-character entries. Multi-character entries must be placed within double quotes (" ") in the MPH or SPH. The string within these quotes may use any of the allowable ASCII character set. Single value characters do not require quotation marks, but are limited to the characters [A..Z], [a..z] and [0..9].

**UNITS:** The use of units is required for numeric values unless the value has no units or the unit type is inherently obvious. For numeric values which do not require units and string-values, the value is followed directly by the terminator character and no units entry is included. When units are deemed necessary, they are placed within angled braces (< >) directly following the last character of the value to which the units apply. No white space is left between the value and the first angled brace, nor is any white space left between the first angled brace and the first character of the units expression. Finally, no white space is left between the last character of the units expression and the closing angled brace. Within the

braces, the units expression may use any allowable ASCII characters and be of any length.

**TERMINATOR:** The terminator character is placed directly after the closing angled brace of the units for entries which have units, or directly after the last character in the value for entries which do not have units attached to them. The terminator value for ENVISAT products is the ASCII newline character (character code 10 in See Decimal Value and corresponding ASCII character). The use of this terminator allows the MPH/SPH structure to be displayed in an easily readable format (one entry per line) on most UNIX text editors.

All ASCII string entries are left-justified within the quotation marks. Therefore, if the string is shorter than the number of characters allocated for it, blank-space ASCII characters are placed after the last character in the string, but before the closing quotation mark.

Note that in the data definitions in this document, the notation is used to indicate the inclusion of an ASCII blank-space character (ASCII character 32).

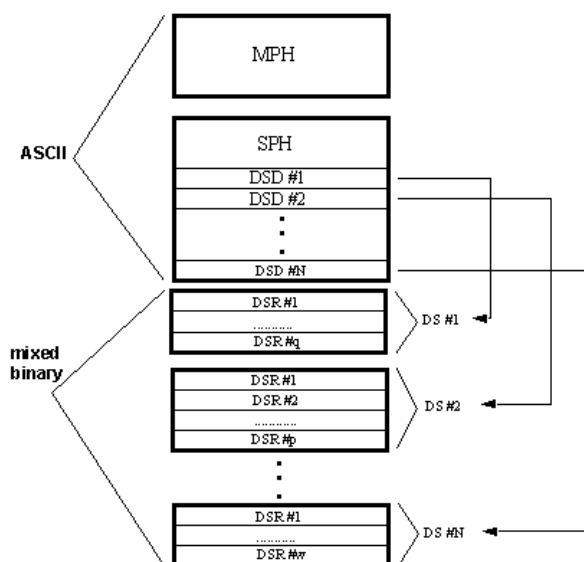


Figure 2.12 Generalised product structure

### 2.3.2.2 Main Product Header (MPH)

The MPH has a fixed length. Its format is identical for all ENVISAT products. The major types of information found in the MPH are:

- product identification (consolidated or unconsolidated, processing stage, reference document describing the product)
- data acquisition and processing
- sensing time (start, stop)

- geolocation (start, stop)
- orbit information (phase, cycle, orbit number, state vector, state vector origin)
- auxiliary time tagging information (UTC/SBT, leap indicator, clock step)
- product confidence data (PCD)
- product size/structure information
- check sum

## Contents

The Main Product Header (MPH) identifies the product and its main characteristics. The Main Product Header is an ASCII structure containing information needed for all ENVISAT sensors. It is of fixed length and format for all products. The MPH contains the following major types of information:

### Product Identification Information

This information includes the file name of the product (which describes most of the essential features of the product, such as instrument, mode, and processing level), the consolidation level of the product, and the document ID number of the documentation describing this product.

### Information Regarding Data Acquisition and Processing

This information identifies where the product was acquired, where it was processed, when it was processed, and what hardware/software performed the processing.

### Information on Time of Data

Included in these fields are the [UTC](#) start and stop time of data sensing.

### Information on ENVISAT Orbit and Position

These fields contain orbit positioning data which allow one to determine the exact position of the satellite at the time of sensing.

### SBT to UTC Conversion Information

This data allows for precise conversion from Satellite Binary Time (SBT), as stored in Instrument Source Packets (ISPs), to the conventional [UTC](#) time system.

### Product Confidence Data

[\(See "Product Confidence Data" above.\) 2.3.1.4.](#)

## Product Size Information

These fields identify the size of various structures within the product so that they may be accurately interpreted. (See "[Processed Product Sizes and Coverage](#)" [2.3.1.6.](#), above.)

### Format

All entries are left justified unless otherwise stated (i.e., any spare characters within an entry are included at the end of the entry). If blank characters are included at the end of a multi-character string, the blanks are written before the closing quotation mark, not after. The fields of the MPH are presented below.

Note: the MPH is common to all sensors and products. It is provided as a separate file within the [Data Formats 6.6.1.](#) section, for easy reference.

### 2.3.2.3 Specific Product Header (SPH)

The Specific Product Header (SPH) is defined for each product and provides additional information, applicable to the whole product, related to the processing. Its length is fixed for a given product. It contains one SPH descriptor (an ASCII string describing the product), and at least one data set descriptor (DSD). The SPH will follow an ASCII keyword value format similar to the MPH. It can contain:

- product descriptor
- time and geolocation of first and last valid DSR
- calibration data
- instrument mode data
- version number of characterisation files
- version number of characterisation look-up tables
- processing algorithms information
- product confidence data (PCD)
- annotations
- data set descriptors (DSDs)

The SPH will follow an ASCII keyword-value<units>-terminator format identical to that of the MPH. The detailed SPH structure and contents are given in the sections where each specific product is described in the handbook.

### 2.3.2.4 Data Set Descriptors (DSD)

The Data Set Descriptors (DSD) are used to describe an attached Data Set or to provide references to external files relevant to the current product (e.g., auxiliary data used in

processing but not included with the product). There must be one DSD per Data Set or per reference to an external file. The DS may be a Measurement Data Set (MDS), an Annotation Data Set (ADS) or a Global Annotation Data Set (GADS).

## Contents

All DSDs have the same format. The DSD is contained within the SPH as shown in [Figure 2.12](#) "Generalised product structure" above. As such, the DSD is also in ASCII format. The DSD contains information specific to a given Data Set within the product. The general contents of a DSD are shown in [Table 2.6](#) below "General DSD format."

## Format

The structure of the DSDs will be the same for all products and all instruments. The ASCII format conventions are the same as those used for the MPH and SPH. This structure is referred to as "dsd" throughout this handbook. The general format is shown in Table 1 below:

Table 2.6 General DSD format

Field #	Description	Units	Byte length	Data Type
1	DS_NAME=	keyword	8	8*uc
	quotation mark ("")	-	1	uc
	Data Set Name Name describing the data set. Characters not used are blanked.	-	28	28*uc
	quotation mark ("")	-	1	uc
	newline character	terminator	1	uc
2	DS_TYPE= note: the "DSD Type" flag has been combined with the "DSD Attachment" flag by allowing more possible letters.	keyword	8	8*uc
	DS Type = M if a Measurement DS is attached. = A if an Annotation DS is attached = G if a Global ADS is attached = R if no DS is attached (reference DSD only)	-	1	uc
	newline character	terminator	1	uc

Field #	Description	Units	Byte length	Data Type
3	FILENAME=	keyword	9	9*uc
	quotation mark ("")	-	1	uc
	External Product Reference If the DS Attachment flag was set to R this field contains the name of the referenced product using the standard naming convention of the MPH. If the DS Attachment Flag was set to A, M, or G, this field may contain the name of the file from which the Data Set was copied, or it may be blank (set to ASCII blank space characters). For a product which was supposed to contain a data set or reference to one, but the file was unavailable, the first 7 characters of this field may be set to MISSING and the rest blanked. If space for a DSD has been set aside in the SPH, but the DSD is not used in the current product, this field may be set to NOT USED.	-	62	62*uc
	quotation mark ("")	-	1	uc
	newline character	terminator	1	uc
	DS_OFFSET=	keyword	10	10*uc
4	DS Offset in bytes Gives the position of the first byte of the corresponding DS with respect to the whole product. Set to 0 if no DS is attached.	bytes	21	Ad
	<bytes>	units	7	7*uc
	newline character	terminator	1	uc
5	DS_SIZE=	keyword	8	8*uc
	Total Size of DS in bytes Length in bytes of the Data Set. Set to zero if no DS is attached.	Bytes	21	Ad
	<bytes>	units	7	7*uc
	newline character	terminator	1	uc
6	NUM_DSR=	keyword	8	8*uc
	Number of DSRs within the DS Number of Data Set Records within the DS, set to zero if no DS is attached.	-	11	Al
	newline character	terminator	1	uc
7	DSR_SIZE=	keyword	9	9*uc
	Length of the DSRs in bytes Length of each DSR if DSR length is constant within the Data Set. 0 = no DSRs attached (i.e. no DS attached) -1 = DSR length is variable.	Bytes	11	Al
	<bytes>	units	7	7*uc
	newline character	terminator	1	uc
8	Spare (blanks)	ASCII	32	32*uc
	newline character	terminator	1	uc
TOTAL			280	

## Example Data Set Descriptors

All DSDs must be the same size. In order to clarify the use of DSDs within the product structure, the 5 possible DSD contents are shown explicitly below. All DSDs should fall into one of the following categories. Note that the symbol is used to denote the ASCII blank space character (ASCII character 32). Values given in the following examples are for illustrative purposes only and may not correspond to the true values.

### DSD Pointing to a Data Set

If the DSD points to a Data Set actually contained within the current product, the contents of the DSD will follow the example given below. The example given below assumes that the ASAR SR/GR ADS is being described, however the same format would be used for any other ADS, MDS or GADS.

```
DS_NAME="SR/GRADS"
DS_TYPE=A
FILENAME=""
DS_OFFSET=+000000000000000012345<bytes>
DS_SIZE=+00000000000000006788<bytes>
NUM_DSR=+0000000002
DSR_SIZE=+0000003394<bytes>
DSD Referencing a File
```

If the DSD is referencing a file external to the current product, the contents of the DSD will follow the example given below. The example below assumes that the ASAR Processor Configuration file is being referenced; however, the same format would be used with any other file.

```
DS_NAME="ASARProcessorConfig.File"
DS_TYPE=R
FILENAME="ASA_CON_AXVPDK19990324_150411_19990325_123000_20001231_101413"
DS_OFFSET=+00000000000000000000000000000000<bytes>
DS_SIZE=+00000000000000000000000000000000<bytes>
NUM_DSR=+0000000000
DSR_SIZE=+0000000000<bytes>
DSD Not Used
```

In some cases, space may be allocated to a DSD in an SPH, but the DSD is not used during normal processing of the current product either due to the nature of the product or due to operator-selected options during product processing. For example, room may be allocated for an ADS, but the ADS is not included normally in the current product. In such cases, the DS\_NAME and DS\_TYPE fields are filled as they normally would be, but the FILENAME entry is set to NOT USED as shown in the example below. The remaining fields are set to values of zero.

The example below is for the ASAR SR/GR ADS and assumes that we are describing an ASAR Single-Look Complex product. This ADS is not included in the ASAR SLC products; however, space for it is included in the ASAR Image Products SPH. Therefore, this is a good example of a DSD which is not used for a certain product. In this case, the DSD would have the following format:

```
DS_NAME="SR/GRADS"
DS_TYPE=A
FILENAME="NOTUSED"
DS_OFFSET=+000000000000000000000000<bytes>
DS_SIZE=+000000000000000000000000<bytes>
NUM_DSR=+0000000000
DSR_SIZE=+0000000000<bytes>
Spare DSD
```

A spare DSD is simply 279 blank space characters () followed by a newline character. This structure is referred to as "dsd\_sp" throughout this handbook.

#### DSD for a Missing Data Set or File

If a Data Set was supposed to be included in the product or an external file was supposed to be referenced, but for some reason was not, the DSD indicates this by setting the FILENAME field to MISSING. Note that this is different from the NOT USED DSD. The MISSING DSD indicates that something unexpected has happened, and a reference or Data Set that was supposed to be included has not been. In contrast, the NOT USED DSD indicates that a file or Data Set is simply not used for this product - nothing unexpected has happened.

Note that for most products, if an auxiliary file could not be read or a Data Set produced, then the entire product will not be produced. Thus the MISSING DSD will only be used in special situations which warrant its use.

The example below assumes the ASAR Chirp parameter ADS was supposed to be in the product, but was not produced for some reason. The following DSD would thus be produced:

```
DS_NAME="CHIRPPARAMSADS"
DS_TYPE=A
FILENAME="MISSING"
DS_OFFSET=+000000000000000000000000<bytes>
```

DS\_SIZE=+00000000000000000000<bytes>

NUM\_DSR=+0000000000

DSR\_SIZE=+0000000000<bytes>

### 2.3.2.5 Data Set (DS)

#### Contents

The data set (DS) contains the instrument's scientific measurements and it is the actual data of interest. The DS is composed of data set records (DSR). There are as many DSRs as necessary to complete a DS within a product and that number will depend on the product type. In addition, the size of Data Sets within a product may vary. There are two types of data sets: measurement data sets (MDS) containing instrument data, known as MDSRs, and annotation data sets (ADS) containing auxiliary data, known as ADSRs. In addition, ADSs may exist in two forms. The basic ADS contains time-stamped ADSRs, which can be used to relate the information to the correspondingly time-stamped MDSRs. Global Annotation Data Sets (GADS), however, contain information which pertains to the full product and thus each GADSR may not be time-stamped.

#### Format

The Data Set is in a mixed-binary format. This may consist of integers, floats, characters (1-byte numbers), or ASCII values and ASCII strings. Note that for ASCII multi-character strings in the Data Sets, quotation marks are not used to enclose the string.

A Data Set is composed of Data Set Records (DSRs), as shown in [Figure 2.12 "Generalised Product Structure."](#) For Level 1B and Level 2 products, the structure includes:

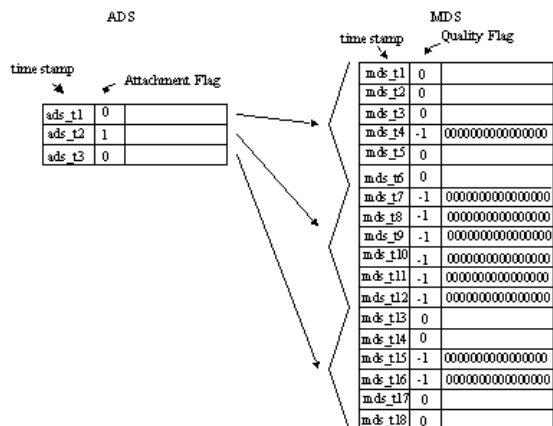
- The start time of the DSR in MJD 2000 (MJD) format.
- The DSR length (optional: include if DSR size is variable within the Data Set).
- Quality Flag: for MDSRs, a signed character is used to indicate the MDSR quality. A value of -1 indicates the MDSR is a blank MDSR (used for Level 1B and Level 2 only).
- Attachment Flag: for ADSRs, a signed character flag may be included to indicate if corresponding MDSRs exist for the ADSR (1 = error, no corresponding MDSRs, 0 = no error). This flag is used to identify large gaps in the sequence of MDSRs. (To simplify processing, this flag is only used for geolocation ADSs (LADSs), and Summary Quality ADSs (SQADSs). In all other cases, it is always set to zero.) In LADSs, this flag identifies empty granules. An example is provided in [Figure 2.13 "Example of Attachment Flag Usage".](#) If an ADS corresponds to more than 1 MDS, the attachment flag is evaluated for each MDS in turn, then combined into 1 flag via

a logical OR operation.

- For GADS, no time stamp or flag is required.
- The data itself.

For Level 0 data, the MDSRs contain Annotated Instrument Source Packets (AISPs) preceded by a time stamp (sensing time) in MJD 2000 format.

Figure 2.13 Example of attachment flag usage



In this example, the ADSR with time stamp ads\_t2 is valid for the MDSRs from mds\_t7 to mds\_t12. However, all these MDSRs have been zero filled due to missing data, as indicated by the fact that their Quality Flags are set to -1. Therefore the Attachment Flag for ads\_t2 is set to 1. The Attachment Flag for the ADSRs with time stamps ads\_t1 and ads\_t3 are not set to 1 since only part of the data is missing. In this way, the Attachment Flag can be used to identify large gaps of missing measurement data.

For the format of the Level 0 SPH and MDSR refer to the "[Data Format \(Chapter 6.\)](#)" section.

## 2.4 Product Evolution History

This section will contain information relating to the newer revisions of the products, as they evolve through time.

## 2.5 ASAR Level 0 Products

### 2.5.1 Introduction

Level 0 data products are derived from the raw data suitable for image processing on other processing sites. They are required by remote sensing scientists for the testing of Synthetic Aperture Radar (SAR) processors and for research institutes interested in full SAR data processing. A description of the Advanced Synthetic Aperture Radar (ASAR) Level 0 product is given in the following subsections (see index)

The general product structure, used in all ENVISAT products, is given in "[Definitions and Conventions](#)." [2.3.2.1.](#)

#### 2.5.1.1 ASAR Instrument Source Packet

The Level 0 product contains Annotated Instrument Source Packets (AISPs). These are Instrument Source Packets as received from the instrument, with a small header attached by the Front End Processor (FEP).

In addition to the AISPs, each Measurement Data Set Record (MDSR) of the Level 0 product contains a time stamp in [MJD](#) 2000 format which gives the on-board sensing time of the ISP which it contains (one MDSR per AISPs).

The MDSRs within the Level 0 product are:

- demultiplexed per instrument (and per mode for some instruments);
- in ascending chronological order;
- without overlap between the real-time and onboard recorder;
- without obsolete data from the onboard recorded data;
- stored on a computer-compatible format, media and interface.

#### 2.5.1.2 Level 0 Products

ASAR products produced from the Level 0 data can be classified as high-rate or low-rate imaging modes or calibration modes (see also the product summary tables presented in the section "[Organisation of Products](#)").

There are nine Level 0 products for ASAR. The first seven correspond to the five main measurement modes, with the AP Level 0 divided into 3 possible products. The final two Level 0 products are the External Characterisation Level 0 and Module Stepping Mode Level 0 products.

The Level 0 products may be Unconsolidated or Consolidated, as described in "[Organisation of Products](#)."

The complete list of Level 0 ASAR products to which the information in this section applies is summarised in [table 2.7](#) below.

Table 2.7 Level 0 ASAR product

Product ID	Description
<a href="#">ASA_WV_0P 2.5.1.2.3.2</a>	Wave Mode
<a href="#">ASA_GM_0P 2.5.1.2.3.1</a>	Global Monitoring Mode
<a href="#">ASA_FC_0P 2.5.1.2.2.4</a>	External Characterisation
<a href="#">ASA_MS_0P 2.5.1.2.3.3</a>	Module Stepping Mode
<a href="#">ASA_IM_0P 2.5.1.2.2.1</a>	Image Mode
<a href="#">ASA_WS_0P 2.5.1.2.2.3</a>	Wide Swath
<a href="#">ASA_APH_0P 2.5.1.2.2.2</a>	Alternating Polarisation (X polar H)
<a href="#">ASA_APV_0P 2.5.1.2.2.2</a>	Alternating Polarisation (X polar V)
<a href="#">ASA_APC_0P 2.5.1.2.2.2</a>	Alternating Polarisation (Copolar)

## 2.5.1.2.1 Processing Performed

The determination of the satellite position and conversion of Satellite Binary Time (SBT) to Universal Time Co-ordinated (UTC) is accomplished using [ESA](#) software. These are the only algorithms applied when forming the Level 0 products.

## 2.5.1.2.2 High Data Rate Level 0 Products

The high data rate Level 0 products, as depicted in [Figure 2.10](#) "ASAR High Data Rate Tree" found in Section "Organisation of Products," are the [Image Mode \(IM\)](#), [Alternating Polarisation Mode \(AP\)](#), and the [Wide Swath Modes \(WS\)](#). There is also a Level 0 External Characterisation product, used for calibration purposes. All of these are discussed below.

### 2.5.1.2.2.1 Image Mode (ASA\_IM\_0P)

The Image Mode Level 0 product consists of time-ordered Annotated Instrument Source Packets (AISPs) collected while the instrument is in Image Mode. The echo samples contained in the AISPs are compressed to 4 bits/sample using Flexible Block Adaptive Quantisation (FBAQ). This is a high-rate, narrow swath mode so data is only acquired for partial orbit segments and may be from one of seven possible image swaths.

Details of extracting level 0 data are explained below and in the [Level 0 Packets](#) section.

The Level 0 product is produced systematically for all data acquired within this mode. The [NRT](#) version of the product is available from the [PDHS](#) 1 day after data acquisition, while the [OFL](#) (fully consolidated) version is available from the [PAC](#) after 2 weeks.

Max size: 22,500 Mbytes

Coverage: 100 km \* 12,000 km (30 min)

Table 2.8 Level 0 ASA\_IM\_0P product

PRODUCT ID	ASA_IM_0P
NAME	ASAR Image Mode source packets Level 0
DESCRIPTION	ASAR Level 0 data of Image Mode. The objective of this product is to offer Level 0 data for possible images processing on an other processing site. It includes some mandatory information for SAR processing.
COVERAGE	Image mode: 56-100 km across-track depending on sub-swath. Along-track coverage depends on the requested time interval (30 min max).
RESOLUTION	N/A
ACCURACY	N/A
SIZE	Depends on the acquired segment: 22,500 Mbytes max (30' of data).
DATASET	MPH + SPH + MDS containing annotated ISP(1) sample = 4 bits I, 4 bits Q (compressed).
AUXILIARY DATA	Orbit data and time correlation parameters, PCD are included. (Noise Measurements, Calibration Pulses P1, P1a, P2, P3, Header content of Source Packet).
NOTES	1. Data decompression is the first step to Level 1 processing

### 2.5.1.2.2.2 Alternating Polarisation (AP) Mode

There are three AP Mode Level 0 products:

- AP Cross-polar H Level 0 (product ID = ASA\_APH\_0P)
- AP Cross-polar V Level 0 (product ID = ASA\_APV\_0P)

- AP Co-polar Level 0 (product ID = ASA\_APC\_0P)

These products contain time-ordered [AISPs](#) corresponding to one of the three possible [polarisation](#) combinations: [HH & HV](#), [VV & VH](#) and HH & VV, respectively). The echo samples in the AISPs have been compressed to 4 bits/sample using [FBAQ](#). This is a high-rate, narrow [swath](#) mode, so data is only acquired for partial orbit segments and may be from one of seven different image swaths.

The Level 0 product is produced systematically for all data acquired within this mode. The [NRT](#) version of the product is available from the [PDHS](#) 1 day after data acquisition, while the [OFL](#), fully consolidated, version is available from the [PAC](#) after 2 weeks.

Max size: 22,500 Mbytes

Coverage: 100 km \* 12,000 km (30 min)

Table 2.9 Level 0 AP Mode products

PRODUCT ID	ASA_APH_0P, ASA_APV_0P, ASA_APC_0P
NAME	ASAR Alternating Polarisation Mode source packets Level 0
DESCRIPTION	ASAR Level 0 data of Alternating Polarisation Mode. Three submodes are existing for this mode: cross-pol H (HH/HV= H transmit H and V received, for ASA_APH_0P), cross-pol V(VV/VH= V transmit V and H received, for ASA_APV_0P), and copol C (HH/VV= H and H received/V transmit and V received for ASA_APC_0P). The objective of this product is to offer Level 0 data for possible images processing on another processing site. It includes mandatory information for SAR processing.
COVERAGE	Alternating polarisation mode: 56-100 km across-track depending on sub-swath. Along-track coverage depends on the requested time interval.
RESOLUTION	N/A
ACCURACY	N/A
SIZE	Depends on the acquired segment: 22,500 Mbytes (30' of data).
DATASET	MPH + SPH + MDS containing annotated ISP(1) sample = 4 bits I, 4 bits Q (compressed).
AUXILIARY DATA	Orbit data and time correlation parameters, PCD are included. (Noise Measurements, Calibration Pulses P1, P1a ,P2 ,P3, Header content of Source Packet).
NOTES	1. Data decompression is the first step to Level 1 processing

### 2.5.1.2.2.3 Wide Swath (WS) Mode (ASA\_WS\_0P)

The WS Mode Level 0 product consists of time-ordered [AISPs](#) collected while the instrument is in WS Mode. The echo samples in the [AISPs](#) have been compressed to 4 bits/sample using [FBAQ](#). This is a high-rate, wide [swath](#) ([ScanSAR](#)) mode so data is only acquired for partial orbit segments and is composed of data from five image swaths (SS1 to SS5). The Level 0 product is produced systematically for all data acquired within this mode. The [NRT](#) version of the product is available from the [PDHS](#) 1 day after data acquisition, while the [OFL](#) (fully consolidated) version is available from the [PAC](#) after 2 weeks.

Max size: 22,500 Mbytes

Coverage: 400 km \* 12,000 km (30 min)

Table 2.10 Level 0 ASA\_WS\_0P product

PRODUCT ID	ASA_WS_0P
NAME	ASAR Wide Swath Mode source packets Level 0
DESCRIPTION	ASAR Level 0 Wide Swath Mode. The objective of this product is to offer Level 0 data for possible images processing on another processing site. It includes mandatory information for SAR processing.
COVERAGE	Wide swath mode: 406 km across-track. Along-track coverage depends on the requested time interval.
RESOLUTION	N/A
ACCURACY	N/A
SIZE	Depends on the acquired segment : 22,500 Mbytes (30' of data).
DATASET	MPH + SPH + MDS containing annotated ISP(1) sample = 4 bits I, 4 bits O (compressed).
AUXILIARY DATA	Orbit data and time correlation parameters, PCD is included. (Noise Measurements, Calibration Pulses P1, P1a, P2, P3 Header content of Source Packet.)
NOTES	1. Data decompression is the first step to Level 1 processing. 2. 10 minutes of acquisition is more typical of operation yielding 1/3 of 22.5GB or 7,500MB.

#### 2.5.1.2.2.4 Level 0 External Characterisation (ASA\_EC\_0P)

The External Characterisation Level 0 product consists of time-ordered [AISPs](#) collected while the instrument is in [External Characterisation Mode](#). All samples in the AISPs are represented by 8 bits/sample. This is a [calibration](#) mode, which allows characterisation in orbit; departures from ground measured characteristics of the [instrument calibration](#) loop and the passive part of the antenna during the overflight of a ground receiver. The Level 0 product is produced systematically for all data acquired within this mode. The [NRT](#) version of the product is available from the [PDHS](#) 1 day after data acquisition, while the [OFL](#) (fully consolidated) version is available from the [PAC](#) after 2 weeks.

The uses for this mode are discussed in the section entitled "[ASAR Characterisation and Calibration](#)" [2.11](#), and in the Chapter 3 section entitled "[In-flight Performance Verification](#)." [3.2.2](#).

#### 2.5.1.2.3 Low Data Rate Level 0 Products

The low data rate Level 0 products, as depicted in [Figure 2.11](#) "ASAR Low Data Rate Tree" found in the section "Organisation of Products," are the [Wave Mode \(WV\)](#) and the [Global](#)

**Monitoring Mode (GM)**. There is also a Level 0 Module [Stepping product 2.5.1.2.3.3.](#), used for calibration purposes. Each of these are discussed below.

### 2.5.1.2.3.1 Global Monitoring (GM) Mode (ASA\_GM\_0P)

The GM Mode Level 0 product consists of time-ordered [AISPs](#) collected while the instrument is in GM Mode. The low data rate is achieved with on-board resampling and filtering. The echo samples in the AISPs have been compressed to 4 bits/sample using [FBAQ](#). This is a low-rate, wide [swath \(ScanSAR\)](#) mode in which data may be acquired over the entire orbit and is composed of data from five image swaths (SS1 to SS5). The Level 0 product is produced systematically for all data acquired within this mode. The [NRT](#) version of the product is available from the [PDHS](#) 1 day after data acquisition, while the [OFL](#) (fully consolidated) version is available from the [PAC](#) after 2 weeks.

Level 0 products include the instrument source packet plus essential input data required for processing.

Max size: 675 Mbytes

Coverage: 400 km \* 40,000 km (1 orbit)

Table 2.11 Level 0 ASA\_GM\_0P product

PRODUCT ID	ASA_GM_0P
NAME	ASAR Global Monitoring Mode low-rate Source Packet Level 0
DESCRIPTION	ASAR Level 0 product annotated Instrument Source Packet collected while the instrument is in Global Monitoring Mode. The objective of this product is to offer Level 0 data for possible images processing on another processing site. It includes mandatory information for SAR processing.
COVERAGE	Up to 100% of the orbit = 40 000 km * 400 km swath.
RESOLUTION	N/A
ACCURACY	N/A
SIZE	Max 675 Mbytes /orbit.
DATASET	MPH + SPH + MDS containing annotated ISP(1) sample = 4 bits I, 4 bits Q (compressed).
AUXILIARY DATA	Orbit data and time correlation parameters, PCDs (Noise Measurements, Calibration Pulses P1, P1a, P2, P3, Header content of Source Packet).
NOTES	Data is resampled from the original measurements.

### 2.5.1.2.3.2 Wave Mode (WV) Level 0 Product (ASA\_WV\_0P)

The WV Mode Level 0 product consists of time-ordered [AISPs](#) collected while the instrument is in WV Mode. The echo samples in the AISPs have been compressed to 2

bits/sample using [FBAQ](#). This is a low-rate mode where data is acquired in small [imagettes](#) (nominally 10 km x 5 km to 5 km x 5 km in size, [high-resolution complex images](#) of ocean scenes) allowing data acquisition to occur periodically (every 100 km) around a full orbit. The Level 0 product is produced systematically for all data acquired within this mode. The [NRT](#) version of the product is available from the [PDHS](#) 1 day after data acquisition, while the [OFL](#) (fully consolidated) version is available from the [PAC](#) after 2 weeks. These are processed to derive spectra of the surface [backscatter](#), and consequently the wavelength and the direction of ocean waves. The vignette can be positioned anywhere in an Image Mode swath. Up to two positions in a single swath, or in different swaths, may be defined with acquisitions alternating between one and the other, which means the vignette will have a separation of 200 km between successive acquisitions at a given position.

The data from this mode is recorded on board and can be obtained anywhere around the orbit when the instrument is not operating in any other mode.

(For a further discussion on Wave Mode products see [Level 1B Wave Products 2.6.2.1.2](#), and [Level 2 Products 2.7.2](#).)

Level 0 products include the instrument source packet plus essential input data required for processing.

Max size: 608 Mbytes

Coverage: 400 \* 5 km \* 5 km (1 orbit)

Table 2.12 Level 0 ASA\_WV\_0P product

PRODUCT ID	ASA_WV_0P
NAME	ASAR Wave Mode low-rate Level 0
DESCRIPTION	ASAR Level 0 source packet of Wave Mode. The objective of this product is to offer Level 0 Source Packet data for possible images processing on another processing site. It includes mandatory information for SAR processing.
COVERAGE	Up to 100% of the orbit (from 6.04 km * 5 km imagette in IS7 to 9.44 km * 5 km Imagette in IS1 depending on swath selection) every 100 km.
RESOLUTION	N/A
ACCURACY	N/A
SIZE	Max 740 Mbytes/orbit based on IS7 subswath
DATASET	MPH + SPH + ISP sample = 2 bits I, bits 2 Q (compressed using the FBAQ).
AUXILIARY DATA	Orbit data and time correlation parameters are included. PCD (Noise Measurements, Calibration Pulses P1, P1a, P2, P3, Header content of Source Packet).
NOTES	(1) Product size derived from IS7 = 1.85 Mbyte for each of up to 400 imagettes/products.

### 2.5.1.2.3.3 Level 0 Module Stepping Mode (ASA\_MS\_0P)

ASAR has a dedicated Module Stepping Mode, which is used to gather data from all of the instrument's 320 Transmit/Receive Modules (TRM) automatically. The entire procedure takes less than one second. The data is downloaded to the ground for processing. After processing, the results are compared with the reference data from on-ground tests in order to determine any TRM gain or phase drifts, temperature behaviour, and any eventual module failures. Using this information, it is possible to implement any necessary correction to the TRM coefficients and eventually re-synthesise the antenna beam patterns if required. See the Chapter 3 subsection entitled the "[ASA Subsystem](#)" for a discussion of the TRM.

The Module Stepping Mode Level 0 product consists of time-ordered [AISPs](#) collected while the instrument is in Module Stepping Mode. All samples contained within the AISPs are represented by 8 bits/sample. This mode provides an internal health checking facility on an individual module basis. The purpose of the mode is to identify malfunctioning modules which may need to be switched off, and to identify modules to which [calibration](#) offsets are to be applied.

The Level 0 product is produced systematically for all data acquired within this mode. The [NRT](#) version of the product is available from the [PDHS](#) 1 day after data acquisition, while the [OFL](#), fully consolidated, version is available from the [PAC](#) after 2 weeks.

The uses for this mode are discussed in the section entitled "[ASAR Characterisation and Calibration](#)" [2.11](#), and in the Chapter 3 section entitled "[In-flight Performance Verification](#)." [3.2.2](#).

### 2.5.1.3 Level 0 Formats

A summary of the general structure of the Level 0 product is shown in [Table 2.13](#) "Level 0 Product Structure" below. Details of the Measurement Data sets are given in the following section [Level0 Source Packet Description](#). [2.5.2](#).

Table 2.13 Level 0 Product Structure

Main Product Header (MPH) (see " <a href="#">Main Product Header</a> " in <a href="#">Data Formats</a> section <a href="#">6.6.1</a> .)
<a href="#">Specific Product Header</a> (SPH)
<a href="#">Data Set Descriptor</a> (DSD) for <a href="#">Measurement Data Set</a> (MDS)
DSD Level 0 Processor Configuration file
DSD for Orbit State Vectors file
DSD - Spare
MDS
Measurement Data Set Record (MDSR) #1
....
Last MDSR

For the description of the Level 0 SPH, including the Data Set Descriptor (DSD) formats, as well as the Level 0 Measurement Data Set (MDS) Format, including a description of the Front End Processor (FEP) Annotations, refer to the [Data Formats \(Chapter 6.\)](#) section.

For Level 0, the only auxiliary data required is the orbit state vectors and the SBT to UTC time conversion parameters.

The maximum size of any product, and the minimum coverage of any product, is given in the section entitled "Definitions and Conventions."

## 2.5.2 Level 0 Instrument Source Packet Description

Processing of raw data from Level 0 packets will require extraction of the Instrument Source Packets from the Level 0 Product.

The following sections describe the packet structure and arrangement for five types of ASAR Level0 products, the [Image mode](#), [Wide Swath mode](#), [Wave mode](#), [Global Monitoring mode](#), and [Alternating Polarisation mode](#). A description of [decompressing FBAQ](#)-coded data is given last.

### Packet Structure

Level 0 Measurement Data Sets consist of Annotation Packet and Instrument Source Packets. The Annotation Packet contains five fields: date code, length of ISP packet, two error counters and a spare word. The Annotations are shown in detail in [table 2.14](#) . The length word in this packet is corrected with any identified transmission errors (as compared to the ISPs) and is more reliable.

Table 2.14 Annotation Packet

Annotation	Time Stamp	12 bytes, MJD2000
	Length of ISP word	Length - 6 - 1
	Count of CRC errors word	Number of errored VCDUs
	Count of RS errors word	Number of errored VCDUs
	spare word	

The Instrument Source Packets consist of a number of 16-bit words arranged in a Header which includes Identification, Sequence Control and Length. The Packet Data field follows

the Header and contains a Data Field (sub-)Header, Source Data Field and optional Packet Error Control.

Bits are displayed left-to-right, numbering from 0, and with least significant byte on the right, as for ordinary numbers. The Packet header is shown in [table 2.15](#) below.

Table 2.15 Packet Header

Packet Header	Packet Identification word	Version, Type, DataField, Application ID
	Packet Sequence Control word	Segment counter (in the 14 LSB)
	Packet Length word	Length minus one
Packet Data	Header Length word	always 30
	Instrument mode word	see <a href="#">table 2.17</a>
	Time Code 5 bytes	Free-running 65536 Hz
	spare byte	
	Mode Packet Count 3 bytes	
	Antenna Beam Set number	6bits, characterised prior to launch
	Compression Ratio	2bits coded
	Echo Flag	1bit, True if Echo data
	Noise Flag	1bit, True if Noise data
	Cal Flag	1bit, True if Calibration data
	Cal Type	1bit, True if Periodic Cal data
	Cycle Packet Count	12bits
	Pulse Repetition Interval word	PRI * RadarSamplingRate
	Window Start Time word	Windowtime * RadarSamplingRate
	Window Length word	Windowlength * RadarSamplingRate
	Upconverter Level word	4bits, 2*Gain (dB)
	Downconverter Level word	5bits, 1*Gain (dB)
	TX Polarisation	1bit, True if Vertical
	RX Polarisation	1bit, True if Vertical
	Calibration Row number	5bits, used during Periodic Cal
	TX Pulse Length	10bits, Pulselength * RadarSampling Rate
	Beam Adjustment Delta	6bits, delta*4096/360+32
	Chirp Pulse Bandwidth	8bits, BW*255/16E6
	Auxiliary TX Monitor Level	8bits,
	Resampling Factor word	values 1 to 64 are valid

In the Identification word, Version, Type, and DataField are constants, with Application ID represented in 11 bits. These vary by instrument mode as shown in [table 2.16](#). The Segment counter represents data segment sequence number and is reset to zero for ASAR mode changes. The Length word represents data lengths from 1 to 65536, except the minimum length is actually 1008 due to data transmission requirements.

The Packet Data entries in the table give details of the settings of the radar during operation. The code words for Pulse Repetition Interval, Window Start-time, etc are described in the third column showing the calculation for the code word. To obtain the actual value, manipulate the algebraic expression, so that PRI = codeword/RadarSamplingRate. For example, codeword=10300, RadarSamplingRate=1/19.2MHz, PRI = 10300/19.2E6=536

---

microseconds.

The compression ratio code is: 00 for 8/4 compression; 01 for 8/4 compression; 10 for 8/3 compression; 11 for 8/2 compression where 8/2 indicates 8 bits compressed to two using FBAQ flexible block-adaptive quantisation.

Table 2.16 Application ID Codes.

Application ID Code	ASAR Mode
578	Wave
56B	Global Monitoring Mode
56D	Module Stepping Mode
614	Image Mode
61B	Wide Swath Mode
607	Alternating Polarisation (co-polar) Mode
608	Alternating Polarisation (Cross-polar H) Mode
60D	Alternating Polarisation (Cross-polar V) Mode

The Application Identification codes listed in [table 2.16](#) appear in the first word of the Packet Header as the least significant 11 bits. The most significant bits are the pattern 10001. Therefore the first word of the packet for Image Mode will be 8E14.

Table 2.17 Instrument Mode Words

Mode Identifier Code	Mode
54	Image Mode
5B	Wide Swath
98	Wave Mode
AB	Global Monitoring Mode
67	AP Co-Polar Mode
68	AP Cross-Polar H
A4	AP Cross-Polar V

### Image Mode Packets

During Image mode a continuous series of pulses and echoes are acquired. The initial transmissions include a calibration sequence, but this changes to interleaved echo measurement and calibration pulses. Figure 1 shows the arrangement of transmissions and echo receptions.

Table 2.18 Image mode Source Packets

Number of Source Packets	Source Packet Contents

---

8	noise
97	initial calibration
1023	echo
1	periodic calibration
1023	echo
1	periodic calibration
...	...
1023	echo
1	periodic calibration
8	noise

Table 2.19 Source Packet Format Echo Data (Averaging Mode)

First Block	64 bytes	8bits	Block ID code
		4bits	I-channel codeword
		4bits	Q-channel codeword
		4bits	I-channel codeword
		4bits	Q-channel codeword
		...	...
		4bits	I-channel codeword #63
		4bits	Q-channel codeword #63
Second Block	64 bytes	8bits	Block ID Code
		4bits	I-channel codeword
		4bits	Q-channel codeword
Last Block	even number of bytes	8bits	Block ID Code
		4bits	I-channel codeword
		4bits	Q-channel codeword
	filler	8bits	to make 972 bytes minimum length and to make length even

[Table 2.19](#) shows the Packet Format for averaging mode (4-bit quantisation). This format applies to both Image Mode and Wide Swath Mode. The filler bytes are added to ensure 972 bytes of source packet plus 6byte packet header and 30 byte packet data header are 1008 bytes or longer. This data size is the minimum transmitted in CCSDS format used in the spacecraft downlink.

Table 2.20 Source Packet Format Calibration Data (8bit quantisation)

Size	8bits	8bits	8bits	8bits	...	8bits	8bits
	I0	Q0	I1	Q1	...	Ilast	Qlast

[Table 2.20](#) shows the format of the Calibration data, which are always quantised to 8 bits. The number of samples in a sampling window is given in the Window Length codeword in [table 2.15](#).

Table 2.21 Noise Data Packet Format

Number of bits	4	4	4	4	...	4	4	e*8
	I	Q	I	Q		I	Q	filler

[Table 2.21](#) shows the format of Noise data. The data are padded to 972 bytes if necessary.

### Wide Swath Mode Packets

Table 2.22 Wide Swath Mode Source Packets

Number of Packets		Source Packet Contents			initial noise and calibration sequence	
8	noise	subswath 1				
97	initial calibration					
8	noise	subswath 2				
97	initial calibration					
...						
8	noise	subswath Q				
97	initial calibration					
R1-2	noise	subswath 1			first cycle	
M1	echo					
1	periodic cal					
R2-2	noise	subswath 2				
M2	echo					
1	periodic cal					
...						
Rp-2	noise	subswath P				
Mp	echo					
1	periodic cal					
...						
R1-2	noise	subswath 1			last cycle	
M1	echo					
1	periodic cal					
R2-2	noise	subswath 2				
M2	echo					
1	periodic cal					
...						
Rp-2	noise	subswath P				
Mp	echo					
1	periodic cal					

In Wide Swath Mode the radar is operated in subswaths,  $Q \leq 6$ , and within a cycle a subswath may be sampled again, up to  $P$  samples per cycle, where  $P \leq 12$ . Each packet shown is comprised of data samples described in [table 2.19](#) Source Packet Format Echo Data. [Table 2.20](#) and [Table 2.21](#) for calibration data, periodic calibration data and noise data also apply.

## Wave Mode Packets

The Wave Mode packets consist of compressed echo packets (compressed 8 to 2), calibration packets and noise packets, interleaved as shown in [table 2.22](#), below.

Table 2.23 Wave Mode Source Packets

Number of Packets		Source Packet Contents		
1	Calibration	first subcycle	first cycle	
1	noise			
1	Calibration sequence			
M1/8	echo			
1	calibration		second cycle	
1	noise			
1	calibration sequence			
M2/8	echo			
1	Calibration			
1	noise			
1	Calibration sequence			
M1/8	echo			
1	calibration	second subcycle		
1	noise			
1	calibration sequence			
M2/8	echo			
last cycle (truncated)				

In Wave Mode there are two calibration intervals, a chirp calibration with 2 windows (called simply "Calibration" in the table), and continuous wave (CW) calibration with 97 windows ("Calibration Sequence" in the table). The echo data is 8 windows and noise data is 8 windows.

Table 2.24 Source Packet Format Echo (8/2 compression mode)

first sampling window	first block	64 bytes	8bits	Block ID Code
			2bits	I-channel codeword
			2bits	Q-channel codeword
			2bits	I-channel codeword
			2bits	Q-channel codeword
			...	
			2bits	I-channel codeword
			2bits	Q-channel codeword
	second block	64 bytes	8bits	Block ID Code
			2bits	I-channel codeword
			2bits	Q-channel codeword
			...	
	last block	c+d bytes	8bits	Block ID Code
			2bits	I-channel codeword
			2bits	Q-channel codeword
			d filler bytes	

second sampling window	first block	64 bytes	8bits	Block ID Code
			2bits	I-channel codeword
			2bits	Q-channel codeword
			2bits	I-channel codeword
			2bits	Q-channel codeword
			...	...
			...	...
			...	...
			...	...
			last block	c+d bytes
			2bits	Q-channel codeword
				d filler bytes

In the wave mode data, each sampling window contains blocks corresponding to PRIs, and sample codewords with quantity specified in the data header. The 2bit codewords are uncompressed in accordance with FBAQ decoding scheme. This is explained in SECTION TBD. Filler bytes are added when necessary to provide 1008 byte blocks when the packet header (36 bytes) is included.

Table 2.25 Wave Mode Calibration Packets

	first calibration window								second window				...	last window	
Number of bits	8	8	8	8	...	8	8	8	8	...	...	8		...	I
	I	Q	I	Q		I	Q	I	Q			I			

Calibration packets in Wave mode appear in either 3 windows or 97 windows depending on the calibration pulse (chirp and CW respectively). The data are quantised to 8 bits not compressed.

Table 2.26 Wave Mode Noise Packet

	first noise window								second window				...	last window	
Number of bits	4	4	4	4	...	4	4	e*8	4	4	...	4		...	4
	I	Q	I	Q		I	Q	filler	I	Q		Q			

The Wave Mode noise packet is formatted to sign and magnitude with fixed exponent. The number of samples is defined in the data header Window Length word, divided by the Resampling factor.

### Global Monitoring Mode

Table 2.27 GM Mode Source Packets

Number of Source Packets	Source Packet Contents			
8	noise	subswath 1	initial noise/calibration sequence	
1	initial cal (97)			
8	noise	subswath 2		
1	initial cal (97)			
...				
8	noise	subswath Q (Q<=6)		
1	initial cal (97)			
1	periodic calibration	first subswath	first subcycle	
1	echo (M1 PRI)			
1	periodic calibration	second subswath		
1	echo (M2 PRI)			
...				
1	periodic calibration	p-th subswath	first cycle (odd)	
1	echo (M2 PRI)			
1	echo (M1 PRI)	first subswath		
1	echo (M2 PRI)	second subswath		
...				
1	echo (Mp PRI)	p-th subswath	second subcycle	
	noise	first subswath		
...				
1	echo (M1 PRI)	pth-subswath		
1	noise	first subswath	S-th subcycle	
1	echo (M1 PRI)			
1	noise	second subswath		
...				
...				
1	periodic cal/noise	first subswath	second cycle (even)	
1	echo (M1 PRI)			
...				
...				
1	periodic cal/noise	first subswath	Nth cycle (odd or even)	
1	echo (M1 PRI)			
...				
...				

GM Mode echo packets are as described in [Table 2.19](#), Averaging Mode.

GM Mode Calibration data are described in [Table 2.20](#).

GM Mode Noise data are described in [Table 2.26](#).

### Alternating Polarisation Mode

In this mode each sampling window contains either echo data, initial calibration, periodic calibration or noise data. The periodic calibration data is four sampling windows. In [table 2.28](#) following, the format for VV-HH (co-polar) mode is shown. Cross-polar modes VV and HH are similar except VV becomes HV and HH becomes VH.

Table 2.28 Alternating Polarisation Mode Source Packets

Number of source packets	Source packet contents		
8	noise (VV)	initial noise/cal sequence	
8	noise (HH)		
97	initial calibration (VV)		
97	initial calibration (HH)		
M-1	echo (VV)	V-cal subcycle	first cycle
1	periodic cal (VV)		
M	echo (HH)		
M	echo (VV)		
M	echo (HH)	H-cal subcycle	
M	echo (VV)		
M-1	echo (HH)		
1	periodic cal (HH)		
M	echo (VV)	V-cal subcycle	last cycle
M	echo (HH)		
M-1	echo (VV)		
1	periodic cal (VV)		
M	echo (HH)	H-cal subcycle	
M	echo (VV)		
M	echo (HH)		
M	echo (VV)		
M-1	echo (HH)		
1	periodic cal (HH)		
M	echo (VV)		
M	echo (HH)		
8	noise (VV)		
8	noise (HH)		

Packet contents for the AP source packets have been described earlier. [Table 2.19](#) describes the echo data, Table 7 calibration, Table 8 for noise.

#### Decompression of FBAQ-coded data

FBAQ compresses the raw SAR echo data from 8 bits per sample to 4, 3 or 2 bits per sample, abbreviated 8/4, 8/3, 8/2. This is a lossy compression method, meaning that distortion in the form of "quantization noise" is added. The distortion is proportional to the degree of compression.

Decompression of FBAQ-coded data is accomplished with the use of look-up-tables, abbreviated LUTs. The LUTs map the codewords to normalized floating-point values. There is one LUT for I-channel and one for the Q-channel when corrections for the differences in analog-to-digital (ADC) converters are applied.

The LUTs are determined from the standard deviation and mean of the SAR data. The threshold values are not uniform but are selected to produce results with minimum least-square error, based on statistics of SAR echoes. The reconstructed value is based on the threshold values and code words. The same tables may be used for positive and negative values (the reconstructed values are symmetric about zero).

[Table 2.29](#) , [table 2.30](#) and [table 2.31](#) show the threshold values for 4-bit, 3-bit and 2-bit reconstruction.

Table 2.29 Constants for 4-bit BAQ

n	Cn	Dn
0	0	0.1284
1	0.2583	0.3882
2	0.5226	0.6569
3	0.7998	0.9426
4	1.0995	1.2565
5	1.4374	1.6183
6	1.8338	2.0693
7	2.4011	2.7328

Table 2.30 Constants for 3-bit BAQ

n	Cn	Dn
0	0	0.2451
1	0.5006	0.7561
2	1.0500	1.3440
3	1.7480	2.1520

Table 2.31 Constants for 2-bit BAQ

n	Cn	Dn
0	0	0.4528
1	0.9816	1.5104

The reconstruction thresholds are

$$R_n = (D_n \cdot \sigma) + \mu \quad \text{eq 2.1}$$

where Dn is given in the tables above, and  $\sigma$  is the standard deviation and  $\mu$  is the mean. For SAR data the mean is zero, and the standard deviation is given in the BlockID.

The decompression algorithm is then

For each range line

For each block in the range line

read the BlockID

Select a LUT corresponding to compression level and BlockID

unpack FBAQ codewords

reconstruct data using codewords and LUT entry

The LUT is an array which is 256 entries across (corresponding to the 8-bit BlockID) and 16-rows (for 4-bit), 8-rows (for 3-bit), and 4-rows (for 2-bit compression). The values of the entries of the six different LUTs (one each for I and Q, three different quantisations) are provided in the [Instrument Characterisation File 6.5.2](#).

## 2.6 Level 1B Products

### 2.6.1 ASAR Level 1B Algorithms

#### 2.6.1.1 ASAR Level 1B Algorithm Physical Justification

##### 2.6.1.1.1 Introduction

The purpose of this section is to provide a basic understanding of the sensor geometry and SAR signal, in order to understand the algorithm descriptions in the succeeding sections.

##### 2.6.1.1.2 Radar Geometry

An imaging [radar](#) such as a SAR is side-looking. (see also "[Imaging Geometry](#)" in the Geometry subsection in the Glossary ). That is, the [radar antenna beam](#) is pointed sideways, typically nearly perpendicular to the flight direction of the spacecraft. The basic side-looking geometry is illustrated in [figure 2.14](#) below. As the transmitted [pulse](#) propagates from the radar, it is reflected from scatterers, or targets, located at increasing distances from the radar along the ground. The received echoes from a single transmitted pulse form one line of SAR data, as a function of the time delay to the scatterers. Thus, one dimension in a [radar image](#) is the distance from the radar to the scatterer, called [range](#). This is not the same as distance along the ground, since the radar is located at some altitude above the ground. Thus the dimension in the image is called [slant range](#), as opposed to [ground range](#), as shown in the figure.

The spacecraft transmits pulses and receives echoes periodically. Because the spacecraft is moving, a pulse is transmitted at different locations along the flight path. Thus, the [along-track](#) direction, or azimuth, is the other dimension in the radar image. Note that the speed of light at which the pulse propagates is much faster than the spacecraft velocity, so the echo of the pulse from the ground is assumed to be received at the same spacecraft position at which the pulse was transmitted.

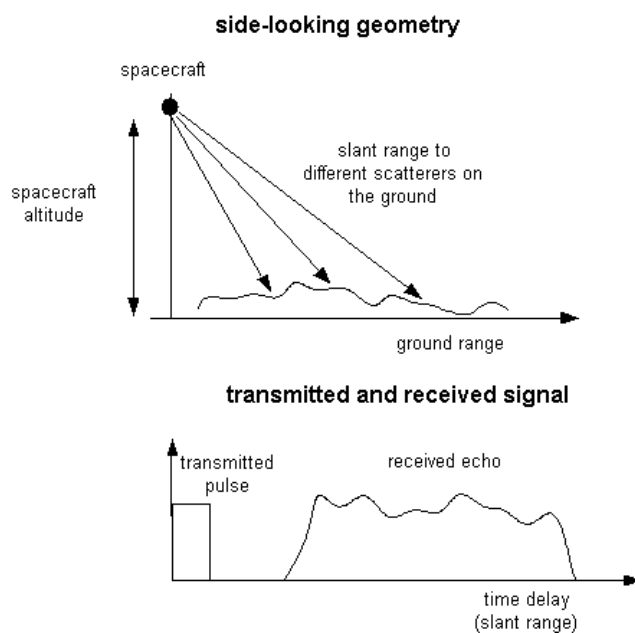


Figure 2.14 Side-looking radar geometry and slant range dimension in line of SAR data.

### 2.6.1.1.3 Pulse Compression

In collecting the SAR data, a long-duration linear [FM](#) pulse is transmitted. This allows the pulse energy to be transmitted with a lower peak power. The linear FM pulse has the property that, when filtered with a matched filter, the result is a narrow pulse in which all the pulse energy has been collected to the peak value. Thus, when a matched filter is applied to the received echo, it is as if a narrow pulse were transmitted, with its corresponding [range resolution](#) and signal-to-noise ratio.

Mathematically, in complex form, a linear FM signal can be represented as:

$$p(\tau) = \exp(i\pi K\tau^2) \quad \text{eq 2.2}$$

where  $i$  is the square root of  $-1$ ,  $\tau$  is time within the pulse, and  $K$  is the [frequency](#) rate. Note the signal has quadratic [phase](#), the derivative of which gives the linearly increasing instantaneous frequency.

Matched filtering is illustrated in the following figure. The linear FM pulse has an instantaneous frequency that increases linearly with time, as shown by the increasing rate of oscillation in the linear FM pulse in the [figure 2.15](#) below. The matched filter can be thought of as a filter with a different time delay for each frequency component of the signal passing through the filter. That is, the different frequency components of the linear FM signal are each delayed so that they all arrive at the same time at the output of the filter. This way, all the signal energy is gathered into a narrow peak in the compressed pulse.

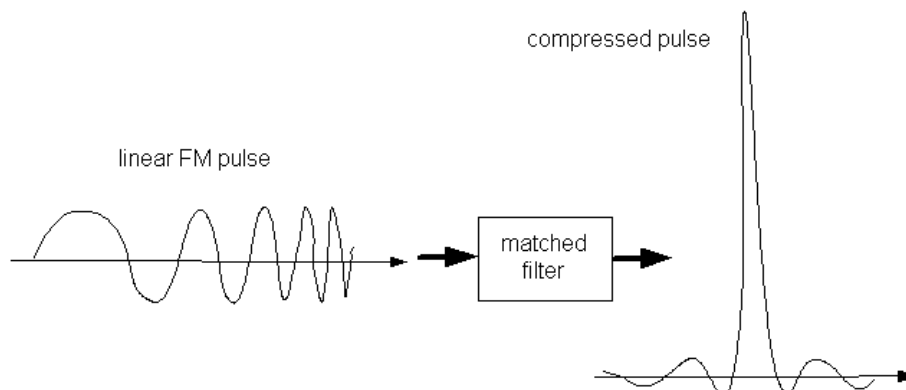


Figure 2.15 Illustration of pulse compression.

#### 2.6.1.1.4 SAR Signal

The sequence of received pulses are arranged in a two-dimensional format, with dimensions of range and azimuth, to form the SAR signal. The signal is typically described by the considering the signal received from a single scatterer on the ground, or point target. In this case, at each azimuth position, a single pulse echo from the point target is received. The delay of the received pulse depends on the distance from the radar to the target, and this distance varies as the spacecraft travels along the flight path. Also, pulses are received for as long as the target is illuminated by the antenna beam. This illumination time determines the azimuth extent of the raw SAR signal from a point target, or synthetic aperture. The changing range, synthetic aperture, and resulting SAR signal are illustrated in the following figure.

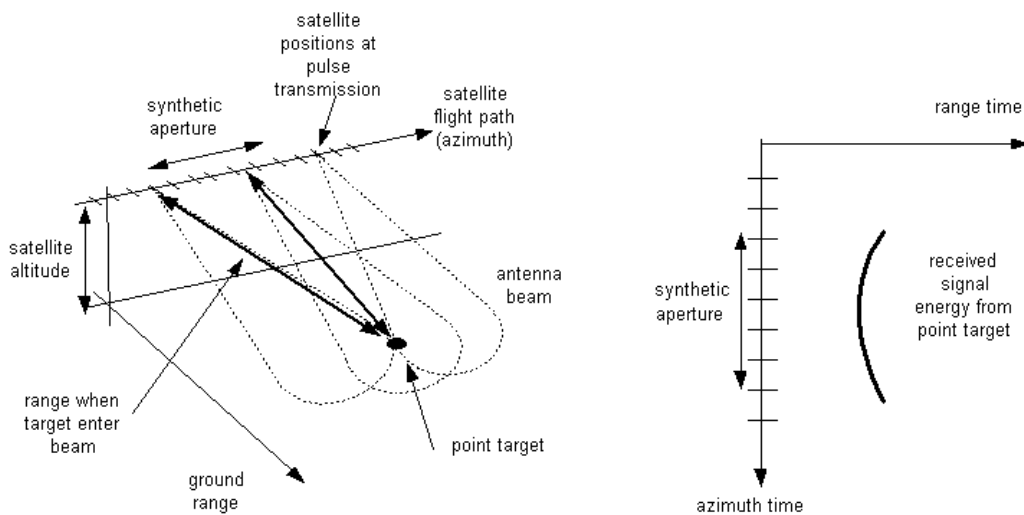


Figure 2.16 Illustration of changing range to scatterer, synthetic aperture, and 2-d SAR signal

In the two-dimensional array, the received signal from a point scatterer (target) follows a trajectory that depends on the changing range to the scatterer, as shown in [figure 2.16](#) above

The changing range to the scatterer also affects the phase of each received pulse. The antenna actually transmits a high frequency, sinusoidal carrier signal, that has been modulated by the transmitted pulse. This carrier signal is reflected by the target, received by the antenna, and demodulated to get the received pulse echo. The delay of the carrier signal due to the range to the target leaves a phase change in the demodulated, received pulse. The coherent demodulation in the radar preserves this phase from pulse to pulse, resulting in an azimuth-varying phase in the SAR signal.

Let  $t$  be time along the flight path (azimuth time) and  $R(t)$  be the distance to the target as a function of azimuth time. Also, let  $\tau$  be the range time within a received pulse (also called fast time), relative to the pulse transmission time. Then, the two-dimensional SAR signal can

be expressed as

$$s(t, \tau) = \exp(i4\pi R(t)/\lambda) p(\tau - 2R(t)/c) \quad \text{eq 2.3}$$

where  $p(\tau)$  is the transmitted pulse,  $c$  is the speed of light, and  $\lambda$  is the [wavelength](#) of the carrier. That is, the delay of the pulse is the round-trip distance divided by the speed of light. Similarly, the phase of the signal due to the delay of the carrier is the round-trip distance divided by the wavelength.

For a straight flight path, the range  $R(t)$  is a hyperbolic function. Typically, it can be approximated by a quadratic function over the length of the synthetic aperture. Thus, the SAR azimuth signal is approximately linear FM, and has an instantaneous frequency that varies with azimuth time. This property allows the azimuth signal to be compressed, as described above for pulse compression, which makes possible the focussing of SAR images.

The varying instantaneous frequency of the azimuth signal is analogous to the varying [Doppler](#) frequency shift of the carrier signal. The Doppler frequency depends on the component of satellite velocity in the line-of-sight direction to the target. This direction changes with each satellite position along the flight path, so the Doppler frequency varies with azimuth time. For this reason, azimuth frequency is often referred to as Doppler frequency.

### 2.6.1.1.5 Continuous versus Burst Data

Different [ASAR modes](#) collect the SAR data in different ways. The fundamental distinction, from the point of view of SAR processing, is whether the data from a [swath](#) on the ground is collected continuously or burst-wise. The continuous model of SAR data applies to [Image Mode \(IM\)](#) data processed with the [range-Doppler 2.6.1.2.3.](#) algorithm. The burst model of SAR data applies to [Alternating Polarisation \(AP\)](#) and [ScanSAR](#) (i.e. [Wide Swath \(WS\)](#) and [Global Monitoring \(GM\)](#)) data, and Image Mode data processed to medium-resolution with the [SPECAN 2.6.1.2.4.](#) algorithm.

Essentially, in continuous mode, all of the received echoes at each azimuth position are used in the focussing of the SAR data. In burst mode, only a certain number of echoes are collected at a time, i.e. bursts of data. The following figure illustrates the SAR signals from several point targets distributed in the azimuth direction, and the data that is actually collected in continuous mode and burst mode.

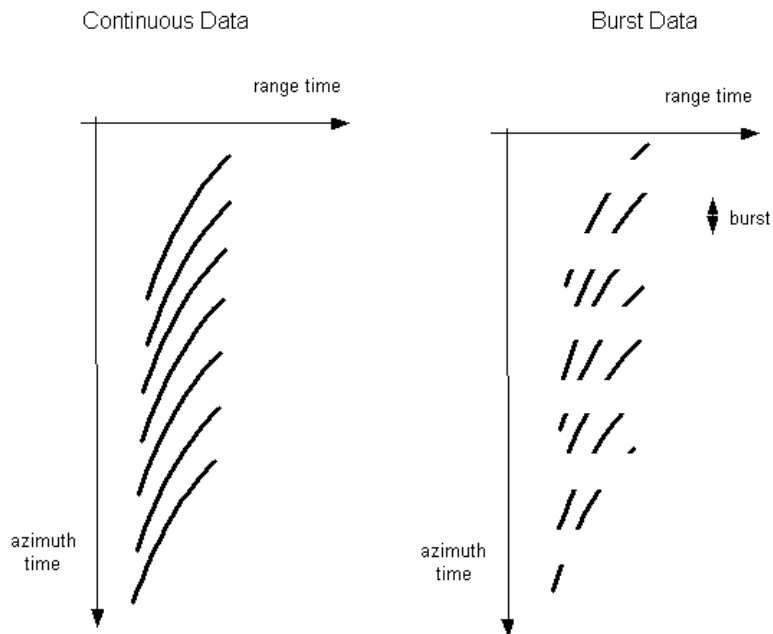


Figure 2.17 Illustration of continuous and burst SAR data

Note that the time between bursts is smaller than the synthetic aperture, so that the signal from one point target shows up in at least two bursts. Thus all the information needed to form an image is still available in the SAR data. Each burst of data can be compressed in the azimuth direction, forming overlapping burst images of the ground.

### 2.6.1.1.6 Image Cross Spectra

The cross spectra of images formed from different azimuth frequency bands are used to estimate the ocean wave spectra from Wave Mode products.

A SAR image of the ocean typically has a striped appearance, corrupted by speckle, as shown in the figure in the [Level 1b Wave Products 2.6.2.1.2](#). section. The stripes correspond to ocean waves. The two-dimensional spectrum of the image will contain energy at the frequency components corresponding to the stripes in the image, and this could be transformed to an estimate the ocean wave spectrum. A problem, however is the 180 degree ambiguity in the direction of the ocean waves. This ambiguity can be resolved by using different look images in the estimation of the ocean wave spectra.

In the SAR signal described above, the azimuth signal has a linear FM character, which means the instantaneous azimuth frequency is related to the azimuth time in the signal. At different azimuth times, the satellite is in different azimuth positions and is viewing a particular point on the earth from different directions. Thus, there is a relationship between azimuth frequency and the viewing angle of the point on the earth.

Given a complex SAR image, a set of images can be formed from different azimuth-frequency bands, or looks. These look-images correspond to different viewing directions of the ocean surface, which allows the ambiguity in the ocean wave direction to be resolved. Instead of using the spectrum of the original SAR detected image, the cross spectra between the look images is transformed to an estimate of the ocean wave spectrum. This method also allows a noise reduction in the derived spectrum.

### 2.6.1.2 ASAR Level 1B Algorithm Descriptions

In general, the algorithms can be broken down into the following categories:

- Preprocessing: ingest and correct the raw ASAR data
- Doppler Centroid Estimation: estimate the centre frequency of the Doppler spectrum of the data, related to the azimuth beam centre
- Image Formation: process the raw data into an image (using [range-Doppler 2.6.1.2.3](#), and [SPECAN 2.6.1.2.4](#), algorithms)

These steps are shown with the flow of the imagery data in the flow diagram below:

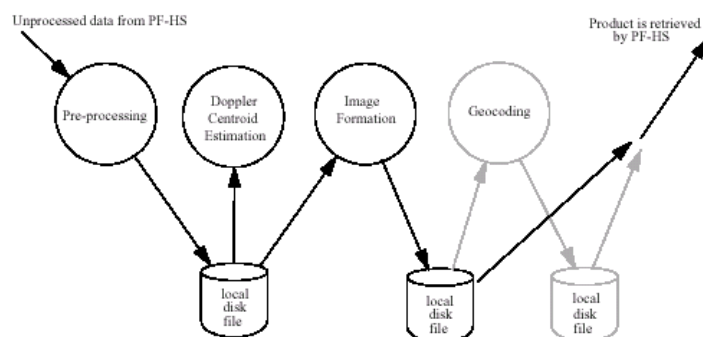


Figure 2.18 Flow of imagery data during processing

The particular algorithms used in each step depend on the type of image product. Table 1 below summarises the algorithms used for each product. (See [Table 2.39 "Level 1B Products"](#), in Section "Level 1B High-Level Organisation of Products" for the complete table of Level 1B products and the corresponding product type description.)

Table 2.32 Processing steps used during generate products

Processing Steps	IM or IM	IMP or IMS	IMG	APM and APB or APP	APS	APG	WSM and WSB	GM1 and GMB	WVI, WVS and WWV
<a href="#">Preprocessing 2.6.1.2.1</a>	X	X	X	X	X	X	X	X	X
<a href="#">Doppler Centroid Estimation (Single Swath) 2.6.1.2.2</a>	X	X	X	X	X	X			
<a href="#">Doppler Centroid Estimation (MultiSwath) 2.6.1.2.2</a>							X	X	
<a href="#">Doppler Refinement 2.6.1.2.2</a>				X	X	X	X		
<a href="#">Range Doppler Image Formation 2.6.1.2.3</a>		X	X		X				
<a href="#">SPECAN Image Formation 2.6.1.2.4</a>	X			X		X	X	X	
Wave Mode Processing (see note 1)									X
Geocoding			X			X			

[Stripline](#) processing is applied to [medium-resolution](#) products and to [Wide Swath](#) (WS) Mode and [Global Monitoring](#) (GM) Mode products.

Note 1: For [Wave Mode](#) (WV) Level 1B products, Wave Mode processing includes [Doppler Centroid Estimation 2.6.1.2.2](#). (DCE) and a [range-Doppler 2.6.1.2.3](#). algorithm to form the [imagette](#) for [cross-spectra](#) estimation.

## 2.6.1.2.1 Preprocessing

Preprocessing is applied to all [raw data](#) before the other parameter estimation and image formation steps are performed.

During preprocessing, [PF-ASAR](#) performs [raw data analysis](#), noise processing, and the processing of the ASAR [calibration pulse](#) data. [Chirp](#) replicas and [antenna pattern gain factors](#) are obtained from the calibration pulse processing. The signal data for all modes is [FBAQ](#) decoded; prior to processing (from 2, 3 or 4 bits back to 8 bits).

Preprocessing includes:

- Ingest and validation of raw ASAR data. Check the data packet headers.
- Block Adaptive Quantisation (BAQ) decoding. Decompress the data from the 2 or 4 bit coded representation to the 8 bit representation. A table look-up operation is used to perform BAQ decoding. This is described further in the [Level 0 Packets](#)

---

### [2.5.2.](#) section.

- Raw Data Analysis. Complex data is collected in in-phase (I) and quadrature-phase (Q) channels. Receiver electronics may introduce biases or cross-coupling (non-orthogonality) between the I and Q channels. This can be estimated by collecting statistics of the I and Q channels. These statistics are collected by accumulating the sums I, Q, I squared and Q squared . Only a fraction of the data set is used.
- Raw Data Correction. I/Q bias removal, I/Q gain imbalance correction, I/Q non-orthogonality correction.
- Replica Construction and Power Estimation. A replica of the transmitted pulse is extracted. This process is also described in [Characterisation 2.11.3.2.](#) .
- Noise Power Estimation. Analysis of noise packets.

## 2.6.1.2.2 Doppler Frequency Estimator

Doppler centroid estimation is a key element in the processing of ASAR data. A full discussion of the various methods used for different product types is given below

### 2.6.1.2.2.1 Introduction

The Doppler centroid frequency of the Synthetic Aperture Radar (SAR) signal is related to location of the [azimuth](#) beam centre, and is an important input parameter when processing SAR imagery. The Doppler centroid locates the azimuth signal energy in the azimuth ([Doppler](#) [frequency](#)) domain, and is required so that all of the signal energy in the Doppler spectrum can be correctly captured by the [azimuth compression](#) filter, providing the best signal-to-noise ratio and azimuth resolution. Also, for modes processed by [SPECAN](#) [2.6.1.2.4.](#) , accurate knowledge of the azimuth beam pointing angle is required in order to correctly apply [radiometric compensation](#) for the azimuth beam pattern.

Even with the use of yaw-steering, and an accurate knowledge of the satellite position and velocity, the pointing angle will have to be dynamically estimated from the SAR data in order to ensure that radiometric requirements of the [PF-ASAR](#) processor are met.

The azimuth pointing angle translates into a Doppler centroid frequency that must be estimated to an accuracy on the order of 25 Hz (for burst-modes including [Alternating Polarisation](#) (AP), [Wide Swath](#) (WS) and [Global Monitoring](#) (GM)), and 50 Hz for all other [modes](#).

There exist a number of algorithms to estimate the Doppler centroid frequency. For the PF-ASAR, the key challenge is to define techniques that will yield sufficiently accurate estimates for all processing modes. In particular, the [burst-mode](#) data products require attention, since their products are inherently more sensitive to Doppler centroid errors.

The Doppler centroid varies with both [range](#) and azimuth. The variation with range depends on the particular satellite attitude and how closely the illuminated footprint on the ground follows an iso-Doppler line on the ground, as a function of range. The variation in azimuth is due to relatively slow changes in satellite attitude as a function of time.

The azimuth signal in SAR is sampled by the [pulse repetition frequency \(PRF\)](#). As with all sampled signals, there is an ambiguity in the location of frequency spectrum, by a multiple of the sampling rate. For this reason, the Doppler centroid is written as

$$f_{\eta_c} = f'_{\eta_c} + MF_a \quad \text{eq 2.4}$$

where the absolute Doppler centroid frequency  $f_{\eta_c}$  is composed of two parts. The fine Doppler centroid frequency  $f'_{\eta_c}$  is sometimes referred to as the fractional part, and is ambiguous to within the azimuth sampling rate,  $F_a$ . (the PRF). The other part is an integer multiple of the azimuth sampling rate  $MF_a$ . Doppler centroid estimation often refers to the estimation of the fine Doppler centroid frequency, which is limited to the range  $\pm F_a/2$ , where  $F_a$  is the pulse repetition frequency (PRF). The Doppler ambiguity,  $M$ , is an integer in the set  $\{..., -2, -1, 0, 1, 2, ...\}$  and the method used to determine this value is known as the Doppler Ambiguity Resolver (DAR). In general, as [ENVISAT](#) is yaw-steered, the expected value of  $M$  is 0; however, the true value may be larger. Usually the two components of the unambiguous Doppler centroid frequency are estimated independently.

Because of the range-variation of the Doppler centroid, the Doppler centroid is estimated at different ranges in the data, and a polynomial function of range is fit to the measurements. The Doppler centroid may also be updated in successive azimuth blocks.

The following sections will discuss the Doppler Centroid Frequency and a number of different methods used to determine both the absolute and the fine Doppler Centroid frequencies. The method used will depend on the type of product being generated:

- For [high-resolution Image Mode \(IM\)](#) and [Wave Mode \(WV\)](#):
- the [MLCC 2.6.1.2.2.3.](#) algorithm [Ref. \[2.1\]](#) is used as an estimator of the absolute Doppler centroid.
- For [Alternating Polarisation \(AP\)](#) Mode and [medium-resolution](#) products processed with SPECAN:
- the MLCC algorithm is used to estimate the absolute Doppler centroid and the fine Doppler centroid estimate is further refined using the [Look Power Balancing 2.6.1.2.2.4.](#) algorithm [Ref. \[2.2\]](#).
- For [Wide Swath \(WS\)](#) mode:
-

the fine Doppler centroid is estimated using [Madsen's method 2.6.1.2.2. Ref. \[2.3\]](#) and then further refined using the Look Power Balancing algorithm. The Doppler ambiguity is resolved using the [PRF diversity method 2.6.1.2.2.5. Ref. \[2.4\]](#).

- For [Global Monitoring \(GM\)](#) mode:
- this is similar to WS mode except the Look Power Balancing method is not used because the amount of data in each azimuth look of GM mode is too little for the Look balancing method.

### 2.6.1.2.2.2 Madsen's Method

Madsen's method is used to estimate the fractional PRF part of the Doppler centroid, or the fine Doppler centroid. It is very simple to implement and it is well suited to the processing of [ScanSAR](#) data. The Madsen method works by estimating the autocorrelation function of the data, and using the fact that the [phase](#) of the autocorrelation function relates to a Doppler shift in the Power Spectral Density function. Madsen's method is very efficient, as it does not require any [Fast Fourier Transforms \(FFTs\)](#) or peak searches to be performed. It also works in raw data or on range compressed data. Madsen's method will be used to derive an initial Doppler centroid estimate in ScanSAR modes, to be refined by the more computationally expensive, but more accurate look balancing techniques described below.

Madsen's method works by calculating the first lag of the autocorrelation function of the data in the azimuth direction. This is the Cross Correlation Coefficient (CCC) of adjacent azimuth samples. The phase of the CCC,  $\phi$ , is related to the Doppler centroid by

$$F_{\eta_c} = \frac{-F_a \phi}{2\pi} \quad \text{eq 2.5}$$

Note that the phase of the CCC is only known within one cycle of 2 pi. From the above equation, one cycle of 2 pi corresponds to one interval of the azimuth sampling rate, so that the method actually estimates the fine Doppler Centroid.

In the estimation algorithm, the CCC is estimated over the azimuth line for each range gate. The result is a complex coefficient for each range gate. The range gates are then divided into groups, and coefficients are then averaged over each group of range gates. This gives an [Average Cross Correlation Coefficient \(ACCC\)](#) for each group of range gates, whose argument is used to calculate the Doppler centroid. The result is an array of fine Doppler centroid estimates as a function of range.

### 2.6.1.2.2.3 Multi-Look Cross Correlation (MLCC) Method

The MLCC Doppler centroid estimator estimates both the integer and fractional parts of the Doppler centroid from the SAR data. The estimator determines the absolute Doppler frequency, without aliasing, obtaining both of the parameters as a function of range.

Knowledge of the beam pointing angles is not needed by the algorithm, except as a cross check.

The MLCC algorithm described here uses the property that the absolute Doppler centroid is a function of the frequency of the transmitted signal. The MLCC algorithm is based on computing the CCC from images formed from two range frequency bands, or looks. That is, the range frequency spectrum is divided into two parts, and [Inverse Fourier Transforms \(IFFTs\)](#) are taken to form complex images corresponding to each of the two range frequency [looks](#). Then, in the range time domain, the ACCC's of two images are computed, and the phase difference between them,

$$\delta\phi = \phi_{L_2} - \phi_{L_1} = \frac{2\pi(K_{a_2} - K_{a_1})\eta_c}{F_a} \quad \text{eq 2.6}$$

is used to compute the absolute Doppler centroid. The absolute Doppler centroid frequency is given by:

$$f_{\eta_c} = \frac{-f_0 F_a \delta\phi}{2\pi\delta f} \quad \text{eq 2.7}$$

where  $f_0$  denotes the centre transmitted frequency. The accuracy of this absolute Doppler centroid is by itself not sufficient, but it can be used to estimate the Doppler ambiguity, as discussed below. The fractional PRF part is obtained from the phases of each of the ACCC's of the two looks,  $\phi_{L_1}$  and  $\phi_{L_2}$ :

$$f'_{\eta_c} = \frac{-F_a}{2\pi} \left( \frac{\phi_{L_1} + \phi_{L_2}}{2} \right) \quad \text{eq 2.8}$$

Note that the phases measured from each look can be in different 2 pi cycles. That is, one or both of the ACCC angles  $\phi_{L_1}, \phi_{L_2}$ , may have been wrapped around. To correct for this, a simple discontinuity detector is used to set  $f'_{\eta_c}$  to within the interval  $\pm f_a/2$ . Similar to Madsen's method, the error tolerance in the two autocorrelation coefficient angles is relatively high; an error of 5° in the autocorrelation coefficient angles causes an error of only 0.014 F a in  $f'_{\eta_c}$ .

Using this method as the Doppler Ambiguity Resolver (DAR), the Doppler ambiguity estimated is:

$$M = \text{round} \left( \frac{f_{\eta_c} - f'_{\eta_c} - f_{\text{offset}}}{F_a} \right) \quad \text{eq 2.9 dop_eq_3_4}$$

where  $f_{\text{offset}}$  is the system offset frequency discussed below.

Finally, given the fine Doppler estimate, the ambiguity M is used to calculate the value of the absolute Doppler centroid  $f_{\eta_c}$ .

Basically, the sum of the two ACCC angles gives the fractional PRF part, and the difference

gives the Doppler ambiguity.

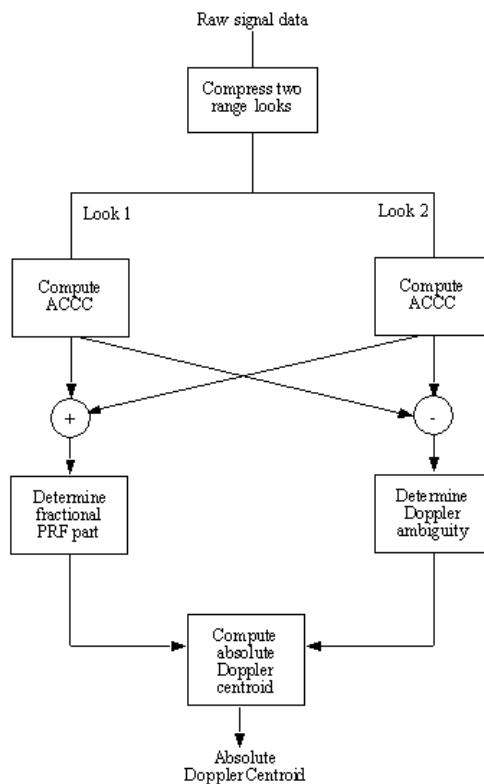


Figure 2.19 The MLCC Algorithm for Doppler Centroid Estimation

The system offset frequency, ( $f_{\text{offset}}$ ), must be subtracted from the measured value of  $f_{\eta_c}$ . This offset frequency depends upon the antenna characteristics, and must be calibrated for each satellite. It originates from the dependence of the antenna pointing angle on transmitted frequency. While the transmitted pulse sweeps across the total bandwidth, the instantaneous antenna pointing angles vary. Since the Doppler centroid frequency depends upon the antenna pointing angles, the instantaneous Doppler centroid frequency varies across the pulse. (The SAR processor requires the average Doppler centroid frequency.) In the MLCC algorithm, the two range looks are extracted each with a different effective carrier frequency. This means that each look has a slightly different Doppler centroid. This effect can be corrected by determining the offset frequency and removing the resulting bias. The system offset frequency can be measured by processing sensor data with a known Doppler ambiguity. The value, before rounding, can be compared to the correct ambiguity. An appropriate offset frequency can be determined by minimising the error between the non-rounded value and  $M$ . These values are output by the processor into a debug file to facilitate this calibration operation. The system offset frequency may be beam dependent.

### 2.6.1.2.2.4 Look Power Balancing

Image products that are formed with the SPECAN algorithm are formed from periodic bursts of SAR data. The burstiness may arise because of the way the data is collected, as in Alternating Polarisation mode or ScanSAR modes (Global Monitoring, Wide Swath), or bursts may be extracted during processing as in the formation of medium-resolution products. Typically a burst is much shorter than the time it takes the azimuth beam to pass over a point on the ground (synthetic aperture time). Thus, during a burst, the portion of the antenna beam that illuminates a target depends on the target position. That is, targets at different azimuth positions are illuminated through different parts of the antenna beam. The azimuth antenna gain pattern then causes an azimuth variation in target intensity in the processed image. The known antenna pattern can be used to compensate for this radiometric variation, but the Doppler centroid, or azimuth beam pointing direction, must be known very accurately. [Figure 2.20](#) illustrates the effect of radiometric correction with the antenna pattern, when the Doppler Centroid is incorrect. The result is an intensity variation across the burst image. When the burst images are stitched together to form the image product, the periodic intensity variation is seen as scalloping in the image. ( For a further discussion of this topic, refer to the section entitled "["Descalloping "](#) [2.6.1.2.4.2.](#)" ).

Typically, there are at least two bursts within a synthetic aperture length, so that multiple bursts contain some data that is received from the same points on the ground. Thus, the images formed from each burst correspond to different looks of overlapping areas on the ground. In forming the final image product, the detected burst images are added together to reduce [speckle](#).

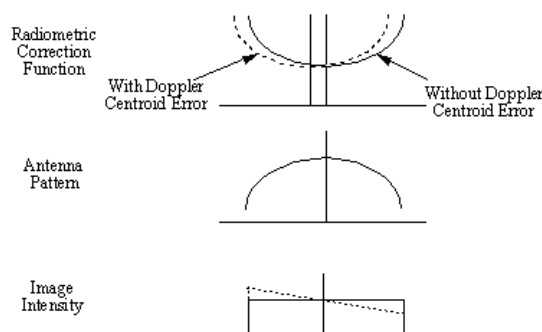


Figure 2.20 Effect of Doppler Centroid Error on Image Intensity

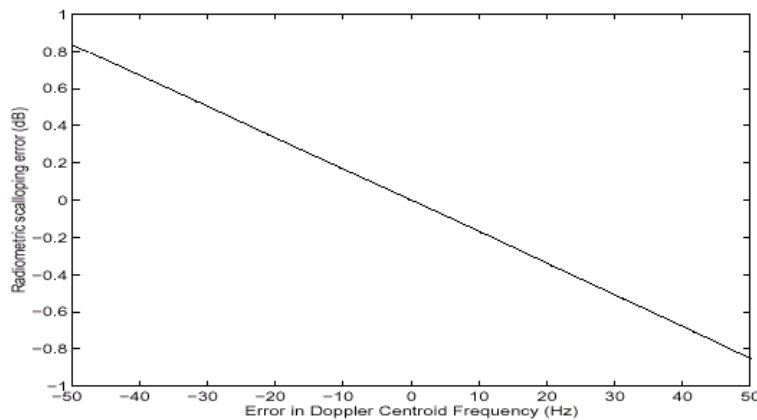


Figure 2.21 Radiometric Error Resulting from Doppler Centroid Error

[Figure 2.21](#) illustrates the residual scalloping error due to a fine Doppler centroid error for the case of two azimuth looks (the graph has been computed assuming a [RADARSAT](#) antenna pattern, although the trends are applicable here). Note that a Doppler centroid accuracy on the order of 25 Hz is required to keep the total scalloping error below 0.4 dB (+/- 0.2 dB from the mean image intensity). The Doppler centroid estimators described above are not expected to meet the accuracy that is required for radiometric correction. Here we will describe a technique for Doppler centroid estimation from burst data which, like those proposed in reference [Ref. \[2.2\]](#), compares the energy in the two extracted looks. The algorithm is based on the fact that the two look images are of the same patch of ground, even they were formed through different parts of the antenna beam. In taking the ratio of the two images, the scene content cancels. Also, the ratio is averaged to reduce the speckle noise. The result is an estimate of the ratio of the azimuth antenna patterns through which the two looks were taken, which depends on the antenna azimuth pointing angle or Doppler centroid.

To describe the method in more detail, we may express the image from look $i$  ( $i = 1, 2$ ) as:

$$X_i(\tau, \eta) = W(\tau, \eta - \eta_i - \eta_c)\sigma(\tau, \eta)\gamma_i(\tau, \eta) \quad \text{eq 2.10}$$

where the dimensions of the images are range time, range time $\tau$ , and azimuth time $\eta$ . The  $W(\tau, \eta - \eta_i - \eta_c)$  denotes the weighting applied by the antenna azimuth beam pattern on the image  $i$ , as a function of azimuth time. The weighting depends on the azimuth time at which the burst occurred,  $\eta_i$ , and the azimuth beam offset time from the zero-Doppler direction (which is related to the The Doppler centroid),  $\eta_c$ .  $\sigma(\tau, \eta)$  is the reflectivity of the ground patch being imaged that is common to both looks, and  $\gamma_i(\tau, \eta)$  is a multiplicative (speckle) noise component, assumed independent from one look to the next. As  $W, \tau, \eta$  and the  $\eta_i$  are known, an estimate of  $\eta_c$  may be derived, with accuracy subject to the constraints imposed by the noise terms.

Taking the ratio of  $W, \tau, \eta, \eta_i, \eta_c, X_1, X_2$  to  $X_1$  removes the dependence on the reflectivity, and taking the log of the ratio makes the function better behaved:

$$\log\left(\frac{X_1}{X_2}\right) = \log\left(\frac{W(\tau, \eta - \eta_2 - \eta_c)}{W(\tau, \eta - \eta_1 - \eta_c)}\right) + \log\left(\frac{\gamma_2(\tau, \eta)}{\gamma_1(\tau, \eta)}\right) = A(\eta_c) + B \quad \text{eq 2.11}$$

The noise term, B, can be reduced by averaging. The basic approach is to estimate  $\eta_c$  by forming an estimate of  $A(\eta_c)$  from the look ratio of the data, and compare it to a set of template functions that has been pre-computed using the known antenna pattern, to find the value of  $\eta_c$  that gives the best fit.

Specifically, we begin with an assumed value of  $\eta_c$  and process the data, including application of the descalloping function ([see note: 1](#)). If the assumed value of  $\eta_c$  is correct, and if B is small relative to  $A(\eta_c)$ , then the expected value of  $A(\eta_c)$  is 0. In general, there will be an offset between the assumed and actual values of  $\eta_c$  which is what the algorithm estimates. The estimate of  $\eta_c$  is generated from the unbiased estimate of  $A(\eta_c)$  by comparing with a number of template functions, each formed by calculating the expected log ratio of the data with a given Doppler centroid offset between the data and the applied descalloping function.

The look power balancing technique requires a sufficiently accurate initial estimate of the fine Doppler centroid in order to work, as it has limited "pull-in". Madsen's method or the MLCC method is used as described above to provide the initial estimate.

**Computation of the Look Ratio** The raw SAR data is fully range and azimuth compressed, and the descalloping correction is applied, using the initial Doppler centroid. Two azimuth looks are extracted from the data; each burst of data produces a Look 2 segment which corresponds to the Look 1 segment from the previous burst.

Once the processor has the two looks corresponding to the same patch on the ground, a boxcar type average of length  $L_{AzAvg}$  in azimuth is applied to the data of each look in order to reduce the variance of the data. After the azimuth averaging, the ratio of the two looks is taken, and the logarithm of the result is generated. In addition to the boxcar filtering performed in azimuth, variance reduction is performed in the range dimension by averaging the resulting log ratios over a number of adjacent range cells,  $L_{Group}$ . The result, as function of azimuth sample, is denoted L(n) and it is this function that we attempt to match to the  $A(\eta_c)$  term.

**Generation of Template Functions** A family of reference functions is defined by calculating the expected radiometry for the individual looks as a function of the offset frequency between the real Doppler centroid and that assumed in calculating the [descalloping 2.6.1.2.4.2.](#) function:

$$y_f(k, n) = \left( \frac{W_f(n)}{W_f(n+k)} \right)^2 \quad \text{eq 2.12}$$

---

where where n is the azimuth sample index (the output from the Specan process), and k is the azimuth offset error, in azimuth samples, which corresponds to the Doppler centroid error . The reference functions are averaged in azimuth with the same boxcar filter. Finally, the logarithm of the ratio is taken resulting in a family of template functions for comparison. Note that for k = 0, there is no Doppler centroid error, and as expected the template is flat with a value of 0. The magnitude of the template functions increases monotonically with k .

**Estimation of the Doppler Centroid Error** The look ratio L(n) is computed for a number of bursts in azimuth. The results are then averaged to obtain the average look ratio, which is then compared against each template function by computing the difference between the functions. An estimate of the Doppler centroid error is determined by the error sample,  $k_{min}$  , which yields the minimum difference between the compute look ratio and the corresponding template function. The error sample is then converted to an estimate of the Doppler Centroid Error (measured in Hertz):

$$F_{offset} = k_{min} \frac{F_a}{L_{FFT}} \quad \text{eq 2.13}$$

Where LFFT is the length of the FFT in the SPECAN algorithm.

The development thus far has assumed that only 2 looks are extracted per burst of data processed. For the 3 and 4 look modes, the method can be easily generalised by comparing the outer pair of looks. These looks are chosen because the variation in the beam pattern is highest at the edges.

This method gives the estimate of the Doppler centroid error at a single range. A low-order polynomial is then fit to the values of  $F_{offset}$  at a number of ranges ( $N_{RangeGroups}$ ) . When combined with the polynomial producing the initial Doppler centroid it yields the absolute value of the Doppler centroid.

### 2.6.1.2.2.5 PRF Diversity Method

In the Wide Swath and Global Monitoring Modes in which ScanSAR is used, a different PRF is used at each of the different range subswaths. This PRF diversity can be used to derive the correct Doppler Ambiguity . [Ref. \[2.4\]](#) Recall the Doppler Ambiguity number, M , is the number of PRF's that must be added to the fine Doppler centroid in order to obtain the absolute Doppler centroid, as described in the Introduction. When different PRF's are used at different range subswaths, the values of the Doppler ambiguity number, M, for the various subswaths must be such that the absolute Doppler centroid is a smooth function of range. In order for this technique to work, the fine Doppler centroid must be known to a resolution less than the difference in PRF's between the subswaths.

Consider two measurements of the fine Doppler centroid, each taken with a different PRF. If the absolute (i.e., actual unambiguous) Doppler centroid is the same for each measurement, then

$$f_{\eta_c} = M_i F_{a_i} + f'_{\eta_{c,i}} \quad \text{eq 2.14}$$

where  $f_{\eta_c}$  is the unambiguous Doppler centroid frequency,  $F_{a_i}$  is the pulse repetition frequency for the  $i^{\text{th}}$  beam, and  $f'_{\eta_{c,i}}$  is the fine Doppler centroid, again for the  $i^{\text{th}}$  beam. The goal of Doppler Ambiguity Resolution is to determine the correct value of  $M_i$ . Given a prior knowledge that the satellite is yaw-steered limits the allowable values of  $M_i$  to be in the set  $\{-2, -1, 0, 1, 2\}$ . ([see note: 2](#)) For a sufficiently large difference between the PRFs, and sufficiently accurate estimates of  $f'_{\eta_{c,i}}$ , the Doppler ambiguity may be derived.

The specific algorithm for deriving the Doppler ambiguity is as follows:

- derive the fine Doppler estimates,  $f'_{\eta_{c,i}}$  for a series of ranges,  $r$ , across the swath
- for each possible value of  $M = -2, -1, 0, 1, 2$ :
- Calculate the unambiguous Doppler centroid for all ranges in the nearest subswath using the appropriate PRF. Ensure the continuity of the absolute Doppler centroid frequency as a function range by incrementing or decrementing  $M$  for each range as necessary.
- For the next subswath, calculate the absolute Doppler centroid frequency, again using the appropriate PRF. Ensure that the correct value of  $M$  is used across the subswath boundary by ensuring that the unambiguous Doppler centroid frequency is reasonably continuous between the beams (i.e. the value of  $M$  may be different than the one used in the step above.)
- Continue outwards through all the ranges for all the subswaths, unwrapping as necessary to ensure a smooth function of the unambiguous Doppler centroid frequency as a function of range.
- Calculate a low order polynomial through the resulting absolute Doppler centroid estimates. Measure the distance between the resulting polynomial and the data points.
- Pick the value(s) of  $M$  that provides the best fit between the polynomial and the data points. Note that ambiguity errors will cause a step in the data that is noticeable, and the polynomial will not be able to do a smooth fit except for when the ambiguity is correct.

### 2.6.1.2.2.6 Notes

1. We assume here that the descalloping or look weighting function is the inverse of the azimuth beampattern. This ensures that the effective number of looks is a constant for all targets. Other approaches exist which lessen the radiometric sensitivity to Doppler centroid estimation errors and ensure constant noise level, but not constant speckle reduction. Note however, that even if an alternate look weighting algorithm were chosen, the inverse beampattern could be used to derive the Doppler centroid estimate as described herein.

2. If the satellite is not yaw-steered, the range of acceptable values will not be centred about 0; however, knowledge of the satellite position and velocity yield an expected value of the Doppler ambiguity, and the uncertainty about that expected value will be  $+/- 2$  prfs.

### 2.6.1.2.2.7 References

#### Ref 2.1

F. H. Wong, I. G. Cumming, A Combined SAR Doppler Scheme Based Upon Signal Phase, IEEE Trans. Geoscience and Remote Sensing, 34 (3): 696-707, May 1996.

#### Ref 2.2

. M.Y. Jin. Optimal Range and Doppler Centroid Estimation for a ScanSAR System, submitted to IEEE Transactions on Geoscience and Remote Sensing.

#### Ref 2.3

. S.N. Madsen. Estimating the Doppler Centroid of SAR Data. IEEE Transactions on Aerospace and Electronic Systems , Vol 25(2):pp 134-140, March 1989.

#### Ref 2.4

C.Y. Chang and J.C. Curlander. Application of the Multiple PRF Technique to Resolve Doppler Centroid Estimation Ambiguity for Spaceborne SAR. IEEE Transactions on Geoscience and Remote Sensing, Vol. GE-30(5): pp 941-949, September, 1992.

### 2.6.1.2.3 Range-Doppler

#### 2.6.1.2.3.1 Introduction

##### 2.6.1.2.3.1.1 Overview

The range-Doppler algorithm is the most commonly used algorithm for processing continuously collected [SAR](#) data into an image (see [Ref. \[2.5 \]](#) and [Ref. \[2.6 \]](#) ). It is computationally efficient and, for typical spaceborne imaging geometries, the range-Doppler algorithm is an accurate approximation to the exact SAR transfer function. Thus, the algorithm is phase-preserving and [Single Look Complex \(SLC\) images](#) formed with the range-Doppler algorithm can be used for applications such as [interferometry](#). The range-Doppler algorithm is designed for continuously collected data, in contrast to [SPECAN 2.6.1.2.4](#), which is best suited to [bursty data](#), and can process the full [azimuth](#) bandwidth.

The range-Doppler algorithm is used for the high-resolution Image Modes (IMS, IMP, IMG) and the high-resolution, single look complex Alternating Polarisation Mode (APS). ( See [Table](#) in the section entitled "Organisation of Products" in chapter 2 ). For the APS

---

mode, the data between bursts is filled with zeros to maintain a continuous-time input to the algorithm, and a modified range-Doppler algorithm is used to produce an [SLC image from AP data 2.6.1.2.3.2.](#)

For the detected (magnitude) image products (IMP, IMG), a technique called [multilooking](#) is incorporated into the algorithm. In this method, separate images are formed from different azimuth spectral bands ([looks](#)), and the magnitude look images are averaged to reduce [speckle](#).

SAR processing is a two-dimensional problem. In the [raw](#) SAR data, the signal energy from a point target is spread in [range](#) and azimuth, and the purpose of SAR focussing is to collect this dispersed energy into a single [pixel](#) in the output image. In range, the signal is spread by duration the linear [FM](#) transmitted pulse. In azimuth, the signal is spread by the duration it is illuminated by the antenna beam, or the [synthetic aperture](#). As a point target passes through the azimuth antenna beam, the range to the target changes. On the scale of the wavelength, this range variation causes a [phase](#) variation in the received signal as a function of azimuth. This phase variation over the synthetic aperture corresponds to the Doppler bandwidth of the azimuth signal, and allows the signal to be compressed in the azimuth direction. The range variation to point target can result in a variation in the range delay to the target that is larger than the range sample spacing, resulting in what is called range migration. This range migration of the signal energy over several range bins must be corrected before azimuth compression can occur. The range-Doppler algorithm performs this correction very efficiently in the range-time, azimuth-frequency domain.

In order to process the correct part of the azimuth frequency spectrum, the range-Doppler algorithm requires as input the Doppler centroid. It is assumed here that Doppler centroid estimation has already been performed, as described in the [Doppler Centroid Estimation 2.6.1.2.2.](#) section. The range-Doppler algorithm also requires knowledge of the transmitted pulse for range compression, and of the [imaging geometry](#) such as the range and satellite velocity for construction of the azimuth matched filter.

The main steps in the version of the range-Doppler algorithm used in ASAR are shown in the block diagram below, and are described in the following sections.

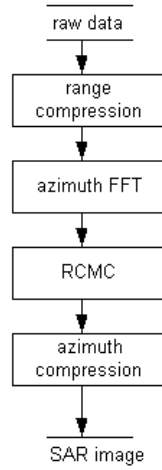


Figure 2.22 Steps of range-Doppler algorithm used in ASAR processing

### 2.6.1.2.3.1.2 Range Compression

In collecting the SAR data, a long-duration linear FM pulse is transmitted. This allows the pulse energy to be transmitted with a lower peak power. The linear FM pulse has the property that, when filtered with a matched filter, the result is a narrow pulse in which all the pulse energy has been collected to the peak value. Thus, when a matched filter is applied to the received echo, it is as if a narrow pulse were transmitted, with its corresponding range resolution and signal-to-noise ratio.

This matched filtering of the received echo is called range compression. Range compression is performed on each range line of SAR data, and can be done efficiently by the use of the [Fast Fourier Transform \(FFT\)](#). The frequency domain range matched filter needs to be generated only once, and it is applied to each range line. The range matched filter may be computed or generated from a replica of the transmitted pulse. In addition, the range matched filter frequency response typically includes an amplitude weighting to control [sidelobes](#) in the range impulse response.

The steps in range compression for each range line are:

- Range FFT: For most products, the range line is divided into two overlapping segments, and an FFT is taken of each segment. The amount of overlap corresponds to the length of the transmitted pulse.
- Range matched (MF) multiply: Each FFT'd segment is multiplied by the frequency response of the matched filter.
- Range Inverse FFT: An inverse FFT is applied to each segment to get the range compressed data. Part of each segment is thrown away since the compressed range data is shorter than the uncompressed range data by the length of the transmitted

pulse. The range matched filter is designed so that the throw-away is at the end of the data after the inverse FFT. The results from each segment are then joined together to get the compressed data for the whole range line.

- Range dependent gain correction: The range compressed data is multiplied by a vector that corrects the effects due to elevation beam pattern and range spreading loss.
- 

#### 2.6.1.2.3.1.3 Azimuth FFT

An FFT is performed in the azimuth direction on each range gate to transform the data into the range Doppler domain. The FFTs are performed on blocks of data overlapped by the azimuth matched filter length.

The range compressed data is stored in range line order. A group FFT algorithm is used which allows azimuth FFTs to be performed while still accessing the data in range line order. Thus the corner turn (transpose to azimuth line order) operation can be delayed until after RCMC.

#### 2.6.1.2.3.1.4 Range Cell Migration Correction (RCMC)

After range compression, the signal energy from a point target follows a trajectory in the two-dimensional SAR data, that depends on the changing range delay to the target as it passes through the antenna beam. This trajectory may cross several range bins. In order to capture all the signal energy for azimuth compression, the signal energy from a point target must be aligned in a signal range bin.

RCMC is the step of correcting for the changing range delay to a point target as the target passes through the antenna beam (range migration). For a given target, this range depends on the closest approach range from the satellite to the target (zero-Doppler range), and on the angle from the satellite to the target, relative to the broadside (zero-Doppler) direction. As targets at the same closest approach range pass through the antenna beam, they all traverse the same interval of angles, and so have the same variation in range from the radar. That is, the signal trajectories from targets at the same closest approach range have the same shape, but are displaced in azimuth because of the different target positions. This is shown in the graph on the left in [figure 2.23](#) below. Because of the relationship between the satellite-to-target angle and Doppler frequency, the range migration of all targets at the same closest approach range can be expressed as a function of Doppler frequency. That is, all signal energy from targets at the same closest approach range is collected into the same trajectory in the range-Doppler domain. This allows RCMC to be performed very efficiently in the range-Doppler domain.

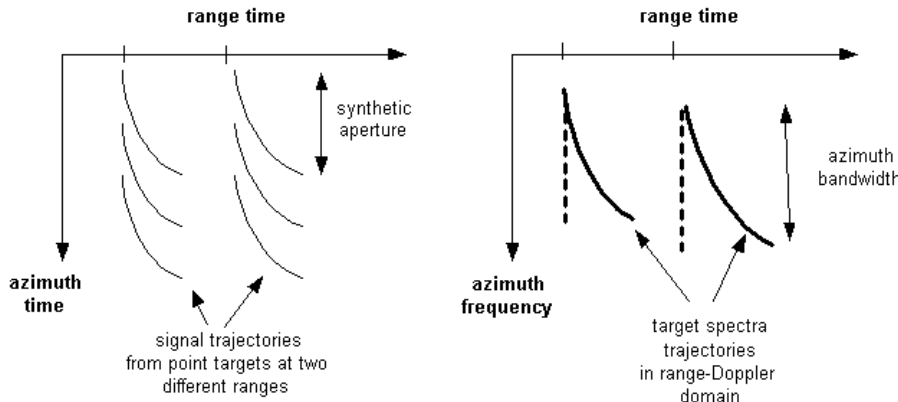


Figure 2.23 Illustration of trajectories in time domain and range-Doppler domain.

The shift in range that is needed to align the signal trajectory in a single range bin is determined for each azimuth frequency bin. This shift is then implemented by an interpolation in the range direction. The straightened trajectories are shown by the dotted lines in the figure.

Other steps in SAR processing that require interpolation in range are slant range to ground range conversion (SR/GR), which converts the distance from the radar (slant range) to distance along the ground, and the range resampling to a desired output pixel spacing. For maximum efficiency, all of these range interpolations are combined into one operation.

### 2.6.1.2.3.1.5 Azimuth Compression

Azimuth compression is a matched filtering of the azimuth signal, performed efficiently using FFT's. Note that the azimuth FFT has already been performed at this point. The azimuth FFT's were performed on blocks of data that overlap in azimuth by the matched filter length. The reason for the overlap is the throw-away after azimuth compression.

The frequency response of the azimuth compression filter is precomputed using the orbital geometry. The azimuth filter also depends on range. Thus the data is divided into range invariance regions, and the same basic matched filter is used over a range interval called the FM rate invariance region. The size of this invariance region must not be large enough to cause severe broadening in the compressed image. Also included is an amplitude weighting to control sidelobes in the azimuth impulse response. Note that the position of the amplitude weighting in the azimuth frequency array depends on the Doppler centroid, which also depends on range.

The way the azimuth compression is implemented depends on the type of image product. For single look complex products (IMS and APS), a single portion of the azimuth bandwidth is multiplied by the azimuth matched filter frequency response, and an inverse FFT is taken of the entire frequency array. The output is complex valued and left at the natural pixel spacing.

For magnitude image products (IMP and IMG), a technique called multilooking is used to reduce speckle noise. In this case, the azimuth frequency spectrum is divided into several portions called looks. The part of the azimuth frequency array for each look is extracted, multiplied by the azimuth matched filter frequency response, and the inverse FFT is performed. The magnitude (detected) look images are then averaged to reduce speckle. This is described in more detail as follows.

The extraction of the looks from the frequency array is illustrated in the figure below. The looks are positioned symmetrically around the Doppler centroid frequency. As the Doppler centroid frequency varies with range, the look frequency positions are different for different range cells. In practice, they are kept constant within the look frequency position invariance region.

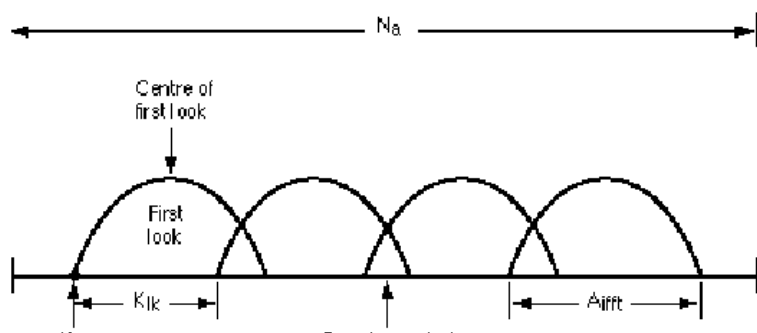


Figure 2.24 Look Position Parameters

The extracted frequency array for each look is multiplied by the matched filter frequency response and the inverse FFT is performed to form the complex look image. The matched filter frequency response is adjusted by a small linear phase ramp for each look. This is equivalent to shifting the compressed look in time, and is required to ensure that the images from different looks are aligned properly for look summation. The amount of azimuth shift is range-dependent. In addition, azimuth interpolation may also be performed after look compression to achieve a desired azimuth pixel spacing, and it is done on each look separately.

After look compression, each of the look images is detected. That is, the power of each complex sample is calculated. The detected azimuth looks are then summed, and the square root of the result is calculated to convert to magnitude.

Finally, for the IMG product, the multilooked image is [geocoded](#). This is a two dimensional resampling operation to convert the image to a desired map projection.

### 2.6.1.2.3.1.6 Summary

The processing steps for each of the types of products processed by the range-Doppler algorithm are summarised below:

- Precision products: All steps (up to and including multilooking) except geocoding are performed.
- Single look complex products: Only the steps up to and including the azimuth IFFT, for only one look, are performed.
- Geocoded products: All steps are performed with the addition of geocoding (The normal square root step is bypassed but is later performed as part of geocoding).
- APS products: A slightly [modified version of the range-Doppler algorithm 2.6.1.2.3.2.](#) is used for the APS product .
- 

### 2.6.1.2.3.1.7 References

#### Ref 2.5

Ian G. Cumming and John R. Bennett. Digital processing of SEASAT SAR data. In Record of the IEEE 1979 International Conference on Acoustics, Speech and Signal Processing , Washington, B.C., April 2-4, 1979.

#### Ref 2.6

J. C. Curlander, R. N. McDonough, Synthetic Aperture Radar: Systems and Signal Processing, John Wiley and Sons, 1991.

## 2.6.1.2.3.2 Processing Algorithms For AP SLC

### 2.6.1.2.3.2.1 Introduction

[PF-ASAR](#) will produce [Single Look Complex](#) (SLC) products from [Alternating Polarisation](#) (AP) mode [SAR](#) data. The primary application for this ASAR APS product is for

---

[Interferometric SAR \(InSAR\)](#), which is a technique that manipulates the relative [phase](#) between a pair of SLC images to extract [topographic](#) information.

This section provides an overview of the processing approach for generating an ASAR APS product that is suitable for InSAR applications. The algorithm is the [range-Doppler 2.6.1.2.3.](#) algorithm, modified to process [bursty](#) data.

### 2.6.1.2.3.2.2 Background

The primary application for this ASAR APS product is for [Interferometric SAR \(InSAR\)](#), for which complex (SLC) image products are required. In SAR Interferometry, the phase difference between two images of the same area is used to compute the topography of the area. The two images are taken from slightly different viewing positions, and for a single satellite, the images are acquired during different passes (repeat-pass interferometry). In the application of APS products for Interferometric SAR, a complex image from [Alternating Polarisation](#) (AP) mode may be combined with another complex image from another pass, in order to retrieve the phase difference between the images which is related to terrain height. The other image be another AP mode image or an [Image Mode](#) (IM) image.

The algorithm used to form the APS product must be capable of preserving the phase information required for SAR Interferometry. Thus, a form of the range-Doppler algorithm is required since in general SPECAN is not phase-preserving. The image quality requirements for the ASAR APS product are derived from the typical requirements for an Image Mode SLC product, which includes phase preservation and adequate [focussing](#). Adequate focussing is typically determined by measurements of the impulse response shape. However, because of the bursty nature of AP data, there are some important considerations in the processing and use of APS data.

Interferometry requires that the two images be well correlated, in order for the phase difference to be an accurate measurement of terrain height. Because of this, the Doppler spectral components must be common to both images. Doppler components that are not common to both images are a source of decorrelation between the images, which introduces phase noise and degrades the accuracy of the terrain height measurement. If two Image Mode images are combined, the full Doppler spectrum is available in both images, and if the antenna pointing is controlled properly then there is sufficient overlap of the Doppler spectra of the two images. In burst mode data, such as AP data or ScanSAR data, the bursts contain only part of the signal from a point target, and thus contain only part of the Doppler spectrum. If an APS image is combined with an IM image, the IM image contains the full Doppler spectrum so again there is sufficient overlap with the Doppler spectrum of APS image.

If the two images are acquired in burst mode, such as two APS images, the amount of Doppler overlap depends on the relative positions of the bursts in the two data sets. If the bursts occurred at the same locations in the two data sets, then the Doppler components overlap. If the bursts do not overlap at all, then there are no common Doppler components, the images are decorrelated, and interferometry cannot be performed. Since the two products are processed without knowledge of the other, it is desired to preserve as much

---

Doppler information as possible. This is referred to as [systematic](#) processing. If systematically generated SLC products are to be used for interferometry, without reverting back to the level 0 data, then azimuth bandpass filtering must be performed on the SLC images to extract the common portions of the Doppler spectrum.

Finally, it should be noted that the [APS](#) product will not be suitable for phase measurements between the interleaved polarisation because the Doppler spectrums of the two focussed images will be disjoint (non-overlapping), which implies that the phases will be completely uncorrelated. The magnitude of the APS product could be used for polarimetry in a similar manner to the [APP](#) product. For this reason the two output [SLC](#) images are co-registered.

This section reviews burst mode interferometry, and presents the considerations in range-Doppler processing of APS data.

#### 2.6.1.2.3.2.3 Burst Mode Interferometry

An illustration of data acquired in discrete bursts as shown in [figure 2.25](#). The figure shows the timing of the bursts, and the exposure times of 16 targets, labelled by  $T_1$  to  $T_{16}$ . The lines for each target represent the exposure time (synthetic aperture time), which is the duration of time during which the target is within the beam footprint. In the case of the AP mode, the azimuth aperture covers a little more than 5 bursts' duration. Any one target is captured from two to three bursts in the same polarisation., thus allowing 2-look processing in forming a [multi-look](#) image (such as APP).

Let us just examine the spectrum of the targets in the burst marked by X. The duration of the Doppler spectrum for each target is shown in [figure 2.26](#) (ignoring the azimuth beam pattern effects). It is clear that the Doppler components contained in this burst, for a given ground target, depend upon the location of the target relative to the burst timeline. The Doppler centroid frequency in this context is the center frequency of the spectrum for a given target.

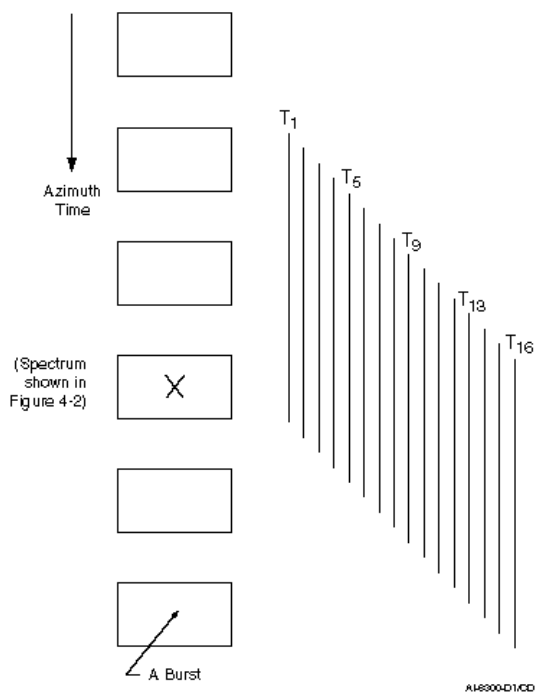


Figure 2.25 Target Exposure Extents Relative to the Burst Timeline

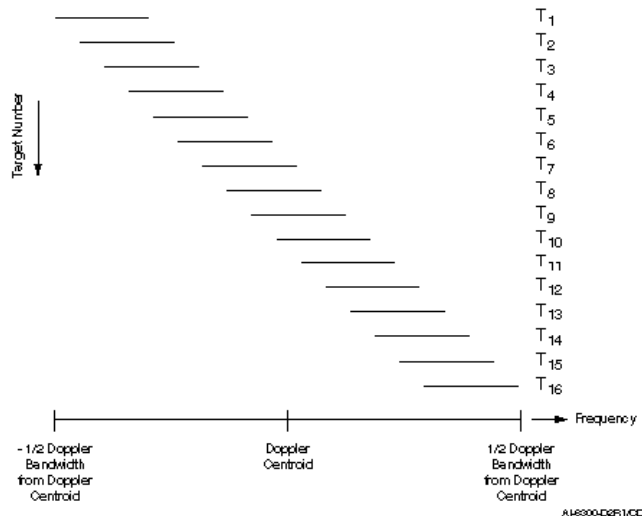


Figure 2.26 Location of Spectra Energy for Targets in Burst X

To preserve the time relationship between the data in different bursts, the level 0 data acquired in burst mode can be stored in the same representation as continuous mode data. That is, range lines during a burst contain the received data for that azimuth time, and range lines between bursts (ie. when the other polarisation is being received) are padded with zeroes.

A problem directly related to the varying Doppler centroid lies in the synchronisation between the two passes. [figure 2.27](#) shows the burst coverage of two typical passes where the bursts are slightly misaligned. If the burst timing of the level 0 data is known, the lines of level 0 data corresponding to non-overlapping areas can be zeroed prior to SAR processing. In this way, only burst data with common Doppler components are retained, so the zeroing out of data is also equivalent to applying a time varying band pass filter to the data in each pass.

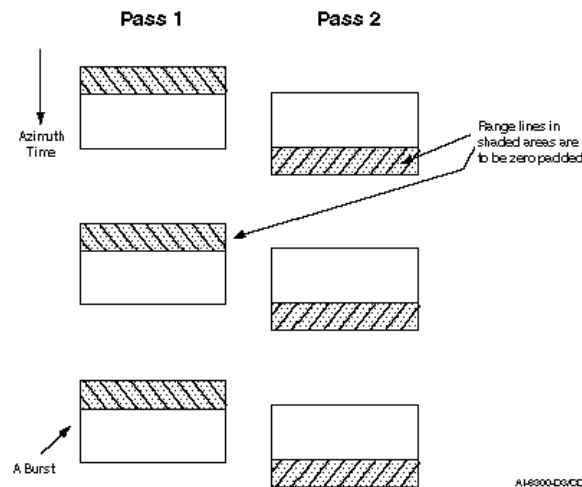


Figure 2.27 Synchronisation of Bursts in Two Slightly Misaligned Passes if Reprocessing from Level 0 Data (the beams are the same)

[Figure 2.28](#) illustrates the spectrum of one burst of data in the two passes, again using the 16 point targets as an example if no level 0 data zeroing is performed. Due to the burst misalignment, the two sets of spectra are also misaligned. The effect of the bandpass filters is to select out the overlapped portion of the spectrum.

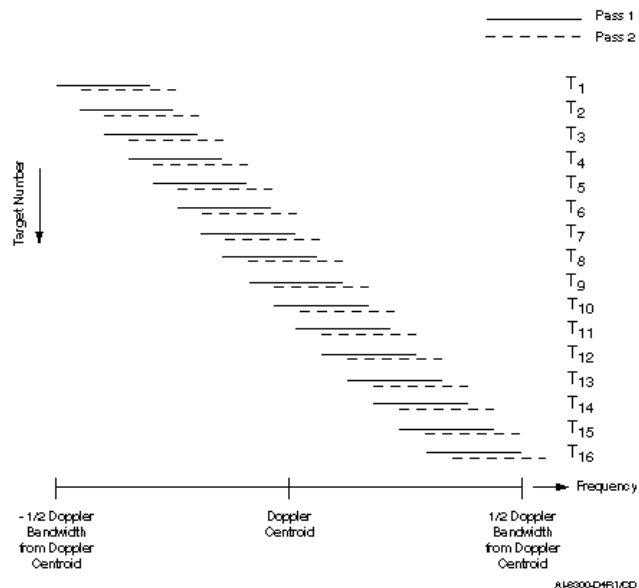


Figure 2.28 Spectra of Targets in a Burst for Two Slightly Misaligned Passes

[Figure 2.29](#) shows the azimuth spectrum for all bursts for a single pass when zeros are inserted in the alternate polarisation. Note that the data from a single target is bursty in nature in both the azimuth time domain and the Doppler frequency domain due to the coupling between time and frequency inherent in linear FM signals. Here it has been assumed that the burst cycle time is an integral multiple of the Pulse Repetition Interval (PRI) which is important for the zero padding to work. This assumption is true for the AP mode but is generally not true for ScanSAR modes.

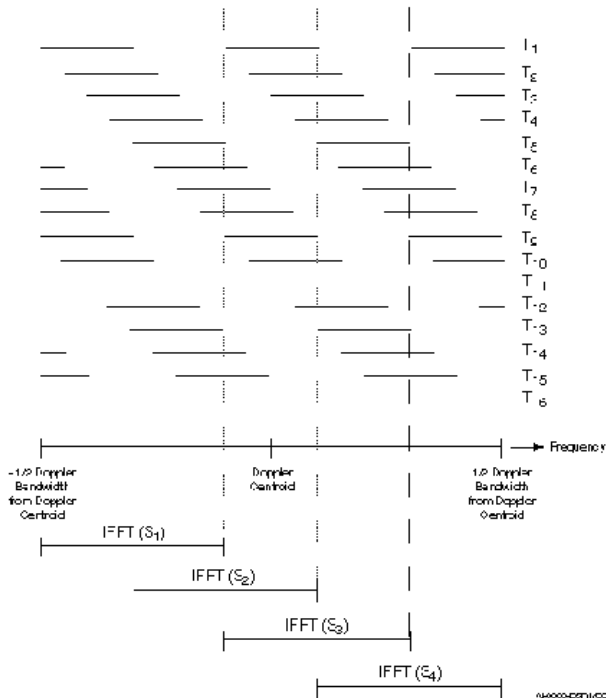


Figure 2.29 Spectra of Targets After Zero Fill Showing IFFT Positions

Since the zero-padded data is stored in the same representation as continuous moded data, it can be processed with the range-Doppler algorithm. Including all the available bursts for a given output point simultaneously ensures that all the Doppler spectrum is maintained for a given target and it can be done independently for both passes. This is discussed in the section below.

During InSAR processing azimuth varying bandpass filters can be used to select out common continuous spectral regions from each image of each pass. This operation has approximately the same result as zero padding the level 0 data prior to SAR processing. This technique has been used successfully to obtain high quality InSAR results ([Guarnieri et al 2.6.1.2.3.2.6.](#) ).

One side-effect of processing the entire Doppler spectrum is that the resulting APS product will have an impulse response that is modulated due to the non-continuous spectrum used for compression. This impulse response shape will not meet the current PF-ASAR requirements for this product but can fully meet the requirements of the InSAR application. In addition, there will be azimuth banding, due to different number of bursts being used to generate the output points. This approach is described further in the algorithm described below and is the recommended version for the PF-ASAR, due to its ability to satisfy the InSAR application requirements, for use with another APS or an IMS, without complicating the ASAR product structure and interpretation.

#### 2.6.1.2.3.2.4 Modifications To Range Doppler Algorithm

The [Range Doppler algorithm 2.6.1.2.3.](#) (RD) is well suited to process continuous data, but can be modified to process data acquired in discrete bursts. This following discusses the modifications required to generate an AP SLC product suitable for InSAR applications.

Let us assume a case in which the beamwidth covers exactly five bursts' duration (closely resembling that in the AP Mode). Now let us focus our discussion on only one polarisation. Each polarisation will be processed separately. The first step is to zero pad the gaps when data of the other polarisation is acquired. Assume 16 equally spaced targets as shown in [figure 2.25](#), and denote them by  $T_1$  to  $T_{16}$ , and assume that they all have the same slant range of closest approach so that they are confined in one range gate after [Range Cell Migration Correction \(RCMC\)](#). Because of the missing data, the spectra of the targets after azimuth Fast Fourier Transform (FFT) and RCMC are bursty, as shown in [figure 2.29](#).

The energy received from a target depends on its position in the antenna azimuth beam during the burst, which corresponds to the position of its Doppler components in the azimuth-frequency domain. To avoid scalloping, the target energy can be corrected by applying the inverse of the azimuth beam pattern to the Doppler spectrum. This is similar to [Descalloping 2.6.1.2.4.2.](#) in SPECAN.

The general steps of the modified RD algorithm are the following:

1. Range compression.
2. Zero pad the missing data to simulate continuous data.
3. Perform an azimuth FFT to transform the data into the Range-Doppler domain.
4. Perform RCMC.
5. Apply inverse of azimuth beam pattern to spectrum.
6. Perform azimuth matched filtering without any windowing applied.
7. Perform the azimuth IFFT.
8. Repeat algorithm for alternate polarisation and include phase ramp term in azimuth matched filter to achieve co-registration.

These steps are quite similar to the basic RD algorithm.

In this approach, a single azimuth IFFT is applied to the Doppler spectrum after application of the matched filter. This approach satisfies the requirements for InSAR processing, but the impulse responses of the APS products suffers from modulation as shown in [figure 2.30](#) below. The modulation arises from the fact that the spectrum of each target is segmented in the IFFT [Ref. \[2.8\]](#)

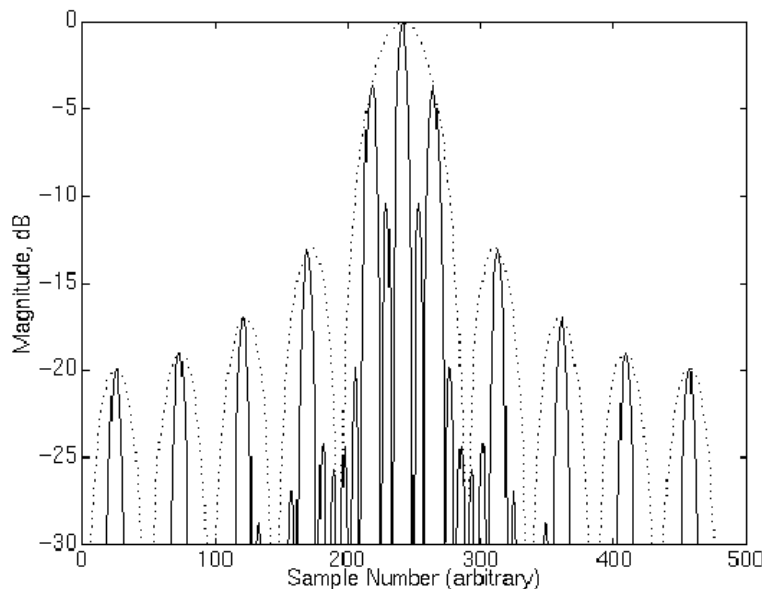


Figure 2.30 Impulse Response from Multiple Burst Processing for Target 1 (dotted curve is envelope of one continuous burst)

If range-Doppler algorithm is used without further modification, the APS product will not meet the radiometric requirements. This is due to the fact that targets have different number of bursts or partial bursts and therefore will have different energies. The energies are modulated along azimuth based upon the target location relative to the burst timeline. This will appear as azimuth banding in the resulting image. This poses a problem if the APS product is to be used for radiometric purposes by forming the magnitude image from the complex samples. It is desirable to attempt to remove this banding if possible.

The azimuth radiometric banding that results in the single IFFT method can be removed by modifying the processed azimuth bandwidth. If the processed bandwidth is exactly four times the burst bandwidth then there will always be the energy from two bursts captured. Therefore, when the inverse beam pattern is applied and there is no weighting applied to the matched filter (i.e. just rectangular window) the total energy processed for each target will be the same. The truncation of the spectrum by the rectangular window will either capture two complete bursts or will capture one complete burst and two partial bursts. In the latter case the two partial bursts add up to a full burst in terms of energy. Since the burst bandwidth is range dependent, the processed bandwidth must be adjusted across range.

There are implications to changing the processed Doppler bandwidth to remove the azimuth radiometric banding:

- Less of the total available Doppler bandwidth is retained for InSAR.
- The azimuth resolution is range dependent (but recall that the impulse response is modulated anyway).

In order to support InSAR filtering it is necessary to supply the following parameters in the product annotation: burst return time, time of the start of a burst for a specified polarisation., Doppler centroid coefficients, azimuth FM rate coefficients, and zero Doppler time of first output line. Using these parameters and knowing that the processed bandwidth is centred at the Doppler centroid with an extent of a specified bandwidth, the location of the available burst spectra can be computed for any pixel in the output image.

### 2.6.1.2.3.2.5 Conclusions

This section has outlined the processing of the AP Mode SLC product, with considerations for performing InSAR. The approach is a range-Doppler algorithm, with an adjustment to the processed bandwidth in the single azimuth IFFT after azimuth compression. The resulting image will pass all phase and geometric image quality requirements. However, there will be an impulse response shape modulation.

In this approach a small amount of Doppler information is lost, with only moderate implications for InSAR, in order remove the radiometric banding in the amplitude image.

During InSAR processing the APS images are azimuth-varying bandpass filtered to achieve common Doppler spectra.

### 2.6.1.2.3.2.6 References

#### Ref 2.7

A. M. Guarnieri, C. Prati and F. Rocca, "Interferometry with ScanSAR", Proceedings of IGARSS '95.

#### Ref 2.8

R. Balmer and M. Eineder," ScanSAR Processing Using Standard High Precision SAR Algorithms", IEEE Transactions on Geoscience and Remote Sensing, Vol. 34, No. 1, January 1996.

### 2.6.1.2.4 SPECAN

## 2.6.1.2.4.1 Introduction

### 2.6.1.2.4.1.1 Overview

The SPECAN algorithm processes periodic [bursts](#) of [SAR](#) data in the [azimuth](#) direction. In [ScanSAR](#) ([Wide Swath](#) (WS) and [Global Monitoring](#) (GM)) and [Alternating Polarisation](#) (AP) modes, the burstiness of the data arises from the way the data is collected. In [medium-resolution](#) Image Modes, periodic bursts are extracted from the continuous data in order to form images very quickly. In either case, if the time between bursts is less than the [synthetic aperture](#) time (time for a target to cross the azimuth antenna beam), then data from all targets on the ground are contained within the bursts and an image can be formed. Because only part of the data from a target is received during a burst however, the full azimuth bandwidth available in the azimuth antenna beam is not used. This results in a lower resolution and/or a smaller number of [looks](#) in the magnitude image product.

Compared to the [range-Doppler 2.6.1.2.3.](#) algorithm, the SPECAN algorithm is not as accurate in matching the exact SAR transfer function, and so is not appropriate for phase-preserving applications. Essentially, the SPECAN algorithm trades resolution, or number of looks, for computational efficiency.

Typically, several bursts occur within a synthetic aperture time. Thus, successive burst images contain overlapping views of the same ground area. These burst images, or looks, are averaged to reduce [speckle](#).

A consequence of SPECAN or burst imaging is an effect called [scalloping](#). During the relatively short burst, targets within the synthetic aperture are viewed through different parts of the azimuth antenna beam. The azimuth beam pattern then results in an azimuth-varying weighting of the target intensity in the image. Given the antenna pattern and the antenna beam centre location ([Doppler centroid 2.6.1.2.2.](#) ), this effect can be corrected. (See [Descalloping 2.6.1.2.4.2.](#) ).

The main steps in the version of the SPECAN algorithm used in ASAR are shown in the block diagram below, and described in the following sections.

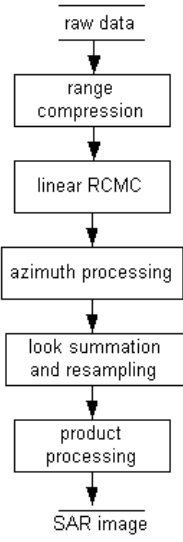


Figure 2.31 Main steps in the version of the SPECAN algorithm used in ASAR

### 2.6.1.2.4.1.2 Range Compression

Range compression is a filtering operation performed on each range line of raw SAR data. It compresses the long transmitted pulse into a narrow pulse with the desired range resolution and higher signal to noise ratio, and can be done efficiently by the use of the [Fast Fourier Transform \(FFT\)](#). It is common to all image formation algorithms, and is described in detail in the section on [range-Doppler 2.6.1.2.3](#).

### 2.6.1.2.4.1.3 Linear Range Cell Migration Correction (RCMC)

After range compression, the signal energy from a point target follows a trajectory in the two-dimensional SAR data, that depends on the changing range delay to the target as it passes through the antenna beam (range migration). This trajectory may cross several range bins. In order to capture all the signal energy for azimuth compression, the signal energy from a point target must be aligned in a single range bin.

In SPECAN processing, the [range migration](#) trajectory is approximated by a straight line of a certain slope in the two-dimensional data array. Thus, [RCMC](#) is done by simply skewing the data - that is, applying a range shift that varies linearly with [azimuth time](#) - in order to align the trajectory from a target in a single range bin. The range shift is done by an interpolation of the range line.

Note that this linear RCMC is done in the range-time, azimuth-time domain, rather than the

range-Doppler domain. While the trajectories of all targets are aligned in single range bins, an effect of linear RCMC in the time domain is that the target range positions are shifted as a function of [azimuth-time](#), resulting in a skewed image. In practice, rather than increasing the size of the data array to hold the skewed data, the skewed data is wrapped around in range in the data array, forming a "barber pole" effect that is undone in the output image. This is illustrated in [figure 2.32](#) below.

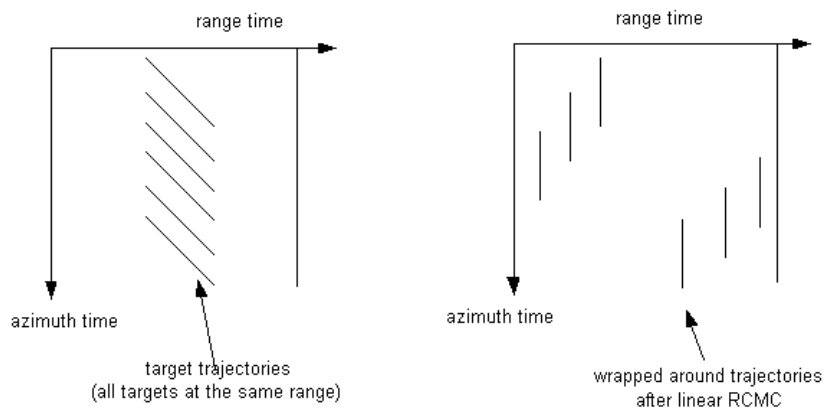


Figure 2.32 Trajectories before and after linear RCMC.

#### 2.6.1.2.4.1.4 Azimuth Processing

SPECAN azimuth processing is based on the concept of deramping linear FM signals [Ref. \[2.9\]](#). The azimuth signal from a point target is approximately a linear FM signal. That is, the instantaneous frequency of the signal varies linearly with time. A burst, then, contains a portion of this linear FM signal from a target. Thus, the instantaneous frequency of the signal varies linearly within the burst, about a mean frequency that depends on the target's position relative to the burst time. Deramping the burst signal refers to the multiplication by a reference linear FM signal whose instantaneous frequency varies linearly at the same rate but with opposite slope. This has the effect of removing the linear frequency variation of the signal, leaving a constant frequency signal with a frequency that is related to the target position. Finally, an [FFT](#) of the deramped signal produces a compressed signal peak at the target position.

A convenient representation of the signal, for purposes of deramping, is the frequency-time diagram. This is a plot of the instantaneous frequency of the signal versus time. For a linear FM signal, it is a sloping straight line, where the slope is the frequency rate. For a sinusoid of constant frequency, the frequency-time diagram is a horizontal line. [figure 2.33](#) below shows the frequency-time diagram of azimuth SAR signals, assumed to be linear FM. Each line represents the signal from a target at a different azimuth position. The portions of the signal

that are contained in the burst are shown. After deramping of the burst, as shown in the bottom part of the figure, the signals have been converted to sinusoids, with frequencies related to the target positions.

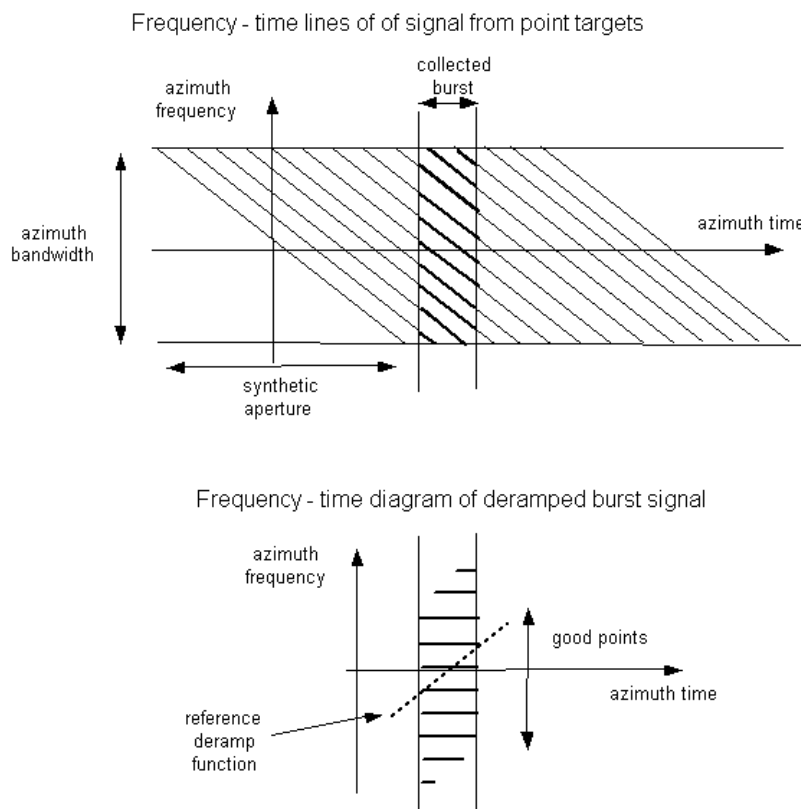


Figure 2.33 Illustration of SPECAN with frequency-time diagrams.

The basic steps of SPECAN, then, are the reference function multiply of the burst in the [azimuth direction](#) (deramp), followed by an azimuth FFT. The FFT length must be as least twice as long as the azimuth block size to achieve the oversampling that is necessary prior to detection. The output of the FFT is the compressed image formed from the burst, and from this image the good points are selected. Good points correspond to targets that were illuminated by the antenna beam during the entire burst. Finally, a [radiometric correction](#) of the burst image is performed with a vector multiply in the azimuth direction. This corrects for a variation in target intensity due to the azimuth antenna beam pattern, as described in the section on [descalloping](#). [2.6.1.2.4.2](#).

The location of a target position depends on the slope of the frequency-time diagram, or the [frequency rate](#) of the linear FM signal. In the SAR azimuth signal, the [azimuth frequency](#)

---

rate depends on range. This geometric distortion needs to be corrected by an azimuth interpolation of the burst image, as described later under resampling.

#### 2.6.1.2.4.1.5 Look Summation and Resampling

After the basic SPECAN azimuth processing to form the burst images, several operations are done to form the image product. These steps are summarised as follows.

First, the burst image is shifted in range to correct for the skew that was applied during linear RCMC. This step is called deskeW. Only the integer portion is corrected in this step. The fractional portion is handled during the SR/GR resampling step.

Next, an optional range multi-looking is applied. This consists of applying a set of range bandpass filters to the image to extract range-look images corresponding to different range frequency bands.

The squared magnitude of the complex burst image for each range look is then computed. This is called detection. The squared magnitude, rather than the magnitude, is taken to avoid aliasing during the following interpolation steps.

The squared magnitude looks are then summed in range. Also, different burst images of the same area of the ground form different azimuth looks, and these are summed. The summation of looks is done to reduce speckle.

The look-summed image is then resampled in range. This is a shift and interpolation to correct for the fractional sample part of the deskeW. At the same time the data is resampled in range in order to convert to ground range and to achieve the required output sample spacing.

Then, azimuth resampling to the desired output pixel spacing. This compensates for the range-depend pixel spacing at the output of deramp and FFT. This may also include averaging to extract additional azimuth looks.

Finally, the square root of the image is taken to obtain the magnitude image.

#### 2.6.1.2.4.1.6 Product Processing

The output at this point is a valid medium-resolution (IMM), ScanSAR (WSM, GM1), or alternating polarisation ([APP](#), [APM](#)) product. ( See [Table](#) in the section entitled "Organisation of Products" in chapter 2 ). Generation of other products require the following steps.

- Block Averaging: The image is averaged and subsampled to form a browse product

(IMB, APB, WSB, GMB). ( See [Table 2.47](#) in the section entitled "Browse Products" ).

- Geocoding: For the [geocoded](#) product (APG), the image is resampled in two dimensions convert the image to a desired map projection.
- 

#### 2.6.1.2.4.1.7 Summary

The processing steps for the products processed by the SPECAN algorithm are summarised below:

- Alternating Polarisation Precision product, and all medium-resolution products: All steps except geocoding and block averaging are performed.
- Geocoded products: All steps except azimuth resampling (resampling is done during geocoding) and block averaging are performed.
- Browse Product: All steps except geocoding are performed.
- 

#### 2.6.1.2.4.1.8 References

##### Ref 2.9

. J. C. Curlander, R. N. McDonough, Synthetic Aperture Radar: Systems and Signal Processing, John Wiley and Sons, 1991.

#### 2.6.1.2.4.2 Descalloping

The purpose of this section is to discuss the problem known as scalloping, and the process used to correct it, known as descalloping.

#### 2.6.1.2.4.2.1 Scalloping

A [radar](#) system can be operated in burst mode such that the sensor is on for a period of time, then off, then on again, and so on, effectively imaging the region of interest in a series of bursts, where each burst consists of a certain number of echoes. In comparison with the conventional strip-mode imaging methods, burst mode operation enables a reduced power consumption and data rate at the expense of the resolution and image quality achieved.

Since a sensor operating in burst mode does not view a scene continuously, achieving uniform image quality over the imaged extent is more difficult for a burst mode imaging system than for a continuous mode one. In particular, burst mode images are subject to cyclic radiometric banding effects as described below.

During [azimuth compression](#), the data in each burst must be adjusted by the proper [azimuth](#) gain correction function. This is due to the fact that the return energy from a single scatterer is modulated in azimuth according to that portion of the antenna gain pattern used in the burst imaging event, an effect known as scalloping [Ref. \[2.11\]](#) (see [figure 2.34](#) Below). In other words, different point targets are illuminated by different positions of the azimuth gain pattern yielding different integrated powers. The amount of scalloping corresponds to the energy difference from the beginning to the end of the processing bandwidth and is generally measured in decibels (dB).

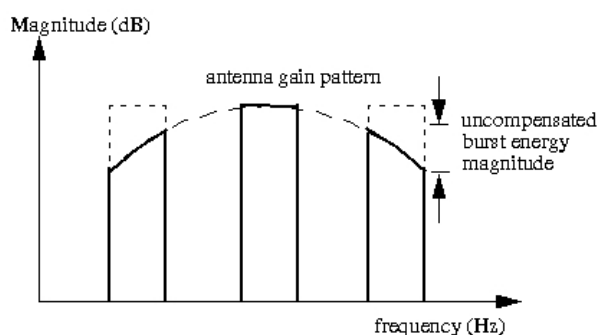


Figure 2.34 Return Energy From a Single Scatterer (3 bursts shown)

One method to correct for azimuth scalloping across individual bursts involves applying descalloping functions which are inversely proportional to the predicted antenna gain pattern function, thus resulting in a constant magnitude in azimuth across the corrected burst, as shown in [figure 2.35](#) a. In this figure, the uncompensated burst energy is drawn as the solid line, and the descalloping (correction) function is drawn as the dotted line. Consequentially, the radiometry is rendered flat in azimuth along the full image extent ([figure 2.35](#) b).

However, an inaccurate estimation of the fractional [Doppler centroid frequency 2.6.1.2.2.](#) leads to a misapplication of each of the azimuth descalloping functions to its corresponding burst image return signal. As a result, the output signal level is rendered non-constant across the azimuth burst as shown in [figure 2.36](#) a below. In this figure, the Doppler centroid error ( $f_{Derror}$ ) causes a cyclic rotation in the uncompensated burst energy function along azimuth (as shown in the solid line), resulting in an incorrect application of the descalloping function (shown as the dotted line). This radiometric variation in azimuth across each burst results in a cyclic radiometric pattern known as residual scalloping across the full image in azimuth, as depicted in [figure 2.36](#) b.

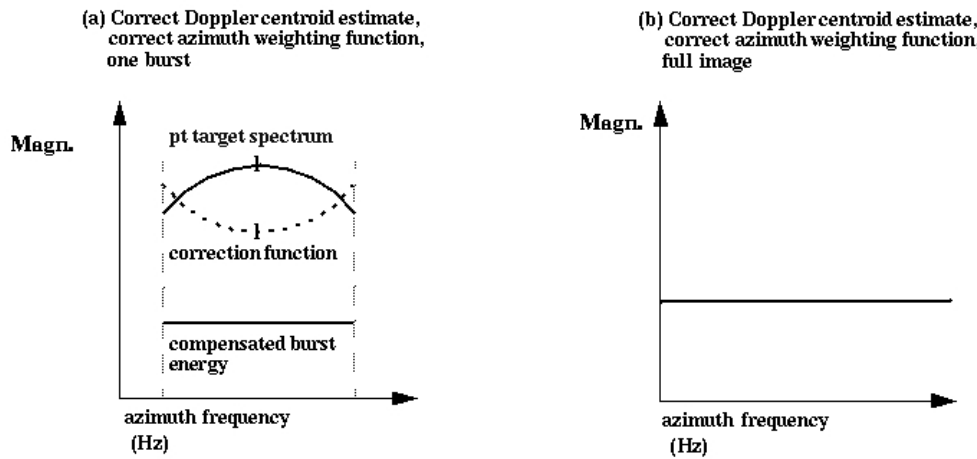


Figure 2.35 The application of a suitable correction function to an azimuth burst with an accurate Doppler centroid frequency estimate

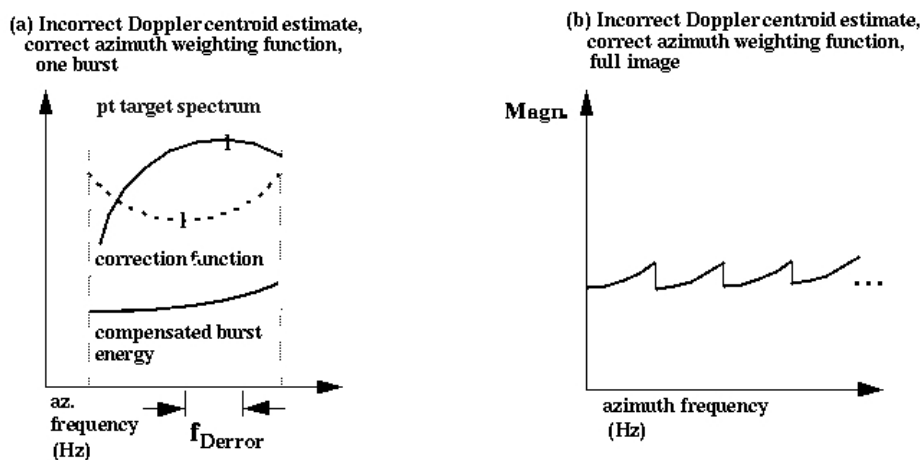


Figure 2.36 The application of a suitable correction function to an azimuth burst in the presence of a Doppler centroid frequency estimation error

### 2.6.1.2.4.2.2 Methods for Scalloping Correction

### 2.6.1.2.4.2.2.1 Azimuth Descalloping Function Application

There are two possible methods that may be selected for calculating the descalloping function: the Inverse Beam Pattern Method and the Constant SNR method.

**Inverse Beam Pattern Descalloping Method** One method to correct for scalloping across azimuth involves applying weighting functions which are inversely proportional to the azimuth antenna gain function. This technique shall be referred to as the Inverse Beam Pattern Method for descalloping.

To apply the correction effectively, the Doppler centroid frequency must be known accurately.

The weighting functions derived using the Inverse Beam Pattern method emphasise the outer looks to equalise the power, thereby maximising the equivalent number of looks, or speckle reduction, over azimuth.

**Constant signal-to-noise ratio (SNR) Descalloping Method** Bamler's "Optimum Look Weighting for Burst-Mode and ScanSAR Processing" ([Ref. \[2.11\]](#)) has developed a set of antenna pattern correction functions for burst mode and ScanSAR processing. The functions are derived to satisfy the following criteria in the multi-look azimuth processing case:

- The image signal energy becomes constant over azimuth,
- The noise energy becomes constant over azimuth, and
- The equivalent number of looks (which describes the amount of [speckle](#) reduction obtained by a weighted [multi-look](#) process) is maximised over azimuth.

The first and second criteria results in a constant signal-to-noise ratio (SNR) over azimuth. By allowing a variation in the signal image level in the derivation of the constant SNR weighting functions, the sensitivity of residual scalloping to Doppler centroid frequency estimation error is reduced. Note that in the case of only two azimuth looks, the signal image level is fixed as there are no degrees of freedom available to maximise.

In addition, the constant SNR method generates weighting functions which de-emphasise the outer looks, so that the equivalent number of looks is not maximised.

### 2.6.1.2.4.2.2.2 Doppler Centroid Frequency Estimation in the context of Burst Mode Data

An accurate [estimate of the Doppler centroid frequency 2.6.1.2.2.](#) is necessary to reduce the effect of residual scalloping, as shown in [figure. 2.36](#)

For both the Inverse Beam Pattern method and the Constant SNR method, the sensitivity to Doppler centroid errors decreases as the number of looks increases.

### 2.6.1.2.4.2.3 Notes

#### Ref 2.10

An approximation in the ASAR implementation of this method is described as follows. The correction at each azimuth location is proportional to the inverse of the midpoint of the azimuth beam pattern over the portion of the beam pattern used in focussing the image at that azimuth location. This is assumed to approximate, at each azimuth location, the inverse of the integral of the azimuth beam pattern over the portion of the beam pattern used in focussing the image at that azimuth location.

### 2.6.1.2.4.2.4 References

#### Ref 2.11

Bamler R, "Optimum Look Weighting for Burst-Mode and ScanSAR Processing", IEEE Transactions on Geoscience and Remote Sensing Vol. 33 No. # pp. 722-725, May 1995.

### 2.6.1.2.4.3 ScanSAR Beam Merging

[ScanSAR](#) multi-beam processing consists of generating independent beam images (called beam buffers) and subsequently combining them into a single output line, as shown in [figure 2.37](#) below:

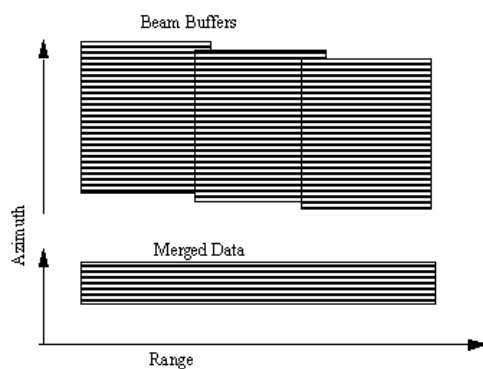


Figure 2.37 Merging Beam Buffers

The beam buffers overlap in range so, in general, the data should be merged to allow the output image line to be continuous.

Data in the merged line is either copied directly from one beam, or the merged line data is a blend of [pixels](#) from the so called blend region of the two beams.

Therefore, the beam merging algorithm consists of three primary steps described ago.

#### 2.6.1.2.4.3.1 Determine a reference point in the blend region

The reference point of the blend region is defined as the pixel corresponding to the range at which the elevation beam patterns for near and far beam intersect. Therefore, the blend region necessarily falls inside the overlap region, which is the region defined by the first pixel of the far beam and the last pixel of the near beam, as indicated in the [figure 2.38](#) below.

#### 2.6.1.2.4.3.2 Determine the limits of the blend region

The nominal size of the blend region, say  $N$  (even number), is specified in a PF-ASAR input parameter file. A number of  $N/2$  points are extracted on either side of the reference point for each (near and far) beam, so the reference point is precisely the centre of the blend region. If necessary,  $N$  will be clipped against the limits of the overlap region.

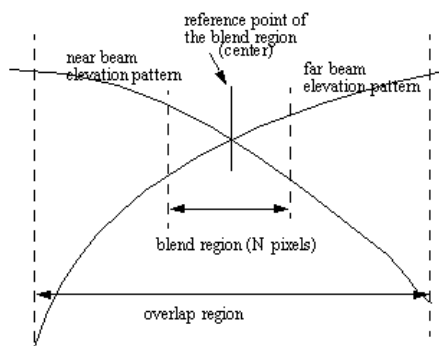


Figure 2.38 The Blend Region and its Reference Point

#### 2.6.1.2.4.3.3 Merge the data in the two beams corresponding to the blend region according to a predefined rule

The merging formula used to complete this third step is designed so that the signal-to-noise ratio of the imagery of the merged data tends to be maximised.

In describing the method, the following notation is used:

$x_{near}(n)$  = the array of near beam pixel power values;

$x_{far}(n)$  = the array of far beam pixel power values and;

$p$  = weight rate

For a given value of  $p$ , the formula used to calculate the merged pixels is given by:

eq 2.15

$$x_{merged}(n) = (1 - (n/N)p) * x_{near}(n) + ((n/N)p) * x_{far}(n),$$

where  $n = 0, 1, \dots, N-1$  and  $p \geq 0$ . The data on the steeper extremities of the beam pattern, where the effects of a bias in the elevation beam pattern correction are more significant, are disregarded while the data on the steeper extremities of the blend region are weighted less by the merging model. This is because the following continuity conditions hold true:

$$x_{merged}(0) = x_{near}(0)$$

$$x_{merged}(N) = x_{far}(N)$$

In particular, if  $x_{far}(n) = x_{near}(n)$  for all  $n = 0, 1, \dots, N-1$ , then

$$x_{merged}(n) = x_{far}(n) = x_{near}(n) \text{ for all } n = 0, 1, \dots, N-1$$

The desired merging scenario can be easily selected by simply setting the weight rate parameter,  $p$ , as shown in the following table:

Table 2.33 Setting Weight Rates Parameter

Parameter $p$	Weighting
$p = 1$	current weighting scenario
$p > 1$	the near beam weighs more (it is favoured)
$0 < p < 1$	the far beam weighs more (it is favoured)
$p = 0$	only the far beam contributes to the merged one
$p = \infty$	only the near beam contributes to the merged one

#### 2.6.1.2.4.4 Global Monitoring Mode Inverse Filter

The transmitted [pulse](#) typically has a rectangular [amplitude](#), and a quadratic phase variation that gives the pulse its linear [FM](#) character. For linear FM pulses, increasing the duration of

the pulse allows greater [frequency](#) variation across the pulse, thus increasing the pulse bandwidth and resulting in a higher resolution after [pulse compression](#). (See the description of range compression in the section on [Range-Doppler 2.6.1.2.3.1.2.](#) processing). Linear FM pulses that are used for pulse compression typically have a large time-bandwidth product, at least 100.

For linear FM pulses with a large time-bandwidth product, there is a time-frequency relationship, such that the amplitude spectrum has the same shape as the pulse amplitude in the time domain. For example, the figure below shows the amplitude of the [Fourier transform \(FFT\)](#) of a large time-bandwidth product pulse with a rectangular shape.

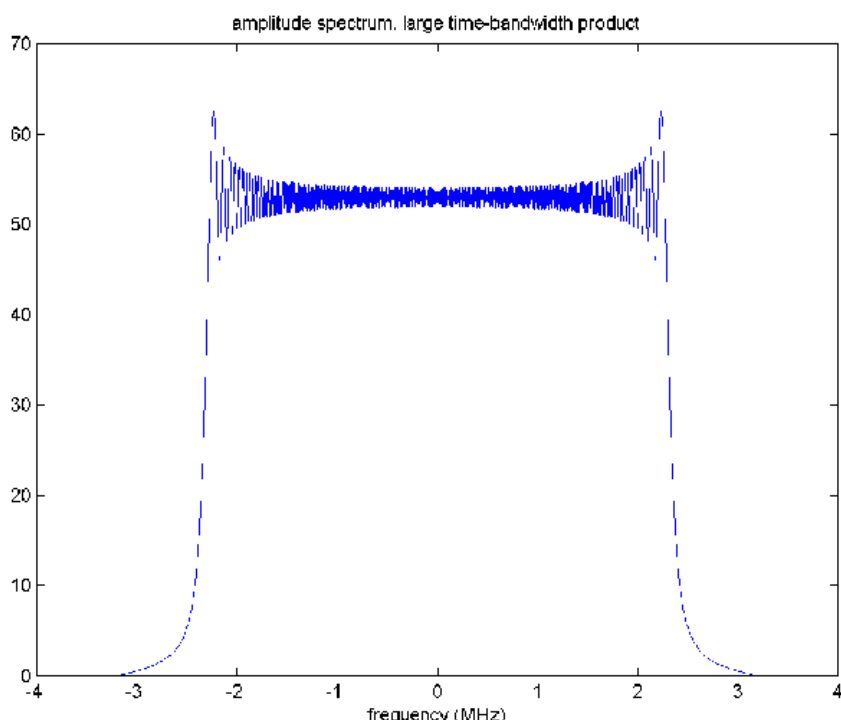


Figure 2.39 Pulse spectrum with large time-bandwidth product.

The [Fourier transform \(FFT\)](#) also has a quadratic phase variation that needs to be removed during [matched filtering](#), in order to compress the pulse. In the frequency domain, the matched filter is defined as the conjugate of the Fourier transform of the pulse. For large time-bandwidth product pulses, multiplication of the pulse spectrum by its conjugate removes the quadratic phase variation, and leaves the amplitude approximately unchanged because of the rectangular shape, resulting in the sinc shaped impulse response.

However, in [Global Monitoring \(GM\)](#) Mode where the required resolution is quite low, a

relatively short pulse with smaller [bandwidth](#) is used. In this case the time-bandwidth product is quite low, on the order of 20, and the time-frequency relationship does not hold as well. For example, the figure below shows the amplitude of the Fourier transform of a pulse used in Global Monitoring Mode. The amplitude is no longer rectangular, and multiplication by the matched filter would worsen the amplitude variation, which affects the shape of the compressed pulse.

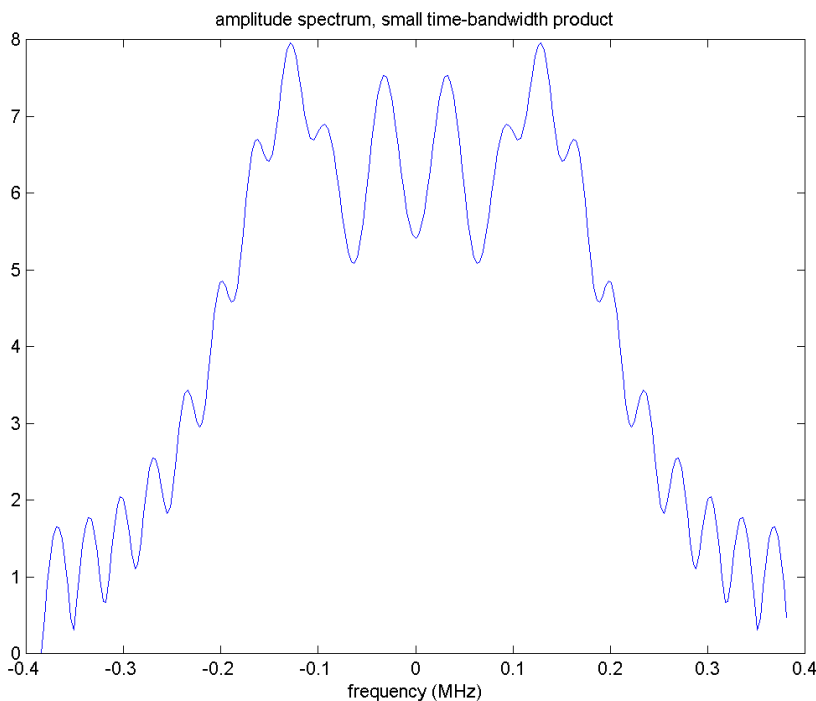


Figure 2.40 Pulse spectrum with small time-bandwidth product.

To solve the problem caused by the shape of the amplitude spectrum when the time bandwidth product is low, the variation of the amplitude spectrum is removed by multiplying the pulse spectrum by the [inverse of the Fourier transform \(IFFT\)](#) of the pulse, rather than the conjugate. This removes the amplitude variation of the spectrum during pulse compression, improving the shape of the compressed pulse.

### 2.6.1.2.5 ASAR Strip Line Product Processing

#### 2.6.1.2.5.1 2.6.1.2.5.1 Introduction

The ASAR Instrument may be operated in one high rate mode continuously (an acquisition segment) for up to ten minutes duration or for up to one orbit duration in a low-rate mode called [Global Monitoring](#) (GM) mode. Stripline products contain image data from an entire acquisition segment, up to a maximum of 10 minutes per product for [IM](#), [AP](#), and [WS](#) and up to a full orbit (100 minutes) for GM. All medium-resolution and [browse products](#) (IMM, IMB, APM, APB, WSM, WSB, GM1, and GMB) are processed as stripline products. The browse products are subsampled versions of the medium-resolution products and are processed at the same time. ( For a further discussion of all of these products refer to the section entitled "[Level 1B Image Products](#)" [2.6.2.1.1.3.](#), and "[Browse Products](#)" [2.6.2.1.3.](#) , which can both be found in chapter 2 ).

The PF-ASAR will systematically generate output parent products, within the time constraints, that cover an entire acquisition segment by processing a number of separate slices and then joining the slices to form the continuous segment. Most long data segments will be processed using more than one processing computer, in order to meet throughput performance requirements. Each computer will be given a portion of the input data segment to process. The output, referred to as slices, from the different computers are then concatenated to produce one long strip product, referred to as stripline product.

This stripline parent product is stored as a single product in the Archive Facility (ARF) and key information about the product is maintained in the inventory database for access by users. After the segment product is archived, a customer may extract a subset, or [child product](#). If a customer orders a [floating scene](#) from within the stripline product the appropriate portion of the archived product, i.e. the [measurement data](#), [annotation data](#), [Specific Product Header](#) (SPH) and [Main Product Header](#) (MPH), will be extracted to form the requested output product. The extracted subset product may start at any point in the segment and shall not contain any radiometric or geometric discontinuities.

Geometric continuity is achieved by ensuring all [PF-ASAR](#) computers establish the same output grid. All PF-ASAR will use the same input parameters (orbit data, earth ellipsoid parameters, centre swath elevation angle, etc.) and the same software to establish the output grid. The projection used for stripline products differs from the normally used for SAR products. SAR products are usually projected such that the first [pixel](#) in [range](#) is kept at a constant range. For stripline products, however, the ground range projection is designed to allow very long [azimuth](#) extent images to be displayed without cutting off any data and with a minimum of black-filled pixels. This is done by keeping the mid-ground range pixels at a constant elevation angle.

Radiometric continuity is achieved by ensuring the Doppler Centroid frequency is continuous along the data segment. The input raw data to the different PF-ASAR computers is overlapped and each PF-ASAR uses the overlap regions (at the beginning and end of the slice) to estimate the Doppler Centroid frequency. The Doppler Centroid frequency that is used within the slice is calculated by interpolation.

The slice size and the overlap depend on the mode (IM, AP, WS or GM). The figure and table below show the minimum and maximum slice sizes and the minimum overlap. The overlap must take into account the amount of data required for Doppler centroid estimation

and processing throw away (matched filter throw-away and azimuth skew).

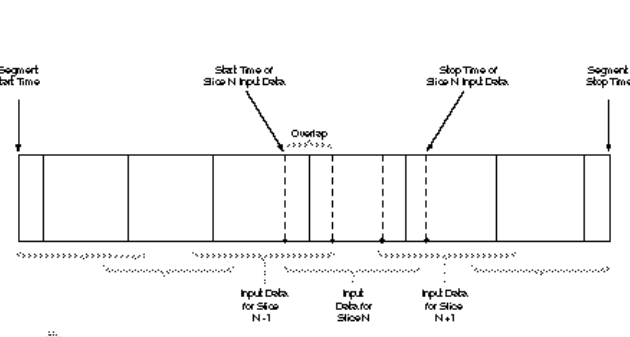


Figure 2.41 Slice Size and Overlap Illustration

Product generation includes the following extra parameters for stripline processing:

- Slice size
- Slice number
- Acquisition start time of the segment
- Overlap size

#### 2.6.1.2.5.1.1 Slice Size and Overlap

Table 2.34 Slice Size and Overlap

Mode	IM	AP	WS	GM
MinimumSlice Size	20.7 sec	37.4 sec	5 sec	30.7 sec
MaximumSlice Size	90 sec	90 sec	90 sec	20 min
MinimumOverlap	2.5 sec	2.5 sec	8.3 sec	54.3 sec

#### 2.6.1.2.5.2 Processing Parameters Affected By Strip Line Product Continuity Requirements

ASAR processing requires the calculation and use of a number of processing parameters whose values vary at different rates. Some parameters may be held constant throughout an acquisition segment while other parameters must be recalculated at intervals and then applied to blocks of data or varied smoothly throughout the segment.

**Table 2.35** below "Processing Parameters Affecting Stripline Products", identifies processing parameters that are important for stripline processing and groups the parameters depending on their source:

- signal data - parameters derived from the SAR raw data;
- auxiliary data - parameters derived from common auxiliary data provided to all ASAR computers;
- ISP header data - parameters extracted from header of downlink data and may vary throughout data segments.

Table 2.35 Processing Parameters Affecting Stripline Products

Processing Parameters from Signal Data	Processing Parameters from Auxiliary Data	Processing Parameters from ISP Header Data
I and Q channel statistics	along-track pixel spacing/start position	First output range sample
Chirp Replica		
Antenna Elevation gain correction	Slant range/ground range interpolation to output grid	
Doppler Centroid Estimate		
Doppler Ambiguity Estimate	FM Rate	

### 2.6.1.2.5.2.1 I And Q Channel Statistics

Channel statistics are calculated from raw data to determine I and Q channel bias and orthogonality adjustments. These adjustments affect radiometric accuracy. ERS experience indicates that channel bias values are relatively slowly varying, therefore statistical analysis of data from any portion of the data segment could be applied to the entire segment, or the analysis could be repeated using any portion of the segment and yield similar results.

Each PF-ASAR computer evaluates I and Q channel statistics from its own [ISP](#) data. The [raw data](#) used for statistics is a subsample of the total raw data taken from samples throughout the input data. The calculated correction factors are applied uniformly for the entire slice.

### 2.6.1.2.5.2.2 Chirp Replica

The [chirp](#) replica is derived by processing the periodic [calibration](#) data. Periodic calibration activities performed by the instrument generate calibration data for segments of the SAR antenna in a cyclic manner and downlinks this data interspersed with the imaging data. The pulse replica is derived from the summation of calibration data from all 32 antenna segments received over a period of time.

During stripline processing the chirp replica is updated whenever a new periodic calibration cycle is found in the input data. If a complete set of calibration pulses from 32 antenna segments is not found, then the nominal chirp is used.

### 2.6.1.2.5.2.3 Antenna Elevation Gain Correction

The antenna elevation gain correction is also derived by processing the periodic calibration data and is also updated whenever a new periodic calibration cycle is found in the input data. If a complete set of calibration pulses from 32 antenna segments is not found, then the nominal antenna elevation gain correction is used.

The antenna elevation pattern is converted to slant range pattern so it can be applied to the range compressed data. This conversion is updated periodically to follow the continuously changing satellite/earth geometry.

### 2.6.1.2.5.2.4 Doppler Centroid Estimation

Doppler centroid estimation is performed by each PF-ASAR computer using the data at the beginning and end of the slice. Linear interpolation using the two estimates is used to compute Doppler centroid frequency at various positions along the slice.

If the overlap data is missing, Doppler centroid estimation is still done using the data at the beginning and end of the available input data. In this case, the Doppler centroid may not be continuous across the adjacent slices. This is acceptable because there is no valid image at the boundary of the slices.

The Doppler centroid frequency maximum variation is about 1.7 Hz/sec. Over a slice of 20 seconds, the Doppler centroid frequency changes by a maximum of 34 Hz and the variation can be approximated as a linear function over a long period.

The ambiguity estimate is performed once per slice and is then applied throughout that slice.

( For a further discussion of the Doppler centroid frequency, ambiguity, and estimation, see the section entitled "[Doppler Centroid Frequency Estimator](#)" [2.6.1.2.2](#) ).

### 2.6.1.2.5.2.5 along-track Pixel Spacing/Start Position

A stripline product is required to have a constant along-track pixel spacing to meet geometric requirements and ease processing of child products (floating scenes extracted from the stripline product). For systematically generated ASAR products (GMM, IMM, WSM, APM, and browse), each output line contains pixels for a specific zero Doppler time and lines are spaced by a constant zero Doppler time interval (rather than constant distance spacing).

Therefore each output line must be placed on a grid with a regular time interval referenced to the start time of the stripline product segment.

The Line Time Interval in seconds (the grid spacing along-track) is pre-defined for each product type and subswath and is a constant throughout the orbit to ensure repeatability of grid spacing from one orbit to the next. (It should be noted that the precise pixel spacing in metres will vary depending on the instantaneous velocity of the satellite.)

Each PF-ASAR calculates the zero Doppler start time of the stripline product segment by converting the acquisition time to zero Doppler time.

Each PF-ASAR then calculates the zero Doppler start time and stop time of its output slice.

### 2.6.1.2.5.2.6 Slant Range/Ground Range (SR/GR) Conversion To Output Grid

The output grid is defined such that the azimuth line of the output product is parallel with the mid swath line, where the mid swath line is the line which has a fixed elevation angle along azimuth. This output grid does not contain any range pixel with a constant range time along azimuth.

As the satellite altitude varies with time, the mid swath line moves closer or farther away from the subsatellite track and the valid data follows the Sampling Window Start Time (SWST).

The number of samples per range lines in the output product is set to be large enough to cover the shift of the valid data along the segment so that no valid data is thrown away.

The valid samples are projected to the output grid using an SR/GR conversion table. PF-ASAR calculates the SR/GR conversion table periodically along the azimuth direction and performs linear interpolation between adjacent SR/GR conversion tables so that a smoothly varying SR/GR can be achieved.

### 2.6.1.2.5.2.7 FM Rate

The Frequency Modulation (FM) Rate must be updated throughout the segment to maintain geometric continuity. The FM rate varies slowly so that calculations at consecutive portions of the segment do not result in discontinuity for medium-resolution products. It is calculated once per slice.

### 2.6.1.2.5.2.8 First Output Range Sample

The location of the first valid output range sample is a function of the Sampling Window Start Time (SWST). PF-ASAR calculates the slant range of this first valid sample using the

SWST and then projects it to the output grid using the smoothly varying SR/GR conversion table.

### 2.6.1.3 Level 1B Accuracies

The following two tables define the product geometric accuracies of the Level1B products.

Table 2.36 ASAR High Resolution Image Accuracy

Product Type	IM (Image Mode)	AP (Alternating Polarisation Mode)	WV (Wave Mode)
Precision Image	Pixel=12.5m Resolution < 28m ENL = 3.9	Pixel=12.5m Resolution < 30m ENL = 1.9	
Single-Look Complex	Pixel=image spacing Resolution=6m (Azimuth) and 9m(Slant Range)	Pixel=image spacing Resolution=12m (Azimuth) and 9m(Slant Range)	
Ellipsoid Geocoded	Pixel=12.5m Resolution < 30m ENL = 3.9	Pixel=12.5m Resolution < 30m ENL > 1.9	
Single-Look Complex Wave Imagette			Pixel=image spacing Resolution=6m (Azimuth) and 9m(Slant Range)

Table 2.37 ASAR Brows, Medium Resolution and Global Monitoring Image Accuracy

Product Type	IM (Image Narrow swath)	AP (Alternating Polarisation)	WS (Wide Swath)	GM (Global Monitoring)
Medium Resolution Image	Resolution < 150m Pixel=75m ENL = 40	Resolution < 150m Pixel=75m ENL = 50	Resolution < 150m Pixel=75m ENL = 11*	
Global Monitoring Image				Resolution < 950m Pixel=500m ENL = 7 to 9*
Browse Image **	Pixel=225m ENL = 80	Pixel=225m ENL = 75	Pixel=900m ENL = 57 to 82	Resolution =2000m Pixel=1000m ENL = 18 to 21

In the tables, Pixel means pixel spacing, Resolution means spatial resolution, ENL is equivalent number of looks (which affects radiometric resolution). The ENL on some images is dependant on the instrument setting, indicated with one asterisk (\*). Browse images are derived from Medium Resolution images.

Table 2.38 Summary of ASAR Predicted Performance with Comparison to ERS

Parameter	Unit	Image	Alternating Polarisation	Wide Swath	Global Monitoring	Wave	ERS-1/2
Polarisation		VV or HH	VV/HH, HH/HV, VV/VH	VV or HH	VV or HH	VV or HH	VV
Spatial resolution (a x r)	m	27.5 x 28.1	28.7 x 29.7	149 x 145	949 x 977	27.5 x 29.6	27.5 x 28.1
Radiometric resolution	dB	1.54	2.46 to 2.50	1.45 to 1.72	1.35 to 1.44	1.54	2.07
PTAR azimuth	dB	25.9 to 29.6	19.1 to 28.0	22.3 to 28.6	26.6 to 29.3	27.3 to 29.6	27.8/24.5
PTAR range	dB	31.6 to 45.8	26.4 to 40.5	25.0 to 33.9	25.0 to 32.2	31.2 to 45.7	>40
DTAR azimuth	dB	22.6 to 24.7	18.1 to 24.5	20.3 to 24.9	24.6 to 27.5	22.6 to 24.7	>25
DTAR range	dB	17.1 to 39.4	17.1 to 39.4	17.1 to 30.8	17.1 to 30.8	21.2 to 47.7	>35
Radiometric stability (1sigma)	dB	0.32 to 0.40	0.50 to 0.55	0.32 to 0.42	0.46 to 0.53	0.55 to 0.60	0.24/0.27
Radiometric accuracy (3sigma)	dB	1.17 to 1.38	1.62 to 1.81	1.20 to 1.45	1.54 to 1.74	1.80 to 1.94	na
Noise Equivalent (sigma-nought)	dB	-19.6 to -22.1	-19.4 to -21.9	-20.8 to -26.2	-31.5 to -35	-19.8 to -22.4	-26.2/-25.2

## 2.6.2 Level 1B Products

### 2.6.2.1 Level 1B High Level Organisation of Products

[Table 2.39](#) below gives a listing of all Level 1B products, as was first disclosed in Section 2.1 "Products and Algorithms Introduction." 2.1.

Table 2.39 Level 1B Products

Mode	Product ID	Product Name
IM	<a href="#">ASA_IMP_IP_2.6.2.1.1.2.1.2.</a>	ASAR Image Mode Precision Image
IM	<a href="#">ASA_IMS_IP_2.6.2.1.1.2.1.1.</a>	ASAR Image Single-Look Complex (SLC)
IM	<a href="#">ASA_IMG_IP_2.6.2.1.1.2.1.3.</a>	ASAR Image Mode ellipsoid geocoded image
IM	<a href="#">ASA_IMM_IP_2.6.2.1.1.3.1.1.</a>	ASAR Image Mode medium-resolution image
AP	<a href="#">ASA_APP_IP_2.6.2.1.1.2.1.5.</a>	ASAR Alternating Polarisation precision image
AP	<a href="#">ASA_APG_IP_2.6.2.1.1.2.1.6.</a>	ASAR Alternating Polarisation Mode ellipsoid geocoded image
AP	<a href="#">ASA_APS_IP_2.6.2.1.1.2.1.4.</a>	ASAR Alternating Polarisation Mode complex image
AP	<a href="#">ASA_APM_IP_2.6.2.1.1.3.1.2.</a>	ASAR Alternating Polarisation medium-resolution image

WS	<a href="#">ASA_WSM_IP 2.6.2.1.1.3.1.3.</a>	ASAR Wide Swath standard image
GM	<a href="#">ASA_GMI_IP 2.6.2.1.1.3.1.4.</a>	ASAR Global Monitoring Mode Image
WV	<a href="#">ASA_WVI_IP 2.6.2.1.2.1.1.</a>	ASAR Wave Mode SLC imagette and Imagette Cross Spectra
WV	<a href="#">ASA_WVS_IP 2.6.2.1.2.1.2.</a>	ASAR Wave Mode Imagette Cross Spectra (Level 1)

ASAR produces Image and Wave products. The details of these products are given in Subsections "[Level 1B Image Products 2.6.2.1.1.](#)" and "[Level 1B Wave Products.](#)" [2.6.2.1.2.](#)

The following processing steps are applied to the Level 0 data to form the SAR Level 1B image:

- data decompression
- replica construction and power estimation
- calibration pulse processing
- noise power estimation
- raw data correction (I/Q bias removal, I/Q gain imbalance correction, I/Q non-orthogonality correction)
- antenna elevation pattern compensation (not applied for SLC images)
- image formation (SPECAN or Range/Doppler)
- geolocation
- conversion to map projection (geocoded products only)

The image formation algorithm used is either the [Range Doppler Algorithm 2.6.1.2.3.](#) or the [SPECAN 2.6.1.2.4.](#) algorithm, depending upon the product requested.

A modified version of the range-Doppler algorithm was developed for the [AP SLC product 2.6.1.2.3.2.](#). The algorithm was chosen such that the output product would be useful for [Interferometric SAR](#) (InSAR). The algorithm is a modified [phase preserving](#) range-Doppler approach. The processed Doppler bandwidth is made equal to four [burst](#) bandwidths (multi-burst processing) so as to keep as much of the signal information as possible while maintaining radiometric quality. The resulting product has a modulated [impulse response](#), but contains all the necessary information required for Interferometric SAR (InSAR). One method to remove the modulation during InSAR post-processing is to use the short [FFT](#) approach to select the common spectra between the two image pairs. ( See also "[Burst Mode Interferometry](#)" in the section entitled "[Processing Algorithms For AP SLC](#)" [2.6.1.2.3.2.3.](#) )

All of the above-mentioned algorithms are discussed in detail in Subsection entitled "[ASAR Level 1B Algorithms.](#)" [2.6.1.](#)

During preprocessing, [PF-ASAR](#) performs [raw data analysis](#), noise processing, and the processing of the ASAR [calibration pulse](#) data. [Chirp](#) replicas and [antenna pattern gain factors](#) are obtained from the calibration pulse processing. The signal data for all modes is [FBAQ](#) decoded; prior to processing (from 2, 3 or 4 bits back to 8 bits).

As far as the [Wave Mode](#) (WV) is concerned, the products generated are not [detected](#), but [Single-Look Complex](#) (SLC). They allow for further Cross Spectra processing, following the algorithm developed by NORUT (Norway) and provide complete [speckle](#) compensation and

---

potential capability to resolve the propagation ambiguity observed on the corresponding [ERS](#) products.

### 2.6.2.1.1 Level 1B Image Products

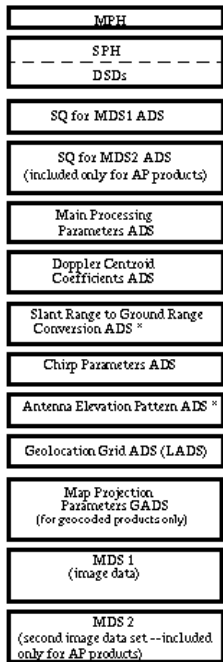
The general product structure, used in all [ENVISAT](#) products, is given in "[Definitions and Conventions](#)." [2.3.2.1](#). For the engineering quantities associated with these products, refer to "[Level 1B Engineering Quantities](#)." [2.6.2.2](#).

Advanced Synthetic Aperture Radar (ASAR) Image Products can be grouped into those produced as [stand-alone products](#) [2.6.2.1.2](#), and those produced as [stripline products](#) [2.6.2.1.3](#). All ASAR Image Products are stored in time-increasing order, except the [geocoded](#) products, which are oriented such that the first [pixel](#) of the first line is the most north-west pixel. Image products can be generated from various [ASAR modes](#), as outlined in the section entitled "[Products and Algorithms Introduction](#)." [2.1](#).

#### 2.6.2.1.1.1 Image Product Structure

All ASAR Image products follow a standard structure as described in [figure 2.42](#), shown below:

Figure 2.42 ASAR image product structure



\* not included for SLC products

The [Main Product Header \(MPH\)](#) is the same as for all ENVISAT products, and it is provided in the [Data Formats 6.6.1.](#) section. The [Specific Product Header \(SPH\)](#) used for image products is also given in the [Data Formats \(Chapter 6.\)](#) section. The [Data Set Names \(DS NAMES\)](#) in [table 2.40](#) below may appear in the ASAR Image Product SPH [Data Set Descriptors \(DSDs\)](#):

Table 2.40 ASAR image products data set descriptor names

Data Set Type	Data Set Name
<a href="#">SQ for MDS 1 ADS</a>	"MDS1 SQ ADS"
SQ for MDS 2 ADS	"MDS2 SQ ADS"
Main Processing parameters ADS	"MAIN PROCESSING PARAMS ADS"
<a href="#">Doppler Centroid parameters 2.6.1.2.2.</a> , ADS	"DOP CENTROID COEFFS ADS"
<a href="#">Slant Range to Ground Range Conversion</a> ADS	"SR GR ADS"
<a href="#">Chirp</a> parameters ADS	"CHIRP PARAMS ADS"
<a href="#">Antenna Elevation Pattern</a> for MDS 1 ADS	"MDS1 ANTENNA ELEV PATT ADS"
Antenna Elevation Pattern for MDS 2 ADS	"MDS2 ANTENNA ELEV PATT "
<a href="#">Geolocation</a> Grid ADS (LADS)	"GEOLOCATION GRID ADS"
Map Projection parameters GADS	"MAP PROJECTION GADS"
Measurement Data Set 1	"MDS1"
Measurement Data Set 2	"MDS2"
<a href="#">DSD</a> referencing the <a href="#">Level 0 product</a> from which this product was created	"LEVEL 0 PRODUCT"
<a href="#">DSD</a> referencing <a href="#">PF-ASAR Processor Configuration file</a>	"ASAR PROCESSOR CONFIG"
<a href="#">DSD</a> referencing <a href="#">Instrument Characterisation</a> file used	"INSTRUMENT CHARACTERISATION"

---

Data Set Type	Data Set Name
DSD referencing <a href="#">External Characterisation</a> file used	"EXTERNAL CHARACTERISATION"
DSD referencing <a href="#">External Calibration</a> file used	"EXTERNAL CALIBRATION"
DSD referencing the <a href="#">Orbit State Vectors</a> file used	"ORBIT STATE VECTOR 1"

### 2.6.2.1.1.1.1 Image Product Data Sets

[Data Sets](#) (DS) are in mixed-binary format. ASCII values may be included in the Data Sets, but they do not follow the Keyword-value format of the [MPH](#) and [SPH](#), nor are they contained within quotation marks.

The Data Sets which make up the ASAR image product structure are the following:

- [Summary Quality ADSs](#)
- Main Processing parameters [ADS](#)
- [Doppler Centroid Coefficients 2.6.1.2.2.](#). ADS
- [Slant Range to Ground Range](#) Conversion ADS
- [Chirp](#) parameters ADS
- [Antenna Elevation Pattern](#) ADS
- [Geolocation](#) Grid ADS (or LADS)
- [Map Projection](#) GADS
- [Measurement Data Set \(MDS\)](#)

The details relating to the layout of each of these [Data Set Records](#) (DSRs), is given in the [Data Formats \(Chapter 6.\)](#) section.

### 2.6.2.1.1.2 Stand-Alone (On-Request) Image Products

Stand-alone image products are produced by request only and are created directly from the Level 0 data. They are ordered as a scene. All of these products share a common format.

[Table 2.41](#) below lists the type of image formation algorithm applied to the various stand-alone products.

Table 2.41 Image formation algorithms for stand-alone products

Product ID	Algorithm Applied
<a href="#">ASA_IMS_1P 2.6.2.1.1.2.1.1.</a>	<a href="#">Range/Doppler 2.6.1.2.3.</a>
<a href="#">ASA_IMP_1P 2.6.2.1.1.2.1.2.</a>	<a href="#">Range/Doppler 2.6.1.2.3.</a>
<a href="#">ASA_IMG_1P 2.6.2.1.1.2.1.3.</a>	<a href="#">Range/Doppler 2.6.1.2.3.</a>
<a href="#">ASA_APS_1P 2.6.2.1.1.2.1.4.</a>	<a href="#">Range/Doppler 2.6.1.2.3.</a>
<a href="#">ASA_APP_1P 2.6.2.1.1.2.1.5.</a>	<a href="#">SPECAN 2.6.1.2.4.</a>
<a href="#">ASA_APG_1P 2.6.2.1.1.2.1.6.</a>	<a href="#">SPECAN 2.6.1.2.4.</a>

## 2.6.2.1.1.2.1 Stand-Alone Product Types

### 2.6.2.1.1.2.1.1 Image Mode Single-Look Complex

The format for this product is given in the [Data Formats \(Chapter 6.\)](#) section, and the engineering quantities are given in the section entitled "[Level 1B Engineering Quantities.](#)" [2.6.2.2.1.2.1.](#)

[Figure 2.43](#) is an example of an ASA\_IMS\_1P product as seen using [EnviView: 1.2.1.2.](#)

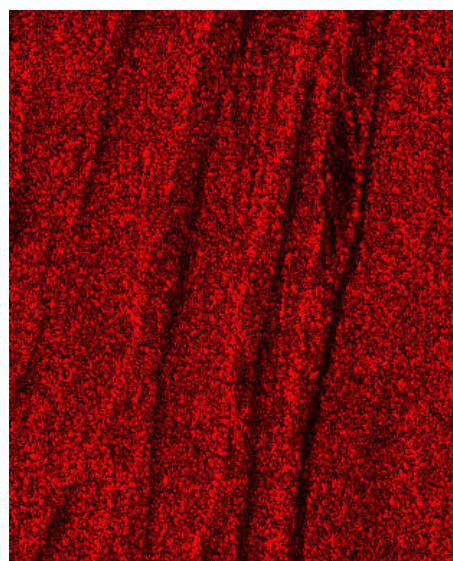


Figure 2.43 ASA\_IMS\_1P sample product (as seen in EnviView)

### 2.6.2.1.2.1.2 Image Mode Precision Image

The format for this product is given in the [Data Formats \(Chapter 6.\)](#) section, and the engineering quantities are given in the section entitled "[Level 1B Engineering Quantities.](#)" [2.6.2.2.1.3.1.](#)

[Figure 2.44](#) is an example of an ASA\_IMP\_1P product as seen using [EnviView 1.2.1.2.](#).

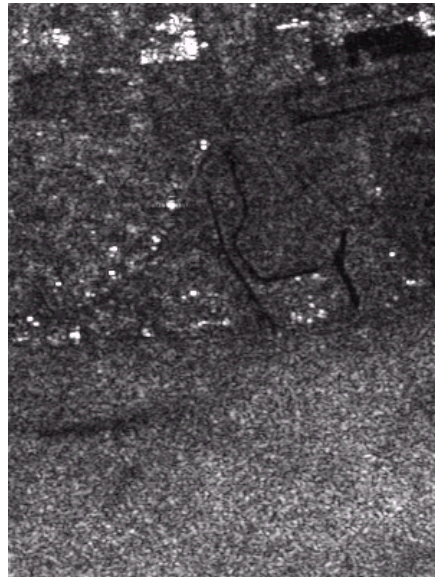


Figure 2.44 ASA\_IM\_1P sample product (as seen with EnviView)

### 2.6.2.1.2.1.3 Image Mode Ellipsoid Geocoded Image

The format for this product is given in the [Data Formats \(Chapter 6.\)](#) section, and the engineering quantities are given in the section entitled "[Level 1B Engineering Quantities](#)" [2.6.2.2.1.4.1.](#)

[Figure 2.45](#) is an example of an ASA\_IMG\_1P product as seen with [EnviView 1.2.1.2.](#)

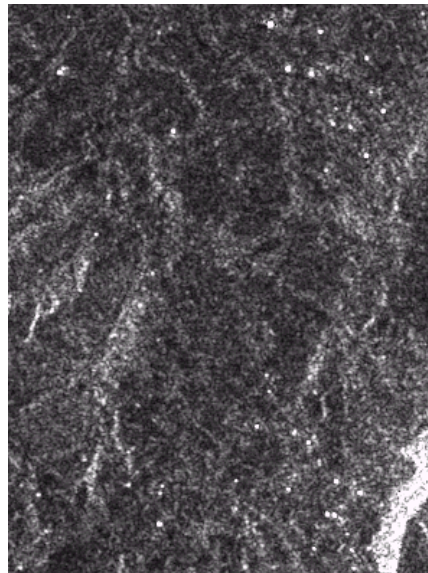


Figure 2.45 ASA\_IMG\_1P sample product (as seen with EnviView)

#### 2.6.2.1.1.2.1.4 Alternating Polarisation Mode Single-Look Complex

The format for this product is given in the [Data Formats \(Chapter 6.\)](#) section, and the engineering quantities are given in the section entitled "[Level 1B Engineering Quantities.](#)" [2.6.2.2.1.2.2.](#)

[Figure 2.46](#) is an example of an ASA\_APS\_1P product as with [EnviView 1.2.1.2.](#)

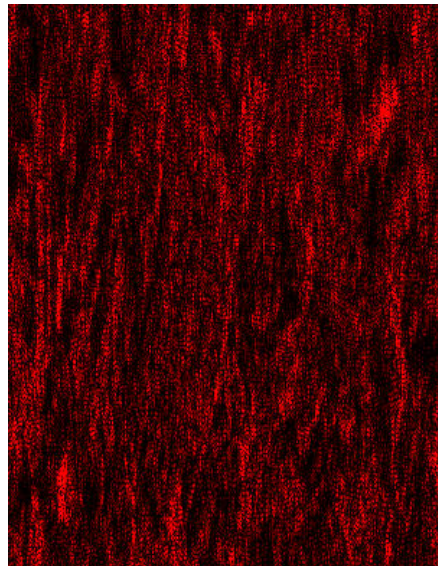


Figure 2.46 ASA\_APS\_1P sample image (as seen in EnviView)

### 2.6.2.1.1.2.1.5 Alternating Polarisation Mode Precision Image

The format for this product is given in the [Data Formats \(Chapter 6.\)](#) section, and the engineering quantities are given in the section entitled "[Level 1B Engineering Quantities.](#)" [2.6.2.2.1.3.2.](#)

[Figure 2.47](#) is an example of as ASA\_APP\_1P product as seen with [EnviView 1.2.1.2.](#) .



Figure 2.47 ASA\_APP\_1P sample product (as seen with EnviView)

#### 2.6.2.1.1.2.1.6 Alternating Polarisation Ellipsoid Geocoded Image

The format for this product is given in the [Data Formats \(Chapter 6.\)](#) section, and the engineering quantities are given in the section entitled "[Level 1B Engineering Quantities.](#)" [2.6.2.2.1.4.2.](#)

[Figure 2.48](#) is an example of an ASA\_APG\_1P product as seen with [EnviView 1.2.1.2.](#).

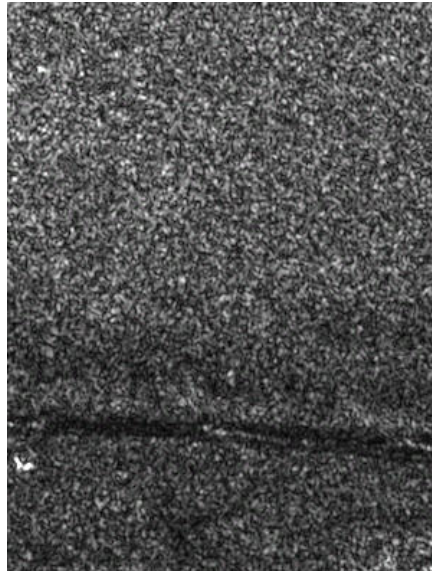


Figure 2.48 ASA\_APG\_1P sample product (as seen with EnviView)

### 2.6.2.1.1.2.2 Input Data

The input for all of the stand-alone products is the Level 0 data corresponding to the particular mode and auxiliary data.

( Refer to [table 2.5.1.2](#). in the section "Level 0 Products" for a listing of the Level 0 products )

### 2.6.2.1.1.2.3 Auxiliary Data Used

The auxiliary data required to create the stand-alone products is listed in [table 2.42](#) shown below. The description of the main auxiliary data records is provided in the "[Auxiliary Data Sets for Level 1B Processing](#)" [2.9.2](#). section, and the formats are provided in the [Data Formats \(Chapter 6.\)](#) section. The description of the orbit state vectors, including their formats, is provided in the section "[Common Auxiliary Data Sets.](#)" [2.9.3](#).

Table 2.42 ASAR auxiliary data for image product processing

Description	Auxiliary Data ID
<a href="#">External Characterisation</a> data file	<a href="#">ASA_XCH_AX</a>
<a href="#">External Calibration</a> data file	<a href="#">ASA_XCA_AX</a>
<a href="#">Instrument Characterisation</a> file	<a href="#">ASA_INS_AX</a>
PF-ASAR Processor Configuration file	<a href="#">ASA_CON_AX</a>
Orbit State Vectors file (one file of five)	<a href="#">AUX_FRO_AX_2.9.3.1</a> <a href="#">AUX_FPO_AX_2.9.3.1</a> DOR_NAV_OP DOR_VOR_AX DOR_POR_AX

### 2.6.2.1.1.3 Stripline Processed Image Products

Stripline image products contain image data for an entire segment, up to a maximum size of 10 minutes per product for IM, AP and WS and up to a full orbit (100 minutes) for GM. The PF-HS concatenates together several sub-images called [slices](#) received from PF-ASAR on a data set basis in order to form the entire stripline image.

Each slice produced by PF-ASAR follows the standard stand-alone image product format described previously. After concatenation of slices to form the stripline, the structure of the stripline image is identical to that of the stand-alone image products except the data sets contain data concatenated from several slices in time ordered sequence.

#### Stripline Formation:

Each slice delivered to the PF-HS is in the form of a separate product (i.e., format shown in [figure 2.42 "ASAR image product structure"](#)). Thus the steps performed by the PF-HS to create the stripline product from the individual slices is as follows:

1. Data Sets of the same type for each slice are concatenated in zero Doppler time order sequence.
2. The SPH from the first slice is adopted as the SPH for the stripline. The following positioning information will be updated to reflect the size of the full stripline product:
  - Stripline continuity indicator (set to 000)
  - Slice number (set to +001)
  - Number of slices (set to 001)
  - Last Zero Doppler Azimuth time of product (can be read from SPH of last slice);
  - Geodetic latitude and longitudes for the first, last, and middle samples of the last line of the stripline image (as read from the SPH of the last slice in the stripline).

In addition, the following parameters must be updated for each DSD describing a data set contained in the product:

- Data set offset (gives location of a data set relative to the start of the product);

- Total size of a data set;
- Number of DSRs within a data set.

3. The MPH from the first slice is adopted for the whole strip. Several fields in the MPH will need to be updated. These fields are:

- sensing stop time (can be read from MPH of last slice); {This is the on-board sensing time of the input source packets used to create each slice. On-board sensing time is also used for the sensing stop time field and to calculate the product duration. The goal is to provide input data times so that the data could be reprocessed at a later date if desired.}
- duration of product sensing (sensing stop time - sensing start time of MPH of first slice);
- total size of product.

Child Product Extraction:

Child product extraction is performed as per specified in the section "[Child Products. 2.1.1.](#)"  
Processing Performed

The same processing steps are applied to stripline products as for stand-alone products. In addition a final concatenation step and MPH/SPH update step is performed by the PF-HS. The image formation algorithm used is the [SPECAN 2.6.1.2.4.](#) algorithm, as shown in [table 2.43](#) below:

Table 2.43 Image formation algorithms for stripline products

Product ID	Algorithm Applied
<a href="#">ASA_IMM_1P 2.6.2.1.1.3.1.1.</a>	<a href="#">SPECAN 2.6.1.2.4.</a>
<a href="#">ASA_APM_1P 2.6.2.1.1.3.1.2.</a>	<a href="#">SPECAN 2.6.1.2.4.</a>
<a href="#">ASA_WSM_1P 2.6.2.1.1.3.1.3.</a>	<a href="#">SPECAN 2.6.1.2.4.</a>
<a href="#">ASA_GMI_1P 2.6.2.1.1.3.1.4.</a>	<a href="#">SPECAN 2.6.1.2.4.</a>

### 2.6.2.1.1.3.1 Stripline Product Types

The medium-resolution products are systematically generated in the [PDHS](#) from Level 0 data collected when the instrument is in Wide Swath Mode (WS), alternating polarisation (AP), or Image Mode (IM) narrow swath. The product covers a continuous area along the imaging swath up to a maximum size of 10 minutes per product.

### 2.6.2.1.3.1.1 Image Mode Medium-resolution Image

The format for this product is given in the [Data Formats \(Chapter 6.\)](#) section, and the engineering quantities are given in the section entitled "[Level 1B Engineering Quantities.](#)" [2.6.2.2.1.1.1.](#)

[Figure 2.49](#) is an example of a simulated ASA\_IMM\_1P product as seen with [EnviView. 1.2.1.2.](#)

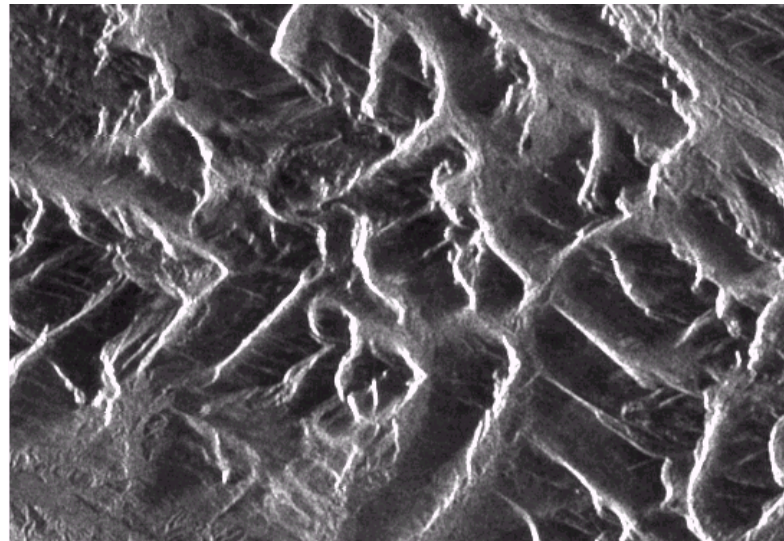


Figure 2.49 ASA\_IMM\_1P sample product (as seen with EnviView)

### 2.6.2.1.3.1.2 Alternating Polarisation Medium-resolution Image

Note: This product may contain only one of the two available polarisations from the original Level 0 data. The format for this product is given in the [Data Formats \(Chapter 6.\)](#) section, and the engineering quantities are given in the section entitled "[Level 1B Engineering Quantities.](#)" [2.6.2.2.1.1.2.](#)

[Figure 2.50](#) is an example of an ASA\_APM\_1P product as seen with [EnviView. 1.2.1.2.](#)

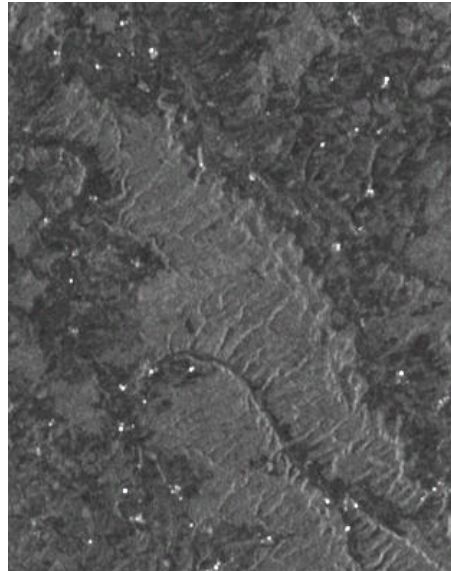


Figure 2.50 ASA\_APM\_1P product sample (as seen in EnviView)

#### 2.6.2.1.1.3.1.3 Wide Swath Medium-resolution Image

The format for this product is given in the [Data Formats \(Chapter 6.\)](#) section, and the engineering quantities are given in the section entitled "[Level 1B Engineering Quantities.](#)" [2.6.2.2.1.1.3.](#)

[Figure 2.51](#) is an example of as ASA\_WSM\_1P product as seen with [EnviView. 1.2.1.2.](#)

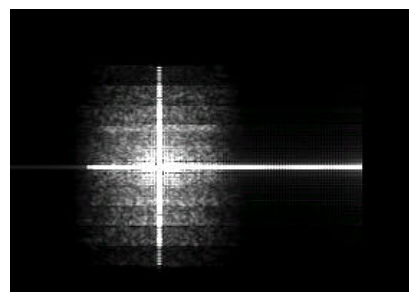


Figure 2.51 ASA\_WSM\_1P sample product (as seen with EnviView)

#### 2.6.2.1.3.1.4 Global Monitoring Mode Image Product

The format for this product is given in the [Data Formats \(Chapter 6.\)](#) section, and the engineering quantities are given in the section entitled "[Level 1B Engineering Quantities.](#)" [2.6.2.2.1.5.1.](#)

[Figure 2.52](#) is an example of an ASA\_GMI\_1P product as seen with [EnviView. 1.2.1.2.](#)

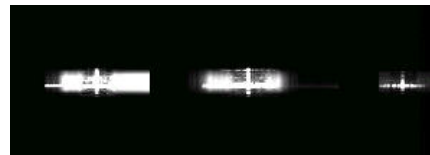


Figure 2.52 ASA\_GMI\_1P sample product (as seen with EnviView)

#### 2.6.2.1.3.2 Input Data

The input for all of the strip-line products is the Level 0 data corresponding to the particular mode and auxiliary data.

( Refer to [table 2.7](#) in the section "Level 0 Products" for a listing of the Level 0 products )

#### 2.6.2.1.3.3 Auxiliary Data Used

The same data used for on-request (stand-alone) products is required for the production of stripline products, as indicated [above 2.42](#). The description of the main auxiliary data records is provided in the "[Auxiliary Data Sets for Level 1B Processing](#)" [2.9.2.](#) section, and the formats are provided in the [Data Formats \(Chapter 6.\)](#) section. The description of the orbit state vectors, including their formats, is provided in the section "[Common Auxiliary Data Sets.](#)" [2.9.3.](#)

#### 2.6.2.1.3.4 Product Structure

The product structure and contents for stripline products is identical to the on-request products. The stripline image product structure is shown in [Figure 2.53](#) below.

For a detailed description of the contents of the data sets refer to the sections for [stand-alone products 2.6.2.1.1.1.1](#), discussed above.

Figure 2.53 Stripline image product structure

MPH	Taken from first slice - some fields updated
SPH ----- DSDs	Identical to slice SPH, some fields updated
SQ ADS for MDS 1	Concatenation of time stamped SQ for MDS 1 ADSs from all slices in strip
SQ ADS for MDS 2*	Concatenation of time stamped SQ for MDS 2 ADSs from all slices in strip
Main Processing Parameters ADS	Concatenation of time stamped Main Proc. Param. ADSs from all slices in strip
Doppler Centroid Coefficients ADS	Concatenation of time stamped Dop. Cent. Coef. ADSs from all slices in strip
Slant Range to Ground Range Conversion ADS	Concatenation of time stamped SR/GR Conversion ADSs from all slices in strip
Chirp Parameters ADS	Concatenation of time stamped Chirp Parameters ADSs from all slices in strip
Antenna Elevation Pattern ADS for MDS 1	Concatenation of time stamped Antenna Elev. Pat. for MDS 1 ADSs from all slices in strip
Antenna Elevation Pattern ADS for MDS 2	Concatenation of time stamped Antenna Elev. Pat. for MDS 2 ADSs from all slices in strip
Geolocation Grid ADS	Concatenation of time stamped Geolocation Grid ADSs from all slices in strip
MDS 1 (image data)	Concatenation of time stamped Image Data MDSs from all slices in strip
MDS 2 (image data for AP only)*	Concatenation of time stamped Image Data MDSs from all slices in strip

\* Not used in the current baseline. DSD is blanked and DS is not included in product.

A by-product of the creation of Strip-line products are the Browse images. A full discussion of these images, identified as: ASA\_IM\_BP, ASA\_AP\_BP, ASA\_WS\_BP and ASA\_GM\_BP, can be found in the section "[Browse Products](#)." [2.6.2.1.3](#). The table which shows the correlation between these two product forms is reproduced here for convenient reference:

Table 2.44 Medium-resolution Level 1B stripline products and corresponding browse images

Level 1B product	Browse product
<a href="#">ASA_IMM_BP 2.6.2.1.1.3.1.1</a>	<a href="#">ASA_IM_BP 2.6.2.1.1.3.1.1</a>
<a href="#">ASA_APM_BP 2.6.2.1.1.3.1.2</a>	<a href="#">ASA_AP_BP 2.6.2.1.1.3.1.2</a>

<a href="#">ASA_WSM_IP 2.6.2.1.1.3.1.3.</a>	<a href="#">ASA_WS_BP 2.6.2.1.3.1.3.</a>
<a href="#">ASA_GM1_IP 2.6.2.1.1.3.1.4.</a>	<a href="#">ASA_GM_BP 2.6.2.1.3.1.4.</a>

## 2.6.2.1.2 Level 1B Wave Products

The general product structure, used in all ENVISAT products, is given in "[Definitions and Conventions](#)." [2.3.2.1](#). For the engineering quantities associated with these products, refer to "[Level 1B Engineering Quantities](#)" [2.6.2.2](#).

**Wave Mode** (WV) products are not [detected](#), but [Single Look Complex](#) (SLC). They allow for further Cross Spectra processing, following the algorithm developed by NORUT (Norway,) and provide complete [speckle](#) compensation and potential capability to resolve the propagation ambiguity observed on the corresponding [ERS](#) products. For a discussion of the processing steps carried out in the generation of the Level 1B products refer to the section entitled "[ASAR Level 1B Algorithm Descriptions](#)." [2.6.1.2](#).

Wave Mode (WV) products are those products produced from data acquired while the ASAR instrument is operating in Wave Mode. During Wave Mode operation, the ASAR instrument acquires small measurements called wave cells which are approximately 5 km along-track by (up to) 10 km in across-track. The wave cells are acquired at 100 km intervals. The cells may have alternating positions in the same swath or be in alternating swaths. In theory, up to 400 of these wave cells may be acquired per orbit, but in practice it is anticipated that the average number of acquisitions per orbit will be substantially lower. Each wave cell is processed into a small SLC image called an imagette and each imagette is further processed using the cross-spectra methodology to produce the cross-spectra of the imagette. In addition, each imagette can be processed to generate the Level 2 ocean wave spectra product.

### 2.6.2.1.2.1 Product Types

The two Level 1B Wave Mode products are shown below:

Table 2.45 Level 1B Wave Mode products

WV	<a href="#">ASA_WVI_IP 2.6.2.1.2.1.1.</a>	ASAR Wave Mode SLC imagette and Imagette Cross-Spectra
WV	<a href="#">ASA_WVS_IP 2.6.2.1.2.1.2.</a>	ASAR Wave Mode Imagette Cross-Spectra (Level 1)

#### 2.6.2.1.2.1.1 Wave Mode SLC Imagette and Imagette Cross-Spectra

---

The format for this product is given in the [Data Formats \(Chapter 6.\)](#) section, and the engineering quantities are given in the section entitled "[Level 1B Engineering Quantities](#)." [2.6.2.2.2.1.1.](#)

[Figure 2.54](#) below is an example of an ASA\_WVI\_1P product as seen using [EnviView: 1.2.1.2.](#)

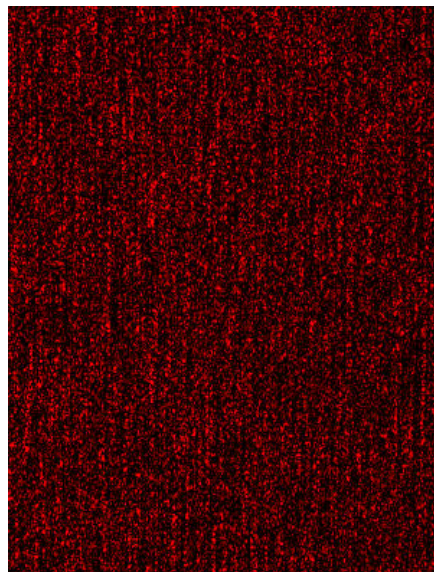


Figure 2.54 ASA\_WVI\_1P sample product (as seen with EnviView)

### 2.6.2.1.2.1.2 Wave Mode Imagette Cross-Spectra

The format for this product is given in the [Data Formats \(Chapter 6.\)](#) section, and the engineering quantities are given in the section entitled "[Level 1B Engineering Quantities](#)" [2.6.2.2.2.1.1.](#)

[Figure 2.55](#) below is an example of an ASA\_WVS\_1P product spectral view ( [see the spectral view section in "EnviView"](#) )

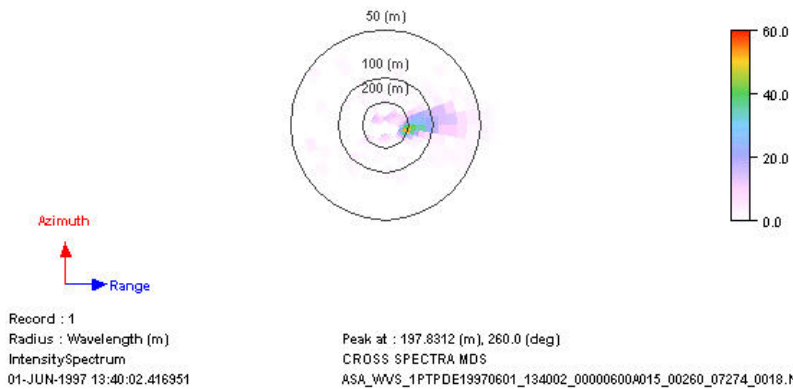


Figure 2.55 ASA\_WVS\_1P spectral view ( as seen with EnviView )

### 2.6.2.1.2.2 Input Data

For the SLC Image and Cross Spectra product, the input data is the Level 0 Wave Mode product ( [ASA\\_WV\\_0P 2.5.1.2.3.2.](#) ) plus auxiliary data. (See [table 2.7](#) in the section entitled "ASAR Level 0 Products" for a listing of all of the Level 0 products.)

The Cross Spectra product is simply an extraction of the Cross Spectra MDS and all ADSs from the SLC Image and Cross Spectra Product.

### 2.6.2.1.2.3 Auxiliary Data Used

The auxiliary data used to create the Wave Mode products is the same as that used to create the on-request SLC Image Mode product (see "[Strip-line Auxiliary Data Used](#)" in "[Level 1b Image Products](#)" [2.6.2.1.1.3.3.](#) ). Auxiliary data formats are described in the section "[Auxiliary Data Sets for Level 1B Processing](#)" [2.9.2.](#) .

### 2.6.2.1.2.4 Processing Performed

The processing steps applied to create the SLC imagette are the same as those used to create the on-request SLC Image Mode product (see the section entitled "[ASAR Strip Line Product](#)

[Processing](#)" [2.6.1.2.5.](#) ). The processing steps required to create the Cross Spectra products are discussed in the section entitled "["ASAR Level 1B Algorithm Descriptions"](#)

#### 2.6.2.1.2.4.1 Wave Mode Error Handling

If PF-ASAR is unable to produce an imagette or cross spectra, the following method is used to indicate the error and the location of the error within the product:

- CASE 1: PF-ASAR is able to produce the imagette but not the cross / wavespectra:
  - The MDSR containing the cross/wave spectra is given the correct time stamp (corresponding to the first line of the imagette), the Quality Flag is set to -1, and all entries pertaining to the cross spectra are set to zero.
  - Fields in all ADSRs pertaining to the cross / wave spectra are set to zero.
  - The Attachment Flags of the SQ ADSR and the Geolocation ADSR corresponding to the wave cell are set to 1.
  - The SPECTRA\_FAILED counter in the SPH is incremented.
- CASE 2: PF-ASAR is unable to produce neither the imagette nor the cross /wave spectra:
  - The MDS which was supposed to hold the imagette is still created. It contains only 1 MDSR which consists only of the time stamp corresponding to the estimated location of where the imagette would have been located, a range line number of 1, and the Quality flag set to -1. If it is not possible to determine the approximate time stamp for the MDSR, the time stamp may be set to zeros.
  - The MDSR which was to have held the cross / wave spectra is still produced, but it is zero filled and the Quality Flag set to -1 (as in CASE 1). The time stamp is identical to that used in the single MDSR of the imagette MDS.
  - Information in all ADSRs is set to zeros, and the Attachment flag of each ADSR is set to 1. The time stamp for each ADSR is identical to that of the single MDSR of the imagette MDS.
  - The SPECTRA\_FAILED and IMAGETTES\_FAILED counters in the SPH are incremented.

The rationale for the error handling described above is that:

1. PF-ASAR should not fail completely just because one imagette or cross /wave spectra in a series could not be produced;
2. for extraction purposes, the number of MDSs containing imagettes and the number of DSRs in the other data sets must be the same;
3. by setting the MDSRs and ADSRs (if appropriate) to zero, a placeholder is inserted in the product which allows one to identify unambiguously which wave cell failed, in both the WV product and in further extracted products.

#### 2.6.2.1.2.5 Product Structure

The standard Wave Mode product structure is shown in [Figure 2.56](#) below:

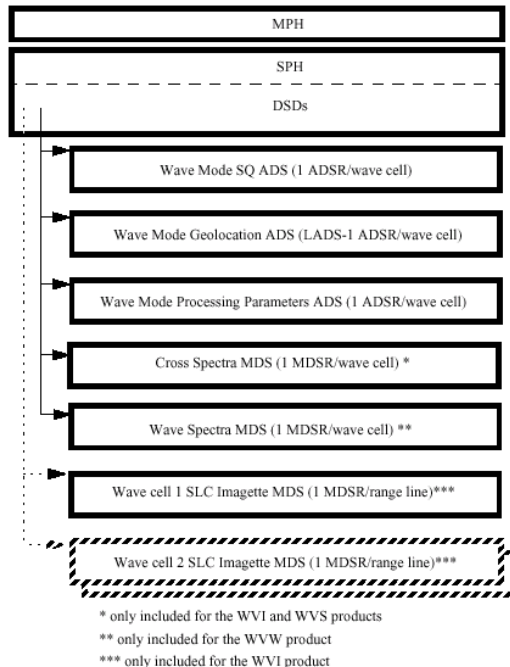


Figure 2.56 Wave Mode Products Structure

#### **2.6.2.1.2.5.1 Main Product Header**

The MPH will be the same as for all ENVISAT products, as discussed in "[Definitions and Conventions](#)" [2.3.2.2.](#).

#### **2.6.2.1.2.5.2 Specific Product Header**

As explained in ["Definitions and Conventions" 2.3.2.3.](#), the SPH is defined for each product and provides additional information, applicable to the whole product, related to the processing. A description of the Level 1B Wave products' SPH, which includes the formulae used to reconstruct the wavelengths as well as the table of related Data Set Descriptors (DSDs), refer to the [ASAR Wave Base SPH in the Data Formats 6.6.22.](#) section.

### 2.6.2.1.2.5.3 Data Set Names

The Data Set Names, shown in [Table 2.46](#) below, may appear in the ASAR Wave Product SPH [Data Set Descriptors \(DSDs\) 2.3.2.4.](#) :

Table 2.46 ASAR Wave Products Data Set Descriptor Names

Data Set Type	Data Set Name
DSD referencing the Level 0 product from which this product was created	"LEVEL 0 PRODUCT"
DSD referencing PF-ASAR Processor Configuration file	"ASAR PROCESSOR CONFIG"
DSD referencing Instrument Characterisation file used	"INSTRUMENT CHARACTERISATION"
DSD referencing External Characterisation file used	"EXTERNAL CHARACTERISATION"
DSD referencing External Calibration file used	"EXTERNAL CALIBRATION"
DSD referencing the Orbit State Vectors file used	"ORBIT STATE VECTOR 1"
DSD referencing the ECWMF file used	"ECWMF"
Wave Mode SQ ADS	"SQ ADS"
Wave Mode Geolocation ADS (LADS)	"GEOLOCATION ADS"
Wave Mode Processing parameters ADS	"PROCESSING PARAMS ADS"
Cross Spectra MDS	"CROSS SPECTRA MDS"
Ocean Wave Spectra MDS	"OCEAN WAVE SPECTRA MDS"
Wave Cell SLC Imagette MDS	"SLC IMAGETTE MDS XXX" where XXX is a counter value from 000 to 999 indicating the cell number corresponding to the given imagette

For the table of DSDs, refer to [ASAR\\_Wave\\_Base\\_SPH in the Data Formats 6.6.22.](#) section.

### 2.6.2.1.2.5.4 Data Sets

The [data sets 2.3.2.5.](#) which make up the ASAR Wave product structure are shown below.

- Cross-Spectrum [MDS](#)
- Wave Mode Processing parameters [ADS](#)
- Wave Mode Geolocation Grid ADS (or [LADS](#))
- Wave Mode Summary Quality Annotation Data Set Records ([SQ ADSRs](#)) - There is one Wave Mode SQ ADSR per wave cell. The ADSR contains information pertaining to both the imagette and the spectrum. This table, known as the ASAR\_Wave\_SQ\_ADSR, consists of the ASAR image SQ information, defined in the table ASAR\_SQ1\_Image\_ADSR, plus new information pertaining to the cross spectra.

The formats for all of these Data Sets can be found in the [Data Formats \(Chapter 6.\)](#) section.

### 2.6.2.1.2.5.4.1 MDS Containing Imagettes

The structure of the Measurement Data Set (MDS) for the [SLC Imagette and Imagette Cross Spectra \(ASA\\_WVI\\_1P\) 2.6.2.1.2.1.1.](#) product, which contains an imagette, will be identical to that specified in the "[Level 1b Image Products" Section 2.6.2.1.1.](#)" Note that there is one MDS per imagette and up to 400 MDSs per product. The MDSs are not included for the [Imagette Cross Spectra \(ASA\\_WVS\\_1P\) 2.6.2.1.2.1.2.](#) product.

If PF-ASAR is unable to produce an imagette, the MDS will consist of only one MDSR with the time stamp corresponding to what the first line of the imagette would have been, a range line number of 1, and the quality flag set to -1.

### 2.6.2.1.3 Browse Products

The general product structure, used in all ENVISAT products, is given in "[Definitions and Conventions." 2.3.2.1.](#)

Browse products are a special form of Stripline product, produced from Level 0 products. As first discussed in the section entitled "[Organisation of Products,"](#) they are decimated images which can be ordered from the ENVISAT inventory.

They are systematically generated at the same time as the corresponding medium-resolution Level 1B, as by-products of this process. For a discussion of the Level 1B Stripline products, refer to "[Level 1B Image Products." 2.6.2.1.1.3.](#)" The Level 1B and browse pairs that are produced together are shown in [table 2.47](#) below:

Table 2.47 Browse products and corresponding Level 1 products

Level 1B product	Browse product
<a href="#">ASA_IMM_1P 2.6.2.1.1.3.1.1.</a>	<a href="#">ASA_IM_BP 2.6.2.1.3.1.1.</a>
<a href="#">ASA_APM_1P 2.6.2.1.1.3.1.2.</a>	<a href="#">ASA_AP_BP 2.6.2.1.3.1.2.</a>
<a href="#">ASA_WSM_1P 2.6.2.1.1.3.1.3.</a>	<a href="#">ASA_WS_BP 2.6.2.1.3.1.3.</a>
<a href="#">ASA_GMI_1P 2.6.2.1.1.3.1.4.</a>	<a href="#">ASA_GM_BP 2.6.2.1.3.1.4.</a>

Browse products are also created as individual slices and then concatenated together by the PF-HS. However, browse products are intended only as a user aid when ordering data. Thus, many of the Annotation Data Sets (ADS) pertaining to detailed processing records may be discarded by the PF-HS for the browse product. There is no additional auxiliary data required.

The 4 browse products listed in [Table 2.47](#) above, are described under the following sections

### 2.6.2.1.3.1 Product Types

#### 2.6.2.1.3.1.1 Image Mode Browse Image

This low-resolution product will be produced systematically together with the Image Mode medium-resolution Product (ASA\_IMM\_1P).

These products will be amenable to dissemination by electronic links in near real-time (NRT). Possible use of data compression algorithms will be considered. The product covers a continuous area along the imaging swath and is derived by block averaging the medium-resolution product.

Table 2.48 Image Mode browse image (ASA\_IM\_BP)

PRODUCT ID	ASA_IM_BP
NAME	ASAR Image Mode browse
DESCRIPTION	ASAR product generated when the instrument is in Image Mode. The product is for browse purpose only. The product is generated from ASA_IMM_1P product.
COVERAGE	Product stripe up to 4000 km 56 -100 km in across-track direction
RADIOMETRIC RESOLUTION	Product ENL ~ 80
PIXEL SPACING	225 m * 225 m (multiple of ASA_IMM pixel spacing)
SIZE	Stripline max 3 Mbytes

The format for this product is given in the [Data Formats \(Chapter 6.\)](#) section.

Below in [Figure 2.57](#) is an example of an ASA\_IM\_BP browse image as seen with [EnviView](#).

#### [1.2.1.2.](#)

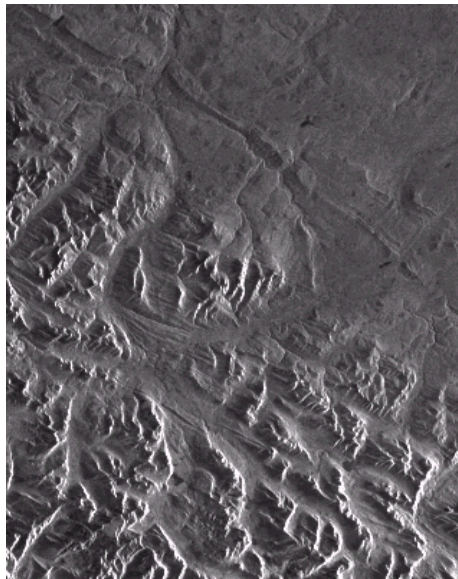


Figure 2.57 ASA\_IM\_BP sample product (as seen with EnviView)

### 2.6.2.1.3.1.2 Alternating Polarisation Browse Image

This low-resolution compressed image product will be produced systematically together with the AP medium-resolution Product. This product will be provided via electronic link in near real-time. The product will contain only one of the polarisation options rather than two. The polarisation used will be that of the MDS1 of the APM product. This means the polarisation may vary depending upon which polarisation option is chosen for MDS1 for the medium-resolution AP product.

Possible use of data compression algorithms will be considered. The product covers a continuous area along the imaging swath and is generated by subsampling from the medium-resolution product.

Note: This product may contain only one of the two available polarisations from the original Level 0 data.

Table 2.49 Alternating Polarisation Browse Image (ASA\_AP\_BP)

PRODUCT ID	ASA_AP_BP
NAME	ASAR alternating polarisation browse

PRODUCT ID	ASA_AP_BP
DESCRIPTION	ASAR product generated when the instrument is in Alternating Polarisation Mode. The product is for browse purposes only. The product is generated from ASA_APM_IP product. It contains one of the two possible polarisation combinations generated in AP mode.
COVERAGE	Product stripe up to 4000 km 56 -100 km in across-track direction
RADIOMETRIC RESOLUTION	Product ENL ~ 75
PIXEL SPACING	225 m * 225 m (multiple of ASA_APM pixel spacing)
SIZE	Stripline max 3 Mbytes

The format for this product is given in the [Data Formats \(Chapter 6.\)](#) section.

Below in [Figure 2.58](#) is an example of an ASA\_AP\_BP browse image as seen with [EnviView. 1.2.1.2.](#)



Figure 2.58 ASA\_AP\_BP sample product (as seen with EnviView)

### 2.6.2.1.3.1.3 Wide Swath Browse Image

This low-resolution product will be produced systematically together with the WS medium-resolution Product.

These products will be amenable to dissemination by electronic links in near real-time. Possible use of data compression algorithm will be considered. The product covers a continuous area along the imaging swath. The product is generated by subsampling from the medium-resolution product.

Table 2.50 Wide Swath browse image (ASA\_WS\_BP)

PRODUCT ID	ASA_WS_BP
NAME	ASAR wide swath browse
DESCRIPTION	ASAR product generated when the instrument is in Wide Swath Mode. The product is for browse purpose only.
COVERAGE	Product stripe up to 4000 km 405 km in across-track direction
RADIOMETRIC RESOLUTION	Product ENL ~ 30 to 48 (TBC)
PIXEL SPACING	900 m * 900 m for WS
SIZE	Stripline max 3 Mbytes

The format for this product is given in the [Data Formats \(Chapter 6.\)](#) section.

#### 2.6.2.1.3.1.4 Global Monitoring Mode Browse Image

This low-resolution product will be produced systematically together with the GM Image Product from Level 0 GM data. The image is intended for browse purposes only (pixel spacing is approximately 1000 m).

These products will be amenable to dissemination by electronic links in near real-time. Possible use of data compression algorithms will be considered. The product covers a continuous area along the imaging swath.

Table 2.51 Global Monitoring Mode browse image (ASA\_GM\_BP)

PRODUCT ID	ASA_GM_BP
NAME	ASAR Global monitoring mode browse
DESCRIPTION	ASAR product generated from the ASA_GM1_1P when the instrument is in Global Monitoring mode. The product is for browse purposes only.
COVERAGE	405 km in across-track direction product stripe up to 40000 km for GM
PIXEL SPACING	1000 m * 1000 m for GM
RADIOMETRIC RESOLUTION	Product ENL ~ 11 -15
SIZE	Stripline max 18 Mbytes

The format for this product is given in the [Data Formats \(Chapter 6.\)](#) section.

#### 2.6.2.1.3.2 Processing Performed

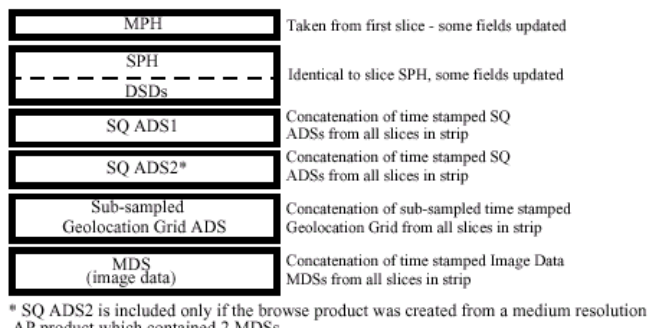
The following processing steps are applied after the medium-resolution slice has been created:

- block averaging of medium-resolution slice (by PF-ASAR)
- concatenation of browse slices by PF-HS

### 2.6.2.1.3.3 Product Structure

The structure of the browse product is the same as for the regular Stripline products except that some data sets have been removed. The structure of the product is shown in [figure 2.59](#) below. For a detailed description of the contents of the data sets, refer to the sections for on-request products in "[Stand-Alone Products](#)" in "[Level 1B High Organisation of Products 2.6.2.1.1.1.](#)"

Figure 2.59 Browse Image Product structure



#### 2.6.2.1.3.3.1 Browse SQ ADS

The SQ ADS for the browse product is simply the SQ for the medium-resolution image from which the browse was created. No fields are updated or changed during the formation of the browse product.

If the browse product is created from an Alternation Polarisation (AP) medium-resolution product containing 2 Measurement Data Sets (MDSs), which means using both polarisations (H and V), then both SQ ADSs are left in the browse product to provide a complete quality record.

#### 2.6.2.1.3.3.2 Subsampled Geolocation Grid ADS

During the formation of the browse product, the Geolocation Grid from the corresponding medium-resolution Image is reduced approximately by a factor of 10 (i.e., approximately every 10th grid entry is left in the ADS, the rest are discarded.) However, the last granule must remain to document the last line of the product.

## 2.6.2.2 Level 1B Engineering Quantities

### 2.6.2.2.1 Image Products

#### 2.6.2.2.1.1 Medium Resolution Products

##### 2.6.2.2.1.1.1 Image Mode Medium-resolution Image (ASA\_IMM\_1P)

This Strip-line ASAR product is systematically generated in the PDHS. This product, processed to approximately 150-m resolution, features an [ENL](#) (radiometric resolution) good enough for ice applications.

Table 2.52 Image Mode Medium-resolution Image (ASA\_IMM\_1P) product

PRODUCT ID	ASA_IMM_1P
NAME	ASAR Image Mode medium-resolution image
DESCRIPTION	ASAR product generated from Level 0 data collected when the instrument is in Image Mode. This product has lower resolution but higher radiometric resolution than the ASA_IMP. The product covers a continuous area along the imaging swath.
COVERAGE	100 km in along-track direction for a scene up to 4000 km for a stripe, 56 - 100 km in across-track direction
GEOMETRIC RESOLUTION	Approximately 150 m * 150 m
RADIOMETRIC RESOLUTION	Product ENL ~ 40
PIXEL SPACING	75 m * 75m
SIZE	4 Mbytes of data for a scene 152 Mbytes for a stripe

##### 2.6.2.2.1.1.2 Alternating Polarisation Medium-resolution Image (ASA\_APM\_1P)

This stripline product is processed to approximately 150 m resolution using the [SPECAN 2.6.1.2.4.](#) algorithm and contains radiometric resolution good enough for ice applications and covers a continuous area along the imaging swath. This product may also be generated on request with one, or both, polarisations included in the product.

Table 2.53 Alternating Polarisation Medium-resolution Image (ASA\_APM\_1P) product

PRODUCT ID	ASA_APM_1P
NAME	ASAR Alternating polarisation medium-resolution image
DESCRIPTION	ASAR product generated from Level 0 data collected when the instrument is in Alternating Polarisation Mode. The product has lower geometric resolution but higher radiometric resolution than ASA_APP. The product contains one or two co-registered images corresponding to one of the three polarisation combination submodes (HH and VV, HH and HV, VV and VH)
COVERAGE	100 km in along-track direction for a scene/up to 4000 km for a stripe, 56 -100 km in across-track direction
GEOMETRIC RESOLUTION	Approximately 150 m * 150 m
RADIOMETRIC RESOLUTION	Product ENL ~ 50
PIXEL SPACING	75m * 75m
SIZE	4 Mbytes for a scene with one polarisation combination

### 2.6.2.2.1.1.3 Wide Swath Medium-resolution Image (ASA\_WSM\_1P)

This is the standard product for ASAR Wide Swath Mode and it is systematically generated in the PDHS using the ScanSAR technique and processed to 150-m resolution. The swath width is approximately 400 km.

Table 2.54 Wide Swath Medium-resolution Image (ASA\_WSM\_1P) product

PRODUCT ID	ASA_WSM_1P
NAME	ASAR wide swath standard image
DESCRIPTION	ASAR product generated from Level 0 data collected when the instrument is in Wide Swath Mode. The product includes slant range to ground range corrections and it covers a continuous area along the imaging swath.
COVERAGE	400 km * 400 km(approximately) for a scene 400 km * 4000 km max for a stripe
GEOMETRIC RESOLUTION	Approximately 150 m * 150 m
RADIOMETRIC RESOLUTION	Product ENL > 11.5
PIXEL SPACING	75 m * 75 m
SIZE	59 Mbytes for a scene 584 Mbytes for a stripe

### 2.6.2.2.1.2 Single-Look Complex (SLC) Products

#### 2.6.2.2.1.2.1 Image Mode Single-Look Complex (ASA\_IMS\_1P)

The Image Mode Single-Look Complex (ASA\_IMS\_1P) products are stand alone, phase-preserved images. They are generated using up-to-date auxiliary parameters (at time of processing), using the [Range-Doppler 2.6.1.2.3.](#) algorithm

Intended use: SAR image quality assessment, calibration and interferometric applications. A minimum number of corrections and interpolations are performed on the data, so as to allow the end-user maximum freedom to derive higher level products. Complex output data is retained to avoid loss of information. Absolute calibration parameters, when available (depending on external calibration activities) shall be provided in the product annotations.

Table 2.55 Image Mode Single-Look Complex (ASA\_IMS\_1P)

PRODUCT ID	ASA_IMS_1P
NAME	ASAR image single-look complex
DESCRIPTION	This is a single-look, complex, slant-range, digital image generated from Level 0 ASAR data collected when the instrument is in Image Mode (7 possible swaths HH or VV polarisation). It is primarily intended for use in SAR quality assessment and calibration, and can be used to derive higher level products.
COVERAGE	100 km along-track * 56-100 km across-track
GEOMETRIC RESOLUTION	Approximately 6 azimuth, programmed chirp bandwidth dependent slant range.
RADIOMETRIC RESOLUTION	1 look in azimuth, 1 look in range
PIXEL SPACING	Natural spacing in both Slant range and Azimuth. Azimuth pixel spacing depends on Earth-Satellite relative velocity and actual PRF.2. Slant range pixel spacing is given by ASAR sampling frequency (19.208 MHz)
SIZE	741 Mbytes

#### 2.6.2.2.1.2.2 Alternating Polarisation Mode Single-Look Complex (ASA\_APS\_1P)

This stand-alone narrow swath product uses the [Range Doppler 2.6.1.2.3.](#) algorithm and the most up to date processing parameters available at the time of processing. The product can be used to derive higher level product.

Intended use: SAR image quality assessment, calibration, and interferometric applications, if allowed by the instrument acquisition. A minimum number of corrections and interpolations

are performed on the data in order to allow the end-user maximum freedom to derive higher level products. Complex output data is retained to avoid loss of information. Absolute calibration parameters, when available (depending on [external calibration](#) activities) shall be provided in the product annotations.

Table 2.56 Alternating Polarisation Mode Single-Look Complex (ASA\_APS\_1P) product

PRODUCT ID	ASA_APS_1P
NAME	ASAR Alternating Polarisation mode complex image
DESCRIPTION	This is a complex, slant-range, digital image generated from Level 0 ASAR data collected when the instrument is in Alternating Polarisation mode. (7 possible swaths). The product contains two CO-registered images corresponding to one of the three polarisation combination submodes (HH and VV, HH and HV, VV and VH)
COVERAGE	100 km along-track, 56 - 100 km across-track
GEOMETRIC RESOLUTION	Approximately TBD azimuth, TBD slant range.
RADIOMETRIC RESOLUTION	1 look in azimuth, 1 look in range
PIXEL SPACING	Natural spacing in both Slant range and Azimuth
SIZE	Max. 1480 Mbytes. Product size will vary function of imaging swath, satellite velocity and actual PRF

### 2.6.2.2.1.3 Precision Image Products

#### 2.6.2.2.1.3.1 Image Mode Precision Image (ASA\_IMP\_1P)

This stand-alone image is generated using the [Range/Doppler 2.6.1.2.3.](#) algorithm. The processing uses up to date (at time of processing) auxiliary parameters and corrects for [antenna elevation gain](#), and range spreading loss.

Engineering corrections and relative [calibration](#) are applied to compensate for well-understood sources of system variability. Absolute calibration parameters, when available (depending on [external calibration](#) activities) shall be provided in the product annotations.

Max size: 134 Mbytes per scene

Coverage: 100 km \* 100 km (max)

Table 2.57 Image Mode Precision Image ASA\_IMG\_1P product

PRODUCT ID	ASA_IMP_1P
NAME	ASAR Image Mode Precision Image
DESCRIPTION	This is a multi-look, ground range, digital image. Generated from Level 0 data collected when the instrument is in Image Mode (7 possible swaths HH or VV polarisation). The product includes slant range to ground range correction as per definition. It is for users wishing to perform applications-oriented analysis. It is intended for multi-temporal imaging and to derive backscattering coefficients. Corrections include: antenna elevation pattern, range spreading loss
COVERAGE	100 km along-track * 56 - 100 km across-track
GEOMETRIC RESOLUTION	Approximately 30 m ground range (except IS1) X 30m azimuth
RADIOMETRIC RESOLUTION	Product ENL > 3
PIXEL SPACING	12.5 m * 12.5 m
SIZE	Up to 134 Mbytes. Product size in the range direction will vary function of imaging swath.

### 2.6.2.2.1.3.2 Alternating Polarisation Mode Precision Image (ASA\_APP\_1P)

This is a stand-alone multi-look, ground range, narrow swath digital image generated using the [SPECAN 2.6.1.2.4](#) algorithm and the most up to date auxiliary information available at the time of processing. Engineering corrections and relative [calibration](#) (antenna elevation gain, range spreading loss) are applied to compensate for well-understood sources of system variability. Generation of this product uses a technique to allow half the looks of an image to be acquired in horizontal [polarisation](#) and the other half in vertical polarisation and processed to 30-m resolution (with the exception of IS1). Absolute calibration parameters, when available (depending on [external calibration](#) activities), shall be provided in the product annotations.

Table 2.58 Alternating Polarisation Mode Precision Image (ASA\_APP\_1P) product

PRODUCT ID	ASA_APP_1P
NAME	ASAR alternating polarisation precision image
DESCRIPTION	ASAR product generated from Level 0 data collected when the instrument is in Alternating Polarisation Mode (7 possible swaths). The product contains two CO-registered images corresponding to one of the three polarisation combination submodes (HH and VV, HH and HV, VV and VH).
COVERAGE	100 km along-track, 56 - 100 km across-track
GEOMETRIC RESOLUTION	Approximately 30 m ground range (except IS1) * 30m azimuth
RADIOMETRIC RESOLUTION	Product ENL > 1.8
PIXEL SPACING	12.5 m * 12.5 m
SIZE	Up to 268 Mbytes. Product size in the range direction will vary function of imaging swath (56 to 100 km).

### 2.6.2.2.1.4 Ellipsoid Geocoded Products

## 2.6.2.2.1.4.1 Image Mode Ellipsoid Geocoded Image (ASA\_IMG\_1P)

This stand-alone Image Mode [Geocoded](#) SAR image is generated in either HH or VV polarisation, using the [Range/Doppler 2.6.1.2.3.](#) algorithm with the best available instrument corrections. The product is intended for mapping applications and other uses requiring map projection images. Absolute [calibration](#) parameters, when available, shall be provided in the product annotation. All processing information in the geocoded product corresponds to the intermediate product created during processing. Only the Geolocation Grid ADS and Map Projection ADS are updated to reflect the map projection information.

The six available map projections are:

- Universal Transverse Mercator
- Universal Polar Stereographic
- Lambert Conformal Conic
- Transverse Mercator
- Mercator
- Polar Stereographic

Engineering corrections and relative calibration are applied to compensate for well-understood sources of system variability. Absolute calibration parameters, when available (depending on [external calibration](#) activities) shall be provided in the product annotations.

Table 2.59 Image Mode Ellipsoid Geocoded Image (ASA\_IMG\_1P) product

PRODUCT ID	ASA_IMG_1P
NAME	ASAR Image Mode ellipsoid geocoded image
DESCRIPTION	ASAR product generated from Level 0 data collected when the instrument is in Image Mode. It is the geocoded version of the PRI product. The product is resampled to a map projection and its orientation is north up. The absolute calibration of the GEC product shall be the same as for the corresponding non-geocoded PRI product.
COVERAGE	100 km * 100 km (corresponding to the input data)
RADIOMETRIC RESOLUTION	Product ENL > 3
GEOMETRIC RESOLUTION	Approximately 30 m ground range (except IS1) * 30m azimuth
PIXEL SPACING	12.5 m * 12.5 m (grid easting and northing)
SIZE	Up to 282 Mbytes. Product size will vary function of imaging swath position.

## 2.6.2.2.1.4.2 Alternating Polarisation Ellipsoid Geocoded Image (ASA\_APG\_1P)

This is a multi-look image generated upon request using the [SPECAN 2.6.1.2.4.](#) algorithm and the most up to date auxiliary information available at the time of processing. Engineering corrections and relative [calibration](#) (antenna elevation gain, range spreading loss) are applied. The product contains two CO-registered images corresponding to one of the three possible [polarisation](#) combinations (HH and VV, HH and HV, VV and VH). Absolute calibration parameters (when available) shall be provided in the product annotation. All processing information in the geocoded product corresponds to the intermediate product created during processing. Only the Geolocation Grid ADS and Map Projection ADS are updated to reflect the map projection information.

Table 2.60 Alternating Polarisation Ellipsoid Geocoded Image (ASA\_APG\_1P) product

PRODUCT ID	ASA_APG_1P
NAME	ASAR Alternating Polarisation mode ellipsoid geocoded image
DESCRIPTION	ASAR product generated from Level 0 data collected when the instrument is in Alternating Polarisation Mode. It is the geocoded version of the PRI product ASA_APP_1P. The product is resampled to a map projection and its orientation is north up.
COVERAGE	100 km * 100 km
GEOMETRIC RESOLUTION	Approximately 30 m ground range (except IS1) * 30m azimuth
RADIOMETRIC RESOLUTION	Product ENL > 1.8
PIXEL SPACING	12.5 m * 12.5 m (grid easting and northing)
SIZE	Up to 563 Mbytes. Product size will vary function of imaging swath position.

## 2.6.2.2.1.5 Global Monitoring Products

### 2.6.2.2.1.5.1 Global Monitoring Mode Image Product (ASA\_GM1\_1P)

This strip-line product is the standard for ASAR Global Monitoring Mode. It is processed to approximately 1 km resolution using the [SPECAN 2.6.1.2.4.](#) algorithm. The swath width is approximately 400 km.

Table 2.61 Global Monitoring Mode Image Product (ASA\_GM1\_1P) product

PRODUCT ID	ASA_GM1_1P
NAME	ASAR Global Monitoring Mode Image
DESCRIPTION	ASAR product generated from Level 0 data collected when the instrument is in Global Monitoring Mode. One product covers a full orbit. The product

PRODUCT ID	ASA_GM1_1P
	includes slant range to ground range correction.
COVERAGE	Up to 40000 km(1 orbit) X 400 km(approximately)
GEOMETRIC RESOLUTION	1 km * 1 km
RADIOMETRIC RESOLUTION	Product ENL ~ 7-9
PIXEL SPACING	500m * 500m
SIZE	Up to 146 Mbytes/orbit extracted scene 2 Mbytes

## 2.6.2.2.2 Wave Products

### 2.6.2.2.2.1 Imagette Cross-Spectra Products

#### 2.6.2.2.2.1.1 Wave Mode SLC Imagette and Imagette Cross-Spectra (ASA\_WVI\_1P)

This is the basic Level 1B Wave Mode product. The product includes up to 400 single-look, complex, slant range, imagettes generated from Level 0 data and up to 400 imagette power spectra computed using the cross-spectra methodology. The auxiliary parameters used are the most up-to-date at the time of processing. A minimum number of corrections and interpolations are performed in order to allow the end-user maximum freedom to derive higher level products. Complex output data is retained to avoid loss of information. Absolute calibration parameters, when available (depending on external calibration activities), shall be provided in the product annotations.

Imagette power spectrum is equivalent to the ERS UWA product with revisited algorithm (cross-spectra) taking into account the higher quality of the SLC imagette.

Note: Starting from an SLC imagette, generation of an ERs UWA-type product might be ensured by a simple look detection and summation.

Table 2.62 Wave Mode SLC Imagette and Imagette Cross-Spectra product (ASA\_WVI\_1P)

PRODUCT ID	ASA_WVI_1P
NAME	ASAR Wave Mode SLC imagette and Imagette Cross-Spectra
DESCRIPTION	The information is retained in complex form to allow derivation of Cross-spectra. Product containing up to 400 imagettes and associated imagettes cross-spectra.
COVERAGE	One product per 400 imagettes with imagette of 5 km x 5 km (min.) every 100 km
GEOMETRIC RESOLUTION	Natural spacing slant range and azimuth azimuth wavelength range from 20 to 1000m in 24 logarithmic steps direction 0-360 degrees in 10 degree steps (only half real part and imaginary part of spectra in product)
RADIOMETRIC RESOLUTION	1 look in azimuth, 1 look in range for the SLC imagette

## PRODUCT ID

ASA\_WVI\_1P

## PIXEL SPACING

Natural pixel spacing in range and azimuth. Azimuth pixel spacing depends on Earth-Satellite relative velocity and actual PRF. Slant range pixel spacing is given by ASAR sampling frequency (19.208 MHz).

## SIZE

Typically 120 Mbytes (20 imagettes and spectra) up to 2394MB (400 imagettes)

## 2.6.2.2.2.2 Single-Look Complex (SLC) Imagette Products

### 2.6.2.2.2.1 Wave Mode Imagette Cross-Spectra (ASA\_WVS\_1P)

This image power spectrum product contains up to 400 cross-spectra extracted from the SLC Imagette and Imagette Cross-Spectra product, shown above. It contains only the cross-spectra derived using cross-spectra methodology.

Table 2.63 Wave Mode Imagette Cross-Spectra product (ASA\_WVS\_1P)

PRODUCT ID	ASA_WVS_1P
NAME	ASAR Wave Mode Imagette Cross Spectra
DESCRIPTION	ASAR Cross-Spectra extracted from the combined SLC and Cross-Spectra product ASA_WVI_1P generated from data collected when the instrument is in Wave Mode. The Product is for Meteo users.
COVERAGE	Up to 20 spectra acquired every 100 km, product coverage 5 km x 5 km minimum
GEOMETRIC RESOLUTION	Wavelength range from 20 to 1000 m in 24 logarithmic steps direction 0-360 degrees in 10 degree steps (only half real part and imaginary part of spectra in product)
PIXEL SPACING	N/A
SIZE	Maximum 2 Mbytes for 400 spectra including auxiliary data.

## 2.6.2.3 Level 1B Essential Product Confidence Data

Product Confidence Data (PCD) data is designed to demonstrate whether the product has met certain minimum quality standards. As such it should be differentiated from mere processing statistics. For example, a processing statistic might be the percentage of pixels in an image which are corrupted. A PCD flag would only be set if the number of bad pixels exceeded a predefined threshold (e.g., 10%).

Product Confidence Data may be located in the MPH, the SPH, and/or within a specific Annotation Data Set attached to a product. A signed character is used at the start of each MDSR in a Data Set to indicate the quality of the DSR (for Level 1B and Level 2 products

only, if needed). The value of -1 is reserved to indicate that the DSR is blank.

Product Confidence Data in the MPH is designed to very simply provide the user with an assessment of the overall product quality by reporting if errors have occurred during the processing. To obtain a detailed description of the errors which occurred, the user refers to the SPH or the detailed PCD structures of the product.

The thresholds used when evaluating PCD information are stored in the processor configuration files for each processor that generates products.

#### PCD in the MPH

The MPH is a generic header (i.e., instrument unspecific), and so any PCD contained within must be applicable to all instrument types.

- PCD applications include:
  - summary quality - high-level quality indicator for product
  - acquisition and de-multiplexing - this is related to the data commutation and downlink performance aspects which are independent of product type
  - processing flag - high-level error detected during product generation
  - error in auxiliary data

#### PCD in the Data Set Record (DSR)

The PCD in the DSR, which was called measurement confidence data (MCD) in ERS, is referred to as PCD in the ENVISAT payload data segment. The DSR PCD provides details on individual source packet quality. It is related directly to the engineering aspects and details of the ground processing algorithms. PCD data includes: error codes, error flags and threshold values for product data, and processor thresholds from processor parameters.

Payload data is found in INSERTLINKTO SQ\_ADSR. The flags are listed in [table 2.64](#) below.

Table 2.64 Product Confidence Flags

Flag	Purpose
input_mean_flag	Input data mean is outside nominal range
input_std_dev_flag	Input data standard deviation is outside nominal range
input_gaps_flag	Significant gaps (more than N missing lines) are present
input_missing_lines_flag	Percentage of missing lines exceeds threshold
dop_cen_flag	Doppler Centroid is uncertain
dop_amb_flag	Doppler Ambiguity estimate is uncertain
output_mean_flag	Output data mean is outside nominal range
output_std_dev_flag	Output data standard deviation is outside nominal range
chirp_flag	Chirp reconstruction failed or is low quality
missing_data_sets_flag	Data sets missing
invalid_downlink_flag	Invalid downlink parameters

Processor thresholds are shown in [ASA\\_CON\\_AX 6.5.1](#). data.

## 2.7 Level 2 Product and Algorithms

There is only one Level 2 ASAR product being produced, which is the "Ocean Wave Spectra Product" (ASA\_WVW\_2P).

### 2.7.1 ASAR Level 2 Algorithms

The Synthetic Aperture [Radar](#) (SAR) is so far the only satellite-borne instrument that can measure the directional characteristics of the ocean wave field. At present, the SAR imaging of ocean waves is fairly well understood. An analytic expression for the non-linear ocean-to-SAR spectral transform exist describing the SAR image [spectrum](#) as a function of the underlying ocean wave field. The transform was derived by Hasselmann and Hasselmann (1991), reformulated by Krogstad (1992), and later extended to the cross-spectral case by Engen and Johnsen (1995). The existing SAR spectral inversion schemes are based on approximations of the nonlinear transform of Hasselmann, and have successfully been applied to [ERS](#) SAR data. The main drawbacks of the algorithms are the need of an a priori wave spectrum in order to solve the propagation ambiguity and find a unique solution for the wave system. The a priori spectrum is usually taken from Wave Models. Extensive validation of the inversion schemes and the impact of assimilation of ERs data into Wave Models has been undertaken (Breivik et. al. 1995). It can be concluded that the impact is on average limited due to sparse data coverage and limited new information in the SAR-derived wave spectra compared to the Wave Model spectra. The latter is partly due to non-optimal processed input SAR data combined with imperfect inversion schemes. By using the cross-spectra methodology the a priori spectrum is no longer needed for solving the ambiguity problem and for finding a unique solution. In addition the contribution from speckle is avoided. The only limitations are the poor [along-track resolution](#) and the limited knowledge of the behaviour of the transfer functions for various sea and wind conditions. The transfer function problem can be overcome where dual-polarised (i.e., simultaneously acquired HH and VV polarisations) data is available by using cross-spectra between different polarisations.

The [wave spectra retrieval](#) algorithms are based on minimizing, with respect to the wave spectrum, the mean square difference between the observed and the computed SAR image spectrum under certain constraints. The computed SAR image spectrum is derived using the nonlinear transform with the current wave spectrum, as input. This transform is for the general case of a multi-channel cross-spectrum derived by Engen (1997). The standard image spectrum, and the single-channel cross-spectrum are just special cases of the general transform.

The discussion of the algorithm used to create the Wave Mode Ocean Wave Spectra product is given below in the following sections.

### 2.7.1.1 General Description

The processing system will access the external input data, which consist of the SLC (Level 1) data and the processing setup data. The setup file may include and estimate of the local wind field. A pre-processing of the data will be done before the core processing is started. The preprocessing consists of inter-look cross-spectral processing. The core processing performs a wave spectral inversion of the cross-spectra with respect to the detected SAR ocean wave-like pattern. This is done by first evaluating the nonlinear contribution to the imaging process assuming that this is caused only by the local wind field, and then to apply a quasi-linear inversion in the most energetic part of the SAR cross-spectrum. The former step is based on the asymptotic development of the full nonlinear SAR mapping transform and its identification in the least energetic SAR observed cross-spectrum. The major requirements for the second step is knowledge of the [Real Aperture Radar](#) Modulation Transfer Function (RAR MTF), the azimuth cut-off (orbital shift variance), and the nonlinear part of the spectra. The RAR [MTF](#) is computed using a backscattering model including non-uniform distribution of scatterers on the long wave field. The [RAR MTF amplitude](#) is provided as part of look-up table used to estimate the nonlinear part of the cross-spectra.

After the core processing is finished, the spectrum is converted to polar grid and an output product is generated and stored on the [ASAR Level 2 WVW format 2.7.2](#), which follows a format similar to the ASAR Level 1 WVS format.. (The wave spectra is substituted with the cross-spectra and the extra header parameters are put into the spare fields.)

### 2.7.1.2 Processing Steps

The main ASAR Level 2 processing steps to create the Wave Mode Ocean Wave Spectra product (ASA\_WVW\_2P) are summarised below in [figure 2.60](#) :

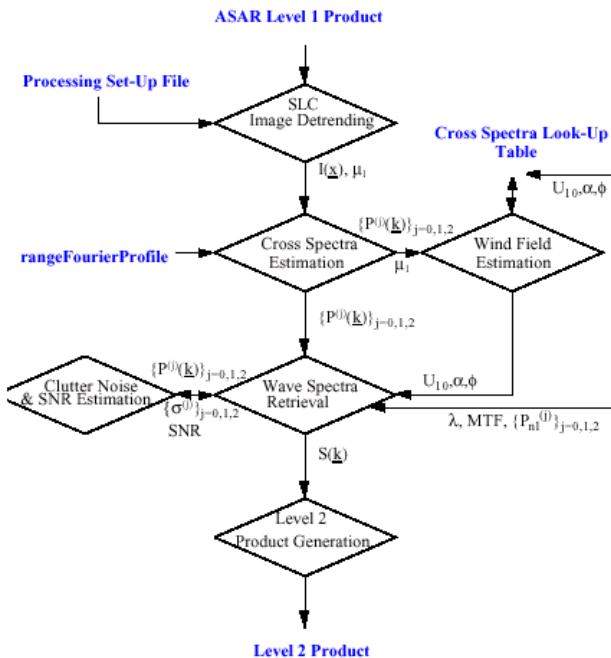


Figure 2.60 Flowchart of the Level 2 processing algorithm

## 1. Data Input

The data input combines the SLC information and the processing set up parameters into a global parameter list required for the processing.

## 2. Look\_Up Table

Lookup tables consisting of a set of simulated cross-spectra are provided with the software, and used to retrieve the nonlinear cross spectra, the smearing parameter, the RAR MTF and the wind field.

One lookup table is provided for each swath and polarisation that will be used for the Wave Mode. The lookup tables are stored on one unformatted data file for each table, and a common formatted information (info) file.

## 3. Processing

The processing module performs the look extraction and cross-spectra estimation according to the steps below:

- Image Detrending - Detrend the input SLC image using a Gaussian low-pass filter operation where the width of  
the filter can be specified in the setup file.

This procedure removes the low frequency effects from the SLC image that are due to non-wave features. This is done by computing a low-pass filtered image from the SLC image and then dividing the SLC image with the square root of the computed low-pass filtered intensity image. The procedure also provides the image intensity of the original input SLC image.

- Image Cross Co-variance Spectrum Estimation - Compute the co-spectrum and the two cross-spectra corresponding to three looks.

This procedure performs the look extraction and computes all combinations of spectra. Default is 3 looks providing 3 spectra - one co-spectrum and two cross-spectra. The spectral processing is based on the periodogram method.

- Estimate and remove the Clutter Bias of the Co-Spectra - Estimate the clutter bias of the co-spectra and remove it from the co-spectra. This procedure gives one unbiased co-spectrum and two cross-spectra generated with two different look separation times -  $\tau$  and  $2\tau$ . All of the spectra are combined statistically and used in the wave spectra retrieval.

#### 4. Parameter Estimation

This module performs the estimation of a set of parameters from the cross-spectra which again are used in combination with the lookup table to generate the RAR MTF, the azimuth cutoff factor, and the nonlinear part of the cross-spectra.

The RAR MTF (Real Aperture Radar Modulation Transfer Function) estimation is based on using the available wind information extracted as part of the fitting of the observed nonlinear part of the cross-spectra to the look-up table, combined with a given backscatter model function incorporating non-uniform distribution of scatterers on the long wave field. The RAR MTF 'amplitude' (i.e., derivative of the phase function taken at Bragg wave-number) is provided within the look-up table.

The estimation procedure also provides an estimate of the local wind speed. The wind speed is estimated from the radar cross-section using CMOD assuming the wind direction is known. The wind direction can be estimated from the phase of the cross-spectra or provided at input.

The computation of the nonlinear SAR image cross-spectrum in the lookup tables is done using an implementation of the full nonlinear SAR transform including a non-uniform distribution of scatterers on the long wave field. The look-up table is used in order to simplify the algorithm and to decrease the processing load.

## 5. Inversion of Quasi-Linear Cross Spectra

The measured SAR image cross-spectrum can be approximated as a sum of a nonlinear part (mainly wind sea driven), a quasi-linear part (detected SAR wave pattern, swell), and a uniform distributed noise term, with known variance.

The procedure for inverting the ASAR Level 1 products with respect to the ocean swell wave spectrum requires the following steps::

- Express the co- and cross-spectra as sums of the nonlinear approximation and the well known quasi-linear part given by the exponential cutoff factor, transfer functions and swell spectrum.
- Remove the nonlinear contribution (using look-up table) and solve the quasi-linear part linearly with respect to the swell spectrum inside the SAR imaging domain, for each of the spectra. Solve for the symmetric and the anti-symmetric spectrum.
- Compute the corresponding clutter noise level of each of the wave spectra solutions.

The signal-to-noise ratio is needed in order to establish the criteria for ambiguity resolution i.e. when combining the symmetric and the anti-symmetric spectra.

- Combine, using the clutter noise level, the solutions of each of the spectra to provide the final estimate of the wave spectrum. Both for the symmetric and the anti-symmetric spectra.
- Compute the clutter noise of the final symmetric and anti-symmetric spectra, combine them with the anti-symmetric spectrum, and use the results to remove the ambiguity of the symmetric spectrum.

The 180 deg. propagation ambiguity in wave spectra can be resolved by combining the symmetric and

the anti-symmetric spectra. The basis idea is to perform an adaptive smoothing (SNR dependent) of

the anti-symmetric spectrum, followed by a detection of the sign for the valid regions defined by the

spectra and their relation to the corresponding noise level. The final wave spectrum is then obtained

by combining the symmetric spectrum and the sign function. The swell inversion procedure will estimate the swell wave spectrum resolved by the SAR. Note that although the extraction of the swell is based on the quasi-linear transform, the inversion is a nonlinear inversion process through the coupling with the nonlinear part.

- Set the inversion confidence measure.

- Convert the final wave spectrum to log-polar grid, compute spectral parameters and transfer the results to the data output module.

The retrieval of ocean wave spectra is then performed on the quasi-linear cross spectra. An example of input and output results of the inversion procedure described above is shown in [figure 2.61](#) below, on Cartesian grid.

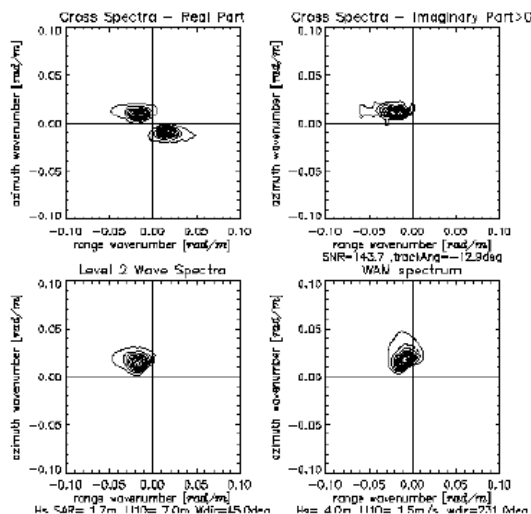


Figure 2.61 Example of ASAR Level 1 cross-spectra (upper plots) and the corresponding wave-spectra (low left) achieved by the inversion procedure described above. Collocated Wave Model (WAM) spectrum shown in lower right plot. Note that here the spectra is shown in Cartesian representation.

The Cartesian to logarithmic polar grid transformation is performed using bi-linear interpolation. The polar grid will be given in wave number-direction representation. The wavelength region is specified in the setup file. The number of wave number and angular bins will be user-selectable with default values 24 and 36, respectively. The wave number samples will be on logarithmic while the angular samples will always be equidistant. The polar spectra is given clockwise relative to north. The Cartesian inverted ocean waveheight spectrum is transformed in to log-polar grid representation.

The spectral peak parameter extraction, discussed below, is to be performed on the polar grid.

The spectral peak period and direction is extracted from the one-dimensional spectra obtained by averaging over direction and wave number, respectively. See [figure 2.62](#) below.

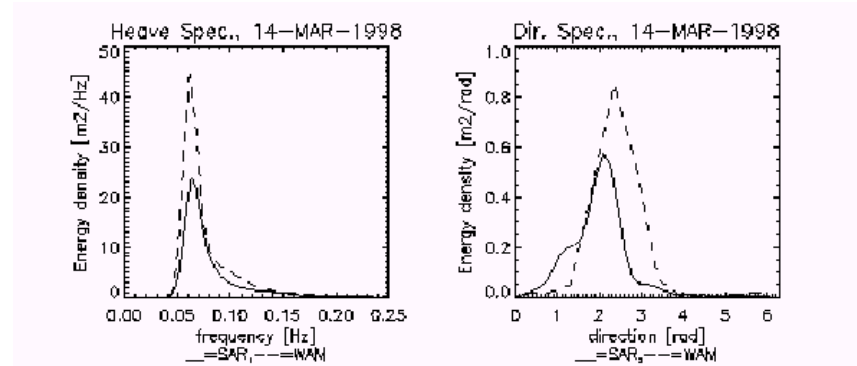


Figure 2.62 Typical non-directional (heave) and directional SAR wave spectra obtained by integrating out the directional and the wave number dependency, respectively. The heave spectrum is used to compute the spectral peak wavelength. The directional spectrum is used to compute the peak propagation direction. The dotted lines are the corresponding spectra derived from collocated WAM (Wave Model) spectra.

## 6. Output Data

The level 2 product that results from the above processing is described in [the section entitled "Level 2 Product" 2.7.2.](#)

### 2.7.2 Level 2 Product

#### Level 2 product (ASA\_WVW\_2P)

The Wave Mode Ocean Wave Spectra product is created by inverting the cross-spectra computed from inter-look processing of the SLC imagettes to derive the directional ocean product ocean wave spectra. Auxiliary ADSs included with the product remains the same as for the Cross-Spectra product. ([see Level 1B Wave Products 2.6.2.1.2.](#))

Table 2.65 Wave Mode Ocean Wave Spectra product

Mode	Product ID	Product Name
WV	ASA_WVW_2P	Wave Mode Ocean Wave Spectra

This is the basic Level 2 product from ASAR Wave Mode. A new Level 2 product is

foreseen, taking into account SAR ocean wave inversion using the cross-spectra methodology.

Below is an example of an ASA\_WVV\_2P product spectral view ([see the section on the EnviView tool](#)):

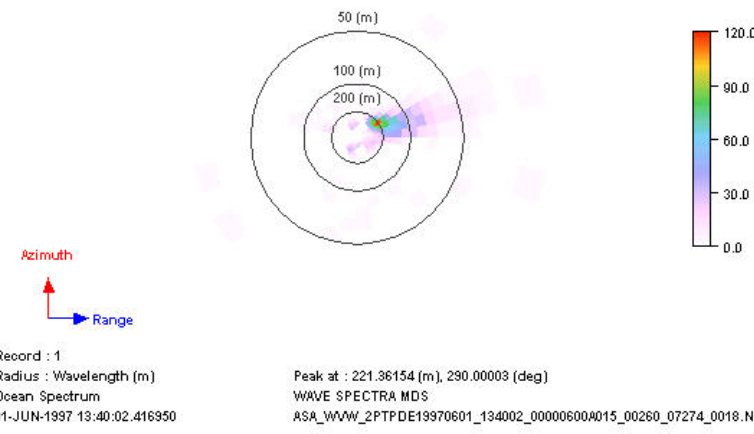


Figure 2.63 ASA\_WVV\_2P spectral view ( as seen in EnviView )

The output product follows the format of the ENVISAT ASAR Level 1B Wave Mode Imagette Cross-Spectra (ASA\_WVS\_1P) product ([see Level 1B Wave Products 2.6.2.1.2](#) ). This is done in order to be compatible with the ground segment products of ENVISAT ASAR.

The products are written in the general form shown in [figure 2.64](#) , below.

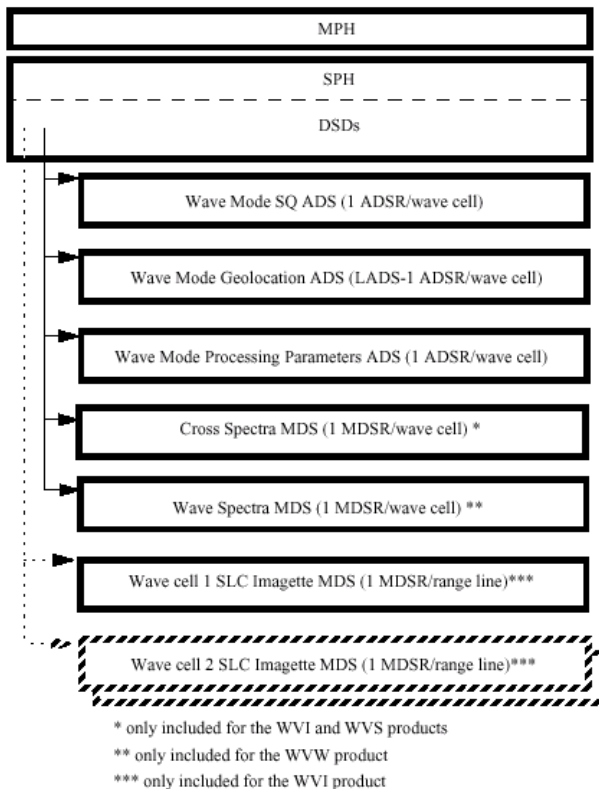


Figure 2.64 Wave Mode Products Structure

The MPH will be the same as described in [section 2.2](#). The ASAR wave mode SPH provides only the information which applies to all wave cells within a product file. The format will be identical for all ASAR wave products, except for the DSD sections.

Table 2.66 ASAR Wave Products Data Set Descriptor Names

Data Set Type	Data Set Name
DSD referencing the Level 0 product from which this product was created	"LEVEL 0 PRODUCT"
DSD referencing PF-ASAR Processor Configuration file	"ASAR PROCESSOR CONFIG"
DSD referencing Instrument Characterization file used	"INSTRUMENT CHARACTERIZATION"
DSD referencing External Characterization file used	"EXTERNAL CHARACTERIZATION"
DSD referencing External Calibration file used	"EXTERNAL CALIBRATION"
DSD referencing the Orbit State Vectors file used	"ORBIT STATE VECTOR 1"



Data Set Type	Data Set Name
DSD referencing the ECMWF file used	"ECMWF"
Wave Mode SQ ADS	"SQ ADS"
Wave Mode Geolocation ADS (LADS)	"GEOLOCATION ADS"
Wave Mode Processing Parameters ADS	"PROCESSING PARAMS ADS"
Cross Spectra MDS	"CROSS SPECTRA MDS"
Ocean Wave Spectra MDS	"OCEAN WAVE SPECTRA MDS"
Wave Cell SLC Imagette MDS	"SLC IMAGETTE MDS XXX" where XXX is a counter value from 000 to 399 indicating the cell number corresponding to the given imagette

## Data Sets

The data sets which make up the ASAR Wave product structure are defined in the following sections. Data Sets are of mixed-binary format. ASCII strings may be included, but are not contained within quotes like for the MPH and SPH.

### Wave Mode SQ ADS

There is one Wave Mode SQ ADSR per wave cell. The ADSR contains information pertaining to both the imagette and the spectrum. This consists of the ASAR image SQ information previously defined in INSERTLINKHERE, plus new information pertaining to the cross spectra.

### Wave Mode Geolocation Grid ADS (or LADS)

Due to the reduced size of the imagettes compared to normal ASAR images, each Wave Mode Geolocation ADSR contains only the geodetic latitude and longitude of the center point of the imagette. One ADSR is produced for each wave cell.

The center point given in the Geolocation ADSR corresponds to the ground range center point of the wave cell. This will not correspond exactly to the latitude and longitude of the center sample of the SLC imagette (in slant range) but provides a more accurate positioning of the location of the cross spectra center point.

Note that the imagettes do not cover a contiguous region geographically. Thus, Wave Mode Geolocation ADS entries may differ substantially for different imagettes.

### Wave Mode Processing Parameters ADS

The Wave Mode Processing parameters ADS details all the parameters used to create the imagette and other parameters specific to Wave Mode Imagette processing. These consist of those found in the Main Processing Parameters ADS of the Image Products format, plus Doppler Centroid parameters, Chirp Parameters, Antenna Elevation Patterns, Slant Range to Ground Range (SR/GR) parameters, Geolocation Grid Tie points, and parameters specific to Wave Mode. Note that the imagette is an SLC image. Therefore the SR/GR parameters and Antenna Elevation parameters pertain to the cross-spectra creation process, not the imagette itself.

---

There is one ADSR per wave cell.

### Cross-Spectrum MDS

This MDS contains the cross spectrum of the imagette. There is one MDSR per wave cell.

The cross spectrum is given in the MDS in complex form on a polar grid. The size of the cross spectrum grid is given in the SPH. Typically this will be 24 by 36 bins in wavelength and direction respectively. As the real part of the polar spectrum is symmetric, and the imaginary part is anti-symmetric, only 0° to 180° need to be given in order to reconstruct the entire spectrum (i.e., only 18 directional bins).

The cross spectrum values shall be stored in an unsigned integer format, each part linearly scaled to the maximum and minimum values of the representation (e.g., 0 to 255). The original maximum and minimum values for each part is reported.

The cross spectrum statistics are derived from a high resolution polar spectrum, prior to encoding for output to the product, or at other intermediate stages of the processing.

If the processor is unable to produce the cross spectra for a given wave cell, the MDSR is time stamped with the time that the cross spectra would have corresponded to, the Quality Flag is set to -1, and the MDSR data fields are all set to zero.

The concept of the Wave Mode cross spectrum product is shown below. The product has 18 sectors with 24 cells each. Because of symmetry the whole circle is not necessary to be supplied. The remaining half is computed according to even- or odd-symmetry of the spectra, as shown below.

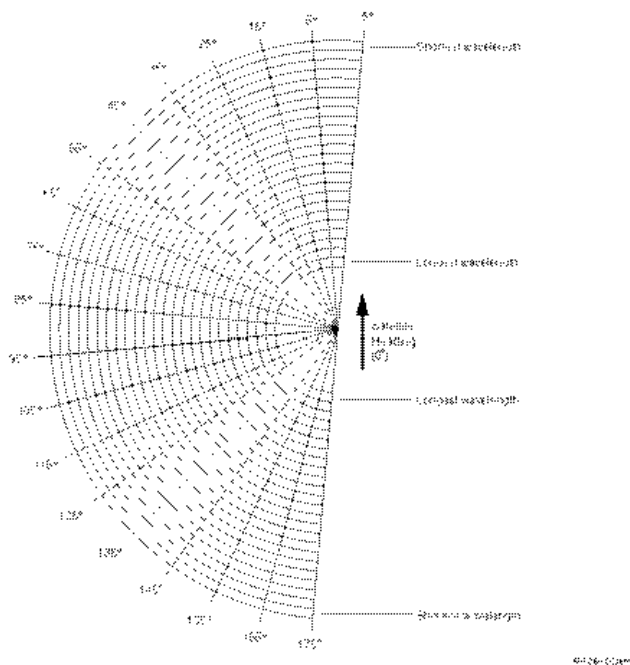


Figure 2.65 Wave Mode Cross Spectra Format

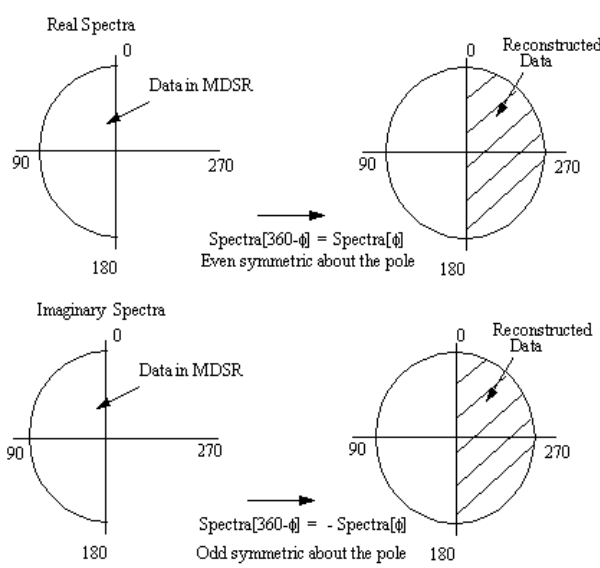


Figure 2.66 Method to Reconstruct Full Cross Spectra

## Ocean Wave-Spectrum MDS

This MDS contains the ocean wave spectrum of the imagette. There is one MDSR per wave cell. The format of the wave-spectrum MDS closely matches that of the cross spectrum MDS where some fields in the cross-spectrum MDS are substituted by new values pertaining to the ocean wave spectrum product. Each ocean wave spectrum MDSR is described below:

The ocean wave spectrum is given in the MDS as real samples distributed on a polar grid. The size of the ocean wave spectrum grid is given in the SPH. Typically this will be 24 by 36 bins in wavelength and direction respectively.

The ocean wave spectrum values shall be stored in an unsigned integer format, each part linearly scaled to the maximum and minimum values of the representation (e.g., 0 to 255). The original maximum and minimum values are reported.

If the processor is unable to produce the ocean wave spectra for a given wave cell, the MDSR is time stamped with the time that the ocean wave spectra would have corresponded to, the Quality Flag is set to -1, and the MDSR data fields are all set to zero.

### MDS Containing Imagettes

The structure of the MDS containing an imagette will be identical to that specified in Section See Measurement Data Set. There is one MDS per imagette. There are up to 400 MDSs per product. The MDSs are not included for WVS and WVW products.

If PF-ASAR is unable to produce an imagette, the MDS will consist of only one MDSR with the time stamp corresponding to what the first line of the imagette would have been, a range line number of 1, and the quality flag set to -1.

## 2.8 Instrument-specific Topics

This topic is described by this entire handbook.

## 2.9 Auxiliary Products

---

Auxiliary data files are all other data files used to produce a product, other than the direct measurements of the instrument. This may include calibration data that was measured on-board but is not part of the main measurement data of the instrument. It may also include external calibration files from sources other than the satellite, processor configuration files, and any other files needed by instrument processors.

A discussion of these files is provided in the following sections.

## 2.9.1 Summary of Auxiliary Data Sets

### 2.9.1.1 Auxiliary Data Files

Auxiliary data files are all other data files used to produce a product other than the direct measurements of the instrument. This may include calibration data that was measured on-board but is not part of the main measurement data of the instrument. It may also include external calibration files from sources other than the satellite, processor configuration files, and any other files needed by instrument processors. For a further discussion of the auxiliary data files refer to the section "[Common Auxiliary Data Sets](#)" 2.9.3, and "[Auxiliary Data Sets for Level 1B Processing](#)" 2.9.2.

### 2.9.1.2 Naming Strategy

The naming strategy for auxiliary data will be similar to the product naming conventions. The first 10 characters will be the auxiliary data ID, and will follow the following format:

WWW\_XXX\_YZ

WWW is the same instrument codes used for specifying product IDs. The instrument ID for auxiliary data indicates the instrument the data is intended for. Auxiliary data intended for several instruments will use the code AUX.

XXX is used to identify the type of auxiliary data.

YZ is always set to the letters AX for auxiliary data.

For auxiliary data, the file name structure contains:

The Auxiliary Data ID as described above (10 characters).

The Processing Stage flag which is used to indicate the quality level of the auxiliary data, using the same method as for the core products with N for preliminary quality up to V for highest quality (1 character).

The Originator ID indicates the source of the auxiliary data (3 characters). If not relevant, set to XXX.

The date and time of the auxiliary data creation (YYYYMMDD\_hhmmss) (15 characters).

Underscore character (1 character).

The date and time when the auxiliary data becomes valid in the PDS (YYYYMMDD\_hhmmss) (15 characters).

Underscore character (1 character).

The date and time when the auxiliary data ceases to be valid in the PDS (YYYYMMDD\_hhmmss) (15 characters).

Note: The filename format above is 61 characters long. When the filename is written to field 1 of the MPH (which is 62 characters long) a blank space character is added at the end of the filename in order to fill the field.

[Table 2.67](#) below provides a list of the auxiliary data files used in the ENVISAT PDS for ASAR processing.

Table 2.67 ENVISAT PDS Auxiliary Data Files used by ASAR

Aux_Data_ID	Approx. Size (MB)	Estimated Update Rate	Used by	Used for	Comments
<a href="#">ASA_CON_AX</a>	0.003	Infrequent	ASAR	L1B	ASAR Processor Configuration file
<a href="#">ASA_INS_AX</a>	0.163	Infrequent	ASAR	L1B	Instrument characterisation file
<a href="#">ASA_XCA_AX</a>	0.010	6 Months	ASAR	L1B	ASAR External calibration data
<a href="#">ASA_XCH_AX</a>	0.003	6 Months	ASAR	L1B	ASAR External characterisation data
<a href="#">AUX_FRO_AX 2.9.3.1</a>	0.195	1 Day	All Instruments	L0, L1B, L2	Restituted orbit state vector
<a href="#">AUX_FPO_AX 2.9.3.1</a>	0.013	1 Day	ASAR and PF-HS	L0, L1B, L2	Predicted orbit state vector
<a href="#">DOR POR_AX 2.9.3.2</a>	0.003	1 day	All Instruments	L1B	DORIS Preliminary Orbit State Vectors
<a href="#">DOR_VOR_AX 2.9.3.3</a>	0.003	1 day	All Instruments	L1B	DORIS Precise Orbit State Vectors

### 2.9.1.3 Auxiliary Data Structure

Auxiliary data files follow the same format guidelines as the PDS products. Every Auxiliary Data file will consist of an MPH, an [SPH](#) and one or more data sets.

Auxiliary data which originates outside the PDS will be wrapped in an MPH and SPH upon entry to the PDS. The actual contents of the foreign file will become those of a GADS, without modification.

#### 2.9.1.4 Auxiliary Data MPH

The MPH used for auxiliary data is the same as that used for products. For auxiliary data which originates from the satellite, most of the MPH fields will be relevant. For auxiliary data which does not originate from the satellite, many sections of the MPH will not be relevant, and MPH fields not pertinent will be blanked or set to zero (depending on the field type) as shown in the [MPH layout provided in the Data Formats 6.6.1](#), section.

Field 1 of the MPH will contain the name of the auxiliary data file using the auxiliary data naming strategy described in [NAMING STRATEGY 2.9.1.2](#), above. Therefore, field 1 of the MPH will be constructed as follows:

Table 2.68 Field 1 of Auxiliary Data MPH Record

Field	Description	Units	Byte Length	Data Type
1	PRODUCT=		keyword	8
	quotation mark ("")			1
	Auxiliary Data File Name (the following fields describe the contents of the auxiliary data filename)			62
	10 character file ID		-	10
	Processing stage flag		-	1
	Originator ID (if not relevant, set to XXX)		-	3
	creation_day (YYYYMMDD UTC creation day of the auxiliary file)		-	8
	underscore character		-	1
	creation_time (HHMMSS UTC creation time of the auxiliary file)		-	6
	underscore character		-	1
	valid_day (YYYYMMDD UTC day the auxiliary file becomes valid)		-	8
	underscore character		-	1
	valid_time (HHMMSS UTC time the auxiliary file becomes valid)		-	6
	underscore character		-	1
	invalid_day (YYYYMMDD UTC day the auxiliary file becomes invalid)		-	8
	underscore character		-	1
	invalid_time (HHMMSS UTC time the auxiliary file becomes invalid)		-	6
	blank space character		-	1
	quotation mark ("")		-	1
	newline character		terminator	1

### 2.9.1.5 Auxiliary Data SPH Structure

The structure of this header file is given in [Data Formats. \(Chapter 6.\)](#)

### 2.9.1.6 Auxiliary Data Sets

The Data Sets may be of any of the types described for PDS Products, and follow identical format rules. Any exceptions are noted in the individual file descriptions.

## 2.9.2 Auxiliary Data Sets for Level 1B Processing

The auxiliary files used by PF-ASAR to create the ASAR products are described in this section. A depiction of the antenna beam characterisation measurements that supply the data for the files discussed here, is given in [figure 2.67](#) below:

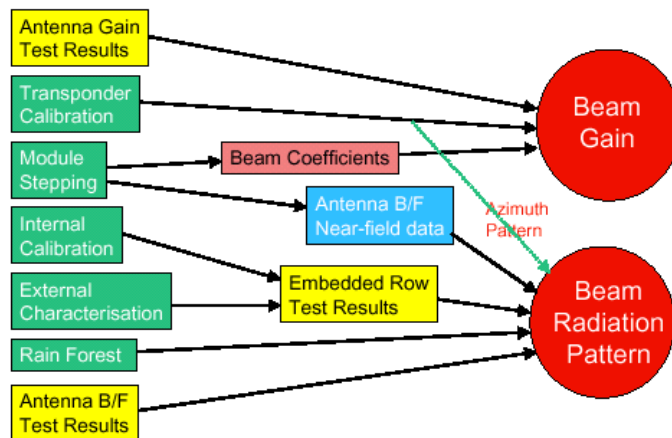


Figure 2.67 Antenna beam characterisation measurements

### External Characterisation Data (ASA\_XCH\_AX)

The ASAR instrument has an External Characterisation Mode which is operated overflying a receiver set up for H or V polarisation located in the ground. During the mode, the ASAR transmits a sequence of pulses from each antenna row in turn. These pulses are received and

digitised on the ground and the data recorded for off-line analysis. Simultaneously during the mode the calibration loop in the instrument is used to couple transmit pulses which are then sampled within a calibration widow in order to provide comparative values. The External characterisation Data file is provided as the output of the external characterisation analysis and is used for internal calibration processing correction. It is updated nominally every 6 months.

The MPH and SPH of these files will follow the standard MPH, SPH structure of all ENVISAT-1 auxiliary data. There is one DSD in the SPH, known as the ASA\_XCH\_AX\_GADS. The formats for all of these records are given in the [Data Formats \(Chapter 6.\)](#) section.

#### External Calibration Data (ASA\_XCA\_AX)

The external calibration scaling factor is determined by ESA using three calibrated transponders, and the in-flight elevation pattern estimates are obtained using natural targets with known properties such as the rainforest. The file is used during image calibration and is updated nominally every 6 months

The MPH and SPH of these files will follow the standard MPH, SPH structure of all ENVISAT-1 auxiliary data. There is one DSD in the SPH, known as the ASA\_XCA\_AX\_GADS. The formats for all of these records are given in the [Data Formats \(Chapter 6.\)](#) section.

#### Processor Configuration File (ASA\_CON\_AX)

This file contains static processing parameters used by the PF-ASAR which includes the threshold values used for setting PCD flags. This file is available in the inventory so a user may check what the processing configuration and threshold values were for the product of interest. The file is updated infrequently, only if static processing parameters change or PCD thresholds are updated.

The MPH and SPH of these files will follow the standard MPH, SPH structure of all ENVISAT-1 auxiliary data. There is one DSD in the SPH, which is a GADS called ASA\_CON\_AX\_GADS. Details of the formats for all of these records are given in the [Data Formats \(Chapter 6.\)](#) section.

#### Instrument Characterisation File (ASA\_INS\_AX)

This file contains key parameters which characterise the instrument. This includes look up tables and other parameters needed in the ground processing. It contains a subset of the data found in the Instrument Characterisation database. The file is updated infrequently, only if instrument operating parameters change.

The MPH and SPH of these files will follow the standard MPH, SPH structure of all ENVISAT-1 auxiliary data. There is one DSD in the SPH called the ASA\_INS\_AX\_GADS. Details of the formats for all of these records are given in the [Data Formats \(Chapter 6.\)](#) section.

## Orbit State Vectors

Vectors may be from the "Flight Operations Segment" (FOS) or from the "Doppler Orbitography and Radiopositioning Integrated by Satellite" (DORIS) instrument. FOS and DORIS vectors are described in "[Common Auxiliary Data Sets](#)" 2.9.3.

Table 2.69

Orbit State Vectors file (one file of five)	<a href="#">AUX_FRO_AX 2.9.3.1.</a> <a href="#">AUX_FPO_AX 2.9.3.1.</a> <a href="#">DOR_NAV_0P 2.9.3.4.</a> <a href="#">DOR_VOR_AX 2.9.3.3.</a> <a href="#">DOR_POR_AX 2.9.3.2.</a>
---	---

### 2.9.3 Common Auxiliary Data Sets

The common auxiliary files used in ASAR processing, that have not already been discussed in previous sections, are provided in this section.

#### 2.9.3.1 FOS Orbit State Vectors

The instrument ground processing software uses the CFI orbit propagator software module and an orbit state vector as input to calculate the satellite position all along the orbit. The following describes the product structure of the "Flight Operations Segment" (FOS) instrument's predicted and restituted orbit state vector files. These are used during ground processing and are updated once per day. FOS Predicted: (AUX\_FPO\_AX) One MDSR per orbit, file contains MPH, SPH and MDS and covers 6 days . FOS Restituted: (AUX\_FRO\_AX) One MDSR per minute, file contains MPH, SPH and MDS and covers 1 day, with approximately a 60 minute overlap.

##### Format

The MPH and SPH of these files will follow the standard MPH, SPH structure of all ENVISAT auxiliary data. The SPH contains a single DSD of type M pointing to the MDS. The file will consist of a single MDS containing several MDSRs. Each MDSR is of the format shown below.

**NOTE THAT ORBIT STATE VECTOR MDSRs DO NOT FOLLOW STANDARD ENVISAT-PDS FORMAT.** The MDSR is in ASCII format and, although common to all ENVISAT instruments, is given here for convenient reference.

Table 2.70 Format of MDSR for orbit State vectors

N	MDSR Contents	Units	Byte Length	DataType	Dim.
1	UTC of Orbit State Vector	UTC	27	uc	27
2	ASCII blank space character	-	1	uc	1
3	Delta UT1 = UT1-UTC	s	8	Ado06	1
4	ASCII blank space character	-	1	uc	1
5	Absolute Orbit number	-	6	As	1
6	ASCII blank space character	-	1	uc	1
7	X position in Earth fixed reference frame	m	12	Ado73	1
8	ASCII blank space character	-	1	uc	1
9	Y position in Earth fixed reference frame	m	12	Ado73	1
10	ASCII blank space character	-	1	uc	1
11	Z position in Earth fixed reference frame	m	12	Ado73	1
12	ASCII blank space character	-	1	uc	1
13	X velocity relative to Earth fixed reference frame	m/s	12	Ado46	1
14	ASCII blank space character	-	1	uc	1
15	Y velocity relative to Earth fixed reference frame	m/s	12	Ado46	1
16	ASCII blank space character	-	1	uc	1
17	Z velocity relative to Earth fixed reference frame	m/s	12	Ado46	1
18	ASCII blank space character	-	1	uc	1
19	Quality Flags (TBD by ESA)	-	6	uc	6
20	ASCII newline character	terminator	1	uc	1
	TOTAL		129		

### 2.9.3.2 DORIS Preliminary Orbit State Vectors

The preliminary orbit reconstruction is the first orbit estimate produced from the "Doppler Orbitography and Radiopositioning Integrated by Satellite" (DORIS) instrument Doppler shift data. It is produced off-line systematically for all DORIS data received, and is intended as an orbit estimate of higher quality than that of the Navigator product. The file is used during ground processing and is updated once per day.

The format is identical to that described above for the [FOS State vectors](#). Each file covers 26 hours, with 1 MDSR per minute. Therefore, there are 1560 MDSRs in the MDS.

### 2.9.3.3 DORIS Precise Orbit State Vectors

The precise orbit reconstruction is the most accurate orbit estimate produced from the



DORIS data. It is produced off-line systematically for all DORIS data received, and is intended as an orbit estimate of the highest quality achievable using DORIS. The file is used during ground processing and is updated once per day.

The format is identical to that described above for the [FOS State vectors](#). Each file covers 26 hours, with 1 MDSR per minute. Therefore, there are 1560 MDSRs in the MDS.

#### 2.9.3.4 DORIS Navigator Level 0

The DORIS Navigator Level 0 product is a file containing time ordered AISPs which are output from the on-board DORIS Navigator software. This product provides the first estimate of satellite positioning available from the DORIS sensor,

the accuracy of which is described in the table below. No further processing is applied to the Level 0 Navigator Product. The NRT version of the product is available within 3 hours of data acquisition. The OFL (fully consolidated) version is available

2 weeks after acquisition.

As with all Level 0 products, it has an MPH and an SPH followed by an MDS containing the annotated instrument source packets. These formats are given in [Data Formats. \(Chapter 6.\)](#)

#### 2.9.3.5 UTC/SBT Time Conversion File

The instrument ground processing software uses the CFI time conversion software module and this file to convert from satellite binary time to UTC time. It is used during ground processing, annotated into MPH and is updated once per orbit.

Format:

The MPH and SPH of these files will follow the standard MPH, SPH structure of all ENVISAT auxiliary data. The SPH contains a single DSD of type G pointing to the GADS. The format of the GADS is shown below:

Table 2.71 Format of GADS for SBT/UTC Time Conversion File

N	Description	Units	Byte Length	Data Type	Dim.
1	Reference UTC time corresponding to SBT time below (currently defined to be	UTC	27	uc	27

	given at the time of the ascending node state vector)				
2	ASCII blank space character	-	1	uc	1
3	Reference Satellite Binary Time (SBT)	-	11	Al	1
4	ASCII blank space character	-	1	uc	1
5	SBT clock step in picoseconds	ps	11	Al	1
6	ASCII newline character	-	1	uc	1
TOTAL			52		

### 2.9.3.6 ECMWF Data Files

The "European Centre for Medium-range Weather Forecasting" (ECMWF) data files contain Meteo information. They are ingested into the PDS ground segment on a regular basis and are used by various instrument processors during the generation of products.

There are two kinds of ECMWF data: Forecast data (AUX\_ECF\_AX) and Analysis data (AUX\_ECA\_AX). Forecast data is used in NRT processing, while Analysis data is used during OFL product generation. Both Forecast data and Analysis data files have the same format. The data from is used in Level 1B processing and L2 processing. The ECMWF files enter the PDS every 6 hours. There are 4 Analysis files and 4 Forecast files, each valid for a 12 hour time period.

ECMWF files enter the PDS every 6 hours. There are 4 Analysis files and 4 Forecast files, each valid for a 12 hour time period.

Format:

The high level breakdown of the file is shown below:

Table 2.72 Schematic Structure of ECMWF Files

MPH
SPH - standard Auxiliary Data SPH with 1 DSD
DSD for the ECMWF GADS
ECMWF GADS

ECMWF data files entering the PDS are encoded in PB-IO format. Upon entry to the PDS, the file is modified to fit the standard ENVISAT PDS file format. This is done by completing the following steps:

1. Place the PB-IO file (without modifying its structure) into a GADS (the ECMWF GADS);
2. Add an Auxiliary Data SPH (with one DSD for the GADS);

- 
3. Add an MPH (fields not relevant set to zero or filled with ASCII blank space characters);
  4. Assign a PDS filename as per the auxiliary data naming convention described earlier in this volume.

## ECMWF GADS

The GADS contains information encoded in PB-IO format. No additions or modifications are made from the original format.

## 2.10 ASAR Latency Throughput and Data Volume

PF-ASAR is an operational SAR processor that is capable of being used for very high throughput processing with no operator intervention. The combination of the processing facility software architecture and the IBM SP-2 allows scalability over a wide range of throughput requirements. This generic architecture allows [PF-ASAR](#) to be installed in many stations (both large and small). PF-ASAR processes data from all ASAR imaging modes and produces a wide range of output products. Some of these products are based on [ERS](#) heritage and some are new. The concept of stripline products allows medium-resolution products with very long azimuth extents to be efficiently produced. All PF-ASAR products meet very high accuracy and quality requirements.

### 2.10.1 Latency

Latency is mainly a factor for the products generated systematically (i.e. the medium resolution products and the wave mode products).

Two categories of product distribution services are provided by the PDS:

- Near real time (NRT) services

NRT services are typically three hours from sensing for data used in forecasting or tactical operations (global and regional products produced and distributed systematically). For applications requiring high resolution images (agriculture, forestry, soil moisture, etc.) NRT products are typically available one to three days from sensing.

- Off-line service

- 

Off-line service (OFL) is typically available from a few days to weeks from data take. Off-line products benefit from superior data on calibration, auxiliary data, and precise orbit data.

## 2.10.2 Throughput

### 2.10.2.1 Product parameters

The parameters shown below are assumed to be constant for all products.

Table 2.73 Parameters common to all products

Description	Value
beam velocity	6800 m/s
sampling frequency	19.208 MHz
transmitted pulse duration	15.0 s
antenna length	10.0 m

The number and type of measurements made per orbit depends on the nature of the user requests for ASAR acquisitions. ASAR can be operated for up to 30 min per orbit for high-rate modes and for the full orbit for low-rate modes.

## 2.10.3 Data Volume

### 2.10.3.1 Product Sizes for Disk Storage

Approximate values of the worst case input, intermediate, and output product sizes for each of the ASAR products is shown below in [table 2.74](#) and [table 2.75](#) below. The table is taken from the processing system specification, and users will be most interested in the Output Data Set Size column. The need for intermediate product storage arises during the processing of [geocoded](#) products

Table 2.74 ASAR approximate image data disk requirements

Product Identifier	Input Data Set Size(MB)	Intermediate Data Set Size(MB)	Output Data Set Size(MB)	Total(MB)
<a href="#">IMP</a>	250	-	128	378
<a href="#">IMS</a>	250	-	690	940
<a href="#">IMG</a>	250	350	280	880
<a href="#">IMM and IMB</a>	250	-	4	254
<a href="#">APP</a>	250	-	256	506
<a href="#">APS</a>	250	-	1380	1630
<a href="#">APG</a>	250	980	560	1790
<a href="#">APM and APB</a>	250	-	8	258
<a href="#">WSM and WSB</a>	800	-	60	860
<a href="#">WVI</a>	740 /orbit	-	2070 / orbit	2810 / orbit
<a href="#">GMI &amp; GMB</a>	675 / orbit	-	140 / orbit	815 / orbit

The table assumes about 20 sec of raw data is required to process both scene and strip mode products with 100 km coverage. 65 sec of data is assumed to be needed for products with 400 km coverage.

Wave mode processing for an entire orbit has the largest disk space requirements. The calculation of the data set sizes for each imagette in Wave Mode are detailed below.

Table 2.75 Data sizes for wave mode imagette

<a href="#">Sub-swath</a>	Ka	PRF(max)	Azimuth matched filter length La	Number of samples per range line (max) Nr	Range matched filter length (min) Lr	Number echoes per imagette (max) Na	Input data set size(MB)Nr*Na/2	Output data set size(MB)(Nr*Lr)*(Na-La)*4
IS1	1969	1677	1143	1164	287	2392	1.33	4.18
IS2	1929	1645	1122	1223	292	2376	1.38	4.45
IS3	1859	2095	1889	1079	226	3080	1.58	3.88
IS4	1789	1680	1262	1305	286	2520	1.56	4.89
IS5	1727	2082	2008	1161	231	3160	1.74	4.09
IS6	1671	1698	1380	1352	283	2648	1.71	5.17
IS7	1619	2070	2117	1215	232	3192	1.85	4.03

## 2.11 ASAR Characterisation and Calibration

### 2.11.1 Introduction

Unlike the [ERS](#) AMI-SAR that operates a passive phased-array antenna, the ENVISAT-1 ASAR encompasses an active one that consists of 320 subarrays each one connected to a transmit/receive module (TRM). The [antenna](#) layout is of 32 rows of 10 subarrays. The subarrays are grouped in 2 x 10 tiles of 16 subarrays each (see figure 1). Each [TRM](#) has two transmit chains, one for horizontal and one for vertical polarisation, and one receive chain for both. The three chains are independently programmable in [amplitude](#) and phase to provide the required elevation [beam](#) patterns. The eight swaths required by the ASAR operation modes are dealt with by the antenna by means of the definition of eight sets of beam coefficients. The beam coefficient set consists of 32 transmit and 32 receive complex coefficients for each polarisation, corresponding to the 32 antenna rows in the [across-track](#) or elevation direction.

Any drift in the gain and phase characteristics of the TRMs can distort the antenna beams. Deviations in antenna pattern and antenna gain will potentially contribute to radiometric errors in the SAR image. The ASAR calibration scheme is, therefore, different to that used for ERS.

In-orbit beam calibration of an active phased-array antenna is a major task and it will include measurements in special modes, like [module stepping](#) and external characterisation, as well as acquisitions over rain forest. A sophisticated antenna model will combine the various data together with the pre-flight characterisation and provide the elevation and azimuth patterns for the ground processor.

Monitoring any instrument gain drifts requires a separate calibration network, to couple out part of the transmit signal or to inject chirp signals into the receiver chain. This data will be included into the high-rate data stream and will be analysed by the ground processor in order to estimate the necessary gain drift corrections.

The absolute overall system gain can be most accurately determined from the image response of point targets with high and well-known [Radar](#) Cross Sections (RCS). ( [for the derivation of backscattering coefficients and RCSs in ASAR products see below 2.11.5.](#) ) ASAR high precision transponders will be deployed in the Netherlands and will serve as the main [external calibration](#) targets. A special transponder operation mode and well-characterised distributed targets will be used for the [low-resolution](#) Global Monitoring mode.

## 2.11.2 Pre-flight Characterisation Measurements

In order to provide the required image quality, the two-way antenna beam pattern should be known to a high degree of accuracy (0.1dB). The transmit and receive antenna patterns have been accurately [measured on ground 2.11.7.](#) for all eight beams (IS1-IS7 and SS1) and both horizontal and vertical polarisations. The radiating performances of the antenna were measured in the Large Planar Near Field Range at Astrium Ltd (Portsmouth). Full

characterisation was performed: 8 beams, two modes (transmit and receive), two polarisations (V and H), in copolar and crosspolar components.

### 2.11.3 Internal Calibration

The ASAR instrument incorporates a very comprehensive system for internal calibration. There is an individual calibration path for each of the 320 transmit/receive modules (T/R modules).



Figure 2.68 T/R Module

Internal calibration will be carried out on a row by row basis for each of the 32 rows. The calibration pulses are included in the instruments timeline during imaging and consist of the following:

Transmit Calibration Pulses P1 (representative of T/R module load)

Since T/R modules of the four adjacent rows share the same power supply, the ten modules of the 'wanted' row are set to their nominal phase and amplitude settings whilst the phase of the modules of the three 'unwanted' rows are set so that their combined contribution out of the calibration network is nominally zero. Thereby minimising their interference to the measurement of the 'wanted' row. The equation for this is given below:

$$a_{1,n}(t) = e^{j\phi_{1,n}(t)} \quad \text{eq 2.16}$$

#### Transmit Calibration Pulse P1A

A second type of transmit pulse is added in order to characterise the residual parasitic contribution of the three unwanted rows during P1. During P1A, the three unwanted rows are set as for P1 and the previously wanted row is now switched off. Even though the load conditions on the power supplies are not exactly representative, the small error introduced into the estimation of P1A is negligible. The equation for this is given below:

eq 2.17

$$a_{1A,n}(t) e^{j\phi_{1A,n}(t)}$$

### Receive Calibration Pulse P2

The receive path of the instrument is also characterised, but since no variation is expected from power supply load variations it is possible to characterise on a row-by-row basis. The equation follows:

eq 2.18

$$a_{2,n}(t) = e^{j\phi_{2,n}(t)}$$

### Central Electronics Calibration Pulse P3

The auxiliary receive and transmit path of the central electronics are included in the P1/P1a and P2 characterisations, respectively. This part of the central electronics is therefore characterised independently by means of P3. The equation is as follows:

eq 2.19

$$a_{3,n}(t) e^{j\phi_{3,n}(t)}$$

Except for WV mode, the individual, mode and beam dependent chirps are used as calibration pulses, i.e. they have the same characteristics as the transmit chirps. WV mode calibration pulses are not chirped (cw-signal).

These calibration pulses are being used to monitor any transmit/receive gain variations and to reconstruct the chirp replica for range compression.

Calibration pulse measurements are being performed at the beginning of an acquisition (so-called initial cal sequence) and also during the acquisition with a mode-dependent repeat cycle of 5 - 35 seconds (periodic cal sequence). The processor is only using the periodic cal sequences.

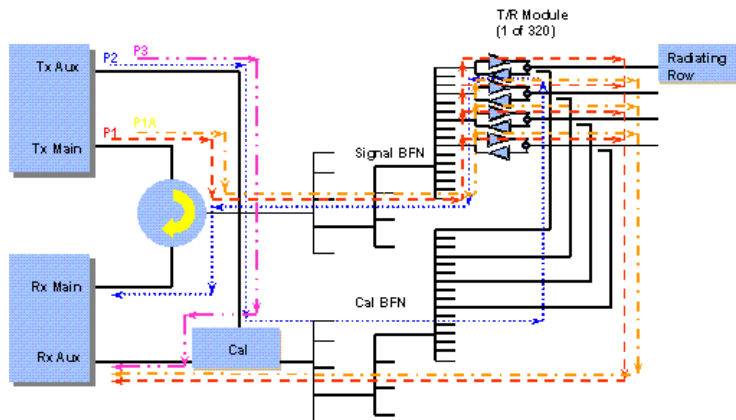


Figure 2.69 Calibration pulse diagram

### 2.11.3.1 Elevation Gain Monitoring

Using the amplitude and phase of the calibration pulses (P1/P1a, P2 and P3) for each row it is first necessary to calculate the amplitude and phase of P2 relative to P3 and to subtract P1a vectorially from P1. From these values for each of the 32 rows and together with the external characterisation factor, it is possible to calculate the elevation beam pattern. This is then used to detect any deviation to the reference instrument gain pattern as characterised on ground. The typical update rate for this calculation is 5 to 35 seconds (mode dependent).

The first step in the elevation gain monitoring is the calculation of amplitude and phase of the individual calibration pulses. Amplitudes are derived by averaging the pulse ([see note 1 below](#)), phase is derived after pulse compression from the peak response (in WV mode by multiplication with a reference cw-signal). Nominal or replica pulses can be used for calibration pulse compression. P1 pulses are then corrected for the P1A contribution and formalised to the nominal P1 pulse value (amplitude only) for beam IS0:

eq 2.20

$$a_{t,n} e^{j\phi_{t,n}} = (a_{1,n} e^{j\phi_{1,n}} - a_{1A,n} e^{j\phi_{1A,n}}) / a_{1,nom,n}^0$$

If necessary, normalisation by the nominal pulses P1 for IS0 can be easily reverted by setting

the values in the ASA\_INS\_AX file to 1.

The P2 pulses are then divided by P3 to correct for contributions from the AUX transmit and receive units, which only affect the cal pulses but not the signal.

eq 2.21

$$a_{n,n} e^{j\phi_{n,n}} = \frac{a_{2,n} e^{j\phi_{2,n}}}{a_{3,n} e^{j\phi_{3,n}}}$$

The antenna gain for an array antenna is given as the weighted coherent sum of the subarray radiation patterns (in our case the so-called embedded row patterns  $f_n$ ). The weights (taper) are given by the calibration pulse measurements. As the calibration pulses do not cover the passive part of the antenna (radiating elements) but are influenced by differences in the calibration network, we have to include the factors  $g_n$ , which are determined in the external characterisation. Calibration pulses,  $f_n$  and  $g_n$  are polarisation dependent.

The transmit/receive gain variation is then calculated at the reference elevation angles:

$$G_t(\theta_0) = \left| \sum_{n=1}^{32} a_{t,n} e^{j\phi_{t,n}} f_n(\theta_0) g_n \right|^2$$

$$G_r(\theta_0) = \left| \sum_{n=1}^{32} a_{r,n} e^{j\phi_{r,n}} f_n(\theta_0) g_n \right|^2$$

eq 2.22

The two-way gain variations are then given by:

eq 2.23

$$G_2(\theta_0) = G_t(\theta_0) G_r(\theta_0)$$

In the current implementation in PF-ASAR we repeat this calculation for a set of nominal pulses for this beam to generate  $G_{2,nom}$  and finally derive the elevation gain change with respect to this nominal gain:

eq 2.24

$$G'_2(\theta_0) = G_2(\theta_0) / G_{2,nom}(\theta_0)$$

If we add a flag in PF-ASAR to set  $G_{2,nom}$  to 1 we can revert this normalisation step. Together with the nominal pulses for IS0 set to 1, we obtain elevation gain factors that reflect the full change in antenna gain from beam to beam with any time/temperature dependent instrument gain variation on top.

### 2.11.3.2 Chirp Replica Construction

A replica of the chirped pulse is calculated from a complete calibration row cycle using the P1/P1a, P2 and P3 measurements, the ground characterised row patterns and the external characterisation data. This is also typically updated every 5 to 35 seconds.

The chirp replica, including the full transmit and receive path of the ASAR instrument, is also reconstructed from the calibration pulses. The chirp replica reconstruction uses the time-dependent signals instead of single pulse amplitude and phase values, but otherwise performs similar operations as in the elevation gain monitoring. The replica is given as the convolution of the P1A-corrected P1 pulse with the P2 pulse. The correction for the AUX transmit and receive units (pulse P3), which only affect the cal pulses but not the signal, is performed by a de-convolution. All these operations are performed in the frequency domain, where convolutions/de-convolutions simplified to multiplications/divisions. The required processing steps are:

eq 2.25

$$a_{t,n}(t) e^{j\phi_{t,n}(t)} = a_{1,n}(t) e^{j\phi_{1,n}(t)} - a_{1A,n}(t) e^{j\phi_{1A,n}(t)}$$

$$r_t(t) = \sum_{n=1}^{32} a_{t,n}(t) e^{j\phi_{t,n}(t)} f_n(\theta_o) g_n$$

|

$$r_r(t) = \sum_{n=1}^{32} a_{2,n}(t) e^{j\phi_{2,n}(t)} f_n(\theta_o) g_n$$

$$R(t) = \text{FFT}^{-1} \left[ \frac{\text{FFT}[r_t(t)] \cdot \text{FFT}[r_r(t)]}{\langle \text{FFT}[a_{3,n}(t) e^{j\phi_{3,n}(t)}] \rangle_n} \right]$$

where the  $\langle \rangle$  operator denotes an average over n. The replica energy is then calculated in PF-ASAR in the frequency domain (assuming a well-normalised FFT-operation):

eq 2.26

$$\text{repEnergy} = \sum |R(f)|^2$$

No normalisation of the transmit pulses for IS0 nominal pulses P1 and no normalisation like  $G_{2,\text{pom}}$  are being performed. If we switch off these two steps in the elevation gain monitoring, we should end up with comparable results, i.e. the elevation gain factor multiplied by the chirp duration should be equivalent to the replica energy.

Despite the comprehensive nature of the internal calibration system, it is not possible to use it to calibrate the passive part of the antenna, which falls outside of the calibration loop. This is achieved through external characterisation by using the ground transponders.

### 2.11.3.3 PF-ASAR Normalisation

PF-ASAR calculates the replica and the elevation gain factor from the calibration pulses in one calibration cycle. Only one calibration cycle is considered in scene products. In stripmap, where multiple cycles are available, the replica and the elevation gain are updated for every calibration cycle.

PF-ASAR uses two different processing algorithms (Range Doppler and the SPECAN), which follow different normalisation implementations. For both algorithms three different cases are considered which are already implemented in the processor:

1. The chirp replica can be reconstructed from the internal calibration pulses contained in the Level 0 and it is used during range compression.
2. The chirp replica cannot be reconstructed from the internal calibration pulses (replica quality measurements fall below the thresholds) and the processor automatically uses the nominal chirp during range compression.
3. The chirp replica can be reconstructed from the internal calibration pulses but the processor is forced to use the nominal chirp reconstructed from the coefficients.

### 2.11.3.4 Module Stepping

ASAR has a dedicated Module Stepping Mode, which is used to gather data from all 320 transmit/receive modules automatically. The entire procedure takes less than one second. The data are downloaded to the ground for processing. After processing, the results are compared with the reference data from on-ground tests in order to determine any T/R Module (TRM) module gain or phase drifts, temperature behaviour and any eventual module failures. Using this information it is possible to implement any necessary correction to the TRM coefficients and eventually re-synthesise the antenna beam patterns if required.

## 2.11.4 External Characterisation

ASAR can be put into External Characterisation Mode while flying over a calibration transponder. This involves sending a series of pulses from each of the 32 rows in turn followed by each of the 10 columns in turn.

These pulses are detected both by the internal calibration loop and the receiver embedded in the transponder. Comparison of these data allows characterising the passive part of the antenna and the calibration network. The baseline is to repeat measurement every six months.

#### 2.11.4.1 Characterisation of the Antenna Beam Pattern

For the characterisation of the antenna beam pattern, images of the Amazon Rain Forest are used. This is because the rain forest is a stable, large-scale, isotropic distributed target with a relatively high backscatter and a well-understood relationship between backscatter and incidence angle.

In order to determine the two-way beam pattern, an uncorrected rain forest image is averaged in the azimuth direction. In the final processed image, the inverted beam pattern is applied and hence the effect of the pattern on the backscatter is removed.

Alternative distributed targets at different latitudes are being investigated. Promising results have been found from ERS data over Lake Vostok in Antarctica. Antenna pattern estimates at different latitudes could be used to verify the round-orbit performance of the ASAR.

#### 2.11.4.2 Gain Calibration

The purpose of the ASAR gain calibration is to provide the users of ASAR data with the possibility to determine the absolute level of backscatter from any target, point ( $s$ ) or distributed ( $s_0$ ). For ASAR this is achieved in fundamentally the same way as for ERS, namely by providing an Absolute gain Calibration Factor (ACF) in the header of the (processed) product. Since ASAR, however, has a total of eight beams and five different modes and up to four polarisations more ACFs will need to be determined for ASAR than for the ERS single beam, single polarisation with two modes.

The method to be used to determine the ACFs is to image a target of known radar cross-section, integrate the power in its Impulse Response Function (IRF) corrected for the associated background (clutter) power and hence calculate the correction (the ACF) which must be applied to the image values in order to arrive at the same cross-section for that target. For this purpose, precision calibration transponders are deployed in the Netherlands.

---

The radar cross-section of these transponders is 65dBm2 and is known to within  $\pm 0.13\text{dB}$  and they are stable to 0.08dB [Ref. \[2.14\]](#). It is necessary to use active radar calibrators (transponders) as opposed to passive ones (e.g. corner reflectors) since the ratio of signal to clutter determines the accuracy to which the calibration can be made.

Once the ACF for a particular configuration has been calculated it will be possible to make a direct comparison with the on-ground measurements of the end-to-end system gain carried out during FM testing.

#### 2.11.4.3 Global Monitoring Mode

This is a special case since the spatial resolution of 10001000m makes the normal use of the transponders unfeasible. For a reasonable calibration to be made (3s value of  $\pm 0.5\text{dB}$ ), a signal to clutter ratio of better than 30dB is required. If the clutter at the calibration sites typically has a sigma nought of -6dB then this would require a transponder RCS greater than 84dBm2. This would inevitably saturate the receiver invalidating the calibration. As a result, it is necessary to come up with an alternative scenario for calibrating this mode.

The first option (baseline) is using the other modes (namely Wide Swath and Image) to calibrate GM mode by means of the Amazonian rain forest. Since the  $s_0$  of the rain forest is stable to within 0.3dB it will be possible to use the  $s_0$  value obtained from a previous (or subsequent) pass in WS or IM to calibrate GM mode. In addition, other relatively stable distributed targets may be used such as the ice caps and specific desert regions (Gibson, Gobi etc).

The second option will allow direct calibration using a special global monitoring mode setting and a modified calibration transponder. The intention is to use the ASAR's digital chirp generator to offset the centre frequency by 5MHz. This is possible since the chirp bandwidth in GM mode is only around 1MHz. In the calibration transponder, the received signal is shifted back by 5MHz allowing it to be received by the ASAR. As the clutter return will all be outside the range of the reduced bandwidth filter in GM mode, only the transponder response will be seen in the processed image against a background of noise. The result of this operation is to provide a transponder signal to clutter ratio of between 25 and 30dB allowing for reliable calibration of Global Monitoring Mode.

#### 2.11.5 The Derivation of Backscattering Coefficients and RCSs in ASAR Products

ASAR detected ground range projected products will be delivered as radar brightness (i.e. elevation antenna pattern and range spreading loss corrected but no incidence angle

compensation) while complex slant-range products will be delivered without any cross-track radiometric corrections.

Distributed targets backscattering coefficients sigma nought:

for ground range projected products:

$$\sigma^0 = \frac{\langle A^2 \rangle}{K} \sin(\alpha_d) \quad \text{eq 2.27}$$

where:

$K$	=	absolute calibration constant
$\langle A^2 \rangle$	=	average pixel intensity
$\sigma^0$	=	distributed target sigma nought
$\alpha_d$	=	distributed target incidence angle

for complex slant-range projected products:

For all complex slant-range projected products except for APS products:

$$\sigma^0 = \frac{\langle A^2 \rangle}{K} \frac{1}{G^2(\theta_d)} \left( \frac{R_d}{R_{ref}} \right)^3 \sin(\alpha_d) \quad \text{eq 2.28}$$

where:

$K$	=	absolute calibration constant
$\langle A^2 \rangle$	=	average pixel intensity
$\sigma^0$	=	distributed target sigma nought
$G^2(\theta_d)$	=	two-way antenna gain at the distributed target look angle $\theta_d$
$R_d$	=	distributed target slant range distance
$R_{ref}$	=	reference slant range distance (800km for all beams and modes)
$\alpha_d$	=	distributed target incidence angle

For APS products, an additional factor ( $R_d/R_{ref}$ ) has to be taken into account:

eq 2.29

$$\sigma^0 = \frac{\langle A^2 \rangle}{K} \frac{1}{G^2(\theta_d)} \left( \frac{R_d}{R_{ref}} \right)^4 \sin(\alpha_d)$$

Point targets radar cross section sigma:

for ground range projected products:

$$\sigma = I_p \cdot \frac{P_{Agr}}{K} \cdot \sin(\alpha_p) \quad \text{eq 2.30}$$

where:

$I_p$	=	background corrected integrated power of the point target. It is obtained as the sum of the pixel intensities – after background intensity correction– over a square area of 20 by 20 resolution cells centred around the peak of the point targets impulse response function.
$K$	=	absolute calibration constant
$P_{Agr}$	=	ground range pixel area
$\alpha_p$	=	incidence angle at transponder position

for complex slant-range projected products:

For all complex slant-range projected products except for APS products:

$$\sigma = I_p \cdot \frac{P_{Asr}}{K} \cdot \left( \frac{R_p}{R_{ref}} \right)^3 \cdot \left( \frac{1}{G^2(\theta_p)} \right) \quad \text{eq 2.31}$$

For APS products, an additional factor  $(R_p/R_{ref})$  has to be taken into account:

eq 2.32

$$\sigma = I_p \cdot \frac{P_{Asr}}{K} \cdot \left( \frac{R_p}{R_{ref}} \right)^4 \cdot \left( \frac{1}{G^2(\theta_p)} \right)$$

## 2.11.6 Notes

[1] P1, P2 and P3 amplitudes are derived by averaging all samples within 3dB of the maximum pulse amplitude. P1A amplitudes are averaged over the whole calibration window length in the current PF-ASAR implementation. In reality P1A pulse levels are significantly above the noise floor and therefore the amplitude averaging should be performed as for the other three calibration pulse types.

## 2.11.7 References

**Ref 2.12**

R. Torres, C. H. Buck, J-L. Suchail, M. Zink, "In-Orbit Calibration and Maintenance of the ENVISAT ASAR Antenna Beams", Proc. of CEOS SAR Workshop 2001, Tokyo, Japan, 2.-5. April 2001.

**Ref 2.13**

J-L. Suchail, C. Buck, A. Schnenberg, R. Torres, M. Zink, ESA/ESTEC. "The ASAR Instrument Verification: Results from the Pre-Flight Test Campaign". Proc. CEOS SAR Workshop April 2001, Tokyo, Japan.

**Ref 2.14**

H Jackson ESA/ESTEC, I. Sinclair, S. Tam. MPB Technologies Inc. "ENVISAT ASAR Precision Transponders". CEOS SAR Workshop 26-29 October 1999, ESA-SP450

**Ref 2.15**

M. Zink & J. Closa & B. Rosich, "ASAR Internal Calibration and PF-ASAR Normalisation". Technical Note 30 November 2001, issue 2, revision 0.

## 2.12 ASAR Data Handling Cookbook

This section of the handbook is to be completed in a future revision. Topics to include the following:

### Hints and Algorithms for Data Use

- Extracting Grid Information To Do Plots
- Locating the Error Information
- Converting Units of Engineering/Geophysical parameters
- Displaying 'Scientific' PCD Information

### Hints and Algorithms for Higher Level Processing

#### 2.12.1 Hints and Algorithms for Data Use

##### 2.12.1.1 Extracting Grid Information To Do Plots

### 2.12.1.2 Locating the Error Information

### 2.12.1.3 Converting Units of Engineering/Geophysical parameters

### 2.12.1.4 Displaying 'Scientific' PCD Information

## 2.12.2 Hints and Algorithms for Higher Level Processing

---

# Chapter 3

## The ASAR Instrument

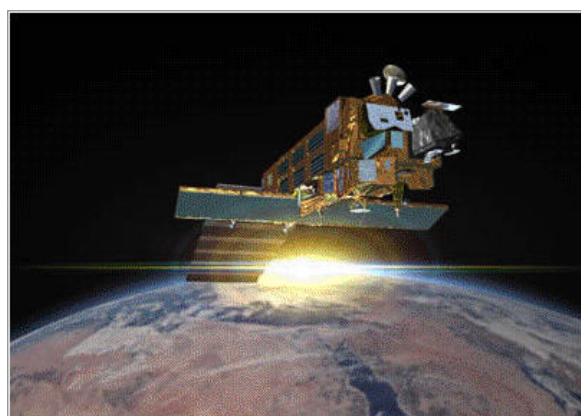


Figure 3.1 Envisat Satellite (Artist's view)

Discussion of the ASAR instrument description, functionality, characteristics, and performance expectations will be found in the following sections.

## 3.1 Instrument Description

### Principle of Operation

The [radar antenna beam](#) illuminates the ground to the right side of the satellite. Due to the satellite motion and the [along-track](#) (azimuth) beamwidth of the antenna, each target element only stays inside the illumination beam for a short time. As part of the on-ground processing, the complex echo signals received during this time are added coherently. This process is equivalent to a long antenna (so called Synthetic Aperture) illuminating the target. This synthetic aperture is equal to the distance the satellite travelled during the integration time.

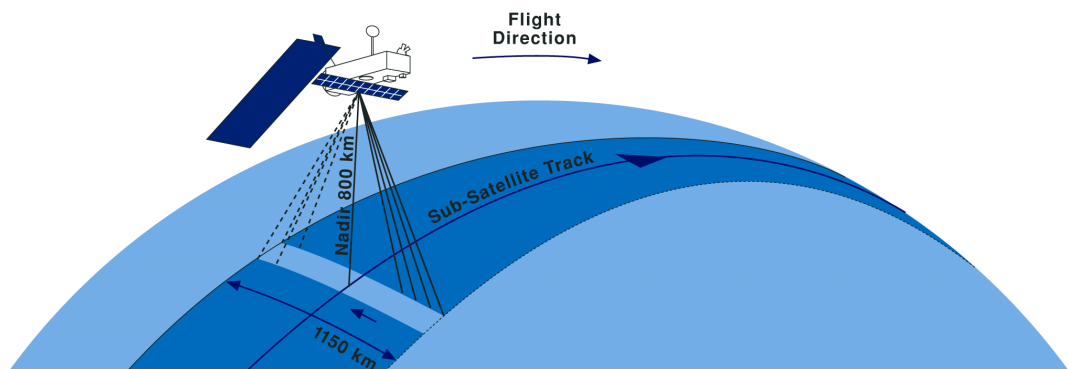


Figure 3.2 Subsatellite Track

The along-track (equivalent to the azimuth in the ground processing) [resolution](#) obtainable with the SAR principle is half the physical antenna length. The achieved resolution can be traded off against other [image](#) quality parameters (such as the radiometric resolution).

The [across-track](#) or [range resolution](#) is a function of the transmitted radar bandwidth. [Pulse compression](#) techniques are used to improve the performance taking into account the instrument peak power capability. The fact that the end-to-end system works coherently means that both the [amplitude](#) and the [phase](#) relationships between the complex transmitted

and received signals are maintained throughout the instruments and the processing chain. This facilitates aperture synthesis, as well as multi-pass radar interferometry, using pairs of images taken over the same area at different times.

### General Description

The Advanced [Synthetic Aperture Radar](#) (ASAR) was built upon the experience gained with the ERS-1/2 [Active Microwave Instrument](#) (AMI) to continue and extend Earth observation with SAR. ASAR is a high-resolution, wide-swath [imaging radar](#) instrument that can be used for site-specific investigations as well as land, sea, ice, and ocean monitoring and surveillance.

Compared to ERS AMI, which is a single-channel, fixed-geometry instrument, the ASAR instrument provides a number of technological improvements. Significant advances have been made in both system flexibility and the scientific value of its data sets, employing a number of new technological developments that allow extended performance. The most challenging advancement has been the replacement of the centralised high-power amplifier, combined with the wave guide slot passive radiator array of the AMI, by an active phased-array antenna system using distributed elements. Transmit/Receive (T/R) modules are arranged across the antenna such that, by adjusting the gain and phase of individual modules, the transmit and receive beams may be steered and shaped, allowing the selection of different [swaths](#) and providing a swath coverage of over 400-km wide using ScanSAR techniques.

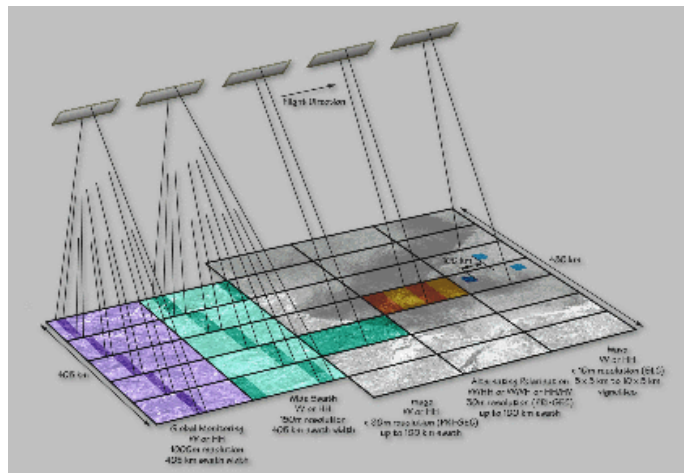


Figure 3.3 ASAR operational mode swaths

ASAR is also equipped with programmable digital waveform generation, which will allow optimisation of the product radiometric quality. Another improvement, compared to ERS, is an 8 bit Analog-to-Digital Converter (ADC) associated with a Flexible Block Adaptive Quantiser (FBAQ) to be used in 8/4 and 8/2 compression ratio that will allow the collection of a larger dynamic range of input signals within the data rate constraints.

The two pictures below show the ASAR Flight Model (FM) Antenna. The first ([figure 3.4](#)) shows the antenna during radiation testing at ASTRIUM Portsmouth and the second ([figure 3.5](#)) shows it after a deployment test.



Figure 3.4 ASAR FM antenna during radiation testing (Image by courtesy of ASTRIUM Ltd)



Figure 3.5 ASAR FM antenna after deployment test (Image by courtesy of ASTRIUM Ltd)

The ASAR instrument comprises two functional groups: the Antenna Subassembly (ASA) and the Central Electronics Subassembly (CESA), with subsystems as shown in the functional block diagram below ([figure 3.6](#)).

The active antenna contains 20 Tiles with 16 Subarrays each equipped with a

Transmit/Receive (T/R) module. The instrument is driven by the [Control Subsystem](#) (CSS), which provides the command and control interface to the spacecraft, manages the distribution of the operational parameters (such as transmit pulse characteristics and antenna beam-set), and generates the instrument operation timeline.

The transmit pulse characteristics are set in the Data Subsystem (DSS) the output of which is an up-chirp pulse centred on the IF carrier (124 MHz). In the [RF Subsystem](#) (RF S/S) the pulse is up-converted to the RF [frequency](#) (5.331 GHz) and amplified. The signal is then passed to the Tile Subsystem (TSS) through a waveguide distribution network (RFPF) and subsequently, within the tile, to each individual [T/R](#) module using a microstrip corporate feed. The T/R modules apply phase and gain characteristic according to the pre-selected beam settings transferred from the Control Sub-System and stored in the Tile Control Interface Unit (TCIU).

In receive the RF-echo signal follows the reciprocal path down to the Data Sub-System where the raw science data are generated and provided to the spacecraft interface.

## ASAR INSTRUMENT SYNOPTIC DIAGRAM

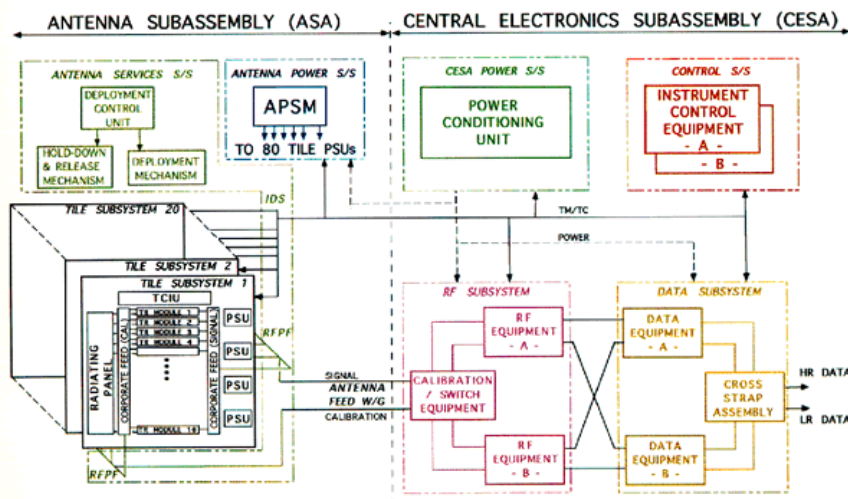


Figure 3.6 ASAR instrument synoptic diagram

The [ASA 3.1.1.1](#), and [CESA 3.1.1.2](#), subsystems, which are described in the "[Payload Description, Position on the Platform](#)" [3.1.1](#), section to follow, are comprised of the following primary components:

### ASA Subsystem

- Antenna Services Subsystem (ASS)
- Tile Subsystem (TSS)

- Antenna Power Switching and Monitoring Subsystem (APSM)
- CESA Subsystem
- Data Subsystem
- Radio Frequency subsystem (RFSS)
- Control Subsystem (CSS)

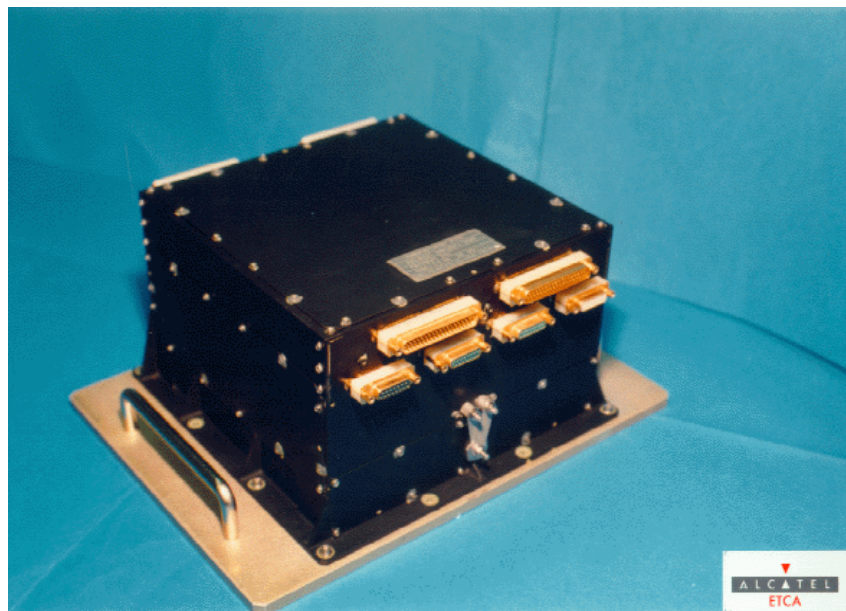


Figure 3.7 Power Conditioning Unit (PCU)

The ENVISAT ASAR system will benefit from the on-board availability of a Solid State Recorder, allowing up to 10 minutes recording of ASAR high rate modes (100 Mbit/s) at any point around the orbit. Finally, the orbit determination system on the DORIS instrument will allow for accurate geolocation of all ASAR products produced in near real-time (NRT) or off-line.

The main new technical features are:

- Instrument enhancements that include a digital chirp generator (programmable from 200 kHz to 16 MHz) and an improved linear dynamic range.
- Flexible swath positioning; offering the choice between several image swath positions at various distances from the subsatellite track, with different incidence angles.
- Dual polarisation; offering horizontal (HH) & vertical (VV) or cross polarisation (HH&HV or VV&VH) operation.
- Wide swath coverage; 405 km swath with 150 m or 1 km resolution.
- Enhanced Wave Mode with imagettes acquired at 100 km intervals along-track.
- Extended operating time at high-resolution (30 minutes of operation; 10 minutes in eclipse).
- Global SAR coverage; possible using the solid state recorder or data relay satellite.

### 3.1.1 Payload Description and Position on the Platform

The Advanced Synthetic Aperture Radar (ASAR), operating at C-band, ensures continuity with the Image Mode (SAR) and the Wave Mode (WM) of the ERS-1/2 sensor. As explained in earlier sections, it features enhanced capability in terms of coverage, range of incidence angles, polarisation, and modes of operation.

The picture below shows the ENVISAT satellite and the relative position of the instruments on board:

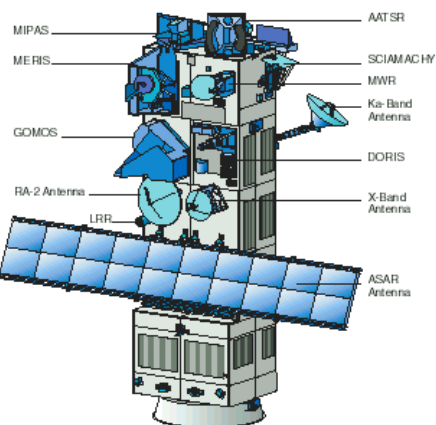


Figure 3.8 ENVISAT payload locations

ASAR consists of a coherent, active phased array antenna that is mounted with the long axis of the antenna aligned with the satellite's flight direction, or Y-axis. ( see [figure 3.2](#) "Subsatellite Track" in the previous section entitled "ASAR Instrument Description" and [Figure 3.9](#) below). The SAR antenna, with its two-dimensional beam pattern, will image a strip of ground to the right side of the flight path which has potentially unlimited content in the direction of motion, which is the azimuth direction, but is bounded in the orthogonal, or range, direction by the antenna elevation beamwidth. The objective of the SAR system is to produce a two-dimensional representation of the scene reflectivity at high-resolution, with axes defined in both the range and azimuth directions.

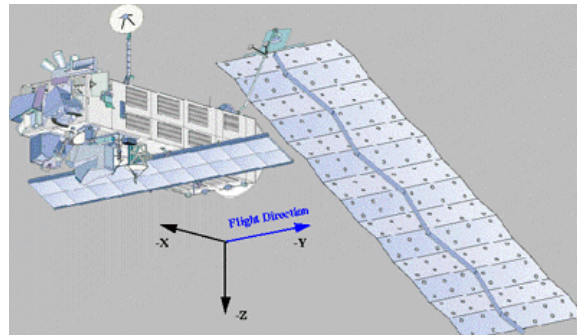


Figure 3.9 ASAR antenna

A coherent, active phased array SAR, is mounted with the antenna long axis aligned with the satellite's flight direction (i.e., Y-axis)

### 3.1.1.1 ASA Subsystem

The ASAR active antenna is a 1.3 m x 10 m phased array. The antenna consists of five 1.3 m x 2 m panels which are folded over for launch. Each panel is formed by four 0.65 m x 1 m tiles mounted together. Each tile consists of 16 linear subarrays of 24 dual-polarised radiating elements. Each subarray is connected to a T/R module with independent connection for the two polarisations.

As indicated in the [synoptic diagram 3.6](#) shown in the previous section entitled "[ASAR Instrument Description 3.1.](#)," the Antenna Subassembly (ASA) consists of three primary components:

- [Antenna Services Subsystem \(ASS\)](#)
- [Tile Subsystem \(TSS\)](#)
- [Antenna Power Switching and Monitoring Subsystem \(APSM\)](#)

It is one of the two main functional subsystems within the ASAR instrument, with the [CESA subsystem 3.1.1.2.](#) working along side it. The primary units of the ASA subsystem are described below.

#### Antenna Services Subsystem (ASS)

The antenna is based on a mechanical structure consisting of five rigid Carbon Fibre Reinforced Plastic (CFRP) frames and a RF distribution network consisting of two similar sets of CFRP waveguides running in parallel along the five panels (RFPF). In launch configuration, the five panels are stowed, folded over a fixed central one, and are held

---

together by eight Hold-Down and Release Mechanisms (HRM) up to a preload of 31 kN. In order to avoid coupling with the launcher, this guarantees the first axial vibration mode frequency to be higher than 42 Hz.

Each HRM consists of a retractable telescopic tube levered by a secondary mechanism based on a non-pyrotechnic device (kevlar cable cut by a redundant thermal knife with a cutting time of less than 120 sec.) derived from well-proven solar array hold-down technology.

After release, the panels are sequentially deployed around four hinge lines by using a stepper motor, each, with 200:1 reduction harmonic drive, thus providing a high motorisation margin (approximately 3 times the expected resistive torque). The final latching is performed with the eight builtin latches to achieve the final antenna planarity of  $\pm 4$  mm in orbit (this including an apportionment of  $\pm 1.5$  mm for the overall thermoelastic effects). Associated to inter-panel contact points, the latches ensure waveguide flange alignment and deployed rigidity of higher than 2.4 Hz to avoid AOCS disturbances. A specific unit (DCU) contains the electronics for driving and controlling the release, deployment and latching operations.

Each HRM consists of a retractable telescopic tube, levered by a secondary mechanism based on a non-pyrotechnic device derived from well-proven solar array hold-down technology

The ASS is comprised of the following primary components:

- Antenna Mechanical Structure (AMS)
- RF Distribution Network (RFPF)
- Hold-Down and Release Mechanism (HRM)
- Deployment Mechanism (DEM)
- Deployment Control Unit (DCU)
- Antenna Harness



Figure 3.10 Antenna Mechanical Structure (AMS)

### Tile Subsystem (TSS)

Each of the twenty tiles is a self-contained full-operating subsystem which contains 4 power units (PSUs), a local control unit (TCIU), 2 RF distribution corporate feeds and 16 subarrays each one fed by a T/R module. The 16 subarrays are mounted together on a panel (the Radiating Panel) that provides the structural and thermal integrity to the tile.

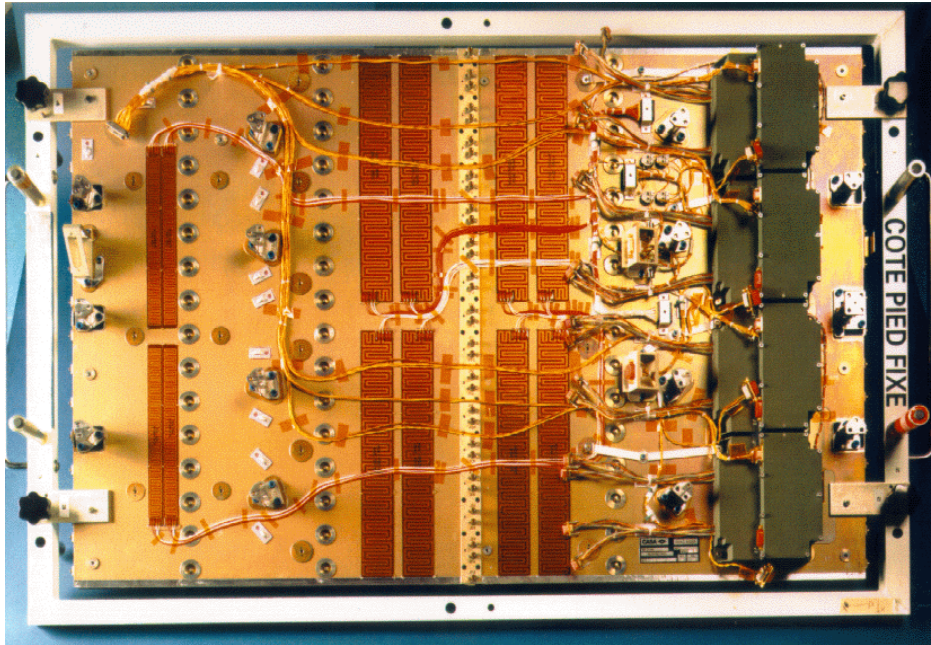


Figure 3.11 Tile (Image courtesy of Alcatel-Telecom)

The corporate feeds (one for signal distribution and another for calibration) are 1:16 power dividers made in microstrip on Duroid 6002. Each of the four Power Supply Units (PSU) provides power to a group of four T/R Modules and the TCIU. The control functions within the Tile are achieved by a Tile Control Interface Unit (TCIU) which is carrying out local control of the T/R Modules including temperature compensation and beamforming setting, it is transferring data and interfacing to the Control Subsystem. There is one TCIU per Tile using internal duplication for redundancy purposes. A picture of one of the ASAR transmit tiles, ready for radiation testing, is shown in [figure 3.12](#) below.

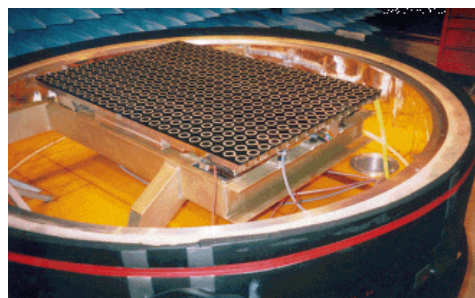


Figure 3.12 ASAR Transmit Tile (Image by courtesy of Alcatel)

## Radiating Panel

The subarrays and the modules are mounted on a supporting plate, thermally and mechanically decoupled. The subarrays are formed by 24 1-diameter ring slot radiating elements, electrically coupled to a dualpolarisation low-loss dispersion-free triplate feeding system which provides a constant phase and amplitude illumination.

The measured radiating characteristics of the subarrays are showing a gain of 20.5 dB, loss of 1.5 dB, VSWR of 18 dB and a very good crosspolarisation better than 35 dB for both polarisations.

## Transmit/Receive Module



Figure 3.13 ASAR Transmit/Receive Module (Image by courtesy of Alcatel)

The T/R module receive signals passed to it from the RF subsystem, within the CESA subsystem. The T/R modules apply phase and gain changes to the signal in accordance with the beam forming characteristics which have been given by the TCIU. For an active antenna, the amplitude and phase characteristics of the T/R Modules vary principally as a function of temperature. To handle this, fluctuation the instrument includes a scheme to compensate for drifts over the temperature range. For this purpose, the temperature of each T/R module is monitored and utilised by the TCIU to compensate for the amplitude and phase variations. This scheme provides the antenna with a high degree of stability. The signal is then power-amplified and passed to the radiator panel.

Echo signals are received through the same antenna array passing to the T/R modules, for low noise amplification and phase and gain changes, which determine the receive beam shape. The outputs from each module are then routed at the RF, via the corporate feed, and the antenna RF distribution system, which acts as a combiner effectively adding signal inputs coherently and noise inputs incoherently.

Each module consists of two (H/V) transmit and one common receive chains, which amplify and control the signal of each individual subarray, in phase and amplitude. These functions are implemented using MMIC's, glued on etched TMM10i circuits, component

---

interconnections performed by using parallel-gap welding (Au and Ag ribbons).

The input Phase Shifter (5 bits) is controlling the Tx/Rx signal, a SP3T switch selects either Tx (H/V) or Rx chains. On the Tx chain a Variable Gain Amplifier (VGA) provides 42 dB of control range, followed by a medium power driver. A Telettra Power Amplifier (SSPA of 10 W at 1 dB compression, 30% efficiency), provides the final output power. The connection to the subarrays is made via a Circulator/Isolator/Passive-Limiter (0.25 dB insertion loss in Tx, 1 dB in Rx, 35 dB isolation). On the receive side, a 1.3 dB NF LNA (CFY67 HEMT) is connected to the limiter, a SPDT switches the V/H chain to the common Rx path which includes a third VGA. For Calibration Purposes, a coupler (-24 dB) has been implemented at the output of the module to the antenna. The T/R Module is commanded by a serial link consisting of 3 signals: a data signal, a gated control signal and a strobe signal. The temperature of each T/R Module is monitored and used for correction of amplitude and phase setting.

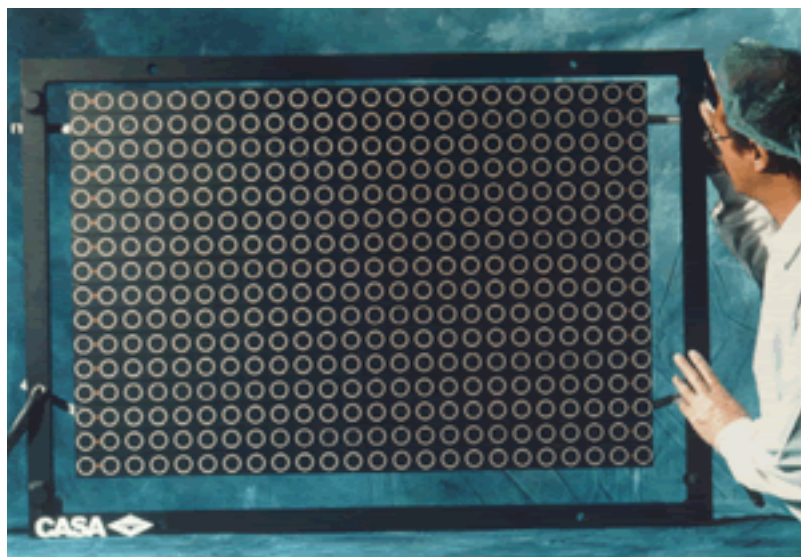


Figure 3.14 Supporting Plate

### Antenna Power Switching and Monitoring Subsystem (APSM)

The APSM forms the heart of the antenna power distribution controlling the power input to 80 tile power supplies. Each tile PSU is independently switched under full control from the instrument central electronics. Current monitoring occurs on two levels. The first, at each tile PSU interface ensures that hazardous loads are disabled autonomously within a few hundred micro-seconds. Secondary protection is provided through current telemetry back to the central processor, which checks against expected limits and commands switch-off in the event

---

that they are exceeded. The setting of the APSM autonomous current trip level required careful attention since it was simultaneously required to guarantee the safety of the tile PSU in the event of anomalous loads, while ensuring adequate availability. That is, not switching off under extreme conditions of component tolerance, temperature or peak ripple current.

### 3.1.1.2 CESA Subsystem

As indicated in the [synoptic diagram 3.6](#) shown in the previous section entitled "ASAR Instrument Description," the Central Electronics Subassembly (CESA) consists of three subsystems:

- Data Subsystem
- Radio Frequency (RF) Subsystem
- Control Subsystem (CSS)

It is one of the two main functional subsystems within the ASAR instrument, with the [ASA subsystem 3.1.1.1](#), working along side it.

The CESA is in charge of generating the transmitted chirp, converting the echo signal into measurement data, as well as controlling and monitoring the whole instrument.

Compared to ERS-1 and ERS-2, which used Surface Acoustic Wave devices for analog chirp generation and On Board Range Compression, ASAR uses digital technologies for on-board chirp generation and data reduction. A fundamental advantage of using digital chirp generation is the inherent flexibility of such a design which allows for chirp versatility in terms of pulse duration and bandwidth, thus accommodating efficiently the various requirements associated with the high number of available operational modes and swaths of the instrument.

In order to optimise raw data transfer, the data equipment also contains science memory, where the echo samples are temporarily stored before their transmission to the on-board recorders.

#### 3.1.1.2.1 Data Subsystem

At reception, the echo signal is first filtered and down-converted in the Radio Frequency (RF) Sub-System, then demodulated into the I & Q components of the carrier. These two signals are then both digitised into 8-bit samples. If required, it is then possible to perform digital decimation of the samples, in order to reduce the data stream, such as in Global Monitoring Mode where the transmit bandwidth is low. Following this decimation, a Flexible Block Adaptive Quantiser (FBAQ) compression scheme is applied to the echo samples.

The transmit pulse characteristics are set within the data subsystem by coefficients in a digital

chirp generator, which supplies in-phase (I) and quadrature (Q) components. The output of the data subsystem is a composite up-chirp centred at the IF carrier.

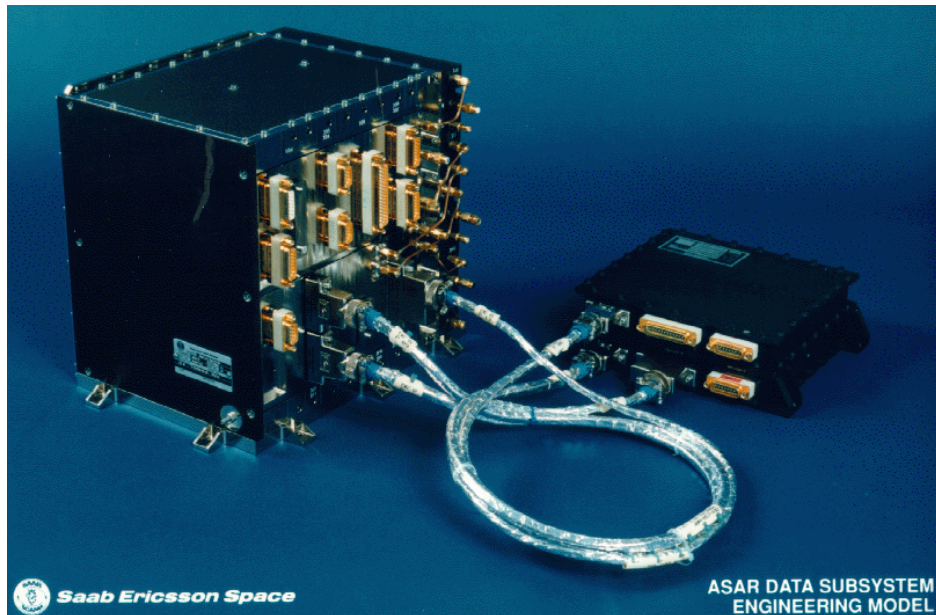


Figure 3.15 Data Subsystem

The signal is then passed on to the RF Subsystem where the coherent RF/IF conversion of the RF echo signals is performed in the downconverter. I/Q detection of the Intermediate Frequency (IF) echo signal is accomplished in the demodulator of the data subsystem. The resulting baseband I/Q signals are further processed in the data subsystem, which performs filtering, digitalization, and compression of this data. After buffering and packetizing, the echo data is transmitted to the measurement data Interface (I/F).

### 3.1.1.2.2 Radio Frequency (RF) Subsystem

When the signal is passed on to the RF Subsystem, it is mixed with the local oscillator frequency to generate the RF signal centred on 5.331 GHz. The upconverted signal is routed via the calibration/switch equipment to the antenna signal feed waveguide.

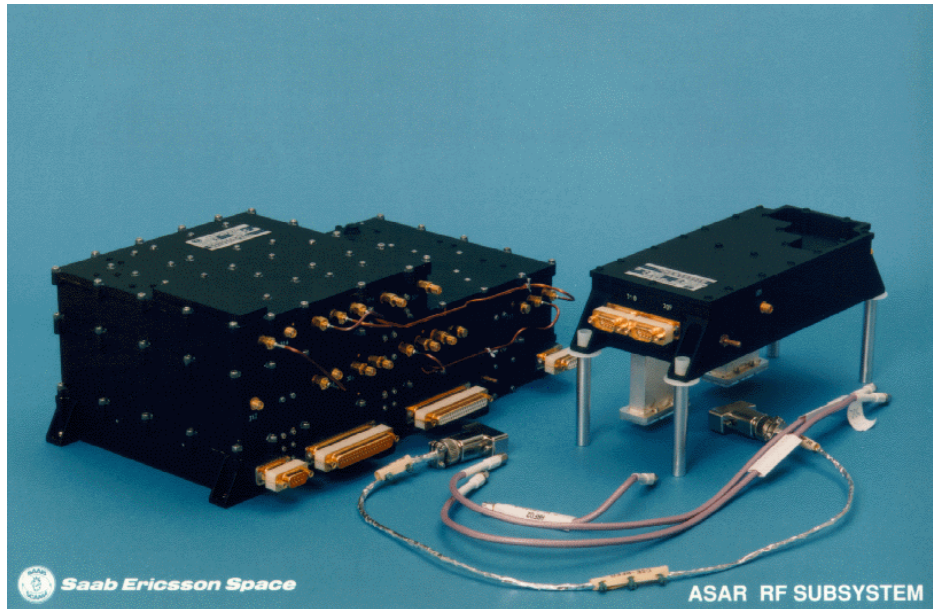


Figure 3.16 RF Subsystem

The upconverted signal is then routed, via the calibration/switch equipment, shown in [figure 3.17](#) below, to the antenna signal feed waveguide. At the antenna the signal is distributed by the RF panel feed waveguide network to the tile subsystems within the ASA Subsystem.

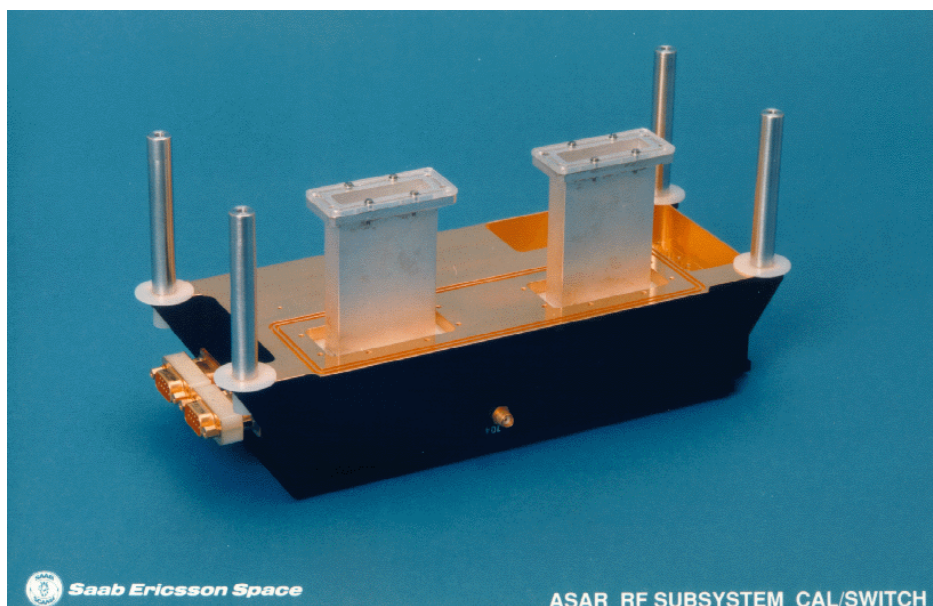


Figure 3.17 Calibration/switch equipment

### 3.1.1.2.3 Control Subsystem (CSS)

The instrument is driven by the Control Subsystem (CSS), which provides the command and control interface to the spacecraft, maintains the database, manages the distribution of the operation parameters, and generates the time-lining of the instrument.

The ASAR instrument is controlled by its instrument control equipment (ICE), which provides the command and control interface to the satellite. Macrocommands are transferred from the payload management computer to the ICE where they are expanded and queued. The ICE maintains and manages a database of operation parameters, such as transmit pulse and beam characteristics, for each swath of each mode as well as timing characteristics, such as pulse repetition frequencies and window timings. The ICE downloads parameters from the database during transition to the operation mode and provides the operational control of the ASAR equipment, including the control of power and telemetry monitoring.

### 3.1.1.2.4 Power Conditioning Unit (PCU)

Shown in [figure 3.18](#) below, provides a regulated supply to the data subsystem and the RF subsystem, as well as auxiliary power to the antenna power switching and monitoring unit.

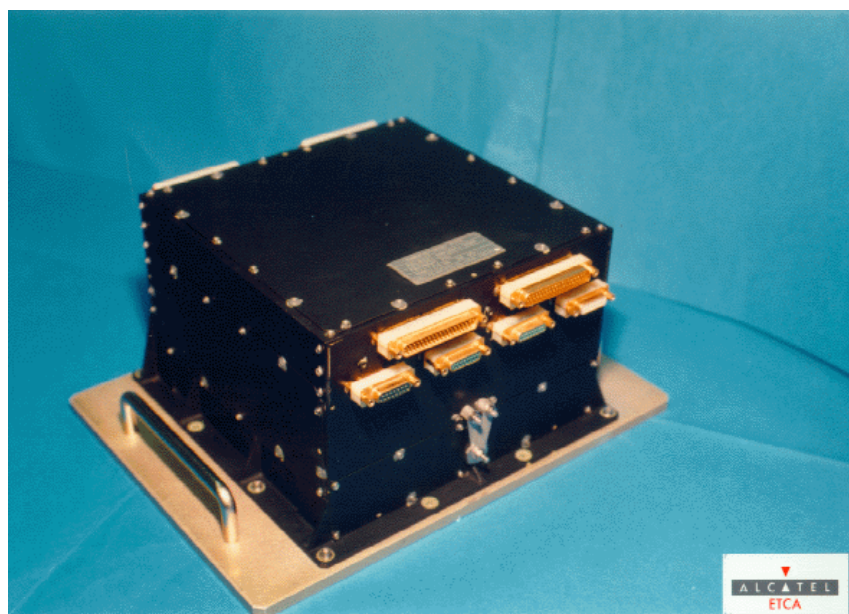


Figure 3.18 Power Conditioning Unit (PCU)

### 3.1.2 ASAR Instrument Functionality

ASAR will provide continuity of the [ERS SAR Image](#) and Wave Modes, but with the opportunity for better temporal [frequency](#) of coverage. The nominal 30 m spatial [resolution](#) and [swath](#) coverage of the ASAR Image Mode (100 km) and Wave Mode (5 km) are the same as the ERS Image Mode, and ASAR will also be on a 35 day repeat orbit.

ASAR has five mutually exclusive modes of operation and offers, by exploiting the combinations of polarisations and incidence angles, 37 different and mutually exclusive operating modes in high, medium (Wide Swath Mode), and reduced (Global Monitoring Mode) resolution. These modes are operated mainly in response to user requests. Wave mode is mutually exclusive with respect to all the other modes. It is a low-rate mode operated systematically over oceans as part of the Global Mission. ( See [figure 3.3](#) in the section entitled "Instrument Description" ).

Global Monitoring and Wave Modes are recorded systematically when operated. ASAR high- and medium-resolution imaging modes are either transmitted on a real-time link (direct [X-band](#) or via Artemis Ka-band link) or recorded on the on-board solid state recorder for ground data recovery. The high- and medium-resolution data is acquired only when required to satisfy either a background mission scenario and/or user requests. The operation modes are divided into two categories:

#### 3.1.2.1 Global Mission

These modes have a low data rate (data generation of 0.9 Mbps) with systematic on-board recording and operational capability of up to 100% of the orbit. The two modes, GM and WV described below, are systematically recorded to an on-board tape recorder that is dumped every orbit under visibility of an ESA Station, such as the Kiruna Station in Sweden or the ESRIN Station, in Italy.

- Global Monitoring Mode (GM)

The [Global Monitoring Mode](#) provides [low-resolution](#) images (1 km) using the [ScanSAR](#) technique, over a 405 km swath, at HH or VV polarisation. As explained above, this mode has a low data rate due to a slightly reduced [along-track](#) duty ratio and the use of digital filtering for reduction in the [across-track](#) direction. The same subswaths as those defined for the [Wide Swath](#) (WS) Mode are used.

- Wave Mode (WV)

In Wave Mode, the ASAR instrument measures the changes in [backscatter](#) from the sea

---

surface due to ocean wave action. Therefore, it will generate vignettes with a minimum size of 5 km x 5 km, similar to the ERS [AMI](#) Wave Mode, spaced 100 km along-track in HH or VV polarisation. The position of the wave vignette across-track being selected as either constant or alternating between two across-track positions over the full swath range.

### 3.1.2.2 Regional Mission

These modes are high data rate (downlink rate of 100 Mbps) modes for narrow swath, like the Image Mode (IM) and [Alternating Polarisation](#) (AP) modes, or for the Wide Swath (WS) mode, with operation time up to 30 minutes per orbit (including 10' in eclipse). The high-rate mode data is recovered according to one of the following schemes:

- real transmission via an X-band link to ESA
- another station
- real-time transmission via tire Ka-band link using the Artemis Data Relay Satellite to the ESA ESRIN Station in Italy
- recorded on board the Solid State Recorder and dump in X- or Ka-band link in visibility of an ESA station
- Image Mode (IM)

In Image Mode, the ASAR generates high spatial resolution products (30 m) similar to the ERS SAR. It will image one of the seven swaths located over a range of incidence angles spanning from 15 to 45 degrees in HH or VV polarisation.

#### Alternating Polarisation Mode (AP)

Alternating Polarisation Mode provides high-resolution products in any swath, as in Image Mode, but with polarisation changing from subaperture to subaperture within the synthetic aperture. Effectively, a ScanSAR technique is used but without varying the subswath. The results are in two images of the same scene in different polarisation combinations (HH/VV or HH/HV or VV/VH) with approximately 30 m resolution (except IS1). Radiometric resolution is reduced compared to Image Mode.

#### Wide Swath Mode (WS)

In the Wide Swath Mode, the ScanSAR technique is used, providing images of a wider strip (405 km) with medium-resolution (150 m) in HH or VV polarisation. The total swath consists of five subswaths and the ASAR transmits bursts of pulses to each of the subswaths in turn in such a way that a continuous along-track image is built up for each subswath.

The ERS high-resolution products PRI, SLC, and GEC will be continued for Image Mode, and generated for Alternating Polarisation Mode on user request. The Wave Mode products are continued, and their quality improved, thanks to cross-spectra algorithms.

Within each mode, several different image swaths may be used. The swath layout is depicted in [figure 3.19](#) below.

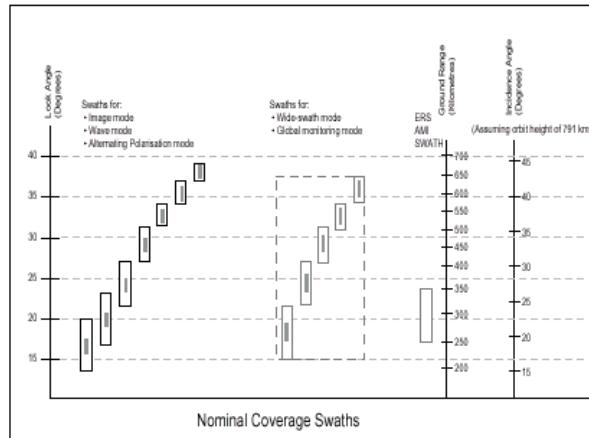


Figure 3.19 ASAR swath designations

In addition, ASAR supports 2 Auxiliary Modes, known as Test Mode and Module Stepping Mode, and one Calibration Mode, known as External Characterisation Mode. As their names imply, these are used for testing, calibration and instrument monitoring. Finally, one of five possible on-board data quantisation methods may be used for each mode, though each has a default choice which will be used in most cases.

The nominal characteristics of the various ASAR measurement modes are summarised in [table 3.1](#) below:

Table 3.1 Nominal ASAR characteristics

Image Mode (IM)	VV or HH polarisation images from any of 7 selectable swaths. Swath width between approximately 56 km (swath 7) and 100 km (swath 1) across-track. Spatial resolution of approximately 30 m (for precision product).
Alternating Polarisation Mode (AP)	Two co-registered images per acquisition, from any of 7 selectable swaths. HH/VV, HH/HV, or VV/VH polarisation pairs possible. Spatial resolution of approximately 30 m (for precision product).
Wide Swath Mode (WS)	400 km by 400 km wide swath image. Spatial resolution of approximately 150 m by 150 m for nominal product. VV or HH polarisation.
Global Monitoring Mode (GM)	Spatial resolution of approximately 1000 m in azimuth by 1000 m in range for nominal product. Up to a full orbit of coverage. HH or VV polarisation.
Wave Mode (WV)	A small imagede (dimensions range between 10 km by 5 km to 5km by 5km) is acquired at regular intervals of 100 km along-track. The imagede can be positioned anywhere in an Image Mode swath. Up to two positions in a single swath or in different swaths may be specified, with acquisitions alternating between one and the other (successive imagedes will hence have a separation of 200 km between acquisitions at a given position). HH or VV polarisation may be chosen. Imagedes are converted to wave spectra for ocean monitoring.

### 3.1.3 Internal Data Flow

#### ASAR Data Processing

All of the ASAR modes of operation are processed on the ASAR Generic Processor to be installed in the ESA Payload Data Handling Stations (PDHS), at Kiruna and ESRIN-Frascati, and to be procured by the ENVISAT Processing and Archiving Centres (PACs) and national stations offering ESA ASAR services. The use of a generic processor will ensure product compatibility between the different processing centres (same format and processing algorithm) and will simplify product validation.

The ASAR generic processor runs on an IBM SP-2 parallel computer system and is designed to ensure a throughput linearly proportional to the number of processing nodes available in the station.

The key feature of the ASAR Generic Processor is the capability to process acquired data to generate medium-resolution products (150 m) or low-resolution product (1 km), and their corresponding browse products, in Stripline without geometric or radiometric discontinuity.

The ASAR ground processor functional block diagram is shown below in [figure 3.20](#).

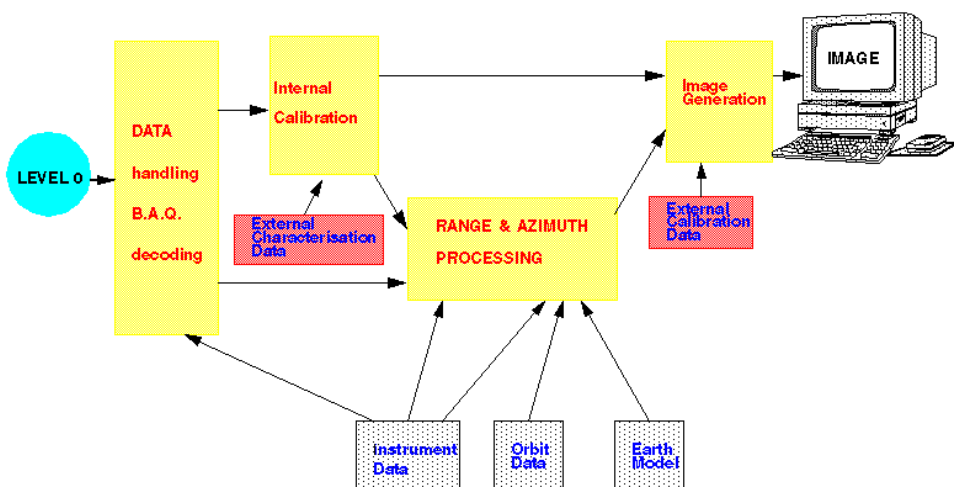


Figure 3.20 ASAR ground processor functional block diagram

#### ASAR User Services

---

The access to user services is provided via the Internet and it includes, in particular, a free access to all browse images and the capability to access the data inventory.

The user services allow ordering of products from acquired data and the ordering of future products to be acquired. The on-line retrieval of small products is also possible.

The delivery of products is performed in Near Real Time (NRT) via satellite links and off-line on physical media.

For a full discussion of the ASAR products, and the processes that produce them, refer to the ["Products and Algorithms" \(Chapter 2.\)](#) section of this handbook.

## 3.2 Instrument Characteristics and Performance

This section of the Reference Guide describes the characteristics and performance of the ASAR instrument. It is split into two sections (see index)

### 3.2.1 Preflight Characteristics and Expected Performance

Compared to the ERS AMI-SAR, ASAR offers five different modes of operation, dual polarization and a total of seven beams with a combined ground-range of 485km covering incidence angles from 15° to 45°. In spite of this substantial increase in functionality, the intention from the outset was that there would be no significant degradation in the various performance parameters such as spatial and radiometric resolution, sensitivity and ambiguity suppression compared to ERS.

As a result and in order to be convinced that this high goal would be met, performance prediction analyses have been repeatedly made and updated since the earliest days of the project using principally the specially developed [PEAS](#) software (Performance Evaluation and Assessment Software).

Confidence in the results obtained using PEAS is high, thanks to independent corroborative analyses and comparison, where possible, of the predictions and measurements made on the

FM instrument.

Performance Objectives are shown in [Level 1B Accuracy 2.6.1.3.](#).

#### Performance Prediction Methodology

The ASAR antenna with its 320 [T/R](#) modules requires a different philosophy when determining performance than say, ERS, since instead of a single point failure it has 320. That being said, it is reasonable to assume that not all of the modules will survive launch and four years of continuous operation. This forms the basis of the performance analysis philosophy the aim of which is to predict the worst case expected performance at end of life following a period of so-called graceful degradation.

To achieve this, two main issues with respect to the T/R modules are considered, namely: module failure and phase and [amplitude](#) setting errors.

#### Module Failure

From assessments of component reliability a figure of 6% failure rate has been estimated by industry for the T/R modules at end-of-life. This corresponds to about 20 failed modules.

#### Module Setting Errors

Each T/R module can be set to provide a certain [phase](#) and amplitude in order to generate the required elevation [beam](#) patterns. Six bits are available the required phase from 0° to 360° and a further six to specify the amplitude in the range 0 to -20dB. From measurements made at component and instrument level it has been determined that the phase setting accuracy is approximately ±5° and the amplitude setting accuracy approximately ±0.5dB..

#### Generating "End-of-Life" Antenna Patterns

In order to model accurately the impact of T/R module failures and setting errors on the ASAR performance it is possible to create a failure/error matrix representing the antenna and use it in producing representative simulated elevation beam patterns. Each pattern thus generated would have a slightly different shape to the one desired with some sidelobes becoming larger and nulls appearing at different look angles. The problem with this approach is clearly the extremely large number of possible permutations of failures and setting errors.

Instead, the method chosen was to calculate a disturbance level which could be applied linearly to the calculated elevation patterns with the effect of increasing sidelobe levels and "filling-in" nulls.

Ideally T/R modules would fail in an evenly distributed random pattern across the antenna. However, the possibility that failures might be clustered could not be ignored. This was accounted for by calculating the variance in the sidelobe level as a result of failures and basing the disturbance level to be applied on a 90% probability (two standard deviations) of the antenna being able to generate the required pattern within the sidelobe levels set ([figure 3.21](#)).

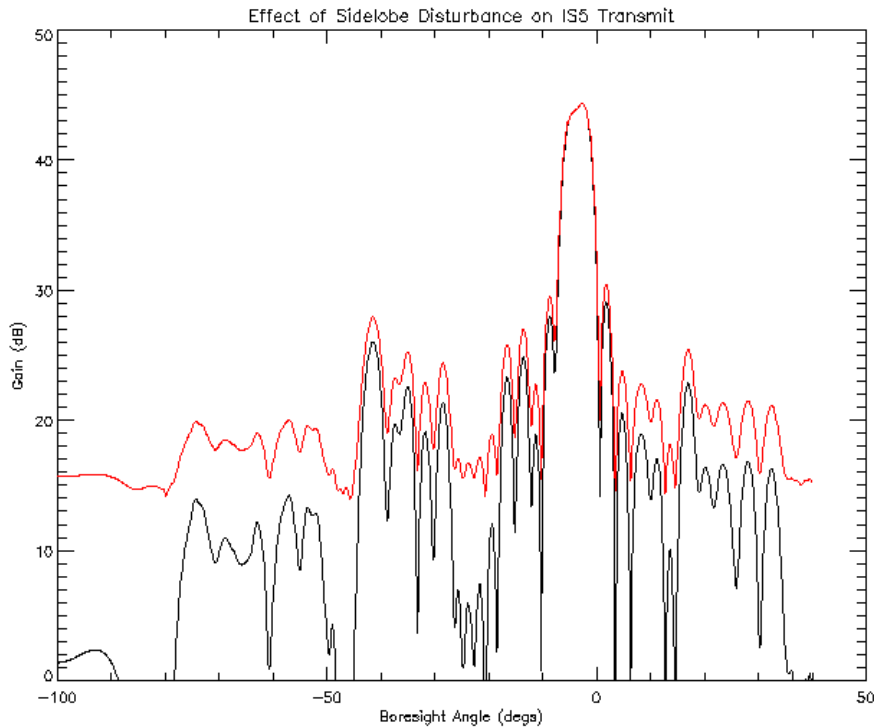


Figure 3.21 Effect of Disturbance Level on Elevation Beam Pattern. Black: FM measured pattern, Red: sidelobe disturbed pattern at 90% probability

### Sigma Nought Model

A similar "worst case" approach was taken in order to determine the distributed target ambiguity suppression ratio with respect to the normalized [radar](#) cross section of the in-swath target region and the ambiguous regions. From measurements provided in the literature ([Ref. \[3.1\]](#)) on C-band [backscatter](#) over land and sea or ice two graphs were produced. In swath, the [sigma](#) nought would be assumed to be the lower of the two curves while outside the swath, the ambiguous regions, would be assumed to have a [sigma nought](#) corresponding to the higher curve (see [figure 3.22](#) ).

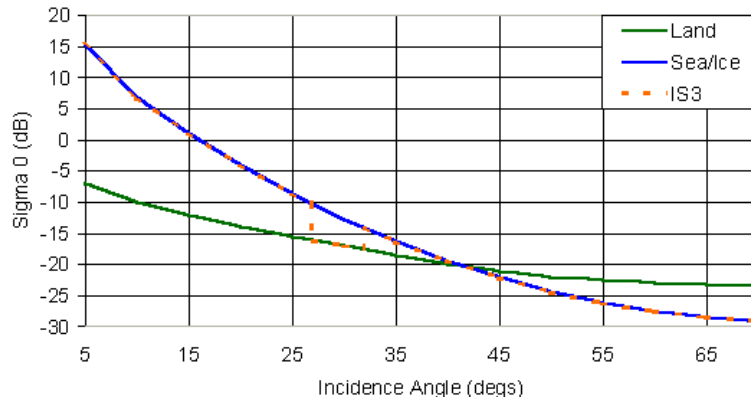


Figure 3.22 ASAR sigma nought model showing the position of the IS3 swath

At low incidence angles this can lead to more than 15dB difference between target and ambiguous region sigma nought which puts extra constraints on the elevation pattern sidelobe levels.

#### Predicted Performance

The predicted performance of ASAR has been determined using the ASAR PEAS software which makes use of algorithms based on those used successfully to predict the performance of the ERS SARs. All FM instrument measured characteristics have been used as input parameters to PEAS together with the sidelobe disturbed FM beam patterns to produce the most accurate possible performance predictions for end-of-life operation.

[Figure 3.23](#) shows the sensitivity expressed as [noise equivalent sigma nought](#) for all [image](#) beams (IS1-IS7) compared to the ASAR sigma nought model. There is several dB margin everywhere for all beams compared to the sigma nought curves with the exception of the [far range](#) of IS5 over land which in any case overlaps with the [near range](#) of IS6.

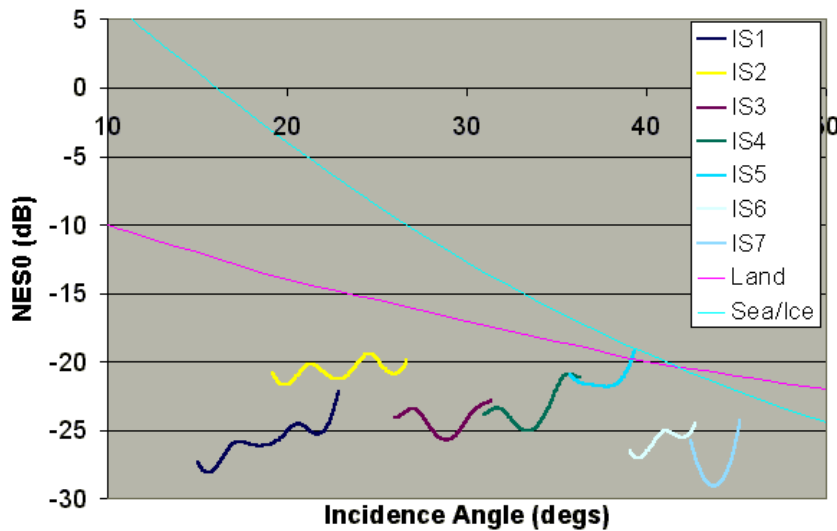


Figure 3.23 Noise Equivalent Sigma Nought for Image Mode beams IS1-IS7

In [figure 3.24](#) the range distributed target ambiguity suppression for beams IS1-IS7 is shown. For each beam the measured FM pattern has been used in the calculation to show the start-of-life situation (lower set of curves) as well as the sidelobe disturbed version of the FM patterns to demonstrate the worst case (90% probability) expected suppression at end-of-life (upper set of curves). This shows that at start-of-life the [DTRAR](#) is better everywhere than about -25dB and even at end-of-life it should never be worse than about -20dB.

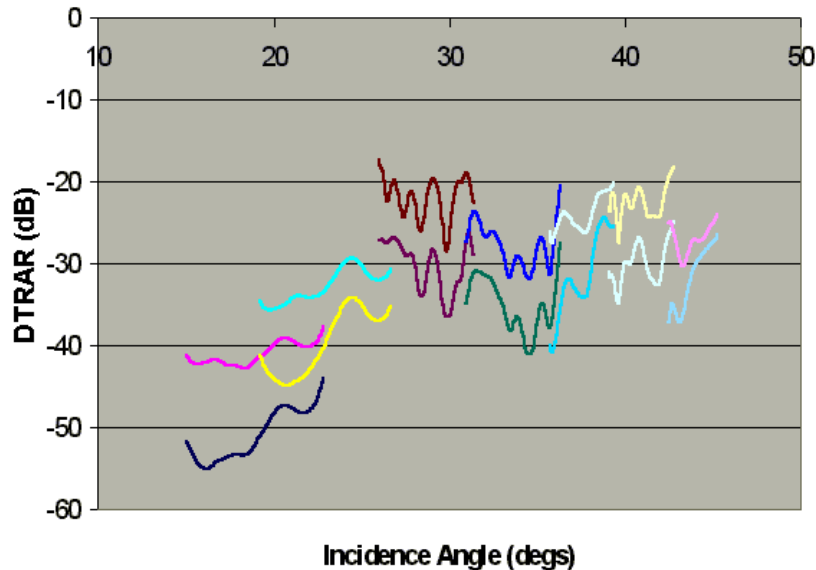


Figure 3.24 Distributed Target Range Ambiguity Ratio

A summary of all the end-of-life performance parameters and how they compare to those calculated or estimated for ERS is given in table 2.

#### Conclusions

Throughout the pre-flight assessment of the performance of the ASAR instrument a worst case scenario has been assumed including all component related issues. The result of this approach is that there is now high confidence that the ASAR will meet all the requirement specifications throughout its planned life. This means that the high standards which were set by the ERS AMI SARs will be maintained allowing ASAR to become a valuable instrument in terms of its potential for applications.

#### REFERENCES

##### Ref 3.1

R. Torres, C. Buck, J. Guijarro and J-L. Suchail (ESA-ESTEC, NL). "ESA's Ground Breaking Synthetic Aperture Radar: The ENVISAT-1 ASAR Active Antenna". APS'99.

##### Ref 3.2

J-L. Suchail, C. Buck, J. Guijarro and R. Torres (ESA-ESTEC, NL). "The Development of ENVISAT-1 Advanced Synthetic Aperture Radar". RADAR'99.

##### Ref 3.3

P. Mancini, J-L. Suchail, R. Torres, J. Guijarro and C. Buck (ESA-ESTEC, NL). "The

---

## ENVISAT-1 Advanced Synthetic Aperture Radar. The Development Status". CEOS'98.

Ref 3.4

J. Guijarro, C. Buck, P. Mancini, J-L. Suchail and R. Torres (ESA-ESTEC, NL). "The Development of the ENVISAT-1 ASAR". IGARSS'96.

### 3.2.2 Inflight Performance Verification

In-orbit beam calibration of an active phased-array antenna is a major task and it will include measurements in special modes, like module stepping and external characterisation, as well as acquisitions over rain forest. A sophisticated antenna model will combine the various data together with the pre-flight characterisation and provide the elevation and azimuth patterns for the ground processor.

Any drift in the gain and phase characteristics of the TRMs can distort the antenna beams. Deviations in antenna pattern and antenna gain will potentially contribute to radiometric errors in the SAR image. [figure 3.25](#) shows an overview of the various processes defined to maintain the calibration of the ASAR antenna beams.

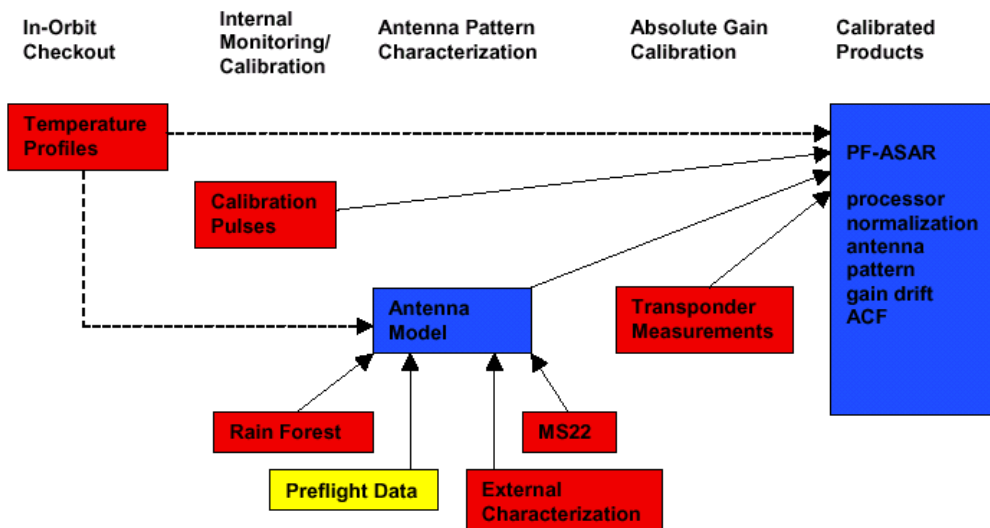


Figure 3.25 ASAR instrument calibration tasks

Monitoring any instrument gain drifts requires a separate calibration network, to couple out

part of the transmit signal or to inject chirp signals into the receiver chain. This data will be included into the high-rate data stream and will be analysed by the ground processor in order to estimate the necessary gain drift corrections.

The absolute overall system gain can be most accurately determined from the [image](#) response of point targets with high and well-known RCS. ASAR high precision transponders will be deployed in the Netherlands and will serve as the main [external calibration](#) targets. A special transponder operation mode and well-characterised distributed targets will be used for the [low-resolution](#) Global Monitoring mode.

In the following sections the pre-flight measurements and the above methods for internal calibration, module stepping, [external characterisation](#) and rainforest measurements and absolute gain calibration will be explained. Furthermore the strategy for maintaining the ASAR antenna beams will be presented.

#### Preflight Characterisation Measurements

In order to provide the required image quality, the two-way antenna beam pattern should be known to a high degree of accuracy (0.1dB). The transmit and receive antenna patterns have been accurately measured on ground [Ref. \[3.5\]](#) for all eight beams (IS1-IS7 and SS1) and both horizontal and vertical polarisations. The radiating performances of the antenna were measured in the Large Planar Near Field Range at Astrium Ltd (Portsmouth). Full characterisation was performed: 8 beams, two modes (transmit and receive), two polarisations (V and H), in copolar and crosspolar components. Example patterns are shown in [figure 3.26](#).

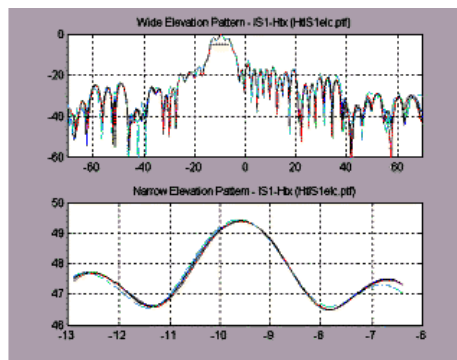


Figure 3.26 FM Elevation Beam Pattern Measurement

#### Internal Calibration

The ASAR instrument incorporates a very comprehensive system for internal calibration. There is an individual calibration path for each of the 320 transmit/receive modules. Internal calibration will be carried out on a row by row basis for each of the 32 rows. The calibration pulses are included in the instruments timeline during imaging and consist of the following

(see also [figure 3.27](#)):

- Transmit Calibration Pulses P1 (representative of T/R module load)

The T/R modules of the four adjacent rows in a tile share the same power supply. In order for the calibration sequence to be representative of the nominal operation, the ten modules of the selected row are set to their nominal phase and amplitude settings whilst the phase of the modules of the three rows sharing the same power supplies, are set so that their combined contribution out of the calibration network is nominally zero. Thereby minimising their interference to the measurement of the selected row.

- Transmit Calibration Pulse P1a

A second type of transmit pulse is added in order to characterise the residual parasitic contribution of the three unwanted rows during P1. During P1a, the three unwanted rows are set as for P1 and the previously wanted row is now switched off. Even though the load conditions on the power supplies are not exactly representative, the small error introduced into the estimation of P1a is negligible.

- Receive Calibration Pulse P2

The receive path of the instrument is also characterised but since no variation is expected from power supply load variations it is possible to characterise on a row by row basis.

- Central Electronics Calibration Pulse P3

The central electronics transmit and receive paths are included in the P1/P1a and P2 characterisations. The central electronics are therefore characterised independently by means of P3.

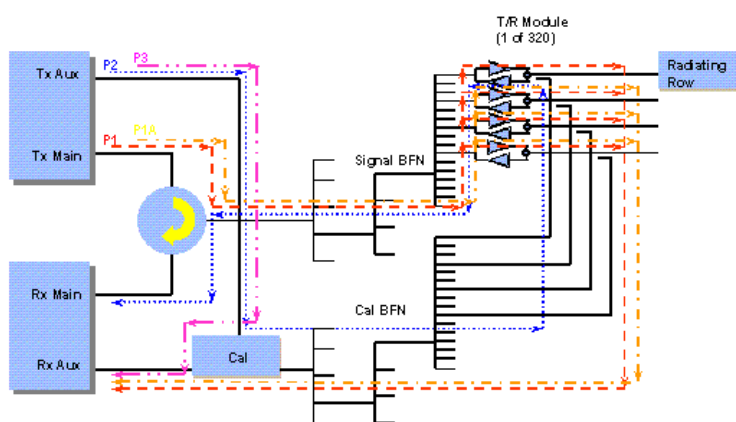


Figure 3.27 ASAR Internal Calibration Diagram

---

Using the amplitude and phase of the calibration pulses (P1/P1a, P2 and P3) for each row it is first necessary to calculate the amplitude and phase of P2 relative to P3 and to subtract P1a vectorially from P1. From these values for each of the 32 rows and together with the external characterisation factor, it is possible to calculate the elevation beam pattern. This is then used to detect any deviation to the reference instrument gain pattern as characterised on ground. The typical update rate for this calculation is 5 to 35 seconds (mode dependent).

A replica of the chirped pulse is calculated from a complete calibration row cycle using the P1/P1a, P2 and P3 measurements, the ground characterised row patterns and the external characterisation data. This is also typically updated every 5 to 35 seconds.

Despite the comprehensive nature of the internal calibration system, it is not possible to use it to calibrate the passive part of the antenna, which falls outside of the calibration loop. This is achieved through external characterisation by using the ground transponders.

#### Module Stepping

ASAR has a dedicated Module Stepping Mode, which is used to gather data from all 320 transmit/receive modules automatically. The entire procedure takes less than one second. The data are downloaded to the ground for processing. After processing, the results are compared with the reference data from on-ground tests in order to determine any TRM module gain or phase drifts, temperature behaviour and any eventual module failures. Using this information it is possible to implement any necessary correction to the TRM coefficients and eventually re-synthesise the antenna beam patterns if required.

#### External Characterisation

ASAR can be put into External Characterisation Mode while flying over a calibration transponder. This involves sending a series of pulses from each of the 32 rows in turn followed by each of the 10 columns in turn. These pulses are detected both by the internal calibration loop and the receiver embedded in the transponder (see [figure 3.28](#) ). Comparison of these data allows characterising the passive part of the antenna and the calibration network. The baseline is to repeat measurement every six months.

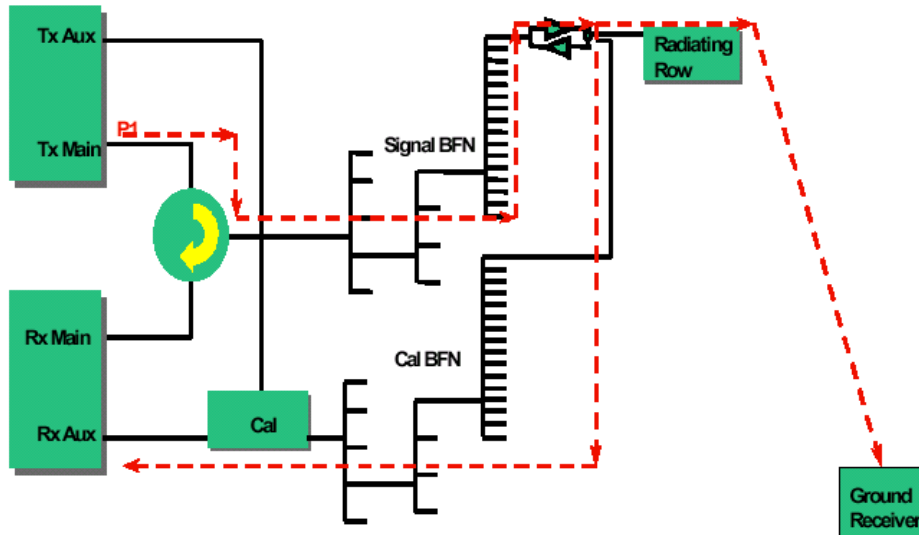


Figure 3.28 External Characterisation

## Rain Forest

The reasons images of the Amazonian rain forest are used for the characterisation of the antenna beam pattern are that it is a stable, large-scale, isotropic distributed target with a relatively high backscatter and a well-understood relationship between backscatter and incidence angle.

In order to determine the two-way beam pattern, an uncorrected rain forest image is averaged in the azimuth direction. In the final processed image, the inverted beam pattern is applied and hence the effect of the pattern on the backscatter is removed.

Alternative distributed targets at different latitudes are being investigated. Promising results have been found from ERS data over Lake Vostok in Antarctica. Antenna pattern estimates at different latitudes could be used to verify the round-orbit performance of the ASAR.  
Gain Calibration

The purpose of the ASAR gain calibration is to provide the users of ASAR data with the possibility to determine the absolute level of backscatter from any target, point ( $s$ ) or distributed ( $s_0$ ). For ASAR this is achieved in fundamentally the same way as for ERS, namely by providing an Absolute gain Calibration Factor (ACF) in the header of the (processed) product. Since ASAR, however, has a total of eight beams and five different modes and up to four polarisations more ACFs will need to be determined for ASAR than for the ERS single beam, single polarisation with two modes.

The method to be used to determine the ACFs is to image a target of known radar cross-section, integrate the power in its Impulse Response Function (IRF) corrected for the associated background (clutter) power and hence calculate the correction (the ACF) which must be applied to the image values in order to arrive at the same cross-section for that target. For this purpose, precision calibration transponders are deployed in the Netherlands. The radar cross-section of these transponders is 65dBm<sup>2</sup> and is known to within  $\pm 0.13\text{dB}$  and they are stable to 0.08dB [Ref. \[3.6 \]](#). It is necessary to use active radar calibrators (transponders) as opposed to passive ones (e.g. corner reflectors) since the ratio of signal to clutter determines the accuracy to which the calibration can be made.

Once the ACF for a particular configuration has been calculated it will be possible to make a direct comparison with the on-ground measurements of the end-to-end system gain carried out during FM testing.

### Global Monitoring Mode

This is a special case since the spatial resolution of 1000x1000m makes the normal use of the transponders unfeasible. For a reasonable calibration to be made (3s value of  $\pm 0.5\text{dB}$ ), a signal to clutter ratio of better than 30dB is required. If the clutter at the calibration sites typically has a sigma nought of -6dB then this would require a transponder RCS greater than 84dBm<sup>2</sup>. This would inevitably saturate the receiver invalidating the calibration. As a result, it is necessary to come up with an alternative scenario for calibrating this mode.

The first option (baseline) is using the other modes (namely Wide Swath and Image) to calibrate GM mode by means of the Amazonian rain forest. Since the sigma nought of the rain forest is stable to within 0.3dB it will be possible to use the sigma-nought value obtained from a previous (or subsequent) pass in WS or IM to calibrate GM mode. In addition, other relatively stable distributed targets may be used such as the ice caps and specific desert regions (Gibson, Gobi etc).

The second option will allow direct calibration using a special global monitoring mode setting and a modified calibration transponder. The intention is to use the ASAR's digital chirp generator to offset the centre frequency by 5MHz. This is possible since the chirp bandwidth in GM mode is only around 1MHz. In the calibration transponder, the received signal is shifted back by 5MHz allowing it to be received by the ASAR. As the clutter return will all be outside the range of the reduced bandwidth filter in GM mode, only the transponder response will be seen in the processed image against a background of noise. The result of this operation is to provide a transponder signal to clutter ratio of between 25 and 30dB allowing for reliable calibration of Global Monitoring Mode.

### Calibration Transponder

Since the commissioning phase is planned to last only six months following switch-on of the instrument it is necessary to make use of every possibility of imaging the transponders during that period. Furthermore the placement of the transponders must be optimised to ensure

---

that each of the seven image mode swaths can be acquired over the transponders sufficiently to allow for reliable calibration of each beam. Based on a detailed coverage analysis four locations in the Netherlands have been selected. Three transponders will be fixed. One mobile unit will be used for calibrating the Wave Mode and to support interferometric investigations during later phases of the ENVISAT mission.

Three precision calibration transponders have been developed by MPB (Canada) based on an ESA prototype and were delivered to ESTEC in April 2000 ([figure 3.29](#)). Validation of the calibration performance will be supported by the four RADARSAT transponders deployed over a latitude range from 45-74° in Canada [3]. As RADARSAT operates at 5.3GHz, the actual RCS of these transponders at 5.331GHz will decrease by about 0.4dB.



Figure 3.29 Prototype ASAR Calibration Transponder Deployed at ESTEC

### Beam Maintenance Strategy

The strategy for beam maintenance throughout the instrument lifetime is schematically shown in [figure 3.30](#). Initially, the on-ground characterisation data will be used. TRM drifts occurring during the first years of operation will be detected during module stepping and compensated for, individually, by applying corresponding offsets, in order to bring the TRMs back to the initial conditions. Should compensation not be sufficient after TRM eventual failures, the antenna beam characterisation data will be updated in the ground processor with a new calculated antenna pattern. At the end of the instrument lifetime, beam optimisation by re-calculation of new sets of beam coefficients will also be possible.

The use of rain forest images, antenna synthesis software based on pre-flight embedded row tests, and eventually the actual near-field raw data acquired during the pre-flight beam characterisation will be used, in parallel, to verify any change.

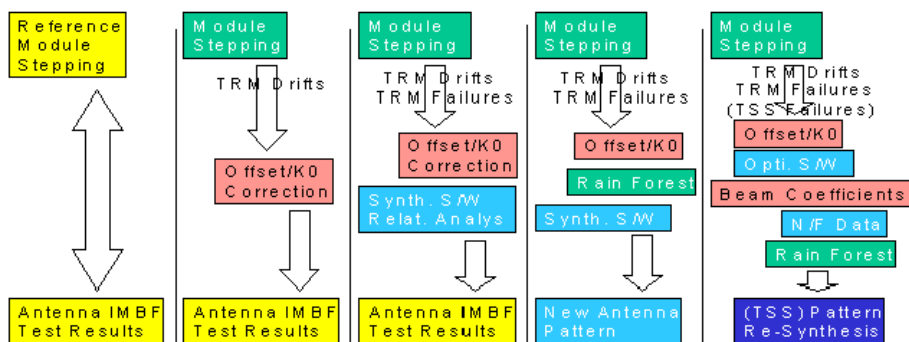


Figure 3.30 ASAR Beam Maintenance Strategy

## Conclusions

ASAR antenna beam calibration is based on combining several inputs: pre-flight characterisation measurements, internal calibration, module stepping and external characterisation, rain forest and transponder measurements. Absolute calibration will rely on ASAR precision transponders. RADARSAT transponders will support the verification of round-orbit calibration performance.

It is the intention to have the Image, Wave and Wide Swath modes calibrated within six months of launch and the all modes within nine months of launch.

## REFERENCES

### Ref 3.5

J-L. Suchail, C. Buck, A. Schnenberg, R. Torres, M. Zink, ESA/ESTEC. "The ASAR Instrument Verification: Results from the Pre-Flight Test Campaign". Proc. CEOS SAR Workshop April 2001, Tokyo, Japan.

### Ref 3.6

H Jackson ESA/ESTEC, I. Sinclair, S. Tam. MPB Technologies Inc. "ENVISAT ASAR Precision Transponders". CEOS SAR Workshop 26-29 October 1999, ESA-SP450

### Ref 3.7

R.K. Hawkins, et al. "RADARSAT Precision Transponders". Adv. Space Res. Vol. 19, No. 9, pp. 1455-1465, 1997.



# Chapter 4

## ASAR Frequently Asked Questions

### This chapter questions

- |              |   |
|--------------|---|
| Question 4.1 | <a href="#"><u>What does synthetic aperture mean?</u></a>   |
| Question 4.2 | <a href="#"><u>Why is radar often used in remote sensing?</u></a>   |
| Question 4.3 | <a href="#"><u>How does radar "see" at night?</u></a>   |
| Question 4.4 | <a href="#"><u>How does radar "see" through clouds?</u></a>   |
| Question 4.5 | <a href="#"><u>How is radar data different from what I would see? Why isn't there any colour?</u></a>   |
| Question 4.6 | <a href="#"><u>Our eyes perceive what is called visible electromagnetic radiation, or electromagnetic radiation with wavelengths between 0.4 and 0.7 microns. Even though we can't see other wavelengths of electromagnetic radiation, they certainly affect us. Ultraviolet radiation, for example, can burn our skin or hurt our eyes, and X-Rays can inform us if we have broken a bone or have developed cavities in our teeth!</u></a> |
| Question 4.7 | <a href="#"><u>What's the smallest object you can see in a SAR image?</u></a>   |
| Question 4.8 | <a href="#"><u>What's the difference between resolution and pixel spacing?</u></a>  |
| Question 4.9 | <a href="#"><u>How is this SAR data used?</u></a>   |

- 
- |               |  |
|---------------|--|
| Question 4.10 | <a href="#"><u>What's the difference between slant range and ground range?</u></a> |
| Question 4.11 | <a href="#"><u>What does geocoded mean?</u></a>                                    |
| Question 4.12 | <a href="#"><u>What does terrain correction mean?</u></a>                          |
| Question 4.13 | <a href="#"><u>What is a look (e.g. 4-look data)? What is speckle?</u></a>         |
| Question 4.14 | <a href="#"><u>What do you mean by "Complex SAR Data"?</u></a>                     |

## Question 4.1 : What does synthetic aperture mean?

In general the larger the antenna, the more unique information you can obtain about a particular viewed object. With more information, you can create a better image of that object (improved resolution). It's prohibitively expensive to place very large radar antennas in space, however, so researchers found another way to obtain fine resolution: they use the spacecraft's motion and advanced signal processing techniques to simulate a larger antenna.

A SAR antenna transmits radar pulses very rapidly. In fact, the SAR is generally able to transmit several hundred pulses while its parent spacecraft passes over a particular object. Many backscattered radar responses are therefore obtained for that object. After intensive signal processing, all of those responses can be manipulated such that the resulting image looks like the data were obtained from a big, stationary antenna. The synthetic aperture in this case, therefore, is the distance traveled by the spacecraft while the radar antenna collected information about the object. Please see the associated graphic [below]

The ERS-1 satellite's SAR sends out around 1700 pulses a second, collects about a thousand backscattered responses from a single object while passing overhead, and the resulting processed image has a resolution near 30 metres. The spacecraft travels around 4 kilometres while an object is "within sight" of the radar, implying that ERS-1's 10 metre x 1 metre radar antenna synthesizes a 4 kilometre-long stationary antenna!

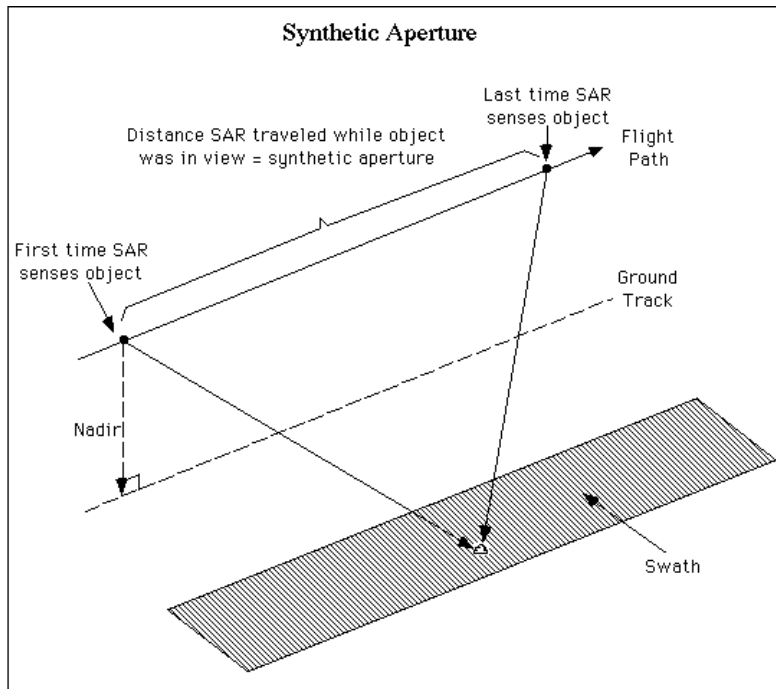


Figure 4.1 Synthetic Aperture

## Question 4.2 : Why is radar often used in remote sensing?

(Why are radio waves, visible light, and infrared radiation the most common forms of electromagnetic radiation sensed by Earth observing satellites?)

The wavelengths of electromagnetic radiation most commonly used for remotely sensing Earth are: the spectrum of visible light, a wide spectrum of radio wavelengths, and several infrared wavelengths. A partial explanation of why these wavelengths are preferable is outlined below. When radar (which employs radio waves) is selected from these possible choices, the decision is usually based upon radar's independence of solar illumination and weather conditions. See the questions: How does radar "see" at night? and How does radar "see" through clouds? for more details.

There is a good reason why our eyes sense the electromagnetic radiation (light) they do: visible light represents a significant portion of the electromagnetic radiation which can pass through Earth's atmosphere and ionosphere. A wide spectrum of radio waves, which radars employ, and some infrared radiation can also pass through to the Earth's surface.

There are many reasons why other wavelengths/frequencies of electromagnetic radiation don't make it through Earth's atmosphere. For example many people know that ozone in Earth's upper atmosphere helps protect us from ultraviolet radiation. This occurs because

the structure of the ozone molecule is particularly sensitive to ultraviolet frequencies; it has a natural resonance near those frequencies. Think of a person swinging; he swings back and forth with a particular frequency. If you push him with the same frequency (every time he comes back) or at a related periodic frequency (say, every other time he comes back), he will keep going higher and higher. Incoming ultraviolet radiation likewise keeps "pushing" the ozone molecule at the structure's resonant frequency - in a sense like pushing the swinging person higher. Soon the ozone molecule breaks into an oxygen atom and an O<sub>2</sub> molecule which go on to other adventures. The incoming ultraviolet radiation's energy was used to break apart the ozone molecule, a process by which we say the radiation was "absorbed." Many molecules in Earth's atmosphere have various kinds of resonances which absorb other frequencies of electromagnetic radiation. The visible spectrum, a wide spectrum of radio frequencies, and some infrared frequencies don't match well with those resonances, however, and thus are not much affected by absorption. These frequencies of electromagnetic radiation are therefore most commonly used for remote sensing purposes.

As a side note - some radar wavelengths reflect off the ionosphere and therefore cannot be used for remote sensing purposes. You may know a HAM radio operator who utilizes this phenomenon to talk to a companion halfway around the world. In this case radio waves are transmitted up to the ionosphere and reflected back down to Earth elsewhere, rather than passing through the ionosphere. This happens because the radio waves cause electrons in the ionosphere to oscillate, and the oscillating electrons in turn radiate electromagnetic waves.

#### Question 4.3 : How does radar "see" at night?

SAR instruments transmit radar signals and then measure how strongly those signals are scattered back. An analogy with photography can be made: when it's dark, a camera's flash sends out light and then the film records objects that the flash illuminates. In both cases the SAR and the camera are not dependent upon the sun because they provide their own illumination.

#### Question 4.4 : How does radar "see" through clouds?

Light does often make it through clouds, but that light has just been scattered all over the place, making it nearly impossible to tell how the light was oriented before it entered the cloud. This is why we can't see objects through clouds. The difference with radar is how much less it's distorted while passing through a cloud.

The reason why clouds scatter visible light while leaving radar undistorted is a matter of relative scale. Radar's longer wavelengths in effect average the properties of air with the properties and shapes of many individual water droplets, making the cloud look homogeneous - i.e. like moist air. Visible light has short enough wavelengths to respond to all the individual boundaries between air and water droplets. At each boundary the light is reflected to a new direction, and by the time it escapes the cloud, information on the light's original direction is hopelessly lost. The radar signals, on the other hand, are only affected while entering and exiting the cloud. Because they don't suffer multiple bounces, the radar waves are relatively undistorted by clouds.

**Question 4.5 : How is radar data different from what I would see? Why isn't there any colour?**

(See the previous question for an explanation of why you don't see clouds in a typical radar image.)

**Question 4.6 : Our eyes perceive what is called visible electromagnetic radiation, or electromagnetic radiation with wavelengths between 0.4 and 0.7 microns. Even though we can't see other wavelengths of electromagnetic radiation, they certainly affect us. Ultraviolet radiation, for example, can burn our skin or hurt our eyes, and X-Rays can inform us if we have broken a bone or have developed cavities in our teeth!**

When we think about all the information light provides us about our world, and about how other electromagnetic waves impact our lives, it seems only natural that people would want to detect and "visualize" many other kinds of electromagnetic radiation. The Earth Observing System does just that; many satellites' instruments "see" certain electromagnetic waves and relay that data to a "brain" (computer), where the information is then converted into an image for humans to interpret. Each wavelength indicates something different about the imaged object, just as you might associate the wavelength corresponding to bright green light with young plants.

Visible light contains a range of wavelengths, but with radar we often measure one very specific wavelength. Just think of how differently things would look if you could only see yellow. Your eyes would only detect how brightly an object scattered yellow, so the reflection's intensity, not the colour, is what would give you new and useful information. Similarly, radar antennas are often made to detect how brightly objects reflect one particular wavelength. Since there are no other "colours" (wavelengths) to mix in, we really only care about the backscatter's intensity and therefore often use greyscale in our visualizations of this data.

**Question 4.7 : What's the smallest object you can see in a SAR image?**

In ASF's full-resolution SAR images, you can distinguish objects as small as about 30 metres wide. Some of the smaller items that we've spotted have been ships and their wakes. When the SAR happens to be aligned at a certain angle, long thin objects such as roads or even the Alaskan oil pipeline can also be seen.

**Question 4.8 : What's the difference between resolution and pixel spacing?**

Pixel spacing represents how much area each pixel covers, while resolution indicates the

---

smallest object you could pick out in an image. Each pixel represents one solid colour, so of course you can't see anything within it. When you place other pixels around it, though, you might notice a few pixels are rather different in colour than surrounding pixels and conclude that you have identified a distinct object. ASF's full-resolution ERS-1 SAR images have 12.5 m pixel spacing and about 30 m resolution. This means that each pixel represents a 12.5 x 12.5 m area on the ground, and you can discern individual objects which are around 30 m wide or larger.

#### Question 4.9 : How is this SAR data used?

SAR's ability to pass relatively unaffected through clouds, illuminate the Earth's surface with its own signals, and precisely measure distances makes it especially useful for the following applications:

- Sea ice monitoring
- Cartography
- Surface deformation detection
- Glacier monitoring
- Crop production forecasting
- Forest cover mapping
- Ocean wave spectra
- Urban planning
- Coastal surveillance (erosion)
- Monitoring disasters such as forest fires, floods, volcanic eruptions, and oil spills

Some of the larger current research projects include: mapping the Antarctic continent; mapping the Amazon rainforest; using interferometric analysis for predicting or analyzing earthquakes and volcanic activity; and generating "Arctic Snapshots" of the Arctic ice extent.

#### Question 4.10 : What's the difference between slant range and ground range?

The time it takes for a transmitted signal to travel to an object and back tells you how far away the object is. If you transmit a signal and receive two separate "echoes," you can use the time difference between when you record the first and second responses to determine the distance between the two sensed objects (dependent on where you stand). In this way the spaceborne SAR measures how far objects are from the spacecraft and the distance between the two objects, along the direction the spacecraft is looking. These distances are said to be recorded in slant range, since they are measured in a direction which is at an angle/slant to the ground.

Often researchers don't really care about distances from the spacecraft; they want to know about distances on the ground. Perhaps they need "real" (ground) distances to determine how much land was used for farming or what percentage of the sea was covered with ice, but the spacecraft samples the returning radar signals at specific time intervals which correspond to discrete distances from the spacecraft. That means that the data are originally in slant range. Given various parameters, the data can be processed such that each data value covers the same amount of area (distance) on the ground. We then say that the data are in ground range.

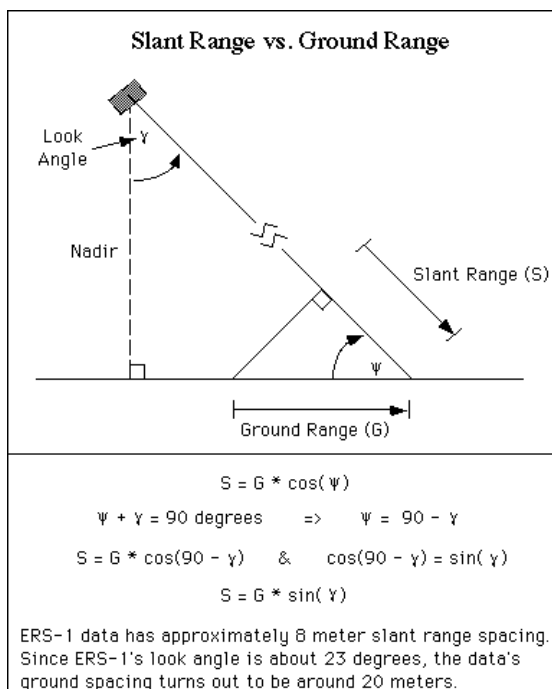


Figure 4.2 Slant Range vs Ground Range

### Question 4.11 : What does geocoded mean?

A standard ASF SAR image has gone through a lot of processing to look "normal." One step in this process involves manipulating the data such that each pixel represents a specific distance on the ground. The latitude and longitude coordinates of each image's centre and corner pixels are also known. Sometimes, however, it's convenient to map the data onto a standard grid - such as a mercator projection. Then the pixels in each row would be evenly spaced in terms of longitude, and the entire row would be located at a specific latitude. The data would then be termed geocoded. It is often much easier to compare/overlay geocoded SAR data with non-SAR data sets.

## Question 4.12 : What does terrain correction mean?

If you have information about a region's topography, like a digital elevation model (DEM), you can make the slant to ground range conversion more sophisticated. In effect this terrain correction can compensate for foreshortening by spreading data representing the mountain's facing side into more pixels and compacting returns from the back face into fewer pixels. It's nearly impossible, though, to reliably extract the separate returns from data values representing the facing slope. Sometimes people try to compensate for shadowing as well. Knowing the mountain's slopes, they can approximate how the strength of backscattered signals were affected by the changed incidence angle and adjust results accordingly. These procedures, though inexact, can greatly improve SAR image analysis.

## Question 4.13 : What is a look (e.g. 4-look data)? What is speckle?

As the spacecraft moves along in its orbit, the radar antenna transmits pulses very rapidly. It can therefore obtain many backscattered radar responses from a particular object while passing overhead. In fact the ERS-1 SAR records about 1,000 responses for a single object. The SAR processor could use all of these responses to obtain the object's radar cross-section (i.e. how brightly the object backscattered the incoming radar), but the result often contains quite a bit of speckle.

Speckle, generally considered to be noise, is due in part to the SAR's fine resolution and its signals' coherency. Speckle can be caused by an object that behaves as a very strong reflector at a particular alignment between itself and the spacecraft, or by a coherent sum of all the various responses within a grid cell which happen to randomly sum (as vectors with magnitude and phase) to a large resultant magnitude at a given phase.

To reduce speckle, the data are sometimes processed in sections which are later combined. With ERS-1's 1,000 samples per object, we might wish to use an object's first 250 responses to determine its radar cross-section. If we then processed the next 250 responses to get another estimate, and so on, we would end up with four estimates of the object's radar cross-section. Combining these four estimates, or looks, together would reduce the amount of speckle.

When an image has been processed as "4-looks": the first 250 (or so) samples of each viewed object were processed to make one image; the next 250 samples for each object were processed to make a second image; the third and fourth images were created with the next chunks of data; and the four images (looks) were combined to create the final result.

The more looks that are used to process an image, the less speckle there is. (The Complex-Format SAR Data Example [given below] demonstrates this.) It must be taken into account that information deemed important is also lost in this process, however, and that resolution is reduced. Several research groups are developing/improving algorithms to reduce speckle while saving as much accurate information as possible.

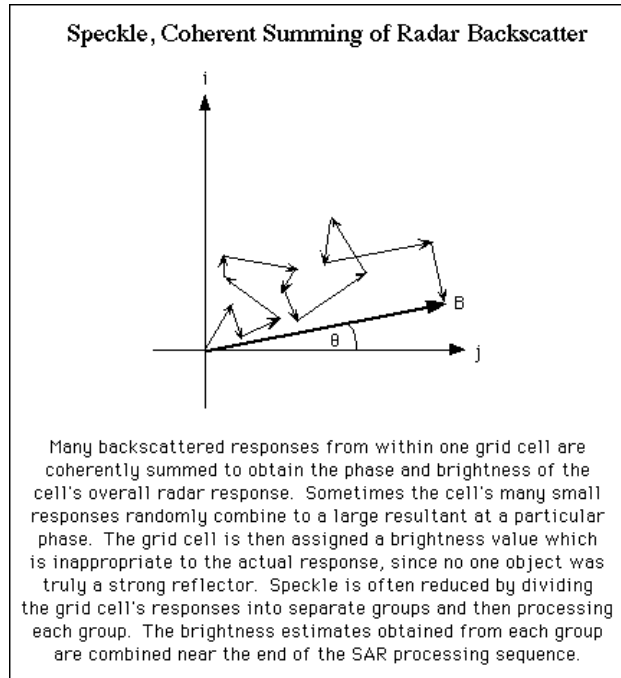


Figure 4.3 Coherent Summing of Radar Backscatter

#### Question 4.14 : What do you mean by "Complex SAR Data"?

Used here the term "complex" refers to complex numbers, or complex-format data. You might be used to hearing of complex numbers with their "real" and "imaginary" components, also known as cosine and sine components. For example a wave might be described in complex format by:  $A^*(\cos(\omega t) + i\sin(\omega t))$ , where ' $\omega$ ' represents the wave's frequency and ' $A$ ' its amplitude. [see below] The cosine value would describe the wave's real component, sine the imaginary component, and the two would combine as vectors to provide the wave's overall phase (inverse tangent of sin/cos) and amplitude.

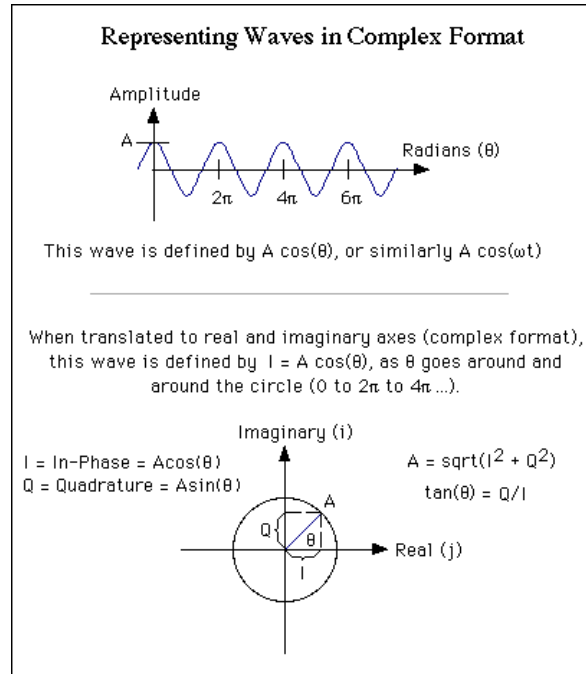


Figure 4.4 Representing Waves in Complex Format

Both the cosine and sine components of backscattered SAR signals are measured and digitized on-board the satellite.

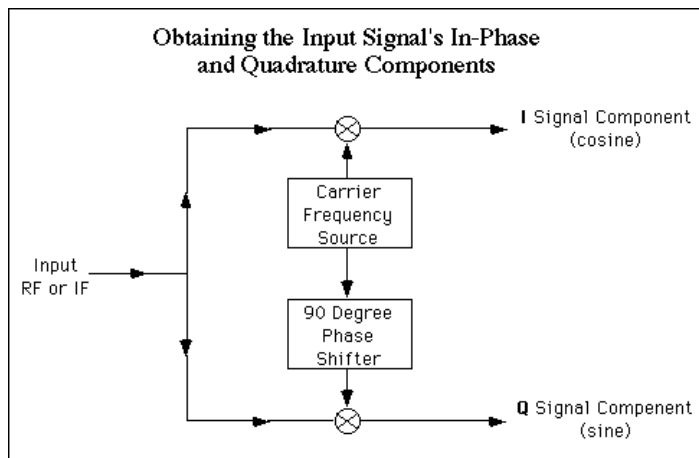


Figure 4.5 Obtaining the Input Signal's In-Phase and Quadrature Components

The two resulting data streams are then transmitted to a ground station for further processing. People sometimes call these the 'I' (representing In-Phase, or the cosine or real component) and 'Q' (representing Quadrature, the 90 degrees shifted, sine or imaginary component) data streams. For standard processing these two data values are combined to obtain the composite signal intensity ( $\sqrt{I^2 + Q^2}$ ). Sometimes, though, it's desired to process the two data streams separately - usually to maintain the signals' phase information. Then ASF distributes the individually-processed I and Q data values for each pixel location, calling this product "Complex SAR Data." A more detailed example/tutorial of complex SAR data is also available.

# Chapter 5

---

## ASAR Glossary Terms

The complete glossary of terms and acronyms for this handbook has been divided into the following subsections (index)

Note: With the notable exception of the "Instrument Glossary", the descriptions found herein have been provided by [MacDonald Dettwiler and Associates \(MDA\)](#), with contributions from the [Canadian Centre for Remote Sensing \(CCRS\)](#) and the [Alaska SAR Facility \(ASF\)](#).

### 5.1 Acronyms and Abbreviations

Table 5.1

AATSR	Advanced Along-track Scanning Radiometer ( <a href="#">ENVISAT</a> )
AC	<a href="#">Across-Track</a>
ACCC	<a href="#">Average Cross Correlation Coefficient</a>
ADC	Analog-To-Digital Converter
ADS	<a href="#">Annotation Data Set</a>
ADSR	Annotation Data Set Record
ADU	Analogue to Digital Unit
AERONET	Aerosol Robotic Network
AGC	Automatic Gain Control
AISP	<a href="#">Annotated Instrument Source Packet</a>
AL	<a href="#">Along-Track</a>
AMI	<a href="#">Active Microwave Instrument</a>
AMT	Atlantic Meridian Transect
AO	Announcement of Opportunity
AOI	Announcement of Opportunity Instrument
AP	<a href="#">Alternating Polarisation Mode</a>
APB	<a href="#">Alternating Polarisation Browse Image</a>
APG	<a href="#">Alternating Polarisation Mode Ellipsoid Geocoded image</a>
API	Application Process Identifier
APM	<a href="#">Alternation Polarisation Medium-Resolution product</a>
APP	<a href="#">Alternating Polarisation Precision Product</a>
APS	<a href="#">Alternating Polarisation Mode Single-look Complex image</a>
APSM	<a href="#">Antenna Power Switching and Monitoring Subsystem</a>
ARF	Archiving Facility
ASA	<a href="#">Antenna Sub-Assembly</a>
ASAR	<a href="#">Advanced Synthetic Aperture Radar</a>
ASCII	American Standard Code for Information Interchange
ASF	Alaska <a href="#">SAR</a> Facility
ASS	<a href="#">Antenna Services Subsystem</a>
AVHRR	Advanced Very High Resolution Radiometer
BAQ	<a href="#">Block Adaptive Quantisation</a>
BB	Black Body
BOA	Bottom Of the Atmosphere
BT	<a href="#">Brightness Temperature</a>
BUFR	Binary Universal Form for meteorological data
Cal/Val	Calibration / Validation
CASI	Compact Airborne Spectrographic Imager
CCD	<a href="#">Charge Coupled Device</a>
CCC	Cross Correlation Coefficient
CCRS	Canadian Centre for Remote Sensing
CESA	<a href="#">Control Electronics Sub-Assembly</a>
CESAR	Cold Atmospheric Emission Spectral Radiometer
CFRP	<a href="#">Carbon Fibre Reinforced Plastic</a>
CHAMP	Comet Halley Active Monitoring programme
CMC	Centre Monitoring and Control element
CNES	Centre National d'Études des Télécommunications, France
COASTLLOC	COAstal Surveillance Through Observation of Ocean Colour
CORINE	Co-ordination of Information on the Environment
CP	Characterisation Parameter --also-- Control Point
CRC	Cyclic Redundancy Code
CSIRO	Commonwealth Scientific and Industrial Research Organisation
CSS	<a href="#">Control Subsystem</a>
CTM	Chemical Transport Model
CW	Continuous Wave
DAR	<a href="#">Doppler Ambiguity Resolver</a>
DCE	<a href="#">Doppler Centroid Estimation 2.6.1.2.2.</a>
DDKP	Detailed Design Key Point
DDT	Data Dictionary Tool
DEM	<a href="#">Digital Elevation Model</a>
DEP	Doppler Estimation Processor
DFT	Discrete Fourier Transform
DINSAR	<a href="#">Differential Interferometric SAR 1.1.5.4.4.</a>
DLR	Deutsche Forschungsanstalt für Raumfahrt, Germany
DMS	Data Measurement Set
DOAS	Differential Optical Absorption Spectrometric (SCIAMACHY)
DORIS	Doppler Orbitography and Radiopositioning Integrated by Satellite
DS	<a href="#">Data Set 2.3.2.5.</a>

DSD	<a href="#">Data Set Descriptor 2.3.2.4.</a>
DSR	<a href="#">Data Set Record 2.3.2.5.</a>
DTRAR	Distributed Target Range Ambiguity Ratio
ECMWF	European Centre for Medium-range Weather Forecasting
ECOC	Electrochemical Ozone Cell
ECP	<a href="#">Extracted Calibration Product</a>
EDI	ESA Developed Instrument
EIH	<a href="#">Extracted Instrument Header</a>
ELHYSA	Etude de L'HYgrométrie Stratosphérique
ENL	Equivalent Number of <a href="#">Looks</a>
ENVISAT	ENVIronnement SATellite
EP	Engineering Parameter
ERS	<a href="#">European Remote Sensing Satellite</a>
ESA	European Space Agency
ESABC	Envisat Stratospheric Aircraft and Balloon Campaign
ESL	Expert Support Laboratory
ESOC	European Space Operations Centre, Darmstadt, Germany
ESOV	Earth Map and Swaths Visualisation tool
ESRIN	ESA's Earth Observation Centre, Frascati, Italy
ESTEC	European Space Research and Technology Centre, Noordwijk, The Netherlands
FBAQ	<a href="#">Flexible Block Adaptive Quantisation</a>
FC	<a href="#">False Colour</a>
FCC	<a href="#">False Colour Composite</a>
FE	Fixed Exponent Quantisation
FEP	Front End Processor
FFT	<a href="#">Fast Fourier Transform</a>
FIR	Finite Impulse Response
FISH	Fast In situ Stratospheric Hygrometer
FM	<a href="#">Frequency Modulation</a> (also Flight Model)
FOS	Flight Operations Segment ( on ground )
FOV	Field Of View
FOZAN	Fast Ozone Analyser
FTIR	<a href="#">Fourier-Transform</a> Infrared Spectrometer
FTS	<a href="#">Fourier-Transform</a> Absorption Spectrometer
FWHM	Full Width at Half Maximum
GADS	<a href="#">Global Annotation Data Set</a>
GCP	<a href="#">Ground Control Point</a>
GDR	Geophysical Data Record
GEC	<a href="#">Geocoded Image</a>
GIS	Geographic Information System
GM	<a href="#">Global Monitoring Mode</a>
GMB	<a href="#">Global Monitoring Mode Browse Image</a>
GMI	<a href="#">Global Monitoring Mode product</a>
GOCE	Gravity and steady-state Ocean Circulation Explorer
GOME	Global Ozone Monitoring Experiment
GOMOS	Global Ozone Monitoring by Occultation of the Stars
GPS	Global Positioning System
GR	Ground Range
GRACE	Gravity Recovery and Climate Experiment
GRIB	Gridded Binary Format (meteorological data interchange format)
GSRT	Ground segment Reference Time
GUV	Ground-based Ultraviolet Radiometer
HEX	Hexadecimal Number Representation
HDF	Hierarchical Data Format
HH	<a href="#">Horizontal Polarisation Transmitted/Horizontal Polarisation Received</a>
HHTML	House Keeping Telemetry Data
HR	High Rate
HV	<a href="#">Horizontal Polarisation Transmitted/Vertical Polarisation Received</a>
HWHM	Half Width at Half Maximum
Hz	Hertz
ICU	Instrument Control Unit
ID	Identifier
IDEFOV	Instantaneous Detector Element Field of View
IECF	Instrument Engineering Calibration Facility
IEEE	Institute of Electrical and Electronics Engineers
IF	Intermediate Frequency
I/F	Interface
IFFT	<a href="#">Inverse Fast Fourier Transform</a>

---

IFOV	Instantaneous Field of View
IGDR	Interim Geophysical Data Record
ILS	Instrument Line Shape
IM	<a href="#">Image Mode</a>
IMB	Image Mode Browse Image
IMG	<a href="#">Image Mode ellipsoid Geocoded image</a>
IMM	<a href="#">Image Mode Medium resolution image</a>
IMP	<a href="#">Image Mode Precision image</a>
IMS	<a href="#">Image Mode Single-Look Complex image</a>
InSAR	Interferometric Synthetic Aperture Radar
IPC	Inter-Process communication
IPF	Instrument Processing Facility
I/Q	<a href="#">In-Phase/Quadrature Channels</a>
IR	Incident Report --also-- InfraRed
IRF	Impulse Response Function
IRW	<a href="#">Impulse Response Width</a>
ISAR	<a href="#">Inverted Synthetic Aperture Radar</a>
ISLR	<a href="#">Integrated Side Lobe Ratio</a>
ISP	<a href="#">Instrument Source Packet</a>
JPL	Jet Propulsion Laboratory
kB	kiloBytes (also: kBytes)
LADS	<a href="#">Location Annotation Data Set</a>
L1b	<a href="#">Level 1b (product)</a>
L2	<a href="#">Level 2 (product)</a>
LCC	<a href="#">Lambert Conformal Conic map projection</a>
LIDAR	LIght Detection And Ranging
LOS	Line-Of-Sight
LR	Low Rate
LSB	Least Significant Bit (or Byte, depending on context)
LST	Land Surface Temperature
LSW	Least Significant Word
LUT	Look-Up Table
LVI	Live Vegetation Index
M-AERI	Marine Atmosphere Emitted Radiance Interferometer
MAVT	<a href="#">MERIS &amp; AATSR Validation Team</a>
MB	MegaBytes (also: Mbytes)
MCD	<a href="#">Measurement Confidence Data</a>
MLCC	Multi-Look Cross Correlation
MDA	MacDonald, Dettwiler and Associates
MDS	<a href="#">Measurement Data Set</a>
MDSR	<a href="#">Measurement Data Set Record</a>
MERIS	MEdium-Resolution Imaging Specrometre
MERC	<a href="#">Mercator map projection</a>
METEOSAT	Meteorological Satellite
MGVI	<a href="#">MERIS Global Vegetation Index</a>
MIPAS	Michelson Interferometer for Passive Atmospheric Sounding
MISR	Multi-angle Imaging Spectrometer
MJD	Modified Julian Day
MLCC	<a href="#">Multi-Look Cross Correlation</a>
MODIS	Moderate-Resolution Imagine Spectrometer
MOE	Medium Accuracy Orbit
MPH	<a href="#">Main Product Header 2.3.2.2.</a>
MSB	Most Significant Bit (or Byte, depending on context)
MSG	Meteosat Second Generation
MSW	Most Significant Word
MTF	Modulation Transfer Function
MWR	Microwave Radiometer
N/A	Not Applicable
NASA	National Aeronautics and Space Administration, USA
NASDA	National Space Development Agency, Japan
NDSC	Network for the Detection of Stratospheric Change
NESR	Noise Equivalent Spectral Radiance
NILU	Norwegian Institute for Air Research
NIR	Near Infrared
NOAA	National Oceanic and Atmospheric Administration
NRT	<a href="#">Near Real Time</a>
NSP	<a href="#">National Systems Projection</a>
NWP	Numerical Weather Predication

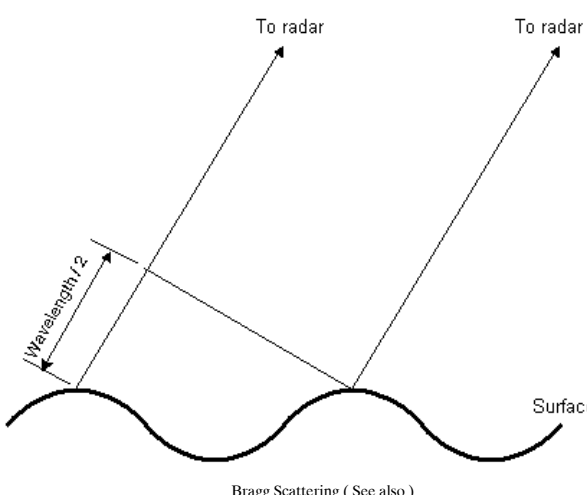
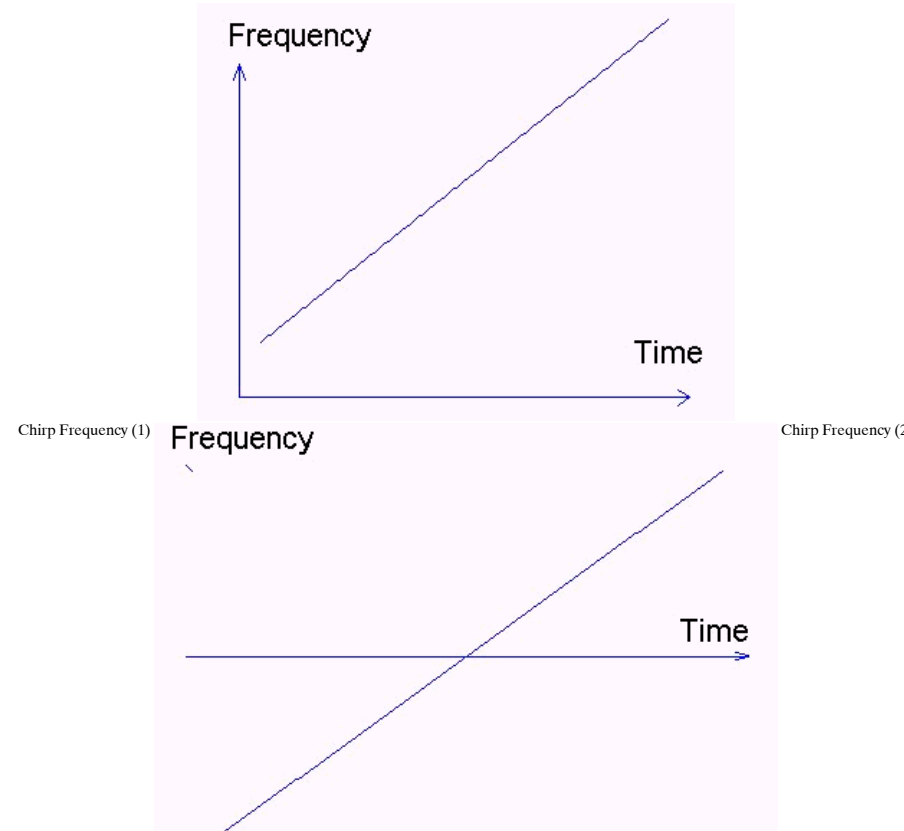
OBDH	On-Board Data Handling
OBR	On-Board Recorder
OBT	On-Board Time
OFL	Off-Line
OL	On Line
OVID	Optical Visible and near Infrared Detector
PAC	Processing and Archiving Centre
PAR	Photosynthetically Active Radiation
PARC	Polarimetric Active Radar Calibrator
PCD	Product Confidence Data
PDHS	Payload Data Handling Station
PDS	Payload Data Segment ( <a href="#">ENVISAT</a> )
PEAS	Performance Evaluation Software
PF	Processing Facility
PF-ASAR	<a href="#">ASAR</a> Processing Facility
PF-HS	Processing Facility Host Structure
PGICD	Payload to Ground Segment Interface Control Document
PI	Principal Investigator
POD	Precise Orbit Determination
POE	Precise Orbit
POLDER	Polarisation and Directionality of Earth's Reflectances
PRF	Pulse Repetition Frequency
PRI	Precision Image (ASAR) also Pulse Repetition Interval
PRN	Pseudo Random Noise
PS	Polar Stereographic map projection
PSLR	Peak Side Lobe Ratio
PTI	Pulse Transmission Interval
PTR	Point Target Response
PTU	Pressure Temperature Humidity
QM	Qualification Model
Quad Pol Radar	Quadrature Polarisation Radar
R/D	<a href="#">Range/Doppler SAR Algorithm 2.6.1.2.3.</a>
RA-2	Radar Altimeter-2
RADAR	<a href="#">Radio Detection And Ranging</a>
RADARSAT	<a href="#">RADAR SATellite</a> ( developed by RADARSAT International, in Canada )
RAL	Rutherford Appleton Laboratory, UK
RAR	Real Aperture Radar
RAR MTF	Real Aperture Radar Modulation Transfer Function
RCS	Radar Cross Section
RCMC	Range Cell Migration Correction
RERV	Radar Estimated Rain Volume
RF	Radio Frequency
RFOV	Reduced Field of View
RISC	Reduced Instruction Set Chip
RHI	Radar Height Indicator (also known as Range Height Indicator)
RM	Range Matched
RMS	Root Mean Squared
RMVT	<a href="#">RA-2 / MWR Validation Team</a>
ROSAR	<a href="#">Rotor-SAR</a>
R/S	Remote Sensing
RS	Reed-Solomon (error correction)
RR	Reduced Resolution
S+M	Sign plus Magnitude (fixed exponent) mode
SAFIRE	Spectroscopy of the Atmosphere Far Infrared Emission
SAR	<a href="#">Synthetic Aperture Radar</a>
SASM	<a href="#">Synthetic Aperture Strip Map</a>
SBT	Satellite Binary Time
SBUV	Solar Backscatter Ultraviolet
ScanSAR	<a href="#">Scanning SAR Imaging Technique (for wide swath coverage)</a>
SCI	Stripline Continuity Indicator
SCIAMACHY	Scanning Imaging Absorption Spectrometre for Atmospheric Cartography
SEASAT	<a href="#">Sea Satellite</a> ( developed by NASA, in the USA )
SeaWiFS	Sea Wide Field-of-view Spectrometre
SFA	Steering Front Assembly
SLADS	Sub-sampled <a href="#">Location Annotation Data Set</a> (LADS)
SLAR	<a href="#">Side-Looking Aperture Radar</a>
SLC	<a href="#">Single Look Complex Image</a>
SLR	Satellite Laser Ranging

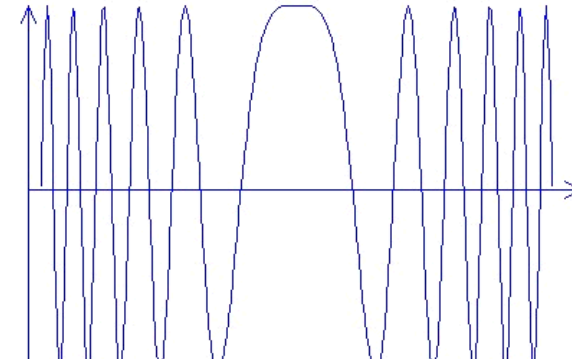
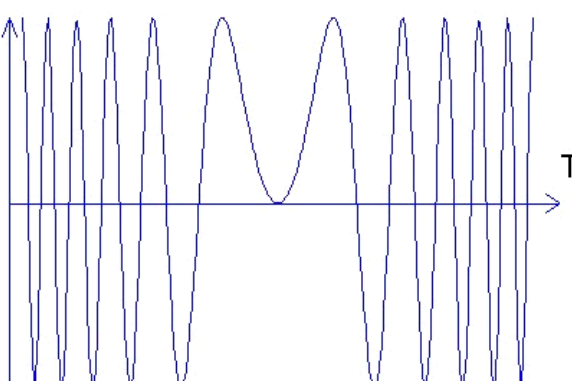
SNR	<a href="#">Signal-to-Noise Ratio</a>
SOAZ	Système d'Analyse par Observations Zéro@Thales
SODAP	Switch-On and Data Acquisition Phased
SPCS	<a href="#">State Plane Co-ordinate System</a>
SPECAN	<a href="#">Spectral Analysis SAR Algorithm 2.6.1.2.4.</a>
SPH	<a href="#">Specific Product Header 2.3.2.3.</a>
SPOT	Satellite pour l'Observation de la Terre ( SPOT Image, in France )
SQ	<a href="#">Summary Quality</a>
SQADS	<a href="#">Summary Quality Auxiliary Data Set</a>
SQADSR	<a href="#">Summary Quality Auxiliary Data Set Record</a>
SR	<a href="#">Slant Range</a>
SR/GR	<a href="#">Slant Range to Ground Range</a>
SS	Sub-Swath
SSST	Skin Sea Surface Temperature
SST	Sea Surface Temperature
STC	<a href="#">Sensitivity Time Control</a>
SWST	Sampling Window Start Time
SZA	Sun Zenith Angle
T/R	Transmit/Receive
TBC	To Be Confirmed
TBD	To Be Determined ALSO To Be Defined
TCIU	<a href="#">Tile Control Interface Unit</a>
TIFF	Tagged Image File Format
TM	<a href="#">Transverse Mercator map projection</a>
TOA	Top Of the Atmosphere
TOAVI TOA	Vegetation Index
TOMS	Total Ozone Mapping Spectrometer
TOPEX	Topography Experiment for Ocean Circulation
TRM	<a href="#">T/R Modules</a>
TSS	Tile Subsystem
UPS	<a href="#">Universal Polar Stereographic</a>
USF	User Service Facility
USO	Ultra Stable Oscillator
UTC	Universal Time Co-ordinated
UTM	<a href="#">Universal Transverse Mercator</a>
UV	Ultraviolet
VCDU	Virtual Channel Data Unit
VH	<a href="#">Vertical Polarisation Transmitted/Horizontal Polarisation Received</a>
VIP	Verification Input parameter
VIS	Visible
VLBI	Very Long Baseline Interferometry
VMR	Volume-Mixing Ratio
VV	<a href="#">Vertical Polarisation Transmitted/Vertical Polarisation Received</a>
WAIS	West Antarctic Ice Sheet
WG84	World Geodetic System 1984
WS	<a href="#">Wide Swath Mode</a>
WSB	<a href="#">Wide Swath Browse Image</a>
WSM	<a href="#">Wide Swath Medium-resolution image</a>
WV	<a href="#">Wave Mode</a>
WVI	<a href="#">Wave Mode SLC imlette and Imlette Cross Spectra image</a>
WVS	<a href="#">Wave Mode Imlette Cross Spectra image</a>

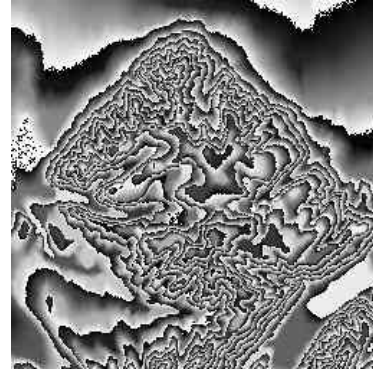
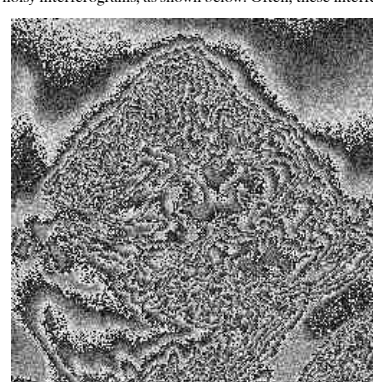
## 5.2 RADAR and SAR Glossary

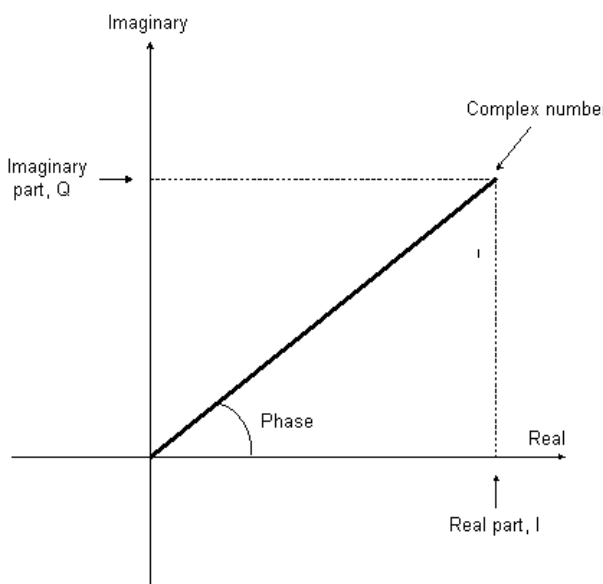
Table 5.2

Across-track	An across-track sensor is one that uses a mirror system that moves from side to side in the <a href="#">range</a> to obtain <a href="#">remote sensing</a> data. ( See also " <a href="#">Imaging Geometry</a> " in the Geometry glossary )
Active Microwave Instrument (AMI)	Ordinarily referred to as a radar, this is the term commonly used to describe the radar instrument onboard the <a href="#">ERS</a> satellites. (See <a href="#">Microwave</a> )
Active Remote Sensing System	A system that provides its own source of energy and illumination (i.e. radar system). A remote sensing system that transmits its own electromagnetic emanations at an object(s) and then records the energy reflected or refracted back to the sensor.
Advanced Synthetic Aperture Radar (ASAR)	This is the newest SAR instrument from <a href="#">ESA</a> . The Advanced Synthetic Aperture Radar ( ASAR ) instrument onboard the <a href="#">ENVISAT</a> satellite extends the mission of the <a href="#">Active Microwave Instrument</a> ( AMI ) <a href="#">Synthetic Aperture Radar</a> ( SAR ) instruments flown on the <a href="#">European Remote Sensing</a> ( ERS ) Satellites ERS-1 and ERS-2. ASAR uses an <a href="#">active phased-array antenna</a> , with <a href="#">incidence angles</a> between 15 and 45 degrees. Applications for this sensor will include the study of ocean waves, sea ice extent and motion, and land surface studies such as deforestation and desertification, to name a few. ( see also chapter 1 " <a href="#">ASAR User Guide</a> " ( <a href="#">Chapter 1</a> .) ).
Along-track	An along-track sensor is made up of a linear detector array of CCDs (Charge Coupled Device) that obtains data in the platform's direction of motion ( <a href="#">azimuth</a> or along-track dimension). The sensor's instantaneous field of view extends the length of the <a href="#">swath</a> width. The dimension parallel to the path of the platform carrying the sensor. The along-track dimension is the imaging direction of the sensor that is parallel to the direction in which the satellite or aircraft is moving. For <a href="#">side-looking radars (SLARS)</a> , this dimension is sometimes called the cross range. The typical two-dimensional <a href="#">remotely sensed</a> image is created by the movement of the platform in the along-track direction, while the sensor scans or aims at the orthogonal direction. ( See also " <a href="#">Imaging Geometry</a> " in the Geometry glossary )
Alternating Polarisation (AP)	These products are similar to Image Mode products but include a second image acquired using a second <a href="#">polarisation</a> combination. The raw data is acquired in bursts of alternating polarisation. See Products glossary <a href="#">AP_MODE</a> .
Amplitude	Measure of the strength of a signal, and in particular the strength or height of an electromagnetic wave (units of voltage). The amplitude may imply a <a href="#">complex signal</a> , including both magnitude and the <a href="#">phase</a> .
Antenna	Part of the radar system, which transmits and/or receives electromagnetic energy. ( <a href="#">See Radar Antenna</a> )
Antenna Array	An arrangement of several individual <a href="#">antennas</a> so spaced and phased that their individual contributions add in the preferred direction and cancel in other directions. SAR systems, employ a short physical antenna, but through modified data recording and processing techniques, they synthesise the effect of a very long antenna. The result of this mode of operation is a very narrow effective antenna beamwidth, even at far ranges, without requiring a physically long antenna or a short operating wavelength. For example, in a SAR system, a 2m antenna can be made effectively 600 m long.
Array Antenna	See <a href="#">Antenna Array</a>
Attenuation	Decrease in the strength of a signal. The decrease in the strength of a signal, is usually described by a multiplicative factor in the mathematical description of signal level. A signal is attenuated by application of a gain less than unity. Common causes of attenuation of an electromagnetic wave include losses through absorption and by volume scattering in a medium as a wave passes through.
Azimuth Ambiguity	A form of ghosting that occurs when the sampling of returned signals is too slow.
Azimuth Bandpass Filtering	Bandpass filtering selects a certain band of <a href="#">frequency</a> components in the signal. <a href="#">Azimuth</a> bandpass filtering refers to filtering in the <a href="#">azimuth direction</a> of the two-dimensional <a href="#">SAR</a> signal. The location of signal energy in the azimuth frequency domain depends on the antenna pointing angle ( <a href="#">Doppler centroid 2.6.1.2.2</a> ), so bandpass filtering is necessary to maximize the signal energy in the processed image.
Azimuth Beam Inversion	The azimuth Impulse Response Function (IRF) has an amplitude which is modulated by the position of the echo in the azimuth beam pattern as the instrument passes the target. This modulation is removed by modifying the reference function by the inverse of the azimuth beam pattern (expressed as a function of <a href="#">Doppler frequency</a> ). This equalises the echo data across the Doppler bandwidth but exaggerates the noise - thereby degrading the noise figure by the so-called Beamshaping loss.
Azimuth Compression	In the SAR signal domain, the raw data is spread out in the range and azimuth directions and must be coherently compressed to realise the full-resolution potential of the instrument. Azimuth compression consists of coherently correlating the received signal with the azimuth replica function. (See <a href="#">Azimuth Beam Inversion</a> ). The appropriate Hamming weighting is applied also to the reference function. Subsequent correlation has the effect of modulating both signal and noise by similar amounts and hence the signal-to-noise ratio is unchanged by this process
Azimuth Descalloping	Radiometric correction (descalloping) is performed with a vector multiply in the azimuth direction. See <a href="#">Descalloping</a> in products glossary.
Azimuth Frequency	See <a href="#">Doppler Frequency</a>
Azimuth Time	The time along the flight path.
Backscatter	Backscatter is the portion of the outgoing radar signal that the target redirects directly back towards the <a href="#">radar antenna</a> . Backscattering is the process by which backscatter is formed. The scattering cross section in the direction toward the radar is called the backscattering cross section; the usual notation is the symbol <a href="#">sigma</a> . It is a measure of the reflective strength of a radar target. The normalised measure of the radar return from a distributed target is called the backscatter coefficient, or <a href="#">sigma nought</a> , and is defined as per unit area on the ground. If the signal formed by backscatter is undesired, it is called clutter. Other portions of the incident radar energy may be reflected and scattered away from the radar or absorbed.
Band	A selection of <a href="#">wavelengths</a> or range of radar <a href="#">frequencies</a> .
Bandwidth	A measure of the span of <a href="#">frequencies</a> available in the signal or passed by the band limiting stages of the system. Bandwidth is a fundamental parameter of any imaging system and determines the ultimate resolution available.
Beam	A focused pulse of energy. The <a href="#">antenna</a> beam of a <a href="#">side-looking radar (SLAR)</a> is directed perpendicular to the flight path and illuminates a <a href="#">swath</a> parallel to the platform ground track. Due to the motion of the satellite, each target element is illuminated by the beam for a period of time, known as the integration time. (See also chapter 1 " <a href="#">Principles of Measurement</a> " <a href="#">1.1.3</a> .)
Beam Mode	The <a href="#">SAR</a> operating configuration defined by the <a href="#">swath</a> width and resolution.
Beam Position	The area within the total possible <a href="#">swath</a> that is actually illuminated while being governed by the characteristics of a specific <a href="#">beam mode</a> .
Beta Nought	( $B^0$ )A radar brightness coefficient. The reflectivity per unit area in slant range which is dimensionless.
Bragg Scattering	Bragg Scattering is the enhanced <a href="#">backscatter</a> due to <a href="#">coherent</a> combinations of signals reflected from a <a href="#">rough</a> surface having features, with periodic distribution in the direction of wave propagation, and whose spacing is equal to half of the <a href="#">wavelength</a> as projected onto the surface.

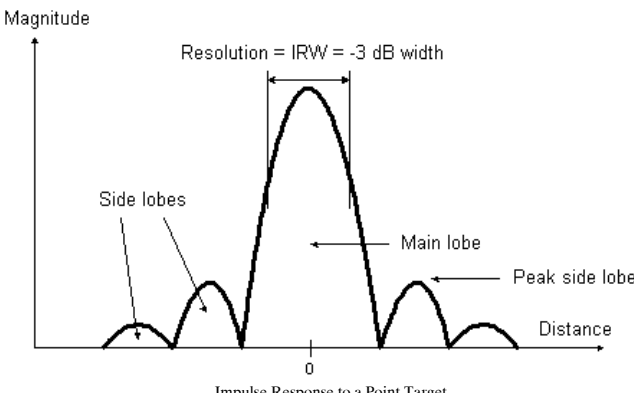
	 <p><b>Bragg Scattering ( See also )</b></p>
Brightness	Property of an image in which the strength of the radar reflectivity is expressed as being proportional to a digital number (digital image file) or to a grey scale (photographic image), which for a photographic positive shows bright as white. The attribute of visual perception in accordance with which an area appears to emit more or less light. Brightness may be a result of variations in tone, texture, or in the case of radar imagery, radar artefacts. The topography and surface roughness of the terrain will affect the image brightness. Where the local incidence angle is large, the image will be dark. Conversely, the image will be brighter where the local incidence angle is small.
Cardinal Effect	A tendency of a radar to produce very strong echoes from a city street pattern or other linear feature oriented perpendicular to the radar beam.
C-Band	A nominal frequency range, from 8 to 4 Ghz (3.75 to 7.5 cm wavelength) within the microwave (radar) portion of the electromagnetic spectrum. C-band has been the frequency of choice for several experimental aircraft SAR systems as well as a series of single-band satellite SAR systems, including the European ERS-1, ERS-2 and Envisat SAR systems and Canada's RADARSAT SAR. The corresponding wavelength for these systems is on the order of 5.6 cm, which has been found useful in sea ice surveillance as well as in other applications. Imaging radars equipped with C-band are generally not hindered by atmospheric effects and are capable of 'seeing' through tropical clouds and rain showers. Its penetration capability with regard to vegetation canopies or soils is limited and is restricted to the top layers. C-band is also used in range instrumentation radars
Chirp	<p>Typical phase coding or modulation applied to the range pulse of an imaging radar designed to achieve a large time-bandwidth product. The resulting phase is quadratic in time, which has a linear derivative. Such coding is often called linear frequency modulation, or linear FM.</p> 

	<p><b>Amplitude</b></p>  <p>The Real Part of Chirp</p> <p><b>Amplitude</b></p>  <p>The Imaginary Part of Chirp</p>
Chirp Compression	<p>The echo signal is correlated with a suitable reference function. This correlation is performed in the frequency domain after suitable Fast Fourier Transform from the time domain.</p> <p>The reference function of interest should represent the chirp signal which illuminates the target.</p> <p>This chirp varies from one swath to another due to the phase and amplitude settings introduced to produce beam steering. The beam steering (and shaping if necessary) is achieved by changing the excitations - phase and/or amplitude - to the many phase centres of the planar array antenna. The reference function should reflect these differences.</p> <p>In ASAR the phase of the excitation to any one row is constant along its length. Thus any row can be considered to be homogeneous. The characteristics of such a row are determined by exciting just that row - and hence deriving a reference function for it. A total reference function can then be derived by combining 32 such reference functions - using the commanded excitation phases.</p>
Circular Polarisation	A polarisation state in which the two perpendicular components of the electric field have equal magnitudes and a 90-degree phase difference. In this case, the tip of the electric field vector traces a circle on a plane that is perpendicular to the wave propagation direction.
Circularly Polarised Antenna	An antenna that is designed to radiate a left-hand or right-hand circularly polarised electromagnetic wave in its far field.
Clutter	Unwanted echoes in a radar return. See also <a href="#">Backscatter</a> .
Coherence	<p>Coherence is the fixed relationship between waves in a beam of electromagnetic (EM) radiation. Two wave trains of EM radiation are coherent when they are in phase. That is, they vibrate in unison. In terms of the application to things like radar, the term coherence is also used to describe systems that preserve the phase of the received signal.</p>
Coherence in an Interferogram	<p>In an <a href="#">interferogram</a>, coherence is a measure of correlation . It ranges from 0.0, where there is no useful information in the interferogram; to 1.0, where there is no noise in the interferogram (a perfect interferogram). Both extremes are rarely seen-- most images lie somewhere in between.</p> <p>Coherence is affected by, (in approximate order):</p> <ul style="list-style-type: none"> <li>Local slope (steep slopes lead to low coherence)</li> <li>Properties of the surface being imaged (vegetated or moving surfaces have low coherence).</li> <li>Time lag between the passes in an interferogram (long lags lead to low coherence)</li> <li>The baseline (large baselines lead to low coherence)</li> </ul> <p>Technical details of the generation of the interferogram (poor co-registration or resampling leads to low coherence)</p> <p>Coherence can serve as a measure of the quality of an interferogram; tell you more about the surface type (vegetated vs. rock); or tell you when a tiny, otherwise invisible change has occurred in the image, and it is only visible in the phase image of an interferogram.</p> <p>High coherence makes for attractive, not-noisy interferograms. Here is a coherent phase image of a mountain.</p>

	 <p>Coherent Phase Image of a Mountain</p> <p>Low coherence makes unattractive, noisy interferograms, as shown below. Often, these interferograms are difficult to phase unwrap.</p>  <p>Incoherent Phase Image of a Mountain</p> <p>Coherence is the magnitude of an interferogram's pixels, divided by the product of the magnitudes of the original image's pixels. It is usually calculated on a small window of pixels at a time, from the complex interferogram and images.</p> <p><b>Interferometric SAR (InSAR)</b> techniques make use of the coherence of the radar signal and the fact that the signal phase is equal to twice the path length between the sensor and the earth's surface. The phase difference between measurements generated from two SAR images with the sensor separated by a baseline, allows measurement of the slant range difference to fractions of a radar wavelength. The slant range difference can be geometrically related to the terrain height. By subtracting two signals, you generate an interference pattern. By subtracting the phases of two co-registered SAR images, you generate an interferogram.</p> <p>There are two basic SAR interferometry methods. In the first, two antennas are placed on the same platform and simultaneously acquire images of the scene from two different angles. The relative phase difference may then be used to construct a Digital Elevation Model (DEM).</p> <p>In the second, a pair of images from the same sensor are taken at different times. This is now a well-proven concept and has been demonstrated with several spaceborne SAR sensors, including RADARSAT. For this repeat-pass interferometry, the scenes are acquired at different times, so there is a time difference as well as viewing geometry to consider. The passes must have rather similar geometry in order to allow extraction of the relative phase difference. This usually requires that the satellite be on an exact repeat orbit.</p>
Coherent Reflector	Simple or complex surface, such as a corner reflector, from which reflected wave components are coherent with respect to each other, and thus combine to yield larger effective power than would be observed from a diffuse scattering surface of the same area.
Complex Number	For radar systems, a complex number implies that the representation of a signal, or data file, needs both magnitude and phase measures. In the digital SAR context, a complex number is often represented by an equivalent pair of numbers, the real in-phase component (I) and the imaginary quadrature component (Q). For coherent systems such as SAR, the role of complex numbers is an essential part of the signal, since signal phase is used in the processor to obtain high-resolution.

	 <p>Complex Number ( See also ).</p>
Conservation of Confusion	Principle, for imagery derived from a given SAR, that the amount of information in the data is a constant. One expression of this rule is that the product of the <a href="#">range</a> and the <a href="#">azimuth</a> resolution divided by the number of statistically independent looks is a constant, which serves as a figure of merit of the system. (In this context, information is related to the statistical degrees of freedom in the data ensemble, and not necessarily to knowledge about objects in the scene.)
Conservation of Co-ordinates	Principle, for Synthetic Aperture Radar (SAR) imagery, that image position is not changed by pitch, roll, or yaw rotations of the radar, since <a href="#">range</a> is determined by the speed of light, and <a href="#">azimuth</a> is determined by the <a href="#">along-track</a> radar velocity.
Conservation of Energy (Radar)	Principle, assuming that all available data is used for each case, that the average value of the estimated reflectivity from a scene is a constant for a given SAR and processor, independent of the number of looks used, and independent of any time varying noncoherence in the scene, such as from a moving surface of water, or in the radar/processor combination.
Co-polarisation Maxima	The antenna polarisation state for which maximum backscattered power is received from a particular target. For co-polarisation, the transmit and receive antennas are the same.
Co-polarisation Nulls	The antenna polarisation state for which zero backscattered power is received from a particular target. For co-polarisation, the transmit and receive antennas are the same. Co-polarisation nulls may not correspond to the maximum cross polarisation received power.
Co-polarisation Signature	The received signature when the transmit and receive antennas have the same polarisation properties.
Corner Reflector	A combination of two or more intersecting specular surfaces that combine to enhance the signal reflected in the direction of the radar. The strongest reflection is obtained for materials having a high conductivity (i.e. ships, bridges).
Cross Polarisation Maxima	The antenna polarisation state for which maximum cross-polarised backscattered power is received from a particular target. Co-polarisation nulls may not correspond to the maximum cross polarisation received power.
Cross Polarisation Nulls	The antenna polarisation state for which zero cross-polarised backscattered power is received from a particular target. For co-polarisation, the transmit and receive antennas are the same. Note that for cross polarisation nulls the co-polarisation power is maximum.
Cross Polarisation Signature	The received signature when the transmit and receive antennas have orthogonal polarisations.
Cross-polarised Waves ( or Orthogonal Waves )	Each wave in a pair of cross-polarised waves are completely polarised. However, an antenna optimised to receive the co-polarisation maximum of one wave will receive no power from the other wave. Note that, in general, an arbitrary wave may be treated as the sum of two cross-polarised waves.
Degree of Polarisation	An electromagnetic wave can have a polarised and a nonpolarised component. The degree of polarisation is given by the ratio of the power in the polarised part of an electromagnetic wave to the total power in the electromagnetic wave
Depolarisation	The polarisation state of an electromagnetic wave can change when the wave scatters from a target. Depolarisation is a measure of the change in the degree of polarisation of a partially polarised wave upon scattering. For example, a target may scatter a wave with a greater degree of polarisation than the incident wave, in which case the depolarisation is negative. Depolarisation is also used to indicate spatial or temporal variation of the degree of polarisation for a completely polarised wave
Detection ( Radar )	Processing stage at which the strength of the signal is determined for each pixel value. Detection removes phase information from the data file. The preferred detection scheme uses a magnitude squared method, which is energy conserving, and has units of voltage squared per pixel.
Dipole Sheet Transform	Also called radon transform. A three dimensional transform used in scattering of radar signals, optical data processing, and the like.
Doppler Frequency	The Doppler frequency depends on the component of satellite velocity in the line-of-sight direction to the target. This direction changes with each satellite position along the flight path, so the Doppler frequency varies with azimuth time. For this reason, azimuth frequency is often referred to as Doppler frequency.
Doppler Radar	A radar system which differentiates between fixed and moving targets by detecting the change in frequency of the reflected wave caused by the doppler effects. The system can also measure target velocity with high accuracy.
Dynamic Range	A description of the variety of signal amplitudes available in a system. Dynamic range is specified either (i) to be within minimum and maximum values or (ii) with respect to the ratio of maximum to minimum values.
Electromagnetic Displacement	Image distortion in the <a href="#">range</a> -direction caused Infra Red, <a href="#">microwave</a> , and <a href="#">radio waves</a> . By terrain features in the scene being above, or below, the reference elevation contour and, in fact, being closer to, or farther from, the <a href="#">radar</a> than their planimetric position. The effect may be used to create radar stereo images.
Electromagnetic Spectrum	The ordered array of known electromagnetic energy extending from the shortest rays, through gamma rays, X-rays, Ultra Violet, visible, Infra Red, microwave, and radio waves. ( <a href="#">see Scientific Background 1.1.2.1</a> .)
Elliptical Polarisation	A polarisation state in which the two perpendicular components of the electric field have unequal magnitudes and a non-zero phase difference. In this case, the tip of the electric field vector traces an ellipse on a plane that is transverse to the wave propagation direction.
Elliptically Polarised Antenna	An antenna that radiates <a href="#">elliptically-polarised</a> electromagnetic waves in its far field
European Remote Sensing (ERS)	Satellite series (ERS-1 and -2) launched by the European Space Agency (ESA) in July 1991 and April 1995. One instrument ( <a href="#">AMI</a> ) includes a <a href="#">C-band SAR</a> , <a href="#">VV polarisation</a> , and 23° <a href="#">incidence angle</a> , and 30-metre resolution. Predecessors to the <a href="#">ENVISAT</a> satellite.
Frequency	Number of oscillations per unit time or number of wavelengths that pass a point per unit time. Rate of oscillation of a wave. In remote sensing, this

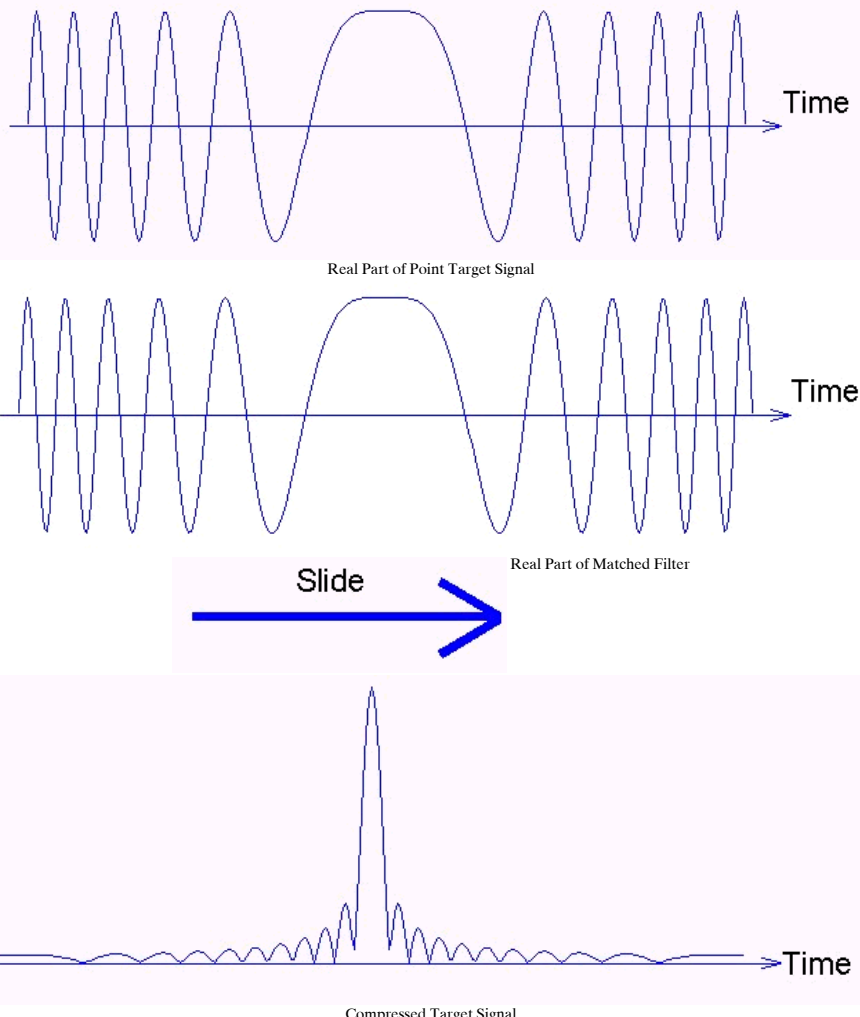
term is most often used with radar. The frequency bands used by radar (radar frequency bands) were first designated by letters for military secrecy. In the microwave region, frequencies are on the order of 1 GHz (Gigahertz) to 100 GHz. ("Giga" implies multiplication by a factor of a billion). For electromagnetic waves, the product of wavelength and frequency is equal to the speed of propagation, which, in free space, is the speed of light.\* In the microwave region, frequencies are on the order of 0.3 GHz-300 GHz, having wavelengths of 1mm - 1 m respectively.

	term is most often used with radar. The frequency bands used by radar (radar frequency bands) were first designated by letters for military secrecy. In the microwave region, frequencies are on the order of 1 GHz (Gigahertz) to 100 GHz. ("Giga" implies multiplication by a factor of a billion). For electromagnetic waves, the product of wavelength and frequency is equal to the speed of propagation, which, in free space, is the speed of light.* In the microwave region, frequencies are on the order of 0.3 GHz-300 GHz, having wavelengths of 1mm - 1 m respectively.
Frequency Assignment	Frequency at which a sensor (especially radar) operates.
Frequency Modulation	A technique in which the frequency of a signal is changed about a fundamental or carrier frequency. FM signals are used in many applications in remote sensing and in the radio broadcasting community. In SAR, the outgoing chirp signal has a linear FM of several megahertz. GPS signals are broadcast in FM.
Frequency Rate	The frequency rate is the coefficient of quadratic phase variation in the linear FM signal
Horizontal Polarisation	Linear polarisation with the lone electric vector oriented in the horizontal direction in antenna co-ordinates.
Horizontal Transmit - Horizontal Receive Polarisation (HH)	A mode of <a href="#">radar polarisation</a> where the <a href="#">microwaves</a> of the electric field are oriented in the horizontal plane for both signal transmission and reception by means of a radar <a href="#">antenna</a> .
Horizontal Transmit - Vertical Receive Polarisation (HV)	A mode of <a href="#">radar polarisation</a> where the <a href="#">microwaves</a> of the electric field are oriented in the horizontal plane for signal transmission, and where the vertically polarised electric field of the <a href="#">backscattered</a> energy is received by the radar <a href="#">antenna</a> .
Imaging Radar	Most imaging radars produce two-dimensional images. The two dimensions are called <a href="#">range</a> , and <a href="#">azimuth</a> .
	Also known as the point spread function, impulse response is the two-dimensional <a href="#">brightness</a> pattern in an image (after processing) corresponding to the signal reflected by an object whose sigma falls within the <a href="#">dynamic range</a> of the system, and for which the width of the imaged pattern is determined by the <a href="#">radar</a> and processor rather than by the size of the object. A trihedral <a href="#">corner reflector</a> is the most commonly used object for generating an impulse response in a test image. A good impulse response has a relatively large value for the <a href="#">pixel</a> that maps the point scatterer location, and very small values for all surrounding pixels. The impulse response is a basic building block in describing a given radar's imaging performance, since an image is built up from the linear combination of impulse responses from all individual scatterers illuminated by the radar. The impulse response width (IRW, or resolution) of the central peak is the most important characteristic of the impulse response, together with the shape of the impulse distribution, both close to and remote from its centre.
Impulse Response	 <p>Magnitude</p> <p>Resolution = IRW = -3 dB width</p> <p>Side lobes</p> <p>Main lobe</p> <p>Peak side lobe</p> <p>Distance</p> <p>0</p> <p>Impulse Response to a Point Target</p>
Incoherent	Property of a signal or data set in which the phases of the constituents are not statistically correlated, or systematically related in any fashion. Also known as non-coherent. ( <a href="#">See Coherence</a> )
In-Phase (I)	The real component of the signal that has the same phase as the complex reference frequency. In-phase is represented by the constant I ( see <a href="#">Complex Number</a> and )
In-Phase/Quadrature Channels (I/Q)	In-phase component of a ( See <a href="#">Complex Number</a> and )
Integrated Side Lobe Ratio (ISLR)	Given a single point scatterer on the ground, the processed <a href="#">SAR</a> image consists of a narrow, strong peak at the location of the scatterer (the mainlobe), surrounded by smaller peaks called <a href="#">sidelobes</a> . The sum of energy in the sidelobes, divided by the sum of energy in the mainlobe, is the Integrated Side Lobe Ratio (ISLR).
Interferometer	Device such as an imaging radar that uses two different paths for imaging, and deduces information from the coherent interference between the two signals. In SAR applications, spatial <a href="#">interferometry</a> has been demonstrated to measure terrain height, and time delay interferometry is used to measure movement in the scene such as oceanic currents.
Interferometric Synthetic Aperture Radar (InSAR)	<p><a href="#">SAR</a> interferometry is a technique involving <a href="#">phase</a> measurements from successive satellite SAR images to infer differential <a href="#">range</a> and range changes for the purpose of detecting very subtle changes on, or of, the earth's surface with unprecedented scale, accuracy and reliability.</p> <p><a href="#">SAR</a> <a href="#">interferometry</a> has been demonstrated successfully in a number of applications, including topographic mapping, measurement of terrain displacement as a result of earthquakes, and measurement of flow rates of glaciers or large ice sheets. The term InSAR, is most commonly associated with repeat-pass interferometry, as discussed in the section entitled "<a href="#">Interferometry 1.1.5.4</a>", in the User Guide. In contrast, D-InSAR is used to describe differential interferometry.</p> <p>( see also the section entitled "<a href="#">Processing Algorithms For AP SLC 2.6.2.1.1.2.1.4</a>", in chapter 2).</p>
Interferometry	A technique that uses the measured differences in the <a href="#">phase</a> of the return signal between two satellite passes to detect slight changes on the Earth's surface. ( see <a href="#">Interferometry</a> ) The combination of two <a href="#">radar</a> measurements of the same point on the ground, taken at the same time, but from slightly different angles, to produce stereo images. Using the cosine rule from trigonometry to calculate the distance between the radar and the Earth's surface, these measurements can produce very accurate height maps, or maps of height changes. Mapping height changes provides information on earthquake damage, volcanic activity, landslides, and glacier movement. ( see also the section entitled " <a href="#">Interferometry</a> " in the <a href="#">User Guide 1.1.5.4</a> .)
Inverse Synthetic Aperture Radar (ISAR)	A SAR system that makes use of the motion of the target to synthesise a large aperture antenna.
Linear Frequency Modulation (FM)	A linear FM signal has a quadratic phase variation with time, so the instantaneous frequency varies linearly with time.
Linear Polarisation	A polarisation state in which one of the perpendicular components of the electric field has zero magnitude. In this case, the polarisation ellipse collapses to a straight line; the tip of the electric field vector traces a straight line on a plane that is transverse to the wave propagation direction.
Linear Range Cell Migration Correction (RCMC)	A shift and interpolation operation is performed in the <a href="#">range</a> direction to correct for linear Range Cell Migration (RCM).
Linearity	Property according to which an operation on a sum of signals is equivalent to the same operation applied to each of the signals individually, and the resulting numbers added together. Linearity, over the dynamic range of the system, is an essential attribute of most measurement devices such as an imaging radar.
Look Direction	The radar <a href="#">look</a> direction defines the angle in the horizontal plane in which the radar antenna is pointing when transmitting a pulse and receiving the return signal from the ground or from an object. The look direction is an angular measurement (in degrees) and is usually made with respect to true North. In <a href="#">side-looking imaging radar (SLAR)</a> , the look direction is often orthogonal (normal) to the flight trajectory ( <a href="#">azimuth</a> ) of the platform carrying the radar and is thus synonymous with the <a href="#">range</a> direction. The radar look direction is an important parameter when analysing features with a preferred orientation, for example fracture patterns in rock formations, regular street patterns, or ocean waves, as these may be enhanced through choice of appropriate radar illumination direction. ( See also " <a href="#">Imaging Geometry</a> " in the geometry glossary ).

**Looks**

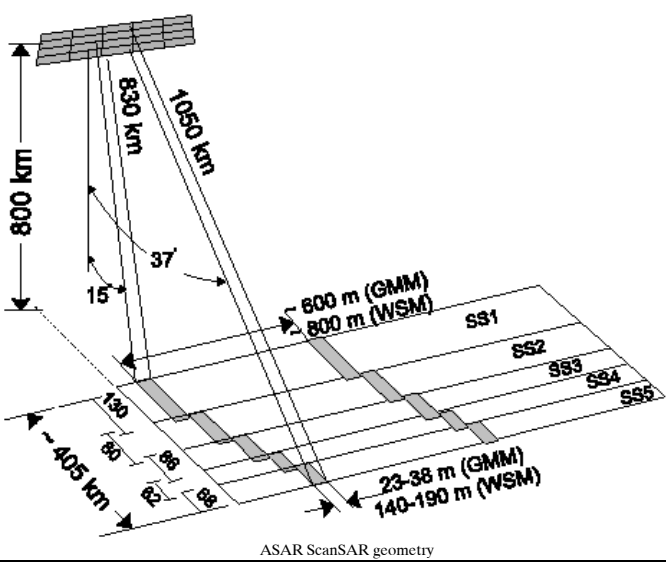
Radar terminology refers to individual looks as groups of signal samples in a SAR processor that splits the full synthetic aperture into several sub-apertures, each representing an independent look of the identical scene. The resulting image formed by incoherent summing of these looks is characterised by reduced speckle and degraded spatial resolution. The SAR signal processor can use the full synthetic aperture and the complete signal data history in order to produce the highest possible resolution, albeit very speckled, single-look complex (SLC) SAR image product. **Multiple looks** may be generated by averaging over range and/or azimuth resolution cells. For an improvement in radiometric resolution using multiple looks there is an associated degradation in spatial resolution. Note that there is a difference between the number of looks physically implemented in a processor, and the effective number of looks as determined by the statistics of the image data. ( See also ).

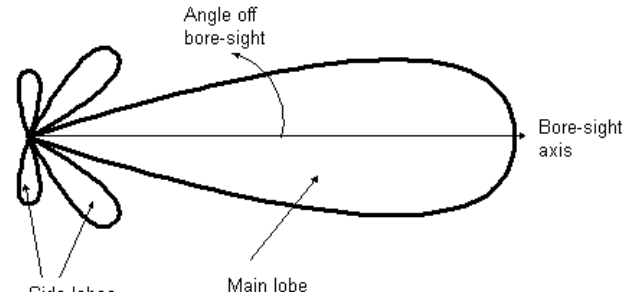
The matched filter can be thought of as a filter with a different time delay for each frequency component of the signal passing through the filter. That is, the different frequency components of the linear FM signal are each delayed so that they all arrive at the same time at the output of the filter. This way, all the signal energy is gathered into a narrow peak in the compressed pulse. ( see also "ASAR Level 1B Algorithm Physical Justification" - Pulse Compression 2.6.1.1.3.)



Looks	<p>Radar terminology refers to individual looks as groups of signal samples in a SAR processor that splits the full synthetic aperture into several sub-apertures, each representing an independent look of the identical scene. The resulting image formed by incoherent summing of these looks is characterised by reduced speckle and degraded spatial resolution. The SAR signal processor can use the full synthetic aperture and the complete signal data history in order to produce the highest possible resolution, albeit very speckled, single-look complex (SLC) SAR image product. <b>Multiple looks</b> may be generated by averaging over range and/or azimuth resolution cells. For an improvement in radiometric resolution using multiple looks there is an associated degradation in spatial resolution. Note that there is a difference between the number of looks physically implemented in a processor, and the effective number of looks as determined by the statistics of the image data. ( See also ).</p>
Matched Filtering	<p>The matched filter can be thought of as a filter with a different time delay for each frequency component of the signal passing through the filter. That is, the different frequency components of the linear FM signal are each delayed so that they all arrive at the same time at the output of the filter. This way, all the signal energy is gathered into a narrow peak in the compressed pulse. ( see also "ASAR Level 1B Algorithm Physical Justification" - Pulse Compression 2.6.1.1.3.)</p>
Microwave	A very short electromagnetic wave. The portion of the <a href="#">electromagnetic spectrum</a> lying between the far infrared (IR) and the conventional radio <a href="#">frequency</a> portion. While not bounded by definition, it is commonly regarded as extending from 1 mm to 1 m in <a href="#">wavelength</a> (300 GHz to 0.3 GHz frequency). Passive systems operating at these wavelengths sometimes are called microwave systems. <a href="#">Active systems</a> are called radar, although the literal definition of <a href="#">radar</a> requires a distance measuring capability not always included in active systems.
Motion Compensation	Adjustment of a sensing system and/or the recorded data to remove effects of platform motion, including rotation and translation, and variations in along-track velocity. Motion compensation is essential for aircraft SARs, but usually is not needed for spacecraft SARs.
Multifrequency Radar	Broadband systems that transmit pulses in a range of frequencies and wavelengths.
Multipolarisation Radar	A radar capable of simultaneously and coherently acquiring several independent complex polarisation measurements for every pixel in the image.
Night Sensing	The collection of non-photographic data during the period of time between sunset and sunrise.
Noise Equivalent Sigma Nought	A measure of the sensitivity of a given <a href="#">SAR</a> . It describes the strength of the (additive) system noise in terms of the equivalent (average) power in the image domain that would result from an idealised distributed scatterer of the stated reflectivity. Smaller noise equivalent sigma nought values are better. Within physical limitations, smaller may be achieved by increasing the power of the radar transmitter, or by decreasing the <a href="#">noise figure</a> of the electronics.
Noise Figure	Factor that describes the noise level in a radar receiver relative to the that in a theoretically perfect receiver. The noise figure, which is always larger than one, is typically two or more, and is usually expressed in decibels.
Optical Correlator	A device that enhances weak signals in noise by performing an optical operation approximating the computation of a correlation function. A radar optical correlator uses the original synthetic aperture radar signal film recording of doppler phase histories to make the radar image by methods that are similar to those used in optical <a href="#">Fourier transformation</a> .
Passive System	Systems that sense naturally available energy.
P-Band	A frequency range from 0.999 to 0.2998 GHz (30 to 100 cm wavelength) within the microwave (radar) portion of the electromagnetic spectrum. P-band is an experimental <a href="#">SAR</a> frequency that has only been used to-date for research and development purposes. It is part of the <a href="#">NASA JPL AIRSAR</a> multi-frequency (C-, L- & P-band) SAR system designed for Earth observation experiments. P-band is not hindered by atmospheric effects and is capable of seeing through heavy rain showers. P-band SAR penetration capabilities are very significant with regard to vegetation.

	canopies, glacier or sea ice, and soil. Its vegetation canopy imaging capability is considered a key element in estimating vegetation biomass by means of remote sensing.
Phase	See <a href="#">Radar Phase</a>
Phase Preserving	When the phase at the peak is correct, the processing algorithm is referred to as phase preserving, regardless of the phase variation across the <a href="#">impulse response</a> .
Phase Unwrap	In <a href="#">SAR interferometry (InSAR)</a> , the <a href="#">phase</a> delay of the carrier signal at a certain point in the interferogram is a function of the terrain height at that point. However, the phase of the carrier signal can only be measured to within one cycle, or 360 degrees. Phase unwrapping refers to converting the measured phase to the absolute phase, by adding the appropriate number of cycles, or multiple of 360 degrees, to the measured phase.
Polarimetric Active Radar Calibrator (PARC)	Device used to receive and retransmit radar <a href="#">pulses</a> . These devices usually consist of a <a href="#">polarisation</a> sensitive receive and transmit antenna and a stable amplifier which boosts the signal level so that the device being <a href="#">calibrated</a> receives a high signal of a given polarisation.
Polarimetric Radar	A radar which permits measurement of the full <a href="#">polarisation</a> signature of every resolution element.
Polarisation	The process of confining the vibrations of the magnetic, or electric field, vector of light or other radiation to one plane. Orientation of the plane of the electric field relative to the Earth's surface. See also <a href="#">Radar Polarisation</a> in Geometry glossary.
Polarisation Beamwidth	For a pair of antennas in a <a href="#">transmit-receive configuration</a> , the polarisation beamwidth is defined as the angle between the two directions from the transmitter at which the polarisation efficiency is one-half of its maximum value.
Polarisation Efficiency	For an electromagnetic wave that is incident upon a receiving antenna, the polarisation efficiency is defined as the ratio of power actually received in an impedance-matched load, to the maximum power that could be received if the antenna had optimum polarisation for the received wave.
Polarisation Ellipse	For an elliptically polarised wave, the tip of the electric field vector traces an ellipse on a plane that is transverse to the wave propagation direction. This polarisation ellipse describes the polarisation properties of the electromagnetic waves, including the ratio of the perpendicular electric field components and their relative phases.
Polarisation Loss	The inverse of <a href="#">polarisation efficiency</a> .
Pulse	A short burst of electromagnetic radiation transmitted by the <a href="#">radar</a> . Also described as a group of waves with a distribution confined to a short interval of time. Such a distribution is described in the time domain, or in spatial dimensions, by its width and its amplitude or magnitude, from which its energy may be found. In radar, use is made of modulated or coded pulses which must be processed to decode or compress the original pulse to achieve the <a href="#">impulse response</a> observed in the image. Coded pulses have a time-bandwidth product that is much larger than unity. The resolution that may be achieved after processing is determined by the bandwidth of the original pulse.
Pulse Compression	In collecting the <a href="#">SAR</a> data, a long-duration linear <a href="#">FM pulse</a> is transmitted. This allows the pulse energy to be transmitted with a lower peak power. The linear FM pulse has the property that, when filtered with a <a href="#">matched filter</a> , the result is a narrow pulse in which all the pulse energy has been collected to the peak value. Thus, when a matched filter is applied to the received echo, it is as if a narrow pulse were transmitted, with its corresponding range resolution and signal-to-noise ratio (SNR). ( see also " <a href="#">ASAR Level 1B Algorithm Physical Justification</a> " - Pulse Compression <a href="#">2.6.1.1.3.</a> )
Pulse Repetition Frequency (PRF)	Rate of recurrence of the <a href="#">pulses</a> transmitted by a <a href="#">radar</a> .
Quadrature (Q) Channel	The signal component that is 90° out of phase with respect to the reference frequency. It is represented by the letter Q. It is the imaginary part, which indicates the magnitude of the signal, of the complex number. See <a href="#">Complex Number</a> .
Quadrature Polarisation Radar (Quad Pol Radar)	A <a href="#">Radar</a> system designed to simultaneously collect imaging data of a scene in two orthogonal <a href="#">polarisation</a> states on transmit and the same two polarisation states on receive. From such a data set a complete scattering matrix of the reflectivity of the scene may be synthesised, leading to the concept of polarisation signature.
Radar	See " <a href="#">Radio Detection and Ranging</a> ".
Radar Angles	A <a href="#">radar</a> echo from a region where there are no visible targets; may be caused by insects, birds, or refractive index variations in the atmosphere.
Radar Antenna	The <a href="#">radar</a> antenna is a structure for transmitting and receiving radiated energy; it is an important subsystem that defines, to a great extent, a radar's operational capabilities and cost. In radar remote sensing the main function of the antenna is to concentrate a radiated <a href="#">microwave</a> energy into a beam of required shape, referred to as the antenna pattern, to transmit it into the desired direction ( <a href="#">look direction</a> ), and to receive the returned energy from surfaces or objects. Radar remote sensing antennas provide scene illumination ( See <a href="#">Active Remote Sensing System</a> ). The main parameters of radar antennas are operating <a href="#">frequency</a> band, antenna pattern shape (directive), power (or antenna-) gain, beam-width, <a href="#">side-lobe</a> level, <a href="#">polarisation</a> , and power handling capability. Moving antennas can be used to form a <a href="#">synthetic aperture</a> , where the physical antenna is small compared to the synthesised antenna, and has a sufficiently wide radiation pattern to illuminate the observed surface over a significant period of platform motion.
Radar Beam	The vertical fan-shaped beam of electromagnetic energy produced by the <a href="#">radar</a> transmitter.
Radar Cross Section (RCS)	Measure of radar reflectivity. The Radar Cross Section (RCS) is expressed in terms of the physical size of an hypothetical uniformly scattering sphere that would give rise to the same level of reflection as that observed from the sample target.
Radar Height Indicator (RHI)	Also known as Range Height Indicator.
Radar Parallax	Apparent change in the position of an object due to an actual change in the point of view of observation. For a <a href="#">SAR</a> , true parallax occurs only with viewpoint changes that are away from the nominal flight path of the radar. In contrast to aerial photography, parallax cannot be created by forward and aft looking exposures. Parallax may be used to create stereo viewing of radar images.
Radar Phase	Phase is a property of a periodic phenomenon, for example a wave, referring to its starting point or advancement (fraction) relative to an arbitrary origin. In radar remote sensing, the concept of phase is usually applied to the oscillation of electromagnetic waves. When viewed as a cyclical phenomenon, like wave motion or the crankshaft motion of a bicycle pedal, phase can be expressed in degrees. One-quarter cycle represents a phase rotation of 90 degrees; completion of one complete cycle corresponds to a phase rotation of 360 degrees. Waves are considered in-phase, if their origins of phase 0 degrees are perfectly aligned; out-of-phase conditions are met when phase 0 and 180 degrees are aligned. Precise knowledge of phase properties in radar signal data is a key element in interferometric as well as in polarimetric SAR.
Radar Transmission	Energy sent by the radar, normally in the form of a sequence of pulses, to illuminate a scene of interest.
Radar Wave Energy	For a waveform of time-limited duration such as a radar pulse reflected by an object, the pulse energy is given by the power of the signal integrated over the duration of the signal. It is expressed in units of watt-seconds = joules = j
RADARSAT-1	RADARSAT-1 is an advanced Earth observation satellite project developed by Canada to monitor environmental change and to support resource sustainability. It is Canada's first Earth observation satellite and the world's first operationally-oriented radar sensor. With a planned lifetime of five years, RADARSAT-1 is equipped with a <a href="#">Synthetic Aperture Radar (SAR)</a> . Launched in November 1995, this <a href="#">C-band</a> SAR satellite includes a steerable beam, which offers a wide selection of image scales and resolutions. It operates at 5.3 GHz. RADARSAT-2 is scheduled for launch in late 2003.
Radio Altimetry	The science and techniques involved in using a radar altimeter for precise measurements of distance between the sensor and the surface or feature. The basic concept of radar altimetry involves a short radar pulse transmitted toward the surface or feature and accurate measurement of the round trip time to the reflecting surface, which yields precise distance. The accuracy, which is generally on the order of several centimetres or tens of centimetres, depends mainly on the sharpness of the pulse, or signal bandwidth, and the footprint of the radar beam. Measurement techniques involve beam-limited and pulse-limited radar altimeters that provide two dimensional, high-resolution height profiles along the flight line. The synthetic aperture approach is also used by SAR altimeters to reduce the size of the footprint along the flight line. Prominent geoscientific applications of radar altimetry include measurement of ocean surface dynamics as well as solid surface topographic mapping.
Radio Band	The range of <a href="#">wavelengths</a> or frequencies of electromagnetic radiation designated as radio waves; approximately 10(4) to 10(9) Hz in frequency.
Radio Detection And Ranging (RADAR)	A method, system or technique, including equipment components, for using beamed, reflected, and timed electromagnetic radiation to detect, locate, and (or) track objects, to measure altitude and to acquire a terrain image. The radio detection instrument consists of a transmitter that sends out high-frequency radio waves and a receiver that picks them up after they have been reflected by an object. Basic building blocks of a radar are the transmitter, the antenna (normally used for both transmission and for reception), the receiver, and the data handling equipment. A synthetic aperture radar system, by implication, includes an image processor, even though it may be remotely located in time or space from the radar electronics. The advantage radar sensors have over other types of sensors, is that microwaves can penetrate clouds, most rain storms, and even dry snow. Therefore, for those parts of the world where cloud and rain present a problem in acquiring images (tropics, coastal/maritime regions), radar is highly beneficial. ( see also , chapter 4)

Radio Echo	The signal reflected by a <a href="#">radar</a> target, or the trace produced by this signal on the screen of the cathode-ray tube in a radar receiver.
Radio Frequency (RF)	A frequency that falls within the <a href="#">radio band</a> : 10(4) to 10(9) Hz.
Radiometer	An instrument for quantitatively measuring the intensity of electromagnetic radiation in any band of wavelengths in any part of the electromagnetic spectrum. Usually used with a modifier, such as an infrared radiometer or a microwave radiometer.
Radiometric Compensation	The sensitivity of the antenna is sensitive to angle and the radiometric compensation adjusts for variation in the received signal due to this effect. See <a href="#">Side Lobes</a> .
Range Time	The fast time within a received pulse, relative to the pulse transmission time
Real Aperture Radar (RAR)	A radar system where the antenna beamwidth is controlled by the physical length of the antenna. Also known as brute force or noncoherent radar. A <a href="#">SLAR</a> system in which azimuth resolution is determined by the physical length of the antenna and by the wavelength. The radar returns are recorded directly to produce images. The advantages of RAR is their simple design and data processing. However, its resolution is poor so RAR are limited to short range, low altitude missions, scanning short wavelengths. The use of the data is limited as shorter wavelengths experience a large amount of atmospheric effects, scattering and dispersion, for example. Because the missions are flown at low altitudes, the coverage is small. The resolution is limited by the length of the antenna. The antenna needs to be many times longer than the wavelength to produce narrow bandwidths. However, it is impractical to design an antenna long enough to produce high-resolution data. ( <a href="#">see also FAOS (Chapter 4.)</a> )
Remote Sensing (R/S)	Group of techniques for collecting image or other forms of data about an object from measurements made at a distance from the object, and the processing and analysis of the data. ( see also , chapter 4).
Repeat Pass Interferometry	Method based on two image acquisitions of the same scene from slightly displaced orbits of a satellite. <a href="#">Phase</a> information of the two image data files are superimposed. The two phase values at each <a href="#">pixel</a> are then subtracted, leading to an interferogram that records only the differences in phase between the two original images. Phase differences can be related to the altitude variation at each position in the <a href="#">swath</a> and enable the production of a <a href="#">Digital Elevation Model (DEM)</a> . For optimum results, there should be no change in the <a href="#">backscatter</a> to maintain <a href="#">coherence</a> ; vegetated sites are therefore a problem. For detection of feature movement (e.g. tracking glaciers) orbits should be as close as possible. Ground control points (GCPs) are required to accurately superimpose the two images. And knowledge of the sensor location is critical. With a good baseline and coherence, this technique can be better than stereo (~10 m vertical accuracy). ( see <a href="#">Interferometry</a> )
Rotor-SAR (ROSAR)	A synthetic aperture radar concept whereby antennas are mounted at the tips of the rotor blades (i.e. helicopter) illuminating a circular ring-shaped swath.
SAR Focusing	In a long synthetic aperture (array), <a href="#">SAR</a> focusing involves the removal and compensation of path length differences from the antenna to the target on the ground. The main advantage of a focused synthetic aperture is that it increases its array length over those <a href="#">radar</a> signals that can be processed, and thus increases potential SAR resolution at any range. SAR focusing is a necessary process when the length of a synthetic array is a significant fraction of the <a href="#">range</a> to ground being imaged, as the lines-of-sight (range) from a particular point on the ground to each individual element of the array differ in distance. These range differences, or path length differences, of the radar signals can affect image quality. In a focused SAR image these <a href="#">phase</a> errors can be compensated for by applying a phase correction to the return signal at each synthetic aperture element. Focusing errors may be introduced by unknown or uncorrected platform motion. In an unfocused SAR image, the usable synthetic aperture length is quite limited.
S-Band	A nominal frequency range from 4 to 2 GHz (7.5 to 15 cm wavelength) within the microwave (radar) portion of the electromagnetic spectrum. S-band radars are used for medium-range meteorological applications, for example rainfall measurements, as well as airport surveillance and specialised tracking tasks.
Scanning Synthetic Aperture Radar (ScanSAR)	A having the capability to illuminate several subswaths by scanning its <a href="#">antenna</a> off- <a href="#">nadir</a> into different positions.  <p>ASAR ScanSAR geometry</p>
Sea Satellite (SEASAT)	<a href="#">NASA</a> ocean research satellite that was in operation July-September of 1978. Seasat was the first (civilian) satellite to carry a <a href="#">SAR</a> . It operated at L-band, using horizontal <a href="#">polarisation</a> at 22° <a href="#">incidence angle</a> . Data from Seasat is still important for applications and processing technique development.
Sensitivity Time Control (STC)	Pre-programmed change in radar <a href="#">amplitude</a> due to weaker <a href="#">backscatter</a> from greater ranges and varying <a href="#">incidence</a> angles across the imaged swath.
Short Pulse Radar	Radar system capable of generating nanosecond pulses of energy at <a href="#">microwave</a> frequencies.
Sidelobes	Non-zero levels in a distribution that are separated from the desired central response. Sidelobes arise naturally in <a href="#">antenna</a> patterns, for example, although in general they are a nuisance, and must be suppressed as much as possible. Large side-lobes may lead to unwanted multiple images of a single feature.

	 <p>( See also <a href="#">Beamwidth</a> in the Geometry glossary )</p>
Side-Looking Aperture Radar (SLAR)	A high-resolution real aperture radar ( <a href="#">RAR</a> ) having antennas aimed to the right or left of the flight path. Also referred to as side-looking radar. An all-weather, day/night remote sensor which is particularly effective in imaging large areas of terrain. It is an active sensor, as it generates its own energy which is transmitted and received to produce a photo-like picture of the ground. It provides high-resolution strip maps with photograph-like detail. ( see also <a href="#">FAQS (Chapter 4.)</a> )
Signal Noise	Signal noise is any unwanted or contaminating signal competing with the desired signal. In a SAR, two common kinds of noise are additive (receiver) noise and signal dependent noise, usually either additive or multiplicative. The relative amount of additive noise is described by the signal-to-noise ratio (SNR). Signal dependent noises, such as azimuth ambiguities or quantization noise, arise from system imperfections, and are dependent on the strength of the signal itself. <a href="#">Speckle</a> is sometimes considered to be a kind of signal dependent multiplicative noise in a SAR system.
Spectral Window	A band of the <a href="#">electromagnetic spectrum</a> which offers maximum transmission and minimal attenuation through a particular medium.
Spectrum	See <a href="#">Electromagnetic Spectrum</a>
Stereo Sensing	Science and techniques used in obtaining stereo imagery (other than aerial photography).
Synthetic Aperture	A synthetic aperture, or virtual <a href="#">antenna</a> , consists of a long <a href="#">array</a> of successive and <a href="#">coherent</a> radar signals that are transmitted and received by a physically short (real) antenna as it moves along a predetermined flight or orbital path. The synthetic aperture is formed by pointing the real radar antenna of relatively small dimensions, which are restricted in size by the satellite platform, broadside to the direction of forward motion of that platform. The points at which successive <a href="#">pulses</a> are transmitted can be thought of as the elements of a long synthetic array, which a signal processor will then use and process to generate a SAR image. This detailed array of radar signal data is the key to achieving high <a href="#">azimuth</a> resolution. This long virtual antenna concept is the basis for synthetic aperture radar, or SAR. ( see also " <a href="#">Scientific Background</a> " <a href="#">1.1.2.</a> )
Synthetic Aperture Radar (SAR)	A <a href="#">synthetic aperture radar</a> , or SAR, is a <a href="#">coherent</a> radar system that generates high-resolution remote sensing imagery. Signal processing uses magnitude and <a href="#">phase</a> of the received signals over successive pulses from elements of a <a href="#">synthetic aperture</a> to create an image. As the line of sight direction changes along the radar platform trajectory, a synthetic aperture is produced by signal processing that has the effect of lengthening the <a href="#">antenna</a> . The achievable <a href="#">azimuth</a> resolution of a SAR is approximately equal to one-half the length of the actual (real) antenna and does not depend on platform altitude (distance). High range resolution is achieved through <a href="#">pulse compression</a> techniques. In order to map the ground surface the radar beam is directed to the side of the platform trajectory; with a sufficiently wide antenna beam width in the <a href="#">along-track</a> direction, an identical target or area may be illuminated a number of times without a change in the antenna <a href="#">look</a> angle. ( see also " <a href="#">Scientific Background</a> " <a href="#">1.1.2.3.</a> )
Synthetic Aperture Time	The time for a target to cross the <a href="#">azimuth</a> antenna beam.
Unpolarised Wave	A polarisation state in which the two perpendicular components of the electric field have equal magnitudes and a random relative phase difference.
Vertical Polarisation	<a href="#">Linear polarisation</a> with the lone electric vector oriented in the vertical direction in <a href="#">antenna</a> co-ordinates.
Vertical Transmit-Horizontal Receive Polarisation (VH)	A mode of <a href="#">radar polarisation</a> where the <a href="#">microwaves</a> of the electric field are oriented in the vertical plane for signal transmission, and where the horizontally polarised electric field of the <a href="#">backscatter</a> energy is received by the radar antenna.
Vertical Transmit-Vertical Receive Polarisation (VV)	A mode of <a href="#">radar polarisation</a> where the <a href="#">microwaves</a> of the electric field are oriented in the vertical plane for both signal transmission and reception by means of a radar <a href="#">antenna</a> . In this case, the plane of the electric field of the microwave energy is designated by the letter V (vertical) for both transmit and receive events, i.e. VV; this transmit-receive polarity is also called like-polarised as opposed to cross-polarised (horizontal transmit - vertical receive, HV). The amount of radar <a href="#">backscatter</a> received at a particular <a href="#">linear polarisation</a> state from a particular ground surface or object depends, in part, on the scattering mechanism and <a href="#">depolarisation</a> effects involved. The transmit-receive acronym is often used in conjunction with the <a href="#">frequency</a> band ( <a href="#">wavelength</a> ) designation of a particular radar system, e.g. C-VV for <a href="#">C-band</a> . Several satellite SAR designs have used single-band, horizontally like-polarised systems, for example the European <a href="#">ERS</a> -1 and ERS-2 (C-VV).
Wavelength	In a periodic wave, the distance between two points of corresponding <a href="#">phase</a> in consecutive cycles
Wavelet	Filter for enhancing and compressing radar images. Wavelets are operators that act both in space (azimuth and range) and in frequency (signal content). The classification and identification of texture and features in images incorporates fractal and multi-fractal models that can parameterise geophysical processes. Wavelets may be tailored to retain desired signal behaviour or to preserve smoothness. They are also used to characterise complex signals.
X-Band	A nominal frequency range from 12.5 to 8 GHz (2.4 to 3.75 cm wavelength) within the microwave (radar) portion of the electromagnetic spectrum. X-band is a suitable frequency for several high-resolution radar applications and has often been used for both experimental and operational airborne SAR systems, designed for military as well as civilian remote sensing applications. The corresponding wavelength for these systems is on the order of 3 cm, which has been found useful for mapping and surveillance tasks.

## 5.3 Product Terms

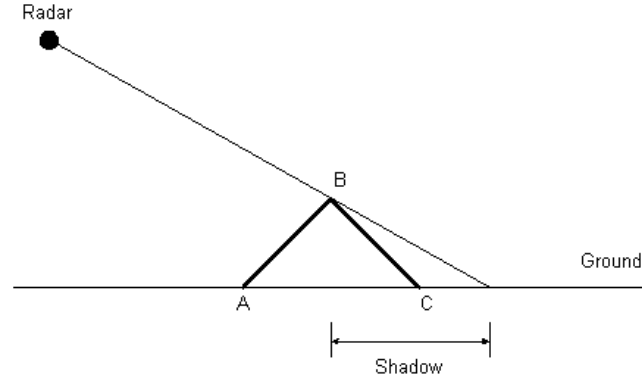
Table 5.3

Alternating Polarisation Mode (APP) Product	Two co-registered images per acquisition, from any of 7 selectable <a href="#">swaths.HH/VV</a> HH/HV or VV/VH polarisation pairs possible. Spatial resolution of approximately 30 m (for Precision product) ( see also " <a href="#">Organisation of Products</a> " ). These products are similar to <a href="#">Image Mode</a> (IM) products but include a second image acquired using a second polarisation combination. The <a href="#">raw data</a> is acquired in bursts of alternating polarisation. (See also <a href="#">Burst Mode Products</a> )
Alternating Polarisation Browse (APB) Image	Alternating Polarisation Browse (APB) image is a low-resolution compressed image product that will be produced systematically together with the <a href="#">AP Medium-resolution product</a> ( see also " <a href="#">Organisation of Products</a> " and " <a href="#">Browse Products</a> " <a href="#">2.6.2.1.3.1.2.</a> )
Alternating Polarisation Medium-Resolution (APM) product	This product is systematically generated in the <a href="#">PDHS</a> from Level 0 data collected when the instrument is in <a href="#">alternating polarisation (AP mode)</a> . The product is processed to approximately 150 m resolution using the <a href="#">SPECAN 2.6.1.2.4.</a> algorithm and contains radiometric resolution good enough for ice applications. The product contains one image corresponding to one of the 4 possible polarisation combinations ( <a href="#">HH</a> , <a href="#">VV</a> , <a href="#">HV</a> , or <a href="#">VH</a> ) when processed systematically in near real-time ( <a href="#">NRT</a> ). This product may also be generated on request with one, or both, polarisations included in the product. ( See also <a href="#">"Organisation of Products"</a> )
Alternating Polarisation Mode Ellipsoid Geocoded (APG) image	The Alternating Polarisation Mode Ellipsoid Geocoded (APG) image is a multi-look image generated upon request using the <a href="#">SPECAN 2.6.1.2.4.</a> algorithm and the most up to date auxiliary information available at the time of processing. ( see also " <a href="#">Organisation of Products</a> " and " <a href="#">Level 1B Image Products</a> " <a href="#">2.6.2.1.1.2.1.6.</a> )
Alternating Polarisation Mode Single-look Complex (APS) image	The <a href="#">Alternating Polarisation Mode</a> Single-look Complex (APS) image is a stand-alone narrow swath product uses the <a href="#">Range Doppler 2.6.1.2.3.</a> algorithm and the most up to date processing parameters available at the time of processing. ( see also " <a href="#">Organisation of Products</a> " and " <a href="#">Level 1B Image Products</a> " <a href="#">2.6.2.1.1.2.1.4.</a> )
Annotation Data Set (ADS)	One of two types of data sets ( Measurement Data Sets (MDS) is the other ) found in the <a href="#">Data Set Records</a> (DSRs) of an <a href="#">ASAR</a> product. See " <a href="#">Definitions and Conventions</a> " <a href="#">2.3.2.</a>
Annotated Instrument Source Packet (AISP)	The <a href="#">Level 0</a> product contains Annotated Instrument Source Packets (AISPs). These are <a href="#">Instrument Source Packets (ISPs)</a> as received from the instrument, with a small header attached by the Front End Processor (FEP).
Antenna Elevation Gain Scaling Factor	( See <a href="#">Antenna Elevation Gain Correction</a> )
Antenna Elevation Pattern	The <a href="#">antenna</a> pattern is the gain of a signal transmitted or received by the antenna, as a function of angle. The Elevation Pattern is the antenna pattern in the elevation, or vertical, direction.
Antenna Elevation Gain Correction	<a href="#">Antenna</a> elevation gain correction is derived by processing the periodic <a href="#">calibration</a> data. Periodic calibration generates <a href="#">calibration data</a> for the 32 rows of the <a href="#">SAR</a> antenna in a cyclic manner and downlinks this data interspersed with the imaging data. The antenna gain correction is derived from the calibration data from all 32 antenna rows received over a period of time. The elevation gain correction is also updated whenever a new periodic calibration cycle is found in the input data.
ASAR Modes	The different operating/measurement modes of the ASAR instrument. They are <a href="#">Image (IM) Mode</a> , <a href="#">Alternating Polarisation (AP) Mode</a> , <a href="#">Wide Swath (WS) Mode</a> , <a href="#">Global Monitoring (GM) Mode</a> , and the <a href="#">Wave (WV) Mode</a> . (See " <a href="#">Products and Algorithms Introduction</a> ")
Attachment Flag	Attachment flags are used within the <a href="#">DSRs</a> of ASAR products. See " <a href="#">Definitions and Conventions</a> " <a href="#">2.13</a>
Auxiliary Data	Product Data other than the instrument measurements which are necessary to the processing. Auxiliary data may come from the satellite itself, sources external to the <a href="#">PDS</a> , or be created by instrument processing facilities within the PDS. ( see also " <a href="#">Auxiliary Products</a> " <a href="#">2.9.</a> )
Average Cross Correlation Coefficient (ACCC)	The Cross Correlation Coefficient that is measured in the <a href="#">Doppler centroid estimation 2.6.1.2.2.</a> algorithm is measured in the <a href="#">azimuth direction</a> . The Average Cross Correlation Coefficient (ACCC) is the average of this Cross Correlation Coefficient over several azimuth lines.
Azimuth Compression	Azimuth compression is a matched filtering of the <a href="#">azimuth</a> signal, performed efficiently using <a href="#">FFT</a> 's. See discussion on " <a href="#">Azimuth Compression</a> " <a href="#">2.6.1.2.3.1.5.</a> in the section entitled Range Doppler in chapter 2.
Azimuth Bin	An azimuth <a href="#">bin</a> refers to a particular azimuth sample number.
Azimuth Fast Fourier Transform ( FFT )	<a href="#">FFT</a> 's are performed in the <a href="#">azimuth</a> direction. The FFT length must be as least twice as long as the azimuth block size to achieve the oversampling that is necessary prior to detection. See section entitled " <a href="#">Range Doppler</a> " <a href="#">2.6.1.2.3.1.3.</a> in chapter 2.
Azimuth Look Extraction	The good points for each <a href="#">azimuth</a> look are selected.
Azimuth Reference Function Multiply (deramp):	The data is multiplied by the <a href="#">azimuth</a> reference function. See also <a href="#">Deramping</a> .
Azimuth Resolution	Resolution characteristic of the <a href="#">azimuth</a> dimension, usually applied to the image domain. Azimuth resolution is fundamentally limited by the Doppler bandwidth of the system. Excess Doppler bandwidth is usually used to allow extra looks, at the expense of azimuth resolution.
Bin	A bin refers to a certain sample of a signal, in the time domain or the frequency domain.
Block Adaptive Quantisation (BAQ) decoding	A table look-up operation is used to perform BAQ decoding. The operation decompresses the data from the 2 or 4 bit coded representation to the 8 bit representation. Data compression using Block Adaptive Quantisation depends on the signals being quasi-random with Gaussian probability distribution function. The calibration pulses are completely deterministic and hence do not follow this assumption. For this the BAQ is effectively switched off giving 8 bits per sample quantisation -the highest accuracy possible.
Browse Averaging	The medium-resolution image is averaged and subsampled to form a browse product. Also referred to as Block Averaging.
Browse Product	Browse products are severely decimated images which can be ordered from the ENVISAT inventory. These products are very small, to support electronic transmission while querying the catalogues. They may be further reduced in size through the use of standardised data compression algorithms. Browse products are produced systematically, as by-products of the generation of the medium-resolution <a href="#">Level 1B</a> Image products, and contain image lines derived from a data segment (up to a full orbit of data). ( see also " <a href="#">Browse Products</a> " <a href="#">2.6.2.1.3.</a> )
Burst Mode Products	Image products that are formed with the <a href="#">SPECAN 2.6.1.2.4.</a> algorithm are formed from periodic bursts of <a href="#">SAR</a> data. The burstiness may arise because of the way the data is collected, as in <a href="#">Alternating Polarisation (AP) mode</a> or <a href="#">ScanSAR</a> modes [ <a href="#">Global Monitoring (GM)</a> , <a href="#">Wide Swath (WS)</a> ], or bursts may be extracted during processing, as in the formation of medium-resolution <a href="#">Image Mode (IM)</a> products. Typically a burst is much shorter than the time it takes the azimuth beam to pass over a point on the ground (synthetic aperture time). In comparison with the conventional <a href="#">stripmap</a> imaging methods, burst mode operation enables a reduced power consumption, and data rate, at the expense of the resolution and image quality achieved. When the burst images are stitched together to form the image product, the periodic intensity variation is seen as <a href="#">scalloping</a> <a href="#">2.6.1.2.4.2.</a> in the image. Scalloping can be corrected by multiplication with a <a href="#">descalloping</a> function.
Butterworth Filter	A particular type of filter frequency response, which is smooth (no ripples) as a function of frequency.
Calibration	Process of comparing an instrument's measurement with that of a known standard. For a discussion on this topic see " <a href="#">ASAR Characterisation and Calibration</a> " <a href="#">2.11.</a> in chapter 2 and " <a href="#">In-flight Performance Verification</a> " <a href="#">3.2.2.</a> in chapter 3.
Calibration Data	ASAR calibration data is considered to be auxiliary data within the <a href="#">PDS</a> . The data may be from <a href="#">Internal (Instrument) Calibration</a> , <a href="#">External Characterisation</a> , or <a href="#">External Calibration</a> .
Child Product	A child is the result of the extraction of a set of data from a parent product ( <a href="#">Level 0</a> , <a href="#">Level 1B</a> , <a href="#">Level 2</a> ). <a href="#">Generation of child products</a> can be formulated in terms of time, <a href="#">data set</a> (DS), or <a href="#">ISP</a> selection; in terms of either segments or scenes.
Complex Factor (fnp)	The fnp is the ground characterised complex factor characterising the path through the calibration loop and from the calibration

	coupler to the antenna face for row n, polarisation p at the swath reference angle for each beam. It is used in calculating the elevation gain function and to reconstruct the replica.
Complex Loop Paths Characterisation Factor (gnp)	The gnp is the complex loop paths characterisation factor relative to free space, where n is the index of the row (1 to 32) and p is the index of the polarisation (H or V). As with the Complex Factor (fnp) it is used in calculating the elevation gain function and to reconstruct the replica.
Complex Product	In a complex product, the extracted frequency array for each <a href="#">look</a> is multiplied by the <a href="#">matched filter</a> frequency response and <a href="#">inverse FFT'd</a> to form the complex look image. The matched filter frequency response is adjusted by a small linear phase ramp for each look. This is equivalent to shifting the compressed look in time, and is required to ensure that the images from different looks are aligned properly for look summation. The amount of <a href="#">azimuth</a> shift is <a href="#">range</a> -dependent. In addition, azimuth interpolation may also be performed after look compression to achieve a desire azimuth <a href="#">pixel</a> spacing, and it is done on each look separately. (see also <a href="#">Detected Product</a> )
Compression	Compression refers to the matched filtering of a linear FM pulse, in which all the energy of a long duration input pulse is gathered together at a peak value of a narrow output pulse.
Compression Algorithm	The compression algorithm that handles the necessary <a href="#">pulse compression</a> . See the discussion on " <a href="#">Pulse Compression</a> " <a href="#">2.6.1.1.3</a> , in chapter 2 entitled "ASAR Level 1B Algorithm Physical Justification".
Cross Correlation Coefficient (CCC)	The Cross Correlation Coefficient (CCC) is used in the <a href="#">Doppler centroid estimation</a> <a href="#">2.6.1.2.2</a> , algorithm. It is the average value of the product of adjacent signal samples, where the sample of a signal is multiplied by the conjugate of the next sample.
Cross Covariance	The average of the product of two signals, with one signal conjugated and shifted with respect to the other. The cross covariance is a function of the relative shift and is used to obtain the cross spectrum for the <a href="#">Level 1B wave products</a> .
Cross Spectra	The cross spectrum is the <a href="#">Fourier transform</a> of the <a href="#">cross covariance</a> .
Data Set (DS)	Data Sets are in mixed-binary format and each consists of one or more Data Set Records (DSRs). (See also " <a href="#">Definitions and Conventions</a> <a href="#">2.3.2.5</a> .)
Data Set Descriptor (DSD)	Data Set Descriptors are used to describe an attached <a href="#">Data Set</a> or to provide reference to external files relevant to the current product (e.g. auxiliary data used in processing but not included with the product). There must be one DSD per Data Set or per reference to an external file. ( see also " <a href="#">Definitions and Conventions</a> <a href="#">2.3.2.4</a> .)
Data Set Record (DSR)	Data Set Records contain information about products or auxiliary data. A number of record types are defined and used according to the type of product.
Deramping	A process whereby burst data is multiplied by the azimuth reference function. See discussion on " <a href="#">Azimuth Processing</a> " <a href="#">2.6.1.2.4.1.4</a> , in the section entitled "SPECAN" in chapter 2.
Descalloping	Descalloping is a radiometric correction of the burst image, performed with a vector multiply in the <a href="#">azimuth</a> direction. See <a href="#">Scalloping</a> . For a further discussion on this topic see the section entitled " <a href="#">Descalloping</a> " <a href="#">2.6.1.2.4.2</a> , in chapter 2.
Deskew	The data is shifted to correct for the skew that was applied during linear RCMC. Only the integer portion is corrected in this step. The fractional portion is handled during the <a href="#">SR/GR</a> resampling step.
Detected Product	( see also <a href="#">Complex Product</a> ). For the detected (magnitude) image products (IMP, IMG), a technique called multilooking is incorporated into the algorithm. In this method, separate images are formed from different azimuth spectral bands (looks), and the magnitude look images are averaged to reduce speckle. See also <a href="#">Detection</a> in Radar and SAR glossary.
Digital	Operating on data represented as a series of binary digits.
Directional Bins	The two-dimensional cross spectrum is converted to polar format, with dimensions of wavenumber and direction. A directional bin refers to a sample of the cross spectrum in at a certain direction.
Doppler Ambiguity Resolver (DAR)	Mathematical model used to determine the Doppler Ambiguity. See chapter 2 " <a href="#">Doppler Frequency Estimator</a> " <a href="#">2.6.1.2.2</a> .
Ellipsoid Geocoded Product	The Ellipsoid Geocoded Image product is similar to a <a href="#">Precision Image</a> , but with the best available instrument corrections applied for precise location and rectification to a map projection.
Extracted Calibration Product (ECP)	The Extracted Calibration Product (ECP) is a child product extracted from a level-0 product. It contains a suite of complete <a href="#">ISPs</a> for a selected time interval, and its structure is the same as the parent <a href="#">level-0 product</a> .
Extracted Instrument Header (EIH)	The Extracted Instrument Header (EIH) child product is extracted from a <a href="#">level-0</a> product. It contains a suite of <a href="#">ISP</a> fields for a selected time interval. It contains an <a href="#">MPH</a> , <a href="#">SPH</a> and <a href="#">MDS</a> .
False Colour (FC)	Using one colour to represent another. A colour imaging process which produces an image of a colour that does not correspond to the true colour of the scene (as seen by our eyes).
False Colour Composite (FCC)	An image produced by displaying multiple spectral bands as colours different from the spectral range they were taken in. It is a method of displaying multi-band (multi-channel) imagery. By assigning three of the image bands to the fundamental colours red, blue and green, you can produce a colour image. The blue band in the original image is often affected by atmospheric effects such as haze, and is therefore usually left out. When the assigned image bands do not correspond to the frequencies of red, blue and green the output image will appear in colours that are not intuitive or natural. For instance, different types of vegetation might appear as blue, red, green or yellow. Intuitively, vegetation would appear green. Such an image is known as a false colour composite. It is useful for extraction information difficult to discern in the original imagery, variations in vegetation species or health, for example.
Fast Fourier Transform (FFT)	A mathematical operation that fits a continuous function through the discrete digital number values, if they were plotted along each row and column of an image. The peaks and valleys along any given row or column can be described mathematically by a combination of sine and cosine waves with various <a href="#">amplitudes</a> , <a href="#">frequencies</a> , and <a href="#">phases</a> . A Fourier Transform results from the calculation of the amplitude and phase for each possible spatial frequency in an image. After an image is separated into its component spatial features, it is possible to display these values in a two-dimentional scatter plot, known as a Fourier Spectrum.
Floating Scene	<a href="#">Floating scene concept on archived products</a>
Flexible Block Adaptive Quantisation (FBAQ) Method	Process used to reduce echo samples. The FBAQ algorithm is an optimum minimum mean square quantizer, meaning it minimizes the value of the mean square of the differences between the original signal data and the FBAQ decoded signal data. One of the properties of this type of quantizer is that the variance of the decoded signal is reduced compared to that of the original signal. (See also <a href="#">Block Adaptive Quantisation (BAQ) decoding</a> and <a href="#">Root Mean Squared (RMS) Equalisation</a> )
Frame	The set of product <a href="#">pixels</a> corresponding to a given satellite position
Frequency Domain	The representation is the <a href="#">Fourier transform</a> of the original distribution. For every distribution f in time there is an equivalent representation F whose independent variable is frequency. F and f are equivalent in the sense that they carry the same information, but expressed in an alternative way. The concept is often generalised to distributions in the space domain, for which the Fourier transform is in the spatial frequency domain, having units of cycles per unit length. The azimuth frequency domain is also known as the Doppler domain.
Fully Consolidated Product	This is a <a href="#">Level 1B ASAR</a> product generated <a href="#">off-line</a> , time ordered, no overlap, no data gaps (except where the instrument has been turned off), fully validated; the basis for any further off-line processing. It has been produced using the most precise <a href="#">auxiliary</a> information available. It is compiled to respect the defined product boundaries (e.g., ascending node to ascending node at the equator for full orbit products).
Gaussian Filter	A filter with a Gaussian-shaped frequency response.
Geocoded	Geographic correction of image data to conform to a map projection. It is the process of resampling the data to conform to a standard map projection with known co-ordinates. Ground Control Points (GCPs) are often used to increase the accuracy of the geocoding process. ( See also ).

Geolocation	Geolocation information is provided in the product header in the form of latitude and longitude information that allow the user to determine the area covered by the data from a simple inspection of the header. For image data, a <a href="#">location</a> grid may also be provided as an attachment to the product to allow for precise pixel geolocation.
Geophysical Calibration Constant (CMOD)	The Geophysical Calibration Constant (CMOD) is an algorithm used for estimating the wind speed from the <a href="#">amplitude</a> of the SAR image. In the <a href="#">Level 2 wave mode</a> algorithm the parameter is used as follows: $\text{sigmaNought} = \sin(\theta\text{etaMid}) * \text{meanVal} / k\text{Cmod};$ In this equation $\text{sigmaNought}$ is the (modelled) radar cross section of the sea surface; $\theta\text{etaMid}$ is the <a href="#">incidence angle</a> at the centre of the <a href="#">imagette</a> , and $\text{meanVal}$ is the mean intensity of the imagette. Therefore, $k\text{Cmod}$ is simply the expected value of : $k\text{Cmod} = \sin(\theta\text{etaMid}) * \text{meanVal} / \text{sigmaNought}$
Georeferenced	The act of registering a map's co-ordinates with the ground's co-ordinates at true scale, also incorporating <a href="#">latitude</a> and <a href="#">longitude</a> information into the <a href="#">image</a> .
Ghosting	A SAR <a href="#">image artefact</a> where a dim copy of a bright target appears offset in <a href="#">range</a> and/or <a href="#">azimuth</a> . Ghosts are visible in the background as dark and invariant (e.g. calm water). Alternatively, ghosts are difficult to detect over variable backgrounds (e.g. forest). Ghosts occur when the desired signal is contaminated by the signal of adjacent targets. There are three types of ghosts: <a href="#">azimuth ambiguity</a> , <a href="#">range ambiguity</a> and <a href="#">nadir ambiguity</a> .
Global Annotation Data Set	Annotation data set ( <a href="#">ADS</a> ) which applies to the entire product.
Global Coverage	A global product contains coverage for the entire length of an orbit.
Global Monitoring Product Mode (GM)	The Global-Monitoring Mode product is a 1 km (low-) resolution image with a 405 km <a href="#">swath</a> width, suitable for dissemination by electronic links in <a href="#">near real-time (NRT)</a> . ( see also " <a href="#">Organisation of Products</a> " )
Global Monitoring Mode Browse (GMB) Image Product	The <a href="#">Global Monitoring Mode</a> Browse (GMB) Image product is a low-resolution product will be produced systematically together with the GM Image Product from Level 0 GM data. ( see also " <a href="#">Organisation of Products</a> " and " <a href="#">Browse Products</a> " <a href="#">2.6.2.1.3.1.4</a> . )
Global Monitoring Mode (GMI) Image Product	This is the standard product for ASAR <a href="#">Global Monitoring Mode</a> . It is processed to approximately 1 km resolution using the <a href="#">SPECAN 2.6.1.2.4</a> . algorithm. The <a href="#">swath</a> width is approximately 400 km. ( see also " <a href="#">Organisation of Products</a> " )
Granule	Granules are a part of the product which corresponds to the time window covered by a <a href="#">Data Set Record (DSR)</a> of the <a href="#">LADS</a> . Product slices are made from integer numbers of granules. See <a href="#">Figure 2.5</a> and <a href="#">Figure 2.6</a> in "Products and Algorithms Introduction"
High-resolution Image	The high-resolution ASAR images are the <a href="#">Image Mode</a> products (IMS, IMP, IMG) and the <a href="#">SLC Alternating Polarisation</a> mode product (APS). See <a href="#">Table</a> in the section entitled "Organisation of Products" in chapter 2.
Image	A pictorial representation acquired in any wavelength of the <a href="#">electromagnetic spectrum</a> . Also defined as: (1) The counterpart of an object produced by the reflection or refraction of light when focused by a lens or mirror. (2) The recorded representation (commonly as a photo-image) of an object produced by optical, electro-optical, optical mechanical, or electronic means. It is generally used when the electromagnetic radiation is emitted or reflected from a scene is not directly recorded on film. For radar, the image tones represent the radar reflectivity of the scene. ( See <a href="#">Radar Image</a> )
Image Artefact - SAR	SAR image artefacts can occur due to platform, sensor, and/or processing problems. Some example of artefacts are: <a href="#">ghosting</a> ( <a href="#">azimuth</a> , <a href="#">range</a> , <a href="#">nadir</a> ), <a href="#">scalloping</a> , and Automatic Gain Control (AGC) effects. Image radiometries and geometries can be affected. Images can sometimes be improved by being reprocessed, though artefacts are sometimes incorrigible.
Imagette	Small, <a href="#">high-resolution</a> , <a href="#">complex image</a> product collected in wave mode.
Imagette Power Spectrum	The <a href="#">imagette</a> power spectrum is the distribution of signal energy in the image over the two-dimensional frequency domain.
Image Mode (IM) Product	These products are <a href="#">high-resolution</a> , narrow swath products based on data acquired at one of seven sub-swaths. Swath width between approximately 56 km (swath 7) and 100 km (swath 1) across-track. Spatial resolution of approximately 30 m (for Precision product). (see also " <a href="#">Organisation of Products</a> " )
Image Mode Browse (IMB) Image	The Image Mode Browse (IMB) image product is a low-resolution product that will be produced systematically together with the <a href="#">Image Mode Medium-resolution product</a> . ( see also " <a href="#">Organisation of Products</a> " and " <a href="#">Browse Products</a> " <a href="#">2.6.2.1.3.1.1</a> . )
Image Mode Ellipsoid Geocoded Image (IMG) Product	The Image Mode Ellipsoid Geocoded Image (IMG) product is stand-alone Image Mode <a href="#">Geocoded</a> SAR image generated in either <a href="#">HH</a> or <a href="#">VV</a> polarisation, using the <a href="#">Range/Doppler 2.6.1.2.3</a> . algorithm with the best available instrument corrections. ( see also " <a href="#">Organisation of Products</a> " and " <a href="#">Level 1B Image Products</a> " <a href="#">2.6.2.1.1.2.1.3</a> . )
Image Mode Medium-Resolution Image (IMM) Product	These products are <a href="#">medium-resolution</a> systematically generated in the <a href="#">PDHS</a> from the Level 0 data collected when the instrument is in <a href="#">Image Mode</a> . This product, processed to approximately 150-m resolution, features an <a href="#">ENL</a> (radiometric resolution) good enough for ice applications. (see also " <a href="#">Organisation of Products</a> " and " <a href="#">Level 1B Image Products</a> " <a href="#">2.6.2.1.1.3.1.1</a> . )
Image Mode Precision Image (IMP) Product	These are <a href="#">high-resolution</a> stand-alone image products created directly from the Level 0 data. The scene size is 100 km <a href="#">along-track</a> by the <a href="#">swath</a> width for the swath from which the data is acquired (between 56 and 100 km wide). This stand-alone image is generated using the <a href="#">Range/Doppler 2.6.1.2.3</a> . algorithm. The processing uses up to date (at time of processing) auxiliary parameters and corrects for <a href="#">antenna elevation gain</a> , and range spreading loss. (see also " <a href="#">Organisation of Products</a> " and " <a href="#">Level 1B Image Products</a> " <a href="#">2.6.2.1.1.2.1.2</a> . )
Image Mode Single-Look Complex (IMS) Product	Single-Look Complex (SLC) image data is a <a href="#">high-resolution</a> , narrow swath products based on data acquired at one of seven subswaths. It is intended for SAR image quality assessment, calibration and interferometric or wind/wave applications. A small number of corrections and interpolations are performed on the data in order to allow freedom in the derivation of higher-level products. (see also " <a href="#">Organisation of Products</a> " and " <a href="#">Level 1B Image Products</a> " <a href="#">2.6.2.1.1.2.1.1</a> . )
Input Data Gap	An input data gap is defined as a contiguous block of N missing lines where the value of N has been predefined for each product.
Invariance Regions	A number of range samples over which processing parameters are held constant
Inverse Fast Fourier Transform (IFFT)	If the Fourier Spectrum [see <a href="#">Fast Fourier Transform (FFT)</a> ] of an image is known, it is possible to regenerate the original image through the application of an Inverse Fourier Transform, which is simply the mathematical reversal of the FFT.
Instrument Source Packet (ISP)	The Instrument Source Packets (ISP) contain the ASAR measurement data codewords, as well as the necessary information to decode the codewords for ground processing. The source packet layout covers the structure of the Packet Header and Packet Data Field, plus the interpretation of the parameters contained within the packet. For a full description of the layout and techniques used for the reconstruction of sampled data refer to the document "ENVISAT-1 ASAR Interpretation of Source Packet Data. PO-TN-MMS-SR-0248".
Level 0	Level 0 data is reformatted, time-ordered satellite data (no overlap), in computer-compatible format. Level 0 is the lowest level product in the <a href="#">ENVISAT PDS</a> . ( See <a href="#">Table 2.7</a> in section entitled "ASAR Level 0 Products" in chapter 2 for a summary of these products).
Level 1B	Level 1B products are <a href="#">geolocated</a> products in which data has been converted into engineering units, auxiliary data has been separated from measurements, and selected <a href="#">calibrations</a> have been applied to the data. These products are the foundation from which higher level products are derived. <a href="#">Level 0</a> products are transformed into Level 1B products by application of algorithms and calibration data to form a baseline engineering product. <a href="#">ASAR</a> Level 1b products may be <a href="#">unconsolidated</a> , <a href="#">fully consolidated</a> , or <a href="#">partially consolidated</a> . ( See <a href="#">Table 2.39</a> in section entitled "Level 1B High Level Organisation of Products" in chapter 2 for a summary of these products).
Level 2	The Level 2 product is a <a href="#">geolocated</a> geophysical product. The <a href="#">Level 1B</a> product is transformed into one, or more, Level 2 products through higher-level processing to convert engineering units into geophysical quantities and to form a data set that is

	easier to interpret. For ASAR there is currently only one Level 2 product (ASA_WVV_2P), referred to as the Ocean Wave Spectra product. (For more detail concerning this product see the section entitled " <a href="#">Level 2 Product and Algorithms</a> " 2.7, in chapter 2)
Line	A line of <a href="#">pixels</a> follows the <a href="#">across-track</a> direction, its numbering starts from one and increases from North to South
Location Annotation Data Set (LADS)	The LADS provides latitude and longitude of image data for wave mode, and a table of geodetic lat/longs at various range/azimuth positions and times for other images. Used to geolocate products.
Main Product Header (MPH)	The Main Product Header (MPH) is in ASCII format and contains information which is common to all <a href="#">ENVISAT</a> instruments. (see " <a href="#">Definitions and Conventions</a> " 2.3.2.2.)
Measurement Confidence Data (MCD)	This was the term used by <a href="#">ERS</a> for what is now referred to as the Product Confidence Data ( <a href="#">PCD</a> ) found in the Specific Product Header ( <a href="#">SPH</a> ) of the product.
Measurement Data Set (MDS)	The Measurement Data Set (MDS) consist of a series of <a href="#">Annotated Instrument Source packets (AISPs)</a> . (see " <a href="#">Definitions and Conventions</a> " 2.3.2.5.)
Medium-resolution Image	A medium-resolution Image product will be available at 150 m resolution, which is specifically aimed at sea ice and oceanography applications.
Module Stepping (MS) Mode	The Module Stepping Mode is used to gather data from all of the instrument's 320 Transmit/Receive Modules (TRM) automatically. This mode provides an internal health checking facility on an individual module basis. The purpose of the mode is to identify malfunctioning modules which may need to be switched off, and to identify modules to which <a href="#">calibration</a> offsets are to be applied. (See also the section entitled " <a href="#">ASAR Level 0 Products</a> 2.5.1.2.3.3," and " <a href="#">ASAR Characterisation and Calibration</a> " 2.11, in chapter 2 and in the section entitled " <a href="#">In-flight Performance Verification</a> " 3.2.2, in chapter 3 ).
Mosaic	A technique whereby multiple satellite images are digitally joined, while correcting for systematic changes in radiometry and geometry, thus creating a seamless image product.
Motion Artefact - Radar	Objects in the scene that are not properly imaged because of motion in the aircraft carrying the sensor (radar).
Multi-Look Cross Correlation (MLCC)	This is a Doppler centroid frequency algorithm that estimates both the integer and fractional parts of the Doppler centroid from the <a href="#">SAR</a> data. The estimator determines the absolute Doppler frequency, without aliasing, obtaining both of the parameters as a function of <a href="#">range</a> . Knowledge of the beam pointing angles is not needed by the algorithm, except as a cross check. (See the section entitled " <a href="#">Doppler Frequency Estimator</a> " 2.6.1.2.2.3, in chapter 2).
Multi-Look Imagery	Resulting image when independent images of the same area are averaged to create a single multi-look image. Such an image has a lower resolution but the <a href="#">speckle</a> has been reduced. ( See also )
Multi-Temporal Imagery	A collection of <a href="#">images</a> of the same area, obtained at different times.
Nadir Ambiguity	A form of <a href="#">ghosting</a> that appears as bright linear features with approximately constant <a href="#">range</a> . They occur when signal returns from <a href="#">nadir</a> are strong due to near-specular reflection from targets within a very narrow <a href="#">slant range</a> distance. This results in bright tone. Due to <a href="#">pulse compression</a> , the bright return is restricted to a small number of range cells. This results in the sharp, linear shape.
Near Real Time (NRT) Products	There are two types of Near Real Time ( NRT ) products: those to be produced within 3 hours and those to be produced within one day.
Ocean Wave Mode	see <a href="#">Level 2</a>
Off-line (OFL) Products	Some products will be processed off-line. The availability time depends on the complexity of the processing and the availability of auxiliary data. Delivery time ranges from two business days to four weeks.
Orbit Designator (Ascending or Descending )	A satellite in a polar orbit, such as ENVISAT, has an Ascending orbital designation when travelling northbound and a Descending orbital designation when travelling southbound. The orbital designation of the SAR data is determined by the satellite position at the start of the imaging activity.
Partially Consolidated Product	This is a <a href="#">Level 1b</a> ASAR product, that has been <a href="#">consolidated</a> in all ways except that it does not use the most precise auxiliary data possible to perform processing. Since several different levels of accuracy exist for auxiliary data (e.g., 5 possible orbit state vector sources) varying levels of consolidation may exist for a product.
Pixel	Picture element, the smallest display element. For a discussion on pixel spacing see <a href="#">FAQs (Chapter 4.)</a> . Product pixels are a matrix of points where 1) lines (frames) correspond to the ASAR sampling instants and cope with the swath at those instants; 2) columns correspond to regular subdivisions of the interval between two adjacent columns of the tie points matrix, i.e. product columns are sampling the <a href="#">swath</a> at constant distance. (See also )
Point Target	A point target is an idealized single scatterer that reflects the transmitted pulse. Used to model the SAR signal for processing.(See also the section entitled " <a href="#">ASAR Level 1B Algorithm Physical Justification</a> " 2.6.1.1.4, in chapter 2).
Precision Image Product (PRI)	The Precision Image product is a <a href="#">multi-look</a> , <a href="#">ground range</a> , digital image (in either <a href="#">HH</a> or <a href="#">VV</a> polarisation) suitable for most applications. It is intended for <a href="#">multi-temporal</a> analysis and for deriving <a href="#">backscatter</a> coefficients. Engineering corrections and <a href="#">relative calibration</a> are applied to compensate for well understood sources of system variability. Absolute calibration parameters are provided in the product annotations.
Preprocessing	Preprocessing is applied to all <a href="#">raw data</a> before the other parameter estimation and image formation steps are performed. (see " <a href="#">Preprocessing</a> 2.6.1.2.1," section in chapter 2)
Product Confidence Data	A flag that simultaneously provides surface type information (land, water or cloud), additional scientific information relevant to the product interpretation (dark vegetation, turbid waters, absorbing aerosols etc.), and confidence information for each product. ( See also " <a href="#">Definitions and Conventions</a> " 2.3.1.4, and " <a href="#">Level 1B Essential Product Confidence Data</a> " 2.6.2.3. )
Quick-look	<a href="#">Imagery</a> produced immediately after data reception. The imagery lacks corrections, but has sufficient resolution and clarity to provide visual information for most users.
Radar Image	A <a href="#">Radar</a> Image is the mapping of the observed radar reflectivity of a scene. For radars with digital image processing, the image consists of a file of digital numbers assigned to spatial positions on a grid of <a href="#">pixels</a> , and presented either as hard copy (such as a photographic print) or soft copy (such as a digital data record). All radar images are subject to statistical variations, mainly <a href="#">speckle</a> and <a href="#">noise</a> , which must be accommodated in either visual or numerical image interpretation. The most commonly used image formats occur after <a href="#">detection</a> .
Radar Processing	Sometimes denoted <a href="#">pre-processing</a> 2.6.1.2.1 , it is the means of converting the received reflected signal into an <a href="#">image</a> . Processing consists of image focusing through <a href="#">matched filter</a> integration, <a href="#">detection</a> , and <a href="#">multi-look</a> summation. The output files of a <a href="#">SAR</a> processor usually are presented with unity aspect ratio (so that <a href="#">range</a> and <a href="#">azimuth</a> image scales are the same). Images may be either in <a href="#">slant range</a> or <a href="#">ground range</a> projection. Both of these spatial adjustments require resampling of the image file. (The algorithms used to generate the different ASAR images are discussed in the sections entitled " <a href="#">ASAR Level 1B Algorithms</a> 2.6.1," and " <a href="#">ASAR Level 2 Algorithm Description</a> " 2.7.1, in chapter 2).
Radiometric Correction	This procedure corrects and <a href="#">calibrates</a> the gain and offset variations in <a href="#">radar imagery</a> .
Range Ambiguities	Unwanted <a href="#">echoes</a> that fall into the image from <a href="#">ranges</a> that, in fact, are outside of the intended <a href="#">swath</a> , due to the range sampling operation of the <a href="#">radar</a> . Range ambiguities may be minimised by antenna pattern and <a href="#">imaging mode</a> control.
Range Bin	An range <a href="#">bin</a> refers to a particular range sample number.
Range Cell Migration Correction (RCMC)	Range Cell Migration Correction (RCMC) is the step of correcting for the changing range delay to a point target as the target passes through the antenna beam (range migration). See the discussion " <a href="#">Range Cell Migration Correction (RCMC)</a> " 2.6.1.2.3.1.4, in the section entitled "Range Doppler" in chapter 2.
Range Compression	Is <a href="#">matched filtering</a> of the received <a href="#">echo</a> . See the discussion " <a href="#">Range Compression</a> " 2.6.1.2.3, in the section entitled "Range Doppler" in chapter 2.

Range Dependent Gain Correction	The <a href="#">range compressed</a> data is multiplied by a vector that corrects the effects due to elevation beam pattern and range spreading loss.
Range Fast Fourier Transform (FFT)	<a href="#">FFTs</a> are performed in the <a href="#">range</a> direction. For most products, this consists of two overlapped FFTs per range line. See the discussion " <a href="#">Range Compression</a> " <a href="#">2.6.1.2.3</a> , in the section entitled "Range Doppler" in chapter 2.
Range Inverse Fast Fourier Transform (IFFT)	<a href="#">IFFTs</a> are performed in the <a href="#">range</a> direction. Again, this usually consists of two overlapped IFFTs. Each segment is inverse FFT'd to get the range compressed data. Part of each segment is thrown away since the compressed range data is shorter than the uncompRESSED range data by the length of the transmitted pulse. The range matched filter is designed so that the throw-away is at the end of the inverse FFTed data. The results from each segment are then joined together to get the compressed data for the whole range line. See the discussion " <a href="#">Range Compression</a> " <a href="#">2.6.1.2.3</a> , in the section entitled "Range Doppler" in chapter 2.
Range Matched (RM) Multiply	The <a href="#">frequency</a> domain data is multiplied with the <a href="#">range matched filter</a> . Each <a href="#">FFT</a> 'd segment is multiplied by the frequency response of the matched filter. See the discussion " <a href="#">Range Compression</a> " <a href="#">2.6.1.2.3</a> , in the section entitled "Range Doppler" in chapter 2.
Range Multi-Looking	A set of band pass filters are applied to the data to extract multiple range looks (if necessary).
Range Resolution	Resolution characteristic of the <a href="#">range</a> dimension, usually applied to the <a href="#">image</a> domain, either in the <a href="#">slant range</a> plane or in the <a href="#">ground range</a> plane. Range resolution is fundamentally determined by the system <a href="#">bandwidth</a> in the range channel.
Raw Data	Raw data is data as received from the satellite (serial data stream, not demultiplexed). Raw data is recorded from the X and Ka band demodulator output interfaces and stored on High-Density Data Tapes (HDDTs). The Raw Data is not considered a product.
Raw Data Analysis	Complex data is collected in-phase (I) and quadrature-phase (Q) channels. Receiver electronics may introduce biases or cross-coupling (non-orthogonality) between the I and Q channels. This can be estimated by collecting statistics of the I and Q channels. These statistics are collected by accumulating the sums I, Q, I squared and Q squared . Only a fraction of the data set is used. ( See also <a href="#">Complex Number</a> in the Radar and SAR glossary )
Raw Data Correction	The following operations are performed for each sample: I/Q bias removal in one of the channels, power balance in one of the channels (I/Q gain imbalance correction), and phase (I/Q non-orthogonality) correction in one of the channels. ( See also <a href="#">Complex Number</a> in the Radar and SAR glossary )
Regional Coverage	A regional product may only cover a specific segment of an orbit.
Resolution	The minimum separation between two objects of equal reflectivity that enables them to appear individually in a processed <a href="#">radar image</a> . Also referred to as spatial resolution. Resolution in a radar system differs in two directions: the <a href="#">azimuth</a> (or <a href="#">along-track</a> ) direction and the <a href="#">range</a> (or <a href="#">across-track</a> ) direction.
Resolution Cell	A two-dimensional cylindrical volume surrounding each point in the scene. The cell <a href="#">range</a> depth is <a href="#">slant range resolution</a> , and its width is <a href="#">azimuth</a> resolution
Root Mean Squared (RMS) Equalisation	The Root Mean Squared (RMS) Equalisation method is an <a href="#">FBAQ</a> decoding option whereby the decoder attempts to make the RMS of the decoded data equal to that of the original signal data. This is done at the expense of mean-squared error performance (i.e. the algorithm is no longer a true optimum minimum mean square quantizer when this option is used). Note that for <a href="#">SAR</a> data, characterized by a zero mean Gaussian distribution, the RMS of the data is equal to the square-root of the variance. Also note that RMS Equalisation is not expected to be used operationally, but may be used for some Wave Mode experiments.
Roughness	Variation of surface height within an <a href="#">imaged resolution cell</a> . For <a href="#">radar images</a> this term describes the average vertical relief of small-scale irregularities of the terrain surface. A surface appears rough to <a href="#">microwave</a> illumination when the height variations become larger than a fraction of the <a href="#">radar wavelength</a> . The fraction is qualitative, but may be shown to decrease with <a href="#">incidence angle</a> .
Scalloping	A corduroy-like radiometric banding across (rangeward) the scene caused by the improper estimation of the Doppler centroid. The image can be reprocessed using better Doppler centroid estimates. For a further discussion on this topic see the section entitled " <a href="#">Descalloping</a> " <a href="#">2.6.1.2.4.2</a> , and " <a href="#">Doppler Frequency Estimator</a> " <a href="#">2.6.1.2.2</a> , in chapter 2).
ScanSAR Beam Merging	<a href="#">ScanSAR</a> multi-beam processing consists of generating independent beam images, called beam buffers and subsequently combining them into a single output line. ( See the section entitled " <a href="#">ScanSAR Beam Merging</a> <a href="#">2.6.1.2.4.3</a> ," in chapter 2).
Scattering Coefficient	The ratio of the average reflected electromagnetic wave power to the incident electromagnetic power, for distributed scattering targets. (See also <a href="#">Sigma Nought</a> )
Scattering Matrix	Array of four <a href="#">complex numbers</a> that describe the transformation of the <a href="#">polarisation</a> of a wave <a href="#">incident</a> upon a reflective medium to the polarisation of the <a href="#">backscattered</a> wave. It is the polarisation vector counterpart to the coefficient of reflectivity.
Shadow - Radar	A radar shadow is the absence of radar illumination because of intervening reflecting or absorbing objects. The occurrence, shape and amount of radar shadow caused by either concave or convex relief features are dependent on several factors. These include radar <a href="#">look direction</a> , <a href="#">incidence angle</a> and platform altitude, as well as terrain (object) configuration, slope angle and slope orientation. Shadow effects are most prominent with large incidence angle illumination; they occur in the down-range direction and may serve as a good indicator of the radar illumination direction, topography, and height. In high relief terrain, radar shadow effects may obscure a significant amount of surface area, which is most obvious in large incidence angle (e.g. >50°) airborne SAR imagery. Satellite-based radar tends to produce far less radar shadow effects, but other important aspects come into play, such as slope <a href="#">foreshortening</a> and <a href="#">lavover</a> . There is no measurable target return signal in radar shadow (other than <a href="#">noise</a> ). 
	Radar Shadow ( See also " <a href="#">Elevation Displacement</a> " in Geometry glossary.)
Sigma	The conventional measure of the strength of a <a href="#">radar</a> signal reflected from a geometric object (natural or manufactured) such as a <a href="#">corner reflector</a> . Sigma specifies the strength of reflection in terms of the geometric cross section of a conducting sphere that would give rise to the same level of reflectivity. (Units of area, such as metres squared). See also <a href="#">Backscatter</a> in radar glossary.
Sigma Nought	<a href="#">Scattering coefficient</a> , or the conventional measure of the strength of <a href="#">radar</a> signals reflected by a distributed scatterer, usually expressed in dB. It is a normalised dimensionless number, comparing the strength observed to that expected from an area of one square metre. Sigma nought is defined with respect to the nominally horizontal plane, and in general has a significant variation

	with <a href="#">incidence angle</a> , <a href="#">wavelength</a> , and <a href="#">polarisation</a> , as well as with properties of the scattering surface itself. See also chapter 3 "Pre-flight Characteristics and Expected Performance" and <a href="#">Backscatter</a> in radar glossary.
Sign + Magnitude Mode (S+M)	The Sign + Magnitude Mode (S+M), or Fixed Exponent mode, is a data compression technique used in ASAR data processing. For a further description of this method, refer to the document "ENVISAT-1 ASAR Interpretation of Source Packet Data. PO-TN-MMS-SR-0248". ( See also <a href="#">Flexible Block Adaptive Quantisation (FBAQ)</a> method ).
Single Look Complex Image (SLC)	Single Look Complex (SLC) image data are intended for <a href="#">SAR</a> image quality assessment, <a href="#">calibration</a> and <a href="#">interferometric</a> or wind/wave applications. A small number of corrections and interpolations are performed on the data in order to allow freedom in the derivation of higher level products. ( See <a href="#">Table 2.39</a> in the section entitled "Level 1B High Level Organisation of Products" )
Slant Range to Ground Range (SR/GR) Conversion	Converts the distance from the radar ( <a href="#">slant range</a> ) to distance along the ground ( <a href="#">ground range</a> ) and the range resampling to a desired output <a href="#">pixel</a> spacing.
Slice	A slice is an integer number of <a href="#">granules</a> . See Figure and Figure in "Products and Algorithms Introduction". In stripline processing, the <a href="#">PF-ASAR</a> will systematically generate output parent products, within the time constraints, that cover an entire acquisition segment by processing a number of separate scenes and then joining the scenes to form the continuous segment. Most long data segments will be processed using more than one processing computer, in order to meet throughput performance requirements. Each computer will be given a portion of the input data segment to process. The output, referred to as slices, from the different computers are then concatenated to produce one long strip product, referred to as " <a href="#">Stripline Product</a> " ( See also <a href="#">Figure 2.2</a> in the section entitled "Products and Algorithms Introduction" in chapter 2).
Specific Product Header (SPH)	The Specific Product Header (SPH) is in ASCII format and contains information which describes the specific product as a whole. It will vary between instruments and between different products for each instrument. The SPH also contains <a href="#">Data Set Descriptors (DSDs)</a> . DSDs are used to point to and describe the various <a href="#">Data Sets</a> which make up a product. ( see also " <a href="#">Definitions and Conventions 2.3.2.3</a> ." )
Speckle	Speckle refers to a noise-like characteristic produced by <a href="#">coherent</a> systems, including <a href="#">synthetic aperture radars (SARs)</a> . It is evident as a random structure of picture elements ( <a href="#">pixels</a> ) caused by the interference of electromagnetic waves scattered from surfaces or objects. When illuminated by the SAR, each target contributes <a href="#">backscatter</a> energy which, along with <a href="#">phase</a> and power changes, is then coherently summed for all scatterers. This summation can be either high or low, depending on constructive or destructive interference. This statistical fluctuation (variance), or uncertainty, associated with the <a href="#">brightness</a> of each pixel in SAR imagery. When transforming SAR signal data into actual imagery, <a href="#">multi-look</a> processing is usually applied. The speckle still inherent in the actual SAR image data can be reduced further through processing tasks such as <a href="#">filtering</a> . Unlike system <a href="#">noise</a> , speckle is a real electromagnetic measurement, which is exploited in <a href="#">SAR interferometry (InSAR)</a> ( See also )
Speckle Filter	A radiometric enhancement technique that reduces <a href="#">speckle</a> with a minimum loss of information. Filtering permits better discrimination of scene targets and easier automatic image segmentation. In addition, after an image has been filtered, classical enhancement techniques can be applied with improved results (e.g. edge detectors, <a href="#">textural</a> classifiers). In homogeneous areas, the filter should preserve radiometric information and the edges between different areas. In textured areas, the filter should preserve radiometric information, and spatial signal variability (textural information).
Stereo Imagery	Two images of the same area taken from different sensor stations so as to afford stereoscopic vision.
Stokes Matrix	A description of the complete <a href="#">polarisation</a> signature of a reflective medium. 4x4 array of real numbers that describes the transformation of the Stokes parameters of the <a href="#">incident</a> wave into the Stokes parameters of the electromagnetic wave reflected by each element of a scene illuminated by a <a href="#">radar</a> .
Stokes parameters	Set of four real numbers that together describe the state of <a href="#">polarisation</a> of an electromagnetic wave.
Stokes Vector	A four component real vector that describes the <a href="#">polarisation</a> state of an electromagnetic wave in terms of combinations of the perpendicular wave components.
Stand-alone Products	Also referred to as "On Request" products, these are not generated unless specifically requested by a user. The <a href="#">ASAR</a> stand-alone products are: <a href="#">Precision</a> , <a href="#">Ellipsoid Geocoded</a> and <a href="#">Single Look Complex</a> images.
Stripline Products	Stripline products are generated along a complete segment or an orbit. Geometric and radiometric continuity are ensured along the complete segment or orbit. Scenes can be ordered from anywhere within a stripline, then extracted and distributed via the <a href="#">PDS</a> User Services (no <a href="#">framing</a> constraint). Stripline processing of <a href="#">browse</a> , <a href="#">medium-resolution</a> and low-resolution data will produce products for up to 10 minutes data acquisition in <a href="#">Image (IM)</a> , <a href="#">Alternating Polarisation (AP)</a> and <a href="#">Wide Swath (WS)</a> <a href="#">Modes</a> , and up to a full orbit for <a href="#">Global Monitoring (GM) Mode</a> . ( See also "Products and Algorithms Introduction" in chapter 2 and " <a href="#">Level 1b Image Products 2.6.2.1.3</a> , in chapter 2).
Strip Map	A strip map is an image formed in width by the <a href="#">swath</a> of the imager and follows the length contour of the flight line of the imager itself. Strip map images are generally not <a href="#">geocoded</a> since they follow the irregular path of the imaging platform.
Sub-look Image Terms	A sub-look image is one of the images formed from one of the azimuth frequency bands (looks) during cross spectra calculation. Mean, variance, skewness, and kurtosis are statistical terms that are defined mathematically. Say x is a sample of a sublook image. It is treated as a random variable. Let E(x) be the mean, or average of x over the image. Denoting this mean value by x', then the other statistics are defined as: $\text{variance} = E((x-x')^2)$ $\text{skewness} = E((x-x')^3)$ $\text{kurtosis} = E((x-x')^4)$ Where the $(\cdot)^n$ notation means to the n <sup>th</sup> power'. That is $x^2$ is x squared.
Surface Roughness	See <a href="#">Roughness</a>
Summary Quality Annotation Data Set (SQADS)	An <a href="#">ADS</a> that contains the Summary Quality (SQ) information of a product, such as the <a href="#">Product Confidence Data (PCDs)</a> .
Swath	The width of an imaged scene in the <a href="#">range</a> dimension, measured in either <a href="#">ground range</a> or <a href="#">slant range</a> on the swath. See also chapter 1 " <a href="#">Principles of Measurement 1.1.3</a> ", and chapter 3 " <a href="#">ASAR Instrument Functionality 3.1.2</a> ," for a further discussion on ASAR swath modes.
Synthetic Aperture Strip Map (SASM)	See <a href="#">Strip Map</a>
Systematic Product	Products that are generated automatically for all received data as opposed to <a href="#">stand-alone</a> .
Texture - Radar	Texture is generally referred to as the detailed spatial pattern of variability of the average reflectivity ( <a href="#">tone</a> ). Image texture is produced by an assembly of features that are too small to be identified individually. <a href="#">SAR</a> image texture is composed of a convolution of <a href="#">speckle</a> with scene texture. Texture is an important radar image interpretation element; its statistical characterisation requires measurement from a finite sampling window rather than estimates from a single picture element ( <a href="#">pixel</a> ). Texture edge detection, or segmentation, is a critical method used for accurate radar image classification. Radar image texture is apparent at various different scale levels. Micro-scale texture is the result of more or less homogeneous, noise-like and random fluctuations of light and dark tone throughout the entire image. Meso-scale texture is produced by spatially and not randomly organised fluctuations of grey tone on the order of several <a href="#">resolution cells</a> , within an otherwise homogeneous unit. Examples of descriptive terms to characterise texture include <a href="#">rough</a> (coarse), <a href="#">smooth</a> (fine), <a href="#">grainy</a> , <a href="#">checkered</a> , or <a href="#">speckled</a> .
Throwaway	After filtering, the output signal samples at the end of the array correspond to incomplete input pulses. These are invalid output samples that are not used in further processing.
Tie Frame	A set of tie points corresponding to a given time and location of the satellite.
Tie Point	Tie points for a given product are a matrix of Earth points, where 1 lines ( <a href="#">tie frames</a> ) correspond to regularly spaced (time-wise)

	instants tf, origin at the first frame of the product. Tie points are located at successive projections at instants tf of the (YS=0) plane in the satellite fixed frame (XS, YS, ZS); 2) the central tie point is at the swath centre, i.e. the projection on the geoid of the axis ZS; 3) tie points at a given instant are spaced at even distance (the same for all tie frames) along the <a href="#">swath</a> .
Tone	Tone refers to each distinguishable grey level from black to white. First order spatial average of image <a href="#">brightness</a> , often defined for a region of nominally constant average reflectivity. It is proportional to the strength of radar <a href="#">backscatter</a> . Relatively smooth targets, like calm water, appear as dark tones. Diffuse targets, like some vegetation, appear as intermediate tones. Man-made targets (buildings, ships) may produce bright tones, depending on their shape, orientation and/or constituent materials. Tone can be interpreted using a computer assisted density slicing technique.
Unconsolidated Product	This is the <a href="#">ASAR Level 1B</a> product produced in <a href="#">NRT</a> using available NRT <a href="#">auxiliary data</a> (i.e. may not be the most precise orbit vectors or <a href="#">calibration</a> information).
Wavelength Bin	An wavelength <a href="#">bin</a> refers to a particular wavelength sample number.
Wave Mode Products (WV)	<a href="#">ASAR</a> Wave Mode (WV) products are based on small <a href="#">high-resolution, complex</a> images of ocean scenes, also called <a href="#">imagettes</a> . These are processed to derive spectra of the ocean <a href="#">backscatter</a> and consequently the <a href="#">wavelength</a> and direction of ocean waves. A small imagette (dimensions range between 10 km by 5 km to 5km by 5km) is acquired at regular intervals of 100 km <a href="#">along-track</a> .The imagette can be positioned anywhere in an <a href="#">Image Mode (IM) swath</a> .Up to two positions in a single swath or in different swaths may be specified, with acquisitions alternating between one and the other (successive imagettes will hence have a separation of 200 km between acquisitions at a given position). <a href="#">HH</a> or <a href="#">VV</a> polarisation may be chosen.Imagettes are converted to wave spectra for ocean monitoring. ( see also " <a href="#">Organisation of Products</a> " )
Wave Mode Imquette Cross Spectra (WVS) Product	The Wave Mode Imquette Cross Spectra (WVS) product is an image power spectrum product that contains up to 400 cross spectra extracted from the <a href="#">SLC Imquette and Imquette Cross Spectra product (WVI)</a> . ( see also " <a href="#">Organisation of Products</a> " and " <a href="#">Level 1B Wave Products</a> " <a href="#">2.6.2.1.2.1.2</a> . )
Wave Mode SLC Imquette and Imquette Cross Spectra (WVI) Product	The Wave Mode SLC Imquette and Imquette Cross Spectra (WVI) product is the basic Level 1B Wave Mode product. The product includes up to 400 single-look, complex, slant range, imagettes generated from Level 0 data and up to 400 imquette power spectra computed using the cross-spectra methodology. ( see also " <a href="#">Organisation of Products</a> " and " <a href="#">Level 1B Wave Products</a> " <a href="#">2.6.2.1.2.1.1</a> . )
Wave Spectra Retrieval	The wave spectra retrieval algorithms are based on minimizing, with respect to the wave spectrum, the mean square difference between the observed and the computed SAR image spectrum under certain constraints. The computed SAR image spectrum is derived using the non-linear transform with the current wave spectrum, as input. ( See the section entitled " <a href="#">ASAR Level 2 Algorithm 2.7.1</a> " for a discussion of this topic).
Wide Swath (WS) Mode product	The Wide Swath Mode (WS) product is a 400 km by 400 km image. Spatial resolution of approximately 150 m by 150 m for nominal product <a href="#">VV</a> or <a href="#">HH</a> polarisation.( see also " <a href="#">Organisation of Products</a> " )
Wide Swath Browse (WSB) Image	The Wide Swath Browse (WSB) image product is the low-resolution product that will be produced systematically together with the <a href="#">WS Medium-resolution (WSM)</a> Product. ( See also " <a href="#">Organisation of Products</a> " and " <a href="#">Browse Products</a> " <a href="#">2.6.2.1.3.1.3</a> . )
Wide Swath Medium-Resolution (WSM) image product	This is the standard product for ASAR <a href="#">Wide Swath Mode</a> and it is systematically generated in the <a href="#">PDHS</a> from Level 0 data collected when the instrument is in Wide Swath Mode using the <a href="#">SCANSAR</a> technique and processed to 150-m resolution. The swath width is approximately 400 km. ( see also " <a href="#">Organisation of Products</a> " and " <a href="#">Level 1B Image Products</a> " <a href="#">2.6.2.1.3.1.3</a> . )
Zero Doppler Time	Zero <a href="#">Doppler</a> time is the <a href="#">along-track (azimuth)</a> time at which a target on the ground would have a Doppler shift of zero with respect to the satellite ( i.e. when the target was perpendicular to the flight path). Also called the closest approach azimuth time. The <a href="#">SAR</a> processor locates targets in the image at the zero-Doppler azimuth time.

## 5.4 ASAR Instrument Glossary

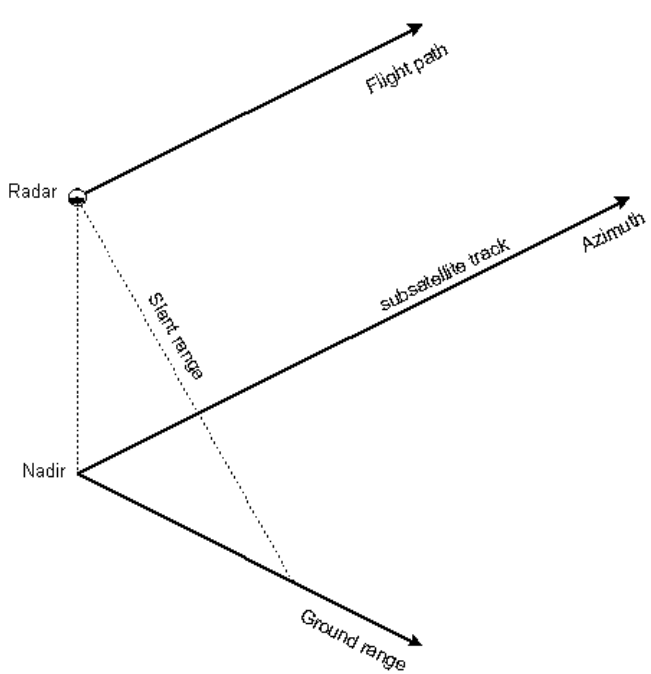
Table 5.4

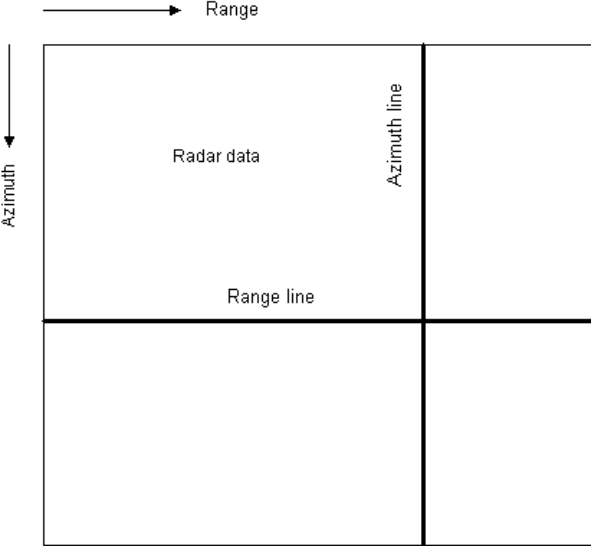
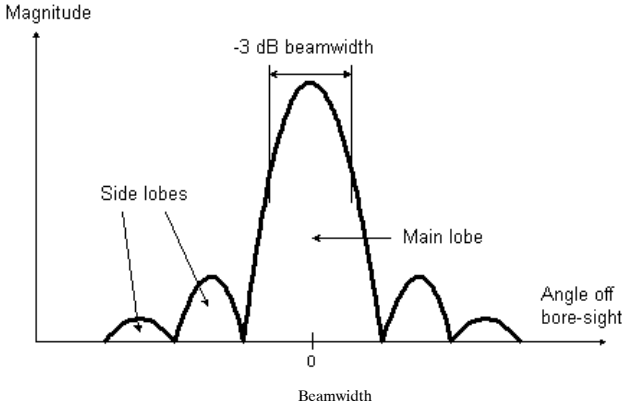
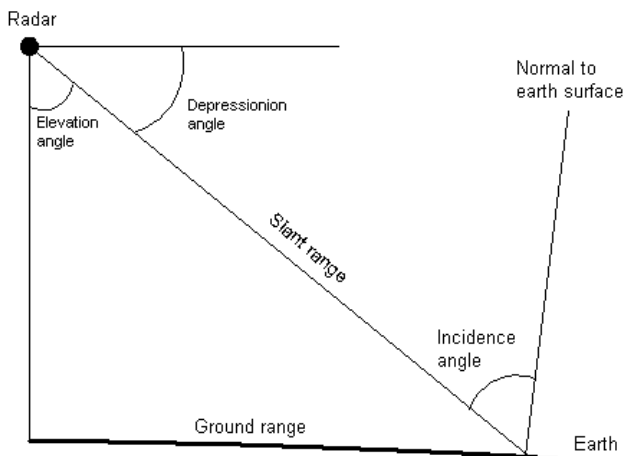
Antenna Power Switching and Monitoring Subsystem (APSM)	The <a href="#">Antenna Power Switching and Monitoring Subsystem (APSM) 3.1.1.1</a> , is part of the <a href="#">Antenna Subassembly (ASA) 3.1.1.1</a> , on the ASAR Instrument
Antenna Services Subsystem (ASS)	The <a href="#">Antenna Services Subsystem (ASS) 3.1.1.1</a> , is part of the <a href="#">Antenna Subassembly (ASA) 3.1.1.1</a> , on the ASAR Instrument
Antenna Subassembly (ASA)	The <a href="#">Antenna Subassembly (ASA) 3.1.1.1</a> , is one of the two functional groups of the <a href="#">ASAR Instrument 3.1</a> . (CESA is the other )
Calibration Loop	The instrument calibration loop is used to perform three distinct functions. Firstly, it is used to characterise the instrument transfer function during the measurement modes. Secondly, it is used to characterise individual T/R modules. Finally, it is used in the special external characterisation mode. ( See the section entitled " <a href="#">ASAR Characterisation and Calibration</a> " <a href="#">2.1.1</a> , in chapter 2)
Carbon Fibre Reinforced Plastic (CFRP)	A very stiff, and lightweight material with negligible thermal expansion coefficient
Control Electronics Sub-Assembly (CESA)	The <a href="#">Control Electronics Sub-Assembly (CESA) 3.1.1.2</a> , is one of the two functional groups of the <a href="#">ASAR Instrument 3.1</a> . ( ASA is the other )
Control Subsystem (CSS)	The <a href="#">Control Subsystem (CSS) 3.1.1.2</a> , drives the ASAR instrument by providing the command and control interface to the spacecraft, maintaining the database, managing the distribution of the operation parameters, and generating the time-lining of the instrument.
External Calibration	Absolute gain calibration of the ASAR using ground calibration transponders. ( see " <a href="#">ASAR Characterisation and Calibration</a> " <a href="#">2.1.1</a> , and " <a href="#">Auxiliary Data Sets for Level 1B Processing</a> " in chapter 2).

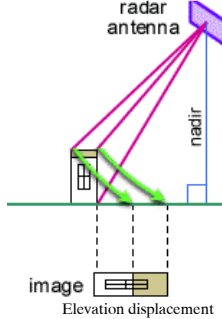
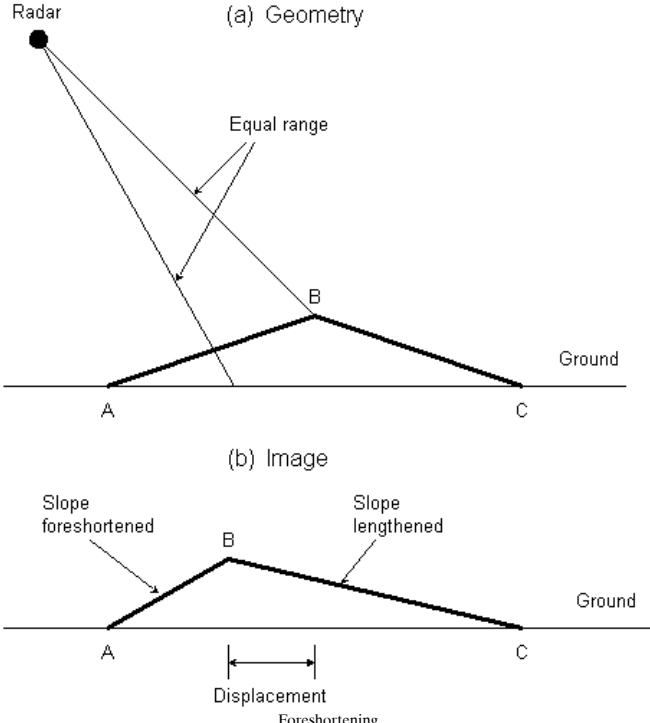
External Characterisation	A <a href="#">calibration</a> scheme used by ASAR that involves sending a series of pulses that are detected both by the internal calibration loop and the receiver embedded in the ground transponder. Used to monitor the passive part of the antenna, the calibration loop and the mechanical pointing of the antenna. (see " <a href="#">ASAR Characterisation and Calibration</a> " 2.11, and " <a href="#">Auxiliary Data Sets for Level 1B Processing</a> " in chapter 2).
Instrument ( or Internal ) Calibration	A <a href="#">calibration</a> scheme with the objective to derive the ASAR instrument internal path transfer function, and to perform noise calibration. This objective is realised by dedicated calibration signal paths and special calibration pulses within the instrument for making the required calibration measurements and by using these measurements to perform corrections within the ground processor. ( see " <a href="#">ASAR Characterisation and Calibration</a> " 2.11, and " <a href="#">Auxiliary Data Sets for Level 1B Processing</a> " in chapter 2).
Receiver Gain Droop	During the receive or echo window the gain droops by up to 0.9dB. The effect has been well characterized preflight and will be automatically corrected in the processor.
Tile Control Interface Unit (TCIU)	Mechanism in the Tile Subsystem (TSS) used to control the individual transmit/receive modules (TRM) of the <a href="#">ASA</a> Subsystem in the ASAR Instrument.
Transmitter/Receiver Polarisation	The <a href="#">polarisation</a> modes handled by ASAR's Active Phased <a href="#">Array Antenna</a> .

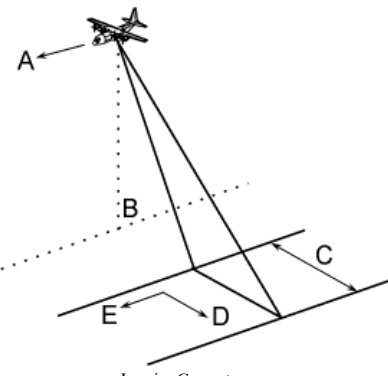
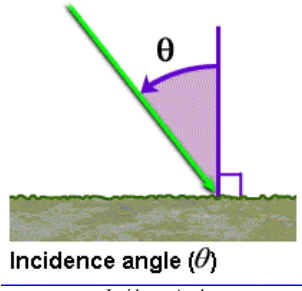
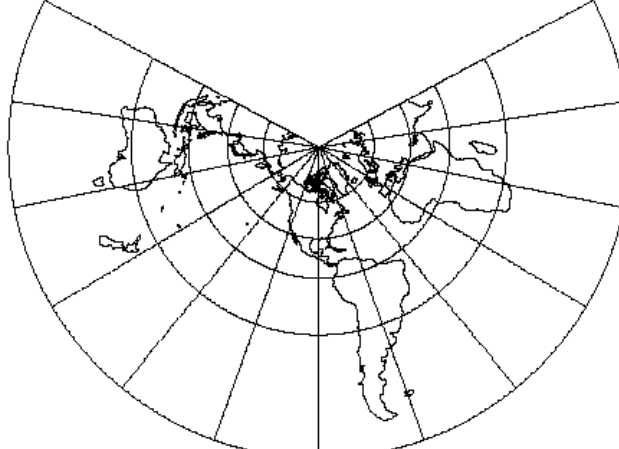
## 5.5 Geometry Glossary

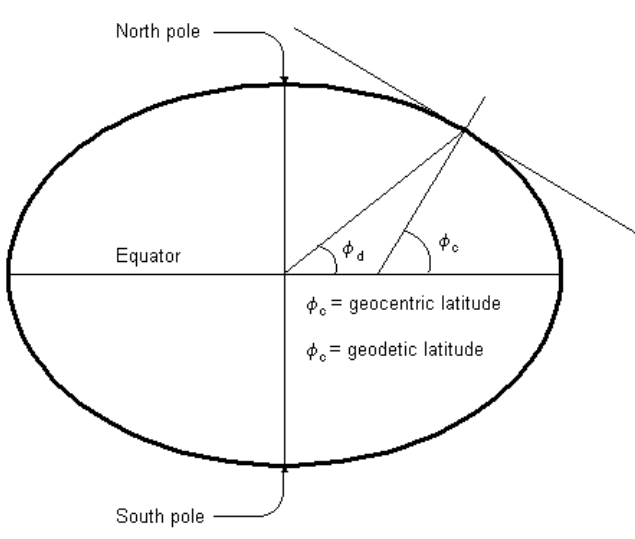
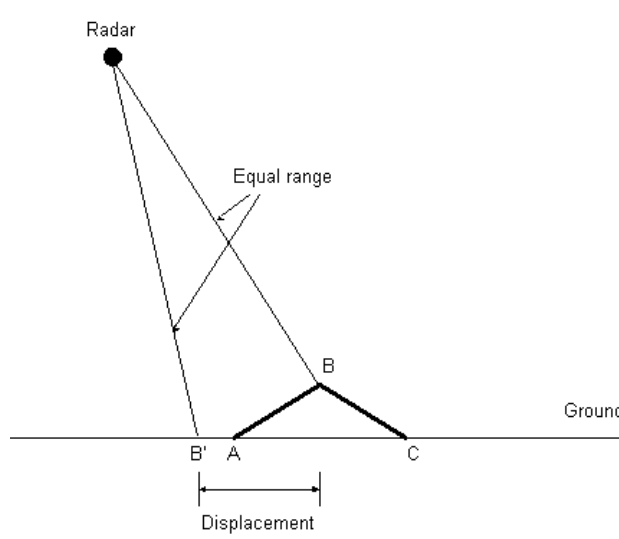
Table 5.5

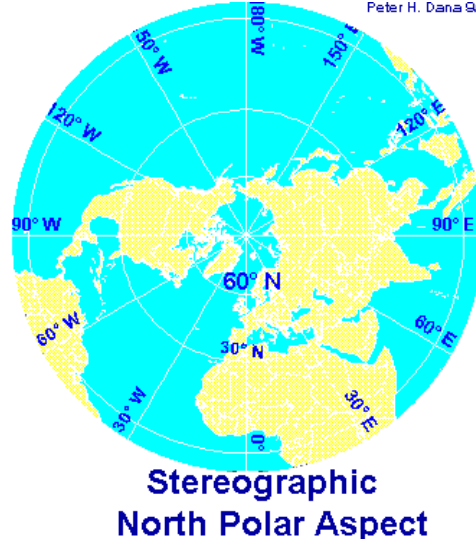
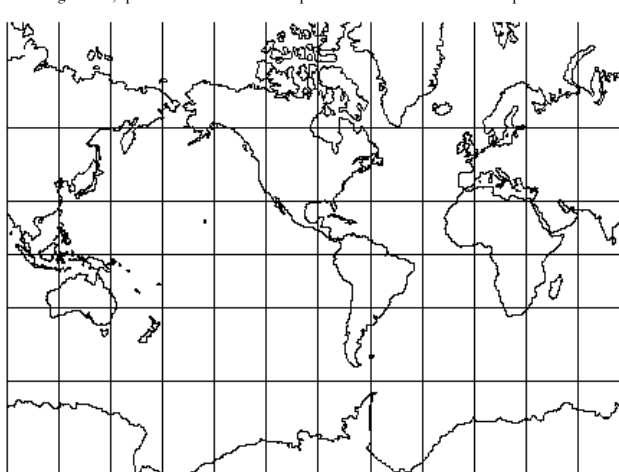
Along Track	See <a href="#">Azimuth</a> below.
Aspect Angle	Description of the geometric orientation in the horizontal plane of an object in the scene with respect to the illuminating wavefront.
Azimuth	<p>The term azimuth is used to indicate linear distance or image scale in the direction parallel to the <a href="#">radar</a> flight path. In an <a href="#">image</a>, azimuth is also known as <a href="#">along-track</a> direction, since it is the relative along-track position of an object within the <a href="#">antenna</a>'s field of view following the radar's line of flight. Azimuth is predominately used in radar terminology. The azimuth direction is perpendicular to the <a href="#">range</a> direction. The resolution of an image in the azimuth directions for a <a href="#">SAR</a> image is constant and is independent of the range. For two objects to be resolved, they must be separated in the azimuth direction by a distance greater than the <a href="#">beamwidth</a> on the ground.</p>  <p>(See also <a href="#">Imaging Geometry</a>)</p>
Azimuth Direction	Direction parallel to the line of flight, also referred to as the <a href="#">along-track</a> direction. (See <a href="#">Azimuth</a> )
Azimuth Line	A line of constant range. Each <a href="#">azimuth</a> line is parallel to the flight path. Note that this usage is not universal; some researchers use 'azimuth line' to refer to what is here called 'range line' (and vice versa).

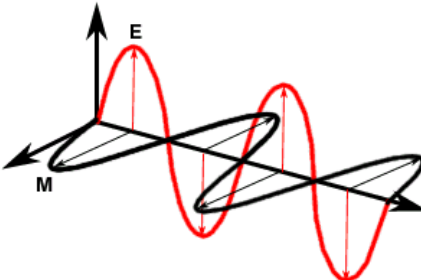
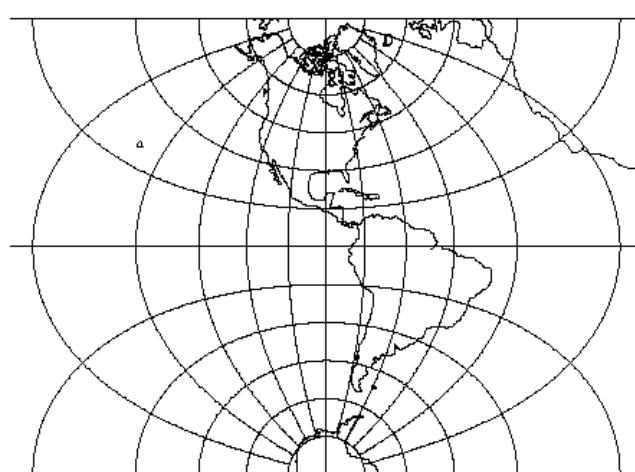
	 <p>The diagram illustrates a rectangular area representing 'Radar data'. A horizontal arrow at the top points to the right and is labeled 'Range'. A vertical arrow on the left points downwards and is labeled 'Azimuth'. A thick black vertical line runs down the center of the rectangle, labeled 'Azimuth line' to its right. A thin horizontal line runs across the middle of the rectangle, labeled 'Range line' below it.</p>
Beamwidth	<p>Beamwidth is a measure of the width of the radiation pattern of an <a href="#">antenna</a>. For <a href="#">SAR</a> applications, both the vertical beamwidth, affecting the width of the illuminated <a href="#">swath</a>, and the horizontal or <a href="#">azimuth</a> pattern, which determines, indirectly, the azimuth resolution, are frequently used. Beamwidth may be measured in the one-way or two-way form, and in either voltage or power.</p>  <p>The graph shows the magnitude of the radiation pattern as a function of the angle off bore-sight. The main lobe is the central peak, and the side lobes are the smaller peaks on either side. The -3 dB beamwidth is indicated by a double-headed arrow across the main lobe. The angle off bore-sight is measured from the horizontal axis.</p> <p>(See also <a href="#">Side-Lobes</a> in Radar and SAR glossary )</p>
Depression Angle	<p>Depression angle usually refers to the line of sight from the radar to an illuminated object as measured from the horizontal plane at the <a href="#">radar</a>. For image interpretation, use of the term is not recommended because it does not account for the effects of Earth curvature, and it does not conveniently include effects of local slope in the scene. It is more appropriate for an engineering description of the vertical <a href="#">antenna</a> pattern at the radar itself.</p>  <p>The diagram shows a cross-section of the Earth's surface. A vertical line represents the 'Normal to earth surface'. A point on the surface is labeled 'Earth'. A horizontal line extends from the radar to the Earth, labeled 'Slant range'. The angle between the normal to the surface and the slant range is the 'Incidence angle'. The angle between the horizontal and the slant range is the 'Depression angle'. The angle between the vertical normal and the horizontal is the 'Elevation angle'.</p>

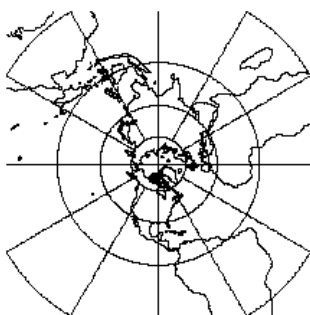
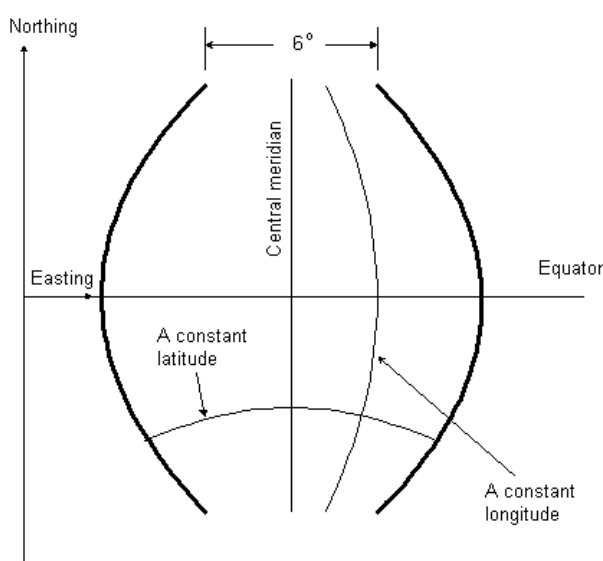
	Depression Angle
Digital Elevation Model ( DEM )	A quantitative model of a landform in digital form, normally given as metres above sea level (including the height of the vegetation), and referenced to a geographic co-ordinate system.
Elevation Angle	The elevation angle is that which is located between the <a href="#">slant range</a> and the <a href="#">nadir</a> . It closely approximates the <a href="#">incidence angle</a> , but there are differences as a result of the curvature of the Earth. (See also <a href="#">Depression Angle</a> and <a href="#">Imaging Geometry</a> )
Elevation Displacement	<p>Elevation displacement, also referred to as geometric distortion, is the image displacement in a <a href="#">remote sensing</a> image toward the <a href="#">nadir</a> point in <a href="#">radar</a> imagery due to sensor/target imaging geometries. In a <a href="#">radar image</a> the displacement is toward the sensor and can become quite large when the sensor is nearly overhead. The displacement increases with decreasing <a href="#">incidence angle</a>. The four characteristics resulting from the geometric relationship between the sensor and the terrain that are unique to radar imagery are <a href="#">foreshortening</a>, <a href="#">pseudo-shadowing</a>, <a href="#">layover</a>, and <a href="#">shadowing</a>. Topographic features like mountains, as well as artificial targets like tall buildings, will be displaced from their desired orthographic position in an image. The effect may be used to create <a href="#">stereo images</a>. It may be removed from an image through independent knowledge of the terrain profile. In many applications, an approximate correction may be derived through shape-from-shading techniques. Elevation displacement will be greater in <a href="#">slant range</a> than <a href="#">ground range</a> due to the fact that the image is more compressed in a slant range presentation. Elevation displacement is also most pronounced at <a href="#">near range</a>.</p> 
Ellipsoid	A model used to describe the shape of the planet Earth, which is not a true sphere but an oblate spheroid compressed along the polar axis and bulging slightly around the equator.
Ellipticity Angle	Defined as the magnitude of the arctangent of the ratio of the polarisation ellipse's minor and major axes. If negative, the ellipse rotation is right-handed; if positive, is the ellipse rotation is left-handed.
Far Range	Portion of the radar image farthest from the flight path. ( See also " <a href="#">Imaging Geometry</a> " )
Foreshortening	<p>Foreshortening is the spatial distortion whereby terrain slopes facing a <a href="#">side-looking radar's (SLAR)</a> illumination are mapped as having a compressed scale relative to its appearance, as if the same terrain were level. Foreshortening is a special case of <a href="#">elevation displacement</a>. The effect is more pronounced for steeper slopes and for radars that use steeper <a href="#">incidence</a> angles. ( See also <a href="#">Shadow</a> in Products glossary.)</p> 
Ground Range	Ground Range is the perpendicular distance from the ground track to a given object on the Earth's surface. Also defined as the range direction of a side-looking radar image as projected onto the nominally horizontal reference plane, similar to the spatial display of conventional maps. Ground range projection requires a geometric transformation from slant range to ground range; for spacecraft data, a geoid model of the Earth is used, whereas for airborne radar data, a planar approximation is sufficient. This can lead to relief or elevation displacement, foreshortening, and layover on radar images. However, if terrain elevation information is used, the effect on viewing geometry can be minimised. ( See also " <a href="#">Imaging Geometry</a> ", " <a href="#">Depression Angle</a> " and " <a href="#">ASAR Level 1B Algorithm Physical Justification - Radar Geometry 2.6.1.1.2</a> " , as well as )
Imaging Geometry	The imaging geometry of a <a href="#">radar</a> system is different from the framing and scanning systems commonly employed for optical remote sensing. Similar to optical systems, the platform travels forward in the flight direction (A) with the <a href="#">nadir</a> (B) directly beneath the platform. The <a href="#">microwave</a> beam is transmitted obliquely at right angles to the direction of flight illuminating a <a href="#">swath</a> (C) which is offset from nadir. <a href="#">Range</a> (D) refers to the <a href="#">across-track</a> dimension perpendicular to the flight direction, while <a href="#">azimuth</a> (E) refers to the <a href="#">along-track</a> dimension parallel to the flight direction. This <a href="#">side-looking</a> viewing geometry is typical of imaging radar systems (airborne or spaceborne).

	 <p><b>Imaging Geometry</b></p> <p>The portion of the image swath closest to the nadir track of the radar platform is called the <b>near range</b> (A) while the portion of the swath farthest from the nadir is called the <b>far range</b> (B). The <b>incidence angle</b> is the angle between the <b>radar beam</b> and ground surface (A) which increases, moving across the swath from near to far range. The look angle (B) is the angle at which the radar <b>looks</b> at the surface. In the near range, the viewing geometry may be referred to as being steep, relative to the far range, where the viewing geometry is shallow. At all ranges the radar <b>antenna</b> measures the radial line of sight distance between the radar and each target on the surface. This is the <b>slant range</b> distance (C). The <b>ground range</b> distance (D) is the true horizontal distance along the ground corresponding to each point measured in slant range.</p>
Incidence Angle	<p>The incidence angle is the angle defined by the incident <b>radar beam</b> and the vertical (normal) to the intercepting surface. In general, reflectivity from distributed scatterers decreases with increasing incidence angle. The incidence angle is commonly used to describe the angular relationship between the radar beam and the ground, surface layer or a target. A change of the radar illumination angle often affects the radar <b>backscattering</b> behaviour of a surface or target. The incidence angle changes across the radar image <b>swath</b>; it increases from <b>near range</b> to <b>far range</b>. In the case of satellite <b>radar imagery</b>, the change of incidence angle for flat terrain across the imaging <b>swath</b> tends to be rather small, usually on the order of several degrees. In the case of an inclined surface (slope), the local incidence angle (<math>I</math>) is defined as the angle between the incident radar beam and a line that is normal to that surface. The local incidence angle determining, in part, the <b>brightness</b>, or <b>image tone</b>, for each picture element (pixel) and slope facet, is a key element in the prominent rendition of terrain features in radar imagery.</p>  <p><b>Incidence angle (<math>\theta</math>)</b></p>
Lambert Conformal Conic (LCC) map projection	<p><b>Microwave</b> interactions with the surface are complex and different scattering mechanisms may occur in different angular regions. Returns due to surface scattering are normally strong at low incidence angles and decrease with increasing incidence angle, with a slower rate of decrease for <b>rougher</b> surfaces. Returns due to volume scattering from an heterogeneous medium with low dielectric constant tend to be more uniform for all incidence angles. Thus, radar backscatter has an angular dependence, and there is potential for choosing optimum configurations for different applications.</p> <p>( See also "<a href="#">"Imaging Geometry"</a>" and the section "<a href="#">"Incidence Angles"</a>" in the User Guide 1.1.5.2.)</p> <p>The Lambert Conformal Conic (LCC) map projection is a <a href="#">State Plane Co-ordinate System</a> that consists of 120 zones designed to optimally represent sections of the individual states. Points on the earth are projected onto a cone that intersects the earth's surface at two parallels of <a href="#">latitude</a>. Along these two circles the scale will be exact. If the parallels are close in a north-south direction, the map scale will be reasonably accurate no matter how far the map is extended in an east-west direction. The Lambert projection is useful for mapping states that are relatively wide in an east-west direction. This projection is said to be conformal because the scales in all directions are equivalent.</p> 
Latitude	Latitude is the number of degrees north or south of the equator, an imaginary circle on the Earth's surface everywhere equidistant between the two poles.

	 <p>Geocentric and Geodetic Latitudes</p>
Layover	<p>Layover is an extreme form of <a href="#">elevation displacement</a> or <a href="#">foreshortening</a> in which the top of a reflecting object, such as mountain, is closer to the <a href="#">radar</a> (in <a href="#">slant range</a>) than are the lower parts of the object. The image of such a feature appears to have fallen over towards the radar. Also defined as the displacement of the top of an elevated feature with respect to its base on the radar image. The peaks look like dip-slopes. The effect is more pronounced for radars having smaller incidence angle. ( See also <a href="#">Shadow</a> in Products glossary.</p>  <p>Layover</p>
Location	<p>Co-ordinates (<a href="#">geodetic latitude</a>, <a href="#">longitude</a>) of a point on the geoid, expressed in the Earth-fixed co-ordinate system.</p>
Longitude	<p>The angular distance on the Earth, or on a globe or map, east or west of the prime meridian at Greenwich, England to the point on the Earth's surface for which the longitude is being ascertained, expressed in degrees, or in hours, minutes and seconds.</p>
Map Projections	<p>ASAR processing supports 6 different map projections: <a href="#">Mercator (MERC)</a>, <a href="#">Transverse Mercator (TM)</a>, <a href="#">Universal Transverse Mercator (UTM)</a>, <a href="#">Polar Stereographic Mercator (PS)</a>, <a href="#">Universal Polar Stereographic (UPS)</a>, and the <a href="#">Lambert Conformal Conic (LCC)</a>.</p> <p>Cylindrical projections are based upon the various methods of projecting the Earth upon a cylinder that is either tangent to the equator (normal or equatorial form), a meridian (transverse) or obliquely aligned. Any of these classes are available in both conformal and equal area form. These projections are best used in mapping applications involving a zone near the line of tangency.[e.g. Mercator, Transverse Mercator (TM), Universal Transverse Mercator (UTM)]. Applications should be limited to equatorial regions, but it is frequently used for navigational charts with latitude of true scale specified within or near the chart's boundaries.</p> <p>Conic projections involve the transformations to a cone either secant or tangent to the Earth's surface.[e.g. Lambert Conformal Conic (LCC)]</p> <p>Stereographic projections are those in which perspective is a point at the opposite end of the globe. In other words, the light is a point source shown from a point on the globe through to the other end of the globe (e.g., a South Pole point of projection would shine light through to the North Pole). An example of a stereographic projection is the North Polar Stereographic Projection shown below:</p>

	 <p>North Polar Stereographic Projection ( image courtesy of Peter H. Dana California State University )  [e.g. Universal Polar Stereographic (UPS) Projection, Polar Stereographic Mercator (PS)]</p>
Mercator (MERC) Map Projection	<p>The Mercator (MERC) map projection, sometimes referred to as the Plain Mercator, is made from the centre of the Earth onto a cylinder surrounding and touching it at the Equator. Therefore, the meridians are equally spaced, parallel and vertical lines, and the parallels of <a href="#">latitude</a> are parallel, horizontal straight lines, spaced farther and farther apart as their distance from the Equator increases.</p>  <p>Mercator map projection</p>
Nadir	<p>Nadir is a single point, or locus of points on the surface of the Earth directly below a sensor as it progresses along its line of flight. Nadir can be both a point and a line. In other words, when a straight line is drawn between the sensor and the centre of the Earth, the nadir is the point where that line intersects the surface of the Earth. When the contiguous nadir points are joined along the ground, they form the nadir line. For <a href="#">radar</a>, the nadir line corresponds to the beginning of the <a href="#">range</a>. ( See also "<a href="#">Imaging Geometry</a>" )</p>
National Systems Projection (NSP)	<p>A National Systems map Projection (NSP) is any of 4 map projections used in ASAR processing, other than the <a href="#">UTM</a> or <a href="#">UPS</a> projections. These are the <a href="#">LCC</a>, <a href="#">TM</a>, <a href="#">MERC</a> and <a href="#">PS</a> projections.</p>
Near Range	<p>Refers to the portion of a radar image closest to the satellite flight path. ( See also "<a href="#">Imaging Geometry</a>" )</p>
One-Way	<p>Numbers relating to only one direction of propagation are denoted as one-way, and the corresponding numbers that include the round trip are called two-way. The <a href="#">radar</a> illuminates the scene through the transmit pattern of the <a href="#">antenna</a>. It receives the <a href="#">backscattered</a> energy through the receive pattern of the antenna. Thus the received <a href="#">pulse</a> must travel two ways, out to each object at <a href="#">range</a>, and back again the same distance. The difference between one-way and two-way is important in measuring effective antenna pattern widths, in signal <a href="#">phase</a>, and in the relationship between two-way delay time and range distance.</p>
Orbit	<p>The path of a satellite as it revolves around the Earth is its orbit. (For the ASAR Orbit State Vectors see the section entitled "<a href="#">Auxiliary Data Sets for Level 1B Processing</a>" in chapter 2).</p>
Pixel Geometry	<p>A set of angles (sun zenith angle, viewing zenith angle and azimuth difference angle) specifying how the <a href="#">pixel</a> is seen from the instrument and from the sun.</p>
Polarisation Signature	<p>A three-dimensional plot of the received <a href="#">backscattered</a> power as a function of the ellipticity and orientation angles of a polarimetric <a href="#">antenna</a>.</p>
Polar Stereographic Mercator (PS) Map projection	<p>( See <a href="#">Map Projections</a> and <a href="#">Mercator Map Projection</a> )</p>
Radar Polarisation	<p><a href="#">Radar</a> polarisation is the orientation of the electric (E) vector in an electromagnetic wave, frequently horizontal or vertical , in conventional imaging radar systems. Polarisation refers to the orientation of the plane of the electric field (E), as opposed to the magnetic field (M)</p>

	 <p>Radar polarisation</p> <p><a href="#">Remote sensing</a> radars are usually designed to transmit either vertically polarised or horizontally polarised radiation. This means that the electric field of the wave is in a vertical plane or a horizontal plane. Likewise, the radar can receive either vertically or horizontally polarised radiation, and sometimes both. The planes of transmitted and received polarisation are designated by the letters H for Horizontal and V for Vertical. Thus the polarisation of a radar image can be <b>HH</b>, for horizontal transmit, horizontal receive, <b>VV</b> for vertical transmit, vertical receive, <b>HV</b> for horizontal transmit vertical receive, and vice versa (<b>VH</b>).</p> <p>When the polarisation of received radiation is the same as the transmitted radiation, the image is said to be like-polarised. When the polarisation of received radiation is the opposite of the transmitted radiation, the image is said to be cross-polarised. Cross polarisation requires multiple scattering by the target and therefore results in weaker <a href="#">backscatter</a> than like-polarisation. Satellite radars generally use like-polarisation because the cross-polarised signals are too weak to produce a good <a href="#">image</a>.</p> <p>Polarisation is established by the <a href="#">antenna</a>, which may be adjusted to be different on transmit and on receive. Reflectivity of <a href="#">microwaves</a> from an object depends on the relationship between the polarisation state and the geometric structure of the object. Possible states of polarisation, in addition to vertical and horizontal, include all angular orientations of the E vector, and time varying orientations leading to elliptical and circular polarisations.</p> <p>( See also the section entitled "<a href="#">Dual Polarisation</a>" <a href="#">1.1.5.1</a>, in chapter 1 ).</p>
Range	Range is the line of sight distance between the <a href="#">radar</a> and each illuminated scatterer (target). In <a href="#">SAR</a> usage, the term is applied to the dimension of an image perpendicular to the line of flight of the radar. <a href="#">Slant range</a> is the distance from the radar, toward each target and measured perpendicular to the line of flight. <a href="#">Ground range</a> is the same distance, projected using a geometrical transformation onto a reference surface such as a map. Radar data are collected in the slant range domain, but usually are projected onto the ground range plane when these data are processed into an image. The resolution of the image in the range direction is dependent on the length of the emitted <a href="#">pulse</a> ; shorter pulses result in finer resolution. ( see also " <a href="#">ASAR Level 1B Algorithm Physical Justification</a> " - <a href="#">Radar Geometry</a> <a href="#">2.6.1.1.2</a> )
Range Curvature	Describes the changing distance between the radar and an object during the time that the object is illuminated by the <a href="#">antenna</a> . Range curvature is more important for long range systems such as satellite <a href="#">SARs</a> , and must be compensated in the processor as a part of image focusing.
Range Gate Bias	
Range Migration	The changing range delay to a point target as the target passes through the antenna beam. See the discussion <a href="#">"Range Cell Migration Correction (RCMC)"</a> <a href="#">2.6.1.2.3.1.4</a> , in the section entitled "Range Doppler" in chapter 2.
Side-Looking	Where the radar antenna beam is pointed sideways, typically nearly perpendicular to the flight direction of the spacecraft. (See also <a href="#">SLAR</a> in the "Radar and SAR glossary" and " <a href="#">ASAR Level 1B Algorithm Physical Justification</a> " - <a href="#">Radar Geometry</a> <a href="#">2.6.1.1.2</a> .)
Slant Range	Represents the distance measured along a line between the radar <a href="#">antenna</a> and the target. Image direction as measured along the sequence of line-of-sight rays from the <a href="#">radar</a> to each and every reflecting point in the illuminated scene. Since a <a href="#">SAR</a> looks down and to the side, the slant range to ground range transformation has an inherent geometric scale which changes across the image <a href="#">swath</a> . (See also " <a href="#">Imaging Geometry</a> " and " <a href="#">ASAR Level 1B Algorithm Physical Justification</a> " - <a href="#">Radar Geometry</a> <a href="#">2.6.1.1.2</a> , as well as )
State Plane Co-ordinate System (SPCS)	The State Plane Co-ordinate System (SPCS), was established in 1935 in the United States. Each of the States have defined, by State legislative action, one or more spcs zones in terms of datum, geographical extent and cartographic projection parameters relating geographic coordinates to the cartesian coordinates used in land surveying.
Swath Angle	An angle sub-tending the arc between <a href="#">swath</a> centre and a point
Transverse Mercator (TM) map projection	<p>The Transverse Mercator (TM) map projection is a <a href="#">State Plane Co-ordinate system</a> that consists of 120 zones designed to optimally represent sections of the individual states. It uses a cylindrical surface that intersects the earth along two lines parallel to a meridian of <a href="#">longitude</a>, called the central meridian. The scale will be exact along the two north-south lines of intersection. This projection is reasonably accurate within a narrow east-west zone, and may be extended indefinitely in a north-south direction. It is therefore useful for states that are narrow in the east-west direction.</p>  <p>Tranverse Mercator (TM) map projection</p>
Trihedral Reflector	<a href="#">Corner reflector</a> formed from three mutually orthogonal surfaces.
Universal Polar Stereographic (UPS) Map Projection	The Universal Polar Stereographic (UPS) map projection is a special case polar aspect of the azimuthal stereographic projection, which is based upon projections to a plane tangent to the Earth's surface.

	 <p>Universal Polar Stereographic (UPS) Map Projection</p>
	<p>The Universal Transverse Mercator (UTM) projection is a special ellipsoidal form of the general <a href="#">Transverse Mercator (TM)</a> projection . It is a planar map projection, that provides a specific geographic coordinate system to which data can be referenced. It is based on a series of 60 zones worldwide, each covering 6 degrees of <a href="#">longitude</a> in a north-south strip.</p>  <p>Universal Transverse Mercator (UTM) Zone</p>
Universal Transverse Mercator (UTM)	
Width - Radar	3dB. Width of a distribution equal to the distance between the outer two points on the distribution having power level half of that at the peak.
Width, Equivalent Rectangle	A standard definition to measure the effective width of a distribution. The width is that of a rectangular distribution with the same amplitude as the maximum of the distribution, and having the same area in the rectangle as is in the measured distribution.
Zero Doppler Direction	The angle from the satellite to the target, relative to the broadside
Zero Doppler Range	The closest approach range from the satellite to the target.

## 5.6 Oceans Glossary

Table 5.6

Oil Spill Detection and Mapping	<p>The presence of oil on water reduces the back scatter over the area of the spill due to the attenuation of the Bragg scale waves and a reduced signal return to the sensor.</p> <p>On the image, the oil spill has a darker tone than the surrounding water. Wind shadows near land, regions of low wind speed, natural surfactants, and grease ice can be mistaken for oil spills and ancillary or multi-temporal information is sometimes</p>
---------------------------------	--

## Oil Spill Emergency Response

needed to discriminate the oil spill from other phenomena. Steep incidence angles are recommended for oil spill detection.

The presence of oil on water reduces the backscatter over the area of the spill due to the attenuation of the Bragg scale waves and a reduced signal return to the sensor. On the image, the oil spill has a darker tone than the surrounding water. Wind shadows near land, regions of low wind speed, natural surfactants, and grease ice can be mistaken for oil spills and ancillary or multi-temporal information is sometimes needed to discriminate the oil spill from other phenomena. Steep incidence angles are recommended for oil spill detection.

## 5.7 Land Glossary

Table 5.7

Burn Delineation	After a forest area is affected by a fire, the affected area dries out and leaves and small twigs fall off the trees resulting in a contrast in moisture levels and structure between the burn area and surrounding forest. Radar is sensitive to differences in these parameters resulting in a contrast in <a href="#">backscatter</a> .
Clear Cuts in Forests	The relatively smooth surface of clear cuts produce little <a href="#">backscatter</a> compared to the <a href="#">rougher</a> canopy of uncut forest. These differences in backscatter allow forest clear cuts to be potentially delineated from uncut forest.
Co-seismic	Co-seismic events are those which occur at the same time as an earthquake, usually in a matter of seconds of the initial event.
Crop Damage Assessment	Damage to crops alters the geometric structure of plants and canopy surface <a href="#">roughness</a> . Damaged areas have different geometric structure/roughness than surrounding areas, therefore producing contrasting <a href="#">backscatter</a> .
Crop Type Determination	Different crops have unique <a href="#">roughness</a> and moisture levels. Radar is sensitive to differences in these parameters resulting in contrasting backscatter.
Crustal Displacement.	Also known as crustal deformation, crustal displacement is induced by the movement of the Earth's tectonic plates. This activity can produce a variety of landforms at the surface of the Earth, depending on the duration of the process involved in their formation.
Flood Extent Mapping	The smooth surface of water bodies acts as a specular reflector which results in a low <a href="#">backscatter</a> return. This contrasts with the <a href="#">rougher</a> surface of the land which is a diffuse scatterer and produces relatively high amounts of backscatter.
Forest Cover Type Discrimination	In some cases different forest types have unique geometric structures, canopy surface <a href="#">roughness</a> and moisture levels. Radar is sensitive to these parameters which potentially results in contrasting <a href="#">backscatter</a> . Different forest types can often be inferred from terrain analysis.
Geological Structure Mapping	Geological structures often have characteristic forms which, if located near the Earth's surface, may be manifested topographically as the <a href="#">side-looking configuration</a> of radar highlights relief.
Landform Delineation	Landforms often have characteristic shapes which may be manifested as topographic relief. The ability to image landforms is a result of the <a href="#">side-looking configuration of radar</a> , which highlights relief.
Landslide Hazard Assessment	Landslide hazard areas are defined when the locations of past landslides are identified. Landslides change the landscape through the transportation of vegetation and soil, thus affected areas have different canopy and soil <a href="#">roughness</a> than surrounding unaffected areas. Radar is sensitive to these variances in roughness, and produces contrasting <a href="#">backscatter</a> between affected and unaffected areas
Subsidence	Subsidence is the sinking of the Earth's surface in response to geological or man-induced causes. ( <a href="#">see also "subsidence" in the section entitled "Land Applications"</a> )
Soil Moisture Assessment	Variations in soil moisture produce changes in dielectric properties of soil. This contrast results in increasing <a href="#">backscatter</a> with increasing soil moisture.
Temporal Change Evaluation	Canopy <a href="#">roughness</a> and moisture content vary over the growing season. Radar is sensitive to these differences in contrasting <a href="#">backscatter</a> during the growing season. This allows for the

	evaluation of change in backscatter over several dates and evaluation of temporal change in crop parameters.
Terrain Analysis	Terrain may manifest as topographic relief. The ability to image topographic relief is a result of the <a href="#">side-looking configuration of radar</a> which highlights topographic differences.
Tillage Practice Determination	Different tillage practices produce unique soil surface <a href="#">roughness</a> . Radar is sensitive to differences in surface roughness resulting in contrasting <a href="#">backscatter</a> .
Topography	The technique of graphically representing the exact physical features of a place or region on a map.

## 5.8 Sea Ice Glossary

Table 5.8

Ice Concentration Estimation	Based on the ability to distinguish ice from open water. The proportion of the ocean surface covered in sea ice may be estimated.
Ice Decay Estimation	Distinct physical properties (salinity, microstructure, moisture content and surface roughness) of different ice types produces contrasting backscatter which allows floes to be differentiated at a single date. Multi-date data comparison allows the identification of location and estimation of rate of ice decay.
Ice Edge Determination	The ice edge is normally distinguishable from open water by a higher backscatter response. In rough seas or at steep incidence angles this contrast is reduced and the presence of ice may be detected as dark features which dampen the bright ocean response.
Ice Motion Estimation	Distinct physical properties (salinity, microstructure, moisture content and surface roughness) of different ice types produces contrasting backscatter which allows floes to be differentiated at a single date. Multi-temporal acquisition allows the magnitude and direction of displacement of floes to be estimated.
Ice Pressure Determination	Ice pressure results in ice topographic features which increase the roughness of the ice surface which in turn, increases radar backscatter.
Ice Type Determination	Different ice types (newly formed ice versus first and multi-year ice) have very different physical properties (salinity, microstructure, moisture content and surface roughness). Radar is sensitive to differences in these parameters which produces differential backscatter. In addition, the shape, size and location of the ice floes give important clues to its physical structure and thickness. These features may be visually interpreted from radar imagery.
Surface Topography Determination	Ice topographic features (ridges, rubble fields, etc.) increase the surface roughness of the ice thus producing an associated increase in radar backscatter which contrasts from smoother surrounding features.

# Chapter 6

---

## ASAR Data Formats Products

### 6.1 Level 2 Products

Table 6.1

## 6.1.1 ASA\_WVW\_2P: ASAR Wave Mode Wave Spectra

Table 6.2

### ASA\_WVW\_2P

ASAR Wave Mode Wave Spectra

#### File Structure

Data Sets

6

<a href="#">MPH 6.6.1.</a>	ENVISAT-1 MPH
<a href="#">SPH 6.6.18.</a>	ASAR Wave Mode Products Base SPH
<a href="#">SQ ADS 6.6.21.</a>	SQ ADSRs
<a href="#">GEOLOCATION ADS 6.6.19.</a>	Wave Mode Geolocation ADS
<a href="#">PROCESSING PARAMS ADS 6.6.20.</a>	Wave Mode processing parameters
<a href="#">OCEAN WAVE SPECTRA MDS 6.6.14.</a>	Ocean Wave Spectra

Format Version 114.0

## 6.2 Level 1 Products

Table 6.3

### 6.2.1 ASA\_APG\_1P: ASAR Alternating Polarization Ellipsoid Geocoded Image

Table 6.4

## ASA\_APG\_1P

ASAR Alternating Polarization Ellipsoid Geocoded Image

### File Structure

Data Sets

14

<a href="#">MPH 6.6.1.</a>	ENVISAT-1 MPH
<a href="#">SPH 6.6.11.</a>	ASAR Image Products SPH
<a href="#">MDS1 SQ ADS 6.6.16.</a>	SQ ADSRs
<a href="#">MDS2 SQ ADS 6.6.16.</a>	SQ ADSRs
<a href="#">MAIN PROCESSING PARAMS ADS 6.6.12.</a>	Main Processing parameters
<a href="#">DOP CENTROID COFFS ADS 6.6.8.</a>	Doppler Centroid parameters
<a href="#">SR GR ADS 6.6.17.</a>	Slant Range to Ground Range conversion parameters
<a href="#">CHIRP PARAMS ADS 6.6.7.</a>	Chirp parameters
<a href="#">MDS1 ANTENNA ELEV PATT ADS 6.6.6.</a>	Antenna Elevation patterns(s)
<a href="#">MDS2 ANTENNA ELEV PATT ADS 6.6.6.</a>	Antenna Elevation patterns(s)
<a href="#">GEOLOCATION GRID ADS 6.6.9.</a>	Geolocation Grid ADSRs
<a href="#">MAP PROJECTION GADS 6.6.13.</a>	Map Projection parameters
<a href="#">MDS1 6.6.10.</a>	Measurement Data Set 5
<a href="#">MDS2 6.6.10.</a>	Measurement Data Set 5

Format Version 114.0

## 6.2.2 ASA\_APM\_1P: ASAR Alternating Polarization Medium Resolution Image product

Table 6.5

## ASA\_APM\_1P

ASAR Alternating Polarization Medium Resolution Image product

## File Structure

Data Sets

13

<a href="#">MPH 6.6.1.</a>	ENVISAT-1 MPH
<a href="#">SPH 6.6.11.</a>	ASAR Image Products SPH
<a href="#">MDS1 SQ ADS 6.6.16.</a>	SQ ADSRs
<a href="#">MDS2 SQ ADS 6.6.16.</a>	SQ ADSRs
<a href="#">MAIN PROCESSING PARAMS ADS 6.6.12.</a>	Main Processing parameters
<a href="#">DOP CENTROID COEFFS ADS 6.6.8.</a>	Doppler Centroid parameters
<a href="#">SR GR ADS 6.6.17.</a>	Slant Range to Ground Range conversion parameters
<a href="#">CHIRP PARAMS ADS 6.6.7.</a>	Chirp parameters
<a href="#">MDS1 ANTENNA ELEV PATT ADS 6.6.6.</a>	Antenna Elevation patterns(s)
<a href="#">MDS2 ANTENNA ELEV PATT ADS 6.6.6.</a>	Antenna Elevation patterns(s)
<a href="#">GEOLOCATION GRID ADS 6.6.9.</a>	Geolocation Grid ADSRs
<a href="#">MDS1 6.6.10.</a>	Measurement Data Set 5
<a href="#">MDS2 6.6.10.</a>	Measurement Data Set 5

Format Version 114.0

## 6.2.3 ASA\_APP\_1P: ASAR Alternating Polarization Mode Precision Image

Table 6.6

## ASA\_APP\_1P

ASAR Alternating Polarization Mode Precision Image

### File Structure

Data Sets

13

<a href="#">MPH 6.6.1.</a>	ENVISAT-1 MPH
<a href="#">SPH 6.6.11.</a>	ASAR Image Products SPH
<a href="#">MDS1 SQ ADS 6.6.16.</a>	SQ ADSRs
<a href="#">MDS2 SQ ADS 6.6.16.</a>	SQ ADSRs
<a href="#">MAIN PROCESSING PARAMS ADS 6.6.12.</a>	Main Processing parameters
<a href="#">DOP CENTROID COEFFS ADS 6.6.8.</a>	Doppler Centroid parameters
<a href="#">SR GR ADS 6.6.17.</a>	Slant Range to Ground Range conversion parameters
<a href="#">CHIRP PARAMS ADS 6.6.7.</a>	Chirp parameters
<a href="#">MDS1 ANTENNA ELEV PATT ADS 6.6.6.</a>	Antenna Elevation patterns(s)
<a href="#">MDS2 ANTENNA ELEV PATT ADS 6.6.6.</a>	Antenna Elevation patterns(s)
<a href="#">GEOLOCATION GRID ADS 6.6.9.</a>	Geolocation Grid ADSRs
<a href="#">MDS1 6.6.10.</a>	Measurement Data Set 5
<a href="#">MDS2 6.6.10.</a>	Measurement Data Set 5

Format Version 114.0

## 6.2.4 ASA\_APS\_1P: ASAR Alternating Polarization Mode Single Look Complex

Table 6.7

### ASA\_APS\_1P

ASAR Alternating Polarization Mode Single Look Complex

#### File Structure

Data Sets

10

<a href="#">MPH 6.6.1.</a>	ENVISAT-1 MPH
<a href="#">SPH 6.6.11.</a>	ASAR Image Products SPH
<a href="#">MDS1 SQ ADS 6.6.16.</a>	SQ ADSRs
<a href="#">MDS2 SQ ADS 6.6.16.</a>	SQ ADSRs
<a href="#">MAIN PROCESSING PARAMS ADS 6.6.12.</a>	Main Processing parameters
<a href="#">DOP CENTROID COEFFS ADS 6.6.8.</a>	Doppler Centroid parameters
<a href="#">CHIRP PARAMS ADS 6.6.7.</a>	Chirp parameters
<a href="#">GEOLOCATION GRID ADS 6.6.9.</a>	Geolocation Grid ADSRs
MDS1	Measurement Data Set for imagette 400
MDS2	Measurement Data Set for imagette 400

Format Version 114.0

## 6.2.5 ASA\_GM1\_1P: ASAR Global Monitoring Mode Image

Table 6.8

---

## ASA\_GM1\_1P

ASAR Global Monitoring Mode Image

**File Structure**

Data Sets

10

<a href="#">MPH 6.6.1.</a>	ENVISAT-1 MPH
<a href="#">SPH 6.6.1L</a>	ASAR Image Products SPH
<a href="#">MDS1 SQ ADS 6.6.16.</a>	SQ ADSRs
<a href="#">MAIN PROCESSING PARAMS ADS 6.6.12.</a>	Main Processing parameters
<a href="#">DOP CENTROID COFFS ADS 6.6.8.</a>	Doppler Centroid parameters
<a href="#">SR GR ADS 6.6.17.</a>	Slant Range to Ground Range conversion parameters
<a href="#">CHIRP PARAMS ADS 6.6.7.</a>	Chirp parameters
<a href="#">MDSLANTENNA ELEV PATT ADS 6.6.6.</a>	Antenna Elevation patterns(s)
<a href="#">GEOLOCATION GRID ADS 6.6.9.</a>	Geolocation Grid ADSRs
<a href="#">MDS1 6.6.10.</a>	Measurement Data Set 5

Format Version 114.0

**6.2.6 ASA\_IMG\_1P: ASAR Image Mode Ellipsoid Geocoded Image**

Table 6.9

**ASA\_IMG\_1P**

ASAR Image Mode Ellipsoid Geocoded Image

**File Structure**

Data Sets

11

<a href="#">MPH 6.6.1.</a>	ENVISAT-1 MPH
<a href="#">SPH 6.6.1L</a>	ASAR Image Products SPH
<a href="#">MDS1 SQ ADS 6.6.16.</a>	SQ ADSRs
<a href="#">MAIN PROCESSING PARAMS ADS 6.6.12.</a>	Main Processing parameters
<a href="#">DOP CENTROID COFFS ADS 6.6.8.</a>	Doppler Centroid parameters
<a href="#">SR GR ADS 6.6.17.</a>	Slant Range to Ground Range conversion parameters
<a href="#">CHIRP PARAMS ADS 6.6.7.</a>	Chirp parameters
<a href="#">MDSLANTENNA ELEV PATT ADS 6.6.6.</a>	Antenna Elevation patterns(s)

<a href="#">GEOLOCATION GRID ADS 6.6.9.</a>	Geolocation Grid ADSRs
<a href="#">MAP PROJECTION GADS 6.6.13.</a>	Map Projection parameters
<a href="#">MDS1 6.6.10.</a>	Measurement Data Set 5

Format Version 114.0

## 6.2.7 ASA\_IMM\_1P: ASAR Image Mode Medium Resolution Image

Table 6.10

### ASA\_IMM\_1P

ASAR Image Mode Medium Resolution Image

#### File Structure

Data Sets

10

<a href="#">MPH 6.6.1.</a>	ENVISAT-1 MPH
<a href="#">SPH 6.6.11.</a>	ASAR Image Products SPH
<a href="#">MDS1 SQ ADS 6.6.16.</a>	SQ ADSRs
<a href="#">MAIN PROCESSING PARAMS ADS 6.6.12.</a>	Main Processing parameters
<a href="#">DOP CENTROID COEFFS ADS 6.6.8.</a>	Doppler Centroid parameters
<a href="#">SR GR ADS 6.6.17.</a>	Slant Range to Ground Range conversion parameters
<a href="#">CHIRP PARAMS ADS 6.6.7.</a>	Chirp parameters
<a href="#">MDS1 ANTENNA ELEV PATT ADS 6.6.6.</a>	Antenna Elevation patterns(s)
<a href="#">GEOLOCATION GRID ADS 6.6.9.</a>	Geolocation Grid ADSRs
<a href="#">MDS1 6.6.10.</a>	Measurement Data Set 5

Format Version 114.0

## 6.2.8 ASA\_IMP\_1P: ASAR Image Mode Precision Image

Table 6.11

## ASA\_IMP\_1P

ASAR Image Mode Precision Image

### File Structure

Data Sets

10

<a href="#">MPH 6.6.1.</a>	ENVISAT-1 MPH
<a href="#">SPH 6.6.11.</a>	ASAR Image Products SPH
<a href="#">MDS1 SQ ADS 6.6.16.</a>	SQ ADSRs
<a href="#">MAIN PROCESSING PARAMS ADS 6.6.12.</a>	Main Processing parameters
<a href="#">DOP CENTROID COFFS ADS 6.6.8.</a>	Doppler Centroid parameters
<a href="#">SR GR ADS 6.6.17.</a>	Slant Range to Ground Range conversion parameters
<a href="#">CHIRP PARAMS ADS 6.6.7.</a>	Chirp parameters
<a href="#">MDS1 ANTENNA ELEV PATT ADS 6.6.6.</a>	Antenna Elevation patterns(s)
<a href="#">GEOLOCATION GRID ADS 6.6.9.</a>	Geolocation Grid ADSRs
<a href="#">MDS1 6.6.10.</a>	Measurement Data Set 5

Format Version 114.0

## 6.2.9 ASA\_IMS\_1P: ASAR Image Mode Single Look Complex

Table 6.12

## ASA\_IMS\_1P

ASAR Image Mode Single Look Complex

### File Structure

Data Sets

8

<a href="#">MPH 6.6.1.</a>	ENVISAT-1 MPH
----------------------------	---------------

[SPH 6.6.11.](#)

ASAR Image Products SPH

[MDS1 SQ ADS 6.6.16.](#)

SQ ADSRs

[MAIN PROCESSING PARAMS ADS 6.6.12.](#)

Main Processing parameters

[DOP CENTROID COFFS ADS 6.6.8.](#)

Doppler Centroid parameters

[CHIRP PARAMS ADS 6.6.7.](#)

Chirp parameters

[GEOLOCATION GRID ADS 6.6.9.](#)

Geolocation Grid ADSRs

MDS1

Measurement Data Set for imagette 400

Format Version 114.0

## 6.2.10 ASA\_WSM\_1P: ASAR Wide Swath Medium Resolution Image

Table 6.13

### ASA\_WSM\_1P

ASAR Wide Swath Medium Resolution Image

#### File Structure

Data Sets

10

<a href="#">MPH 6.6.1.</a>	ENVISAT-1 MPH
<a href="#">SPH 6.6.11.</a>	ASAR Image Products SPH
<a href="#">MDS1 SQ ADS 6.6.16.</a>	SQ ADSRs
<a href="#">MAIN PROCESSING PARAMS ADS 6.6.12.</a>	Main Processing parameters
<a href="#">DOP CENTROID COFFS ADS 6.6.8.</a>	Doppler Centroid parameters
<a href="#">SR GR ADS 6.6.17.</a>	Slant Range to Ground Range conversion parameters
<a href="#">CHIRP PARAMS ADS 6.6.7.</a>	Chirp parameters
<a href="#">MDS1 ANTENNA ELEV PATT ADS 6.6.6.</a>	Antenna Elevation patterns(s)
<a href="#">GEOLOCATION GRID ADS 6.6.9.</a>	Geolocation Grid ADSRs
<a href="#">MDS1 6.6.10.</a>	Measurement Data Set 5

Format Version 114.0

## 6.2.11 ASA\_WVI\_1P: ASAR Wave Mode SLC Imagette and

## Imagette Cross Spectra

Table 6.14

### ASA\_WVI\_1P

ASAR Wave Mode SLC Imagette and Imagette Cross Spectra

#### File Structure

Data Sets

406

<a href="#">MPH 6.6.1.</a>	ENVISAT-1 MPH
<a href="#">SPH 6.6.22.</a>	ASAR WVI Product SPH
<a href="#">SQ ADS 6.6.21.</a>	SQ ADSRs
<a href="#">GEOLOCATION ADS 6.6.19.</a>	Wave Mode Geolocation ADS
<a href="#">PROCESSING PARAMS ADS 6.6.20.</a>	Wave Mode processing parameters
<a href="#">CROSS SPECTRA MDS 6.6.15.</a>	Measurement Data Set containing spectra. 1 MDSR per spectra.
SLC IMAGETTE MDS 000	Measurement Data Set for imagette 400
SLC IMAGETTE MDS 001	Measurement Data Set for imagette 400
SLC IMAGETTE MDS 002	Measurement Data Set for imagette 400
SLC IMAGETTE MDS 003	Measurement Data Set for imagette 400
SLC IMAGETTE MDS 004	Measurement Data Set for imagette 400
SLC IMAGETTE MDS 005	Measurement Data Set for imagette 400
SLC IMAGETTE MDS 006	Measurement Data Set for imagette 400
SLC IMAGETTE MDS 007	Measurement Data Set for imagette 400
SLC IMAGETTE MDS 008	Measurement Data Set for imagette 400
SLC IMAGETTE MDS 009	Measurement Data Set for imagette 400
SLC IMAGETTE MDS 010	Measurement Data Set for imagette 400
SLC IMAGETTE MDS 011	Measurement Data Set for imagette 400
SLC IMAGETTE MDS 012	Measurement Data Set for imagette 400
SLC IMAGETTE MDS 013	Measurement Data Set for imagette 400
SLC IMAGETTE MDS 014	Measurement Data Set for imagette 400
SLC IMAGETTE MDS 015	Measurement Data Set for imagette 400
SLC IMAGETTE MDS 016	Measurement Data Set for imagette 400
SLC IMAGETTE MDS 017	Measurement Data Set for imagette 400
SLC IMAGETTE MDS 018	Measurement Data Set for imagette 400
SLC IMAGETTE MDS 019	Measurement Data Set for imagette 400
SLC IMAGETTE MDS 020	Measurement Data Set for imagette 400
SLC IMAGETTE MDS 021	Measurement Data Set for imagette 400
SLC IMAGETTE MDS 022	Measurement Data Set for imagette 400
SLC IMAGETTE MDS 023	Measurement Data Set for imagette 400
SLC IMAGETTE MDS 024	Measurement Data Set for imagette 400
SLC IMAGETTE MDS 025	Measurement Data Set for imagette 400
SLC IMAGETTE MDS 026	Measurement Data Set for imagette 400
SLC IMAGETTE MDS 027	Measurement Data Set for imagette 400
SLC IMAGETTE MDS 028	Measurement Data Set for imagette 400
SLC IMAGETTE MDS 029	Measurement Data Set for imagette 400
SLC IMAGETTE MDS 030	Measurement Data Set for imagette 400
SLC IMAGETTE MDS 031	Measurement Data Set for imagette 400
SLC IMAGETTE MDS 032	Measurement Data Set for imagette 400
SLC IMAGETTE MDS 033	Measurement Data Set for imagette 400
SLC IMAGETTE MDS 034	Measurement Data Set for imagette 400
SLC IMAGETTE MDS 035	Measurement Data Set for imagette 400
SLC IMAGETTE MDS 036	Measurement Data Set for imagette 400
SLC IMAGETTE MDS 037	Measurement Data Set for imagette 400











SLC IMAGETTE MDS 378	Measurement Data Set for imagette 400
SLC IMAGETTE MDS 379	Measurement Data Set for imagette 400
SLC IMAGETTE MDS 380	Measurement Data Set for imagette 400
SLC IMAGETTE MDS 381	Measurement Data Set for imagette 400
SLC IMAGETTE MDS 382	Measurement Data Set for imagette 400
SLC IMAGETTE MDS 383	Measurement Data Set for imagette 400
SLC IMAGETTE MDS 384	Measurement Data Set for imagette 400
SLC IMAGETTE MDS 385	Measurement Data Set for imagette 400
SLC IMAGETTE MDS 386	Measurement Data Set for imagette 400
SLC IMAGETTE MDS 387	Measurement Data Set for imagette 400
SLC IMAGETTE MDS 388	Measurement Data Set for imagette 400
SLC IMAGETTE MDS 389	Measurement Data Set for imagette 400
SLC IMAGETTE MDS 390	Measurement Data Set for imagette 400
SLC IMAGETTE MDS 391	Measurement Data Set for imagette 400
SLC IMAGETTE MDS 392	Measurement Data Set for imagette 400
SLC IMAGETTE MDS 393	Measurement Data Set for imagette 400
SLC IMAGETTE MDS 394	Measurement Data Set for imagette 400
SLC IMAGETTE MDS 395	Measurement Data Set for imagette 400
SLC IMAGETTE MDS 396	Measurement Data Set for imagette 400
SLC IMAGETTE MDS 397	Measurement Data Set for imagette 400
SLC IMAGETTE MDS 398	Measurement Data Set for imagette 400
SLC IMAGETTE MDS 399	Measurement Data Set for imagette 400

Format Version 114.0

## 6.2.12 ASA\_WVS\_1P: ASAR Wave Mode Imagette Cross Spectra

Table 6.15

### ASA\_WVS\_1P

ASAR Wave Mode Imagette Cross Spectra

#### File Structure

Data Sets

6

<a href="#">MPH 6.6.1.</a>	ENVISAT-1 MPH
<a href="#">SPH 6.6.18.</a>	ASAR Wave Mode Products Base SPH
<a href="#">SQ ADS 6.6.21.</a>	SQ ADSRs
<a href="#">GEOLOCATION ADS 6.6.19.</a>	Wave Mode Geolocation ADS
<a href="#">PROCESSING PARAMS ADS 6.6.20.</a>	Wave Mode processing parameters
<a href="#">CROSS SPECTRA MDS 6.6.15.</a>	Measurement Data Set containing spectra. 1 MDSR per spectra.

---

Format Version 114.0

## 6.2.13 ASA\_WSS\_1P: Wide Swath Mode SLC Image

Table 6.16

### ASA\_WSS\_1P

ASAR Wide Swath Medium Resolution Image

#### File Structure

Data Sets

15

<a href="#"><u>MPH 6.6.1.</u></a>	ENVISAT-1 MPH
<a href="#"><u>SPH 6.6.11.</u></a>	ASAR Image Products SPH
<a href="#"><u>MDS1 SQ ADS 6.6.16.</u></a>	SQ ADSRs
<a href="#"><u>MAIN PROCESSING PARAMS ADS 6.6.12.</u></a>	Main Processing parameters
<a href="#"><u>DOP CENTROID COEFFS ADS 6.6.8.</u></a>	Doppler Centroid parameters
<a href="#"><u>SR GR ADS 6.6.17.</u></a>	Slant Range to Ground Range conversion parameters
<a href="#"><u>CHIRP PARAMS ADS 6.6.7.</u></a>	Chirp parameters
<a href="#"><u>MDS1 ANTENNA ELEV PATT ADS 6.6.6.</u></a>	Antenna Elevation patterns(s)
<a href="#"><u>GEOLOCATION GRID ADS 6.6.9.</u></a>	Geolocation Grid ADSRs
<a href="#"><u>DOP CENTROID GRID ADS 6.6.26.</u></a>	Doppler Centroid Grid ADS
<a href="#"><u>MDS1 6.6.10.</u></a>	Measurement Data Set 5
<a href="#"><u>MDS2 6.6.10.</u></a>	Measurement Data Set 5
<a href="#"><u>MDS3 6.6.10.</u></a>	Measurement Data Set 5
<a href="#"><u>MDS4 6.6.10.</u></a>	Measurement Data Set 5
<a href="#"><u>MDS5 6.6.10.</u></a>	Measurement Data Set 5

Format Version 114.0

## 6.3 Level 0 Products

Table 6.17

### 6.3.1 ASA\_APC\_0P: ASAR Alternating Polarization Level 0 (Copolar)

Table 6.18

## ASA\_APC\_0P

ASAR Alternating Polarization Level 0 (Copolar)

### File Structure

Data Sets	3
<a href="#">MPH 6.6.1</a>	ENVISAT-1 MPH
<a href="#">SPH 6.6.25</a>	Level 0 SPH
<a href="#">ASAR_SOURCE_PACKETS 6.6.24</a>	Level 0 MDSR

Format Version 114.0

### 6.3.2 ASAAPH\_0P: ASAR Alternating Polarization Level 0 (Cross polar H)

Table 6.19

## ASA\_APH\_OP

ASAR Alternating Polarization Level 0 (Cross polar H)

### File Structure

Data Sets

3

<a href="#">MPH 6.6.1.</a>	ENVISAT-1 MPH
<a href="#">SPH 6.6.25.</a>	Level 0 SPH
<a href="#">ASAR_SOURCE_PACKETS 6.6.24.</a>	Level 0 MDSR

Format Version 114.0

### 6.3.3 ASA\_APV\_OP: ASAR Alternating Polarization Level 0 (Cross polar V)

Table 6.20

## ASA\_APV\_OP

ASAR Alternating Polarization Level 0 (Cross polar V)

### File Structure

Data Sets

3

<a href="#">MPH 6.6.1.</a>	ENVISAT-1 MPH
<a href="#">SPH 6.6.25.</a>	Level 0 SPH
<a href="#">ASAR_SOURCE_PACKETS 6.6.24.</a>	Level 0 MDSR

Format Version 114.0

## 6.3.4 ASA\_EC\_0P: ASAR Level 0 External Characterization

Table 6.21

### ASA\_EC\_0P

ASAR Level 0 External Characterization

#### File Structure

Data Sets

3

<a href="#">MPH 6.6.1.</a>	ENVISAT-1 MPH
<a href="#">SPH 6.6.25.</a>	Level 0 SPH
<a href="#">ASAR_SOURCE_PACKETS 6.6.24.</a>	Level 0 MDSR

Format Version 114.0

## 6.3.5 ASA\_GM\_0P: ASAR Global Monitoring Mode Level 0

Table 6.22

### ASA\_GM\_0P

ASAR Global Monitoring Mode Level 0

#### File Structure

Data Sets

3

<a href="#">MPH 6.6.1.</a>	ENVISAT-1 MPH
<a href="#">SPH 6.6.25.</a>	Level 0 SPH



<a href="#">ASAR_SOURCE_PACKETS 6.6.24.</a>	Level 0 MDSR
---	--------------

Format Version 114.0

### 6.3.6 ASA\_IM\_0P: ASAR Image Mode Level 0

Table 6.23

## ASA\_IM\_0P

ASAR Image Mode Level 0

### File Structure

Data Sets

3

<a href="#">MPH 6.6.1.</a>	ENVISAT-1 MPH
<a href="#">SPH 6.6.25.</a>	Level 0 SPH
<a href="#">ASAR_SOURCE_PACKETS 6.6.24.</a>	Level 0 MDSR

Format Version 114.0

### 6.3.7 ASA\_MS\_0P: ASAR Level 0 Module Stepping Mode

Table 6.24

## ASA\_MS\_0P

ASAR Level 0 Module Stepping Mode

---

## File Structure

Data Sets

3

<a href="#">MPH 6.6.1.</a>	ENVISAT-1 MPH
<a href="#">SPH 6.6.25.</a>	Level 0 SPH
<a href="#">ASAR_SOURCE_PACKETS 6.6.24.</a>	Level 0 MDSR

Format Version 114.0

### 6.3.8 ASA\_WS\_\_OP: ASAR Wide Swath Mode Level 0

Table 6.25

## ASA\_WS\_\_OP

ASAR Wide Swath Mode Level 0

### File Structure

Data Sets

3

<a href="#">MPH 6.6.1.</a>	ENVISAT-1 MPH
<a href="#">SPH 6.6.25.</a>	Level 0 SPH
<a href="#">ASAR_SOURCE_PACKETS 6.6.24.</a>	Level 0 MDSR

Format Version 114.0

### 6.3.9 ASA\_WV\_\_OP: ASAR Wave Mode Level 0

Table 6.26

## ASA\_WV\_0P

ASAR Wave Mode Level 0

### File Structure

Data Sets

3

<a href="#">MPH 6.6.1.</a>	ENVISAT-1 MPH
<a href="#">SPH 6.6.25.</a>	Level 0 SPH
<a href="#">ASAR_SOURCE_PACKETS 6.6.24.</a>	Level 0 MDSR

Format Version 114.0

## 6.4 Browse Products

Table 6.27

### 6.4.1 ASA\_AP\_BP: ASAR Alternating Polarization Browse Image

Table 6.28

## ASA\_AP\_BP

ASAR Alternating Polarization Browse Image

### File Structure

<a href="#">MPH 6.6.1.</a>	ENVISAT-1 MPH
<a href="#">SPH 6.6.11.</a>	ASAR Image Products SPH
<a href="#">MDS1 SO ADS 6.6.16.</a>	SQ ADSRs
<a href="#">MDS2 SQ ADS 6.6.16.</a>	SQ ADSRs
<a href="#">GEOLOCATION GRID ADS 6.6.9.</a>	Geolocation Grid ADSRs
MDS1	Measurement Data Set 1

Format Version 114.0

## 6.4.2 ASA\_GM\_BP: ASAR Global Monitoring Mode Browse Image

### File Structure

Table 6.29

<a href="#">MPH 6.6.1.</a>	Main Product Header
<a href="#">SPH 6.6.11.</a>	ASAR Image Products SPH
<a href="#">MDS1 SO ADS 6.6.16.</a>	SQ ADSRs
<a href="#">GEOLOCATION GRID ADS 6.6.9.</a>	Geolocation Grid ADSRs
MDS1	Measurement Data Set 1

Format Version DDT v100.2 EV 2.0.1 (11/02/2002)

## 6.4.3 ASA\_IM\_BP: ASAR Image Mode Browse Image

Table 6.30

## ASA\_IM\_BP

ASAR Image Mode Browse Image

### File Structure

Data Sets

5

<a href="#">MPH 6.6.1.</a>	ENVISAT-1 MPH
<a href="#">SPH 6.6.11.</a>	ASAR Image Products SPH
<a href="#">MDS1 SQ ADS 6.6.16.</a>	SQ ADSRs
<a href="#">GEOLOCATION GRID ADS 6.6.9.</a>	Geolocation Grid ADSRs
MDS1	Measurement Data Set 1

Format Version 114.0

### 6.4.4 ASA\_WS\_BP: ASAR Wide Swath Browse Image

Table 6.31

## ASA\_WS\_BP

ASAR Wide Swath Browse Image

### File Structure

Data Sets

5

<a href="#">MPH 6.6.1.</a>	ENVISAT-1 MPH
<a href="#">SPH 6.6.11.</a>	ASAR Image Products SPH
<a href="#">MDS1 SQ ADS 6.6.16.</a>	SQ ADSRs
<a href="#">GEOLOCATION GRID ADS 6.6.9.</a>	Geolocation Grid ADSRs
MDS1	Measurement Data Set 1

Format Version 114.0

## 6.5 Auxilliary Products

Table 6.32

### 6.5.1 ASA\_CON\_AX: ASAR Processor Configuration

Table 6.33

## ASA\_CON\_AX

ASAR Processor Configuration

### File Structure

Data Sets

3

<a href="#">MPH 6.6.1.</a>	ENVISAT-1 MPH
<a href="#">SPH 6.6.23.</a>	SPH for auxiliary data with N=1 DSDs
<a href="#">Asar auxiliary data 6.6.2.</a>	Contains ASAR processor configuration data

Format Version 114.0

### 6.5.2 ASA\_INS\_AX: ASAR Instrument characterization

Table 6.34

## ASA\_INS\_AX

ASAR Instrument characterization

### File Structure

Data Sets

3

<a href="#">MPH 6.6.1.</a>	ENVISAT-1 MPH
<a href="#">SPH 6.6.23.</a>	SPH for auxiliary data with N=1 DSDs
<a href="#">Asar auxiliary data 6.6.3.</a>	Contains ASAR instrument characterization data

Format Version 114.0

## 6.5.3 ASA\_XCA\_AX: ASAR External calibration data

Table 6.35

## ASA\_XCA\_AX

ASAR External calibration data

### File Structure

Data Sets

3

<a href="#">MPH 6.6.1.</a>	ENVISAT-1 MPH
<a href="#">SPH 6.6.23.</a>	SPH for auxiliary data with N=1 DSDs
<a href="#">Asar auxiliary data 6.6.4.</a>	Contains ASAR external calibration data

---

Format Version 114.0

## 6.5.4 ASA\_XCH\_AX: ASAR External characterization data

### File Structure

Data Sets

3

Table 6.36

<a href="#">MPH 6.6.1.</a>	Main Product Header
<a href="#">SPH 6.6.23.</a>	SPH for auxiliary data with N=1 DSDs
<a href="#">Asar auxiliary data 6.6.5.</a>	Contains ASAR external characterization data

Format Version DDT v100.2 EV 2.0.1 (11/02/2002)

## 6.6 Records

### 6.6.1 Main Product Header

Table 6.37 Main Product Header

## ENVISAT-1 MPH

#	Description	Units	Count	Type	Size
Data Record					
0	product_name_title	keyword	1	AsciiString	8 byte(s)



#	Description	Units	Count	Type	Size
	PRODUCT=				
1	quote_1 quotation mark ("")	ascii	1	AsciiString	1 byte(s)
2	product Product File name	ascii	1	AsciiString	62 byte(s)
3	quote_2 quotation mark ("")	ascii	1	AsciiString	1 byte(s)
4	newline_char_1 newline character	terminator	1	AsciiString	1 byte(s)
5	processing_stage_title PROC_STAGE=	keyword	1	AsciiString	11 byte(s)
6	proc_stage Processing Stage FlagN = Near Real Time, T = test product, V = fully validated (fully consolidated) product, S = special product. Letters between N and V (with the exception of T and S) indicate steps in the consolidation process, with letters closer to V	ascii	1	AsciiString	1 byte(s)
7	newline_char_2 newline character	terminator	1	AsciiString	1 byte(s)
8	reference_doc_title REF_DOC=	keyword	1	AsciiString	8 byte(s)
9	quote_3 quotation mark ("")	ascii	1	AsciiString	1 byte(s)
10	ref_doc Reference Document Describing Product AA-BB-CCC-DD-EEEE_V/I?? (23 characters, including blank space characters) where AA-BB-CCC-DD-EEEE is the ESA standard document no. and V/I is the Version / Issue. If the reference document is the Products Specifications PO-RS-MDA-GS-2009, the version and revision have to refer to the volume 1 of the document, where the status (version/revision) of all volumes can be found. If not used, set to ??????????????????????	ascii	1	AsciiString	23 byte(s)
11	quote_4 quotation mark ("")	ascii	1	AsciiString	1 byte(s)
12	newline_char_3 newline character	terminator	1	AsciiString	1 byte(s)
13	spare_1 Spare	-	1	SpareField	41 byte(s)
14	acquisition_station_id_title ACQUISITION_STATION=	keyword	1	AsciiString	20 byte(s)
15	quote_5 quotation mark ("")	ascii	1	AsciiString	1 byte(s)
16	acquisition_station Acquisition Station ID (up to 3 codes) If not used, set to ????????????????????	ascii	1	AsciiString	20 byte(s)
17	quote_6 quotation mark ("")	ascii	1	AsciiString	1 byte(s)
18	newline_char_5 newline character	terminator	1	AsciiString	1 byte(s)
19	processing_center_title PROC_CENTER=	keyword	1	AsciiString	12 byte(s)
20	quote_7 quotation mark ("")	ascii	1	AsciiString	1 byte(s)
21	proc_center Processing Center ID which generated current product If not used, set to ???????	ascii	1	AsciiString	6 byte(s)
22	quote_8 quotation mark ("")	ascii	1	AsciiString	1 byte(s)
23	newline_char_6 newline character	terminator	1	AsciiString	1 byte(s)
24	processing_time_title PROC_TIME=	keyword	1	AsciiString	10 byte(s)
25	quote_9 quotation mark ("")	ascii	1	AsciiString	1 byte(s)
26	proc_time UTC Time of Processing (product generation time) UTC Time format. If not used, set to ????????????????????????????	UTC	1	UtcExternal	27 byte(s)
27	quote_10 quotation mark ("")	ascii	1	AsciiString	1 byte(s)
28	newline_char_7 newline character	terminator	1	AsciiString	1 byte(s)
29	software_version_title SOFTWARE_VER=	keyword	1	AsciiString	13 byte(s)
30	quote_11 quotation mark ("")	ascii	1	AsciiString	1 byte(s)
31	software_ver Software Version number of processing softwareFormat: Name of processor (up	ascii	1	AsciiString	14 byte(s)



#	Description	Units	Count	Type	Size
	to 10 characters)/version number (4 characters)--left justified (any blanks added at end). If not used, set to ??????????????.e.g. MIPAS/2.31????				
32	quote_12 quotation mark ("")	ascii	1	AsciiString	1 byte(s)
33	newline_char_8 newline character	terminator	1	AsciiString	1 byte(s)
34	spare_2 Spare	-	1	SpareField	41 byte(s)
35	sensing_start_title SENSING_START=	keyword	1	AsciiString	14 byte(s)
36	quote_13 quotation mark ("")	ascii	1	AsciiString	1 byte(s)
37	sensing_start UTC start time of data sensing (first measurement in first data record) UTC Time format. If not used, set to ????????????????????????????	UTC	1	UtcExternal	27 byte(s)
38	quote_14 quotation mark ("")	ascii	1	AsciiString	1 byte(s)
39	newline_char_10 newline character	terminator	1	AsciiString	1 byte(s)
40	sensing_stop_title SENSING_STOP=	keyword	1	AsciiString	13 byte(s)
41	quote_15 quotation mark ("")	ascii	1	AsciiString	1 byte(s)
42	sensing_stop UTC stop time of data sensing (last measurements last data record) UTC Time format. If not used, set to ????????????????????????????	UTC	1	UtcExternal	27 byte(s)
43	quote_16 quotation mark ("")	ascii	1	AsciiString	1 byte(s)
44	newline_char_11 newline character	terminator	1	AsciiString	1 byte(s)
45	spare_3 Spare	-	1	SpareField	41 byte(s)
46	phase_title PHASE=	keyword	1	AsciiString	6 byte(s)
47	phase Phasephase letter. If not used, set to X.	ascii	1	AsciiString	1 byte(s)
48	newline_char_13 newline character	terminator	1	AsciiString	1 byte(s)
49	cycle_title CYCLE=	keyword	1	AsciiString	6 byte(s)
50	cycle CycleCycle number. If not used, set to +000.	-	1	AsciiIntegerAuc	4 byte(s)
51	newline_char_14 newline character	terminator	1	AsciiString	1 byte(s)
52	relative_orbit_title REL_ORBIT=	keyword	1	AsciiString	10 byte(s)
53	rel_orbit Start relative orbit number If not used, set to +00000	-	1	As	6 byte(s)
54	newline_char_15 newline character	terminator	1	AsciiString	1 byte(s)
55	absolute_orbit_title ABS_ORBIT=	keyword	1	AsciiString	10 byte(s)
56	abs_orbit Start absolute orbit number. If not used, set to +00000.	-	1	As	6 byte(s)
57	newline_char_16 newline character	terminator	1	AsciiString	1 byte(s)
58	state_vector_time_title STATE_VECTOR_TIME=	keyword	1	AsciiString	18 byte(s)
59	quote_17 quotation mark ("")	ascii	1	AsciiString	1 byte(s)
60	state_vector_time UTC of ENVISAT state vector. UTC time format. If not used, set to ????????????????????????	UTC	1	UtcExternal	27 byte(s)
61	quote_18 quotation mark ("")	ascii	1	AsciiString	1 byte(s)
62	newline_char_17 newline character	terminator	1	AsciiString	1 byte(s)
63	delta_ut1_title DELTA_UT1=	keyword	1	AsciiString	10 byte(s)
64	delta_ut1 DUT1=UT1-UTC. If not used, set to +.000000.	s	1	Ado06	8 byte(s)

#	Description	Units	Count	Type	Size
65	delta_ut1_units <>	units	1	AsciiString	3 byte(s)
66	newline_char_18 newline character	terminator	1	AsciiString	1 byte(s)
67	x_position_title X_POSITION=	keyword	1	AsciiString	11 byte(s)
68	x_position X Position in Earth-Fixed reference. If not used, set to +0000000.000.	m	1	Ado73	12 byte(s)
69	x_position_units <m>	units	1	AsciiString	3 byte(s)
70	newline_char_19 newline character	terminator	1	AsciiString	1 byte(s)
71	y_position_title Y_POSITION=	keyword	1	AsciiString	11 byte(s)
72	y_position Y Position in Earth-Fixed reference. If not used, set to +0000000.000.	m	1	Ado73	12 byte(s)
73	y_position_units <m>	units	1	AsciiString	3 byte(s)
74	newline_char_20 newline character	terminator	1	AsciiString	1 byte(s)
75	z_position_title Z_POSITION=	keyword	1	AsciiString	11 byte(s)
76	z_position Z Position in Earth-Fixed reference. If not used, set to +0000000.000.	m	1	Ado73	12 byte(s)
77	z_position_units <m>	units	1	AsciiString	3 byte(s)
78	newline_char_21 newline character	terminator	1	AsciiString	1 byte(s)
79	x_velocity_title X_VELOCITY=	keyword	1	AsciiString	11 byte(s)
80	x_velocity X velocity in Earth fixed reference. If not used, set to +0000.000000.	m/s	1	Ado46	12 byte(s)
81	x_velocity_units <m/s>	units	1	AsciiString	5 byte(s)
82	newline_char_22 newline character	terminator	1	AsciiString	1 byte(s)
83	y_velocity_title Y_VELOCITY=	keyword	1	AsciiString	11 byte(s)
84	y_velocity Y velocity in Earth fixed reference. If not used, set to +0000.000000.	m/s	1	Ado46	12 byte(s)
85	y_velocity_units <m/s>	units	1	AsciiString	5 byte(s)
86	newline_char_23 newline character	terminator	1	AsciiString	1 byte(s)
87	z_velocity_title Z_VELOCITY=	keyword	1	AsciiString	11 byte(s)
88	z_velocity Z velocity in Earth fixed reference. If not used, set to +0000.000000.	m/s	1	Ado46	12 byte(s)
89	z_velocity_units <m/s>	units	1	AsciiString	5 byte(s)
90	newline_char_24 newline character	terminator	1	AsciiString	1 byte(s)
91	vector_source_title VECTOR_SOURCE=	keyword	1	AsciiString	14 byte(s)
92	quote_19 quotation mark ("")	ascii	1	AsciiString	1 byte(s)
93	vector_source Source of Orbit Vectors	ascii	1	AsciiString	2 byte(s)
94	quote_20 quotation mark ("")	ascii	1	AsciiString	1 byte(s)
95	newline_char_25 newline character	terminator	1	AsciiString	1 byte(s)
96	spare_4 Spare	-	1	SpareField	41 byte(s)
97	utc_sbt_time_title UTC_SBT_TIME=	keyword	1	AsciiString	13 byte(s)
98	quote_21 quotation mark ("")	ascii	1	AsciiString	1 byte(s)
99	utc_sbt_time UTC time corresponding to SBT below(currently defined to be given at the time	UTC	1	UtcExternal	27 byte(s)

#	Description	Units	Count	Type	Size
	of the ascending node state vector). If not used, set to ??????????????????????????.				
100	quote_22 quotation mark ("")	ascii	1	AsciiString	1 byte(s)
101	newline_char_28 newline character	terminator	1	AsciiString	1 byte(s)
102	sat_binary_time_title SAT_BINARY_TIME=	keyword	1	AsciiString	16 byte(s)
103	sat_binary_time Satellite Binary Time (SBT) 32bit integer time of satellite clock. Its value is unsigned (= >0). If not used, set to +0000000000.	-	1	AsciiIntegerAul	11 byte(s)
104	newline_char_29 newline character	terminator	1	AsciiString	1 byte(s)
105	clock_step_title CLOCK_STEP=	keyword	1	AsciiString	11 byte(s)
106	clock_step Clock Step Sizeclock step in picoseconds. Its value is unsigned (= >0). If not used, set to +0000000000.	psec.	1	AsciiIntegerAul	11 byte(s)
107	clock_step_units <ps>	units	1	AsciiString	4 byte(s)
108	newline_char_30 newline character	terminator	1	AsciiString	1 byte(s)
109	spare_5 Spare	-	1	SpareField	33 byte(s)
110	leap_utc_title LEAP_UTC=	keyword	1	AsciiString	9 byte(s)
111	quote_23 quotation mark ("")	ascii	1	AsciiString	1 byte(s)
112	leap_utc UTC time of the occurrence of the Leap SecondSet to ?????????????????????????? if not used.	UTC	1	UtcExternal	27 byte(s)
113	quote_24 quotation mark ("")	ascii	1	AsciiString	1 byte(s)
114	newline_char_302 newline character	terminator	1	AsciiString	1 byte(s)
115	leap_sign_title LEAP_SIGN=	keyword	1	AsciiString	10 byte(s)
116	leap_sign Leap second sign(+001 if positive Leap Second, -001 if negative)Set to +000 if not used.	s	1	Ac	4 byte(s)
117	newline_char_303 newline character	terminator	1	AsciiString	1 byte(s)
118	leap_err_title LEAP_ERR=	keyword	1	AsciiString	9 byte(s)
119	leap_err Leap second errorif leap second occurs within processing segment = 1, otherwise = 0If not used, set to 0.	ascii	1	AsciiString	1 byte(s)
120	newline_char_304 newline character	terminator	1	AsciiString	1 byte(s)
121	spare_6 Spare	-	1	SpareField	41 byte(s)
122	product_err_title PRODUCT_ERR=	keyword	1	AsciiString	12 byte(s)
123	product_err 1 or 0. If 1, errors have been reported in the product. User should then refer to the SPH or Summary Quality ADS of the product for details of the error condition. If not used, set to 0.	ascii	1	AsciiString	1 byte(s)
124	newline_char_33 newline character	terminator	1	AsciiString	1 byte(s)
125	total_size_title TOT_SIZE=	keyword	1	AsciiString	9 byte(s)
126	tot_size Total Size Of Product (# bytes DSR + SPH + MPH)	bytes	1	Ad	21 byte(s)
127	total_size_units <bytes>	units	1	AsciiString	7 byte(s)
128	newline_char_34 newline character	terminator	1	AsciiString	1 byte(s)
129	sph_size_title SPH_SIZE=	keyword	1	AsciiString	9 byte(s)
130	sph_size Length Of SPH(# bytes in SPH)	bytes	1	Al	11 byte(s)
131	sph_size_units	units	1	AsciiString	7 byte(s)



#	Description	Units	Count	Type	Size
	<bytes>				
132	newline_char_35 newline character	terminator	1	AsciiString	1 byte(s)
133	number_of_dsd_title NUM_DSD=	keyword	1	AsciiString	8 byte(s)
134	num_dsd Number of DSDs(# DSDs)	-	1	AI	11 byte(s)
135	newline_char_36 newline character	terminator	1	AsciiString	1 byte(s)
136	size_of_dsd_title DSD_SIZE=	keyword	1	AsciiString	9 byte(s)
137	dsd_size Length of Each DSD(# bytes for each DSD, all DSDs shall have the same length)	-	1	AI	11 byte(s)
138	size_of_dsd_units <bytes>	units	1	AsciiString	7 byte(s)
139	newline_char_37 newline character	terminator	1	AsciiString	1 byte(s)
140	number_of_ds_att_title NUM_DATA_SETS=	keyword	1	AsciiString	14 byte(s)
141	num_data_sets Number of DSs attached(not all DSDs have a DS attached)	-	1	AI	11 byte(s)
142	newline_char_38 newline character	terminator	1	AsciiString	1 byte(s)
143	spare_7 Spare	-	1	SpareField	41 byte(s)

Record Length : 1247

DS\_NAME : ENVISAT-1 MPH

Format Version 114.0

## 6.6.2 ASAR processor configuration data

The Processor Configuration Auxiliary file contains static processing parameters used by the PF-ASAR which includes the threshold values used for setting PCD flags. This file is available in the inventory so a user may check what the processing configuration and threshold values were for the product of interest.

USE: Used during image formation for level 1b and level 2 products.

UPDATED: infrequently, only if static processing parameters change or PCD thresholds are updated.

SIZE: MPH(1247 bytes) + SPH (378 bytes) + GADS (796 bytes)

The MPH and SPH of these files will follow the standard MPH, SPH structure of all Envisat-1 auxiliary data. There is one DSD in the SPH: a GADS called

ASA\_CON\_AX\_GADS. The format of this GADS file is shown below:

Table 6.38 ASAR processor configuration data

## Contains ASAR processor configuration data

#	Description	Units	Count	Type	Size
Data Record					
0	dsr_time Time of creation MJD time	MJD	1	mjd	12 byte(s)
1	dsr_length DSR length Length of this DSR in bytes	bytes	1	ul	4 byte(s)
2	thresh_chirp_broadening Threshold for setting the chirp quality flag Maximum percentage broadening permitted in cross-correlation pulse width compared to theoretical width	samples	1	fl	4 byte(s)
3	thresh_chirp_sidelobe Threshold for setting the chirp quality flag First sidelobe of the chirp cross correlation function	dB	1	fl	4 byte(s)
4	thresh_chirp_islr Threshold for setting the chirp quality flag ISLR of the chirp cross correlation function	dB	1	fl	4 byte(s)
5	thresh_input_mean Threshold for setting the mean of input data quality flag For an expected mean value of x, this is the value T, such that the measured mean must fall between the x-T and x+T. Used for both I and Q channels.	-	1	fl	4 byte(s)
6	thresh_input_std_dev Threshold for setting the standard deviation of input data quality flag For an expected std. dev. value of y, this is the value D, such that the measured std. dev. must fall between the y-D and y+D. Used for both I and Q channels.	-	1	fl	4 byte(s)
7	thresh_dop_cen Threshold for setting the Doppler Centroid quality flag Threshold for Doppler Centroid confidence	-	1	fl	4 byte(s)
8	thresh_dop_amb Threshold for setting the Doppler Centroid ambiguity quality flag Threshold for setting the Doppler Centroid ambiguity confidence flag	-	1	fl	4 byte(s)
9	thresh_output_mean Threshold for setting the mean of output data quality flag For an expected mean value of x, this is the value T, such that the measured mean must fall between the x-T and x+T.	-	1	fl	4 byte(s)
10	thresh_output_std_dev Threshold for setting the standard deviation of output data quality flag For an expected std. dev. value of y, this is the value D, such that the measured std. dev. must fall between the y-D and y+D.	-	1	fl	4 byte(s)
11	thresh_missing_lines Threshold for setting the missing lines quality flag Maximum percentage of missing lines to total lines	-	1	fl	4 byte(s)
12	thresh_gaps Threshold for setting the missing gaps quality flag Maximum number of gaps allowed	-	1	fl	4 byte(s)
13	spare_1 Spare	-	1	SpareField	64 byte(s)
14	lines_per_gap Number of missing lines which constitute a gap	lines	1	ul	4 byte(s)
15	exp_im_mean Expected mean of I and Q samples for (IM) and (WV) SLC images Image Mode and Wave Mode	-	1	fl	4 byte(s)
16	exp_im_std_dev	-	1	fl	4 byte(s)

#	Description	Units	Count	Type	Size
	Expected standard deviation of I and Q samples for (IM) and (WV) SLC images Image Mode and Wave Mode				
17	exp_ap_mean Expected mean of I and Q samples for (AP) SLC images Alternating Polarisation Mode	-	1	fl	4 byte(s)
18	exp_ap_std_dev Expected standard deviation of I and Q samples for (AP) SLC images Alternating Polarisation Mode	-	1	fl	4 byte(s)
19	exp_imp_mean Expected mean of (IM) PRI samples Image Mode Precision	-	1	fl	4 byte(s)
20	exp_imp_std_dev Expected standard deviation of (IM) PRI samples Image Mode Precision	-	1	fl	4 byte(s)
21	exp_app_mean Expected mean of (AP) PRI samples Alternating Polarisation Precision	-	1	fl	4 byte(s)
22	exp_app_std_dev Expected standard deviation of (AP) PRI samples Alternating Polarisation Precision	-	1	fl	4 byte(s)
23	exp_immm_mean Expected mean of (IMM) samples Image Mode Medium-resolution product	-	1	fl	4 byte(s)
24	exp_immm_std_dev Expected standard deviation of (IMM) samples Image Mode Medium-resolution product	-	1	fl	4 byte(s)
25	exp_apm_mean Expected mean of (APM) samples Alternating Polarisation Medium-resolution image	-	1	fl	4 byte(s)
26	exp_apm_std_dev Expected standard deviation of (APM) samples Alternating Polarisation Medium-resolution image	-	1	fl	4 byte(s)
27	exp_wsm_mean Expected mean of (WSM) samples Wide Swath Medium-resolution standard image	-	1	fl	4 byte(s)
28	exp_wsm_std_dev Expected standard deviation of (WSM) samples Wide Swath Medium-resolution standard image	-	1	fl	4 byte(s)
29	exp_gm1_mean Expected mean of (GM1) samples Global Monitoring Mode Image	-	1	fl	4 byte(s)
30	exp_gm1_std_dev Expected standard deviation of (GM1) samples Global Monitoring Mode Image	-	1	fl	4 byte(s)
31	input_mean Expected I and Q input mean	-	1	fl	4 byte(s)
32	expected_input_std_dev Expected I and Q input std dev.	-	1	fl	4 byte(s)
33	look_conf_thresh Look image statistics confidence parameter thresholds Minimum and maximum	-	2	fl	2*4 byte(s)
34	inter_look_conf_thresh Inter-look confidence statistics confidence parameter threshold	-	1	fl	4 byte(s)
35	az_cutoff_thresh Azimuth cut-off convergence measure threshold	-	1	fl	4 byte(s)
36	az_cutoff_iterations_thresh Azimuth cut-off Iteration count overflow threshold	-	1	fl	4 byte(s)
37	phs_peak_thresh Phase information confidence measure threshold for the spectral peak	-	1	fl	4 byte(s)
38	phs_cross_thresh Phase information confidence measure threshold for the cross covariance peak offset	m	1	fl	4 byte(s)
39	spare_2 Spare	-	1	SpareField	64 byte(s)
40	apply_gain_corr_flag Apply Receive Gain Droop correction (0=not applied; 1=applied).	flag	1	BooleanFlag	1 byte(s)
41	apply_gc_cal_p2_flag Apply Receive Gain Droop correction to Calibration Pulse P2. (0=not applied; 1=applied).	flag	1	BooleanFlag	1 byte(s)
42	apply_gc_delay_cal_p2_flag Apply Receive Gain Droop correction nominal delay to Calibration Pulse P2.	flag	1	BooleanFlag	1 byte(s)



#	Description		Units	Count	Type	Size
(0=not applied; 1=applied).						
43	spare_3 Spare		-	1	SpareField	65 byte(s)
44	chirp_val_im Reference chirp energy values for IM values. Parameters are arranged in four lists (1list for each HH.VV),each list containing 7 values for IS1 to IS7.		dB	14	fl	14*4 byte(s)
45	chirp_val_ap Reference chirp energy values for AP values.Parameters are arranged in four lists (1list for each HH.VV),each list containing 7 values for IS1 to IS7.		dB	28	fl	28*4 byte(s)
46	chirp_val_wv Reference chirp energy values for WV values. Parameters are arranged in four lists (1list for each HH.VV),each list containing 7 values for IS1 to IS7.		dB	14	fl	14*4 byte(s)
47	chirp_val_ws Reference chirp energy values for WS values. Parameters are arranged in four lists (1list for each HH.VV),each list containing 7 values for IS1 to IS7.		dB	10	fl	10*4 byte(s)
48	chirp_val_gm Reference chirp energy values for GS values. Parameters are arranged in four lists (1list for each HH.VV),each list containing 7 values for IS1 to IS7.		dB	10	fl	10*4 byte(s)
49	rep_eng_thres_im Replica Energy Threshold for chirp energy comparison for IM		dB	1	fl	4 byte(s)
50	rep_eng_thres_ap Replica Energy Threshold for chirp energy comparison for AP		dB	1	fl	4 byte(s)
51	rep_eng_thres_wv Replica Energy Threshold for chirp energy comparison for WV		dB	1	fl	4 byte(s)
52	rep_eng_thres_ws Replica Energy Threshold for chirp energy comparison for WS		dB	1	fl	4 byte(s)
53	rep_eng_thres_gm Replica Energy Threshold for chirp energy comparison for GM		dB	1	fl	4 byte(s)
54	norm_im Normalisation for IM		-	1	norm_imStruct	8.0 byte(s)
	a	perform_norm Perform Normalisation Flag (1=yes,0=no)	-	1	uc	1 byte(s)
	b	norm_type Normalisation Type( only used if flag set to 1):REPLICA or REF0000 or EQV0000	-	1	AsciiString	7 byte(s)
55	norm_ap Normalisation for AP		-	1	norm_apStruct	8.0 byte(s)
	a	perform_norm Perform Normalisation Flag (1=yes,0=no)	-	1	uc	1 byte(s)
	b	norm_type Normalisation Type( only used if flag set to 1):REPLICA or REF0000 or EQV0000	-	1	AsciiString	7 byte(s)
56	norm_wv Normalisation for WV		-	1	norm_wvStruct	8.0 byte(s)
	a	perform_norm Perform Normalisation Flag (1=yes,0=no)	-	1	uc	1 byte(s)
	b	norm_type Normalisation Type( only used if flag set to 1):REPLICA or REF0000 or EQV0000	-	1	AsciiString	7 byte(s)
57	norm_ws Normalisation for WS		-	1	norm_wsStruct	8.0 byte(s)
	a	perform_norm Perform Normalisation Flag (1=yes,0=no)	-	1	uc	1 byte(s)
	b	norm_type Normalisation Type( only used if flag set to 1):REPLICA or REF0000 or EQV0000	-	1	AsciiString	7 byte(s)

#	Description		Units	Count	Type	Size
	or EQV0000					
58	norm_gm Normalisation for GM		-	1	norm_gmStruct	8.0 byte(s)
	a	perform_norm Perform Normalisation Flag (1=yes,0=no)	-	1	uc	1 byte(s)
	b	norm_type Normalisation Type( only used if flag set to 1):REPLICA or REF0000 or EQV0000	-	1	AsciiString	7 byte(s)
59	rep_re_cutoff_im Replica reconstruction cutoff threshold for IM		-	1	fl	4 byte(s)
60	rep_re_cutoff_ap Replica reconstruction cutoff threshold for AP		-	1	fl	4 byte(s)
61	rep_re_cutoff_wv Replica reconstruction cutoff threshold for WV		-	1	fl	4 byte(s)
62	rep_re_cutoff_ws Replica reconstruction cutoff threshold for WS		-	1	fl	4 byte(s)
63	rep_re_cutoff_gm Replica reconstruction cutoff threshold for GM		-	1	fl	4 byte(s)
64	cal_pluse_apl_thres_im Calibration Pulse Amplitude Threshold for IM		dB	1	fl	4 byte(s)
65	cal_pluse_apl_thres_ap Calibration Pulse Amplitude Threshold for AP		dB	1	fl	4 byte(s)
66	cal_pluse_apl_thres_wv Calibration Pulse Amplitude Threshold for WV		dB	1	fl	4 byte(s)
67	cal_pluse_apl_thres_ws Calibration Pulse Amplitude Threshold for WS		dB	1	fl	4 byte(s)
68	cal_pluse_apl_thres_gm Calibration Pulse Amplitude Threshold for GM		dB	1	fl	4 byte(s)
69	spare_4 Spare		-	1	SpareField	256 byte(s)
70	proces_gain_imp Processing gain values for IMP products.(7 values from swath IS1 to IS7)		linear	7	fl	7*4 byte(s)
71	proces_gain_ims Processing gain values for IMS products.(7 values from swath IS1 to IS7)		linear	7	fl	7*4 byte(s)
72	proces_gain_img Processing gain values for IMG products.(7 values from swath IS1 to IS7)		linear	7	fl	7*4 byte(s)
73	proces_gain_immm Processing gain values for IMM products.(7 values from swath IS1 to IS7)		dB	7	fl	7*4 byte(s)
74	proces_gain_app Processing gain values for APP products.(7 values from swath IS1 to IS7)		dB	7	fl	7*4 byte(s)
75	proces_gain_aps Processing gain values for APS products.(7 values from swath IS1 to IS7)		linear	7	fl	7*4 byte(s)
76	proces_gain_apg Processing gain values for APG products.(7 values from swath IS1 to IS7)		dB	7	fl	7*4 byte(s)
77	proces_gain_apm Processing gain values for APM products.(7 values from swath IS1 to IS7)		linear	7	fl	7*4 byte(s)
78	proces_gain_wvv Processing gain values for WV products.(7 values from swath IS1 to IS7)		linear	7	fl	7*4 byte(s)
79	proces_gain_wss Processing gain values for WSS products.(7 values from swath IS1 to IS7)		linear	5	fl	5*4 byte(s)
80	proces_gain_wsm Processing gain values for WSM products.(7 values from swath IS1 to IS7)		dB	5	fl	5*4 byte(s)
81	proces_gain_gmone Processing gain values for GM1 products.(7 values from swath IS1 to IS7)		dB	5	fl	5*4 byte(s)
82	range_look_bandw_imp Range Look Bandwidth values for IMP products.(7 values from swath IS1 to IS7)		Hz	7	fl	7*4 byte(s)
83	range_look_bandw_ims Range Look Bandwidth values for IMS products.(7 values from swath IS1 to IS7)		Hz	7	fl	7*4 byte(s)
84	range_look_bandw_img Range Look Bandwidth values for IMG products.(7 values from swath IS1 to IS7)		Hz	7	fl	7*4 byte(s)
85	range_look_bandw_immm Range Look Bandwidth values for IMM products.(7 values from swath IS1 to IS7)		Hz	7	fl	7*4 byte(s)
86	range_look_bandw_app Range Look Bandwidth values for APP products.(7 values from swath IS1 to IS7)		Hz	7	fl	7*4 byte(s)

#	Description	Units	Count	Type	Size
87	range_look_bandw_aps Range Look Bandwidth values for APS products.(7 values from swath IS1 to IS7)	Hz	7	fl	7*4 byte(s)
88	range_look_bandw_apg Range Look Bandwidth values for APG products.(7 values from swath IS1 to IS7)	Hz	7	fl	7*4 byte(s)
89	range_look_bandw_apm Range Look Bandwidth values for APM products.(7 values from swath IS1 to IS7)	Hz	7	fl	7*4 byte(s)
90	range_look_bandw_wss Range Look Bandwidth values for WSS products.(7 values from swath IS1 to IS7)	Hz	5	fl	5*4 byte(s)
91	range_look_bandw_wsm Range Look Bandwidth values for WSM products.(7 values from swath IS1 to IS7)	Hz	5	fl	5*4 byte(s)
92	range_look_bandw_gmone Range Look Bandwidth values for GM1 products.(7 values from swath IS1 to IS7)	Hz	5	fl	5*4 byte(s)
93	total_range_bandw_imp Total Range Bandwidth values for IMP products.(7 values from swath IS1 to IS7)	Hz	7	fl	7*4 byte(s)
94	total_range_bandw_ims Total Range Bandwidth values for IMS products.(7 values from swath IS1 to IS7)	Hz	7	fl	7*4 byte(s)
95	total_range_bandw_img Total Range Bandwidth values for IMG products.(7 values from swath IS1 to IS7)	Hz	7	fl	7*4 byte(s)
96	total_range_bandw_imm Total Range Bandwidth values for IMM products.(7 values from swath IS1 to IS7)	Hz	7	fl	7*4 byte(s)
97	total_range_bandw_app Total Range Bandwidth values for APP products.(7 values from swath IS1 to IS7)	Hz	7	fl	7*4 byte(s)
98	total_range_bandw_aps Total Range Bandwidth values for APS products.(7 values from swath IS1 to IS7)	Hz	7	fl	7*4 byte(s)
99	total_range_bandw_apg Total Range Bandwidth values for APG products.(7 values from swath IS1 to IS7)	Hz	7	fl	7*4 byte(s)
100	total_range_bandw_apm Total Range Bandwidth values for APM products.(7 values from swath IS1 to IS7)	Hz	7	fl	7*4 byte(s)
101	total_range_bandw_wv Total Range Bandwidth values for WV products.(7 values from swath IS1 to IS7)	Hz	7	fl	7*4 byte(s)
102	total_range_bandw_wss Total Range Bandwidth values for WSS products.(7 values from swath IS1 to IS7)	Hz	5	fl	5*4 byte(s)
103	total_range_bandw_wsm Total Range Bandwidth values for WSM products.(7 values from swath IS1 to IS7)	Hz	5	fl	5*4 byte(s)
104	total_range_bandw_gmone Total Range Bandwidth values for GM1 products.(7 values from swath IS1 to IS7)	Hz	5	fl	5*4 byte(s)
105	num_range_looks_imp Number of Range Looks for IMP products.(7 values from swath IS1 to IS7)	looks	7	ul	7*4 byte(s)
106	num_range_looks_ims Number of Range Looks for IMS products.(7 values from swath IS1 to IS7)	looks	7	ul	7*4 byte(s)
107	num_range_looks_img Number of Range Looks for IMG products.(7 values from swath IS1 to IS7)	looks	7	ul	7*4 byte(s)
108	num_range_looks_imm Number of Range Looks for IMM products.(7 values from swath IS1 to IS7)	looks	7	ul	7*4 byte(s)
109	num_range_looks_app Number of Range Looks for APP products.(7 values from swath IS1 to IS7)	looks	7	ul	7*4 byte(s)
110	num_range_looks_aps Number of Range Looks for APS products.(7 values from swath IS1 to IS7)	looks	7	ul	7*4 byte(s)
111	num_range_looks_apg Number of Range Looks for APG products.(7 values from swath IS1 to IS7)	looks	7	ul	7*4 byte(s)
112	num_range_looks_apm Number of Range Looks for APM products.(7 values from swath IS1 to IS7)	looks	7	ul	7*4 byte(s)
113	num_range_looks_wss Number of Range Looks for WSS products.(7 values from swath IS1 to IS7)	looks	5	ul	5*4 byte(s)
114	num_range_looks_wsm Number of Range Looks for WSM products.(7 values from swath IS1 to IS7)	looks	5	ul	5*4 byte(s)
115	num_range_looks_gmone Number of Range Looks for GM1 products.(7 values from swath IS1 to IS7)	looks	5	ul	5*4 byte(s)
116	azimuth_look_bandw_imp Azimuth Look Bandwidth values for IMP products.(7 values from swath IS1 to IS7)	Hz	7	fl	7*4 byte(s)
117	azimuth_look_bandw_ims Azimuth Look Bandwidth values for IMS products.(7 values from swath IS1 to IS7)	Hz	7	fl	7*4 byte(s)
118	azimuth_look_bandw_img Azimuth Look Bandwidth values for IMG products.(7 values from swath IS1 to IS7)	Hz	7	fl	7*4 byte(s)
119	azimuth_look_bandw_aps Azimuth Look Bandwidth values for APS products.(7 values from swath IS1 to IS7)	Hz	7	fl	7*4 byte(s)



#	Description	Units	Count	Type	Size
120	tot_azimuth_bandw_imp Total Azimuth Bandwidth values for IMP products.(7 values from swath IS1 to IS7)	Hz	7	fl	7*4 byte(s)
121	tot_azimuth_bandw_ims Total Azimuth Bandwidth values for IMS products.(7 values from swath IS1 to IS7)	Hz	7	fl	7*4 byte(s)
122	tot_azimuth_bandw_img Total Azimuth Bandwidth values for IMG products.(7 values from swath IS1 to IS7)	Hz	7	fl	7*4 byte(s)
123	tot_azimuth_bandw_aps Total Azimuth Bandwidth values for APS products.For APS products this value corresponds to the AP burst bandwidth.(7 values from swath IS1 to IS7)	Hz	7	fl	7*4 byte(s)
124	tot_azimuth_bandw_wv Total Azimuth Bandwidth values for WV products.(7 values from swath IS1 to IS7)	Hz	7	fl	7*4 byte(s)
125	num_azimuth_look_imp Number of Azimuth Looks for IMP products.(7 values from swath IS1 to IS7)	looks	7	ul	7*4 byte(s)
126	num_azimuth_look_ims Number of Azimuth Looks for IMS products.(7 values from swath IS1 to IS7)	looks	7	ul	7*4 byte(s)
127	num_azimuth_look_img Number of Azimuth Looks for IMG products.(7 values from swath IS1 to IS7)	looks	7	ul	7*4 byte(s)
128	num_azimuth_look_imm Number of Azimuth Looks for IMM products.(7 values from swath IS1 to IS7)	looks	7	ul	7*4 byte(s)
129	num_azimuth_look_app Number of Azimuth Looks for APP products.(7 values from swath IS1 to IS7)	looks	7	ul	7*4 byte(s)
130	num_azimuth_look_aps Number of Azimuth Looks for APS products.(7 values from swath IS1 to IS7)	looks	7	ul	7*4 byte(s)
131	num_azimuth_look_apg Number of Azimuth Looks for APG products.(7 values from swath IS1 to IS7)	looks	7	ul	7*4 byte(s)
132	num_azimuth_look_apm Number of Azimuth Looks for APM products.(7 values from swath IS1 to IS7)	looks	7	ul	7*4 byte(s)
133	num_azimuth_look_wss Number of Azimuth Looks for WSS products.	looks	1	ul	4 byte(s)
134	num_azimuth_look_wsm Number of Azimuth Looks for WSM products.	looks	1	ul	4 byte(s)
135	num_azimuth_look_gmone Number of Azimuth Looks for GM1 products.	looks	1	ul	4 byte(s)
136	descalloping_flag_imm Descalloping flag for IMM products. 1 = descalloping correction applied 0 = descalloping correction NOT applied	-	1	uc	1 byte(s)
137	descalloping_flag_app Descalloping flag for APP products. 1 = descalloping correction applied 0 = descalloping correction NOT applied	-	1	uc	1 byte(s)
138	descalloping_flag_apg Descalloping flag for APG products. 1 = descalloping correction applied 0 = descalloping correction NOT applied	-	1	uc	1 byte(s)
139	descalloping_flag_apm Descalloping flag for APM products. 1 = descalloping correction applied 0 = descalloping correction NOT applied	-	1	uc	1 byte(s)
140	spare_5 Spare	-	1	SpareField	1 byte(s)
141	descalloping_flag_wsm Descalloping flag for WSM products. 1 = descalloping correction applied 0 = descalloping correction NOT applied	-	1	uc	1 byte(s)
142	descalloping_flag_gmone Descalloping flag for GM1 products. 1 = descalloping correction applied 0 = descalloping correction NOT applied	-	1	uc	1 byte(s)
143	const_snr_filter_flag_imm Constant SNR filter flag for IMM products. 1 = use constant SNR descalloping 0 = use constant ENL	-	1	uc	1 byte(s)
144	const_snr_filter_flag_app Constant SNR filter flag for APP products. 1 = use constant SNR descalloping 0 = use constant ENL	-	1	uc	1 byte(s)
145	const_snr_filter_flag_apg Constant SNR filter flag for APG products. 1 = use constant SNR descalloping 0 = use constant ENL	-	1	uc	1 byte(s)
146	const_snr_filter_flag_apm Constant SNR filter flag for APM products. 1 = use constant SNR descalloping 0 = use constant ENL	-	1	uc	1 byte(s)
147	spare_6 Spare	-	1	SpareField	1 byte(s)
148	const_snr_filter_flag_wsm Constant SNR filter flag for WSM products. 1 = use constant SNR descalloping 0 = use constant ENL	-	1	uc	1 byte(s)
149	const_snr_filter_flag_gmone	-	1	uc	1 byte(s)



#	Description		Units	Count	Type	Size
	Constant SNR filter flag for GM1 products, 1 = use constant SNR desclopping 0 = use constant ENL					
150	azimuth_win_type_imp Azimuth Window Type and coefficients for IMP products		-	1	azimuth_win_type_impsStruct	11.0 byte(s)
	a	window_type Window Type: HAMMING or KAISER0 or NONE000	-	1	AsciiString	7 byte(s)
	b	window_coeff Window Coefficients	-	1	fl	4 byte(s)
151	azimuth_win_type_ims Azimuth Window Type and coefficients for IMS products		-	1	azimuth_win_type_imsStruct	11.0 byte(s)
	a	window_type Window Type: HAMMING or KAISER0 or NONE000	-	1	AsciiString	7 byte(s)
	b	window_coeff Window Coefficients	-	1	fl	4 byte(s)
152	azimuth_win_type_img Azimuth Window Type and coefficients for IMG products		-	1	azimuth_win_type_imgStruct	11.0 byte(s)
	a	window_type Window Type: HAMMING or KAISER0 or NONE000	-	1	AsciiString	7 byte(s)
	b	window_coeff Window Coefficients	-	1	fl	4 byte(s)
153	azimuth_win_type_imm Azimuth Window Type and coefficients for IMM products		-	1	azimuth_win_type_immStruct	11.0 byte(s)
	a	window_type Window Type: HAMMING or KAISER0 or NONE000	-	1	AsciiString	7 byte(s)
	b	window_coeff Window Coefficients	-	1	fl	4 byte(s)
154	azimuth_win_type_app Azimuth Window Type and coefficients for APP products		-	1	azimuth_win_type_appStruct	11.0 byte(s)
	a	window_type Window Type: HAMMING or KAISER0 or NONE000	-	1	AsciiString	7 byte(s)
	b	window_coeff Window Coefficients	-	1	fl	4 byte(s)
155	azimuth_win_type_aps Azimuth Window Type and coefficients for APS products		-	1	azimuth_win_type_apsStruct	11.0 byte(s)
	a	window_type Window Type: HAMMING or KAISER0 or NONE000	-	1	AsciiString	7 byte(s)
	b	window_coeff Window Coefficients	-	1	fl	4 byte(s)
156	azimuth_win_type_apg Azimuth Window Type and coefficients for APG products		-	1	azimuth_win_type_apgStruct	11.0 byte(s)
	a	window_type Window Type: HAMMING or KAISER0 or NONE000	-	1	AsciiString	7 byte(s)
	b	window_coeff Window Coefficients	-	1	fl	4 byte(s)

#	Description			Units	Count	Type	Size
157	azimuth_win_type_apm Azimuth Window Type and coefficients for APM products			-	1	azimuth_win_type_apmStruct	11.0 byte(s)
	a	window_type Window Type: HAMMING or KAISER0 or NONE000	-	1	AsciiString	7 byte(s)	
	b	window_coeff Window Coefficients	-	1	fl	4 byte(s)	
158	azimuth_win_type_wv Azimuth Window Type and coefficients for WV products			-	1	azimuth_win_type_wvStruct	11.0 byte(s)
	a	window_type Window Type: HAMMING or KAISER0 or NONE000	-	1	AsciiString	7 byte(s)	
	b	window_coeff Window Coefficients	-	1	fl	4 byte(s)	
159	azimuth_win_type_wss Azimuth Window Type and coefficients for ASS products			-	1	azimuth_win_type_wssStruct	11.0 byte(s)
	a	window_type Window Type: HAMMING or KAISER0 or NONE000	-	1	AsciiString	7 byte(s)	
	b	window_coeff Window Coefficients	-	1	fl	4 byte(s)	
160	azimuth_win_type_wsm Azimuth Window Type and coefficients for ASM products			-	1	azimuth_win_type_wsmStruct	11.0 byte(s)
	a	window_type Window Type: HAMMING or KAISER0 or NONE000	-	1	AsciiString	7 byte(s)	
	b	window_coeff Window Coefficients	-	1	fl	4 byte(s)	
161	azimuth_win_type_gmone Azimuth Window Type and coefficients for GM1 products			-	1	azimuth_win_type_gmoneStruct	11.0 byte(s)
	a	window_type Window Type: HAMMING or KAISER0 or NONE000	-	1	AsciiString	7 byte(s)	
	b	window_coeff Window Coefficients	-	1	fl	4 byte(s)	
162	range_win_type_imp Range Window Type and coefficients for IMP products			-	1	range_win_type_impStruct	11.0 byte(s)
	a	window_type Window Type: HAMMING or KAISER0 or NONE000	-	1	AsciiString	7 byte(s)	
	b	window_coeff Window Coefficients	-	1	fl	4 byte(s)	
163	range_win_type_ims Range Window Type and coefficients for IMS products			-	1	range_win_type_imsStruct	11.0 byte(s)
	a	window_type Window Type: HAMMING or KAISER0 or NONE000	-	1	AsciiString	7 byte(s)	
	b	window_coeff Window Coefficients	-	1	fl	4 byte(s)	

#	Description			Units	Count	Type	Size
164	range_win_type_img Range Window Type and coefficients for IMG products			-	1	range_win_type_imgStruct	11.0 byte(s)
	a	window_type Window Type: HAMMING or KAISER0 or NONE000	-	1	AsciiString	7 byte(s)	
	b	window_coeff Window Coefficients	-	1	fl	4 byte(s)	
165	range_win_type_imm Range Window Type and coefficients for IMM products			-	1	range_win_type_immStruct	11.0 byte(s)
	a	window_type Window Type: HAMMING or KAISER0 or NONE000	-	1	AsciiString	7 byte(s)	
	b	window_coeff Window Coefficients	-	1	fl	4 byte(s)	
166	range_win_type_app Range Window Type and coefficients for APP products			-	1	range_win_type_appStruct	11.0 byte(s)
	a	window_type Window Type: HAMMING or KAISER0 or NONE000	-	1	AsciiString	7 byte(s)	
	b	window_coeff Window Coefficients	-	1	fl	4 byte(s)	
167	range_win_type_aps Range Window Type and coefficients for APS products			-	1	range_win_type_apsStruct	11.0 byte(s)
	a	window_type Window Type: HAMMING or KAISER0 or NONE000	-	1	AsciiString	7 byte(s)	
	b	window_coeff Window Coefficients	-	1	fl	4 byte(s)	
168	range_win_type_apg Range Window Type and coefficients for APG products			-	1	range_win_type_apgStruct	11.0 byte(s)
	a	window_type Window Type: HAMMING or KAISER0 or NONE000	-	1	AsciiString	7 byte(s)	
	b	window_coeff Window Coefficients	-	1	fl	4 byte(s)	
169	range_win_type_apm Range Window Type and coefficients for APM products			-	1	range_win_type_apmStruct	11.0 byte(s)
	a	window_type Window Type: HAMMING or KAISER0 or NONE000	-	1	AsciiString	7 byte(s)	
	b	window_coeff Window Coefficients	-	1	fl	4 byte(s)	
170	range_win_type_wv Range Window Type and coefficients for WV products			-	1	range_win_type_wvStruct	11.0 byte(s)
	a	window_type Window Type: HAMMING or KAISER0 or NONE000	-	1	AsciiString	7 byte(s)	
	b	window_coeff Window Coefficients	-	1	fl	4 byte(s)	

#	Description		Units	Count	Type	Size
171	range_win_type_wss Range Window Type and coefficients for WSS products		-	1	range_win_type_wssStruct	11.0 byte(s)
	a	window_type Window Type: HAMMING or KAISER0 or NONE000	-	1	AsciiString	7 byte(s)
	b	window_coeff Window Coefficients	-	1	fl	4 byte(s)
172	range_win_type_wsm Range Window Type and coefficients for WSM products		-	1	range_win_type_wsmStruct	11.0 byte(s)
	a	window_type Window Type: HAMMING or KAISER0 or NONE000	-	1	AsciiString	7 byte(s)
	b	window_coeff Window Coefficients	-	1	fl	4 byte(s)
173	range_win_type_gm_one Range Window Type and coefficients for GM1 products		-	1	range_win_type_gm_oneStruct	11.0 byte(s)
	a	window_type Window Type: HAMMING or KAISER0 or NONE000	-	1	AsciiString	7 byte(s)
	b	window_coeff Window Coefficients	-	1	fl	4 byte(s)
174	thres_terr_height_std_dev_imp Threshold for terrain height standard deviation for IMP products		m	1	us	2 byte(s)
175	thres_terr_height_std_dev_ims Threshold for terrain height standard deviation for IMS products		m	1	us	2 byte(s)
176	thres_terr_height_std_dev_img Threshold for terrain height standard deviation for IMG products		m	1	us	2 byte(s)
177	thres_terr_height_std_dev_imm Threshold for terrain height standard deviation for IMM products		m	1	us	2 byte(s)
178	thres_terr_height_std_dev_app Threshold for terrain height standard deviation for APP products		m	1	us	2 byte(s)
179	thres_terr_height_std_dev_aps Threshold for terrain height standard deviation for APS products		m	1	us	2 byte(s)
180	thres_terr_height_std_dev_apg Threshold for terrain height standard deviation for APG products		m	1	us	2 byte(s)
181	thres_terr_height_std_dev_apm Threshold for terrain height standard deviation for APM products		m	1	us	2 byte(s)
182	thres_terr_height_std_dev_wss Threshold for terrain height standard deviation for WSS products		m	1	us	2 byte(s)
183	thres_terr_height_std_dev_wsm Threshold for terrain height standard deviation for WSM products		m	1	us	2 byte(s)
184	thres_terr_height_std_dev_gmone Threshold for terrain height standard deviation for GM1 products		m	1	us	2 byte(s)
185	spare_7 Spare		-	1	SpareField	1002 byte(s)
186	dop_cen_est_flag_imp Doppler Centriod Estimation flag for IMP products 1=yes 0=no		-	1	uc	1 byte(s)
187	dop_cen_est_flag_ims Doppler Centriod Estimation flag for IMS products 1=yes 0=no		-	1	uc	1 byte(s)
188	dop_cen_est_flag_img Doppler Centriod Estimation flag for IMG products 1=yes 0=no		-	1	uc	1 byte(s)
189	dop_cen_est_flag_imm Doppler Centriod Estimation flag for IMM products 1=yes 0=no		-	1	uc	1 byte(s)
190	dop_cen_est_flag_app Doppler Centriod Estimation flag for APP products 1=yes 0=no		-	1	uc	1 byte(s)
191	dop_cen_est_flag_aps Doppler Centriod Estimation flag for APS products 1=yes 0=no		-	1	uc	1 byte(s)
192	dop_cen_est_flag_apg Doppler Centriod Estimation flag for APG products 1=yes 0=no		-	1	uc	1 byte(s)
193	dop_cen_est_flag_apm Doppler Centriod Estimation flag for APM products 1=yes 0=no		-	1	uc	1 byte(s)

#	Description	Units	Count	Type	Size
194	dop_cen_est_flag_wv Doppler Centriod Estimation flag for WV products 1=yes 0=no	-	1	uc	1 byte(s)
195	dop_cen_est_flag_wss Doppler Centriod Estimation flag for WSS products 1=yes 0=no	-	1	uc	1 byte(s)
196	dop_cen_est_flag_wsm Doppler Centriod Estimation flag for WSM products 1=yes 0=no	-	1	uc	1 byte(s)
197	dop_cen_est_flag_gmone Doppler Centriod Estimation flag for GM1 products 1=yes 0=no	-	1	uc	1 byte(s)
198	per_dop_amb_est_flag_imp Perform Doppler Ambiguity Estimation flag for IMP products 1=yes 0=no	-	1	uc	1 byte(s)
199	per_dop_amb_est_flag_ims Perform Doppler Ambiguity Estimation flag for IMS products 1=yes 0=no	-	1	uc	1 byte(s)
200	per_dop_amb_est_flag_img Perform Doppler Ambiguity Estimation flag for IMG products 1=yes 0=no	-	1	uc	1 byte(s)
201	per_dop_amb_est_flag_immm Perform Doppler Ambiguity Estimation flag for IMM products 1=yes 0=no	-	1	uc	1 byte(s)
202	per_dop_amb_est_flag_app Perform Doppler Ambiguity Estimation flag for APP products 1=yes 0=no	-	1	uc	1 byte(s)
203	per_dop_amb_est_flag_aps Perform Doppler Ambiguity Estimation flag for APS products 1=yes 0=no	-	1	uc	1 byte(s)
204	per_dop_amb_est_flag_apg Perform Doppler Ambiguity Estimation flag for APG products 1=yes 0=no	-	1	uc	1 byte(s)
205	per_dop_amb_est_flag_apm Perform Doppler Ambiguity Estimation flag for APM products 1=yes 0=no	-	1	uc	1 byte(s)
206	per_dop_amb_est_flag_wv Perform Doppler Ambiguity Estimation flag for WV products 1=yes 0=no	-	1	uc	1 byte(s)
207	per_dop_amb_est_flag_wss Perform Doppler Ambiguity Estimation flag for WSS products 1=yes 0=no	-	1	uc	1 byte(s)
208	per_dop_amb_est_flag_wsm Perform Doppler Ambiguity Estimation flag for WSM products 1=yes 0=no	-	1	uc	1 byte(s)
209	per_dop_amb_est_flag_gmone Perform Doppler Ambiguity Estimation flag for GM1 products 1=yes 0=no	-	1	uc	1 byte(s)
210	dop_refine_flag_app Doppler Refinement flag for APP products 1=yes 0=no	-	1	uc	1 byte(s)
211	dop_refine_flag_aps Doppler Refinement flag for APS products 1=yes 0=no	-	1	uc	1 byte(s)
212	dop_refine_flag_apg Doppler Refinement flag for APG products 1=yes 0=no	-	1	uc	1 byte(s)
213	dop_refine_flag_apm Doppler Refinement flag for APM products 1=yes 0=no	-	1	uc	1 byte(s)
214	dop_refine_flag_wss Doppler Refinement flag for APP products 1=yes 0=no	-	1	uc	1 byte(s)
215	dop_refine_flag_wsm Doppler Refinement flag for WSM products 1=yes 0=no	-	1	uc	1 byte(s)
216	per_dop_grid_estm_flag_imp Perform Doppler Grid Estimation flag for IMP products 1=yes 0=no	-	1	uc	1 byte(s)
217	per_dop_grid_estm_flag_ims Perform Doppler Grid Estimation flag for IMS products 1=yes 0=no	-	1	uc	1 byte(s)
218	per_dop_grid_estm_flag_immm Perform Doppler Grid Estimation flag for IMM products 1=yes 0=no	-	1	uc	1 byte(s)
219	per_dop_grid_estm_flag_app Perform Doppler Grid Estimation flag for APP products 1=yes 0=no	-	1	uc	1 byte(s)
220	per_dop_grid_estm_flag_aps Perform Doppler Grid Estimation flag for APS products 1=yes 0=no	-	1	uc	1 byte(s)
221	per_dop_grid_estm_flag_apm Perform Doppler Grid Estimation flag for APM products 1=yes 0=no	-	1	uc	1 byte(s)
222	per_dop_grid_estm_flag_wss Perform Doppler Grid Estimation flag for WSS products 1=yes 0=no	-	1	uc	1 byte(s)
223	per_dop_grid_estm_flag_wsm Perform Doppler Grid Estimation flag for WSM products 1=yes 0=no	-	1	uc	1 byte(s)
224	per_dop_grid_estm_flag_gmone Perform Doppler Grid Estimation flag for GM1 products 1=yes 0=no	-	1	uc	1 byte(s)
225	spare_8 Spare	-	1	SpareField	55 byte(s)

Record Length : 4096

DS\_NAME : Contains ASAR processor configuration data

Format Version 114.0

Mathematical notation for the various fields within the ASA\_CON\_AX\_GADS:

Field# 34 - Look image statistics confidence parameter thresholds (minimum and maximum) mathematical expression:  $[d_{IS}^{\min}, d_{IS}^{\max}]$

Field# 35 - Inter-look confidence statistics confidence parameter threshold mathematical expression:  $|d_{IL}|$

Field# 36 - Azimuth cut-off convergence measure threshold mathematical expression:  $|\Delta\lambda_c^{\lim}|$

Field# 37 - Azimuth cut-off Iteration count overflow threshold mathematical expression:  $|N_{iter}|$

Field# 38 - Phase information confidence measure threshold for the spectral peak mathematical expression:  $|d_{PI}|$

Field# 39 - Phase information confidence measure threshold for the cross covariance peak offset mathematical expression:  $|d_{CI}|$

### 6.6.3 ASAR instrument characterization data

This Global Auxiliary Data Set (GADS) is the only [Data Set Descriptor \(DSD\)](#) associated with the [Instrument Characterisation Auxiliary File](#). The format of this GADS is given below:

Table 6.39 ASAR instrument characterization data

## Contains ASAR instrument characterization data

#	Description	Units	Count	Type	Size
Data Record					
0	dsr_time Time of creation	MJD	1	mjd	12 byte(s)
1	dsr_length	bytes	1	ul	4 byte(s)

#	Description		Units	Count	Type	Size
	Length of this DSR in bytes					
2	radar_freq Radar Frequency		Hz	1	fl	4 byte(s)
3	samp_rate Radar Sampling Rate		Hz	1	fl	4 byte(s)
4	offset_freq Offset frequency for wave mode calibration pulses		Hz	1	fl	4 byte(s)
5	cal_pulse_im0_tx_h_1 Image mode transmit H polarisation calibration data for pulse 1, swath IS0.		-	1	cal_pulse_im0_tx_h_1Struct	256.0 byte(s)
	a	nom_amplitude Nominal amplitude (ax,n,nom) for antenna row 1 to antenna row 32 (where x is the pulse number)	LSB	32	fl	32*4 byte(s)
	b	nom_phase Nominal value of phase (fx,n,nom) for antenna row 1 to antenna row 32 (where x is the pulse number)	deg	32	fl	32*4 byte(s)
6	cal_pulse_im0_tx_v_1 Image mode transmit V polarisation calibration data for pulse 1, swath IS0.		-	1	cal_pulse_im0_tx_v_1Struct	256.0 byte(s)
	a	nom_amplitude Nominal amplitude (ax,n,nom) for antenna row 1 to antenna row 32 (where x is the pulse number)	LSB	32	fl	32*4 byte(s)
	b	nom_phase Nominal value of phase (fx,n,nom) for antenna row 1 to antenna row 32 (where x is the pulse number)	deg	32	fl	32*4 byte(s)
7	cal_pulse_im0_tx_h_1a Image mode transmit H polarisation calibration data for pulse 1A, swath IS0.		-	1	cal_pulse_im0_tx_h_1aStruct	256.0 byte(s)
	a	nom_amplitude Nominal amplitude (ax,n,nom) for antenna row 1 to antenna row 32 (where x is the pulse number)	LSB	32	fl	32*4 byte(s)
	b	nom_phase Nominal value of phase (fx,n,nom) for antenna row 1 to antenna row 32 (where x is the pulse number)	deg	32	fl	32*4 byte(s)
8	cal_pulse_im0_tx_v_1a Image mode transmit V polarisation calibration data for pulse 1A, swath IS0.		-	1	cal_pulse_im0_tx_v_1aStruct	256.0 byte(s)
	a	nom_amplitude Nominal amplitude (ax,n,nom) for antenna row 1 to antenna row 32 (where x is the pulse number)	LSB	32	fl	32*4 byte(s)
	b	nom_phase Nominal value of phase (fx,n,nom) for antenna row 1 to antenna row 32 (where x is the pulse number)	deg	32	fl	32*4 byte(s)
9	cal_pulse_im0_rx_h_2 Image mode receive H polarisation calibration data for pulse 2, swath IS0.		-	1	cal_pulse_im0_rx_h_2Struct	256.0 byte(s)
	a	nom_amplitude Nominal amplitude (ax,n,nom) for antenna	LSB	32	fl	32*4 byte(s)



#	Description			Units	Count	Type	Size
	row 1 to antenna row 32 (where x is the pulse number)						
	b	nom_phase Nominal value of phase (fx,n,nom) for antenna row 1 to antenna row 32 (where x is the pulse number)	deg	32	fl		32*4 byte(s)
10	cal_pulse_im0_rx_v_2 Image mode receive V polarisation calibration data for pulse 2, swath IS0.			-	1	cal_pulse_im0_rx_v_2Struct	256.0 byte(s)
	a	nom_amplitude Nominal amplitude (ax,n,nom) for antenna row 1 to antenna row 32 (where x is the pulse number)	LSB	32	fl		32*4 byte(s)
	b	nom_phase Nominal value of phase (fx,n,nom) for antenna row 1 to antenna row 32 (where x is the pulse number)	deg	32	fl		32*4 byte(s)
11	cal_pulse_im0_h_3 Image mode H polarisation calibration data for pulse 3, swaths IS0.			-	1	cal_pulse_im0_h_3Struct	256.0 byte(s)
a	nom_amplitude Nominal amplitude (ax,n,nom) for antenna row 1 to antenna row 32 (where x is the pulse number)	LSB	32	fl		32*4 byte(s)	
	b	nom_phase Nominal value of phase (fx,n,nom) for antenna row 1 to antenna row 32 (where x is the pulse number)	deg	32	fl		32*4 byte(s)
12	cal_pulse_im0_v_3 Image mode V polarisation calibration data for pulse 3, swaths IS0.			-	1	cal_pulse_im0_v_3Struct	256.0 byte(s)
a	nom_amplitude Nominal amplitude (ax,n,nom) for antenna row 1 to antenna row 32 (where x is the pulse number)	LSB	32	fl		32*4 byte(s)	
b	nom_phase Nominal value of phase (fx,n,nom) for antenna row 1 to antenna row 32 (where x is the pulse number)	deg	32	fl		32*4 byte(s)	
13	cal_pulse_im_tx_h_1 Image mode transmit H polarisation calibration data for pulse 1, swaths IS1 to IS7.			-	7	cal_pulse_im_tx_h_1Struct	7*256.0 byte(s)
	a	nom_amplitude Nominal amplitude (ax,n,nom) for antenna row 1 to antenna row 32 (where x is the pulse number)	LSB	32	fl		32*4 byte(s)
	b	nom_phase Nominal value of phase (fx,n,nom) for antenna row 1 to antenna row 32 (where x is the pulse number)	deg	32	fl		32*4 byte(s)
14	cal_pulse_im_tx_v_1 Image mode transmit V polarisation calibration data for pulse 1, swaths IS1 to IS7.			-	7	cal_pulse_im_tx_v_1Struct	7*256.0 byte(s)



#	Description			Units	Count	Type	Size
	a	nom_amplitude Nominal amplitude (ax,n,nom) for antenna row 1 to antenna row 32 (where x is the pulse number)	LSB	32	fl		32*4 byte(s)
	b	nom_phase Nominal value of phase (fx,n,nom) for antenna row 1 to antenna row 32 (where x is the pulse number)	deg	32	fl		32*4 byte(s)
15	cal_pulse_im_tx_h_1a Image mode transmit H polarisation calibration data for pulse 1A, swaths IS1 to IS7.		-	7	cal_pulse_im_tx_h_1aStruct		7*256.0 byte(s)
	a	nom_amplitude Nominal amplitude (ax,n,nom) for antenna row 1 to antenna row 32 (where x is the pulse number)	LSB	32	fl		32*4 byte(s)
	b	nom_phase Nominal value of phase (fx,n,nom) for antenna row 1 to antenna row 32 (where x is the pulse number)	deg	32	fl		32*4 byte(s)
16	cal_pulse_im_tx_v_1a Image mode transmit V polarisation calibration data for pulse 1A, swaths IS1 to IS7.		-	7	cal_pulse_im_tx_v_1aStruct		7*256.0 byte(s)
	a	nom_amplitude Nominal amplitude (ax,n,nom) for antenna row 1 to antenna row 32 (where x is the pulse number)	LSB	32	fl		32*4 byte(s)
	b	nom_phase Nominal value of phase (fx,n,nom) for antenna row 1 to antenna row 32 (where x is the pulse number)	deg	32	fl		32*4 byte(s)
17	cal_pulse_im_rx_h_2 Image mode receive H polarisation calibration data for pulse 2, swaths IS1 to IS7.		-	7	cal_pulse_im_rx_h_2Struct		7*256.0 byte(s)
	a	nom_amplitude Nominal amplitude (ax,n,nom) for antenna row 1 to antenna row 32 (where x is the pulse number)	LSB	32	fl		32*4 byte(s)
	b	nom_phase Nominal value of phase (fx,n,nom) for antenna row 1 to antenna row 32 (where x is the pulse number)	deg	32	fl		32*4 byte(s)
18	cal_pulse_im_rx_v_2 Image mode receive V polarisation calibration data for pulse 2, swaths IS1 to IS7.		-	7	cal_pulse_im_rx_v_2Struct		7*256.0 byte(s)
	a	nom_amplitude Nominal amplitude (ax,n,nom) for antenna row 1 to antenna row 32 (where x is the pulse number)	LSB	32	fl		32*4 byte(s)
	b	nom_phase Nominal value of phase (fx,n,nom) for antenna row 1 to antenna row 32 (where x is the pulse number)	deg	32	fl		32*4 byte(s)

#	Description			Units	Count	Type	Size
19	cal_pulse_im_h_3 Image mode H polarisation calibration data for pulse 3, swaths IS1 to IS7.			-	7	cal_pulse_im_h_3Struct	7*256.0 byte(s)
	a	nom_amplitude Nominal amplitude (ax,n,nom) for antenna row 1 to antenna row 32 (where x is the pulse number)	LSB	32	fl		32*4 byte(s)
	b	nom_phase Nominal value of phase (fx,n,nom) for antenna row 1 to antenna row 32 (where x is the pulse number)	deg	32	fl		32*4 byte(s)
20	cal_pulse_im_v_3 Image mode V polarisation calibration data for pulse 3, swaths IS1 to IS7.			-	7	cal_pulse_im_v_3Struct	7*256.0 byte(s)
	a	nom_amplitude Nominal amplitude (ax,n,nom) for antenna row 1 to antenna row 32 (where x is the pulse number)	LSB	32	fl		32*4 byte(s)
	b	nom_phase Nominal value of phase (fx,n,nom) for antenna row 1 to antenna row 32 (where x is the pulse number)	deg	32	fl		32*4 byte(s)
21	cal_pulse_ap_tx_h_1 AP mode transmit H polarisation calibration data for pulse 1, swaths IS1 to IS7.			-	7	cal_pulse_ap_tx_h_1Struct	7*256.0 byte(s)
	a	nom_amplitude Nominal amplitude (ax,n,nom) for antenna row 1 to antenna row 32 (where x is the pulse number)	LSB	32	fl		32*4 byte(s)
	b	nom_phase Nominal value of phase (fx,n,nom) for antenna row 1 to antenna row 32 (where x is the pulse number)	deg	32	fl		32*4 byte(s)
22	cal_pulse_ap_tx_v_1 AP mode transmit V polarisation calibration data for pulse 1, swaths IS1 to IS7.			-	7	cal_pulse_ap_tx_v_1Struct	7*256.0 byte(s)
	a	nom_amplitude Nominal amplitude (ax,n,nom) for antenna row 1 to antenna row 32 (where x is the pulse number)	LSB	32	fl		32*4 byte(s)
	b	nom_phase Nominal value of phase (fx,n,nom) for antenna row 1 to antenna row 32 (where x is the pulse number)	deg	32	fl		32*4 byte(s)
23	cal_pulse_ap_tx_h_1a AP mode transmit H polarisation calibration data for pulse 1A, swaths IS1 to IS7.			-	7	cal_pulse_ap_tx_h_1aStruct	7*256.0 byte(s)
	a	nom_amplitude Nominal amplitude (ax,n,nom) for antenna row 1 to antenna row 32 (where x is the pulse number)	LSB	32	fl		32*4 byte(s)
	b	nom_phase Nominal value of phase (fx,n,nom) for antenna row 1 to antenna row 32 (where x is the pulse number)	deg	32	fl		32*4 byte(s)



#	Description			Units	Count	Type	Size
24	cal_pulse_ap_tx_v_1a AP mode transmit V polarisation calibration data for pulse 1A, swaths IS1 to IS7.			-	7	cal_pulse_ap_tx_v_1aStruct	7*256.0 byte(s)
	a	nom_amplitude Nominal amplitude (ax,n,nom) for antenna row 1 to antenna row 32 (where x is the pulse number)	LSB	32	fl		32*4 byte(s)
	b	nom_phase Nominal value of phase (fx,n,nom) for antenna row 1 to antenna row 32 (where x is the pulse number)	deg	32	fl		32*4 byte(s)
25	cal_pulse_ap_rx_h_2 AP mode receive H polarisation calibration data for pulse 2, swaths IS1 to IS7.			-	7	cal_pulse_ap_rx_h_2Struct	7*256.0 byte(s)
	a	nom_amplitude Nominal amplitude (ax,n,nom) for antenna row 1 to antenna row 32 (where x is the pulse number)	LSB	32	fl		32*4 byte(s)
	b	nom_phase Nominal value of phase (fx,n,nom) for antenna row 1 to antenna row 32 (where x is the pulse number)	deg	32	fl		32*4 byte(s)
26	cal_pulse_ap_rx_v_2 AP mode receive V polarisation calibration data for pulse 2, swaths IS1 to IS7.			-	7	cal_pulse_ap_rx_v_2Struct	7*256.0 byte(s)
	a	nom_amplitude Nominal amplitude (ax,n,nom) for antenna row 1 to antenna row 32 (where x is the pulse number)	LSB	32	fl		32*4 byte(s)
	b	nom_phase Nominal value of phase (fx,n,nom) for antenna row 1 to antenna row 32 (where x is the pulse number)	deg	32	fl		32*4 byte(s)
27	cal_pulse_ap_h_3 AP mode H polarisation calibration data for pulse 3, swaths IS1 to IS7.			-	7	cal_pulse_ap_h_3Struct	7*256.0 byte(s)
	a	nom_amplitude Nominal amplitude (ax,n,nom) for antenna row 1 to antenna row 32 (where x is the pulse number)	LSB	32	fl		32*4 byte(s)
	b	nom_phase Nominal value of phase (fx,n,nom) for antenna row 1 to antenna row 32 (where x is the pulse number)	deg	32	fl		32*4 byte(s)
28	cal_pulse_ap_v_3 AP mode V polarisation calibration data for pulse 3, swaths IS1 to IS7.			-	7	cal_pulse_ap_v_3Struct	7*256.0 byte(s)
	a	nom_amplitude Nominal amplitude (ax,n,nom) for antenna row 1 to antenna row 32 (where x is the pulse number)	LSB	32	fl		32*4 byte(s)
	b	nom_phase Nominal value of phase (fx,n,nom) for antenna row 1 to antenna row 32 (where x is the pulse number)	deg	32	fl		32*4 byte(s)

#	Description			Units	Count	Type	Size
29	cal_pulse_wv_tx_h_1 WV mode transmit H polarisation calibration data for pulse 1, swaths IS1 to IS7.			-	7	cal_pulse_wv_tx_h_1Struct	7*256.0 byte(s)
	a	nom_amplitude Nominal amplitude (ax,n,nom) for antenna row 1 to antenna row 32 (where x is the pulse number)	LSB	32	fl		32*4 byte(s)
	b	nom_phase Nominal value of phase (fx,n,nom) for antenna row 1 to antenna row 32 (where x is the pulse number)	deg	32	fl		32*4 byte(s)
30	cal_pulse_wv_tx_v_1 WV mode transmit V polarisation calibration data for pulse 1, swaths IS1 to IS7.			-	7	cal_pulse_wv_tx_v_1Struct	7*256.0 byte(s)
	a	nom_amplitude Nominal amplitude (ax,n,nom) for antenna row 1 to antenna row 32 (where x is the pulse number)	LSB	32	fl		32*4 byte(s)
	b	nom_phase Nominal value of phase (fx,n,nom) for antenna row 1 to antenna row 32 (where x is the pulse number)	deg	32	fl		32*4 byte(s)
31	cal_pulse_wv_tx_h_1a WV mode transmit H polarisation calibration data for pulse 1A, swaths IS1 to IS7.			-	7	cal_pulse_wv_tx_h_1aStruct	7*256.0 byte(s)
	a	nom_amplitude Nominal amplitude (ax,n,nom) for antenna row 1 to antenna row 32 (where x is the pulse number)	LSB	32	fl		32*4 byte(s)
	b	nom_phase Nominal value of phase (fx,n,nom) for antenna row 1 to antenna row 32 (where x is the pulse number)	deg	32	fl		32*4 byte(s)
32	cal_pulse_wv_tx_v_1a WV mode transmit V polarisation calibration data for pulse 1A, swaths IS1 to IS7.			-	7	cal_pulse_wv_tx_v_1aStruct	7*256.0 byte(s)
	a	nom_amplitude Nominal amplitude (ax,n,nom) for antenna row 1 to antenna row 32 (where x is the pulse number)	LSB	32	fl		32*4 byte(s)
	b	nom_phase Nominal value of phase (fx,n,nom) for antenna row 1 to antenna row 32 (where x is the pulse number)	deg	32	fl		32*4 byte(s)
33	cal_pulse_wv_rx_h_2 WV mode receive H polarisation calibration data for pulse 2, swaths IS1 to IS7.			-	7	cal_pulse_wv_rx_h_2Struct	7*256.0 byte(s)
	a	nom_amplitude Nominal amplitude (ax,n,nom) for antenna row 1 to antenna row 32 (where x is the pulse number)	LSB	32	fl		32*4 byte(s)
	b	nom_phase Nominal value of phase (fx,n,nom) for antenna row 1 to antenna row 32 (where x is the pulse number)	deg	32	fl		32*4 byte(s)



#	Description			Units	Count	Type	Size
34	cal_pulse_wv_rx_v_2 WV mode receive V polarisation calibration data for pulse 2, swaths IS1 to IS7.			-	7	cal_pulse_wv_rx_v_2Struct	7*256.0 byte(s)
	a	nom_amplitude Nominal amplitude (ax,n,nom) for antenna row 1 to antenna row 32 (where x is the pulse number)	LSB	32	fl		32*4 byte(s)
	b	nom_phase Nominal value of phase (fx,n,nom) for antenna row 1 to antenna row 32 (where x is the pulse number)	deg	32	fl		32*4 byte(s)
35	cal_pulse_wv_h_3 WV mode H polarisation calibration data for pulse 3, swaths IS1 to IS7.			-	7	cal_pulse_wv_h_3Struct	7*256.0 byte(s)
	a	nom_amplitude Nominal amplitude (ax,n,nom) for antenna row 1 to antenna row 32 (where x is the pulse number)	LSB	32	fl		32*4 byte(s)
	b	nom_phase Nominal value of phase (fx,n,nom) for antenna row 1 to antenna row 32 (where x is the pulse number)	deg	32	fl		32*4 byte(s)
36	cal_pulse_wv_v_3 WV mode V polarisation calibration data for pulse 3, swaths IS1 to IS7.			-	7	cal_pulse_wv_v_3Struct	7*256.0 byte(s)
	a	nom_amplitude Nominal amplitude (ax,n,nom) for antenna row 1 to antenna row 32 (where x is the pulse number)	LSB	32	fl		32*4 byte(s)
	b	nom_phase Nominal value of phase (fx,n,nom) for antenna row 1 to antenna row 32 (where x is the pulse number)	deg	32	fl		32*4 byte(s)
37	cal_pulse_ws_tx_h_1 WS mode transmit H polarisation calibration data for pulse 1, swaths SS1 to SS5.			-	5	cal_pulse_ws_tx_h_1Struct	5*256.0 byte(s)
	a	nom_amplitude Nominal amplitude (ax,n,nom) for antenna row 1 to antenna row 32 (where x is the pulse number)	LSB	32	fl		32*4 byte(s)
	b	nom_phase Nominal value of phase (fx,n,nom) for antenna row 1 to antenna row 32 (where x is the pulse number)	deg	32	fl		32*4 byte(s)
38	cal_pulse_ws_tx_v_1 WS mode transmit V polarisation calibration data for pulse 1, swaths SS1 to SS5.			-	5	cal_pulse_ws_tx_v_1Struct	5*256.0 byte(s)
	a	nom_amplitude Nominal amplitude (ax,n,nom) for antenna row 1 to antenna row 32 (where x is the pulse number)	LSB	32	fl		32*4 byte(s)
	b	nom_phase Nominal value of phase (fx,n,nom) for antenna row 1 to antenna row 32 (where x is the pulse number)	deg	32	fl		32*4 byte(s)



#	Description			Units	Count	Type	Size
39	cal_pulse_ws_tx_h_1a WS mode transmit H polarisation calibration data for pulse 1A, swaths SS1 to SS5.			-	5	cal_pulse_ws_tx_h_1aStruct	5*256.0 byte(s)
	a	nom_amplitude Nominal amplitude (ax,n,nom) for antenna row 1 to antenna row 32 (where x is the pulse number)	LSB	32	fl		32*4 byte(s)
	b	nom_phase Nominal value of phase (fx,n,nom) for antenna row 1 to antenna row 32 (where x is the pulse number)	deg	32	fl		32*4 byte(s)
40	cal_pulse_ws_tx_v_1a WS mode transmit V polarisation calibration data for pulse 1A, swaths SS1 to SS5.			-	5	cal_pulse_ws_tx_v_1aStruct	5*256.0 byte(s)
	a	nom_amplitude Nominal amplitude (ax,n,nom) for antenna row 1 to antenna row 32 (where x is the pulse number)	LSB	32	fl		32*4 byte(s)
	b	nom_phase Nominal value of phase (fx,n,nom) for antenna row 1 to antenna row 32 (where x is the pulse number)	deg	32	fl		32*4 byte(s)
41	cal_pulse_ws_rx_h_2 WS mode receive H polarisation calibration data for pulse 2, swaths SS1 to SS5.			-	5	cal_pulse_ws_rx_h_2Struct	5*256.0 byte(s)
	a	nom_amplitude Nominal amplitude (ax,n,nom) for antenna row 1 to antenna row 32 (where x is the pulse number)	LSB	32	fl		32*4 byte(s)
	b	nom_phase Nominal value of phase (fx,n,nom) for antenna row 1 to antenna row 32 (where x is the pulse number)	deg	32	fl		32*4 byte(s)
42	cal_pulse_ws_rx_v_2 WS mode receive V polarisation calibration data for pulse 2, swaths SS1 to SS5.			-	5	cal_pulse_ws_rx_v_2Struct	5*256.0 byte(s)
	a	nom_amplitude Nominal amplitude (ax,n,nom) for antenna row 1 to antenna row 32 (where x is the pulse number)	LSB	32	fl		32*4 byte(s)
	b	nom_phase Nominal value of phase (fx,n,nom) for antenna row 1 to antenna row 32 (where x is the pulse number)	deg	32	fl		32*4 byte(s)
43	cal_pulse_ws_h_3 WS mode H polarisation calibration data for pulse 3, swaths SS1 to SS5.			-	5	cal_pulse_ws_h_3Struct	5*256.0 byte(s)
	a	nom_amplitude Nominal amplitude (ax,n,nom) for antenna row 1 to antenna row 32 (where x is the pulse number)	LSB	32	fl		32*4 byte(s)
	b	nom_phase Nominal value of phase (fx,n,nom) for antenna row 1 to antenna row 32	deg	32	fl		32*4 byte(s)

#	Description		Units	Count	Type	Size
	(where x is the pulse number)					
44	cal_pulse_ws_v_3 WS mode V polarisation calibration data for pulse 3, swaths SS1 to SS5.		-	5	cal_pulse_ws_v_3Struct	5*256.0 byte(s)
	a	nom_amplitude Nominal amplitude (ax,n,nom) for antenna row 1 to antenna row 32 (where x is the pulse number)	LSB	32	fl	32*4 byte(s)
	b	nom_phase Nominal value of phase (fx,n,nom) for antenna row 1 to antenna row 32 (where x is the pulse number)	deg	32	fl	32*4 byte(s)
45	cal_pulse_gm_tx_h_1 GM mode transmit H polarisation calibration data for pulse 1, swaths SS1 to SS5.		-	5	cal_pulse_gm_tx_h_1Struct	5*256.0 byte(s)
	a	nom_amplitude Nominal amplitude (ax,n,nom) for antenna row 1 to antenna row 32 (where x is the pulse number)	LSB	32	fl	32*4 byte(s)
	b	nom_phase Nominal value of phase (fx,n,nom) for antenna row 1 to antenna row 32 (where x is the pulse number)	deg	32	fl	32*4 byte(s)
46	cal_pulse_gm_tx_v_1 GM mode transmit V polarisation calibration data for pulse 1, swaths SS1 to SS5.		-	5	cal_pulse_gm_tx_v_1Struct	5*256.0 byte(s)
	a	nom_amplitude Nominal amplitude (ax,n,nom) for antenna row 1 to antenna row 32 (where x is the pulse number)	LSB	32	fl	32*4 byte(s)
	b	nom_phase Nominal value of phase (fx,n,nom) for antenna row 1 to antenna row 32 (where x is the pulse number)	deg	32	fl	32*4 byte(s)
47	cal_pulse_gm_tx_h_1a GM mode transmit H polarisation calibration data for pulse 1A, swaths SS1 to SS5.		-	5	cal_pulse_gm_tx_h_1aStruct	5*256.0 byte(s)
	a	nom_amplitude Nominal amplitude (ax,n,nom) for antenna row 1 to antenna row 32 (where x is the pulse number)	LSB	32	fl	32*4 byte(s)
	b	nom_phase Nominal value of phase (fx,n,nom) for antenna row 1 to antenna row 32 (where x is the pulse number)	deg	32	fl	32*4 byte(s)
48	cal_pulse_gm_tx_v_1a GM mode transmit V polarisation calibration data for pulse 1A, swaths SS1 to SS5.		-	5	cal_pulse_gm_tx_v_1aStruct	5*256.0 byte(s)
	a	nom_amplitude Nominal amplitude (ax,n,nom) for antenna row 1 to antenna row 32 (where x is the pulse number)	LSB	32	fl	32*4 byte(s)

#	Description			Units	Count	Type	Size
			nom_phase Nominal value of phase (fx,n,nom) for antenna row 1 to antenna row 32 (where x is the pulse number)	deg	32	fl	32*4 byte(s)
49	cal_pulse_gm_rx_h_2 GM mode receive H polarisation calibration data for pulse 2, swaths SS1 to SS5.		-	5	cal_pulse_gm_rx_h_2Struct		5*256.0 byte(s)
			a nom_amplitude Nominal amplitude (ax,n,nom) for antenna row 1 to antenna row 32 (where x is the pulse number)	LSB	32	fl	32*4 byte(s)
			b nom_phase Nominal value of phase (fx,n,nom) for antenna row 1 to antenna row 32 (where x is the pulse number)	deg	32	fl	32*4 byte(s)
50	cal_pulse_gm_rx_v_2 GM mode receive V polarisation calibration data for pulse 2, swaths SS1 to SS5.		-	5	cal_pulse_gm_rx_v_2Struct		5*256.0 byte(s)
			a nom_amplitude Nominal amplitude (ax,n,nom) for antenna row 1 to antenna row 32 (where x is the pulse number)	LSB	32	fl	32*4 byte(s)
			b nom_phase Nominal value of phase (fx,n,nom) for antenna row 1 to antenna row 32 (where x is the pulse number)	deg	32	fl	32*4 byte(s)
51	cal_pulse_gm_h_3 GM mode H polarisation calibration data for pulse 3, swaths SS1 to SS5.		-	5	cal_pulse_gm_h_3Struct		5*256.0 byte(s)
			a nom_amplitude Nominal amplitude (ax,n,nom) for antenna row 1 to antenna row 32 (where x is the pulse number)	LSB	32	fl	32*4 byte(s)
			b nom_phase Nominal value of phase (fx,n,nom) for antenna row 1 to antenna row 32 (where x is the pulse number)	deg	32	fl	32*4 byte(s)
52	cal_pulse_gm_v_3 GM mode V polarisation calibration data for pulse 3, swaths SS1 to SS5.		-	5	cal_pulse_gm_v_3Struct		5*256.0 byte(s)
			a nom_amplitude Nominal amplitude (ax,n,nom) for antenna row 1 to antenna row 32 (where x is the pulse number)	LSB	32	fl	32*4 byte(s)
			b nom_phase Nominal value of phase (fx,n,nom) for antenna row 1 to antenna row 32 (where x is the pulse number)	deg	32	fl	32*4 byte(s)
53	nom_pulse_im Nominal values of amplitude and phase of the transmitted chirp for Image Mode. Parameters repeated for each swath (7 times), from swath IS1 to IS7:		-	7	nom_pulse_imStruct		7*36.0 byte(s)
			a pulse_amp_coeff 4 pulse amplitude coefficients	-, s-1, s-2, s-3	4	fl	4*4 byte(s)

#	Description			Units	Count	Type	Size	
	b	pulse_phs_coeff 4 pulse phase coefficients	cyclesHz,Hz/s,Hz/s2		4	fl	4*4 byte(s)	
	c	pulse_duration Nominal pulse duration	s		1	fl	4 byte(s)	
54	nom_pulse_ap		Nominal values of amplitude and phase of the transmitted chirp for AP Mode. Parameters repeated for each swath (7 times), from swath IS1 to IS7:		-	7	nom_pulse_apStruct 7*36.0 byte(s)	
	a	pulse_amp_coeff 4 pulse amplitude coefficients	-, s-1, s-2, s-3		4	fl	4*4 byte(s)	
	b	pulse_phs_coeff 4 pulse phase coefficients	cyclesHz,Hz/s,Hz/s2		4	fl	4*4 byte(s)	
	c	pulse_duration Nominal pulse duration	s		1	fl	4 byte(s)	
55	nom_pulse_wv		Nominal values of amplitude and phase of the transmitted chirp for WV Mode. Parameters repeated for each swath (7 times), from swath IS1 to IS7:		-	7	nom_pulse_wvStruct 7*36.0 byte(s)	
	a	pulse_amp_coeff 4 pulse amplitude coefficients	-, s-1, s-2, s-3		4	fl	4*4 byte(s)	
	b	pulse_phs_coeff 4 pulse phase coefficients	cyclesHz,Hz/s,Hz/s2		4	fl	4*4 byte(s)	
	c	pulse_duration Nominal pulse duration	s		1	fl	4 byte(s)	
56	nom_pulse_ws		Nominal values of amplitude and phase of the transmitted chirp for WS Mode. Parameters repeated for each sub-swath (5 times), from swath SS1 to SS5:		-	5	nom_pulse_wsStruct 5*36.0 byte(s)	
	a	pulse_amp_coeff 4 pulse amplitude coefficients	-, s-1, s-2, s-3		4	fl	4*4 byte(s)	
	b	pulse_phs_coeff 4 pulse phase coefficients	cyclesHz,Hz/s,Hz/s2		4	fl	4*4 byte(s)	
	c	pulse_duration Nominal pulse duration	s		1	fl	4 byte(s)	
57	nom_pulse_gm		Nominal values of amplitude and phase of the transmitted chirp for GM Mode. Parameters repeated for each sub-swath (5 times), from swath SS1 to SS5:		-	5	nom_pulse_gmStruct 5*36.0 byte(s)	
	a	pulse_amp_coeff 4 pulse amplitude coefficients	-, s-1, s-2, s-3		4	fl	4*4 byte(s)	
	b	pulse_phs_coeff 4 pulse phase coefficients	cyclesHz,Hz/s,Hz/s2		4	fl	4*4 byte(s)	
	c	pulse_duration Nominal pulse duration	s		1	fl	4 byte(s)	
58	az_pattern_is1		2 way antenna azimuth pattern for swath IS1. Pattern values are from beam center - 0.25 deg to beam center + 0.25 deg. in 0.005 degree steps.		dB	101	fl	101*4 byte(s)
59	az_pattern_is2		2 way antenna azimuth pattern for swath IS2. Pattern values are from beam center - 0.25 deg to beam center + 0.25 deg. in 0.005 degree steps.		dB	101	fl	101*4 byte(s)
60	az_pattern_is3_ss2		2 way antenna azimuth pattern for swath IS3/SS2. Pattern values are from beam center - 0.25 deg to beam center + 0.25 deg. in 0.005 degree steps.		dB	101	fl	101*4 byte(s)
61	az_pattern_is4_ss3		2 way antenna azimuth pattern for swath IS4/SS3. Pattern values are from beam center - 0.25 deg to beam center + 0.25 deg. in 0.005 degree steps.		dB	101	fl	101*4 byte(s)
62	az_pattern_is5_ss4		2 way antenna azimuth pattern for swath IS5. Pattern values are from beam center - 0.25 deg to beam center + 0.25 deg. in 0.005 degree steps.		dB	101	fl	101*4 byte(s)
63	az_pattern_is6_ss5		2 way antenna azimuth pattern for swath IS6. Pattern values are from beam center - 0.25 deg to beam center + 0.25 deg. in 0.005 degree steps.		dB	101	fl	101*4 byte(s)
64	az_pattern_is7				dB	101	fl	101*4 byte(s)

#	Description	Units	Count	Type	Size
	2 way antenna azimuth pattern for swath IS7. Pattern values are from beam center - 0.25 deg to beam center + 0.25 deg. in 0.005 degree steps.				
65	az_pattern_ss1 2 way antenna azimuth pattern for swath SS1. Pattern values are from beam center - 0.25 deg to beam center + 0.25 deg. in 0.005 degree steps.	dB	101	fl	101*4 byte(s)
66	range_gate_bias Range Gate bias	s	1	fl	4 byte(s)
67	range_gate_bias_gm Range Gate bias for reduced bandwidth filter (GM mode only).	s	1	fl	4 byte(s)
68	adc_lut_i Look Up Table for ADC Characterization (I Channel). Contains 255 normalised amplitude levels corresponding to voltage thresholds. First value in LUT is for -127, last value is for +127.	-	255	fl	255*4 byte(s)
69	adc_lut_q Look Up Table for ADC Characterization (Q Channel). Contains 255 normalised amplitude levels corresponding to voltage thresholds. First value in LUT is for -127, last value is for +127.	-	255	fl	255*4 byte(s)
70	spare_1 Spare	-	1	SpareField	648 byte(s)
71	full8_lut_i Reconstruction Look Up Table for Full 8-bit Quantisation (I Channel). Contains normalised amplitude levels corresponding to sample codewords. First value in LUT is for codeword 0, last value is for +255 (binary offset format). Contains normalised amplitude levels corresponding to sample codewords. First value in LUT is for codeword 0, last value is for +255 (binary offset format). Table values account for Analog-to-Digital Converter (ADC) correction.	-	256	fl	256*4 byte(s)
72	full8_lut_q Reconstruction Look Up Table for Full 8-bit Quantisation (Q Channel). Contains normalized amplitude levels corresponding to sample codewords. First value in LUT is for codeword 0, last value is for +255 (binary offset format). Table values account for ADC correction.	-	256	fl	256*4 byte(s)
73	fbaq4_lut_i Reconstruction Look Up Table for FBAQ 4-bit Quantisation (I Channel). Gives 4096 normalised amplitude reconstruction levels which include ADC correction.	-	4096	fl	4096*4 byte(s)
74	fbaq3_lut_i Reconstruction Look Up Table for FBAQ 3-bit Quantisation (I Channel). Gives 2048 normalised amplitude reconstruction levels which include ADC correction.	-	2048	fl	2048*4 byte(s)
75	fbaq2_lut_i Reconstruction Look Up Table for FBAQ 2-bit Quantisation (I Channel). Gives 1024 normalised amplitude reconstruction levels which include ADC correction.	-	1024	fl	1024*4 byte(s)
76	fbaq4_lut_q Reconstruction Look Up Table for FBAQ 4-bit Quantisation (Q Channel). Gives 4096 normalised amplitude reconstruction levels which include ADC correction.	-	4096	fl	4096*4 byte(s)
77	fbaq3_lut_q Reconstruction Look Up Table for FBAQ 3-bit Quantisation (Q Channel). Gives 2048 normalised amplitude reconstruction levels which include ADC correction.	-	2048	fl	2048*4 byte(s)
78	fbaq2_lut_q Reconstruction Look Up Table for FBAQ 2-bit Quantisation (Q Channel). Gives 1024 normalised amplitude reconstruction levels which include ADC correction.	-	1024	fl	1024*4 byte(s)
79	fbaq4_no_adc Reconstruction Look Up Table for FBAQ 4-bit Quantisation (no ADC). This is the FBAQ reconstruction LUT which does not have ADC correction incorporated into it. It gives 4096 reconstruction levels which decodes FBAQ codewords to floating point values on the 8-bit range (-128 to +127). This table is used for RMS Equalisation. The format of this table is identical to that of the FBAQ 4-bit Reconstruction LUT for the I channel, as given in document ENVISAT-1 ASAR Interpretation of Source Packet Data. PO-TN-MMS-SR-0248.	-	4096	fl	4096*4 byte(s)
80	fbaq3_no_adc Reconstruction Look Up Table for FBAQ 3-bit Quantisation (no ADC). This is the FBAQ reconstruction LUT which does not have ADC correction incorporated into it. It gives 2048 reconstruction levels which decodes FBAQ codewords to floating point values on the 8-bit range (-128 to +127). This table is used for RMS Equalisation. The format of this table is identical to that of the FBAQ 3-bit Reconstruction LUT for the I channel, as given in document ENVISAT-1 ASAR Interpretation of Source Packet Data. PO-TN-MMS-SR-0248	-	2048	fl	2048*4 byte(s)
81	fbaq2_no_adc Reconstruction Look Up Table for FBAQ 2-bit Quantisation (No ADC). This is the FBAQ reconstruction LUT which does not have ADC correction incorporated into it. It gives 1024 reconstruction levels which decodes FBAQ codewords to floating point values on the 8-bit range (-128 to +127). This table is used for RMS Equalisation. The format of this table is identical to that of the	-	1024	fl	1024*4 byte(s)

#	Description		Units	Count	Type	Size
	FBAQ 2-bit Reconstruction LUT for the I channel, as given in document ENVISAT-1 ASAR Interpretation of Source Packet Data. PO-TN-MMS-SR-0248.					
82	sm_lut_i Reconstruction Look Up Table for Sign + Magnitude Quantisation (I Channel). Contains normalised amplitude reconstruction levels corresponding to sample codewords. First value in LUT is for threshold -7, last value is for threshold +7.		-	16	fl	16*4 byte(s)
83	sm_lut_q Reconstruction Look Up Table for Sign + Magnitude Quantisation (Q Channel). Contains normalised amplitude reconstruction levels corresponding to sample codewords. First value in LUT is for threshold -7, last value is for threshold +7.		-	16	fl	16*4 byte(s)
84	data_config_im Default data processing configuration table for Image Mode (IM)		-	1	data_config_imStruct	32.0 byte(s)
	a	echo_comp_method Compression Method used for echo samples FBAQ, S+M?, NONE	ascii	1	AsciiString	4 byte(s)
	b	echo_comp_ratio Compression Ratio for echo samples: 8/4, 8/3, 8/2, 8/8	ascii	1	AsciiString	3 byte(s)
	c	echo_resamp_flag Resampling applied to echo samples? (1=yes, 0=no)	flag	1	BooleanFlag	1 byte(s)
	d	init_cal_comp_method Compression Method used for initial calibration samples FBAQ, S+M?, NONE	ascii	1	AsciiString	4 byte(s)
	e	init_cal_comp_ratio Compression Ratio for initial calibration samples 8/4, 8/3, 8/2, 8/8	ascii	1	AsciiString	3 byte(s)
	f	init_cal_resamp_flag Resampling applied to initial calibration samples? (1=yes, 0=no)	flag	1	BooleanFlag	1 byte(s)
	g	per_cal_comp_method Compression Method used for periodic calibration samples FBAQ, S+M?, NONE	ascii	1	AsciiString	4 byte(s)
	h	per_cal_comp_ratio Compression Ratio for periodic calibration samples: 8/4, 8/3, 8/2, 8/8	ascii	1	AsciiString	3 byte(s)
	i	per_cal_resamp_flag Resampling applied to periodic calibration samples? (1=yes, 0=no)	flag	1	BooleanFlag	1 byte(s)
	j	noise_comp_method Compression Method used for noise samples FBAQ, S+M?, NONE	ascii	1	AsciiString	4 byte(s)
	k	noise_comp_ratio Compression Ratio for noise samples: 8/4, 8/3, 8/2, 8/8	ascii	1	AsciiString	3 byte(s)
	l	noise_resamp_flag Resampling applied to noise samples? (1=yes, 0=no)	flag	1	BooleanFlag	1 byte(s)
85	data_config_ap Default data processing configuration table for Alternating Polarisation (AP) mode		-	1	data_config_apStruct	32.0 byte(s)
	a	echo_comp_method Compression Method used for echo samples FBAQ, S+M?, NONE	ascii	1	AsciiString	4 byte(s)
	b	echo_comp_ratio Compression Ratio for echo samples: 8/4, 8/3, 8/2, 8/8	ascii	1	AsciiString	3 byte(s)
	c	echo_resamp_flag Resampling applied to	flag	1	BooleanFlag	1 byte(s)

#	Description			Units	Count	Type	Size
86		echo samples? (1=yes, 0=no)					
	d	init_cal_comp_method Compression Method used for initial calibration samples FBAQ, S+M?, NONE	ascii		1	AsciiString	4 byte(s)
	e	init_cal_comp_ratio Compression Ratio for initial calibration samples 8/4, 8/3, 8/2, 8/8	ascii		1	AsciiString	3 byte(s)
	f	init_cal_resamp_flag Resampling applied to initial calibration samples? (1=yes, 0=no)	flag		1	BooleanFlag	1 byte(s)
	g	per_cal_comp_method Compression Method used for periodic calibration samples FBAQ, S+M?, NONE	ascii		1	AsciiString	4 byte(s)
	h	per_cal_comp_ratio Compression Ratio for periodic calibration samples: 8/4, 8/3, 8/2, 8/8	ascii		1	AsciiString	3 byte(s)
	i	per_cal_resamp_flag Resampling applied to periodic calibration samples? (1=yes, 0=no)	flag		1	BooleanFlag	1 byte(s)
	j	noise_comp_method Compression Method used for noise samples FBAQ, S+M?, NONE	ascii		1	AsciiString	4 byte(s)
	k	noise_comp_ratio Compression Ratio for noise samples: 8/4, 8/3, 8/2, 8/8	ascii		1	AsciiString	3 byte(s)
	l	noise_resamp_flag Resampling applied to noise samples? (1=yes, 0=no)	flag		1	BooleanFlag	1 byte(s)
data_config_ws Default data processing configuration table for Wide Swath (WS) mode			-	1	data_config_wsStruct	32.0 byte(s)	
86	a	echo_comp_method Compression Method used for echo samples FBAQ, S+M?, NONE	ascii		1	AsciiString	4 byte(s)
	b	echo_comp_ratio Compression Ratio for echo samples: 8/4, 8/3, 8/2, 8/8	ascii		1	AsciiString	3 byte(s)
	c	echo_resamp_flag Resampling applied to echo samples? (1=yes, 0=no)	flag		1	BooleanFlag	1 byte(s)
	d	init_cal_comp_method Compression Method used for initial calibration samples FBAQ, S+M?, NONE	ascii		1	AsciiString	4 byte(s)
	e	init_cal_comp_ratio Compression Ratio for initial calibration samples 8/4, 8/3, 8/2, 8/8	ascii		1	AsciiString	3 byte(s)
	f	init_cal_resamp_flag Resampling applied to initial calibration samples? (1=yes, 0=no)	flag		1	BooleanFlag	1 byte(s)
	g	per_cal_comp_method Compression Method used for periodic calibration samples FBAQ, S+M?, NONE	ascii		1	AsciiString	4 byte(s)
	h	per_cal_comp_ratio Compression Ratio for periodic calibration samples: 8/4, 8/3, 8/2, 8/8	ascii		1	AsciiString	3 byte(s)
	i	per_cal_resamp_flag Resampling applied to periodic calibration	flag		1	BooleanFlag	1 byte(s)

#	Description			Units	Count	Type	Size
87	samples? (1=yes, 0=no)						
	j	noise_comp_method Compression Method used for noise samples FBAQ, S+M?, NONE	ascii		1	AsciiString	4 byte(s)
	k	noise_comp_ratio Compression Ratio for noise samples: 8/4, 8/3, 8/2, 8/8	ascii		1	AsciiString	3 byte(s)
	l	noise_resamp_flag Resampling applied to noise samples? (1=yes, 0=no)	flag		1	BooleanFlag	1 byte(s)
data_config_gm			-	1	data_config_gmStruct	32.0 byte(s)	
88	a	echo_comp_method Compression Method used for echo samples FBAQ, S+M?, NONE	ascii		1	AsciiString	4 byte(s)
	b	echo_comp_ratio Compression Ratio for echo samples: 8/4, 8/3, 8/2, 8/8	ascii		1	AsciiString	3 byte(s)
	c	echo_resamp_flag Resampling applied to echo samples? (1=yes, 0=no)	flag		1	BooleanFlag	1 byte(s)
	d	init_cal_comp_method Compression Method used for initial calibration samples FBAQ, S+M?, NONE	ascii		1	AsciiString	4 byte(s)
	e	init_cal_comp_ratio Compression Ratio for initial calibration samples 8/4, 8/3, 8/2, 8/8	ascii		1	AsciiString	3 byte(s)
	f	init_cal_resamp_flag Resampling applied to initial calibration samples? (1=yes, 0=no)	flag		1	BooleanFlag	1 byte(s)
	g	per_cal_comp_method Compression Method used for periodic calibration samples FBAQ, S+M?, NONE	ascii		1	AsciiString	4 byte(s)
	h	per_cal_comp_ratio Compression Ratio for periodic calibration samples: 8/4, 8/3, 8/2, 8/8	ascii		1	AsciiString	3 byte(s)
	i	per_cal_resamp_flag Resampling applied to periodic calibration samples? (1=yes, 0=no)	flag		1	BooleanFlag	1 byte(s)
	j	noise_comp_method Compression Method used for noise samples FBAQ, S+M?, NONE	ascii		1	AsciiString	4 byte(s)
	k	noise_comp_ratio Compression Ratio for noise samples: 8/4, 8/3, 8/2, 8/8	ascii		1	AsciiString	3 byte(s)
	l	noise_resamp_flag Resampling applied to noise samples? (1=yes, 0=no)	flag		1	BooleanFlag	1 byte(s)
data_config_wv			-	1	data_config_wvStruct	32.0 byte(s)	
	a	echo_comp_method Compression Method used for echo samples FBAQ, S+M?, NONE	ascii		1	AsciiString	4 byte(s)
	b	echo_comp_ratio Compression Ratio for echo samples: 8/4, 8/3, 8/2, 8/8	ascii		1	AsciiString	3 byte(s)

#	Description			Units	Count	Type	Size
89	c	echo_resamp_flag Resampling applied to echo samples? (1=yes, 0=no)	flag		1	BooleanFlag	1 byte(s)
	d	init_cal_comp_method Compression Method used for initial calibration samples FBAQ, S+M?, NONE	ascii		1	AsciiString	4 byte(s)
	e	init_cal_comp_ratio Compression Ratio for initial calibration samples 8/4, 8/3, 8/2, 8/8	ascii		1	AsciiString	3 byte(s)
	f	init_cal_resamp_flag Resampling applied to initial calibration samples? (1=yes, 0=no)	flag		1	BooleanFlag	1 byte(s)
	g	per_cal_comp_method Compression Method used for periodic calibration samples FBAQ, S+M?, NONE	ascii		1	AsciiString	4 byte(s)
	h	per_cal_comp_ratio Compression Ratio for periodic calibration samples: 8/4, 8/3, 8/2, 8/8	ascii		1	AsciiString	3 byte(s)
	i	per_cal_resamp_flag Resampling applied to periodic calibration samples? (1=yes, 0=no)	flag		1	BooleanFlag	1 byte(s)
	j	noise_comp_method Compression Method used for noise samples FBAQ, S+M?, NONE	ascii		1	AsciiString	4 byte(s)
	k	noise_comp_ratio Compression Ratio for noise samples: 8/4, 8/3, 8/2, 8/8	ascii		1	AsciiString	3 byte(s)
	l	noise_resamp_flag Resampling applied to noise samples? (1=yes, 0=no)	flag		1	BooleanFlag	1 byte(s)
89	swath_config_im Default Swath configuration table for Image Mode (IM)			-	1	swath_config_imStruct	84.0 byte(s)
90	a	num_samp_windows_echo Number of sample windows per source packet for echo samples, initial calibration samples (from beam 1 (IS1 or SS1) to beam 7 (IS7))	-	7	us		7*2 byte(s)
	b	num_samp_windows_init_cal Number of sample windows per source packet for initial calibration samples (from beam 1 to beam 7)	-	7	us		7*2 byte(s)
	c	num_samp_windows_per_ca Number of sample windows per source packet for periodic calibration samples (from beam 1 to beam 7)	-	7	us		7*2 byte(s)
	d	num_samp_windows_noise Number of sample windows per source packet for noise samples (from beam 1 to beam 7)	-	7	us		7*2 byte(s)
	e	resample_factor Resampling factor (beam 1 to beam 7)	-	7	fl		7*4 byte(s)
90	swath_config_ap Default Swath configuration table for Alternating Polarisation (AP)			-	1	swath_config_apStruct	84.0 byte(s)
	a	num_samp_windows_echo Number of sample windows per source	-	7	us		7*2 byte(s)



#	Description			Units	Count	Type	Size
91		packet for echo samples, initial calibration samples (from beam 1 (IS1 or SS1) to beam 7 (IS7))					
	b	num_samp_windows_init_cal Number of sample windows per source packet for initial calibration samples (from beam 1 to beam 7)	-	7	us		7*2 byte(s)
	c	num_samp_windows_per_cal Number of sample windows per source packet for periodic calibration samples (from beam 1 to beam 7)	-	7	us		7*2 byte(s)
	d	num_samp_windows_noise Number of sample windows per source packet for noise samples (from beam 1 to beam 7)	-	7	us		7*2 byte(s)
	e	resample_factor Resampling factor (beam 1 to beam 7)	-	7	fl		7*4 byte(s)
swath_config_ws Default Swath configuration table for Wide Swath (WS) note last two fields of each entry are set to zero			-	1	swath_config_wsStruct		84.0 byte(s)
92	a	num_samp_windows_echo Number of sample windows per source packet for echo samples, initial calibration samples (from beam 1 (IS1 or SS1) to beam 7 (IS7))	-	7	us		7*2 byte(s)
	b	num_samp_windows_init_cal Number of sample windows per source packet for initial calibration samples (from beam 1 to beam 7)	-	7	us		7*2 byte(s)
	c	num_samp_windows_per_cal Number of sample windows per source packet for periodic calibration samples (from beam 1 to beam 7)	-	7	us		7*2 byte(s)
	d	num_samp_windows_noise Number of sample windows per source packet for noise samples (from beam 1 to beam 7)	-	7	us		7*2 byte(s)
	e	resample_factor Resampling factor (beam 1 to beam 7)	-	7	fl		7*4 byte(s)
swath_config_gm Default Swath configuration table for Global Monitoring (GM) mode note last two fields of each entry are set to zero			-	1	swath_config_gmStruct		84.0 byte(s)
93	a	num_samp_windows_echo Number of sample windows per source packet for echo samples, initial calibration samples (from beam 1 (IS1 or SS1) to beam 7 (IS7))	-	7	us		7*2 byte(s)
	b	num_samp_windows_init_cal Number of sample windows per source packet for initial calibration samples (from beam 1 to beam 7)	-	7	us		7*2 byte(s)
	c	num_samp_windows_per_cal Number of sample windows per source packet for periodic calibration samples (from beam 1 to beam 7)	-	7	us		7*2 byte(s)
	d	num_samp_windows_noise	-	7	us		7*2 byte(s)

#	Description			Units	Count	Type	Size
		Number of sample windows per source packet for noise samples (from beam 1 to beam 7)					
	e	resample_factor Resampling factor (beam 1 to beam 7)	-	7	fl		7*4 byte(s)
93	swath_config_wv Default Swath configuration table for Wave Mode (WV)			-	1	swath_config_wvStruct	84.0 byte(s)
	a	num_samp_windows_echo Number of sample windows per source packet for echo samples, initial calibration samples (from beam 1 (IS1 or SS1) to beam 7 (IS7))	-	7	us		7*2 byte(s)
	b	num_samp_windows_init_ca Number of sample windows per source packet for initial calibration samples (from beam 1 to beam 7)	-	7	us		7*2 byte(s)
	c	num_samp_windows_per_ca Number of sample windows per source packet for periodic calibration samples (from beam 1 to beam 7)	-	7	us		7*2 byte(s)
	d	num_samp_windows_noise Number of sample windows per source packet for noise samples (from beam 1 to beam 7)	-	7	us		7*2 byte(s)
	e	resample_factor Resampling factor (beam 1 to beam 7)	-	7	fl		7*4 byte(s)
94	per_cal_widows_ec Number of periodic calibration sample windows per source packet for External Characterisation mode			-	1	us	2 byte(s)
95	per_cal_windows_ms Number of periodic calibration sample windows per source packet for Module Stepping mode			-	1	us	2 byte(s)
96	swath_id_im Default Swath Identification Table for Image Mode (IM) The default swaths corresponding to the Antenna Beam Set Parameter may be changed by macro-command during the mission			-	1	swath_id_imStruct	28.0 byte(s)
	a	swath_num Swath numbers (IS1 to IS7 or SS1 to SS5)	-	7	us		7*2 byte(s)
	b	beam_set_num Antenna Beam Set numbers (IS1 to IS7 or SS1 to SS5)	-	7	us		7*2 byte(s)
97	swath_id_ap Default Swath Identification Table for Alternating Polarisation (AP) The default swaths corresponding to the Antenna Beam Set Parameter may be changed by macro-command during the mission			-	1	swath_id_apStruct	28.0 byte(s)
	a	swath_num Swath numbers (IS1 to IS7 or SS1 to SS5)	-	7	us		7*2 byte(s)
	b	beam_set_num Antenna Beam Set numbers (IS1 to IS7 or SS1 to SS5)	-	7	us		7*2 byte(s)
98	swath_id_ws Default Swath Identification Table for Wide Swath (WS) mode The default swaths corresponding to the Antenna Beam Set Parameter may be changed by macro-command during the mission			-	1	swath_id_wsStruct	28.0 byte(s)
	a	swath_num	-	7	us		7*2 byte(s)

#	Description			Units	Count	Type	Size
99	Swath numbers (IS1 to IS7 or SS1 to SS5)						
	b	beam_set_num Antenna Beam Set numbers (IS1 to IS7 or SS1 to SS5)	-	7	us	7*2 byte(s)	
100	swath_id_gm Default Swath Identification Table for Global Monitoring (GM) mode The default swaths corresponding to the Antenna Beam Set Parameter may be changed by macro-command during the mission			-	1	swath_id_gmStruct	28.0 byte(s)
101	swath_num Swath numbers (IS1 to IS7 or SS1 to SS5)			7	us	7*2 byte(s)	
	b	beam_set_num Antenna Beam Set numbers (IS1 to IS7 or SS1 to SS5)	-	7	us	7*2 byte(s)	
102	swath_id_wv Default Swath Identification Table for Wave Mode (WV) The default swaths corresponding to the Antenna Beam Set Parameter may be changed by macro-command during the mission			-	1	swath_id_wvStruct	28.0 byte(s)
103	swath_num Swath numbers (IS1 to IS7 or SS1 to SS5)			7	us	7*2 byte(s)	
	b	beam_set_num Antenna Beam Set numbers (IS1 to IS7 or SS1 to SS5)	-	7	us	7*2 byte(s)	
104	init_cal_beam_set_wv Beam Set number for Wave Mode initial calibration			-	1	us	2 byte(s)
105	beam_set_ec Beam Set number for External Characterisation Mode			-	1	us	2 byte(s)
106	beam_set_ms Beam Set number for Module Stepping Mode			-	1	us	2 byte(s)
107	cal_seq Calibration Row Sequence Table. 32 numbers give the Row number sequence used during initial and periodic calibration.			-	32	us	32*2 byte(s)
108	timeline_im Mode timelines for Image Mode (IM)			-	1	timeline_imStruct	56.0 byte(s)
109	a swath_nums Swath numbers (IS1 to IS7 or SS1 to SS5)			7	us	7*2 byte(s)	
	b	m_values M values (IS1 to IS7 or SS1 to SS5) M is the number of echo sampling PTIs in a cycle or subcycle	-	7	us	7*2 byte(s)	
	c	r_values R values (IS1 to IS7 or SS1 to SS5) R is the rank (i.e., the number of PRI between transmitted pulse and return echo)	-	7	us	7*2 byte(s)	
	d	g_values G values (IS1 to IS7 or SS1 to SS5) G is the inter swath gap.	-	7	us	7*2 byte(s)	
110	timeline_ap Mode timelines for Alternating Polarisation (AP) mode			-	1	timeline_apStruct	56.0 byte(s)
111	a swath_nums Swath numbers (IS1 to IS7 or SS1 to SS5)			7	us	7*2 byte(s)	
	b	m_values M values (IS1 to IS7 or SS1 to SS5) M is the number of echo sampling PTIs in a cycle or subcycle	-	7	us	7*2 byte(s)	



#	Description			Units	Count	Type	Size
	c	r_values R values (IS1 to IS7 or SS1 to SS5) R is the rank (i.e., the number of PRI between transmitted pulse and return echo)	-	-	7	us	7*2 byte(s)
	d	g_values G values (IS1 to IS7 or SS1 to SS5) G is the inter swath gap.	-	-	7	us	7*2 byte(s)
107	timeline_ws Mode timelines for Wide Swath (WS) mode Note entries for IS6 and IS7 not included			-	1	timeline_wsStruct	56.0 byte(s)
	a	swath_nums Swath numbers (IS1 to IS7 or SS1 to SS5)	-	-	7	us	7*2 byte(s)
	b	m_values M values (IS1 to IS7 or SS1 to SS5) M is the number of echo sampling PTIs in a cycle or subcycle	-	-	7	us	7*2 byte(s)
	c	r_values R values (IS1 to IS7 or SS1 to SS5) R is the rank (i.e., the number of PRI between transmitted pulse and return echo)	-	-	7	us	7*2 byte(s)
	d	g_values G values (IS1 to IS7 or SS1 to SS5) G is the inter swath gap.	-	-	7	us	7*2 byte(s)
108	timeline_gm Mode timelines for Global Monitoring (GM) mode Note entries for IS6 and IS7 not included			-	1	timeline_gmStruct	56.0 byte(s)
	a	swath_nums Swath numbers (IS1 to IS7 or SS1 to SS5)	-	-	7	us	7*2 byte(s)
	b	m_values M values (IS1 to IS7 or SS1 to SS5) M is the number of echo sampling PTIs in a cycle or subcycle	-	-	7	us	7*2 byte(s)
	c	r_values R values (IS1 to IS7 or SS1 to SS5) R is the rank (i.e., the number of PRI between transmitted pulse and return echo)	-	-	7	us	7*2 byte(s)
	d	g_values G values (IS1 to IS7 or SS1 to SS5) G is the inter swath gap.	-	-	7	us	7*2 byte(s)
109	timeline_wv Mode timelines for Wave Mode (WV)			-	1	timeline_wvStruct	56.0 byte(s)
	a	swath_nums Swath numbers (IS1 to IS7 or SS1 to SS5)	-	-	7	us	7*2 byte(s)
	b	m_values M values (IS1 to IS7 or SS1 to SS5) M is the number of echo sampling PTIs in a cycle or subcycle	-	-	7	us	7*2 byte(s)
	c	r_values R values (IS1 to IS7 or SS1 to SS5) R is the rank (i.e., the number of PRI between transmitted pulse and return echo)	-	-	7	us	7*2 byte(s)
	d	g_values G values (IS1 to IS7 or SS1 to SS5) G is the inter swath gap.	-	-	7	us	7*2 byte(s)

#	Description	Units	Count	Type	Size
110	m_ec M value for External Characterization The number of echo sampling PTIs in a cycle or subcycle.	-	1	us	2 byte(s)
111	spare_2 Spare	-	1	SpareField	44 byte(s)
112	ref_elev_angle_is1 Reference elevation angle for IS1	deg.	1	fl	4 byte(s)
113	ref_elev_angle_is2 Reference elevation angle for IS2	deg.	1	fl	4 byte(s)
114	ref_elev_angle_is3_ss2 Reference elevation angle for IS3 / SS2	deg.	1	fl	4 byte(s)
115	ref_elev_angle_is4_ss3 Reference elevation angle for IS4 / SS3	deg.	1	fl	4 byte(s)
116	ref_elev_angle_is5_ss4 Reference elevation angle for IS5 / SS4	deg.	1	fl	4 byte(s)
117	ref_elev_angle_is6_ss5 Reference elevation angle for IS6 / SS5	deg.	1	fl	4 byte(s)
118	ref_elev_angle_is7 Reference elevation angle for IS7	deg.	1	fl	4 byte(s)
119	ref_elev_angle_ss1 Reference elevation angle for SS1	deg.	1	fl	4 byte(s)
120	spare_3 Spare	-	1	SpareField	64 byte(s)
121	cal_loop_ref_is1 Ground Characterised Complex Amplitude Fnp at the swath reference elevation angle for IS1. Complex factor characterising the path through the calibration loop and from the calibration coupler to the antenna face) 32 complex values for H polarisation, followed by 32 complex values for V polarisation	-	128	fl	128*4 byte(s)
122	cal_loop_ref_is2 Ground Characterised Complex Amplitude Fnp at the swath reference elevation angle for IS2. Complex factor characterising the path through the calibration loop and from the calibration coupler to the antenna face) 32 complex values for H polarisation, followed by 32 complex values for V polarisation	-	128	fl	128*4 byte(s)
123	cal_loop_ref_is3_ss2 Ground Characterised Complex Amplitude Fnp at the swath reference elevation angle for IS3/SS2. Complex factor characterising the path through the calibration loop and from the calibration coupler to the antenna face) 32 complex values for H polarisation, followed by 32 complex values for V polarisation	-	128	fl	128*4 byte(s)
124	cal_loop_ref_is4_ss3 Ground Characterised Complex Amplitude Fnp at the swath reference elevation angle for IS4/SS3. Complex factor characterising the path through the calibration loop and from the calibration coupler to the antenna face) 32 complex values for H polarisation, followed by 32 complex values for V polarisation	-	128	fl	128*4 byte(s)
125	cal_loop_ref_is5_ss4 Ground Characterised Complex Amplitude Fnp at the swath reference elevation angle for IS5/SS4. Complex factor characterising the path through the calibration loop and from the calibration coupler to the antenna face) 32 complex values for H polarisation, followed by 32 complex values for V polarisation	-	128	fl	128*4 byte(s)
126	cal_loop_ref_is6_ss5 Ground Characterised Complex Amplitude Fnp at the swath reference elevation angle for IS6/SS5. Complex factor characterising the path through the calibration loop and from the calibration coupler to the antenna face) 32 complex values for H polarisation, followed by 32 complex values for V polarisation	-	128	fl	128*4 byte(s)
127	cal_loop_ref_is7 Ground Characterised Complex Amplitude Fnp at the swath reference elevation angle for IS7. Complex factor characterising the path through the calibration loop and from the calibration coupler to the antenna face) 32 complex values for H polarisation, followed by 32 complex values for V polarisation	-	128	fl	128*4 byte(s)
128	cal_loop_ref_ss1 Ground Characterised Complex Amplitude Fnp at the swath reference elevation angle for SS1. Complex factor characterising the path through the calibration loop and from the calibration coupler to the antenna face) 32 complex values for H polarisation, followed by 32 complex values for V polarisation	-	128	fl	128*4 byte(s)
129	spare_4 Spare	-	1	SpareField	5120 byte(s)
130	im_operating_temp Operating temperature for Image Mode (IM) mode	deg C	1	fl	4 byte(s)
131	im_rx_gain_droop_coeff Coefficients of receiver gain droop curve for IM mode	-	8	db	8*8 byte(s)

#	Description	Units	Count	Type	Size
132	ap_operating_temp Operating temperature for Alternating Polarisation (AP) mode	deg C	1	fl	4 byte(s)
133	ap_rx_gain_droop_coeff Coefficients of receiver gain droop curve for AP mode	-	8	db	8*8 byte(s)
134	ws_operating_temp Operating temperature for Wide Swath (WS) mode	deg C	1	fl	4 byte(s)
135	ws_rx_gain_droop_coeff Coefficients of receiver gain droop curve for WS mode	-	8	db	8*8 byte(s)
136	gm_operating_temp Operating temperature for Global Monitoring (GM) mode	deg C	1	fl	4 byte(s)
137	gm_rx_gain_droop_coeff Coefficients of receiver gain droop curve for GM mode	-	8	db	8*8 byte(s)
138	wv_operating_temp Operating temperature for Wave Mode (WV) mode	deg C	1	fl	4 byte(s)
139	wv_rx_gain_droop_coeff Coefficients of receiver gain droop curve for WV mode	-	8	db	8*8 byte(s)
140	swst_cal_p2 Fixed SWST offset for calibration pulse P2 order zero. The fixed time delay of the calibration pulse order 0 from the start of the receive window.	-	1	fl	4 byte(s)
141	spare_5 Spare	-	1	SpareField	72 byte(s)

Record Length : 171648

DS\_NAME : Contains ASAR instrument characterization data

Format Version 114.0

Note 1: As opposed to the other 3 pulses, the P3 pulse does not characterise the transmit or the receive path, but rather the electronics part of the whole [calibration](#) path.

- Calibration pulses are included in the instrument timeline as initial calibration sequences as well as

during imaging and consist of: a transmit calibration pulse P1/P1a (actually split into two due to the fact that four T/R modules share a single power supply unit, see below),

a receive calibration pulse P2 and

a central electronics calibration pulse P3

See [chapter 3.3.1.](#) for a discussion of the ASAR instrument components and their roles.

Note 2: Format for data found within Fields# 69 and # 70, as well as Fields# 72 - 84 are as is given in document " ENVISAT-1 ASAR Interpretation of Source Packet Data. PO-TN-MMS-SR-0248 " ( document available from ENVISAT). Mathematical notation associated with fields within the ASA\_INS\_AX\_GADS:

## 6.6.4 ASAR external calibration data

The [external calibration](#) scaling factor is determined by [ESA](#) using three calibrated transponders, and the in-flight [elevation pattern](#) estimates are obtained using natural targets with known properties, such as the rainforest. This information is captured in the External Calibration Data file.

SIZE: MPH(1247 bytes) + SPH (378 bytes) + GADS (26552 bytes).

The [MPH](#) and [SPH](#) of these files will follow the standard MPH, SPH structure of all [ENVISAT-1 auxiliary data](#). There is one [DSD](#) in the SPH, known as the ASA\_XCA\_AX\_GADS, and the format for this record is given below.

Note that information is provided for all 5 of the ASAR product modes, which are the [Image \(IM\) mode](#), [Alternating Polarisation \(AP\) mode](#), [Wide Swath \(WS\) mode](#), [Global Monitoring \(GM\) mode](#), and the [Wave \(WV\) mode](#), and for all [swaths](#) IS1 to IS7 as well as the sub-swaths SS1 to SS5.

Table 6.40 ASAR external calibration data

## Contains ASAR external calibration data

#	Description	Units	Count	Type	Size
Data Record					
0	dsr_time Time of creation of this file	MJD	1	mjd	12 byte(s)
1	dsr_length DSR Length Length of this DSR in bytes	bytes	1	ul	4 byte(s)
2	ext_cal_im_hh External Calibration scaling factors for IM mode, SLC image, HH polar. (7 values from swath IS1 to IS7)	-	7	fl	7*4 byte(s)
3	ext_cal_im_vv External Calibration scaling factors for IM mode, SLC image, VV polar. (7 values from swath IS1 to IS7)	-	7	fl	7*4 byte(s)
4	ext_cal_im_pri_hh External Calibration scaling factors for IM mode, Precision Image, HH polar. (7 values from swath IS1 to IS7)	-	7	fl	7*4 byte(s)
5	ext_cal_im_pri_vv External Calibration scaling factors for IM mode, Precision Image, VV polar. (7 values from swath IS1 to IS7)	-	7	fl	7*4 byte(s)
6	ext_cal_im_geo_hh External Calibration scaling factors for IM mode, Geocoded Image, HH polar. (7 values from swath IS1 to IS7)	-	7	fl	7*4 byte(s)
7	ext_cal_im_geo_vv	-	7	fl	7*4 byte(s)

#	Description	Units	Count	Type	Size
	External Calibration scaling factors for IM mode, Geocoded Image, VV polar. (7 values from swath IS1 to IS7)				
8	ext_cal_im_med_hh External Calibration scaling factors for IM mode, Medium Resolution Image, HH polarisation (7 values from swath IS1 to IS7)	-	7	fl	7*4 byte(s)
9	ext_cal_im_med_vv External Calibration scaling factors for IM mode, Medium Resolution Image, VV polarisation (7 values from swath IS1 to IS7)	-	7	fl	7*4 byte(s)
10	ext_cal_ap_hh External Calibration scaling factors for AP mode, SLC image, HH polar. (7 values from swath IS1 to IS7)	-	7	fl	7*4 byte(s)
11	ext_cal_ap_vv External Calibration scaling factors for AP mode, SLC image, VV polar. (7 values from swath IS1 to IS7)	-	7	fl	7*4 byte(s)
12	ext_cal_ap_hv External Calibration scaling factors for AP mode, SLC image, HV polar. (7 values from swath IS1 to IS7)	-	7	fl	7*4 byte(s)
13	ext_cal_ap_vh External Calibration scaling factors for AP mode, SLC image, VH polar. (7 values from swath IS1 to IS7)	-	7	fl	7*4 byte(s)
14	ext_cal_ap_pri_hh External Calibration scaling factors for AP mode, Precision Image, HH polar. (7 values from swath IS1 to IS7)	-	7	fl	7*4 byte(s)
15	ext_cal_ap_pri_vv External Calibration scaling factors for AP mode, Precision Image, VV polar. (7 values from swath IS1 to IS7)	-	7	fl	7*4 byte(s)
16	ext_cal_ap_pri_hv External Calibration scaling factors for AP mode, Precision Image, HV polar. (7 values from swath IS1 to IS7)	-	7	fl	7*4 byte(s)
17	ext_cal_ap_pri_vh External Calibration scaling factors for AP mode, Precision Image, VH polar. (7 values from swath IS1 to IS7)	-	7	fl	7*4 byte(s)
18	ext_cal_ap_geo_hh External Calibration scaling factors for AP mode, Geocoded Image, HH polar. (7 values from swath IS1 to IS7)	-	7	fl	7*4 byte(s)
19	ext_cal_ap_geo_vv External Calibration scaling factors for AP mode, Geocoded Image, VV polar. (7 values from swath IS1 to IS7)	-	7	fl	7*4 byte(s)
20	ext_cal_ap_geo_hv External Calibration scaling factors for AP mode, Geocoded Image, HV polarisation (7 values from swath IS1 to IS7)	-	7	fl	7*4 byte(s)
21	ext_cal_ap_geo_vh External Calibration scaling factors for AP mode, Geocoded Image, VH polar. (7 values from swath IS1 to IS7)	-	7	fl	7*4 byte(s)
22	ext_cal_ap_med_hh External Calibration scaling factors for AP mode, Medium Resolution Image, HH polarisation (7 values from swath IS1 to IS7)	-	7	fl	7*4 byte(s)
23	ext_cal_ap_med_vv External Calibration scaling factors for AP mode, Medium Resolution Image, VV polarisation (7 values from swath IS1 to IS7)	-	7	fl	7*4 byte(s)
24	ext_cal_ap_med_hv External Calibration scaling factors for AP mode, Medium Resolution Image, HV polarisation (7 values from swath IS1 to IS7)	-	7	fl	7*4 byte(s)
25	ext_cal_ap_med_vh External Calibration scaling factors for AP mode, Medium Resolution Image, VH polarisation (7 values from swath IS1 to IS7)	-	7	fl	7*4 byte(s)
26	ext_cal_wv_hh External Calibration scaling factors for WV mode, HH polarisation (7 values from swath IS1 to IS7)	-	7	fl	7*4 byte(s)
27	ext_cal_wv_vv External Calibration scaling factors for WV mode, VV polar. (7 values from swath IS1 to IS7)	-	7	fl	7*4 byte(s)
28	ext_cal_ws_hh External Calibration scaling factors for WS mode, detected image 111HH polar.	-	1	fl	4 byte(s)
29	ext_cal_ws_vv External Calibration scaling factors for WS mode, detected image ,VV polar.	-	1	fl	4 byte(s)
30	ext_cal_gm_hh External Calibration scaling factors for GM mode, HH polar.	-	1	fl	4 byte(s)
31	ext_cal_gm_vv	-	1	fl	4 byte(s)

#	Description	Units	Count	Type	Size
	External Calibration scaling factors for GM mode, VV polar.				
32	elev_ang_is1 Reference elevation angle for IS1	deg.	1	fl	4 byte(s)
33	elev_ang_is2 Reference elevation angle for IS2	deg.	1	fl	4 byte(s)
34	elev_ang_is3_ss2 Reference elevation angle for IS3 / SS2	deg.	1	fl	4 byte(s)
35	elev_ang_is4_ss3 Reference elevation angle for IS4 / SS3	deg.	1	fl	4 byte(s)
36	elev_ang_is5_ss4 Reference elevation angle for IS5 / SS4	deg.	1	fl	4 byte(s)
37	elev_ang_is6_ss5 Reference elevation angle for IS6 / SS5	deg.	1	fl	4 byte(s)
38	elev_ang_is7 Reference elevation angle for IS7	deg.	1	fl	4 byte(s)
39	elev_ang_ss1 Reference elevation angle for SS1	deg.	1	fl	4 byte(s)
40	pattern_is1 Two-way Antenna Elevation Pattern Gain Table for IS1. Four tables, 1 for each HH, VV, HV, VH polarisation. The pattern is defined from reference elevation angle - 5 deg. to reference elevation angle + 5 deg. in 0.05 degree steps.	dB	4*201	fl	4*201*4 byte(s)
41	pattern_is2 Two-way Antenna Elevation Pattern Gain Table for IS2. Four tables, 1 for each HH, VV, HV, VH polarisation. The pattern is defined from reference elevation angle - 5 deg. to reference elevation angle + 5 deg. in 0.05 degree steps.	dB	4*201	fl	4*201*4 byte(s)
42	pattern_is3_ss2 Two-way Antenna Elevation Pattern Gain Table for IS3/SS2. Four tables, 1 for each HH, VV, HV, VH polarisation. The pattern is defined from reference elevation angle - 5 deg. to reference elevation angle + 5 deg. in 0.05 degree steps.	dB	4*201	fl	4*201*4 byte(s)
43	pattern_is4_ss3 Two-way Antenna Elevation Pattern Gain Table for IS4/SS3. Four tables, 1 for each HH, VV, HV, VH polarisation. The pattern is defined from reference elevation angle - 5 deg. to reference elevation angle + 5 deg. in 0.05 degree steps.	dB	4*201	fl	4*201*4 byte(s)
44	pattern_is5_ss4 Two-way Antenna Elevation Pattern Gain Table for IS5/SS4. Four tables, 1 for each HH, VV, HV, VH polarisation. The pattern is defined from reference elevation angle - 5 deg. to reference elevation angle + 5 deg. in 0.05 degree steps.	dB	4*201	fl	4*201*4 byte(s)
45	pattern_is6_ss5 Two-way Antenna Elevation Pattern Gain Table for IS6/SS5. Four tables, 1 for each HH, VV, HV, VH polarisation. The pattern is defined from reference elevation angle - 5 deg. to reference elevation angle + 5 deg. in 0.05 degree steps.	dB	4*201	fl	4*201*4 byte(s)
46	pattern_is7 Two-way Antenna Elevation Pattern Gain Table for IS7. Four tables, 1 for each HH, VV, HV, VH polarisation. The pattern is defined from reference elevation angle - 5 deg. to reference elevation angle + 5 deg. in 0.05 degree steps.	dB	4*201	fl	4*201*4 byte(s)
47	pattern_ss1 Two-way Antenna Elevation Pattern Gain Table for SS1. Four tables, 1 for each HH, VV, HV, VH polarisation. The pattern is defined from reference elevation angle - 5 deg. to reference elevation angle + 5 deg. in 0.05 degree steps.	dB	4*201	fl	4*201*4 byte(s)
48	ext_cal_ws_slc_hh External Calibration scaling factors for WS mode, SLC Image HH polar.	-	1	fl	4 byte(s)
49	ext_cal_ws_slc_vv External Calibration scaling factors for WS mode, SLC Image VV polar	-	1	fl	4 byte(s)
50	spare_1 Spare	-	1	SpareField	24 byte(s)

Record Length : 26552

DS\_NAME : Contains ASAR external calibration data

Format Version 114.0

## 6.6.5 ASAR external characterization data

The [ASAR](#) instrument has an [External Characterisation Mode](#) which is operated overflying a receiver setup for H or V [polarisation](#) located in the ground. During the mode, the ASAR transmits a sequence of [pulses](#) from each [antenna](#) row in turn.

These pulses are received and digitized on the ground and the data recorded for [off-line](#) analysis. Simultaneously during the mode the [calibration loop](#) in the instrument is used to couple transmit pulses which are then sampled within a calibration widow

in order to provide comparative values. The [External Characterisation Data](#) file is provided as the output of the external characterisation analysis and is used for [internal calibration](#) processing correction. It is updated nominally every 6 months.

SIZE: MPH(1247 bytes) + SPH (378 bytes) + GADS (596 bytes)

The [MPH](#) and [SPH](#) of these files will follow the standard MPH, SPH structure of all [ENVISAT](#) -1 [auxiliary](#) data. There is one [Data Set Descriptor \(DSD\)](#) in the SPH, known as the ASA\_XCH\_AX\_GADS, and its format is given below:

Table 6.41 ASAR external characterization data

## Contains ASAR external characterization data

#	Description	Units	Count	Type	Size
Data Record					
0	dsr_time Time of characterisation	MJD	1	mjd	12 byte(s)
1	dsr_length Length of this DSR in bytes	bytes	1	ul	4 byte(s)
2	complex_loop_factors Complex loop paths characterisation factors relative to free space (from External Characterisation data). gnp where n is the index of the row (1 to 32) and p is the index of the polarisation (H or V). Arranged H: 1 to 32, V: 1-32). Values are complex (I,Q) pairs.	-	128	fl	128*4 byte(s)
3	pointing_error Antenna pointing error (from External Characterisation data) This is used to calculate the elevation angle: elevation angle = reference elevation angle	deg	1	fl	4 byte(s)
4	spare_1 Spare	-	1	SpareField	64 byte(s)

Record Length : 596

DS\_NAME : Contains ASAR external characterization data

---

Format Version 114.0

Note: relating to field# 4 within this table :

As a mathematical expression, the antenna pointing error is given  $\Delta p_1$  elevation angle = reference elevation angle  $+ \Delta p_1$

## 6.6.6 Antenna Elevation pattern

The antenna elevation pattern values are updated several times along the [azimuth](#) direction. Each update is time stamped with the [zero Doppler time](#) to which the update applies. The values continue to apply until a new update is made, and new values are added to the [Annotation Data Set \(ADS\)](#) with a new time stamp. The contents of each update (each update is a single [ADSR](#) within the ADS) are as follows. This ADS is not included for [SLC](#) products. The format for the [Antenna Elevation Pattern](#) ADSR (ASAR\_Antenna\_ADSR) is given below.

Note, for [Wide Swath \(WS\)](#) and [Global Monitoring \(GM\)](#) products, there is a separate ADSR for each [beam](#). The ADSRs are ordered according to their time stamps. If the time stamps of several ADSRs are identical, the ADSRs are ordered by beam number from SS1 to SS5.

Table 6.42 Antenna Elevation pattern

## Antenna Elevation patterns(s)

#	Description	Units	Count	Type	Size
Data Record					
0	zero_doppler_time Zero Doppler azimuth time at which pattern applies	MJD	1	mjd	12 byte(s)
1	attach_flag Attachment Flag Always set to zero for this ADSR	flag	1	BooleanFlag	1 byte(s)
2	swath Beam ID to which pattern applies SS1 to SSS or NS	ascii	1	AsciiString	3 byte(s)
3	elevation_pattern Antenna Elevation Pattern The following fields each contain 11 values spaced evenly across the image	-	1	elevation_patternStruct	132.0 byte(s)
	a	slant_range_time	ns	11	fl 11*4 byte(s)

#	Description		Units	Count	Type	Size
b	2 way slant range times					
	b	elevation_angles Corresponding elevation angles	degrees	11	fl	11*4 byte(s)
	c	antenna_pattern Corresponding two-way antenna elevation pattern values	dB	11	fl	11*4 byte(s)
4	spare_1 Spare		-	1	SpareField	14 byte(s)

Record Length : 162

DS\_NAME : Antenna Elevation patterns(s)

Format Version 114.0

## 6.6.7 Chirp parameters

The [chirp](#) parameters derived from the [calibration](#) pulses may be updated more than once per product, or [slice](#). Each update is stamped with the [zero Doppler time](#) to which the update applies, the [swath](#) to which it applies, and [polarisation](#) of the image

to which it applies. This time stamping allows for unambiguous recording of the chirp parameters, which were used for at any part of the image (for both [MDS 1](#) and [MDS 2](#) for [Alternating Polarisation \(AP\)](#) products) and for any [beam](#). The coefficients continue to apply until a new update is made, and new values added to the [ADS](#) with a new time stamp. The contents of each update (each update is a single ADSR within the ADS) are as provided in the ASAR\_Chirp\_ADSR table, provided below.

Note, for [Global Monitoring \(GM\)](#) and [Wide Swath \(WS\)](#) products, there is a separate ADSR for each beam. The ADSRs are ordered according to their time stamps. If the time stamps of several ADSRs are identical, the ADSRs are ordered by beam number from SS1 to SS5.

Table 6.43 Chirp parameters

# Chirp parameters

#	Description	Units	Count	Type	Size	
Data Record						
0	zero_doppler_time Zero doppler azimuth time in azimuth at which estimate applies	MJD	1	mjd	12 byte(s)	
1	attach_flag Attachment Flag Always set to zero for this ADSR	flag	1	BooleanFlag	1 byte(s)	
2	swath Beam ID SS1, SS2, SS3, SS4, or SS5 for WS and GM images. Set to NS for AP, IM, and WV images.	ascii	1	AsciiString	3 byte(s)	
3	polar Tx/Rx polarisation H/H, H/V, V/V, or V/H	ascii	1	AsciiString	3 byte(s)	
4	chirp_width 3-dB pulse width of chirp replica cross-correlation function between reconstructed chirp and nominal chirp	samples	1	fl	4 byte(s)	
5	chirp_sidelobe First side lobe level of chirp replica cross-correlation function between reconstructed chirp and nominal chirp	dB	1	fl	4 byte(s)	
6	chirp_islr ISLR of chirp replica cross-correlation function between reconstructed chirp and nominal chirp	dB	1	fl	4 byte(s)	
7	chirp_peak_loc Peak location of cross-correlation function between reconstructed chirp and nominal chirp	samples	1	fl	4 byte(s)	
8	re_chirp_power Reconstructed Chirp power	dB	1	fl	4 byte(s)	
9	elev_chirp_power Equivalent chirp Power	dB	1	fl	4 byte(s)	
10	chirp_quality_flag Reconstructed chirp exceeds quality thresholds. 0 = reconstructed chirp below quality thresholds, current chirp is the nominal chirp. 1 = reconstructed chirp above quality thresholds, current chirp is the reconstructed chirp.	flag	1	BooleanFlag	1 byte(s)	
11	ref_chirp_power Reference chirp Power	dB	1	fl	4 byte(s)	
12	normalization_source Normalization source REPLICA, REF0000, EQV0000, NONE0000	-	1	AsciiString	7 byte(s)	
13	spare_1 Spare	-	1	SpareField	4 byte(s)	
14	cal_pulse_info This structure is repeated 32 times: once for each antenna row	-	32	cal_pulse_infoStruct	32*44.0 byte(s)	
	a	max_cal Max of Cal pulses 1, 2, and 3 amplitude	-	3	fl	3*4 byte(s)
	b	avg_cal Average of Cal pulse 1, 2, and 3 amplitude over the 3 dB on either side of the max amplitude	-	3	fl	3*4 byte(s)
	c	avg_val_1a Average of Cal pulse 1A over the sample window	-	1	fl	4 byte(s)
	d	phs_cal Extracted phase for calibration pulse 1, 1A, 2, and 3	degrees	4	fl	4*4 byte(s)
15	spare_2 Spare	-	1	SpareField	16 byte(s)	

Record Length : 1483

DS\_NAME : Chirp parameters

Format Version 114.0

## 6.6.8 Doppler Centroid parameters

The [Doppler centroid 2.6.1.2.2](#) of the image is estimated once for [stand-alone products](#), and is hence reported once. For [stripline](#), however, a Doppler centroid estimate is performed at least at the start and at the end of a [slice](#). To ensure the user is given a

complete record of the Doppler parameters used during processing, the Doppler Centroid Coefficients [ADS](#) is updated with a new ADSR at every [granule](#) for stripline processing. Each update is time stamped with the [zero Doppler time](#) to which the update applies. The Doppler centroid coefficients used on [range](#) lines between two updates are found by linear interpolation between the updated and previous values. The contents of each update (each update is a single ADSR within the ADS) are as shown in the table below:

Table 6.44 Doppler Centroid parameters

## Doppler Centroid parameters

#	Description	Units	Count	Type	Size
Data Record					
0	zero_doppler_time Zero Doppler azimuth time at which estimate applies	MJD	1	mjd	12 byte(s)
1	attach_flag Attachment Flag Always set to zero for this ADSR	flag	1	BooleanFlag	1 byte(s)
2	slant_range_time 2-way slant range time origin (t0)	ns	1	fl	4 byte(s)
3	dop_coeff Doppler centroid coefficients as a function of slant range time: D0, D1, D2, D3, and D4. Where Doppler Centroid = D0 + D1(tSR-t0) + D2(tSR-t0)2 + D3(tSR-t0)3 + D4(tSR-t0)4	Hz/Hz/sHz/s2Hz/s3Hz/s4	5	fl	5*4 byte(s)
4	dop_conf Doppler Centroid Confidence Measure. Value between 0 and 1, 0 = poorest confidence, 1= highest confidence	-	1	fl	4 byte(s)
5	dop_conf_below_thresh_flag Doppler Centroid Confidence below threshold flag. 0=confidence above threshold, centroid calculated from data; 1=confidence below threshold, centroid calculated from orbit parameters	flag	1	BooleanFlag	1 byte(s)
6	delta_dopp_coeff Delta Doppler coefficients DelatD0(SS1), DelatD0(SS2) DelatD0(SS3) DelatD0(SS4) DelatD0(SS5)	-	5	ss	5*2 byte(s)
7	spare_1 Spare	-	1	SpareField	3 byte(s)

Record Length : 55

DS\_NAME : Doppler Centroid parameters

Format Version 114.0

Note: For Field# 5:

Doppler Centroid Confidence Measure:

Value between 0 and 1, 0 = poorest confidence, 1= highest confidence

If multiple Doppler Centroid estimates were performed, this value is the lowest confidence value attained.

Doppler Confidence Below Threshold Flag

0 = confidence above threshold, Doppler Centroid calculated from data

1 = confidence below threshold, Doppler Centroid calculated from orbit parameters

For a discussion of the Doppler Centroid estimation algorithms, refer to the included technote "[Doppler Centroid Frequency Estimator](#)". [2.6.1.2.2](#). See also "[Level 1B Essential Product Confidence Data](#)" [2.6.2.3](#), in chapter 2.

## 6.6.9 Geolocation Grid ADSRs

The Geolocation Grid is a table which lists the slant range time, incidence angle, and geodetic latitude and longitude positions at various range/azimuth positions within the image. The location of each tie point (or grid point) in the image is specified by

a line and sample co-ordinate system. Tie point locations in azimuth are specified using the Zero Doppler Time stamp found at the start of each range line in the MDS. The location in range is specified by the number of range samples. Tie points must

be placed at points corresponding to an integer number of range samples, and tie points must be located at least the following 3 points within those reported: the first range sample of the range line, the mid swath range sample, and the last range

sample of the range line.

For Geocoded products, the Zero Doppler Time stamp does not apply. Therefore, it is set to zero, and only the range line number is used to index the grid entries.

The grid spacing in azimuth defines the granule size of the ASAR product. That is, a grid line provides tie points for the first line and last line of a granule. There will be 11 grid updates in range per ADSR. In azimuth, a new ADSR will be added to the ADS nominally every:

- 10 km in azimuth for IM and AP;
- 40 km in azimuth for WS and GM.

The contents of a Geolocation Grid ADSR are shown below:

Table 6.45 Geolocation Grid ADSRs

## Geolocation Grid ADSRs

#	Description	Units	Count	Type	Size
Data Record					
0	first_zero_doppler_time Zero doppler time in azimuth of first line of the granule Gives azimuth location of grid line for first line of the granule.	MJD	1	mjd	12 byte(s)
1	attach_flag Attachment Flag Set to 1 if all MDSRs corresponding to this ADSR are blank, set to zero otherwise	flag	1	BooleanFlag	1 byte(s)
2	line_num Range line number corresponding to the first line of the granule within the slice. Warning: (1) This is not always the record number of the corresponding image MDSR. Use the number of lines per granule field to determine the image MDS record corresponding to each record of tie points.(2) For a stripline product, which may consist of multiple slices in a single MDS, this number is reset to 1 at the beginning of each slice.(3) For child products, which are subsets of a full product, the range line number in the first record may not be 1.	-	1	ul	4 byte(s)
3	num_lines Number of output lines in this granule	lines	1	ul	4 byte(s)
4	sub_sat_track Subsatellite track heading (relative to North) for first line of granule This is the heading on the ground (includes Earth rotation)	deg.	1	fl	4 byte(s)
5	first_line_tie_points First Line Tie Points The following fields each contain 11 values corresponding to 11 tie points in the first line of the granule	-	1	first_line_tie_pointsStruct	220.0 byte(s)
	a samp_numbers Range sample number Gives the range location of the grid points. First range sample is 1, last is M	-	11	ul	11*4 byte(s)
	b slant_range_times 2 way slant range time to range sample	ns	11	fl	11*4 byte(s)
	c angles Incidence Angle at range sample	deg.	11	fl	11*4 byte(s)
	d lats geodetic latitude (positive north)	(1e-6) degrees	11	GeoCoordinate	11*4 byte(s)
	e longs geodetic longitude (positive east)	(1e-6) degrees	11	GeoCoordinate	11*4 byte(s)
6	spare_1 Spare	-	1	SpareField	22 byte(s)

#	Description	Units	Count	Type	Size																													
7	last_zero_doppler_time Zero doppler time for the last line of the granule	MJD	1	mjd	12 byte(s)																													
8	last_line_tie_points Last Line Tie Points The following fields each contain 11 values corresponding to 11 tie points in the last line of the granule	-	1	last_line_tie_pointsStruct	220.0 byte(s)																													
	<table border="1"> <tr> <td>a</td><td>samp_numbers Range sample number Gives the range location of the grid points. First range sample is 1, last is M</td><td>-</td><td>11</td><td>ul</td><td>11*4 byte(s)</td></tr> <tr> <td>b</td><td>slant_range_times 2 way slant range time to range sample</td><td>ns</td><td>11</td><td>fl</td><td>11*4 byte(s)</td></tr> <tr> <td>c</td><td>angles Incidence Angle at range sample</td><td>deg.</td><td>11</td><td>fl</td><td>11*4 byte(s)</td></tr> <tr> <td>d</td><td>lats geodetic latitude (positive north)</td><td>(1e-6) degrees</td><td>11</td><td>GeoCoordinate</td><td>11*4 byte(s)</td></tr> <tr> <td>e</td><td>longs geodetic longitude (positive east)</td><td>(1e-6) degrees</td><td>11</td><td>GeoCoordinate</td><td>11*4 byte(s)</td></tr> </table>	a	samp_numbers Range sample number Gives the range location of the grid points. First range sample is 1, last is M	-	11	ul	11*4 byte(s)	b	slant_range_times 2 way slant range time to range sample	ns	11	fl	11*4 byte(s)	c	angles Incidence Angle at range sample	deg.	11	fl	11*4 byte(s)	d	lats geodetic latitude (positive north)	(1e-6) degrees	11	GeoCoordinate	11*4 byte(s)	e	longs geodetic longitude (positive east)	(1e-6) degrees	11	GeoCoordinate	11*4 byte(s)			
a	samp_numbers Range sample number Gives the range location of the grid points. First range sample is 1, last is M	-	11	ul	11*4 byte(s)																													
b	slant_range_times 2 way slant range time to range sample	ns	11	fl	11*4 byte(s)																													
c	angles Incidence Angle at range sample	deg.	11	fl	11*4 byte(s)																													
d	lats geodetic latitude (positive north)	(1e-6) degrees	11	GeoCoordinate	11*4 byte(s)																													
e	longs geodetic longitude (positive east)	(1e-6) degrees	11	GeoCoordinate	11*4 byte(s)																													
9	spare_2 Spare	-	1	SpareField	22 byte(s)																													

Record Length : 521

## DS\_NAME : Geolocation Grid ADSRs

Format Version 114.0

### 6.6.10 Measurement Data Set 1

The [Measurement Data Set \(MDS\)](#) consists of several Measurement Data Set Records (MDSRs) and each MDSR contains the processed [SAR](#) data for one [range](#) line. The number of MDSRs within a given product depends on the number of range lines contained within the data set. The length of each MDSR depends on the product, the [swath](#), and the data format used to represent the samples.

Each MDSR consists of a small header, followed by the processed SAR data. Note that for the [geocoded](#) products there is no correlation between the MDSR and [zero Doppler time](#), so the time entry is set to zero. Zero Doppler times in the [Annotation Data Sets \(ADSS\)](#) of the geocoded product refer to those of the intermediate image created before geocoding. For [detected images](#) the SAR data consists of real valued samples.

Table 6.46 Measurement Data Set 1

## Measurement Data Set 5

#	Description	Units	Count	Type	Size
Data Record					
0	zero_doppler_time Zero Doppler Time in azimuth MJD format	MJD	1	mjd	12 byte(s)
1	quality_flag Quality Indicator Set to -1 if all entries in MDSR are zero, set to zero otherwise	flag	1	BooleanFlag	1 byte(s)
2	line_num Range line number. Numbered sequentially, for each product (or slice) first range line in MDS is 1. Warning: (1) For a striplice product, which may consist of multiple slices in a single MDS, this number is reset to 1 at the beginning of each slice. (2) For child products, which are subsets of a full product, the range line number in the first record may not be 1	-	1	ul	4 byte(s)
3	proc_data SAR Processed Data. Real samples (detected products)	-	-	-	0 byte(s)

Record Length : 17

DS\_NAME : Measurement Data Set 5

Format Version 114.0

### 6.6.11 ASAR Image Products SPH

The [Specific Product Header \(SPH\)](#) is a one record, fixed length and format, ASCII header that contains general information applicable to the whole product. ( See "[Definitions and Conventions](#) " 2.3, in chapter 2 ).

The philosophy of the [ASAR](#) SPH is to provide only basic information needed to evaluate the product, and only information which applies to both an individual [stand-alone product](#) or a full [striplice product](#). Thus, the image products SPH contents, other than positioning information and some minor [Data Set Descriptor \(DSD\)](#) values, will not need to be updated during striplice formation or [child product](#) extraction. The format will be identical for all ASAR image products, whether they are stand-alone, [slice](#) , archived striplice, or child

products extracted from a stripline. The description of the image product SPH is shown below:

Note that the symbol " " is used throughout this handbook to denote a blank space.

Table 6.47 ASAR Image Products SPH

## ASAR Image Products SPH

#	Description	Units	Count	Type	Size
Data Record					
0	sph_descriptor_title SPH_DESCRIPTOR=	keyword	1	AsciiString	15 byte(s)
1	quote_1 quotation mark ("")	ascii	1	AsciiString	1 byte(s)
2	sph_descriptor SPH Descriptor ASCII string describing the product	ascii	1	AsciiString	28 byte(s)
3	quote_2 quotation mark ("")	ascii	1	AsciiString	1 byte(s)
4	newline_char_1 newline character	terminator	1	AsciiString	1 byte(s)
5	strip_cont_ind_title STRIPLINE_CONTINUITY_INDICATOR=	keyword	1	AsciiString	31 byte(s)
6	stripline_continuity_indicator Strip line continuity indicator Value = +000 for no stripline, otherwise is incremented for each stripline product in the orbit	-	1	Ac	4 byte(s)
7	newline_char_101 newline character	terminator	1	AsciiString	1 byte(s)
8	slice_pos_title SLICE_POSITION=	keyword	1	AsciiString	15 byte(s)
9	slice_position Slice position in the stripline Value: +001 to NUM_SLICES, Set to +001 if not stripline	-	1	Ac	4 byte(s)
10	newline_char_102 newline character	terminator	1	AsciiString	1 byte(s)
11	num_slices_title NUM_SLICES=	keyword	1	AsciiString	11 byte(s)
12	num_slices Number of slices in the stripline. Default = +001 for non-stripline product	-	1	Ac	4 byte(s)
13	newline_char_103 newline character	terminator	1	AsciiString	1 byte(s)
14	first_line_time_title FIRST_LINE_TIME=	keyword	1	AsciiString	16 byte(s)
15	quote_3 quotation mark ("")	ascii	1	AsciiString	1 byte(s)
16	first_line_time First Zero Doppler Azimuth time of product UTC Time of first range line in the MDS of this product.	UTC	1	UtcExternal	27 byte(s)
17	quote_4 quotation mark ("")	ascii	1	AsciiString	1 byte(s)
18	newline_char_2 newline character	terminator	1	AsciiString	1 byte(s)
19	last_line_time_title LAST_LINE_TIME=	keyword	1	AsciiString	15 byte(s)
20	quote_5	ascii	1	AsciiString	1 byte(s)

#	Description	Units	Count	Type	Size
	quotation mark ("")				
21	last_line_time Last Zero Doppler Azimuth time of product Time of last range line in the MDS of this product.	UTC	1	UtcExternal	27 byte(s)
22	quote_6 quotation mark ("")	ascii	1	AsciiString	1 byte(s)
23	newline_char_3 newline character	terminator	1	AsciiString	1 byte(s)
24	first_near_lat_title FIRST_NEAR_LAT=	keyword	1	AsciiString	15 byte(s)
25	first_near_lat Geodetic Latitude of the first sample of the first line A negative value denotes south latitude, a positive value denotes North latitude	(1e-6) degrees	1	AsciiGeoCoordinate	11 byte(s)
26	first_near_lat_units <10-6degN>	units	1	AsciiString	10 byte(s)
27	newline_char_4 newline character	terminator	1	AsciiString	1 byte(s)
28	first_near_long_title FIRST_NEAR_LONG=	keyword	1	AsciiString	16 byte(s)
29	first_near_long East geodetic longitude of the first sample of the first line.Positive values East of Greenwich, negative values west of Greenwich.	(1e-6) degrees	1	AsciiGeoCoordinate	11 byte(s)
30	first_near_long_units <10-6degE>	units	1	AsciiString	10 byte(s)
31	newline_char_5 newline character	terminator	1	AsciiString	1 byte(s)
32	first_mid_lat_title FIRST_MID_LAT=	keyword	1	AsciiString	14 byte(s)
33	first_mid_lat Geodetic Latitude of the middle sample of the first line A negative value denotes south latitude, a positive value denotes North latitude	(1e-6) degrees	1	AsciiGeoCoordinate	11 byte(s)
34	first_mid_lat_units <10-6degN>	units	1	AsciiString	10 byte(s)
35	newline_char_6 newline character	terminator	1	AsciiString	1 byte(s)
36	first_mid_long_title FIRST_MID_LONG=	keyword	1	AsciiString	15 byte(s)
37	first_mid_long East geodetic longitude of the middle sample of the first line.Positive values East of Greenwich, negative values west of Greenwich.	(1e-6) degrees	1	AsciiGeoCoordinate	11 byte(s)
38	first_mid_long_units <10-6degE>	units	1	AsciiString	10 byte(s)
39	newline_char_7 newline character	terminator	1	AsciiString	1 byte(s)
40	first_far_lat_title FIRST_FAR_LAT=	keyword	1	AsciiString	14 byte(s)
41	first_far_lat Geodetic Latitude of the last sample of the first line A negative value denotes south latitude, a positive value denotes North latitude	(1e-6) degrees	1	AsciiGeoCoordinate	11 byte(s)
42	first_far_lat_units <10-6degN>	units	1	AsciiString	10 byte(s)
43	newline_char_8 newline character	terminator	1	AsciiString	1 byte(s)
44	first_far_long_title FIRST_FAR_LONG=	keyword	1	AsciiString	15 byte(s)
45	first_far_long East geodetic longitude of the last sample of the first line.Positive values East of Greenwich, negative values west of Greenwich.	(1e-6) degrees	1	AsciiGeoCoordinate	11 byte(s)
46	first_far_long_units <10-6degE>	units	1	AsciiString	10 byte(s)
47	newline_char_9 newline character	terminator	1	AsciiString	1 byte(s)
48	last_near_lat_title LAST_NEAR_LAT=	keyword	1	AsciiString	14 byte(s)
49	last_near_lat Geodetic Latitude of the first sample of the last line A negative value denotes south latitude, a positive value denotes North latitude	(1e-6) degrees	1	AsciiGeoCoordinate	11 byte(s)
50	last_near_lat_units <10-6degN>	units	1	AsciiString	10 byte(s)
51	newline_char_10 newline character	terminator	1	AsciiString	1 byte(s)
52	last_near_long_title	keyword	1	AsciiString	15 byte(s)

#	Description	Units	Count	Type	Size
	LAST_NEAR_LONG=				
53	last_near_long East geodetic longitude of the first sample of the last line. Positive values East of Greenwich, negative values west of Greenwich.	(1e-6) degrees	1	AsciiGeoCoordinate	11 byte(s)
54	last_near_long_units <10-6degE>	units	1	AsciiString	10 byte(s)
55	newline_char_11 newline character	terminator	1	AsciiString	1 byte(s)
56	last_mid_lat_title LAST_MID_LAT=	keyword	1	AsciiString	13 byte(s)
57	last_mid_lat Geodetic Latitude of the middle sample of the last line A negative value denotes south latitude, a positive value denotes North latitude A negative value denotes south latitude, a positive value denotes North latitude	(1e-6) degrees	1	AsciiGeoCoordinate	11 byte(s)
58	last_mid_lat_units <10-6degN>	units	1	AsciiString	10 byte(s)
59	newline_char_12 newline character	terminator	1	AsciiString	1 byte(s)
60	last_mid_long_title LAST_MID_LONG=	keyword	1	AsciiString	14 byte(s)
61	last_mid_long East geodetic longitude of the middle sample of the last line. Positive values East of Greenwich, negative values west of Greenwich.	(1e-6) degrees	1	AsciiGeoCoordinate	11 byte(s)
62	last_mid_long_units <10-6degE>	units	1	AsciiString	10 byte(s)
63	newline_char_13 newline character	terminator	1	AsciiString	1 byte(s)
64	last_far_lat_title LAST_FAR_LAT=	keyword	1	AsciiString	13 byte(s)
65	last_far_lat Geodetic Latitude of the last sample of the last line A negative value denotes south latitude, a positive value denotes North latitude A negative value denotes south latitude, a positive value denotes North latitude	(1e-6) degrees	1	AsciiGeoCoordinate	11 byte(s)
66	last_far_lat_units <10-6degN>	units	1	AsciiString	10 byte(s)
67	newline_char_14 newline character	terminator	1	AsciiString	1 byte(s)
68	last_far_long_title LAST_FAR_LONG=	keyword	1	AsciiString	14 byte(s)
69	last_far_long East geodetic longitude of the last sample of the last line. Positive values East of Greenwich, negative values west of Greenwich.	(1e-6) degrees	1	AsciiGeoCoordinate	11 byte(s)
70	last_far_long_units <10-6degE>	units	1	AsciiString	10 byte(s)
71	newline_char_15 newline character	terminator	1	AsciiString	1 byte(s)
72	spare_1 Spare	-	1	SpareField	36 byte(s)
73	swath_title SWATH=	keyword	1	AsciiString	6 byte(s)
74	quote_7 quotation mark ("")	ascii	1	AsciiString	1 byte(s)
75	swath Swath number IS1, IS2, IS3, IS4, IS5, IS6, or IS7 for IM, and AP modes. Set to WS for WS and GM modes.	ascii	1	AsciiString	3 byte(s)
76	quote_8 quotation mark ("")	ascii	1	AsciiString	1 byte(s)
77	newline_char_17 newline character	terminator	1	AsciiString	1 byte(s)
78	pass_title PASS=	keyword	1	AsciiString	5 byte(s)
79	quote_9 quotation mark ("")	ascii	1	AsciiString	1 byte(s)
80	pass Ascending or descending orbit designator (defined at start of time pass) ASCENDING , DESCENDING or FULL_ORBIT	ascii	1	AsciiString	10 byte(s)
81	quote_10 quotation mark ("")	ascii	1	AsciiString	1 byte(s)
82	newline_char_18 newline character	terminator	1	AsciiString	1 byte(s)
83	sample_type_title	keyword	1	AsciiString	12 byte(s)

#	Description	Units	Count	Type	Size
	SAMPLE_TYPE=				
84	quote_11 quotation mark ("")	ascii	1	AsciiString	1 byte(s)
85	sample_type Detected or complex sample type designator DETECTED or COMPLEX	ascii	1	AsciiString	8 byte(s)
86	quote_12 quotation mark ("")	ascii	1	AsciiString	1 byte(s)
87	newline_char_19 newline character	terminator	1	AsciiString	1 byte(s)
88	algorithm_title ALGORITHM=	keyword	1	AsciiString	10 byte(s)
89	quote_13 quotation mark ("")	ascii	1	AsciiString	1 byte(s)
90	algorithm Processing Algorithm Used RAN/DOP or SPECAN	ascii	1	AsciiString	7 byte(s)
91	quote_14 quotation mark ("")	ascii	1	AsciiString	1 byte(s)
92	newline_char_20 newline character	terminator	1	AsciiString	1 byte(s)
93	mds1_polar_title MDS1_TX_RX_POLAR=	keyword	1	AsciiString	17 byte(s)
94	quote_15 quotation mark ("")	ascii	1	AsciiString	1 byte(s)
95	mds1_tx_rx_polar Transmitter / Receiver Polarisation for MDS1 H/V or H/H or V/H or V/V	ascii	1	AsciiString	3 byte(s)
96	quote_16 quotation mark ("")	ascii	1	AsciiString	1 byte(s)
97	newline_char_21 newline character	terminator	1	AsciiString	1 byte(s)
98	mds2_polar_title MDS2_TX_RX_POLAR=	keyword	1	AsciiString	17 byte(s)
99	quote_17 quotation mark ("")	ascii	1	AsciiString	1 byte(s)
100	mds2_tx_rx_polar Transmitter/ Receiver Polarisation for MDS2 H/V or H/H or V/H or V/V or blank ( ) for all modes with only one MDS.	ascii	1	AsciiString	3 byte(s)
101	quote_18 quotation mark ("")	ascii	1	AsciiString	1 byte(s)
102	newline_char_22 newline character	terminator	1	AsciiString	1 byte(s)
103	compression_title COMPRESSION=	keyword	1	AsciiString	12 byte(s)
104	quote_19 quotation mark ("")	ascii	1	AsciiString	1 byte(s)
105	compression Compression algorithm used on echo data on-board the satellite FBAQ2, FBAQ3, FBAQ4 (FBAQ: 8 bits reduced to 2, 3, and 4 bits respectively). Others: S&M4 , and NONE	ascii	1	AsciiString	5 byte(s)
106	quote_20 quotation mark ("")	ascii	1	AsciiString	1 byte(s)
107	newline_char_23 newline character	terminator	1	AsciiString	1 byte(s)
108	azimuth_looks_title AZIMUTH_LOOKS=	keyword	1	AsciiString	14 byte(s)
109	azimuth_looks Number of Looks in Azimuth	looks	1	Ac	4 byte(s)
110	newline_char_24 newline character	terminator	1	AsciiString	1 byte(s)
111	range_looks_title RANGE_LOOKS=	keyword	1	AsciiString	12 byte(s)
112	range_looks Number of Looks in Range	looks	1	Ac	4 byte(s)
113	newline_char_25 newline character	terminator	1	AsciiString	1 byte(s)
114	range_spacing_title RANGE_SPACING=	keyword	1	AsciiString	14 byte(s)
115	range_spacing Range sample spacing in meters	m	1	Afl	15 byte(s)

#	Description	Units	Count	Type	Size
116	range_spacing_units <m>	units	1	AsciiString	3 byte(s)
117	newline_char_26 newline character	terminator	1	AsciiString	1 byte(s)
118	azimuth_spacing_title AZIMUTH_SPACING=	keyword	1	AsciiString	16 byte(s)
119	azimuth_spacing Nominal azimuth sample spacing in meters	m	1	Afl	15 byte(s)
120	azimuth_spacing_units <m>	units	1	AsciiString	3 byte(s)
121	newline_char_27 newline character	terminator	1	AsciiString	1 byte(s)
122	line_time_interval_title LINE_TIME_INTERVAL=	keyword	1	AsciiString	19 byte(s)
123	line_time_interval Azimuth sample spacing in time (Line Time Interval)	s	1	Afl	15 byte(s)
124	line_time_interval_units <s>	units	1	AsciiString	3 byte(s)
125	newline_char_28 newline character	terminator	1	AsciiString	1 byte(s)
126	line_length_title LINE_LENGTH=	keyword	1	AsciiString	12 byte(s)
127	line_length Number of samples per output line (includes zero filled samples) If a complex product, 1 sample = 1 I,Q pair, for a detected product, 1 sample = 1 pixel.	samples	1	As	6 byte(s)
128	line_length_units <samples>	units	1	AsciiString	9 byte(s)
129	newline_char_29 newline character	terminator	1	AsciiString	1 byte(s)
130	data_type_title DATA_TYPE=	keyword	1	AsciiString	10 byte(s)
131	quote_21 quotation mark ("")	ascii	1	AsciiString	1 byte(s)
132	data_type Output data type SWORD, UWORLD, or UBYTE. The definition of a word here is a 16 bit integer	ascii	1	AsciiString	5 byte(s)
133	quote_22 quotation mark ("")	ascii	1	AsciiString	1 byte(s)
134	newline_char_30 newline character	terminator	1	AsciiString	1 byte(s)
135	spare_2 Spare	-	1	SpareField	51 byte(s)

Record Length : 1059

DS\_NAME : ASAR Image Products SPH

Format Version 114.0

Note: following field# 34, within the SPH header, are the [Data Set Descriptors \(DSDs\)](#) . What follows here are those DSDs, beginning at field# 35:

Table 6.48

## 6.6.12 Main Processing parameters

The Main Processing parameters [ADS](#) contains a summary of the parameters used to process a product that are constant over the length of the product (i.e., over the length of the [slice](#) in [stripline](#) processing). As such, one ADSR containing these

parameters, preceded by a time stamp, is issued per output product (per slice for stripline). The contents of each ADSR is shown below.

Note : the symbol " " is used to denote a blank space throughout this handbook.

Table 6.49 Main Processing parameters

## Main Processing parameters

#	Description	Units	Count	Type	Size
Data Record					
0	first_zero_doppler_time First Zero Doppler Azimuth time of MDS which this data set describesTime of first range line in the MDS described by this data set	MJD	1	mjd	12 byte(s)
1	attach_flag Attachment Flag Always set to zero for this ADSR	flag	1	BooleanFlag	1 byte(s)
2	last_zero_doppler_time Last Zero Doppler Azimuth time of MDS which this data set describesTime of last range line in the MDS described by this data set	MJD	1	mjd	12 byte(s)
3	work_order_id Work Order ID (left-justified)	ascii	1	AsciiString	12 byte(s)
4	time_diff Time difference between sensing time of first input line and zero Doppler time of first output image line (tdelta). May be used during child product extraction from a stripline product. Left blank (set to zero) for non-stripline products	s	1	fl	4 byte(s)
5	swath_num Swath number IS1, IS2, IS3, IS4, IS5, IS6, or IS7 for IM, WV and AP modes. SS1, SS2, SS3, SS4, SS5 for WSS Products. WS0 for WS and GM modes where only one ADSR for the whole scene is provided	ascii	1	AsciiString	3 byte(s)
6	range_spacing Range sample spacing	m	1	fl	4 byte(s)
7	azimuth_spacing Azimuth sample spacing at image center	m	1	fl	4 byte(s)
8	line_time_interval Azimuth sample spacing in time (Line Time Interval)	s	1	fl	4 byte(s)
9	num_output_lines Number of output range lines in the image. For WSS products this number will vary for each sub swath	lines	1	ul	4 byte(s)
10	num_samples_per_line	samples	1	ul	4 byte(s)



#	Description	Units	Count	Type	Size
	Number of samples per output range line includes zero filled samples				
11	data_type Output data type SWORD, UWORD, or UBYTE	ascii	1	AsciiString	5 byte(s)
12	num_range_lines_per_burst Number of output range lines per burst. Not used for single-beam products	lines	1	ul	4 byte(s)
13	time_diff_zero_doppler Time difference between zero Doppler time and acquisition time of output image lines	s	1	fl	4 byte(s)
14	spare_1 Spare	-	1	SpareField	43 byte(s)
15	data_analysis_flag Raw Data Analysis used for Raw Data Correction 0 = correction done using default parameters 1 = correction done using raw data analysis results	flag	1	BooleanFlag	1 byte(s)
16	ant_elev_corr_flag Antenna Elevation Pattern Correction Applied 0 = no correction applied 1 = correction applied	flag	1	BooleanFlag	1 byte(s)
17	chirp_extract_flag Reconstructed Chirp to be used (if reconstruction successful) 0 = nominal chirp replica to be used 1 = reconstructed chirp to be used	flag	1	BooleanFlag	1 byte(s)
18	srg_flag Slant Range to Ground Range Conversion Applied 0 = no conversion applied 1 = conversion applied	flag	1	BooleanFlag	1 byte(s)
19	dop_cen_flag Doppler Centroid Estimation Performed 0 = no estimation done 1 = estimation done	flag	1	BooleanFlag	1 byte(s)
20	dop_amb_flag Doppler Ambiguity Estimation Performed 0 = no estimate done 1 = estimate done	flag	1	BooleanFlag	1 byte(s)
21	range_spread_comp_flag Range-spreading loss compensation Applied 0 = no compensation applied 1 = compensation applied	flag	1	BooleanFlag	1 byte(s)
22	detected_flag Detection Applied 0 = output product is complex 1 = output product was detected	flag	1	BooleanFlag	1 byte(s)
23	look_sum_flag Look Summation Performed 0 = product is single look 1 = product is multi-looked	flag	1	BooleanFlag	1 byte(s)
24	rms_equal_flag RMS Equalisation performed 0= rms equalization not performed during FBAQ decoding, 1 = rms equalization performed during FBAQ decoding	flag	1	BooleanFlag	1 byte(s)
25	ant_scal_flag Antenna Elevation Gain Scaling Factor applied 0= no scaling factor applied, 1 = scaling factor applied	flag	1	BooleanFlag	1 byte(s)
26	vga_com_echo_flag Receive Gain Droop Compensation applied to Echo. 0=no compression, 1=compensation applied.	flag	1	BooleanFlag	1 byte(s)
27	vga_com_cal_flag Receive Gain Droop Compensation applied to Calibration Pulse P2. 0=no compression, 1=compensation applied.	flag	1	BooleanFlag	1 byte(s)
28	vga_com_nom_time_flag Nominal time delay applied for Receive Gain Droop Compensation of Calibration Pulse P2 order zero. 0=do not use nominal time delay (compensation depends on P2 time delay), 1 = use nominal time delay (constant)	flag	1	BooleanFlag	1 byte(s)
29	gm_range_comp_inverse_filter_flag Inverse filter used for range compression. (GM Mode only). 0 = matched filter used for range compression 1 = inverse filter used for range compression	flag	1	BooleanFlag	1 byte(s)
30	spare_2 Spare	-	1	SpareField	6 byte(s)
31	raw_data_analysis The following 26 parameters form a structure which is repeated twice, once for MDS 1 and once for MDS 2 If MDS 2 is not included with the product the second set of values is blanked (all values set to zero)	-	2	raw_data_analysisStruct	2*92.0 byte(s)
	a	num_gaps Number of input data gaps (a gap is defined as a predetermined number of range lines)	gaps	1	ul 4 byte(s)
	b	num_missing_lines	lines	1	ul 4 byte(s)

#	Description		Units	Count	Type	Size
	Number of missing lines, excluding data gaps					
c	range_samp_skip Range sample skipping factor for raw data analysis		samples	1	ul	4 byte(s)
d	range_lines_skip Range lines skipping factor for raw data analysis		lines	1	ul	4 byte(s)
e	calc_i_bias Calculated I channel bias		-	1	fl	4 byte(s)
f	calc_q_bias Calculated Q channel bias		-	1	fl	4 byte(s)
g	calc_i_std_dev Calculated I channel standard deviation		-	1	fl	4 byte(s)
h	calc_q_std_dev Calculated Q channel standard deviation		-	1	fl	4 byte(s)
i	calc_gain Calculated I/Q gain imbalance		-	1	fl	4 byte(s)
j	calc_quad Calculated I/Q quadrature departure		-	1	fl	4 byte(s)
k	i_bias_max I bias upper bound		-	1	fl	4 byte(s)
l	i_bias_min I bias lower bound		-	1	fl	4 byte(s)
m	q_bias_max Q bias upper bound		-	1	fl	4 byte(s)
n	q_bias_min Q bias lower bound		-	1	fl	4 byte(s)
o	gain_min I/Q gain lower bound		-	1	fl	4 byte(s)
p	gain_max I/Q gain upper bound		-	1	fl	4 byte(s)
q	quad_min I/Q quadrature departure lower bound		-	1	fl	4 byte(s)
r	quad_max I/Q quadrature departure upper bound		-	1	fl	4 byte(s)
s	i_bias_flag I bias significance0 = I bias falls within acceptable range1 = I bias falls outside acceptable range		flag	1	BooleanFlag	1 byte(s)
t	q_bias_flag Q bias Significance0 = Q bias falls within acceptable range1 = Q bias falls outside acceptable range		flag	1	BooleanFlag	1 byte(s)
u	gain_flag I/Q Gain Significance0 = Gain falls within acceptable range1 = Gain falls outside acceptable range		flag	1	BooleanFlag	1 byte(s)
v	quad_flag I/Q Quadrature Departure Significance0 = Quadrature departure falls within acceptable range1 = Quadrature departure falls outside acceptable range		flag	1	BooleanFlag	1 byte(s)
w	used_i_bias I channel bias used for correction (may be different from measured value)		-	1	fl	4 byte(s)
x	used_q_bias Q channel bias used for correction (may be different from measured value)		-	1	fl	4 byte(s)
y	used_gain		-	1	fl	4 byte(s)

#	Description			Units	Count	Type	Size
32		I/Q gain imbalance used for correction(may be different from measured value)					
	z	used_quad I/Q quadrature departure used for correction(may be different from measured value)	-		1	fl	4 byte(s)
32	spare_3 Spare			-	1	SpareField	32 byte(s)
33	start_time  The following 2 parameters form a structure which is repeated twice. Once for values pertaining to MDS 1 and once for values pertaining to MDS 2. If MDS 2 is not included in the product the fields in the second group are blanked (all values are set to zero).			-	2	start_timeStruct	2*20.0 byte(s)
34	a	first_obi On-board binary time of first input line processedLSB accurate to 15.26 ms. (Contained in two long integers)	-		2	ul	2*4 byte(s)
	b	first_mjd Sensing time (MJD format) of first input line processedconverted from satellite binary time	MJD		1	mjd	12 byte(s)
34	parameter_codes  Following fields each contain room for 5 values  Only one value is filled for each for IM and WV modes. Two values are filled (MDS1 and MDS2) if 2 MDSs are included in the product. Five values are filled for WS and GM modes (for SS1 to SS5, respectively). Unused values are set to zero			-	1	parameter_codesStruct	120.0 byte(s)
35	a	swst_code Sampling Window Start time code of first processed line	code	5	us		5*2 byte(s)
	b	last_swst_code Sampling Window Start time code of last processed line	code	5	us		5*2 byte(s)
	c	pri_code Pulse Repetition Interval code	code	5	us		5*2 byte(s)
	d	tx_pulse_len_code Tx pulse length	code	5	us		5*2 byte(s)
	e	tx_bw_code Tx pulse bandwidth	code	5	us		5*2 byte(s)
	f	echo_win_len_code Echo Window Length	code	5	us		5*2 byte(s)
	g	up_code Upconverter Level - Upconverter gain set on the instrument	code	5	us		5*2 byte(s)
	h	down_code Downconverter Level - Downconverter gain set on the instrument	code	5	us		5*2 byte(s)
	i	resamp_code Resampling factor for echo data	code	5	us		5*2 byte(s)
	j	beam_adj_code Beam adjustment delta	code	5	us		5*2 byte(s)
	k	beam_set_num_code Antenna Beam Set Number	code	5	us		5*2 byte(s)
	l	tx_monitor_code Auxiliary Tx Monitor Level	code	5	us		5*2 byte(s)
35	spare_4 Spare			-	1	SpareField	60 byte(s)
36	error_counters			-	1	error_countersStruct	40.0 byte(s)



#	Description		Units	Count	Type	Size
	Error counters					
	Each input line is analyzed for errors in the header using a majority polling technique. Errors are logged for each field of the header in the fields below.					
	a	num_err_swst Number of errors detected in Sampling Window start time field.	-	1	ul	4 byte(s)
	b	num_err_pri Number of errors detected in PRI code field	-	1	ul	4 byte(s)
	c	num_err_tx_pulse_len Number of errors detected in Tx pulse length field	-	1	ul	4 byte(s)
	d	num_err_tx_pulse_bw Number of errors detected in Tx pulse bandwidth field.	-	1	ul	4 byte(s)
	e	num_err_echo_win_len Number of errors detected in Echo Window Length field.	-	1	ul	4 byte(s)
	f	num_err_up Number of errors detected in Upconverter Level field.	-	1	ul	4 byte(s)
	g	num_err_down Number of errors detected in Downconverter Level field.	-	1	ul	4 byte(s)
	h	num_err_resamp Number of errors detected in Resampling factor for echo data field.	-	1	ul	4 byte(s)
	i	num_err_beam_adj Number of errors detected in Beam adjustment delta field.	-	1	ul	4 byte(s)
	j	num_err_beam_set_num Number of errors detected in Antenna Beam Set Number field.	-	1	ul	4 byte(s)
37	spare_5 Spare		-	1	SpareField	26 byte(s)
38	image_parameters Image Data Set parameters Following fields each contain room for 5 values. Only one value is filled for each for IM and WV modes. Two values are filled (MDS1 and MDS2) if 2 MDSs are included in the product. Five values are filled for WS and GM modes (for SS1 to SS5, respectively). Unused values are set to zero		-	1	image_parametersStruct	270.0 byte(s)
	a	swst_value Sampling Window Start time of first processed line	s	5	fl	5*4 byte(s)
	b	last_swst_value Sampling Window Start time of last processed line	s	5	fl	5*4 byte(s)
	c	swst_changes Number of Sample Window Start Time changes within a beam	-	5	ul	5*4 byte(s)
	d	prf_value Pulse Repetition Frequency	Hz	5	fl	5*4 byte(s)
	e	tx_pulse_len_value Tx pulse length	s	5	fl	5*4 byte(s)
	f	tx_pulse_bw_value Tx pulse bandwidth	Hz	5	fl	5*4 byte(s)
	g	echo_win_len_value Echo Window Length	s	5	fl	5*4 byte(s)
	h	up_value Upconverter Level - Upconverter gain set on the instrument	dB	5	fl	5*4 byte(s)
	i	down_value	dB	5	fl	5*4 byte(s)

#	Description			Units	Count	Type	Size
39		Downconverter Level - Downconverter gain set on the instrument					
	j	resamp_value Resampling factor	-	5	fl	5*4 byte(s)	
	k	beam_adj_value Beam adjustment delta	deg.	5	fl	5*4 byte(s)	
	l	beam_set_value Antenna Beam Set Number	-	5	us	5*2 byte(s)	
	m	tx_monitor_value Auxiliary Tx Monitor Level	-	5	fl	5*4 byte(s)	
	n	rank Number of PRI between transmitted pulse and return echo	-	5	ul	5*4 byte(s)	
39	spare_6 Spare			-	1	SpareField	62 byte(s)
40	first_proc_range_samp First processed input range sample, first sample is 1			samples	1	ul	4 byte(s)
41	range_ref Range spreading loss reference range			m	1	fl	4 byte(s)
42	range_samp_rate Range sampling rate			Hz	1	fl	4 byte(s)
43	radar_freq Radar Frequency			Hz	1	fl	4 byte(s)
44	num_looks_range Number of range looks			looks	1	us	2 byte(s)
45	filter_range Matched filter window type HAMMING or KAISER or NONE			ascii	1	AsciiString	7 byte(s)
46	filter_coef_range Window coefficient for range-matched filter			-	1	fl	4 byte(s)
47	bandwidth Bandwidth Following fields each contain room for 5 values. Only one value is filled for each for AP, IM, and WV modes. Five values are filled for WS and GM modes (for SS1 to SS5, respectively). Unused values are set to zero			-	1	bandwidthStruct	40.0 byte(s)
48	a	look_bw_range Range Look Bandwidth (null to null)	Hz	5	fl	5*4 byte(s)	
	b	tot_bw_range Total processed range bandwidth (null to null)	Hz	5	fl	5*4 byte(s)	
48	nominal_chirp Nominal Chirp Following 2 parameters form a structure which is repeated 5 times (one set for each WS beam, SS1 first, to SS5 last -- only one set of values given for narrow swath images)			-	5	nominal_chirpStruct	5*32.0 byte(s)
49	a	nom_chirp_amp 4 nominal chirp amplitude coefficients	-, s-1, s-2, s-3	4	fl	4*4 byte(s)	
	b	nom_chirp_phs 4 nominal chirp phase coefficients	cycles,Hz,Hz/s,Hz/s2	4	fl	4*4 byte(s)	
49	spare_7 Spare			-	1	SpareField	60 byte(s)
50	num_lines_proc Number of input lines processed			lines	1	ul	4 byte(s)
51	num_look_az Number of Azimuth Looks			looks	1	us	2 byte(s)
52	look_bw_az Azimuth Look Bandwidth (null to null)			Hz	1	fl	4 byte(s)
53	to_bw_az Processed Azimuth bandwidth (null to null)			Hz	1	fl	4 byte(s)



#	Description	Units	Count	Type	Size
54	filter_az Matched filter window type HAMMING or KAISER or NONE	ascii	1	AsciiString	7 byte(s)
55	filter_coef_az Window coefficient for azimuth-matched filter	-	1	fl	4 byte(s)
56	az_fm_rate 3 co-efficients for Azimuth FM rate Azimuth FM rate = C0 + C1(tSR-t0) + C2(tSR - t0)2 tSR = 2 way slant range time	Hz/sHz/s2Hz/s3	3	fl	3*4 byte(s)
57	ax_fm_origin 2 way slant range time origin (t0) for Azimuth FM rate calculation	ns	1	fl	4 byte(s)
58	dop_amb_conf Doppler Centroid Ambiguity Confidence MeasureValue between 0 and 1, 0 = poorest confidence, 1= highest confidence	-	1	fl	4 byte(s)
59	spare_8 Spare	-	1	SpareField	68 byte(s)
60	calibration_factors Calibration factors The following 2 parameters form a structure which is repeated twice. Once for values pertaining to MDS 1 and once for values pertaining to MDS 2. If MDS 2 is not included in the product the fields in the second group are set to zero	-	2	calibration_factorsStruct	2*8.0 byte(s)
	a proc_scaling_fact Processor scaling factor	-	1	fl	4 byte(s)
	b ext_cal_fact External Calibration Scaling Factor (mode/swath/polarization dependent)	-	1	fl	4 byte(s)
61	noise_estimation Noise Estimation Following fields each contain room for 5 values. Five values are filled for WS and GM modes (for SS1 to SS5, respectively). Up to 5 values may be provided for IM mode, each one is a separate noise estimate. For AP mode, up to 4 values may be provided in the order: first estimate for MDS1, second estimate for MDS1, first estimate for MDS2, second estimate for MDS2. For WV, there is one estimate provided.	-	1	noise_estimationStruct	40.0 byte(s)
	a noise_power_corr Noise power correction factors	-	5	fl	5*4 byte(s)
	b num_noise_lines Number of noise lines used to calculate factors	-	5	ul	5*4 byte(s)
62	spare_9 Spare	-	1	SpareField	64 byte(s)
63	spare_10 Spare	-	1	SpareField	12 byte(s)
64	output_statistics Output Data Statistics The following 4 parameters form a structure which is repeated twice. Once for values pertaining to MDS 1 and once for values pertaining to MDS 2. If MDS 2 is not included in the product the fields in the second group are set to zero.	-	2	output_statisticsStruct	2*16.0 byte(s)
	a out_mean Output data mean Magnitude for detected products, real sample mean for SLC products	-	1	fl	4 byte(s)
	b out_imag_mean Output imaginary data mean Used for SLC products only (set to zero otherwise)	-	1	fl	4 byte(s)
	c out_std_dev Output data standard deviation Magnitude std. dev. for detected products, real sample std. dev. for SLC products	-	1	fl	4 byte(s)
	d out_imag_std_dev Output imaginary data standard deviation Used for SLC products only (set to zero otherwise)	-	1	fl	4 byte(s)



#	Description	Units	Count	Type	Size	
65	avg_scene_height_ellipsoid Average scene height above ellipsoid used for processing	m	1	fl	4 byte(s)	
66	spare_11 Spare	-	1	SpareField	48 byte(s)	
67	echo_comp Compression Method used for echo samples FBAQ, S&M ,NONE	ascii	1	AsciiString	4 byte(s)	
68	echo_comp_ratio Compression Ratio for echo samples8/4, 8/3, 8/2, or 8/8	ascii	1	AsciiString	3 byte(s)	
69	init_cal_comp Compression Method used for initial calibration samples FBAQ, S&M ,NONE	ascii	1	AsciiString	4 byte(s)	
70	init_cal_ratio Compression Ratio for initial calibration samples8/4, 8/3, 8/2, or 8/8	ascii	1	AsciiString	3 byte(s)	
71	per_cal_comp Compression Method used for periodic calibration samples FBAQ, S&M ,NONE	ascii	1	AsciiString	4 byte(s)	
72	per_cal_ratio Compression Ratio for periodic calibration samples8/4, 8/3, 8/2, or 8/8	ascii	1	AsciiString	3 byte(s)	
73	noise_comp Compression Method used for noise samples FBAQ, S&M ,NONE	ascii	1	AsciiString	4 byte(s)	
74	noise_comp_ratio Compression Ratio for noise samples8/4, 8/3, 8/2, or 8/8	ascii	1	AsciiString	3 byte(s)	
75	spare_12 Spare	-	1	SpareField	64 byte(s)	
76	beam_overlap Number of slant range samples in beam merging One value per merge region (1-2, 2-3, 3-4, 4-5). This parameter is equivalent to N in the following beam merging formula: xmerged(n) = (1 - (n/N)P * xnear(n)) + ((n/N)P * xfar(n))	-	4	ul	4*4 byte(s)	
77	beam_param Beam merge algorithm parameter used for beam merging One value per merge region (1-2, 2-3, 3-4, 4-5). This parameter is equivalent to P in the above beam merging formula, and different values have the following effect: P = 1, linear weighting of the two beams (near and far). P = -1, (which represents infinity in the beam merging formula) only near beam contributes to the merged one P = 0, only far beam contributes to the merged one P > 1, near beam is favoured 0 < P < 1, far beam is favoured.	-	4	fl	4*4 byte(s)	
78	lines_per_burst Number of lines per burst for this image. 5 values for beams SS1 to SS5 in WS and GM modes. Two values for AP mode, all others set to zero.	lines	5	ul	5*4 byte(s)	
79	time_first_SS1_echo Time of first SS1 Echo Source Packet	mjd	1	mjd	12 byte(s)	
80	spare_13 Spare	-	1	SpareField	16 byte(s)	
81	orbit_state_vectors Orbit State Vectors Information The following 7 parameters form a structure which is repeated 5 times, thus allowing the inclusion of up to 5 orbit state vectors which span the scene (or slice) to which this ADSR pertains.	-	5	orbit_state_vectorsStruct	5*36.0 byte(s)	
	a	state_vect_time_1 Time of state vector	MJD	1	mjd	12 byte(s)
	b	x_pos_1 X position in Earth fixed reference frame	10 -2m	1	sl	4 byte(s)
	c	y_pos_1 Y position in Earth fixed reference frame	10 -2m	1	sl	4 byte(s)
	d	z_pos_1 Z position in Earth fixed reference frame	10 -2m	1	sl	4 byte(s)
	e	x_vel_1 X velocity relative to Earth fixed reference frame	10 -5m/s	1	sl	4 byte(s)
	f	y_vel_1 Y velocity relative to Earth fixed reference frame	10 -5m/s	1	sl	4 byte(s)
	g	z_vel_1 Z velocity relative to Earth fixed reference	10 -5m/s	1	sl	4 byte(s)

#	Description		Units	Count	Type	Size
	frame					
82	spare_14 Spare		-	1	SpareField	64 byte(s)

Record Length : 2009

DS\_NAME : Main Processing parameters

Format Version 114.0

## 6.6.13 Map Projection parameters

If geocoding of the data set is performed (i.e., data is resampled to a map projection ), a GADS containing all necessary information to describe the map projection used is included. Geocoding is only performed for stand-alone products .

The PF-ASAR processor supports 6 map projections:

1. Universal Transverse Mercator (UTM)
2. Universal Polar Stereographic (UPS)
3. Lambert Conformal Conic (LCC)
4. Transverse Mercator (TM)
5. Mercator (MERC)
6. Polar Stereographic (PS)

Therefore, the values given for the map descriptor in Field# 1, in the layout for the ASAR\_Map\_GADS that is provided below, will be one of the following:

1. UNIVERSAL\_TRANSVERSE\_MERCATOR
2. UNIVERSAL\_POLAR\_STEREOGRAPHIC
3. LAMBERT\_CONFORMAL\_CONIC
4. TRANSVERSE\_MERCATOR
5. MERCATOR
6. POLAR\_STEREOGRAPHIC

where the symbol " " denotes a blank space.

Table 6.50 Map Projection parameters

# Map Projection parameters

#	Description	Units	Count	Type	Size
<b>Data Record</b>					
0	map_descriptor Map projection descriptor.	ascii	1	AsciiString	32 byte(s)
1	samples Number of samples per line	-	1	ul	4 byte(s)
2	lines Number of lines	-	1	ul	4 byte(s)
3	sample_spacing Nominal inter-sample distance	m	1	fl	4 byte(s)
4	line_spacing Nominal inter-line distance	m	1	fl	4 byte(s)
5	orientation Output scene centre orientation	deg	1	fl	4 byte(s)
6	spare_1 Spare	-	1	SpareField	40 byte(s)
7	heading Platform heading, degrees	deg	1	fl	4 byte(s)
8	ellipsoid_name Reference ellipsoid name	ascii	1	AsciiString	32 byte(s)
9	semi_major Ellipsoid semi-major axis, metres	m	1	fl	4 byte(s)
10	semi_minor Ellipsoid semi-minor axis, metres	m	1	fl	4 byte(s)
11	shift_dx Datum shift parameter referenced to Greenwich: dx (metres)	m	1	fl	4 byte(s)
12	shift_dy Datum shift parameter perpendicular to Greenwich: dy (metres)	m	1	fl	4 byte(s)
13	shift_dz Datum shift parameter direction of the rotation axis: dz (metres)	m	1	fl	4 byte(s)
14	avg_height Average scene height above ellipsoid used for geocoding	-	1	fl	4 byte(s)
15	spare_2 Spare	-	1	SpareField	12 byte(s)
16	projection_description Map projection alphanumeric description	ascii	1	AsciiString	32 byte(s)
17	utm_descriptor UTM descriptor <b>UNIVERSAL_TRANSVERSE_MERCATOR</b>	ascii	1	AsciiString	32 byte(s)
18	utm_zone UTM zone signature	ascii	1	AsciiString	4 byte(s)
19	utm_origin_easting Map origin, false easting	m	1	fl	4 byte(s)
20	utm_origin_northing Map origin, false northing	m	1	fl	4 byte(s)
21	utm_center_long Projection centre longitude, deg	(1e-6) degrees	1	GeoCoordinate	4 byte(s)
22	utm_center_lat Projection centre latitude, deg	(1e-6) degrees	1	GeoCoordinate	4 byte(s)
23	utm_para1 1st standard parallel, deg	deg	1	fl	4 byte(s)
24	utm_para2 2nd standard parallel, deg	deg	1	fl	4 byte(s)
25	utm_scale Scale factor	-	1	fl	4 byte(s)
26	ups_descriptor UPS descriptor <b>UNIVERSAL_POLAR_STEREOGRAPHIC</b>	ascii	1	AsciiString	32 byte(s)
27	ups_center_long Projection centre longitude, deg	(1e-6) degrees	1	GeoCoordinate	4 byte(s)
28	ups_center_lat Projection centre latitude, deg	(1e-6) degrees	1	GeoCoordinate	4 byte(s)



#	Description		Units	Count	Type	Size
29	ups_scale Scale factor		-	1	fl	4 byte(s)
30	nsp_descriptor NSP descriptor One of: LAMBERT_CONFORMAL_CONIC TRANSVERSE_MERCATOR MERCATOR POLAR_STEREOGRAPHIC		ascii	1	AsciiString	32 byte(s)
31	origin_easting Map origin, false easting		m	1	fl	4 byte(s)
32	origin_northing Map origin, false northing		m	1	fl	4 byte(s)
33	center_long Projection centre longitude, deg		(1e-6) degrees	1	GeoCoordinate	4 byte(s)
34	center_lat Projection centre latitude, deg		(1e-6) degrees	1	GeoCoordinate	4 byte(s)
35	standard_parallel_parameters Standard Parallel parameters		-	1	standard_parallel_parametersStruct	16.0 byte(s)
	a	para1 Latitude of first standard parallel (for Lambert Conformal Conic projection only, otherwise zero).	deg	1	fl	4 byte(s)
	b	para2 Latitude of second standard parallel (for Lambert Conformal Conic projection only, otherwise zero).	deg	1	fl	4 byte(s)
	c	spare_3 Spare	-	1	SpareField	8 byte(s)
36	central_meridian_parameters Central meridian parameters		-	1	central_meridian_parametersStruct	12.0 byte(s)
	a	central_m1 Longitude of the central meridian (or for Polar Stereographic projection Longitude down below pole of map).	deg	1	fl	4 byte(s)
	b	spare_4 Spare	-	1	SpareField	8 byte(s)
37	projection_parameters Projection dependent parameters		-	1	projection_parametersStruct	16.0 byte(s)
	a	proj1 Scale factor at central meridian (for Transverse Mercator projection only, otherwise zero).	-	1	fl	4 byte(s)
	b	spare_5 Spare	-	1	SpareField	12 byte(s)
38	position_northings_eastings Positioning Information in Northings and Eastings		-	1	position_northings_eastingsStruct	32.0 byte(s)
	a	tl_northing Top left corner northing, meters;	m	1	fl	4 byte(s)
	b	tl_easting Top left corner easting, meters;	m	1	fl	4 byte(s)
	c	tr_northing Top right corner northing, meters;	m	1	fl	4 byte(s)
	d	tr_easting Top right corner easting, meters;	m	1	fl	4 byte(s)
	e	br_northing Bottom right corner northing, meters;	m	1	fl	4 byte(s)

#	Description			Units	Count	Type	Size
	f	br_easting Bottom right corner casting, meters;	m	1	1	fl	4 byte(s)
	g	bl_northing Bottom left corner northing, meters;	m	1	1	fl	4 byte(s)
	h	bl_easting Bottom left corner easting, meters;	m	1	1	fl	4 byte(s)
39	position_lat_long Positioning Information in Latitude Longitude		-	1	position_lat_longStruct	32.0 byte(s)	
	a	tl_lat Top left corner latitude	(1e-6) degrees	1	GeoCoordinate	4 byte(s)	
	b	tl_long Top left corner longitude	(1e-6) degrees	1	GeoCoordinate	4 byte(s)	
	c	tr_lat Top right corner latitude	(1e-6) degrees	1	GeoCoordinate	4 byte(s)	
	d	tr_long Top right corner longitude	(1e-6) degrees	1	GeoCoordinate	4 byte(s)	
	e	br_lat Bottom right corner latitude	(1e-6) degrees	1	GeoCoordinate	4 byte(s)	
	f	br_long Bottom right corner longitude	(1e-6) degrees	1	GeoCoordinate	4 byte(s)	
	g	bl_lat Bottom left corner latitude	(1e-6) degrees	1	GeoCoordinate	4 byte(s)	
	h	bl_long Bottom left corner longitude	(1e-6) degrees	1	GeoCoordinate	4 byte(s)	
40	spare_6 Spare		-	1	SpareField	32 byte(s)	
41	image_to_map_coefs 8 coefficients to convert a line(L) and sample(S) position to the map projection frame of reference, say (E,N)E = A11 + A12*L + A13 *S + A14 *L*S = A21 + A22*L + A23 *S + A24 *L*S		-	8	fl	8*4 byte(s)	
42	map_to_image_coefs 8 coefficients to convert from the map projection (E,N) to line (L) and sample(S) position in the imageL = B11 + B12*E + B13 *N + B14 *E*NS = B21 + B22*E + B23 *N + B24 *E*N		-	8	fl	8*4 byte(s)	
43	spare_7 Spare		-	1	SpareField	35 byte(s)	

Record Length : 591

DS\_NAME : Map Projection parameters

Format Version 114.0

## 6.6.14 Ocean Wave Spectra

This [MDS](#) contains the [ocean wave spectrum](#) of the [imagette](#). There is one MDSR per wave cell. The format of the wave-spectrum MDS closely matches that of the [cross spectrum](#) MDS

where some fields in the cross-spectrum MDS are substituted

by new values pertaining to the ocean wave spectrum product. Each ocean wave spectrum MDSR is described below:

Table 6.51 Ocean Wave Spectra

## Ocean Wave Spectra

#	Description	Units	Count	Type	Size
Data Record					
0	zero_doppler_time First Zero Doppler Azimuth time of the wave cell. Time of first range line in the SLC Imagette MDS described by this data set	MJD	1	mjd	12 byte(s)
1	quality_flag Quality Indicator. (-1 for blank MDSR, 0 otherwise)	flag	1	BooleanFlag	1 byte(s)
2	range_spectral_res Range spectral bin size of the cartesian cross spectrum	-	1	fl	4 byte(s)
3	az_spectral_res Azimuth spectral bin size of the cartesian cross spectrum	-	1	fl	4 byte(s)
4	spare_1 Spare	-	1	SpareField	4 byte(s)
5	spec_tot_energy Spectrum Total Energy	-	1	fl	4 byte(s)
6	spec_max_energy Spectrum Max Energy	-	1	fl	4 byte(s)
7	spec_max_dir Direction of Spectrum Max (deg) Direction is given clockwise from north in the direction the wave propagates	deg	1	fl	4 byte(s)
8	spec_max_wl Wavelength of Spectrum Max (m) On higher resolution grid.	m	1	fl	4 byte(s)
9	az_image_shift_var Variance of the azimuth image shift caused by the orbital velocity	$m^2$	1	fl	4 byte(s)
10	az_cutoff Azimuthal Clutter Cut-off wavelength (m)	m	1	fl	4 byte(s)
11	nonlinear_spectral_width Spectral width of the non-linear part of the cross spectra	m	1	fl	4 byte(s)
12	image_intensity Image Intensity	-	1	fl	4 byte(s)
13	image_variance Normalised image variance	-	1	fl	4 byte(s)
14	spare_2 Spare	-	1	SpareField	56 byte(s)
15	min_spectrum Min value of ocean wave spectrum	$m^4$	1	fl	4 byte(s)
16	max_spectrum Max value of ocean wave spectrum	$m^4$	1	fl	4 byte(s)
17	spare_3 Spare	-	1	SpareField	8 byte(s)
18	wind_speed Wind speed used in the wave spectra retrieval (m/s)	m/s	1	fl	4 byte(s)
19	wind_direction Wind direction used in the wave spectra retrieval. (clockwise from north from where the wind from if confidence is 0, relative to	deg	1	fl	4 byte(s)

#	Description	Units	Count	Type	Size
	range otherwise) (deg)				
20	norm_inv_wave_age Normalised inverse wave age	-	1	fl	4 byte(s)
21	SAR_wave_height SAR swell wave height	m	1	fl	4 byte(s)
22	SAR_az_shift_var Variance of the azimuth shift computed from the SAR swell wave spectra	$m^2$	1	fl	4 byte(s)
23	backscatter Radar backscatter cross section	dB	1	fl	4 byte(s)
24	confidence_swell Confidence measure of the swell inversion. 0 = inversion successful (a unique spectrum in terms of propagation direction); 1 = inversion not successful (symmetric spectrum)	-	1	us	2 byte(s)
25	signal_to_noise Average signal-to-noise ratio	-	1	fl	4 byte(s)
26	radar_vel_corr Radar velocity off-set correction	m/s	1	fl	4 byte(s)
27	cmod_cal_const Geophysical Calibration constant - CMOD	-	1	fl	4 byte(s)
28	confidence_wind Confidence measure of the wind retrieval. 0 = external wind direction used during inversion; 1 = external wind direction not used during inversion.	-	1	us	2 byte(s)
29	spare_4 Spare	-	1	SpareField	24 byte(s)
30	ocean_spectra Ocean Wave Swell spectra polar grid. Number of bins in wavelength and direction defined in SPH (nominally 24 by 36). Arranged as 24 wavelength cells from longest to shortest wavelength, for zero degrees, then 10 degrees, up to 350 degrees (i.e clockwise direction).	-		uc	1 byte(s)

Record Length : 196

## DS\_NAME : Ocean Wave Spectra

Format Version 114.0

The ocean wave spectrum is given in the [MDS](#) as real samples distributed on a polar grid. The size of the ocean wave spectrum grid is given in the [SPH](#). Typically this will be 24 by 36 [bins](#) in [wavelength](#) and direction respectively.

The ocean wave spectrum values shall be stored in an unsigned integer format, each part linearly scaled to the maximum and minimum values of the representation (e.g., 0 to 255). The original maximum and minimum values are reported.

The detected spectrum statistics are derived from a high-resolution polar spectrum, prior to encoding for output to the product, or at other intermediate stages of the processing.

If the processor is unable to produce the ocean wave spectra for a given wave cell, the MDSR is time stamped with the time that the ocean wave spectra would have corresponded to, the [Quality Flag](#) is set to -1, and the MDSR data fields are all set

to zero.

## 6.6.15 Measurement Data Set containing spectra. 1 MDSR per spectra.

This [Measurement Data Set \(MDS\)](#) contains the [cross spectrum](#) of the [imagette](#). There is one MDSR per wave cell. The format of each MDSR is described in the table below:

Table 6.52 Measurement Data Set containing spectra. 1 MDSR per spectra

## Measurement Data Set containing spectra. 1 MDSR per spectra.

#	Description	Units	Count	Type	Size
Data Record					
0	zero_doppler_time First Zero Doppler Azimuth time of the wave cell/Time of first range line in the SLC Imagette MDS described by this data set	MJD	1	mjd	12 byte(s)
1	quality_flag Quality Indicator (-1 for blank MDSR, 0 otherwise)	flag	1	BooleanFlag	1 byte(s)
2	range_spectral_res Range bin size of the cartesian cross spectrum	-	1	fl	4 byte(s)
3	az_spectral_res Azimuth bin size of the cartesian cross spectrum	-	1	fl	4 byte(s)
4	spare_1 Spare	-	1	SpareField	4 byte(s)
5	spec_tot_energy Spectrum Total Energy	-	1	fl	4 byte(s)
6	spec_max_energy Spectrum Max Energy	-	1	fl	4 byte(s)
7	spec_max_dir Direction of Spectrum Max (deg) On higher resolution grid. Direction is counter-clockwise from satellite track heading	deg	1	fl	4 byte(s)
8	spec_max_wl Wavelength of Spectrum Max (m) On higher resolution grid	m	1	fl	4 byte(s)
9	clutter_noise Clutter Noise	-	1	fl	4 byte(s)
10	az_cutoff Azimuthal Clutter Cut-off length (m)	m	1	fl	4 byte(s)
11	num_iterations Number of iterations to compute Azimuthal Clutter Cut-off	-	1	fl	4 byte(s)
12	range_offset Range offset of peak of cross covariance function (m)	m	1	fl	4 byte(s)
13	ax_offset Azimuth offset of peak of cross covariance function (m)	m	1	fl	4 byte(s)
14	cc_range_res	m	1	fl	4 byte(s)

#	Description	Units	Count	Type	Size
	Range bin size of cross covariance function (m)				
15	cc_azimuth_res Azimuth bin size of cross covariance function (m)	m	1	fl	4 byte(s)
16	sublook_means 1st and last Sub-look Image Means	-	2	fl	2*4 byte(s)
17	sublook_variance 1st and last Sub-look Image Variance	-	2	fl	2*4 byte(s)
18	sublook_skewness 1st and last Sub-look Image Skewness	-	2	fl	2*4 byte(s)
19	sublook_kurtosis 1st and last Sub-look Image Kurtosis	-	2	fl	2*4 byte(s)
20	range_sublook_detrend_coeff 1st and last Sub-look de-trend coefficient in range	-	2	fl	2*4 byte(s)
21	az_sublook_detrend_coeff 1st and last Sub-look de-trend coefficient in azimuth	-	2	fl	2*4 byte(s)
22	min_imag Min value of Imaginary part of cross spectrum	-	1	fl	4 byte(s)
23	max_imag Max value of Imaginary part of cross spectrum	-	1	fl	4 byte(s)
24	min_real Min value of Real part of cross spectrum	-	1	fl	4 byte(s)
25	max_real Max value of Real part of cross spectrum	-	1	fl	4 byte(s)
26	spare_2 Spare	-	1	SpareField	64 byte(s)
27	real_spectra Real part of cross spectra polar grid  Number of bins in wavelength and direction defined in SPH (nominally 24 by 36). However, only 0 to 180 degree of the spectrum need be supplied (24 by 18). Arranged as: 24 wavelength values for [-5,5] deg. sector, 24 values for [5,15] deg. sector, ..., 24 values for [165,175] deg. sector, in the counter-clockwise direction. The 24 values for each sector are given in order from longest to shortest wavelength.	-		uc	1 byte(s)
28	imag_spectra Complex part of cross spectra polar grid  Number of bins in wavelength and direction defined in SPH (nominally 24 by 36). However, only 0 to 180 degrees of the spectrum need be supplied (24 by 18). Arranged as: 24 wavelength values for [-5,5] deg. sector, 24 values for [5,15] deg. sector, ..., 24 values for [165,175] deg. sector, in the counter-clockwise direction. The 24 values for each sector are given in order from longest to shortest wavelength.	-		uc	1 byte(s)

Record Length : 195

DS\_NAME : Measurement Data Set containing spectra. 1 MDSR per spectra.

Format Version 114.0

**Notes:**

The cross spectrum is given in the MDS in complex form on a polar grid. The size of the cross spectrum grid is given in the [SPH](#). Typically this will be 24 by 36 [bins in wavelength](#) and [direction](#) respectively. As the real part of the polar spectrum is symmetric, and the imaginary part is anti-symmetric, only 0 to 180 need to be given in order to reconstruct the entire spectrum (i.e., only 18 directional bins).

The cross spectrum values shall be stored in an unsigned integer format, each part linearly scaled to the maximum and minimum values of the representation (e.g., 0 to 255). The

original maximum and minimum values for each part is reported.

The cross spectrum statistics are derived from a high-resolution polar spectrum, prior to encoding for output to the product, or at other intermediate stages of the processing.

If the processor is unable to produce the cross spectra for a given wave cell, the MDSR is time stamped with the time that the cross spectra would have corresponded to, the [Quality Flag](#) is set to -1, and the MDSR data fields are all set to zero.

The format of the Wave Mode cross spectrum product is given in the section entitled "[Wave Spectra](#)". [1.59](#)

### 6.6.16 SQ ADSRs

There are two Summary Quality (SQ) [ADS](#)s. The first contains information pertaining to [MDS](#) 1 and the second contains information pertaining to MDS 2. The format of each SQ ADS is identical, however the values may differ as each describes a separate MDS.

The information contained in the SQ ADS is a summary of parameters used to establish the quality of the product. This includes [Product Confidence Data \(PCD\)](#) flags, the thresholds used to evaluate the flags, and numerical quality parameters.

For the basic image product, the SQ information ADS is updated once per product (i.e., updated once per [slice](#) for [stripline](#)). Each ADSR is time stamped with the [zero Doppler time](#) at which it was issued. The SQ ADS is included in the inventory so

that the user may evaluate the quality of the product prior to ordering.

The product statistics which are evaluated at each time stamp (each ADSR) and the error message generated will be as follows.

Table 6.53 SQ ADSRs

## SQ ADSRs

#	Description	Units	Count	Type	Size
Data Record					
0	zero_doppler_time Zero doppler time at which Summary Quality information applies	MJD	1	mjd	12 byte(s)
1	attach_flag Attachment Flag Set to 1 if all MDSRs corresponding to this ADSR are blank, set to zero otherwise. This flag will always be zero because this ADSR is updated once per slice or scene. Therefore, if there are no MDSRs, this ADSR is not produced at all.	flag	1	BooleanFlag	1 byte(s)
2	input_mean_flag Input data mean outside nominal range flag 0 = mean of I and Q input values are both within specified range from expected mean. For expected mean of x, the measured mean must fall between x-threshold to x+threshold. 1 = otherwise	flag	1	BooleanFlag	1 byte(s)
3	input_std_dev_flag Input data standard deviation outside nominal range flag 0 = standard deviation values of I and Q input values are both within specified range of expected standard deviation. For expected std. dev. x, the measured std. dev. must fall between x-threshold to x+threshold. 1 = otherwise	flag	1	BooleanFlag	1 byte(s)
4	input_gaps_flag Significant gaps in the input data flag 0 = number of input gaps <= threshold value 1 = number of input data gaps > threshold value.	flag	1	BooleanFlag	1 byte(s)
5	input_missing_lines_flag Missing lines significant flag 0 = percentage of missing lines <= threshold value 1 = percentage of missing lines > threshold value. The number of missing lines is the number of lines missing from the input data, excluding data gaps.	flag	1	BooleanFlag	1 byte(s)
6	dop_cen_flag Doppler Centroid Uncertain flag 0 = confidence measure >= specified value 1 = confidence measure < specified value. If more than one Doppler centroid estimation is performed in a slice, the flag is set if any confidence measure is less than the threshold.	flag	1	BooleanFlag	1 byte(s)
7	dop_amb_flag Doppler ambiguity estimate uncertain flag 0 = confidence measure >= specified value 1 = confidence measure < specified value	flag	1	BooleanFlag	1 byte(s)
8	output_mean_flag Output data mean outside nominal range flag 0 = mean of I and Q output values for SLC image or mean of detected pixels for a detected product, are both within specified range from expected mean. For expected mean of x, the measured mean must fall between x-threshold to x+threshold. 1 = otherwise.	flag	1	BooleanFlag	1 byte(s)
9	output_std_dev_flag Output data standard deviation outside nominal range flag 0 = mean of I and Q output values for SLC image or mean of detected pixels for a detected product, are both within specified range from expected mean. For expected mean of x, the measured mean must fall between x-threshold to x+threshold. 1 = otherwise	flag	1	BooleanFlag	1 byte(s)
10	chirp_flag Chirp extraction failed or is of low quality flag 0 = able to reconstruct all chirps or chirp reconstruction not requested (nominal chirp used) AND all quality measures were acceptable. 1 = unable to reconstruct a chirp during processing and chirp reconstruction was requested or the quality is below the acceptable levels. When value = 1, (i.e. unable to reconstruct a chirp during processing and chirp reconstruction was requested or the quality is below the acceptable levels), PF-ASAR uses the nominal range pulse for processing and a nominal elevation beam scaling factor.	flag	1	BooleanFlag	1 byte(s)
11	missing_data_sets_flag Data sets missing flag 0 = all data sets which are supposed to be in the product are present 1 = any data sets (including ADSs) are missing from the product which are supposed to be included under normal circumstances. When value = 1 (i.e any data sets, including ADSs, are missing from the product which are supposed to be included under normal circumstances), which data sets are missing can be determined by an examination of the DSDs in the SPH.	flag	1	BooleanFlag	1 byte(s)
12	invalid_downlink_flag Invalid downlink parameters flag 0 = all parameters read from the downlinked data were valid 1 = displayed if any downlink parameter is out of range and therefore a default value has been used during processing.	flag	1	BooleanFlag	1 byte(s)

#	Description	Units	Count	Type	Size
13	spare_1 Spare	-	1	SpareField	7 byte(s)
14	thresh_chirp_broadening Threshold for setting the chirp quality flag. Maximum percentage broadening permitted in cross-correlation pulse width compared to theoretical width.	%	1	fl	4 byte(s)
15	thresh_chirp_sidelobe Threshold for setting the chirp quality flag First sidelobe of the chirp cross correlation function	dB	1	fl	4 byte(s)
16	thresh_chirp_islr Threshold for setting the chirp quality flag ISLR of the chirp cross correlation function	dB	1	fl	4 byte(s)
17	thresh_input_mean Threshold for setting the mean of input data quality flag For an expected mean value of x, this is the value T, such that the measured mean must fall between the x-T and x+T.	-	1	fl	4 byte(s)
18	exp_input_mean Expected mean input value for this product for both I and Q.	-	1	fl	4 byte(s)
19	thresh_input_std_dev Threshold for setting the standard deviation of input data quality flag For an expected standard deviation value of y, this is the value D, such that the measured standard deviation must fall between the y-D and y+D.	-	1	fl	4 byte(s)
20	exp_input_std_dev Expected input std. dev. for this product for both I and Q.	-	1	fl	4 byte(s)
21	thresh_dop_cen Threshold for setting the Doppler Centroid quality flag Threshold for Doppler Centroid confidence	-	1	fl	4 byte(s)
22	thresh_dop_amb Threshold for setting the Doppler Centroid ambiguity quality flag Threshold for setting the Doppler Centroid ambiguity confidence flag	-	1	fl	4 byte(s)
23	thresh_output_mean Threshold for setting the mean of output data quality flag For an expected mean value of x, this is the value T, such that the measured mean must fall between the x-T and x+T.	-	1	fl	4 byte(s)
24	exp_output_mean Expected mean output value for this product. For an SLC product this is the expected mean of both the I and Q values.	-	1	fl	4 byte(s)
25	thresh_output_std_dev Threshold for setting the standard deviation of output data quality flag For an expected standard deviation value of y, this is the value D, such that the measured standard deviation must fall between the y-D and y+D.	-	1	fl	4 byte(s)
26	exp_output_std_dev Expected output std. dev. for this product. For an SLC product this is the expected output std. dev. for both I and Q values.	-	1	fl	4 byte(s)
27	thresh_input_missing_lines Threshold for setting the missing lines quality flag Maximum percentage of missing lines to total lines.	%	1	fl	4 byte(s)
28	thresh_input_gaps Threshold for setting the missing gaps quality flag Maximum number of missing gaps allowed.	-	1	fl	4 byte(s)
29	lines_per_gaps Number of missing lines which constitute a gap	lines	1	ul	4 byte(s)
30	spare_2 Spare	-	1	SpareField	15 byte(s)
31	input_mean Input data mean I channel, Q channel	-	2	fl	2*4 byte(s)
32	input_std_dev Input data standard deviation I channel, Q channel	-	2	fl	2*4 byte(s)
33	num_gaps Number of gaps Composed of a predetermined number of consecutive missing lines	-	1	fl	4 byte(s)
34	num_missing_lines Number of missing lines Excluding gaps	-	1	fl	4 byte(s)
35	output_mean Output data mean For SLC products, first value is for the I channel, second is for the Q channel. For detected products, second value is set to zero	-	2	fl	2*4 byte(s)
36	output_std_dev Output data standard deviation For SLC products, first value is for the I channel, second is for the Q channel. For	-	2	fl	2*4 byte(s)

---

#	Description	Units	Count	Type	Size
	detected products, second value is set to zero				
37	tot_errors Total number of errors detected in isp headers	-	1	ul	4 byte(s)
38	Spare_3 Spare	-	1	SpareField	16 byte(s)

Record Length : 170

DS\_NAME : SQ ADSRs

Format Version 114.0

Note : Each of these fields (#15, 16 and 17 ) will all contain values for the " Threshold for setting the chirp quality flag " . A [chirp](#) is reconstructed from information in the downlink , which is then validated against a theoretical chirp, which generates a number of quality measures. These quality measures are then compared to thresholds to determine if the reconstructed chirp is OK

---

### 6.6.17 Slant Range to Ground Range conversion parameters

The [Slant Range-to-Ground Range \(SR/GR\)](#) conversion coefficients may be updated more than once per product (or [slice](#) ). Each update is time stamped with the [zero Doppler time](#) to which the update applies. For [stripline](#) products, the updates occur once for each [granule](#) . The SR/GR coefficients used on [range lines](#) between two updates are found by linear interpolation between the updated and previous values. The contents of each update (each update is a single ADSR within the [ADS](#) ) are as follows. This ADS is not included for [SLC](#) products for which SR/GR conversion is not performed, or for [Geocoded](#) products.

Table 6.54 Slant Range to Ground Range conversion parameters

## Slant Range to Ground Range conversion parameters

#	Description	Units	Count	Type	Size
Data Record					
0	zero_doppler_time Zero Doppler Time in azimuth from which parameters apply	MJD	1	mjd	12 byte(s)
1	attach_flag Attachment Flag Always set to zero for this ADSR	flag	1	BooleanFlag	1 byte(s)
2	slant_range_time 2 way slant range time to first range sample	ns	1	fl	4 byte(s)
3	ground_range_origin Ground range origin of the polynomial (GR0) Measured from the first pixel of the line	m	1	fl	4 byte(s)
4	sgr_coeff The coefficients S0, S1, S2, S3, and S4 of the ground range to slant range conversion polynomial. Slant range = S0 + S1(GR-GR0) + S2(GR-GR0)^2 + S3(GR-GR0)^3 + S4(GR-GR0)^4, where GR is the ground range distance from the first pixel of the range line.	m, -, m-1, m-2	5	fl	5*4 byte(s)
5	spare_1 Spare	-	1	SpareField	14 byte(s)

Record Length : 55

DS\_NAME : Slant Range to Ground Range conversion parameters

Format Version 114.0

## 6.6.18 ASAR Wave Mode Products Base SPH

The ASAR [Wave Mode \(WV\) Specific Product Header \(SPH\)](#) provides only the information which applies to all wave cells within a product file. The format will be identical for all ASAR wave products, except for the [Data Set Descriptors \(DSD\)](#) sections.

The ASAR Wave Mode Products SPH contents are shown below:

Table 6.55 ASAR Wave Mode Products Base SPH

## ASAR Wave Mode Products Base SPH

#	Description	Units	Count	Type	Size
Data Record					
0	sph_descriptor_title	keyword	1	AsciiString	15 byte(s)

#	Description	Units	Count	Type	Size
	SPH_DESCRIPTOR=				
1	quote_1 quotation mark ("")	ascii	1	AsciiString	1 byte(s)
2	sph_descriptor SPH Descriptor ASCII string describing the product	ascii	1	AsciiString	28 byte(s)
3	quote_2 quotation mark ("")	ascii	1	AsciiString	1 byte(s)
4	newline_char_1 newline character	terminator	1	AsciiString	1 byte(s)
5	first_cell_time_title FIRST_CELL_TIME=	keyword	1	AsciiString	16 byte(s)
6	quote_3 quotation mark ("")	ascii	1	AsciiString	1 byte(s)
7	first_cell_time First Zero Doppler Azimuth time of first line of first imagette UTC Time of first range line in the MDS containing the first imagette used to produce product.	UTC	1	UtcExternal	27 byte(s)
8	quote_4 quotation mark ("")	ascii	1	AsciiString	1 byte(s)
9	newline_char_2 newline character	terminator	1	AsciiString	1 byte(s)
10	last_cell_time_title LAST_CELL_TIME=	keyword	1	AsciiString	15 byte(s)
11	quote_5 quotation mark ("")	ascii	1	AsciiString	1 byte(s)
12	last_cell_time Last Zero Doppler Azimuth time of first line of last imagette UTC Time of the first range line in the MDS containing the last imagette used to produce this product.	UTC	1	UtcExternal	27 byte(s)
13	quote_6 quotation mark ("")	ascii	1	AsciiString	1 byte(s)
14	newline_char_3 newline character	terminator	1	AsciiString	1 byte(s)
15	spare_1 Spare	-	1	SpareField	51 byte(s)
16	swath1_title SWATH_1=	keyword	1	AsciiString	8 byte(s)
17	quote_7 quotation mark ("")	ascii	1	AsciiString	1 byte(s)
18	swath1_1 First sub-cycle swath number IS1, IS2, IS3, IS4, IS5, IS6, or IS7.	ascii	1	AsciiString	3 byte(s)
19	quote_8 quotation mark ("")	ascii	1	AsciiString	1 byte(s)
20	newline_char_5 newline character	terminator	1	AsciiString	1 byte(s)
21	swath2_title SWATH_2=	keyword	1	AsciiString	8 byte(s)
22	quote_9 quotation mark ("")	ascii	1	AsciiString	1 byte(s)
23	swath2_2 Second sub-cycle swath number IS1, IS2, IS3, IS4, IS5, IS6, or IS7.	ascii	1	AsciiString	3 byte(s)
24	quote_10 quotation mark ("")	ascii	1	AsciiString	1 byte(s)
25	newline_char_6 newline character	terminator	1	AsciiString	1 byte(s)
26	pass_title PASS=	keyword	1	AsciiString	5 byte(s)
27	quote_11 quotation mark ("")	ascii	1	AsciiString	1 byte(s)
28	pass Ascending or descending orbit designator (defined at start of time pass) ASCENDING , DESCENDING or FULL_ORBIT	ascii	1	AsciiString	10 byte(s)
29	quote_12 quotation mark ("")	ascii	1	AsciiString	1 byte(s)
30	newline_char_7 newline character	terminator	1	AsciiString	1 byte(s)
31	polar_title TX_RX_POLAR=	keyword	1	AsciiString	12 byte(s)
32	quote_13 quotation mark ("")	ascii	1	AsciiString	1 byte(s)
33	tx_rx_polar	ascii	1	AsciiString	3 byte(s)

#	Description	Units	Count	Type	Size
	Transmitter / Receiver Polarisation for MDS 1 H/V or H/H or V/H or V/V				
34	quote_14 quotation mark ("")	ascii	1	AsciiString	1 byte(s)
35	newline_char_8 newline character	terminator	1	AsciiString	1 byte(s)
36	compression_title COMPRESSION=	keyword	1	AsciiString	12 byte(s)
37	quote_15 quotation mark ("")	ascii	1	AsciiString	1 byte(s)
38	compression Compression algorithm used on echo data on-board the satellite. FBAQ2, FBAQ3, FBAQ4 (FBAQ: 8 bits reduced to 2, 3, and 4 bits respectively) others: S&M , and NONE	ascii	1	AsciiString	5 byte(s)
39	quote_16 quotation mark ("")	ascii	1	AsciiString	1 byte(s)
40	newline_char_9 newline character	terminator	1	AsciiString	1 byte(s)
41	spare_2 Spare	-	1	SpareField	51 byte(s)
42	num_dir_bins_title NUM_DIR_BINS=	keyword	1	AsciiString	13 byte(s)
43	num_dir_bins Number of Directional Bins	-	1	Ac	4 byte(s)
44	newline_char_11 newline character	terminator	1	AsciiString	1 byte(s)
45	num_wl_bins_title NUM_WL_BINS=	keyword	1	AsciiString	12 byte(s)
46	num_wl_bins Number of Wavelength Bins	-	1	Ac	4 byte(s)
47	newline_char_12 newline character	terminator	1	AsciiString	1 byte(s)
48	first_dir_bin_title FIRST_DIR_BIN=	keyword	1	AsciiString	14 byte(s)
49	first_dir_bin First Directional Bin	degrees	1	Afl	15 byte(s)
50	first_dir_units <degrees>	units	1	AsciiString	9 byte(s)
51	newline_char_13 newline character	terminator	1	AsciiString	1 byte(s)
52	dir_bin_step_title DIR_BIN_STEP=	keyword	1	AsciiString	13 byte(s)
53	dir_bin_step Directional Bin Step	degrees	1	Afl	15 byte(s)
54	die_bin_step_units <degrees>	units	1	AsciiString	9 byte(s)
55	newline_char_14 newline character	terminator	1	AsciiString	1 byte(s)
56	first_wl_bin_title FIRST_WL_BIN=	keyword	1	AsciiString	13 byte(s)
57	first_wl_bin First Wavelength Bin Longest Wavelength	m	1	Afl	15 byte(s)
58	first_wl_bin_units <m>	units	1	AsciiString	3 byte(s)
59	newline_char_15 newline character	terminator	1	AsciiString	1 byte(s)
60	last_wl_bin_title LAST_WL_BIN=	keyword	1	AsciiString	12 byte(s)
61	last_wl_bin Last Wavelength Bin Shortest Wavelength (NOTE: Logarithmic steps)	m	1	Afl	15 byte(s)
62	last_wl_bin_units <m>	units	1	AsciiString	3 byte(s)
63	newline_char_16 newline character	terminator	1	AsciiString	1 byte(s)
64	spare_3 Spare	-	1	SpareField	51 byte(s)
65	look_sep_title LOOK_SEP=	keyword	1	AsciiString	9 byte(s)
66	look_sep	s	1	Afl	15 byte(s)

#	Description	Units	Count	Type	Size
	Look Separation period in seconds (second = 1/Hz). For the Ocean Wave Spectra, this is the time period between first and last looks.				
67	look_sep_units <s>	units	1	AsciiString	3 byte(s)
68	newline_char_18 newline character	terminator	1	AsciiString	1 byte(s)
69	look_bw_title LOOK_BW=	keyword	1	AsciiString	8 byte(s)
70	look_bw Look bandwidth used during spectra processing	Hz	1	Afl	15 byte(s)
71	look_bw_units <Hz>	units	1	AsciiString	4 byte(s)
72	newline_char_19 newline character	terminator	1	AsciiString	1 byte(s)
73	filter_order_title FILTER_ORDER=	keyword	1	AsciiString	13 byte(s)
74	filter_order Order of Butterworth filter used during cross-spectra processingIf set to zero, a Gaussian filter was applied	-	1	Ac	4 byte(s)
75	newline_char_20 newline character	terminator	1	AsciiString	1 byte(s)
76	trend_removal_title TREND_REMOVAL=	keyword	1	AsciiString	14 byte(s)
77	trend_removal Trend Removal applied during cross spectra computation0 = trend removal not applied1 = trend removal applied	ascii	1	AsciiString	1 byte(s)
78	newline_char_21 newline character	terminator	1	AsciiString	1 byte(s)
79	antenna_corr_title ANTENNA_CORR=	keyword	1	AsciiString	13 byte(s)
80	antenna_corr Antenna gain correction applied during cross spectra computation (note: Antenna Elevation gain correction is never applied to the SLC imagette) 0 = not applied 1 = applied	ascii	1	AsciiString	1 byte(s)
81	newline_char_22 newline character	terminator	1	AsciiString	1 byte(s)
82	srg_title SR_GR=	keyword	1	AsciiString	6 byte(s)
83	sr_gr Slant range to ground range conversion applied during cross spectra computation (note: Slant range to ground range conversion is never applied to the SLC imagette) 0 = not applied 1 = applied	ascii	1	AsciiString	1 byte(s)
84	newline_char_23 newline character	terminator	1	AsciiString	1 byte(s)
85	cc_window_title CC_WINDOW=	keyword	1	AsciiString	10 byte(s)
86	cc_window Cross covariance window function was applied during cross spectra computation 0 = not applied 1 = applied	ascii	1	AsciiString	1 byte(s)
87	newline_char_24 newline character	terminator	1	AsciiString	1 byte(s)
88	spare_4 Spare	-	1	SpareField	30 byte(s)
89	num_look_pairs_title NUM_LOOK_PAIRS=	keyword	1	AsciiString	15 byte(s)
90	num_look_pairs Number of look pairs in cross spectrum processing	-	1	Ac	4 byte(s)
91	newline_char_26 newline character	terminator	1	AsciiString	1 byte(s)
92	cc_range_bins_title CC_RANGE_BINS=	keyword	1	AsciiString	14 byte(s)
93	cc_range_bins Range bins in Cross covariance estimation	-	1	Al	11 byte(s)
94	newline_char_27 newline character	terminator	1	AsciiString	1 byte(s)
95	cc_az_bins_title CC_AZIMUTH_BINS=	keyword	1	AsciiString	16 byte(s)
96	cc_azimuth_bins Azimuth bins in Cross covariance estimation	-	1	Al	11 byte(s)
97	newline_char_28 newline character	terminator	1	AsciiString	1 byte(s)

#	Description	Units	Count	Type	Size
98	cc_half_width_title CC_HALF_WIDTH=	keyword	1	AsciiString	14 byte(s)
99	cc_half_width Half-width of the cross-covariance window function	m	1	Afl	15 byte(s)
100	cc_half_width_units <m>	units	1	AsciiString	3 byte(s)
101	newline_char_29 newline character	terminator	1	AsciiString	1 byte(s)
102	imagettes_failed_title IMAGETTES FAILED=	keyword	1	AsciiString	17 byte(s)
103	imagettes_failed Number of imagettes PF-ASAR failed to produce in this product	-	1	Ac	4 byte(s)
104	newline_char_30 newline character	terminator	1	AsciiString	1 byte(s)
105	spectra_failed_title SPECTRA FAILED=	keyword	1	AsciiString	15 byte(s)
106	spectra_failed Number of cross or ocean wave spectra PF-ASAR failed to produce in this product	-	1	Ac	4 byte(s)
107	newline_char_31 newline character	terminator	1	AsciiString	1 byte(s)
108	imagettes_made_title IMAGETTES MADE=	keyword	1	AsciiString	15 byte(s)
109	imagettes_made number of imagettes successfully produced by the PF-ASAR processor	-	1	Ac	4 byte(s)
110	newline_char_32 newline character	terminator	1	AsciiString	1 byte(s)
111	spectra_made_title SPECTRA MADE=	keyword	1	AsciiString	13 byte(s)
112	spectra_made Number of cross spectra or ocean wave spectra successfully produced by PF-ASAR in this product	-	1	Ac	4 byte(s)
113	newline_char_33 newline character	terminator	1	AsciiString	1 byte(s)
114	spare_5 Spare	-	1	SpareField	10 byte(s)

Record Length : 901

DS\_NAME : ASAR Wave Mode Products Base SPH

Format Version 114.0

The [ASA\\_WVI 2.6.2.1.2](#). product [SPH](#) contains up to a maximum of 411 [DSD](#) s (including the spare DSD). The actual number of [SLC Imnette](#) DSDs is determined at run time and can be derived from the SPH as the sum of Fields #32 and #30 (i.e. as the sum of the number of Imagettes\_Made and the number of Imagettes\_Failed respectively).

Note that the SLC Imnette [Measurement Data Set \(MDS\)](#) size and number of Measurement Data Set Records (MDSRs) may differ from cell to cell.

Fields #15 and #16 of the SPH give the [wavelengths](#) ,  $\lambda_0$  and  $\lambda_{N_k-1}$  , of the first and last [wavelength bins](#) . Field 12 gives the number of bins,  $N_k$  . The formula for reconstructing the wavelengths,  $\lambda_m$  , for each wavelength bin, m , from these first and last values is as follows:

For Level 1 WVI and WVS products:

$$\lambda_m = \frac{\lambda_0}{\left(\frac{\lambda_0}{\lambda_{N_k-1}}\right)^{\frac{2m}{2N_k-1}}} \quad \text{for} \quad m \in [0, N_k - 1]$$

For Level 2 WVW products:

$$\lambda_m = \frac{\lambda_0}{\left(\frac{\lambda_0}{\lambda_{N_k-1}}\right)^{\frac{m}{N_k-1}}} \quad \text{for} \quad m \in [0, N_k - 1]$$

Table 6.56

For a further discussion of this product, and the associated [Data Sets \(DS\)](#) refer to the section entitled "[Level 1B Wave Products](#)" [2.6.2.1.2.](#)

## 6.6.19 Wave Mode Geolocation ADS

Due to the reduced size of the [imagettes](#) compared to normal ASAR images, each [Wave Mode Geolocation](#) Annotation Data Set Record (ADSR) contains only the geodetic [latitude](#) and [longitude](#) of the centre point of the imagette. One ADSR is produced for each wave cell.

The centre point given in the Geolocation ADSR corresponds to the [ground range](#) centre point of the wave cell. This will not correspond exactly to the latitude and longitude of the centre sample of the [SLC](#) imagette (in [slant range](#)), but provides a

more accurate positioning of the location of the [cross spectra](#) centre point.

Note that the imagettes do not cover a contiguous region geographically. Thus, Wave Mode Geolocation ADS entries may differ substantially for different imagettes.

Table 6.57 Wave Mode Geolocation ADS

## Wave Mode Geolocation ADS

#	Description	Units	Count	Type	Size
Data Record					
0	zero_doppler_time Zero Doppler Time of first line of the first line of the imagette	MJD	1	mjd	12 byte(s)
1	attach_flag Attachment Flag Set to 1 if unable to compute the cross spectra for a given SLC imagette (I.e. no Cross Spectra MDSR corresponding to this ADSR), set to 0 otherwise.	flag	1	BooleanFlag	1 byte(s)
2	center_lat Geodetic latitude of center point (positive north) This is the center point of the wave cell.	(1e-6) degrees	1	GeoCoordinate	4 byte(s)
3	center_long Geodetic longitude of center point (positive east) This is the center point of the wave cell.	(1e-6) degrees	1	GeoCoordinate	4 byte(s)
4	heading Subsatellite Track Heading. Relative to North of centre point.	-	1	f1	4 byte(s)

Record Length : 25

DS\_NAME : Wave Mode Geolocation ADS

Format Version 114.0

Note for both fields # 3 and #4, the centre point of the wave cell is calculated after the cross spectra processing, and thus may differ from the centre sample latitude of the SLC imagette if slant range to ground range conversion was performed during the cross spectra calculation.

### 6.6.20 Wave Mode processing parameters

The [Wave Mode \(WV\)](#) Processing parameters [Annotation Data Set \(ADS\)](#) details all the

parameters used to create the [SLC imagette](#) and other parameters specific to Wave Mode Imagette processing. These consist of those found in the Main Processing parameters ADS of the Image Products format ( field# 1- 79 have the identical format as that given by the ASAR\_Main\_ADSR ), plus [Doppler Centroid](#) parameters, [Chirp](#) parameters, [Antenna Elevation Patterns](#) , [Slant Range to Ground Range \(SR/GR\)](#) parameters, [Geolocation](#) Grid [Tie points](#) , and parameters specific to Wave Mode. Since the imagette is an SLC image, the SR/GR parameters and Antenna Elevation parameters pertain to the [cross spectra](#) creation process, not the imagette itself.

There is one ADSR per wave cell, which provides a complete record of the processing parameters and values used during image formation. The table for these ADSRs is given below:

Table 6.58 Wave Mode processing parameters

## Wave Mode processing parameters

#	Description	Units	Count	Type	Size
<b>Data Record</b>					
0	first_zero_doppler_time First Zero Doppler Azimuth time of MDS which this data set describesTime of first range line in the MDS described by this data set	MJD	1	mjd	12 byte(s)
1	attach_flag Attachment Flag Always set to zero for this ADSR	flag	1	BooleanFlag	1 byte(s)
2	last_zero_doppler_time Last Zero Doppler Azimuth time of MDS which this data set describesTime of last range line in the MDS described by this data set	MJD	1	mjd	12 byte(s)
3	work_order_id Work Order ID (left-justified)	ascii	1	AsciiString	12 byte(s)
4	time_diff Time difference between sensing time of first input line and zero Doppler time of first output image line (tdelta). May be used during child product extraction from a stripline product. Left blank (set to zero) for non-stripline products	s	1	fl	4 byte(s)
5	swath_num Swath number IS1, IS2, IS3, IS4, IS5, IS6, or IS7 for IM, WV and AP modes.SS1 ,SS2, SS3, SS4, SS5 for WSS Products.Ws0 for WS and GM modes where only one ADSR for the whole scene is provided	ascii	1	AsciiString	3 byte(s)
6	range_spacing Range sample spacing	m	1	fl	4 byte(s)
7	azimuth_spacing Azimuth sample spacing at image center	m	1	fl	4 byte(s)
8	line_time_interval Azimuth sample spacing in time (Line Time Interval)	s	1	fl	4 byte(s)
9	num_output_lines Number of output range lines in the image.For WSS products this number will vary for each sub swath	lines	1	ul	4 byte(s)
10	num_samples_per_line Number of samples per output range line includes zero filled samples	samples	1	ul	4 byte(s)
11	data_type	ascii	1	AsciiString	5 byte(s)



#	Description	Units	Count	Type	Size	
	Output data type SWORD, UWORD, or UBYTE					
12	<b>num_range_lines_per_burst</b> Number of output range lines per burst. Not used for single-beam products	lines	1	ul	4 byte(s)	
13	<b>time_diff_zero_doppler</b> Time difference between zero Doppler time and acquisition time of output image lines	s	1	fl	4 byte(s)	
14	<b>spare_1</b> Spare	-	1	SpareField	43 byte(s)	
15	<b>data_analysis_flag</b> Raw Data Analysis used for Raw Data Correction 0 = correction done using default parameters 1 = correction done using raw data analysis results	flag	1	BooleanFlag	1 byte(s)	
16	<b>ant_elev_corr_flag</b> Antenna Elevation Pattern Correction Applied 0 = no correction applied 1 = correction applied	flag	1	BooleanFlag	1 byte(s)	
17	<b>chirp_extract_flag</b> Reconstructed Chirp used 0 = nominal chirp replica used 1 = reconstructed chirp used	flag	1	BooleanFlag	1 byte(s)	
18	<b>srg_flag</b> Slant Range to Ground Range Conversion Applied 0 = no conversion applied 1 = conversion applied	flag	1	BooleanFlag	1 byte(s)	
19	<b>dop_cen_flag</b> Doppler Centroid Estimation Performed 0 = no estimation done 1 = estimation done	flag	1	BooleanFlag	1 byte(s)	
20	<b>dop_amb_flag</b> Doppler Ambiguity Estimation Performed 0 = no estimate done 1 = estimate done	flag	1	BooleanFlag	1 byte(s)	
21	<b>range_spread_comp_flag</b> Range-spreading loss compensation Applied 0 = no compensation applied 1 = compensation applied	flag	1	BooleanFlag	1 byte(s)	
22	<b>detected_flag</b> Detection Applied 0 = output product is complex 1 = output product was detected	flag	1	BooleanFlag	1 byte(s)	
23	<b>look_sum_flag</b> Look Summation Performed 0 = product is single look 1 = product is multi-looked	flag	1	BooleanFlag	1 byte(s)	
24	<b>rms_equal_flag</b> RMS Equalisation performed 0= rms equalization not performed during FBAQ decoding, 1 = rms equalization performed during FBAQ decoding	flag	1	BooleanFlag	1 byte(s)	
25	<b>ant_scal_flag</b> Antenna Elevation Gain Scaling Factor applied 0= no scaling factor applied, 1 = scaling factor applied	flag	1	BooleanFlag	1 byte(s)	
26	<b>vga_com_echo_flag</b> Receive Gain Droop Compensation applied to Echo. 0=no compression, 1=compensation applied.	flag	1	BooleanFlag	1 byte(s)	
27	<b>vga_com_cal_flag</b> Receive Gain Droop Compensation applied to Calibration Pulse P2. 0=no compression, 1=compensation applied.	flag	1	BooleanFlag	1 byte(s)	
28	<b>vga_com_nom_time_flag</b> Nominal time delay applied for Receive Gain Droop Compensation of Calibration Pulse P2 order zero. 0=do not use nominal time delay (compensation depends on P2 time delay), 1 = use nominal time delay (constant)	flag	1	BooleanFlag	1 byte(s)	
29	<b>gm_range_comp_inverse_filter_flag</b> Inverse filter used for range compression. (GM Mode only). 0 = matched filter used for range compression 1 = inverse filter used for range compression	flag	1	BooleanFlag	1 byte(s)	
30	<b>spare_2</b> Spare	-	1	SpareField	6 byte(s)	
31	<b>raw_data_analysis</b> The following 26 parameters form a structure which is repeated twice, once for MDS 1 and once for MDS 2 If MDS 2 is not included with the product the second set of values is blanked (all values set to zero)	-	2	raw_data_analysisStruct	2*92.0 byte(s)	
	a	<b>num_gaps</b> Number of input data gaps (a gap is defined as a predetermined number of range lines)	gaps	1	ul	4 byte(s)
	b	<b>num_missing_lines</b> Number of missing lines, excluding data gaps	lines	1	ul	4 byte(s)
	c	<b>range_samp_skip</b> Range sample skipping	samples	1	ul	4 byte(s)

#	Description		Units	Count	Type	Size
		factor for raw data analysis				
d	range_lines_skip	Range lines skipping factor for raw data analysis	lines	1	ul	4 byte(s)
e	calc_i_bias	Calculated I channel bias	-	1	fl	4 byte(s)
f	calc_q_bias	Calculated Q channel bias	-	1	fl	4 byte(s)
g	calc_i_std_dev	Calculated I channel standard deviation	-	1	fl	4 byte(s)
h	calc_q_std_dev	Calculated Q channel standard deviation	-	1	fl	4 byte(s)
i	calc_gain	Calculated I/Q gain imbalance	-	1	fl	4 byte(s)
j	calc_quad	Calculated I/Q quadrature departure	-	1	fl	4 byte(s)
k	i_bias_max	I bias upper bound	-	1	fl	4 byte(s)
l	i_bias_min	I bias lower bound	-	1	fl	4 byte(s)
m	q_bias_max	Q bias upper bound	-	1	fl	4 byte(s)
n	q_bias_min	Q bias lower bound	-	1	fl	4 byte(s)
o	gain_min	I/Q gain lower bound	-	1	fl	4 byte(s)
p	gain_max	I/Q gain upper bound	-	1	fl	4 byte(s)
q	quad_min	I/Q quadrature departure lower bound	-	1	fl	4 byte(s)
r	quad_max	I/Q quadrature departure upper bound	-	1	fl	4 byte(s)
s	i_bias_flag	I bias significance0 = I bias falls within acceptable range1 = I bias falls outside acceptable range	flag	1	BooleanFlag	1 byte(s)
t	q_bias_flag	Q bias Significance0 = Q bias falls within acceptable range1 = Q bias falls outside acceptable range	flag	1	BooleanFlag	1 byte(s)
u	gain_flag	I/Q Gain Significance0 = Gain falls within acceptable range1 = Gain falls outside acceptable range	flag	1	BooleanFlag	1 byte(s)
v	quad_flag	I/Q Quadrature Departure Significance0 = Quadrature departure falls within acceptable range1 = Quadrature departure falls outside acceptable range	flag	1	BooleanFlag	1 byte(s)
w	used_i_bias	I channel bias used for correction (may be different from measured value)	-	1	fl	4 byte(s)
x	used_q_bias	Q channel bias used for correction (may be different from measured value)	-	1	fl	4 byte(s)
y	used_gain	I/Q gain imbalance used for correction (may be different from measured value)	-	1	fl	4 byte(s)



#	Description			Units	Count	Type	Size																																																																							
	z		used_quad I/Q quadrature departure used for correction(may be different from measured value)	-	1	fl	4 byte(s)																																																																							
32	spare_3 Spare			-	1	SpareField	32 byte(s)																																																																							
33	start_time  The following 2 parameters form a structure which is repeated twice. Once for values pertaining to MDS 1 and once for values pertaining to MDS 2. If MDS 2 is not included in the product the fields in the second group are blanked (all values are set to zero).			-	2	start_timeStruct	2*20.0 byte(s)																																																																							
	<table border="1"> <tr> <td>a</td> <td>first_oft On-board binary time of first input line processedLSB accurate to 15.26 ms. (Contained in two long integers)</td> <td>-</td> <td>2</td> <td>ul</td> <td>2*4 byte(s)</td> </tr> <tr> <td>b</td> <td>first_mjd Sensing time (MJD format) of first input line processedconverted from satellite binary time</td> <td>MJD</td> <td>1</td> <td>mjd</td> <td>12 byte(s)</td> </tr> </table>		a	first_oft On-board binary time of first input line processedLSB accurate to 15.26 ms. (Contained in two long integers)	-	2	ul	2*4 byte(s)	b	first_mjd Sensing time (MJD format) of first input line processedconverted from satellite binary time	MJD	1	mjd	12 byte(s)																																																																
a	first_oft On-board binary time of first input line processedLSB accurate to 15.26 ms. (Contained in two long integers)	-	2	ul	2*4 byte(s)																																																																									
b	first_mjd Sensing time (MJD format) of first input line processedconverted from satellite binary time	MJD	1	mjd	12 byte(s)																																																																									
34	parameter_codes  Following fields each contain room for 5 values Only one value is filled for each for (IM) and (WV) modes. Two values are filled for (AP) mode (for MDS1 and MDS2). Five values are filled for (WS) and (GM) modes (for SS1 to SS5, respectively). Unused values are set to zero		-	1	parameter_codesStruct		120.0 byte(s)																																																																							
	<table border="1"> <tr> <td>a</td> <td>swst_code Sampling Window Start time code of first processed line</td> <td>code</td> <td>5</td> <td>us</td> <td>5*2 byte(s)</td> </tr> <tr> <td>b</td> <td>last_swst_code Sampling Window Start time code of last processed line</td> <td>code</td> <td>5</td> <td>us</td> <td>5*2 byte(s)</td> </tr> <tr> <td>c</td> <td>pri_code Pulse Repetition Interval code</td> <td>code</td> <td>5</td> <td>us</td> <td>5*2 byte(s)</td> </tr> <tr> <td>d</td> <td>tx_pulse_len_code Tx pulse length</td> <td>code</td> <td>5</td> <td>us</td> <td>5*2 byte(s)</td> </tr> <tr> <td>e</td> <td>tx_bw_code Tx pulse bandwidth</td> <td>code</td> <td>5</td> <td>us</td> <td>5*2 byte(s)</td> </tr> <tr> <td>f</td> <td>echo_win_len_code Echo Window Length</td> <td>code</td> <td>5</td> <td>us</td> <td>5*2 byte(s)</td> </tr> <tr> <td>g</td> <td>up_code Upconverter Level - Upconverter gain set on the instrument</td> <td>code</td> <td>5</td> <td>us</td> <td>5*2 byte(s)</td> </tr> <tr> <td>h</td> <td>down_code Downconverter Level - Downconverter gain set on the instrument</td> <td>code</td> <td>5</td> <td>us</td> <td>5*2 byte(s)</td> </tr> <tr> <td>i</td> <td>resamp_code Resampling factor for echo data</td> <td>code</td> <td>5</td> <td>us</td> <td>5*2 byte(s)</td> </tr> <tr> <td>j</td> <td>beam_adj_code Beam adjustment delta</td> <td>code</td> <td>5</td> <td>us</td> <td>5*2 byte(s)</td> </tr> <tr> <td>k</td> <td>beam_set_num_code Antenna Beam Set Number</td> <td>code</td> <td>5</td> <td>us</td> <td>5*2 byte(s)</td> </tr> <tr> <td>l</td> <td>tx_monitor_code Auxiliary Tx Monitor Level</td> <td>code</td> <td>5</td> <td>us</td> <td>5*2 byte(s)</td> </tr> </table>		a	swst_code Sampling Window Start time code of first processed line	code	5	us	5*2 byte(s)	b	last_swst_code Sampling Window Start time code of last processed line	code	5	us	5*2 byte(s)	c	pri_code Pulse Repetition Interval code	code	5	us	5*2 byte(s)	d	tx_pulse_len_code Tx pulse length	code	5	us	5*2 byte(s)	e	tx_bw_code Tx pulse bandwidth	code	5	us	5*2 byte(s)	f	echo_win_len_code Echo Window Length	code	5	us	5*2 byte(s)	g	up_code Upconverter Level - Upconverter gain set on the instrument	code	5	us	5*2 byte(s)	h	down_code Downconverter Level - Downconverter gain set on the instrument	code	5	us	5*2 byte(s)	i	resamp_code Resampling factor for echo data	code	5	us	5*2 byte(s)	j	beam_adj_code Beam adjustment delta	code	5	us	5*2 byte(s)	k	beam_set_num_code Antenna Beam Set Number	code	5	us	5*2 byte(s)	l	tx_monitor_code Auxiliary Tx Monitor Level	code	5	us	5*2 byte(s)				
a	swst_code Sampling Window Start time code of first processed line	code	5	us	5*2 byte(s)																																																																									
b	last_swst_code Sampling Window Start time code of last processed line	code	5	us	5*2 byte(s)																																																																									
c	pri_code Pulse Repetition Interval code	code	5	us	5*2 byte(s)																																																																									
d	tx_pulse_len_code Tx pulse length	code	5	us	5*2 byte(s)																																																																									
e	tx_bw_code Tx pulse bandwidth	code	5	us	5*2 byte(s)																																																																									
f	echo_win_len_code Echo Window Length	code	5	us	5*2 byte(s)																																																																									
g	up_code Upconverter Level - Upconverter gain set on the instrument	code	5	us	5*2 byte(s)																																																																									
h	down_code Downconverter Level - Downconverter gain set on the instrument	code	5	us	5*2 byte(s)																																																																									
i	resamp_code Resampling factor for echo data	code	5	us	5*2 byte(s)																																																																									
j	beam_adj_code Beam adjustment delta	code	5	us	5*2 byte(s)																																																																									
k	beam_set_num_code Antenna Beam Set Number	code	5	us	5*2 byte(s)																																																																									
l	tx_monitor_code Auxiliary Tx Monitor Level	code	5	us	5*2 byte(s)																																																																									
35	spare_4 Spare			-	1	SpareField	60 byte(s)																																																																							
36	error_counters Error counters  Each input line is analyzed for errors in the header using a majority polling technique. Errors are logged for each field of the header in the fields below.			-	1	error_countersStruct	40.0 byte(s)																																																																							

#	Description			Units	Count	Type	Size
37	a	num_err_swt Number of errors detected in Sampling Window start time field.	-		1	ul	4 byte(s)
	b	num_err_pri Number of errors detected in PRI code field	-		1	ul	4 byte(s)
	c	num_err_tx_pulse_len Number of errors detected in Tx pulse length field	-		1	ul	4 byte(s)
	d	num_err_tx_pulse_bw Number of errors detected in Tx pulse bandwidth field.	-		1	ul	4 byte(s)
	e	num_err_echo_win_len Number of errors detected in Echo Window Length field.	-		1	ul	4 byte(s)
	f	num_err_up Number of errors detected in Upconverter Level field.	-		1	ul	4 byte(s)
	g	num_err_down Number of errors detected in Downconverter Level field.	-		1	ul	4 byte(s)
	h	num_err_resamp Number of errors detected in Resampling factor for echo data field.	-		1	ul	4 byte(s)
	i	num_err_beam_adj Number of errors detected in Beam adjustment delta field.	-		1	ul	4 byte(s)
	j	num_err_beam_set_num Number of errors detected in Antenna Beam Set Number field.	-		1	ul	4 byte(s)
37	spare_5 Spare			-	1	SpareField	26 byte(s)
38	image_parameters Image Data Set parameters			-	1	image_parametersStruct	270.0 byte(s)
39	a	swst_value Sampling Window Start time of first processed line	s	5	fl		5*4 byte(s)
	b	last_swst_value Sampling Window Start time of last processed line	s	5	fl		5*4 byte(s)
	c	swst_changes Number of Sample Window Start Time changes within a beam	-	5	ul		5*4 byte(s)
	d	prf_value Pulse Repetition Frequency	Hz	5	fl		5*4 byte(s)
	e	tx_pulse_len_value Tx pulse length	s	5	fl		5*4 byte(s)
	f	tx_pulse_bw_value Tx pulse bandwidth	Hz	5	fl		5*4 byte(s)
	g	echo_win_len_value Echo Window Length	s	5	fl		5*4 byte(s)
	h	up_value Upconverter Level - Upconverter gain set on the instrument	dB	5	fl		5*4 byte(s)
	i	down_value Downconverter Level - Downconverter gain set on the instrument	dB	5	fl		5*4 byte(s)

#	Description			Units	Count	Type	Size
	j	resamp_value Resampling factor	-	5	1	fl	5*4 byte(s)
	k	beam_adj_value Beam adjustment delta	deg.	5	1	fl	5*4 byte(s)
	l	beam_set_value Antenna Beam Set Number	-	5	1	us	5*2 byte(s)
	m	tx_monitor_value Auxiliary Tx Monitor Level	-	5	1	fl	5*4 byte(s)
	n	rank Number of PRI between transmitted pulse and return echo	-	5	1	ul	5*4 byte(s)
39	spare_6 Spare			-	1	SpareField	62 byte(s)
40	first_proc_range_samp First processed input range sample, first sample is 1			samples	1	ul	4 byte(s)
41	range_ref Range spreading loss reference range			m	1	fl	4 byte(s)
42	range_samp_rate Range sampling rate			Hz	1	fl	4 byte(s)
43	radar_freq Radar Frequency			Hz	1	fl	4 byte(s)
44	num_looks_range Number of range looks			looks	1	us	2 byte(s)
45	filter_range Matched filter window type HAMMING or KAISER or NONE			ascii	1	AsciiString	7 byte(s)
46	filter_coef_range Window coefficient for range-matched filter			-	1	fl	4 byte(s)
47	bandwidth Bandwidth Following fields each contain room for 5 values. Only one value is filled for each for AP, IM, and WV modes. Five values are filled for WS and GM modes (for SS1 to SS5, respectively). Unused values are set to zero			-	1	bandwidthStruct	40.0 byte(s)
	a	look_bw_range Range Look Bandwidth (null to null)	Hz	5	1	fl	5*4 byte(s)
	b	tot_bw_range Total processed range bandwidth (null to null)	Hz	5	1	fl	5*4 byte(s)
48	nominal_chirp Nominal Chirp Following 2 parameters form a structure which is repeated 5 times (one set for each WS beam, SS1 first, to SS5 last -- only one set of values given for narrow swath images)			-	5	nominal_chirpStruct	5*32.0 byte(s)
	a	nom_chirp_amp 4 nominal chirp amplitude coefficients	-, s-1, s-2, s-3	4	1	fl	4*4 byte(s)
	b	nom_chirp_phs 4 nominal chirp phase coefficients	cycles,Hz,Hz/s,Hz/s2	4	1	fl	4*4 byte(s)
49	spare_7 Spare			-	1	SpareField	60 byte(s)
50	num_lines_proc Number of input lines processed			lines	1	ul	4 byte(s)
51	num_look_az Number of Azimuth Looks			looks	1	us	2 byte(s)
52	look_bw_az Azimuth Look Bandwidth (null to null) (null to null)			Hz	1	fl	4 byte(s)
53	to_bw_az Processed Azimuth bandwidth (null to null)			Hz	1	fl	4 byte(s)
54	filter_az Matched filter window type HAMMING or KAISER or NONE			ascii	1	AsciiString	7 byte(s)



#	Description		Units	Count	Type	Size
55	filter_coeff_az Window coefficient for azimuth-matched filter		-	1	fl	4 byte(s)
56	az_fm_rate 3 co-efficients for Azimuth FM rate Azimuth FM rate = C0 + C1(SR-t0) + C2(SR - t0)t SR = 2 way slant range time		Hz/sHz/s2Hz/s3	3	fl	3*4 byte(s)
57	ax_fm_origin 2 way slant range time origin (t0) for Azimuth FM rate calculation		ns	1	fl	4 byte(s)
58	dop_amb_conf Doppler Centroid Ambiguity Confidence MeasureValue between 0 and 1, 0 = poorest confidence, 1= highest confidence		-	1	fl	4 byte(s)
59	spare_8 Spare		-	1	SpareField	68 byte(s)
60	calibration_factors Calibration factors  The following 2 parameters form a structure which is repeated twice. Once for values pertaining to MDS 1 and once for values pertaining to MDS 2. If MDS 2 is not included in the product the fields in the second group are set to zero		-	2	calibration_factorsStruct	2*8.0 byte(s)
	a	proc_scaling_fact Processor scaling factor	-	1	fl	4 byte(s)
	b	ext_cal_fact External Calibration Scaling Factor (mode/swath/polarization dependent)	-	1	fl	4 byte(s)
61	noise_estimation Noise Estimation  Following fields each contain room for 5 values. Five values are filled for WS and GM modes (for SS1 to SS5, respectively). Up to 5 values may be provided for IM mode, each one is a separate noise estimate. For AP mode, up to 4 values may be provided in the order: first estimate for MDS1, second estimate for MDS1, first estimate for MDS2, second estimate for MDS2. For WV, there is one estimate provided.		-	1	noise_estimationStruct	40.0 byte(s)
	a	noise_power_corr Noise power correction factors	-	5	fl	5*4 byte(s)
	b	num_noise_lines Number of noise lines used to calculate factors	-	5	ul	5*4 byte(s)
62	spare_9 Spare		-	1	SpareField	64 byte(s)
63	spare_10 Spare		-	1	SpareField	12 byte(s)
64	output_statistics Output Data Statistics  The following 4 parameters form a structure which is repeated twice. Once for values pertaining to MDS 1 and once for values pertaining to MDS 2. If MDS 2 is not included in the product the fields in the second group are set to zero.		-	2	output_statisticsStruct	2*16.0 byte(s)
	a	out_mean Output data mean Magnitude for detected products, real sample mean for SLC products	-	1	fl	4 byte(s)
	b	out_imag_mean Output imaginary data mean Used for SLC products only (set to zero otherwise)	-	1	fl	4 byte(s)
	c	out_std_dev Output data standard deviation Magnitude std. dev. for detected products, real sample std. dev. for SLC products	-	1	fl	4 byte(s)
	d	out_imag_std_dev Output imaginary data standard deviation Used for SLC products only (set to zero otherwise)	-	1	fl	4 byte(s)
65	avg_scene_height_ellipsoid		m	1	fl	4 byte(s)

#	Description	Units	Count	Type	Size	
	Average scene height above ellipsoid used for processing					
66	spare_11 Spare	-	1	SpareField	48 byte(s)	
67	echo_comp Compression Method used for echo samples FBAQ, S&M ,NONE	ascii	1	AsciiString	4 byte(s)	
68	echo_comp_ratio Compression Ratio for echo samples8/4, 8/3, 8/2, or 8/8	ascii	1	AsciiString	3 byte(s)	
69	init_cal_comp Compression Method used for initial calibration samples FBAQ, S&M ,NONE	ascii	1	AsciiString	4 byte(s)	
70	init_cal_ratio Compression Ratio for initial calibration samples8/4, 8/3, 8/2, or 8/8	ascii	1	AsciiString	3 byte(s)	
71	per_cal_comp Compression Method used for periodic calibration samples FBAQ, S&M ,NONE	ascii	1	AsciiString	4 byte(s)	
72	per_cal_ratio Compression Ratio for periodic calibration samples8/4, 8/3, 8/2, or 8/8	ascii	1	AsciiString	3 byte(s)	
73	noise_comp Compression Method used for noise samples FBAQ, S&M ,NONE	ascii	1	AsciiString	4 byte(s)	
74	noise_comp_ratio Compression Ratio for noise samples8/4, 8/3, 8/2, or 8/8	ascii	1	AsciiString	3 byte(s)	
75	spare_12 Spare	-	1	SpareField	64 byte(s)	
76	beam_overlap Number of slant range samples in beam merging One value per merge region (1-2, 2-3, 3-4, 4-5). This parameter is equivalent to N in the following beam merging formula: $x_{merged}(n) = (1 - (n/N)P * xnear(n)) + ((n/N)P * xfar(n))$	-	4	ul	4*4 byte(s)	
77	beam_param Beam merge algorithm parameter used for beam merging One value per merge region (1-2, 2-3, 3-4, 4-5). This parameter is equivalent to P in the above beam merging formula, and different values have the following effect: P = 1, linear weighting of the two beams (near and far). P = -1, (which represents infinity in the beam merging formula) only near beam contributes to the merged one P = 0, only far beam contributes to the merged one P > 1, near beam is favoured 0 < P < 1, far beam is favoured.	-	4	fl	4*4 byte(s)	
78	lines_per_burst Number of lines per burst for this image. 5 values for beams SS1 to SS5 in WS and GM modes. Two values for AP mode, all others set to zero.	lines	5	ul	5*4 byte(s)	
79	time_first_SS1_echo Time of first SS1 Echo Source Packet	mjd	1	mjd	12 byte(s)	
80	spare_13 Spare	-	1	SpareField	16 byte(s)	
81	orbit_state_vectors Orbit State Vectors Information The following 7 parameters form a structure which is repeated 5 times, thus allowing the inclusion of up to 5 orbit state vectors which span the scene (or slice) to which this ADSR pertains.	-	5	orbit_state_vectorsStruct	5*36.0 byte(s)	
	a	state_vect_time_1 Time of state vector	MJD	1	mjd	12 byte(s)
	b	x_pos_1 X position in Earth fixed reference frame	10 -2m	1	sl	4 byte(s)
	c	y_pos_1 Y position in Earth fixed reference frame	10 -2m	1	sl	4 byte(s)
	d	z_pos_1 Z position in Earth fixed reference frame	10 -2m	1	sl	4 byte(s)
	e	x_vel_1 X velocity relative to Earth fixed reference frame	10 -5m/s	1	sl	4 byte(s)
	f	y_vel_1 Y velocity relative to Earth fixed reference frame	10 -5m/s	1	sl	4 byte(s)
	g	z_vel_1 Z velocity relative to Earth fixed reference frame	10 -5m/s	1	sl	4 byte(s)

#	Description	Units	Count	Type	Size	
82	spare_14 Spare	-	1	SpareField	64 byte(s)	
83	slant_range_time 2-way slant range time origin (t0)	ns	1	fl	4 byte(s)	
84	dop_coeff Doppler centroid coefficients as a function of slant range time: D0, D1, D2, D3, and D4. Where Doppler Centroid = D0 + D1(tSR-t0) + D2(tSR-t0)2 + D3(tSR-t0)3 + D4(tSR-t0)4	Hz/Hz/s/Hz/s2Hz/s3Hz/s4	5	fl	5*4 byte(s)	
85	dop_conf Doppler Centroid Confidence Measure. Value between 0 and 1, 0 = poorest confidence, 1= highest confidence	-	1	fl	4 byte(s)	
86	dop_conf_below_thresh Doppler Centroid Confidence below threshold flag. 0=confidence above threshold, centroid calculated from data; 1=confidence below threshold, centroid calculated from orbit.	-	1	uc	1 byte(s)	
87	spare_15 Spare	-	1	SpareField	13 byte(s)	
88	chirp_width 3-dB pulse width of chirp replica cross-correlation function between extract chirp and nominal chirp	samples	1	fl	4 byte(s)	
89	chirp_sidelobe First side lobe level of chirp replica cross-correlation function between reconstructed chirp and nominal chirp	dB	1	fl	4 byte(s)	
90	chirp_islr ISLR of chirp replica cross-correlation function between reconstructed chirp and nominal chirp	dB	1	fl	4 byte(s)	
91	chirp_peak_loc Peak location of cross correlation function between reconstructed chirp and nominal chirp	samples	1	fl	4 byte(s)	
92	chirp_power Chirp power	-	1	fl	4 byte(s)	
93	eq_chirp_power Equivalent Chirp power	dB	1	fl	4 byte(s)	
94	rec_chirp_exceedsqua_thres Reconstructed chirp exceeds quality thresholds 0=Reconstructed chirp does not meet quality thresholds 1=Reconstructed chirp does meet quality thresholds	-	1	uc	1 byte(s)	
95	ref_chirp_power Reference Chirp power	dB	1	fl	4 byte(s)	
96	norm_source Normalisation source REPLICA REF0000 EQV0000 or NONE000 ( if normalisation not applied )	ascii	1	AsciiString	7 byte(s)	
97	spare_16 Spare	-	1	SpareField	4 byte(s)	
98	cal_info Calibration pulse information The following 4 parameters form a structure that is repeated 32 times (once for each row). Each repetition consists of a total of 11 measurements of 4 different types as described below.	-	32	cal_infoStruct	32*44.0 byte(s)	
	a	max_cal Max of Cal pulses 1, 2, and 3 amplitude	-	3	fl	3*4 byte(s)
	b	avg_cal Average of Cal pulse 1, 2, and 3 amplitude over the 3 dB on either side of the max amplitude	-	3	fl	3*4 byte(s)
	c	avg_val_1a Average of Cal pulse 1A over the sample window	-	1	fl	4 byte(s)
	d	phs_cal Extracted phase for calibration pulse 1, 1A, 2, and 3	degrees	4	fl	4*4 byte(s)
99	spare_17 Spare	-	1	SpareField	16 byte(s)	
100	first_line_time Zero Doppler Time at first line of imagette	MJD	1	mjd	12 byte(s)	
101	first_line_tie_points Imagette First Line Tie Points	-	1	first_line_tie_pointsStruct	60.0 byte(s)	
	a	range_samp_nums Range sample number	-	3	ul	3*4 byte(s)



#	Description			Units	Count	Type	Size
101	a	Gives the range location of the grid points. First range sample is 1, is M (includes zero filled samples)					
	b	slant_range_times 2 way slant range time to range sample	ns	3		fl	3*4 byte(s)
	c	inc_angles Incidence Angle at range sample	deg.	3		fl	3*4 byte(s)
	d	lats geodetic latitude of range sample (positive north)	(1e-6) degrees	3		GeoCoordinate	3*4 byte(s)
	e	longs geodetic longitude of range sample (positive east)	(1e-6) degrees	3		GeoCoordinate	3*4 byte(s)
102	mid_line_time Zero Doppler Time at centre line of imagette			MJD	1	mjd	12 byte(s)
103	mid_range_line_nums Range line number of the center range line			-	1	ul	4 byte(s)
104	mid_line_tie_points Imagette Mid Line Tie Points			-	1	mid_line_tie_pointsStruct	60.0 byte(s)
105	a	range_samp_nums Range sample number Gives the range location of the grid points. First range sample is 1, is M (includes zero filled samples)	-	3		ul	3*4 byte(s)
	b	slant_range_times 2 way slant range time to range sample	ns	3		fl	3*4 byte(s)
	c	inc_angles Incidence Angle at range sample	deg.	3		fl	3*4 byte(s)
	d	lats geodetic latitude of range sample (positive north)	(1e-6) degrees	3		GeoCoordinate	3*4 byte(s)
	e	longs geodetic longitude of range sample (positive east)	(1e-6) degrees	3		GeoCoordinate	3*4 byte(s)
106	last_line_time Zero Doppler Time at last line of imagette			MJD	1	mjd	12 byte(s)
107	last_line_num Range line number of the last range line			-	1	ul	4 byte(s)
108	last_line_tie_points Imagette Last Line Tie Points			-	1	last_line_tie_pointsStruct	60.0 byte(s)
109	a	range_samp_nums Range sample number Gives the range location of the grid points. First range sample is 1, is M (includes zero filled samples)	-	3		ul	3*4 byte(s)
	b	slant_range_times 2 way slant range time to range sample	ns	3		fl	3*4 byte(s)
	c	inc_angles Incidence Angle at range sample	deg.	3		fl	3*4 byte(s)
	d	lats geodetic latitude of range sample (positive north)	(1e-6) degrees	3		GeoCoordinate	3*4 byte(s)
	e	longs geodetic longitude of range sample (positive east)	(1e-6) degrees	3		GeoCoordinate	3*4 byte(s)
110	swst_offset Wave cell SWST offset			ns	1	fl	4 byte(s)

#	Description	Units	Count	Type	Size	
	From centre of the sub-swath to start of imagette. 208 ns increments					
109	ground_range_bias Wave cell Ground range bias From centre of the sub-swath to the centre of the imagette (Ground range, km)	km	1	fl	4 byte(s)	
110	elev_angle_bias Wave cell elevation angle bias From centre of the sub-swath elevation to the centre of the imagette (deg)	deg	1	fl	4 byte(s)	
111	imagette_range_len Imagette length in range (m)	m	1	fl	4 byte(s)	
112	imagette_az_len Imagette length in azimuth (m)	m	1	fl	4 byte(s)	
113	imagette_range_res Nominal Imagette resolution in slant range (m)	m	1	fl	4 byte(s)	
114	ground_res Nominal resolution in ground range	m	1	fl	4 byte(s)	
115	imagette_az_res Nominal Imagette resolution in azimuth (m)	m	1	fl	4 byte(s)	
116	platform_alt Altitude (platform to ellipsoid) in metres (centre of wave cell)	m	1	fl	4 byte(s)	
117	ground_vel Ground Velocity, w.r.t moving earth	m/s	1	fl	4 byte(s)	
118	slant_range Range to centre of imagette (m) From platform to target	m	1	fl	4 byte(s)	
119	cw_drift CW signal drift	-	1	fl	4 byte(s)	
120	wave_subcycle Wave sub-cycle (1 or 2) of this wave cell	-	1	us	2 byte(s)	
121	earth_radius Earth Radius at imagette center sample	m	1	fl	4 byte(s)	
122	sat_height Satellite distance to earth center	m	1	fl	4 byte(s)	
123	first_sample_slant_range Distance from satellite to first range pixel in the full SLC image	m	1	fl	4 byte(s)	
124	spare_18 Spare	-	1	SpareField	12 byte(s)	
125	elevation_pattern Antenna Elevation Pattern	-	1	elevation_patternStruct	132.0 byte(s)	
	a	slant_range_time 2 way slant range times	ns	11	fl	11*4 byte(s)
	b	elevation_angles Corresponding elevation angles	degrees	11	fl	11*4 byte(s)
	c	antenna_pattern Corresponding two-way antenna elevation pattern values	dB	11	fl	11*4 byte(s)
126	spare_19 Spare	-	1	SpareField	14 byte(s)	

Record Length : 3959

## DS\_NAME : Wave Mode processing parameters

Format Version 114.0

Note: the Spectrum SR/GR parameters and the Antenna Elevation parameters pertain to the creation of the [Cross Spectra](#) ([slant range to ground range conversion](#) and [antenna elevation correction](#)). These operations have NOT been applied to the [SLC](#) imagette contained within the [WVI product](#). They are applied during the computation of the cross

spectra.

## 6.6.21 SQ ADSRs

There is one [Wave Mode \(WV\)](#) Summary Quality (SQ) Annotation Data Set Record (ADSR) per wave cell. The ADSR contains information pertaining to both the [imagette](#) and the spectrum. The ASAR\_Wave\_SQ\_ADSR table shown below consists of the ASAR image SQ information, (found in field# 1 - 39) defined in the table [ASAR\\_SO1\\_Image\\_ADSR \(Chapter 6.\)](#), plus new information pertaining to the [cross spectra](#).

There are two Summary Quality (SQ) [ADS](#)s. The first contains information pertaining to [MDS](#) 1 and the second contains information pertaining to MDS 2. The format of each SQ ADS is identical, however the values may differ as each describes a separate MDS.

The information contained in the SQ ADS is a summary of parameters used to establish the quality of the product. This includes [Product Confidence Data \(PCD\)](#) flags, the thresholds used to evaluate the [flags](#), and numerical quality parameters.

The product statistics which are evaluated at each time stamp (each ADSR) and the error message generated will be as follows.

Table 6.59 SQ ADSRs

## SQ ADSRs

#	Description	Units	Count	Type	Size
Data Record					
0	zero_doppler_time Zero doppler time at which Summary Quality information applies	MJD	1	mjd	12 byte(s)
1	attach_flag Attachment Flag Set to 1 if all MDSRs corresponding to this ADSR are blank, set to zero otherwise. This flag will always be zero because this ADSR is updated once per slice or scene. Therefore, if there are no MDSRs, this ADSR is not produced at all.	flag	1	BooleanFlag	1 byte(s)
2	input_mean_flag Input data mean outside nominal range flag 0 = mean of I and Q input values are both within specified range from expected mean. For expected mean of x, the measured mean must fall between x-threshold to x+threshold. 1 = otherwise	flag	1	BooleanFlag	1 byte(s)

#	Description	Units	Count	Type	Size
3	<b>input_std_dev_flag</b> Input data standard deviation outside nominal range flag 0 = standard deviation values of I and Q input values are both within specified range of expected standard deviation. For expected std. dev. x, the measured std. dev. must fall between x-threshold to x+threshold. 1 = otherwise	flag	1	BooleanFlag	1 byte(s)
4	<b>input_gaps_flag</b> Significant gaps in the input data flag 0 = number of input gaps <= threshold value 1 = number of input data gaps > threshold value.	flag	1	BooleanFlag	1 byte(s)
5	<b>input_missing_lines_flag</b> Missing lines significant flag 0 = percentage of missing lines <= threshold value 1 = percentage of missing lines > threshold value. The number of missing lines is the number of lines missing from the input data, excluding data gaps.	flag	1	BooleanFlag	1 byte(s)
6	<b>dop_cen_flag</b> Doppler Centroid Uncertain flag 0 = confidence measure >= specified value 1 = confidence measure < specified value. If more than one Doppler centroid estimation is performed in a slice, the flag is set if any confidence measure is less than the threshold.	flag	1	BooleanFlag	1 byte(s)
7	<b>dop_amb_flag</b> Doppler ambiguity estimate uncertain flag 0 = confidence measure >= specified value 1 = confidence measure < specified value	flag	1	BooleanFlag	1 byte(s)
8	<b>output_mean_flag</b> Output data mean outside nominal range flag 0 = mean of I and Q output values for SLC image or mean of detected pixels for a detected product, are both within specified range from expected mean. For expected mean of x, the measured mean must fall between x-threshold to x+threshold. 1 = otherwise.	flag	1	BooleanFlag	1 byte(s)
9	<b>output_std_dev_flag</b> Output data standard deviation outside nominal range flag 0 = mean of I and Q output values for SLC image or mean of detected pixels for a detected product, are both within specified range from expected mean. For expected mean of x, the measured mean must fall between x-threshold to x+threshold. 1 = otherwise	flag	1	BooleanFlag	1 byte(s)
10	<b>chirp_flag</b> Chirp extraction failed or is of low quality flag 0 = able to reconstruct all chirps or chirp reconstruction not requested (nominal chirp used) AND all quality measures were acceptable. 1 = unable to reconstruct a chirp during processing and chirp reconstruction was requested or the quality is below the acceptable levels. When value = 1, (i.e. unable to reconstruct a chirp during processing and chirp reconstruction was requested or the quality is below the acceptable levels), PF-ASAR uses the nominal range pulse for processing and a nominal elevation beam scaling factor.	flag	1	BooleanFlag	1 byte(s)
11	<b>missing_data_sets_flag</b> Data sets missing flag 0 = all data sets which are supposed to be in the product are present 1 = any data sets (including ADSs) are missing from the product which are supposed to be included under normal circumstances. When value = 1 (i.e any data sets, including ADSs, are missing from the product which are supposed to be included under normal circumstances), which data sets are missing can be determined by an examination of the DSDs in the SPH.	flag	1	BooleanFlag	1 byte(s)
12	<b>invalid_downlink_flag</b> Invalid downlink parameters flag 0 = all parameters read from the downlinked data were valid 1 = displayed if any downlink parameter is out of range and therefore a default value has been used during processing.	flag	1	BooleanFlag	1 byte(s)
13	<b>spare_1</b> <b>Spare</b>	-	1	SpareField	7 byte(s)
14	<b>thresh_chirp_broadening</b> Threshold for setting the chirp quality flag. Maximum percentage broadening permitted in cross-correlation pulse width compared to theoretical width.	%	1	fl	4 byte(s)
15	<b>thresh_chirp_sidelobe</b> Threshold for setting the chirp quality flag First sidelobe of the chirp cross correlation function	dB	1	fl	4 byte(s)
16	<b>thresh_chirp_islr</b> Threshold for setting the chirp quality flag ISLR of the chirp cross correlation function	dB	1	fl	4 byte(s)
17	<b>thresh_input_mean</b> Threshold for setting the mean of input data quality flag For an expected mean value of x, this is the value T, such that the measured mean must fall between the x-T and x+T.	-	1	fl	4 byte(s)
18	<b>exp_input_mean</b> Expected mean input value for this product for both I and Q.	-	1	fl	4 byte(s)
19	<b>thresh_input_std_dev</b> Threshold for setting the standard deviation of input data quality flag For an expected standard deviation value of y, this is the value D, such that the measured standard deviation must fall between the y-D and y+D.	-	1	fl	4 byte(s)

#	Description	Units	Count	Type	Size
20	exp_input_std_dev Expected input std. dev. for this product for both I and Q.	-	1	fl	4 byte(s)
21	thresh_dop_cen Threshold for setting the Doppler Centroid quality flag Threshold for Doppler Centroid confidence	-	1	fl	4 byte(s)
22	thresh_dop_amb Threshold for setting the Doppler Centroid ambiguity quality flag Threshold for setting the Doppler Centroid ambiguity confidence flag	-	1	fl	4 byte(s)
23	thresh_output_mean Threshold for setting the mean of output data quality flag For an expected mean value of x, this is the value T, such that the measured mean must fall between the x-T and x+T.	-	1	fl	4 byte(s)
24	exp_output_mean Expected mean output value for this product. For an SLC product this is the expected mean of both the I and Q values.	-	1	fl	4 byte(s)
25	thresh_output_std_dev Threshold for setting the standard deviation of output data quality flag For an expected standard deviation value of y, this is the value D, such that the measured standard deviation must fall between the y-D and y+D.	-	1	fl	4 byte(s)
26	exp_output_std_dev Expected output std. dev. for this product. For an SLC product this is the expected output std. dev. for both I and Q values.	-	1	fl	4 byte(s)
27	thresh_input_missing_lines Threshold for setting the missing lines quality flag Maximum percentage of missing lines to total lines.	%	1	fl	4 byte(s)
28	thresh_input_gaps Threshold for setting the missing gaps quality flag Maximum number of missing gaps allowed.	-	1	fl	4 byte(s)
29	lines_per_gaps Number of missing lines which constitute a gap	lines	1	ul	4 byte(s)
30	spare_2 Spare	-	1	SpareField	15 byte(s)
31	input_mean Input data mean I channel, Q channel	-	2	fl	2*4 byte(s)
32	input_std_dev Input data standard deviation I channel, Q channel	-	2	fl	2*4 byte(s)
33	num_gaps Number of gaps Composed of a predetermined number of consecutive missing lines	-	1	fl	4 byte(s)
34	num_missing_lines Number of missing lines Excluding gaps	-	1	fl	4 byte(s)
35	output_mean Output data mean For detected products: second value is set to zero, or I channel followed by Q channel for SLC	-	2	fl	2*4 byte(s)
36	output_std_dev Output data standard deviation For detected products: second value is set to zero, or I channel followed by Q channel for SLC	-	2	fl	2*4 byte(s)
37	tot_errors Total number of errors detected in isp headers	-	1	ul	4 byte(s)
38	Spare_3 Spare	-	1	SpareField	16 byte(s)
39	land_flag Land Flag 0 = no land in imagette 1 = land in imagette	flag	1	BooleanFlag	1 byte(s)
40	look_conf_flag Look image statistics confidence parameter flag 1 = The ratio of the standard deviation to the mean of the first look image is outside the range given by a minimum and a maximum threshold. 0 = otherwise	flag	1	BooleanFlag	1 byte(s)
41	inter_look_conf_flag Inter-look confidence statistics confidence parameter flag 1 = The normalised deviation of the two inter-look sub-images is greater than a maximum threshold. 0 = otherwise	flag	1	BooleanFlag	1 byte(s)
42	az_cutoff_flag Azimuth cut-off convergence measure flag 1 = The normalised RMS error between the fitted co-variance profile is greater than a maximum threshold. 0 = otherwise	flag	1	BooleanFlag	1 byte(s)
43	az_cutoff_iteration_flag Azimuth cut-off Iteration count overflow flag	flag	1	BooleanFlag	1 byte(s)

#	Description	Units	Count	Type	Size
	1 = The Azimuth cut-off fit did not converge within a minimum number of iterations. 0 = otherwise				
44	phase_flag Phase information confidence measure flag 1 = The imaginary spectral peak is less than a minimum threshold, and the zero lag shift is greater than a minimum threshold. 0 = otherwise	flag	1	BooleanFlag	1 byte(s)
45	spare_4 Spare	-	1	SpareField	4 byte(s)
46	look_conf_thresh Look image statistics confidence parameter thresholds (minimum and maximum)	-	2	fl	2*4 byte(s)
47	inter_look_conf_thresh Inter-look confidence statistics confidence parameter threshold	-	1	fl	4 byte(s)
48	az_cutoff_thresh Azimuth cut-off convergence measure threshold	-	1	fl	4 byte(s)
49	az_cutoff_iterations_thresh Azimuth cut-off Iteration count overflow threshold	-	1	ul	4 byte(s)
50	phase_peak_thresh Phase information confidence measure threshold for the spectral peak	-	1	fl	4 byte(s)
51	phase_cross_thresh Phase information confidence measure threshold for cross covariance peak offset	m	1	fl	4 byte(s)
52	spare_5 Spare	-	1	SpareField	12 byte(s)
53	look_conf Look image statistics confidence parameter The ratio of the standard deviation to the mean of the first look image.	-	1	fl	4 byte(s)
54	inter_look_conf Inter-look confidence statistics confidence parameter.The normalised deviation of the two inter-look sub-images	-	1	fl	4 byte(s)
55	az_cutoff Azimuth cut-off convergence measure The normalised RMS error between the fitted co-variance profile.	-	1	fl	4 byte(s)
56	phase_peak_conf Phase information confidence measure for the spectral peakThe imaginary spectral peak	-	1	fl	4 byte(s)
57	phase_cross_conf Phase information confidence measure for cross covariance peak offset	m	1	fl	4 byte(s)
58	spare_6 Spare	-	1	SpareField	12 byte(s)

Record Length : 252

DS\_NAME : SQ ADSRs

Format Version 114.0

## 6.6.22 ASAR WV Product SPH

The ASAR [Wave Mode \(WV\) Specific Product Header \(SPH\)](#) provides only the information which applies to all wave cells within a product file. The format will be identical for all ASAR wave products, except for the [Data Set Descriptors \(DSD\)](#) sections.

The ASAR Wave Mode Products SPH contents are shown below:

Table 6.60 ASAR WVI Product SPH

## ASAR WVI Product SPH

#	Description	Units	Count	Type	Size
Data Record					
0	sph_descriptor_title SPH_DESCRIPTOR=	keyword	1	AsciiString	15 byte(s)
1	quote_1 quotation mark ("")	ascii	1	AsciiString	1 byte(s)
2	sph_descriptor SPH Descriptor ASCII string describing the product	ascii	1	AsciiString	28 byte(s)
3	quote_2 quotation mark ("")	ascii	1	AsciiString	1 byte(s)
4	newline_char_1 newline character	terminator	1	AsciiString	1 byte(s)
5	first_cell_time_title FIRST_CELL_TIME=	keyword	1	AsciiString	16 byte(s)
6	quote_3 quotation mark ("")	ascii	1	AsciiString	1 byte(s)
7	first_cell_time First Zero Doppler Azimuth time of first line of first imagette UTC Time of first range line in the MDS containing the first imagette used to produce product.	UTC	1	UtcExternal	27 byte(s)
8	quote_4 quotation mark ("")	ascii	1	AsciiString	1 byte(s)
9	newline_char_2 newline character	terminator	1	AsciiString	1 byte(s)
10	last_cell_time_title LAST_CELL_TIME=	keyword	1	AsciiString	15 byte(s)
11	quote_5 quotation mark ("")	ascii	1	AsciiString	1 byte(s)
12	last_cell_time Last Zero Doppler Azimuth time of first line of last imagette UTC Time of the first range line in the MDS containing the last imagette used to produce this product.	UTC	1	UtcExternal	27 byte(s)
13	quote_6 quotation mark ("")	ascii	1	AsciiString	1 byte(s)
14	newline_char_3 newline character	terminator	1	AsciiString	1 byte(s)
15	spare_1 Spare	-	1	SpareField	51 byte(s)
16	swath1_title SWATH_1=	keyword	1	AsciiString	8 byte(s)
17	quote_7 quotation mark ("")	ascii	1	AsciiString	1 byte(s)
18	swath_1 First sub-cycle swath number IS1, IS2, IS3, IS4, IS5, IS6, or IS7.	ascii	1	AsciiString	3 byte(s)
19	quote_8 quotation mark ("")	ascii	1	AsciiString	1 byte(s)
20	newline_char_5 newline character	terminator	1	AsciiString	1 byte(s)
21	swath2_title SWATH_2=	keyword	1	AsciiString	8 byte(s)
22	quote_9 quotation mark ("")	ascii	1	AsciiString	1 byte(s)
23	swath_2 Second sub-cycle swath number IS1, IS2, IS3, IS4, IS5, IS6, or IS7.	ascii	1	AsciiString	3 byte(s)
24	quote_10	ascii	1	AsciiString	1 byte(s)



#	Description	Units	Count	Type	Size
	quotation mark ("")				
25	newline_char_6 newline character	terminator	1	AsciiString	1 byte(s)
26	pass_title PASS=	keyword	1	AsciiString	5 byte(s)
27	quote_11 quotation mark ("")	ascii	1	AsciiString	1 byte(s)
28	pass Ascending or descending orbit designator (defined at start of time pass) ASCENDING , DESCENDING or FULL ORBIT	ascii	1	AsciiString	10 byte(s)
29	quote_12 quotation mark ("")	ascii	1	AsciiString	1 byte(s)
30	newline_char_7 newline character	terminator	1	AsciiString	1 byte(s)
31	polar_title TX_RX_POLAR=	keyword	1	AsciiString	12 byte(s)
32	quote_13 quotation mark ("")	ascii	1	AsciiString	1 byte(s)
33	tx_rx_polar Transmitter / Receiver Polarisation for MDS 1 H/V or H/H or V/H or V/V	ascii	1	AsciiString	3 byte(s)
34	quote_14 quotation mark ("")	ascii	1	AsciiString	1 byte(s)
35	newline_char_8 newline character	terminator	1	AsciiString	1 byte(s)
36	compression_title COMPRESSION=	keyword	1	AsciiString	12 byte(s)
37	quote_15 quotation mark ("")	ascii	1	AsciiString	1 byte(s)
38	compression Compression algorithm used on echo data on-board the satellite. FBAQ2, FBAQ3, FBAQ4 (FBAQ: 8 bits reduced to 2, 3, and 4 bits respectively)others: S&M , and NONE	ascii	1	AsciiString	5 byte(s)
39	quote_16 quotation mark ("")	ascii	1	AsciiString	1 byte(s)
40	newline_char_9 newline character	terminator	1	AsciiString	1 byte(s)
41	spare_2 Spare	-	1	SpareField	51 byte(s)
42	num_dir_bins_title NUM_DIR_BINS=	keyword	1	AsciiString	13 byte(s)
43	num_dir_bins Number of Directional Bins	-	1	Ac	4 byte(s)
44	newline_char_11 newline character	terminator	1	AsciiString	1 byte(s)
45	num_wl_bins_title NUM_WL_BINS=	keyword	1	AsciiString	12 byte(s)
46	num_wl_bins Number of Wavelength Bins	-	1	Ac	4 byte(s)
47	newline_char_12 newline character	terminator	1	AsciiString	1 byte(s)
48	first_dir_bin_title FIRST_DIR_BIN=	keyword	1	AsciiString	14 byte(s)
49	first_dir_bin First Directional Bin	degrees	1	Afl	15 byte(s)
50	first_dir_units <degrees>	units	1	AsciiString	9 byte(s)
51	newline_char_13 newline character	terminator	1	AsciiString	1 byte(s)
52	dir_bin_step_title DIR_BIN_STEP=	keyword	1	AsciiString	13 byte(s)
53	dir_bin_step Directional Bin Step	degrees	1	Afl	15 byte(s)
54	die_bin_step_units <degrees>	units	1	AsciiString	9 byte(s)
55	newline_char_14 newline character	terminator	1	AsciiString	1 byte(s)
56	first_wl_bin_title FIRST_WL_BIN=	keyword	1	AsciiString	13 byte(s)
57	first_wl_bin First Wavelength Bin	m	1	Afl	15 byte(s)

#	Description	Units	Count	Type	Size
	Longest Wavelength				
58	first_wl_bin_units <m>	units	1	AsciiString	3 byte(s)
59	newline_char_15 newline character	terminator	1	AsciiString	1 byte(s)
60	last_wl_bin_title LAST_WL_BIN=	keyword	1	AsciiString	12 byte(s)
61	last_wl_bin Last Wavelength Bin	m	1	Afl	15 byte(s)
	Shortest Wavelength (NOTE: Logarithmic steps)				
62	last_wl_bin_units <m>	units	1	AsciiString	3 byte(s)
63	newline_char_16 newline character	terminator	1	AsciiString	1 byte(s)
64	spare_3 Spare	-	1	SpareField	51 byte(s)
65	look_sep_title LOOK_SEP=	keyword	1	AsciiString	9 byte(s)
66	look_sep Look Separation period in seconds (second = 1/Hz). For the Ocean Wave Spectra, this is the time period between first and last looks.	s	1	Afl	15 byte(s)
67	look_sep_units <>	units	1	AsciiString	3 byte(s)
68	newline_char_18 newline character	terminator	1	AsciiString	1 byte(s)
69	look_bw_title LOOK_BW=	keyword	1	AsciiString	8 byte(s)
70	look_bw Look bandwidth used during spectra processing	Hz	1	Afl	15 byte(s)
71	look_bw_units <Hz>	units	1	AsciiString	4 byte(s)
72	newline_char_19 newline character	terminator	1	AsciiString	1 byte(s)
73	filter_order_title FILTER_ORDER=	keyword	1	AsciiString	13 byte(s)
74	filter_order Order of Butterworth filter used during cross-spectra processingIf set to zero, a Gaussian filter was applied	-	1	Ac	4 byte(s)
75	newline_char_20 newline character	terminator	1	AsciiString	1 byte(s)
76	trend_removal_title TREND_REMOVAL=	keyword	1	AsciiString	14 byte(s)
77	trend_removal Trend Removal applied during cross spectra computation0 = trend removal not applied1 = trend removal applied	ascii	1	AsciiString	1 byte(s)
78	newline_char_21 newline character	terminator	1	AsciiString	1 byte(s)
79	antenna_corr_title ANTENNA_CORR=	keyword	1	AsciiString	13 byte(s)
80	antenna_corr Antenna gain correction applied during cross spectra computation (note: Antenna Elevation gain correction is never applied to the SLC imagette)0 = not applied 1 = applied	ascii	1	AsciiString	1 byte(s)
81	newline_char_22 newline character	terminator	1	AsciiString	1 byte(s)
82	srgr_title SR_GR=	keyword	1	AsciiString	6 byte(s)
83	sr_gr Slant range to ground range conversion applied during cross spectra computation (note: Slant range to ground range conversion is never applied to the SLC imagette)0 = not applied 1 = applied	ascii	1	AsciiString	1 byte(s)
84	newline_char_23 newline character	terminator	1	AsciiString	1 byte(s)
85	cc_window_title CC_WINDOW=	keyword	1	AsciiString	10 byte(s)
86	cc_window Cross covariance window function was applied during cross spectra computation 0 = not applied 1 = applied	ascii	1	AsciiString	1 byte(s)
87	newline_char_24 newline character	terminator	1	AsciiString	1 byte(s)
88	spare_4	-	1	SpareField	30 byte(s)

#	Description	Units	Count	Type	Size
	Spare				
89	num_look_pairs_title NUM_LOOK_PAIRS=	keyword	1	AsciiString	15 byte(s)
90	num_look_pairs Number of look pairs in cross spectrum processing	-	1	Ac	4 byte(s)
91	newline_char_26 newline character	terminator	1	AsciiString	1 byte(s)
92	cc_range_bins_title CC_RANGE_BINS=	keyword	1	AsciiString	14 byte(s)
93	cc_range_bins Range bins in Cross covariance estimation	-	1	Al	11 byte(s)
94	newline_char_27 newline character	terminator	1	AsciiString	1 byte(s)
95	cc_az_bins_title CC_AZIMUTH_BINS=	keyword	1	AsciiString	16 byte(s)
96	cc_azimuth_bins Azimuth bins in Cross covariance estimation	-	1	Al	11 byte(s)
97	newline_char_28 newline character	terminator	1	AsciiString	1 byte(s)
98	cc_half_width_title CC_HALF_WIDTH=	keyword	1	AsciiString	14 byte(s)
99	cc_half_width Half-width of the cross-covariance window function	m	1	Afl	15 byte(s)
100	cc_half_width_units <m>	units	1	AsciiString	3 byte(s)
101	newline_char_29 newline character	terminator	1	AsciiString	1 byte(s)
102	imagettes_failed_title IMAGETTES FAILED=	keyword	1	AsciiString	17 byte(s)
103	imagettes_failed Number of imagettes PF-ASAR failed to produce in this product	-	1	Ac	4 byte(s)
104	newline_char_30 newline character	terminator	1	AsciiString	1 byte(s)
105	spectra_failed_title SPECTRA FAILED=	keyword	1	AsciiString	15 byte(s)
106	spectra_failed Number of cross or ocean wave spectra PF-ASAR failed to produce in this product	-	1	Ac	4 byte(s)
107	newline_char_31 newline character	terminator	1	AsciiString	1 byte(s)
108	imagettes_made_title IMAGETTES MADE=	keyword	1	AsciiString	15 byte(s)
109	imagettes_made number of imagettes successfully produced by the PF-ASAR processor	-	1	Ac	4 byte(s)
110	newline_char_32 newline character	terminator	1	AsciiString	1 byte(s)
111	spectra_made_title SPECTRA MADE=	keyword	1	AsciiString	13 byte(s)
112	spectra_made Number of cross spectra or ocean wave spectra successfully produced by PF-ASAR in this product	-	1	Ac	4 byte(s)
113	newline_char_33 newline character	terminator	1	AsciiString	1 byte(s)
114	spare_5 Spare	-	1	SpareField	10 byte(s)

Record Length : 901

DS\_NAME : ASAR WVI Product SPH

Format Version 114.0

The [ASA\\_WVI 2.6.2.1.2.](#) product [SPH](#) contains up to a maximum of 411 [DSD](#)s (including the spare DSD). The actual number of [SLC Imagette](#) DSDs is determined at run time and can be derived from the SPH as the sum of Fields #32 and #30 (i.e. as the sum of the number of [Imagettes\\_Made](#) and the number of [Imagettes\\_Failed](#) respectively).

Note that the SLC Imagette [Measurement Data Set \(MDS\)](#) size and number of Measurement Data Set Records (MDSRs) may differ from cell to cell.

Fields #15 and #16 of the SPH give the [wavelengths](#),  $\lambda_0$  and  $\lambda_{N_k-1}$ , of the first and last [wavelength bins](#). Field 12 gives the number of bins,  $N_k$ . The formula for reconstructing the wavelengths,  $\lambda_m$ , for each wavelength bin, m, from these first and last values is as follows:

For Level 1 WVI and WVS products:

$$\lambda_m = \frac{\lambda_0}{\left(\frac{\lambda_0}{\lambda_{N_k-1}}\right)^{\frac{2m}{N_k-1}}} \quad \text{for} \quad m \in [0, N_k - 1]$$

For Level 2 WVW products:

$$\lambda_m = \frac{\lambda_0}{\left(\frac{\lambda_0}{\lambda_{N_k-1}}\right)^{\frac{m}{N_k-1}}} \quad \text{for} \quad m \in [0, N_k - 1]$$

Table 6.61

For a further discussion of this product, and the associated [Data Sets \(DS\)](#) refer to the section entitled ["Level 1B Wave Products" 2.6.2.1.2.](#)

## 6.6.23 SPH for auxiliary data with N=1 DSDs

In order to maintain a degree of conformity across the [Auxiliary Data](#) files, the [Specific Product Header \(SPH\)](#) contains only the SPH Descriptor and a spare field, other than the [Data Set Descriptors \(DSDs\)](#). The number of DSDs in the SPH may vary.

The Auxiliary Data file SPH is defined below. The ASCII conventions used are defined in the "Definitions and Conventions" section.

Table 6.62 SPH for auxiliary data with N=1 DSDs

## SPH for auxiliary data with N=1 DSDs

#	Description	Units	Count	Type	Size
Data Record					
0	sph_descriptor_title SPH_DESCRIPTOR=	keyword	1	AsciiString	15 byte(s)
1	quote_1 quotation mark ("")	ascii	1	AsciiString	1 byte(s)
2	sph_descriptor SPH descriptor ASCII string describing the product	ascii	1	AsciiString	28 byte(s)
3	quote_2 quotation mark ("")	ascii	1	AsciiString	1 byte(s)
4	newline_char_1 newline character	terminator	1	AsciiString	1 byte(s)
5	spare_1 Spare	-	1	SpareField	52 byte(s)

Record Length : 98

DS\_NAME : SPH for auxiliary data with N=1 DSDs

Format Version 114.0

## 6.6.24 Level 0 MDSR

The [Level 0 Measurement Data Set \(MDS\)](#) will consist of a series of [Annotated Instrument Source Packets \(AISPs\)](#). The annotation consists of the header added to the [ISP](#) by the Front End Processor (FEP) plus the sensing time added by the Level 0 processor, as converted from the Satellite Binary Time (SBT) counter embedded in each ISP. This stamp allows for later extraction of specific regions of the MDS.

The exact contents of the Level 0 MDSRs is instrument and mode specific, however it will follow a common structure as shown below.

Table 6.63

## Level 0 MDSR

#	Description	Units	Count	Type	Size
Data Record					
0	dsr_time MJD of sensing time as extracted from Aisp	MJD	1	mjd	12 byte(s)
1	gsrt Ground station reference time	MJD	1	mjd	12 byte(s)
2	isp_length Length of the isp = length of the source packet - 7 bytes	bytes	1	us	2 byte(s)
3	crc_errs Number of VCDUs in the isp which contain a CRC error	VCDU	1	us	2 byte(s)
4	rs_errs Number of VCDUs in the isp for which an RS correction was performed	VCDU	1	us	2 byte(s)
5	spare_1 spare	-	1	SpareField	2 byte(s)
6	source_packet downlinked source packet	-	1	source_packetStruct	-1.0 byte(s)
	a Isp_Fields Instrument Source Packet	-		uc	1 byte(s)

Record Length : 31

DS\_NAME : Level 0 MDSR

Format Version 114.0

## Front End Processor (FEP) Annotations

The FEP annotations describe the quality of the [ISP](#) reconstruction process. The FEP Header will follow the structure shown below:

Table 6.64

Note 2 - This field uses the same definition as the Packet Length field of the Packet Header.

## 6.6.25 Level 0 SPH

A standard [Specific Product Header \(SPH\)](#) format has been defined for all [ENVISAT Level 0](#) data. The format shown below follows the same ASCII format conventions of the [Main Product Header \(MPH\)](#).

Note that the symbol " " denotes a blank space throughout this handbook.

Table 6.65 Level 0 SPH

## Level 0 SPH

#	Description	Units	Count	Type	Size
Data Record					
0	sph_descriptor_title SPH_DESCRIPTOR=	keyword	1	AsciiString	15 byte(s)
1	quote_1 quotation mark ("")	ascii	1	AsciiString	1 byte(s)
2	sph_descriptor SPH descriptor ASCII string describing the product	ascii	1	AsciiString	28 byte(s)

#	Description	Units	Count	Type	Size
3	quote_2 quotation mark ("")	ascii	1	AsciiString	1 byte(s)
4	newline_char_1 newline character	terminator	1	AsciiString	1 byte(s)
5	start_lat_title START_LAT=	keyword	1	AsciiString	10 byte(s)
6	start_lat WGS84 latitude of first satellite nadir point at the sensing start time of the MPH A negative value denotes south latitude; a positive value denotes north latitude.	(1e-6) degrees	1	AsciiGeoCoordinate	11 byte(s)
7	start_lat_units <10-6degN>	units	1	AsciiString	10 byte(s)
8	newline_char_2 newline character	terminator	1	AsciiString	1 byte(s)
9	start_long_title START_LONG=	keyword	1	AsciiString	11 byte(s)
10	start_long WGS84 longitude of first satellite nadir point at the sensing start time of the MPH A positive value denotes east of Greenwich; a negative value denotes west of Greenwich.	(1e-6) degrees	1	AsciiGeoCoordinate	11 byte(s)
11	start_long_units <10-6degE>	units	1	AsciiString	10 byte(s)
12	newline_char_3 newline character	terminator	1	AsciiString	1 byte(s)
13	stop_lat_title STOP_LAT=	keyword	1	AsciiString	9 byte(s)
14	stop_lat WGS84 latitude of first satellite nadir point at the sensing stop time of the MPH A negative value denotes south latitude; a positive value denotes north latitude.	(1e-6) degrees	1	AsciiGeoCoordinate	11 byte(s)
15	stop_lat_units <10-6degN>	units	1	AsciiString	10 byte(s)
16	newline_char_4 newline character	terminator	1	AsciiString	1 byte(s)
17	stop_long_title STOP_LONG=	keyword	1	AsciiString	10 byte(s)
18	stop_long WGS84 longitude of first satellite nadir point at the sensing stop time of the MPH A positive value denotes east of Greenwich; a negative value denotes west of Greenwich.	(1e-6) degrees	1	AsciiGeoCoordinate	11 byte(s)
19	stop_long_units <10-6degE>	units	1	AsciiString	10 byte(s)
20	newline_char_5 newline character	terminator	1	AsciiString	1 byte(s)
21	sat_track_title SAT_TRACK=	keyword	1	AsciiString	10 byte(s)
22	sat_track Sub-satellite track heading at the sensing start time in the MPH.	degrees	1	Afl	15 byte(s)
23	sat_track_units <deg>	units	1	AsciiString	5 byte(s)
24	newline_char_6 newline character	terminator	1	AsciiString	1 byte(s)
25	spare_1 Spare	-	1	SpareField	51 byte(s)
26	isp_errors_sig_title ISP_ERRORS_SIGNIFICANT=	keyword	1	AsciiString	23 byte(s)
27	isp_errors_significant 1 or 0.1 if number of ISPs with CRC errors exceeds threshold	ascii	1	AsciiString	1 byte(s)
28	newline_char_8 newline character	terminator	1	AsciiString	1 byte(s)
29	missing_isps_sig_title MISSING_ISPS_SIGNIFICANT=	keyword	1	AsciiString	25 byte(s)
30	missing_isps_significant 1 or 0.1 if number of missing ISPs exceeds threshold	ascii	1	AsciiString	1 byte(s)
31	newline_char_9 newline character	terminator	1	AsciiString	1 byte(s)
32	isp_discard_sig_title ISP_DISCARDED_SIGNIFICANT=	keyword	1	AsciiString	26 byte(s)
33	isp_discarded_significant 1 or 0.1 if number of ISPs discarded by the PF-HS exceeds threshold	ascii	1	AsciiString	1 byte(s)
34	newline_char_10 newline character	terminator	1	AsciiString	1 byte(s)
35	rs_sig_title	keyword	1	AsciiString	15 byte(s)

#	Description	Units	Count	Type	Size
	RS_SIGNIFICANT=				
36	rs_significant 1 or 0.1 if number of ISPs with Reed Solomon corrections exceeds threshold	ascii	1	AsciiString	1 byte(s)
37	newline_char_11 newline character	terminator	1	AsciiString	1 byte(s)
38	spare_2 Spare	-	1	SpareField	51 byte(s)
39	num_err_isps_title NUM_ERROR_ISPS=	keyword	1	AsciiString	15 byte(s)
40	num_error_isps Number of ISPs containing CRC errors as reported by the FEP	ISPs	1	Al	11 byte(s)
41	newline_char_13 newline character	terminator	1	AsciiString	1 byte(s)
42	err_isp_thresh_title ERROR_ISPS_THRESH=	keyword	1	AsciiString	18 byte(s)
43	error_isps_thresh Threshold at which number of ISPs containing CRC errors is considered significant	percent	1	Afl	15 byte(s)
44	err_isp_thresh_units <%>	units	1	AsciiString	3 byte(s)
45	newline_char_14 newline character	terminator	1	AsciiString	1 byte(s)
46	num_missing_isps_title NUM_MISSING_ISPS=	keyword	1	AsciiString	17 byte(s)
47	num_missing_isps Number of missing ISPs	ISPs	1	Al	11 byte(s)
48	newline_char_15 newline character	terminator	1	AsciiString	1 byte(s)
49	missing_isps_thresh_title MISSING_ISPS_THRESH=	keyword	1	AsciiString	20 byte(s)
50	missing_isps_thresh Threshold at which number of ISPs missing is considered significant	percent	1	Afl	15 byte(s)
51	missing_isps_thresh_units <%>	units	1	AsciiString	3 byte(s)
52	newline_char_16 newline character	terminator	1	AsciiString	1 byte(s)
53	num_discard_title NUM_DISCARDED_ISPS=	keyword	1	AsciiString	19 byte(s)
54	num_discarded_isps Number of ISPs discarded by PF-HS	ISPs	1	Al	11 byte(s)
55	newline_char_17 newline character	terminator	1	AsciiString	1 byte(s)
56	discard_thresh_title DISCARDED_ISPS_THRESH=	keyword	1	AsciiString	22 byte(s)
57	discarded_isps_thresh Threshold at which number of ISPs discarded by PF-HS is considered significant	percent	1	Afl	15 byte(s)
58	discard_thresh_units <%>	units	1	AsciiString	3 byte(s)
59	newline_char_18 newline character	terminator	1	AsciiString	1 byte(s)
60	num_rs_title NUM_RS_ISPS=	keyword	1	AsciiString	12 byte(s)
61	num_rs_isps Number of ISPs with Reed Solomon corrections	ISPs	1	Al	11 byte(s)
62	newline_char_19 newline character	terminator	1	AsciiString	1 byte(s)
63	rs_thresh_title RS_THRESH=	keyword	1	AsciiString	10 byte(s)
64	rs_thresh Threshold at which number of ISPs discarded by PF-HS is considered significant	percent	1	Afl	15 byte(s)
65	rs_thresh_units <%>	units	1	AsciiString	3 byte(s)
66	newline_char_20 newline character	terminator	1	AsciiString	1 byte(s)
67	spare_3 Spare	-	1	SpareField	101 byte(s)
68	tx_polar_title TX_RX_POLAR=	keyword	1	AsciiString	12 byte(s)
69	quote_3 quotation mark ("")	ascii	1	AsciiString	1 byte(s)

#	Description	Units	Count	Type	Size
70	tx_rx_polar Transmitter/receiver polarization (used for ASAR only) for non-ASAR products	ascii	1	AsciiString	5 byte(s)
71	quote_4 quotation mark ("")	ascii	1	AsciiString	1 byte(s)
72	newline_char_22 newline character	terminator	1	AsciiString	1 byte(s)
73	swath_title SWATH=	keyword	1	AsciiString	6 byte(s)
74	quote_5 quotation mark ("")	ascii	1	AsciiString	1 byte(s)
75	swath Swath number (used for ASAR only) for non-ASAR products	ascii	1	AsciiString	3 byte(s)
76	quote_6 quotation mark ("")	ascii	1	AsciiString	1 byte(s)
77	newline_char_23 newline character	terminator	1	AsciiString	1 byte(s)
78	spare_4 Spare	-	1	SpareField	42 byte(s)
79	dsd_spare_5 DSD Spare	-	1	dsd_sp	0 byte(s)

Record Length : 836

**DS\_NAME : Level 0 SPH**

Format Version 114.0

Within each SPH ( and not shown by the SPH Format Table ) are the following [Data Set Descriptors \(DSDs\)](#), which begin in field# 25 of the SPH.

Table 6.66

**Level 0 DSD Format**

There will be 4 DSDs in the Level 0 SPH. The first DSD describes the [Measurement Data Set](#) (the [Instrument Source Packets](#)) the second is a reference DSD which contains the name of the Level 0 Processor Configuration File used to create the product, and the third is a reference DSD which contains the name of the Orbit State Vector file used to create the product. Finally, the fourth is a spare DSD, reserved to allow future additions to the product if needed. A general DSD structure has been defined as in --broken link-- the table " General DSD Format " found in the " Definitions and Conventions " section. The fields of the Level 0 DSD are filled as follows:

DSD for the MDS:

DS\_NAME= " ASAR\_SOURCE\_PACKETS "

**DS\_TYPE =M**

**FILENAME= "**

**"**

**DS\_OFFSET= (MPH length + SPH length including DSDs) < bytes >**

**DS\_SIZE= (data dependent) < bytes >**

**NUM\_DSR=(data dependent)**

**DSR\_SIZE=(data dependent, set to -1 if size is variable) < bytes >**

DSD Referencing the Level 0 Config. file, or the Orbit State Vector file:

**DS\_NAME= " LEVEL\_0\_CONFIGURATION\_FILE "      " or      "**  
**ORBIT\_STATE\_VECTOR\_FILE "**

**DS\_TYPE=R**

**FILENAME= " (filename) " { note: the filename is left justified within the quotation marks, with any blank spaces added before the closing quote }**

**DS\_OFFSET=+000000000000000000000000 < bytes >**

**DS\_SIZE=+000000000000000000000000 < bytes >**

**NUM\_DSR=+0000000000**

**DSR\_SIZE=+0000000000 < bytes >**

**DSD - Spare**

This DSD is simply 279 ASCII blank space characters followed by 1 ASCII newline character

## 6.6.26 Doppler Centroid parameters

Table 6.67

# Doppler Centroid Grid ADS

#	Description	Units	Count	Type	Size
<b>Data Record</b>					
<b>0</b>	<b>first_zero_doppler_time</b> First Zero Doppler Azimuth time of raw signal data used for this estimates	MJD	1	mjd	12 byte(s)
<b>1</b>	<b>attach_flag</b> Attachment Flag (always set to zero for this ADSR)	flag	1	BooleanFlag	1 byte(s)
<b>2</b>	<b>slant_range_time</b> 2-way slant range time origin (t0)	ns	100	fl	100*4 byte(s)
<b>3</b>	<b>dop_coef</b> Fine Doppler centroid frequency estimate. This is the original estimated Doppler centroid frequncy befor any polynomial fitting is applied	Hz	100	fl	100*4 byte(s)
<b>4</b>	<b>last_zero_doppler_time</b> Last Zero Doppler Azimuth time of raw signal data used for this estimates	MJD	1	mjd	12 byte(s)
<b>5</b>	<b>spare_1</b> Spare	-	1	SpareField	388 byte(s)

**Record Length : 1213**

**DS\_NAME : Doppler Centroid Grid ADS**

**Format Version 116.0**

---

# Chapter 7

---

## Credits

The following organisations have contributed data or information to this document:



European Space Agency

8-10 rue Mario Nikis

75738 Paris

Cedex 15



France

Tel: + 33 1 5369 7155

Fax: + 33 1 5369 7690

ESA website:

ENVISAT website:

Contacts: Mr. Guido Levrini, Instrument System Analysis Manager

e-mail: [guido.levrini@esa.int](mailto:guido.levrini@esa.int)

Mr. Manfred Zink

e-mail: [manfred.zink@esa.int](mailto:manfred.zink@esa.int)



European Space Research and Technology Centre ( ESTEC )

Keplerlaan 1

Postbus 299

2200 AG Noordwijk (The Netherlands) Phone: +31 71 565.6565

Fax: +31 71 565.6040

ESTEC website: [www.estec.esa.nl/pr/index.php3](http://www.estec.esa.nl/pr/index.php3)



MacDonald, Dettwiler and Associates



13800 Commerce Parkway

Richmond, British Columbia

Canada V6V 2J3

Tel: +1-604-278-3411

Fax: +1-604-278-0531

Web site: [www.mda.ca/index.shtml](http://www.mda.ca/index.shtml)

Contact person: Mr. Ian McLeod, Senior Engineer

e-mail: [ianm@mda.ca](mailto:ianm@mda.ca)



13800 Commerce Parkway

MacDonald Dettwiler Building

Richmond, British Columbia

V6V 2J3

CANADA

Tel: (604) 231-5000

Fax: (604) 231-4900

Email: [info@rsi.ca](mailto:info@rsi.ca)

contact person: Mr. Adrian Bohane





Contact: Mr. Edryd Shaw

Tel: (613) 947-1393

Fax: (613) 947-1382

E-Mail: [Ed.Shaw@GeoCan.NRCan.gc.ca](mailto:Ed.Shaw@GeoCan.NRCan.gc.ca)

Director General's Office

588 Booth Street , Room 330

Ottawa , Ontario

K1A 0Y7



**THE ALASKA SAR FACILITY**  
SYNTHETIC APERTURE RADAR DATA

Alaska SAR Facility - User Services

Geophysical Institute

University of Alaska Fairbanks

P.O. Box 757320

Fairbanks, AK 99775-7320

web-site: [www.asf.alaska.edu](http://www.asf.alaska.edu)

E-MAIL: [uso@ASF.alaska.edu](mailto:uso@ASF.alaska.edu)

PHONE: 907-474-6166

FAX: 907-474-2665

(alternate: 907-474-5195 ATTN: ASF USO )

The Envisat Product Handbook Publishing Infrastructure Project (EPHPI) was developed by PLD Communications Ltd (a Pildo Cntg. company):



Pildo Labs Barcelona: Fernando Nuñez, JC Jardinier, Pildo Labs Geneva: R. Ramos, J. Lucas, P. Carrasco, C. Serra

Pildo Labs

Llacuna 162

Barcelona

080018

Spain

Tel: +34 934019782

Fax: +34 934019783

Email: [fernando.nunez@pildo.com](mailto:fernando.nunez@pildo.com)

Email: [julie.andrews@pildo.com](mailto:julie.andrews@pildo.com) (no relation)